The Psychopharmacology of Novel Synthetic Cannabinoids

Richard C. Kevin

A thesis submitted in fulfilment of the requirements for the degree of

Doctor of Philosophy

School of Psychology

Faculty of Science

The University of Sydney

2017

Table of contents

Acknowledgements

Science is a fundamentally collaborative effort, and there are a great many people without whom this thesis could never have happened.

First and foremost, I need to thank my PhD supervisor, Iain McGregor, for his unwavering and amazing support throughout my time as a research student. It is a rare thing to find a supervisor who is not only passionate about his student's work, but also fully prepared to support them in all endeavours, from harebrained schemes to international travel for conferences or visits to other research groups. More than that, the bravery required to let an untrained student loose on expensive analytical instruments is certainly worthy of acknowledgement!

The support of my lab colleagues (formerly the McGregor psychopharmacology lab, now the Lambert Initiative) has been crucial over the past four years. There are too many wonderful people to mention individually, although I feel it necessary to give special thanks to Jordyn Stuart, my analytical chemistry buddy and fellow hater of O-rings, and to Katie Wood, for her excellent work as a research assistant.

To Brian Thomas and the folks over at the Research Triangle Institute, thank you for your generosity, your hard work, and incredible hospitality during my visit. I am certain that the skills and friendships I developed during my visit will be invaluable moving forward, and I hope to continue our collaboration in the years ahead. Speaking of collaborations, I also need to thank Samuel Banister for his scientific expertise, synthesis of many of the compounds in this thesis, and valuable advice at key moments.

A very special thanks goes to my parents, Christine and Peter Kevin, who have done so much for me over the years. They have supported me throughout my entire life and have encouraged me in all endeavours, academic or otherwise, and I cannot thank them enough for that. And thanks also to my grandmother Shirley Page for her financial support, home-cooked meals, and tasty biscuits.

And finally, my endless thanks and gratitude go to Peter Wylie, my ever-patient and amazing partner in all things. You mean everything to me.

List of figures

List of tables

Statement of originality

This thesis is submitted to the University of Sydney in fulfilment of the requirement for the Degree of Doctor of Philosophy.

The work presented in this thesis is, to the best of my knowledge and belief, original except as acknowledged in the text. I hereby declare that I have not submitted this material, either in full or in part, for a degree at this or any other institution.

Richard C. Kevin

Signature:  Date: 30/03/2017

Authorship attribution statement

I, Mr. Richard C. Kevin, was the primary author of the publications featured in Chapters 3, 4, and 5. For these publications, I took the lead role in the conception and design of the research, conducting the research, data analysis and interpretation, and the writing and appraisal of manuscripts.

I made a substantial contribution to each of the three publications featured in Chapter 2. In each publication, I performed the experiment concerned with *in vivo* evaluation of synthetic cannabinoids in rats using biotelemetry. For this part of each publication, I took the lead role in experimental design, conducting the experiment, data analysis and interpretation, and writing and appraising the parts of the manuscript concerning biotelemetric assessment. The other experiments concerning compound synthesis and *in vitro* evaluation were designed and carried out by the co-authors of these publications.

In addition to the statements above, in cases where I am not the corresponding author of a published item, permission to include the published material has been granted by the corresponding author.

Richard C. Kevin

Signature:  Date: 30/03/2017

As supervisor for the candidature upon which this thesis is based, I can confirm that the authorship attribution statements above are correct.

Prof. Iain S. Mcgregor

Signature:  Date: 30/03/2017

Publications

The following publications form the main content of this thesis:

Kevin, R. C., Lefever, T. W., Patel, P., Synder, R., Fennel, T. R., Wiley, J. L., McGregor, I. S., & Thomas, B. F. (2017). In vitro and in vivo pharmacokinetics and metabolism of synthetic cannabinoids CUMYL-PICA and 5F-CUMYL-PICA. *Forensic Toxicology,* doi:10.1007/s11419-017-0361-1

(Chapter 3)

Kevin, R. C., Wood, K. E., Stuart, J., Mitchell, A. J., Moir, M., Banister, S. D., Kassiou, M., & McGregor, I. S. (2017). Acute and lasting residual effects resulting from exposure to the novel synthetic cannabinoids AB-PINACA and AB-FUBINACA in adolescent rats. *Journal of Psychopharmacology,* doi: 10.1177/0269881116684336

(Chapter 4)

Kevin, R. C., Allsop, D. J., Lintzeris, N., Dunlop, A. J., Booth, J., & McGregor, I. S. (2017). Urinary cannabinoid levels during Nabiximols (Sativex™)-medicated inpatient cannabis withdrawal. *Forensic Toxicology, 35,* 33-44.

(Chapter 5)

Banister, S. D., Longworth, M., **Kevin, R. C.,** Shivani, S., Santiago, M., Stuart, J., Mack, J., Glass, M., McGregor, I. S., Connor, M., & Kassiou, M. (2016). The pharmacology of valinate and tert-leucinate synthetic cannabinoids 5F-AMBICA, 5F-AMB, 5F-ADB, AMB-FUBINACA, MDMB-FUBINACA, MDMB-CHMICA, and their analogues. *ACS Chemical Neuroscience, 7(9),* 1241-1254.

(Part of Chapter 2)

Banister, S. D., Moir, M., Stuart, J., **Kevin, R. C.**, Wood, K. E., Wilkinson, S. M., Longworth, M., Beinat, C., Buchanan, A., Glass, M., Connor, M., McGregor, I. S., & Kassiou, M. (2015). The pharmacology of indole and indazole synthetic cannabinoid designer drugs AB-FUBINACA, ADB-FUBINACA, AB-PINACA, ADB-PINACA, 5F-AB-PINACA, 5F-ADB-PINACA, ADBICA and 5F-ADBICA. *ACS Chemical Neuroscience, 6(9),* 1546-1559.

(Part of Chapter 2)

Banister, S. D., Stuart, J., **Kevin, R. C.**, Edington, A., Longworth, M., Wilkinson, S. M., Beinat, C., Buchanan, A. S., Hibbs, D. E., Glass, M., Connor, M., McGregor, I. S., & Kassiou, M. (2015). The effects of bioisosteric fluorine in synthetic cannabinoid designer drugs JWH-018, AM-2201, UR-144, XLR-11, PB-22, 5F-PB-22, APICA, and STS-135. *ACS Chemical Neuroscience, 6(8),* 1445-1458.

(Part of Chapter 2)

Additional publications

During my PhD candidature, I contributed to the following publications which are complimentary to this thesis, but do not form part of its content:

Book Chapters

Allsop, D. J., **Kevin, R. C.**, & Arnold, J. (2016). Cannabis: The pharmacokinetics and pharmacodynamics of recreational and medicinal cannabis. In Wolff, K., White, J., & Karch S. (Eds.) *The SAGE Handbook of Drug & Alcohol Studies: Biological Approaches*, 194-212.

Original Research

Banister, S. D., Stuart, J., Conroy, T., Longworth, M., Manohar, M., Beinat, C., Wilkinson, S. M., **Kevin, R. C.**, Hibbs, D. E., Glass, M., Connor, M., McGregor, I. S., & Kassiou, M. (2015). Structure-activity relationships (SARs) of synthetic cannabinoid designer drug RCS-4 and its regioisomers and C4-homologs. *Forensic Toxicology, 33(2),* 355-366.

Lefever, T. W., Marusich, J. A., Thomas, B. F., Barrus, D. G., Peiper, N. C., **Kevin, R. C.**, & Wiley, J. L. (2017). Vaping synthetic cannabinoids: A novel preclinical model of E-cigarette use in mice. *Substance Abuse: Research and Treatment.*

Thomas, B. F., Lefever, T. W., Cortes, R. A., Kovach, A. L., Cox, A. O., Patel, P. R., Pollard, G. T., Marusich, J. A., **Kevin, R. C.**, Gamage, T. F., & Wiley, J. L. (2017). Thermolytic degradation of synthetic cannabinoids: Chemical exposures and pharmacological consequences. *The Journal of Pharmacology and Experimental Therapeutics.*

List of abbreviations

11-OH-THC	11-hydroxy-Δ^9-tetrahydrocannabinol
5F-AB-PINACA	*N*-[(1S)-1-(aminocarbonyl)-2-methylpropyl]-1-(5-fluoropentyl)-1*H*-indazole-3-carboxamide
5F-ADB-PINACA	*N*-[1-(aminocarbonyl)-2,2-dimethylpropyl]-1-(5-fluoropentyl)-1*H*-indazole-3-carboxamide
5F-ADB	*N*-[[1-(5-fluoropentyl)-1H-indazol-3-yl]carbonyl]-3-methyl-*D*-valine, methyl ester
5F-ADBICA	*N*-[1-(aminocarbonyl)-2,2-dimethylpropyl]-1-(5-fluoropentyl)-1*H*-indole-3-carboxamide
5F-AMB	*N*-[(1-(5-fluoropentyl)-1H-indazol-3-yl)carbonyl]-L-valine, methyl ester
5F-AMBICA	*N*-(1-amino-3-methyl-1-oxobutan-2-yl)-1-(5-fluoropentyl)-1*H*-indol-3-carboxamide
5F-CUMYL-PICA	1-(5-Fluoropentyl)-*N*-(2-phenylpropan-2-yl)-1*H*-indole-3-carboxamide
5F-PB-22	1-fluoropentyl-1*H*-indole-3-carboxylic acid 8-quinolinyl ester
7-OH-CBD	7-hydroxy-cannabidiol
Δ^9-THC	(-)-trans-Δ^9-tetrahydrocannabinol
AB-001	1-pentyl-3-(1-adamantoyl)indole
AB-CHMINACA	*N*-[(1*S*)-1-(aminocarbonyl)-2-methylpropyl]-1-(cyclohexylmethyl)-1*H*-indazole-3-carboxamide
AB-FUBINACA	*N*-[(2*S*)-1-amino-3-methyl-1-oxobutan-2-yl]-1-[(4-fluorophenyl) methyl]indazole-3-carboxamide
AB-PINACA	*N*-[(1*S*)-1-(aminocarbonyl)-2-methylpropyl]-1-pentyl-1*H*-indazole-3-carboxamide
ACN	acetonitrile
ADB-FUBINACA	*N*-[1-(aminocarbonyl)-2,2-dimethylpropyl]-1-[(4-fluorophenyl)methyl]-1*H*-indazole-3-carboxamide
ADB-PINACA	*N*-[1-(aminocarbonyl)-2,2-dimethylpropyl]-1-pentyl-1*H*-indazole-3-carboxamide
ADBICA	*N*-(1-amino-3,3-dimethyl-1-oxobutan-2-yl)-1-pentyl-1*H*-indole-3-carboxamide
AEA	*N*-arachidonoylethanolamine; anandamide
AM-2201	1-(5-fluoropentyl)-3-(1-naphthoyl)indole

AMB-FUBINACA	methyl (1-(4-fluorobenzyl)-1*H*-indazole-3-carbonyl)-*L*-valinate
ANOVA	analysis of variance
APICA	see SDB-001
CB_1	cannabinoid 1 (receptor)
CB_2	cannabinoid 2 (receptor)
CBD	cannabidiol
CBDA	cannabidiolic acid
CBG	cannabigerol
CBN	cannabinol
CP-47,497	2[(1*S*,3*R*)-3-hydroxycyclohexyl]-5-(2-methyloctan-2-yl)phenol
CP-55,940	2-[(1*R*,2*R*,5*R*)-5-hydroxy-2-(3-hydroxypropyl) cyclohexyl]-5-(2-methyloctan-2-yl)phenol
CPP	conditioned place preference
CUMYL-PICA	1-pentyl-*N*-(2-phenylpropan-2-yl)-1*H*-indole-3-carboxamide
EG-018	naphthalen-1-yl(9-pentyl-9*H*-carbazol-3-yl)methanone
EPM	elevated plus maze
EtOH	ethanol
FA	formic acid
FAAH	fatty acid amide hydrolase
FUBIMINA	(1-(5-fluoropentyl)-1*H*-benzo[*d*]imidazol-2-yl)(naphthalen-1-yl)methanone
GC-MS	gas chromatrography-mass spectrometry
GM-CSF	granulocyte macrophage colony-stimulating factor
GPR55	G-protein coupled receptor 55
HU-210	1,1-dimethylheptyl- 11-hydroxytetrahydrocannabinol
IFNγ	interferon gamma
IL	interleukin
i.p.	intraperitoneal
JWH-018	1-pentyl-3-(1-naphthoyl)indole
JWH-073	1-butyl-3-(1-naphthoyl)indole
JWH-200	[1-[2-(4-morpholinyl)ethyl]-1*H*-indol-3-yl]-1-naphthalenyl-methanone
LC-MS/MS	liquid chromatography-tandem mass spectrometry

MDMB-CHMINACA	*N*-[[1-(cyclohexylmethyl)-1*H*-indazol-3-yl]carbonyl]-3-methyl-*L*-valine, methyl ester
MDMB-FUBINACA	*N*-[[1-[(4-fluorophenyl)methyl]-1H-indazol-3-yl]carbonyl]-3-methyl-*L*-valine, methyl ester
MeOH	methanol
NOR	novel object recognition
NPS	novel psychoactive substance
OF	open field
SAR	structure-activity relationship
SC	synthetic cannabinoid
SDB-001	*N*-(1-adamantyl)-1-pentyl-1*H*-indole-3-carboxamide
SI	social interaction
STS-135	*N*-(1-adamantyl)-1-(5-fluoropentyl)-1*H*-indole-3-carboxamide
PB-22	1-pentyl-1*H*-indole-3-carboxylic acid 8-quinolinyl ester
THCA	tetrahydrocannabinolic acid
THC-COOH	11-*nor*-9-carboxy-Δ^9-tetrahydrocannabinol
THCV	tetrahydrocannabivarin
TNFα	tumor necrosis factor alpha
THJ-018	1-naphthalenyl(1-pentyl-1*H*-indazol-3-yl)-methanone
TRP	transient receptor potential channel
UR-144	1-(pentyl-1*H*-indol-3-yl)(2,2,3,3-tetramethylcyclopropyl)-methanone
VEH	vehicle
WIN-48,098	pravadoline; (4-methoxyphenyl)[2-methyl]-1-[2-(4-morpholinyl)ethyl]-1*H*-indol-3-yl]-methanone
XLR-11	1-(5-fluoropentyl)-1*H*-indol-3-yl)(2,2,3,3-tetramethylcyclopropyl)methanone
WIN-55,212-2	[(3*R*)-2,3-dihydro-5-methyl-3-(4-morpholinylmethyl)pyrrolo[1,2,3-de]-1,4-benzoxazin-6-yl]-1-naphthalenyl-methanone

Thesis abstract

Over recent years, the rapid proliferation of novel psychoactive substances (NPS) has presented significant challenges to health professionals, regulators, and forensic scientists alike. Of the many different classes of NPS, synthetic cannabinoids comprise an increasingly prevalent and diverse class of compounds that are used by many people around the world for recreational purposes. These compounds act on CB_1 and CB_2 cannabinoid receptors, similar to endogenous cannabinoid receptor ligands and to the prototypical cannabis-derived receptor agonist Δ^9-tetrahydrocannabinol (Δ^9-THC). Recreationally used synthetic cannabinoids tend to produce psychoactive effects similar to, but stronger than, those of Δ^9-THC. The majority of modern synthetic cannabinoids have never been systematically assessed for their effects in humans, meaning that their psychopharmacological and toxicological effects remain largely uncharacterised. Unfortunately, but perhaps not surprisingly, these compounds are implicated in scores of toxic and fatal episodes worldwide.

This thesis presents a series of studies aimed at building new knowledge regarding the behavioural and physiological effects of specific synthetic cannabinoids, their potency and metabolism, their long-term effects on cognitive function and brain neurochemistry, and analytical techniques that may be useful in the development of agonist substitution therapies to assist with synthetic cannabinoid withdrawal.

Chapter 1 consists of a comprehensive review of what is currently known and unknown about modern synthetic cannabinoids. It presents an outline of general cannabinoid pharmacology and reviews the acute effects and toxicity of synthetic cannabinoids, their metabolism, potential for thermal degradation, and the limited

data available regarding their long-tern health-related effects. This review introduces the rationale for the studies presented in the subsequent chapters.

Chapter 2 presents three studies that describe the synthesis of twelve novel synthetic cannabinoids, the affinity and efficacy of these compounds at CB_1 and CB_2 receptors, and their *in vivo* effects on body temperature and heart rate across specific dose ranges. These *in vivo* dose-response relationships were used to inform dosing in subsequent chapters. Radiotelemetric probes were surgically implanted into adult male rats to enable the real-time monitoring of body temperature and heart rate following synthetic cannabinoid administration. All of the tested compounds produced hypothermic effects, although the required dose, magnitude of effect, and duration of effect varied as a function of molecular structure. In some cases, *in vivo* potency exceeded or fell short of predictions derived from *in vitro* cannabinoid receptor binding assays and user reports. These findings suggest that while cannabinoid receptor binding is an important determinant of *in* vivo efficacy of synthetic cannabinoids, metabolic transformation and thermolytic degradation into cannabinoid receptor active compounds most likely play additional important roles in determining *in vivo* potency.

Accordingly, Chapter 3 focuses on the metabolism of the two recently identified synthetic cannabinoids CUMYL-PICA and 5F-CUMYL-PICA, aiming to establish pharmacokinetic parameters and metabolic pathways for these compounds. A total of 56 novel metabolites were described. Major and minor metabolic pathways were postulated, and useful analytical targets were identified as putative markers of consumption. Additionally, this study compared i*n vitro* pharmacokinetic parameters, obtained with *in vitro* microsomal and hepatocyte assays, to data collected *in vivo* in

rats, finding that *in vitro* clearance estimates greatly exceeded actual *in vivo* elimination rates. It is argued that lipid solubility and protein binding are factors that may require consideration during interpretation of similar *in vitro* estimates in the wider literature.

Given the dearth of information regarding the long-term consequences of synthetic cannabinoid use, Chapter 4 investigates the acute and long-term effects of repeated administration of synthetic cannabinoids AB-PINACA and AB-FUBINACA to adolescent male rats. These effects were compared to those of Δ^9-THC. Acute effects included dose-dependent reductions in locomotor activity, increases in anxiety and an absence of conditioned place preference or aversion. Weeks after the cessation of dosing, long-term residual deficits in recognition memory are described, as well as complex ligand-specific effects on cerebellar endocannabinoids and plasma cytokines. Interestingly, most effects caused by either synthetic cannabinoid were similar to those of Δ^9-THC, and no unusual toxidrome was observed in Chapters 2, 3 or 4 with synthetic cannabinoid administration. The inability of rodent models to capture the human toxicity described in numerous case studies in puzzling, and may reflect factors specific to human use, such as product contamination, use of extreme doses, or species differences in pharmacokinetics.

Reports of synthetic cannabinoid withdrawal and addiction are increasingly found in media reports and case studies, suggesting a need for novel clinical treatments for these conditions. One option is agonist substitution therapy, which might involve products such as nabiximols (Sativex™), a buccal spray consisting of equal parts Δ^9-THC and cannabidiol (CBD). CBD is a non-psychoactive constituent of cannabis with anxiolytic and neuroprotective properties. The viability of this

approach depends on being able to administer the treatment at appropriate concentrations, and being able to accurately monitor patient pharmacokinetics. Chapter 5 reports use of a novel method of cannabinoid urinalysis in a population of cannabis-dependent treatment-seeking users treated with nabiximols during inpatient withdrawal. β-glucuronidase hydrolysis was used to increase the concentrations of key cannabinoids and metabolites in urine samples, allowing for enhanced detection of Δ^9-THC and CBD. The study provides evidence that cannabinoid urinalysis can substitute for plasma analysis, which may provide a less invasive sampling method for future studies. Moreover, this study showed that after hydrolysis cannabinoid concentrations were greater in urine than in plasma, such that cannabinoid urinalysis could be used for analysis of trace cannabinoids that may go undetected in blood. This technique might also prove useful for the analysis of urinary synthetic cannabinoid metabolites in future studies.

Chapter 6 provides a general discussion of the results obtained in this thesis and describes how the results represent an advance in several areas of cannabinoid research. The results obtained from Chapters 2, 3, and the wider literature are combined to identify *in vivo* structure-activity and structure-metabolism relationships for a wide variety of synthetic cannabinoids. These relationships may prove useful for the prediction of the psychopharmacological properties and metabolic pathways of future novel synthetic cannabinoids that are detected by authorities, reducing the burden involved in testing large numbers of novel compounds individually. Second, potential implications of chronic synthetic cannabinoid use in humans are discussed. Specifically, long-lasting cognitive impairments and subtle biochemical modulations are predicted in chronic synthetic cannabinoid users. Finally, analytical techniques for

evaluating and monitoring agonist replacement therapy for synthetic cannabinoid withdrawal are established. Taken together, the research presented in this thesis sheds light on the physiological, psychopharmacological, and pharmacokinetic properties of several recreationally used synthetic cannabinoids, and establishes key methodology for future research into specific and efficacious treatments for synthetic cannabinoid withdrawal.

Chapter 1. General introduction and literature review

1.1 Preface

As our understanding of pharmacological processes evolves, so do the tools used to carry out pharmacological investigations. For example, we can design more targeted and efficacious agonists, antagonists, and modulators of systems of interest. These tools may further boost our pharmacological understanding and even provide superior therapeutics for injuries or diseases. Sometimes, these new discoveries involve systems that can produce psychoactive effects. And sometimes, the syntheses of novel, targeted, ultra-potent compounds are published for the world to see. And sometimes, chemists get creative with their business practices.

Thus it comes as little surprise that recent decades have seen the emergence of vast numbers of novel psychoactive substances – compounds that are specifically designed to act on neural systems to produce psychoactive effects (Power, 2014). Scientists, health professionals, and legislators are faced with the emergence of hundreds of such drugs, each possessing largely uncharacterised psychopharmalogical and toxicological properties (EMCDDA, 2015). From “bath salts” to “fake weed” to the misnomer “synthetic LSD”, recent evolutions in psychoactive drugs have challenged health systems, drug legislation, and our understanding of recreational drug use.

Novel drugs are nothing new – improved medications, for example, are introduced all the time. But the typical modern therapeutic has years of research behind it: *in vitro* screening, controlled trials in animals, extensive toxicological and metabolic studies, and often long-term follow-ups (Balunas & Kinghorn, 2005). Each drug, barring exceptional circumstances, has undergone extensive screening before ever being used by a person. For emerging novel psychoactive substances, this process is reversed – the first major discovery is that people are using the substance. From

there, researchers must work backwards, deriving the basic pharmacological properties of the substance after the fact.

Of the many classes of novel psychoactive substances, this thesis focuses on synthetic cannabinoids – compounds designed to act on cannabinoid receptors. In particular, it focuses on a range of synthetic cannabinoids that produce psychoactive effects and that are frequently used recreationally for that purpose. While these drugs are superficially innocuous compared to other novel psychoactive substances like synthetic opiates or designer cathinones, some compounds (but intriguingly, not all) have nevertheless produced toxic and even fatal outcomes worldwide (Louh & Freeman, 2014; Schwartz et al., 2015; Trecki, Gerona, & Schwartz, 2015).

When a novel synthetic cannabinoid is first detected in recreational products, there exist a number of very important but unanswered questions. How does this compound produce its effects? Is there a safe dose, and what is it? Is it inherently toxic? If so, what is the mechanism underlying that toxicity? How is it metabolised? How can it be identified forensically? Does it degrade when heated? How long do the effects last, and are they harmful in the long term? Is it addictive, and if so, can that addiction be treated? The work presented in this thesis is designed to answer some of these questions.

Synthetic cannabinoids exert their effects - at least partially - via mimicry of the action of exogenous phytocannabinoids found in *Cannabis sativa* and the endogenous cannabinoids ("endocannabinoids") occurring naturally throughout the body. Therefore, this introductory chapter begins with a brief review of the history of cannabinoid science, endocannabinoid science and general cannabinoid pharmacology. Following this, the emergence of synthetic cannabinoids as

recreationally used and abused novel psychoactive substances is explored. The chemical structures, structure-activity relationships, and recreational use of synthetic cannabinoids are discussed, before moving to a review of what is currently understood about the psychopharmacology of synthetic cannabinoids. This discussion focuses on their acute physiological and behavioural effects, their toxicity, metabolism and thermal stability, and the limited data concerning their long-term effects. The chapter then moves to a discussion of legislative and forensic responses to the emergence of synthetic cannabinoids, and possible treatments for those burdened with their multifarious adverse effects. Finally, a variety of research is introduced, which is designed to answer important questions surrounding the psychopharmacology and toxicity of synthetic cannabinoids.

1.2 A brief history of *Cannabis sativa* and cannabinoid pharmacology

1.2.1 The discovery and classification of cannabinoids

Cannabis sativa (cannabis; marijuana) is a robust dioecious annual plant that has been utilised for a range of human purposes. It has seen use as a textile (*i.e.* hemp), as herbal medicine, in religious ceremonies, and as a psychoactive drug. The plant's origins can be traced to Central Asia, wherefrom it spread via trade to India, Western Asia, and eventually Europe and beyond (Zuardi, 2006). It was used in Egypt for pain relief around 1500 BC and in China for recreational purposes as early as 2737 BC (Russo, 2007). The success of the plant, which can now be found growing in every inhabited continent, speaks to the historical value of cannabis to human populations. It is therefore somewhat surprising that a basic pharmacological understanding of cannabis has only been achieved recently compared to other psychoactive plants such as the opium poppy (*Papaverus somniferum)* or coca bush (*Erthoxylum coca*).

The delayed development of cannabis pharmacology is underpinned by the chemical properties of the "cannabinoids", which were first defined as a "group of oxygen containing C_{21} aromatic hydrocarbon compounds typical of and present in *Cannabis sativa*" (Mechoulam & Gaoni, 1967, p. 177). Compared to opium or coca constituents like morphine and cocaine, respectively, cannabinoids are difficult to purify and separate. Cannabinoids are numerous and structurally similar, and generally lack distinct functional groups which are easily manipulated in order to chemically separate them from one another (ElSohly & Slade, 2005; Mechoulam et al.,

2014). While opium and coca constituents and derivatives were isolated, purified, and medically studied (e.g. codeine, an opioid medication used as for pain relief; or lignocaine, a local anaesthetic, structurally related to cocaine), cannabis could only be classed as a "drug" with unknown pharmacology for most of the 20th century. It took until the 1960s for analytical techniques to advance sufficiently to correctly identify the psychoactive components of cannabis, and until the 1990s to identify the molecular targets of exogenous cannabinoids and endocannabinoids within the brain and body (Devane et al., 1992; Gaoni & Mechoulam, 1964). It was only then that the pharmacological properties of cannabinoids could be studied directly.

Cannabidiol (CBD) and cannabinol (CBN) were the first cannabinoids isolated from *Cannabis sativa* (Wollner et al., 1942). However, the molecular structures of these cannabinoids could not be accurately elucidated at the time, and they were mistakenly thought to be the psychoactive components of cannabis. The synthetic compound $\Delta^{6a,10a}$-tetrahydrocannabinol possessed pharmacological activity similar to cannabis extracts, so it was assumed that it must be structurally related to the true psychoactive compound(s) (Mechoulam et al., 2014). Finally, in 1964, Δ^{9}-tetrahydrocannabinol (Δ^{9}-THC) was correctly identified as the primary psychoactive component of cannabis, and the correct structures of Δ^{9}-THC and CBD were elucidated (Gaoni & Mechoulam, 1964).

Since this early work, growing understanding of cannabinoid pharmacology has necessitated a broadening of the definition of cannabinoids to include several additional chemical classes beyond the components first identified in the cannabis plant. Cannabinoids now include the carboxylic acid precursors of THC, CBD, and other cannabis-derived cannabinoids (together termed "phytocannabinoids"),

cannabinoid metabolites, synthetic cannabinoids, and endogenous cannabinoids (endocannabinoids). Of these, discovery of the endocannabinoids was a particularly significant breakthrough in cannabinoid pharmacology.

1.2.2 The endocannabinoid system

When Δ^9-THC was first isolated, it had no established molecular target or mechanism of action, although it was clear that phytocannabinoids must act on some endogenous system in order to produce their effects. The basic components of the endocannabinoid system - cannabinoid receptors and their endogenous ligands – were subsequently discovered in the early 1990s (Devane et al., 1992; Matsuda et al., 1990). The endocannabinoid system is comprised of two G-protein coupled receptors termed cannabinoid 1 (CB_1) and 2 (CB_2) receptors, and the endocannabinoids that act on those receptors (Matsuda et al., 1990). The CB_1 receptor was first cloned in 1990 followed shortly by CB_2 receptors in 1993 (Matsuda et al., 1990; Munro, Thomas, & Abu-Shaar, 1993). Both proved resistant to crystallisation, such that the crystal structure of the human CB_1 receptor was only obtained in 2016 (Hua et al., 2016). The endocannabinoid system can be further expanded to include enzymes that synthesise or degrade endocannabinoids (e.g. monoacylglyceral lipase, diacylglycerol lipase) and membrane transporters (Reggio, 2010). G-protein coupled receptor 55 (GPR55) is also activated by some exogenous and endogenous cannabinoid ligands and can be considered a putative cannabinoid receptor (Ryberg et al., 2007).

The first endocannabinoid to be discovered was *N*-arachidonoylethanolamide (AEA; anandamide)(Devane et al., 1992). AEA is a fatty acid neurotransmitter that is a partial agonist for CB_1 and CB_2 receptors, and is primarily degraded by fatty acid amide

hydrolase (FAAH) (Deutsch & Chin, 1993; Mechoulam et al., 2014). A second endocannabinoid, 2-arachidonoylglycerol (2-AG), was identified shortly after the discovery of AEA (Mechoulam et al., 1995; Sugiura et al., 1995). 2-AG acts as a full agonist at CB_1 and CB_2 receptors, and has been found at brain concentrations 170 times that of AEA (Gonsiorek et al., 2000; Stella, Schweitzer, & Piomelli, 1997).

CB_1 receptors are highly expressed throughout the central nervous system, such that CB_1 is one of the most abundantly expressed receptors identified in mammalian brain (Mackie, 2005). It is also found less abundantly in peripheral tissues (Tsou et al., 1998). CB_1 receptor expression is particularly dense in the hippocampus, amygdala, molecular layer of the cerebellum, periaqueductal gray, and dorsal horn of the spinal cord (Farquhar-Smith et al., 2000; Glass, Faull, & Dragunow, 1997; Herkenham et al., 1991; Westlake et al., 1994).

In neural systems, endocannabinoids (particularly 2-AG) activate CB_1 receptors via retrograde (post-synaptic to pre-synaptic) transmission (Freund, Katona, & Piomelli, 2003; Wilson & Nicoll, 2001). Endocannabinoids are synthesised and released when intracellular calcium concentrations rise, such that synaptic endocannabinoid concentrations increase alongside neuronal activation (Mechoulam et al., 2014; Wilson & Nicoll, 2001). Endocannabinoids then bind to presynaptic CB_1 receptors, which inhibit presynaptic firing. Accordingly, the endocannabinoid system appears to be important for maintaining homeostasis across a number of physiological systems. These include appetite (Colombo et al., 1998; Mattes et al., 1994), pain regulation (Guindon & Hohmann, 2009), anxiety (Hill & Tasker, 2012), memory formation and learning (Marsicano & Lafenetre, 2009), mood (Witkin, Tzavara, & Nomikos, 2005), and sleep (Gates, Albertella, & Copeland, 2014; Mechoulam et al.,

1997). However, it should be noted that presynaptic CB_1 receptor activation does not necessarily produce net inhibition across a neural system – for example, inhibition of GABAergic neurons could produce net excitation.

The endocannabinoid system is probably involved in such a plethora of physiological functions because cannabinoid receptors are abundantly distributed (Malfitano et al., 2014; Svizenska, Dubovy, & Sulcova, 2008). It should also be noted that AEA and 2-AG may also act on non-cannabinoid receptors, including transient receptor potential (TRP) channels (Di Marzo & De Petrocellis, 2010), specifically TRPV1 (Ross et al., 2001), peroxisome proliferator-activated receptors (Rockwell et al., 2006), and GPR55 (Ryberg et al., 2007). Consequently the total "footprint" of the endocannabinoid system may extend beyond that of systems presently known to express cannabinoid receptors.

Crucially, CB_1 receptor activation produces the psychoactive effects associated with cannabis. Frequently reported effects of CB_1 receptor agonists in humans are lethargy, increased appetite, xerostomia, and mild euphoria (Heishman et al., 1990; Wachtel et al., 2002). In rodents, CB_1 receptor agonists produce a well-defined behavioural "tetrad": catalepsy, analgesia, hypomotility, and hypothermia (Martin et al., 1991). Tetrad effects can typically be blocked by CB_1 receptor antagonists (Huestis et al., 2001; Rinaldi-Carmona et al., 1995), and are largely absent in CB_1 genetic knockout models (Zimmer et al., 1999). Thus CB_1 receptors are well established as the molecular target underlying these effects. These effects are further reviewed in Sections 1.2.3 and 1.4.1.

CB_2 receptor-mediated effects are less well established than those of CB_1, but nevertheless CB_2 receptors may be involved in the regulation of a large number of

bodily systems and disease states (Malfitano et al., 2014). CB_2 receptors have been found in microglial cells within the CNS, and somewhat controversially, in neuronal tissue (Onaivi, 2011; Stempel et al., 2016). However, CB_2 receptors are generally found in peripheral immune tissues (Svizenska et al., 2008). In particular, CB_2 receptors are highly expressed in tonsils, spleen, and thymus. Although CB_2 receptor activation could theoretically be problematic for immune responses against infectious diseases, some researchers have found evidence for a therapeutic role for CB_2 receptor agonists in treating autoimmune disorders or injury where inflammation plays a major role (Maresz et al., 2007; Zhang et al., 2007). For example, selective CB_2 receptor agonists O-3853 and O-1966 can decrease cerebral infarction following ischemic stroke in mice (Zhang et al., 2007). The therapeutic potential of CB_2 receptors remains an emerging and active area of research.

1.2.3 Δ^9-tetrahydrocannabinol, the prototypical CB_1 receptor agonist

Since its discovery in 1964, the effects of Δ^9-THC (psychoactive or otherwise) have been extensively studied. It was first identified in a hexane extract of hashish, from which it was chromatographically separated from other phytocannabinoids, purified and tested for psychoactivity in dogs (Gaoni & Mechoulam, 1964). Similar assessments revealed that Δ^8-tetrahydrocannabinol is also psychoactive, but that Δ^9-THC is more potent *in vivo* and more prevalent in cannabis (Pertwee, 1988). Δ^9-THC is therefore generally considered the principle psychoactive component of cannabis.

The complete biosynthesis of Δ^9-THC and other phytocannabinoids in the plant is complex and beyond the scope of this thesis (for review see Flores-Sanchez and Verpoorte (2008)), but briefly, the carboxylic acid precursor to Δ^9-THC,

tetrahydrocannabinolic acid (THCA), is biosynthesised from cannabigerolic acid (CBGA) by THCA synthase, and concentrated in the glandular trichomes of cannabis (Flores-Sanchez & Verpoorte, 2008; Taura et al., 2007). THCA, which is not psychoactive, is readily converted by light and heat to Δ^9-THC, and this typically occurs when cannabis or cannabis extracts are smoked, vaporised, or baked (McPartland et al., 2015).

Δ^9-THC content (including THCA) typically ranges from 0 - 35 % of dry plant weight (Bruci et al., 2012; Burgdorf, Kilmer, & Pacula, 2011; Swift et al., 2013). This variance is a result of plant genetics (including plant gender), growing conditions, and the portion of the plant analysed. Repeated selection of plant strains with high Δ^9-THC content for recreational purposes has produced an increase in cannabis potency (*i.e.* Δ^9-THC content) in Europe, the US, the UK, New Zealand, and Australia (Cascini, Aiello, & Di Tanna, 2012; Swift et al., 2013).

After intake of Δ^9-THC via smoking, vaporisation, or ingestion, Δ^9-THC circulates in blood, crosses the blood-brain-barrier and activates CB_1 receptors, producing the classic cannabis "high". As reviewed in the previous section, CB_1 receptor activation affects a variety of physiological systems, such that Δ^9-THC can increase appetite, reduce pain, modulate anxiety, impair memory formation and learning, and alter mood (Pertwee & Cascio, 2014). It also produces "tetrad" effects in rodents (Compton et al., 1993; Martin et al., 1991; Wiley et al., 2007).

In humans and rodents, Δ^9-THC is metabolised to a variety of oxidized derivatives by cytochrome P450 2C9 and 2C19 isoenzymes (Watanabe et al., 2007). The predominant metabolic pathway proceeds via hydroxylation to 11-hydroxy-Δ^9-THC (11-OH-THC) and then further oxidation to 11-*nor*-9-carboxy-THC (THC-COOH)

(Huestis, 2007). Interestingly, 11-OH-THC is more potent at CB_1 receptors than Δ^9-THC, whereas THC-COOH lacks psychoactive effects (Lemberger et al., 1971; Watanabe et al., 1990). 11-OH-THC is more readily formed following oral administration of Δ^9-THC, and as a major metabolite, 11-OH-THC likely contributes to the overall psychoactive effects usually ascribed to Δ^9-THC (Huestis, 2007).

Δ^9-THC produces rewarding effects, as demonstrated by user reports and by animal studies showing self-administration (Braida et al., 2004; Tanda, Munzar, & Goldberg, 2000). Approximately 10% of cannabis users develop dependence (Crean, Crane, & Mason, 2011). The rewarding effects of Δ^9-THC appear to be mediated by activation of dopaminergic reward circuitry involving the ventral tegmental area (VTA) and nucleus accumbens (NAc) (Gardner, 2014). In brief, dopaminergic neurons in the VTA innervate neurons in the NAc, and activation of this circuitry underlies the rewarding effects of a number of drugs of abuse (Fields & Margolis, 2015). Δ^9-THC increases firing of dopaminergic VTA neurons, which may occur indirectly via inhibition of GABAergic projections onto those neurons (Gardner, 2014). However, excitatory glutamatergic neurons that express presynaptic CB_1 also project onto dopaminergic neurons in the VTA (Lupica, Riegel, & Hoffman, 2004). Activation of these receptors would tend to decrease dopaminergic firing. Therefore, the effects of Δ^9-THC in the VTA are likely mediated by a complex interaction between competing neural circuitry. Nevertheless, antagonist studies provide some valuable mechanistic information. For example, the effects of Δ^9-THC in the VTA can be blocked with CB_1 receptor antagonists, pointing to a CB_1-dependent mechanism and involvement of the endocannabinoid system. Infusions of Δ^9-THC directly into the NAc also increases NAc dopamine, which can be blocked not only by CB_1 receptor antagonists but also by

opioid antagonist/inverse agonist naloxone (Tanda, Pontieri, & Chiara, 1997). Thus, multiple receptor systems are involved in mediating cannabinoid reward.

Repeated Δ^9-THC exposure can produce homeostatic compensations in the endocannabinoid system, leading to tolerance. Animal studies show that repeated Δ^9-THC administration decreases CB_1 receptor density in hippocampal and striatal regions (Sim-Selley et al., 2006). Similarly, human cannabis users show down-regulation of cortical CB_1 receptors as measured by positron emission tomography, which positively correlates with the number of years of cannabis use (Hirvonen et al., 2012). AEA concentrations in cerebrospinal fluid are also reduced by cannabis use in humans, in proportion to the amount of cannabis used (Morgan et al., 2013). However, these changes are reversible following cessation of Δ^9-THC (Hirvonen et al., 2012; Sim-Selley et al., 2006), and are less clearly characterised in other biological matrices.

Although the precise mechanism underlying cannabinoid reward is not fully understood, it is noteworthy that abrupt cessation of cannabis use can produce a withdrawal syndrome (Allsop et al., 2011; Volkow et al., 2014). This is usually mild compared to opioid or alcohol withdrawal, but can present an obstacle to the reduction of cannabis use and impair normal daily activities (Allsop et al., 2012). Symptoms include irritability, cravings, decreased appetite, sleep disturbance, depression, anxiety, and headache (Allsop et al., 2015). These symptoms usually resolve after an extended period of cannabis/Δ^9-THC abstinence, perhaps related to the normalisation of receptor density and endocannabinoid concentrations as discussed above.

Δ^9-THC can influence neuronal plasticity and associated learning, likely as a result of high CB_1 receptor density in the prefrontal cortex and hippocampus. In

particular, Δ^9-THC exposure can reduce neuron size and synaptic density in rat hippocampus (Scallet, 1991), and impairs episodic and working memory in infrequent cannabis users (Curran et al., 2002). This may occur via a reduction of blood flow to these brain regions (or conversely, inhibition of the prefrontal cortex and hippocampus may reduce blood flow). In rodents, these effects are more pronounced and enduring in adolescents (Higuera-Matas, Ucha, & Ambrosio, 2015). Adolescent rats show greater residual memory deficits than adults following chronic administration of Δ^9-THC (Quinn et al., 2008).

Peripherally, Δ^9-THC produces tachycardia in humans via increases in diastolic blood pressure. Increases in resting heart-rate occur in a dose-dependent manner (Mittleman et al., 2001; Weiss et al., 1972). However, Δ^9-THC can also produce bradycardia in tolerant human users. Moreover, in rodents, CB_1 agonists including Δ^9-THC produce bradycardia in non-tolerant animals (Banister et al., 2013). Thus, the effect of Δ^9-THC and cannabinoids generally on heart-rate is not fully understood.

Δ^9-THC can also bind to CB_2 receptors, although the outcomes of CB_2 activation are less established than for CB_1. However, the action of Δ^9-THC on CB_2 receptors with respect to immune and inflammatory responses has received some attention. For example, Δ^9-THC can decrease the growth rate of CB_1 and CB_2 receptor expressing breast cancer tumors (Caffarel et al., 2010). This effect was blocked with CB_2-selective antagonist SR144528, but not CB1-selective inverse agonist/antagonist rimonabant (SR141716A), indicating a specifically CB_2 mediated mechanism. Δ^9-THC can also reduce signs of paw pain in a rat arthritis model, and this effect is reduced by SR144528. However, this effect is also partially CB_1-dependent as it is also attenuated by rimonabant (Cox, Haller, & Welch, 2007).

Δ^9-THC does not exist in isolation within cannabis, and a variety of research focuses on potential interactions between Δ^9-THC, other phytocannabinoids, and phytochemicals generally. These interactions are numerous and seem to occur via a number of indirect modulatory mechanisms. Because Δ^9-THC is a CB_1 receptor agonist, these interactions are potentially relevant to synthetic CB_1 agonists, and are briefly reviewed in the following sections.

1.2.4 Interactions between Δ^9-tetrahydrocannabinol and cannabidiol

Cannabis biosynthesises over one hundred phytocannabinoids beyond Δ^9-THC (ElSohly & Gul, 2014). Of these, CBD has recently moved to the forefront of therapeutic cannabinoid research. Ongoing research has indicated applications in the treatment of anxiety (Blessing et al., 2015), epilepsy (Friedman & Devinsky, 2015), schizophrenia (Zuardi et al., 2012), pain (Notcutt et al., 2004), and cannabis withdrawal (Allsop et al., 2015).

CBD is biosynthesied in a similar manner to Δ^9-THC. CBGA (the precursor to THCA) is also a substrate for cannabidiolic acid (CBDA) synthase, which produces CBDA. Like THCA, CBDA is most concentrated in the glandular trichomes of cannabis, and can be decarboxylated to CBD via light and heat (Flores-Sanchez & Verpoorte, 2008). The molecular structure of CBD differs only slightly from Δ^9-THC, yet this difference is sufficient to completely alter its pharmacology. Unlike Δ^9-THC, CBD has poor binding affinity on both CB_1 and CB_2 receptors. CBD does not produce psychoactive effects in humans, and does not produce tetrad effects in rodents (Cascio & Pertwee, 2014). Instead, CBD appears to act via a range of mechanisms on several alternate molecular targets. It may indirectly modulate the effects of CB_1 and CB_2

agonists, is an antagonist at GPR55 (Ryberg et al., 2007), a partial agonist on serotonin $(5\text{-HT})_{1A}$ receptors (Russo et al., 2005), and an allosteric modulator of μ and δ-opioid, dopamine D_2, and γ-aminobutyric acid $(GABA)_A$ receptors (Kathmann et al., 2006).

The interaction of CBD with Δ^9-THC is an area of continuing research. Animal studies have suggested that CBD can both potentiate and attenuate the effects of Δ^9-THC (Cascio & Pertwee, 2014; Klein et al., 2011). CBD has been shown to dose-dependently increase the effects of Δ^9-THC on locomotor activity, rectal temperature, and spatial memory (Hayakawa et al., 2008; Reid & Bornheim, 2001). It can also potentiate Δ^9-THC-produced inhibition of weight gain, anxiogenic effects, and decreases in social interaction in rats (Klein et al., 2011). Potentiation of Δ^9-THC effects may occur through inhibition of enzymes belonging to the cytochrome P450 2C and 3A subfamilies (Bornheim & Correia, 1989, 1990, 1991). On the other hand, CBD has been sometimes shown to attenuate the effects of Δ^9-THC on operant behaviour (Zuardi et al., 1981), social interaction (Malone, Jongejan, & Taylor, 2009), and conditioned place aversion (Vann et al., 2008).

In humans, a similar mix of potentiation and attenuation is observed. Studies have shown that CBD can attenuate some, but not all, of the psychoactive effects of Δ^9-THC. For example, CBD reduces anxiety and subjective ratings of intoxication produced by Δ^9-THC in adults, but does not block tachycardic effects (Zuardi et al., 1982). Studies have also shown that CBD can potentiate pleasurable Δ^9-THC effects (Karniol et al., 1974), in addition to cardiac effects (Hollister & Gillespie, 1975). However, a more recent study found no difference in subjective or cardiac effects between Δ^9-THC and a 50:50 mix of Δ^9-THC and CBD (Sativex®) (Karschner et al., 2011). The doses of Δ^9-THC and CBD and the timing of dosing in the aforementioned

studies also vary widely. Thus, it appears that the relationship between CBD and Δ^9-THC is complex and can change based on the specific effect studied (e.g. anxiety vs heart-rate), on the dose of CBD and/or ratio of CBD to Δ^9-THC, on the timing of dosing, and between species (e.g. human vs rat).

It remains an interesting possibility that CBD could interact with other CB_1 agonists, including synthetic cannabinoids. If CBD can reduce some of the negative effects of Δ^9-THC, then perhaps it can do the same for synthetic CB_1 agonists, providing a possible intervention for synthetic cannabinoid intoxication. Conversely, the absence of CBD from synthetic cannabinoid preparations could possibly be detrimental. Continued research on the interaction between CBD and CB_1 agonists could prove fruitful.

1.2.5 Interactions between Δ^9-tetrahydrocannabinol and other phytochemicals in *Cannabis sativa*

Beyond the phytocannabinoids, cannabis produces an extensive range of terpenoid compounds. Unlike phytocannabinoids, terpenoids are found in a wide variety of flowering plants. Interestingly, these compounds may pharmacologically interact with Δ^9-THC, CBD, and other phytocannabinoids. By extension, they could also interact with synthetic cannabinoids.

Terpenoids are diverse and abundant compounds that are largely responsible for the characteristic odours of most flowering plants (Knudsen et al., 1993), including cannabis. In addition to providing possible anti-fungal and pesticidal benefits for the plant (Gershenzon and Dudareva, 2007; Langenheim, 1994), terpenoid compounds have a variety of putative beneficial properties in humans and produce analgesic

(Lorenzetti et al., 1991), anxiolytic (Komiya et al., 2006), and sedative effects (do Vale et al., 2002). Like the phytocannabinoids, terpenoids are concentrated in the trichomes of the plant, and interestingly, phytocannabinoids and terpenoids are biosynthetically related. Terpenes are biosynthesised via combinations of five carbon isoprene units, and these same units are used in the biosynthesis of phytocannabinoids. Indeed, phytocannabinoids are "terpenophenolic" compounds; that is, they are synthesised via the combination of terpenes and phenols.

Terpenoids may act directly or indirectly to modulate phytocannabinoid effects (Russo, 2011). For example, the terpene β-caryophyllene is a CB_2 agonist *in vitro* (Gertsch et al., 2008). Direct action of terpenoids on CB_1 receptors is unlikely, since a comparison of pure Δ^9-THC and cannabis smoke (containing terpenoids) yielded no overall difference in CB_1 binding *in vitro* (Fischedick et al., 2010a), and the subjective effects of pure Δ^9-THC and cannabis are similar at low doses (Cooper et al., 2013; Wachtel et al., 2002). Nevertheless, interactions between terpenoids and phytocannabinoids via indirect mechanisms have been reported; for example, β-linalool shows antinociceptive effects via adenosine A_1 and A_{2A} receptors (Peana et al., 2006), as does β-myrcene via PGE-2 (Lorenzetti et al., 1991). These interactions have been collectively termed "the entourage effect" (Russo, 2011), although more research is needed to conclusively determine if terpenoids produce physiologically relevant interactive effects at concentrations found in cannabis. Nevertheless, if terpenoids can modulate the effects of Δ^9-THC, then they may also modulate the effects of synthetic cannabinoids. Thus, as was the case for CBD, the total pharmacological effect of synthetic preparations may be influenced by the presence or absence of terpenoids.

1.3 The discovery and evolution of synthetic cannabinoids

1.3.1 Early bicyclic synthetic cannabinoids

The structures of Δ^9-THC and similar phytocannabinoids were used as templates for the first synthetic, *i.e.* human-designed, cannabinoids. These compounds were designed in order to investigate the endocannabinoid system, with the goals of building a mechanistic understanding of the system and discovering novel therapeutics. The earliest compounds were bicyclic synthetic cannabinoids that resulted from alterations to the chemical structure of Δ^9-THC (Figure 1A). These include HU-210 and CP-47,497 (Figure 1B and 1C) which both possess greater affinity for CB_1 and CB_2 receptors than Δ^9-THC (Stern & Lambert, 2007; Titishov, Mechoulam, & Zimmerman, 1989; Weissman, Milne, & Melvin, 1982). Compounds of this type usually contain two six-membered rings and a hydrocarbon "tail" in a configuration similar to that of Δ^9-THC.

These compounds have been used with success in scientific investigations of cannabinoid pharmacology (Ottani & Giuliani, 2001). For example, competitive binding assays with radiolabelled CP-55,940 (a potent CB_1 and CB_2 receptor agonist) have been used to characterise the binding strength of a range of cannabinoid agonists (Thomas et al., 1998). Moreover, radiolabelled CP-55,940 was used to localise cannabinoid receptors in the central nervous system (Herkenham et al., 1990).

The psychopharmacology of the early bicyclics has also been investigated, largely using rodent models. As expected, HU-210 and CP-55,940 produce tetrad effects in rats (Fox et al., 2001), which can be blocked by rimonabant (Chaperon & Thiébot, 1999). HU-210 can also impair rat learning in the water maze task when

administered daily at 50 μg/kg or higher (Ferrari et al., 1999), and can produce anxiogenic-like effects following sub-chronic treatment (Giuliani, Ferrari, & Ottani, 2000). CP-55,940 can produce aversive effects in rats, as measured by conditioned place preference and conditioned taste aversion (McGregor, Issakidis, & Prior, 1996), although some studies have found mild rewarding effects, depending on dose and testing schedule (Braida et al., 2001). Chronic dosing with CP-55,940 can also produce lasting memory impairments in adolescent rats (O'Shea et al., 2004).

Overall, the early bicyclic synthetic cannabinoids act similarly to Δ^9-THC via action at CB_1 receptors, although the available evidence suggests that some can produce more extreme effects, particularly on learning and memory (Higuera-Matas et al., 2015). This is presumably a result of the high potency of these compounds at CB_1 receptors. However, this relatively simplistic picture has since been complicated by the discovery of additional classes of cannabimimetic compounds that are structurally dissimilar to Δ^9-THC and the early bicyclic synthetic cannabinoids. Such discoveries produced large increases in both the number and potency of synthetic cannabinoids, which has seemingly broadened the range of potential psychopharmacological and toxicological effects produced by these compounds.

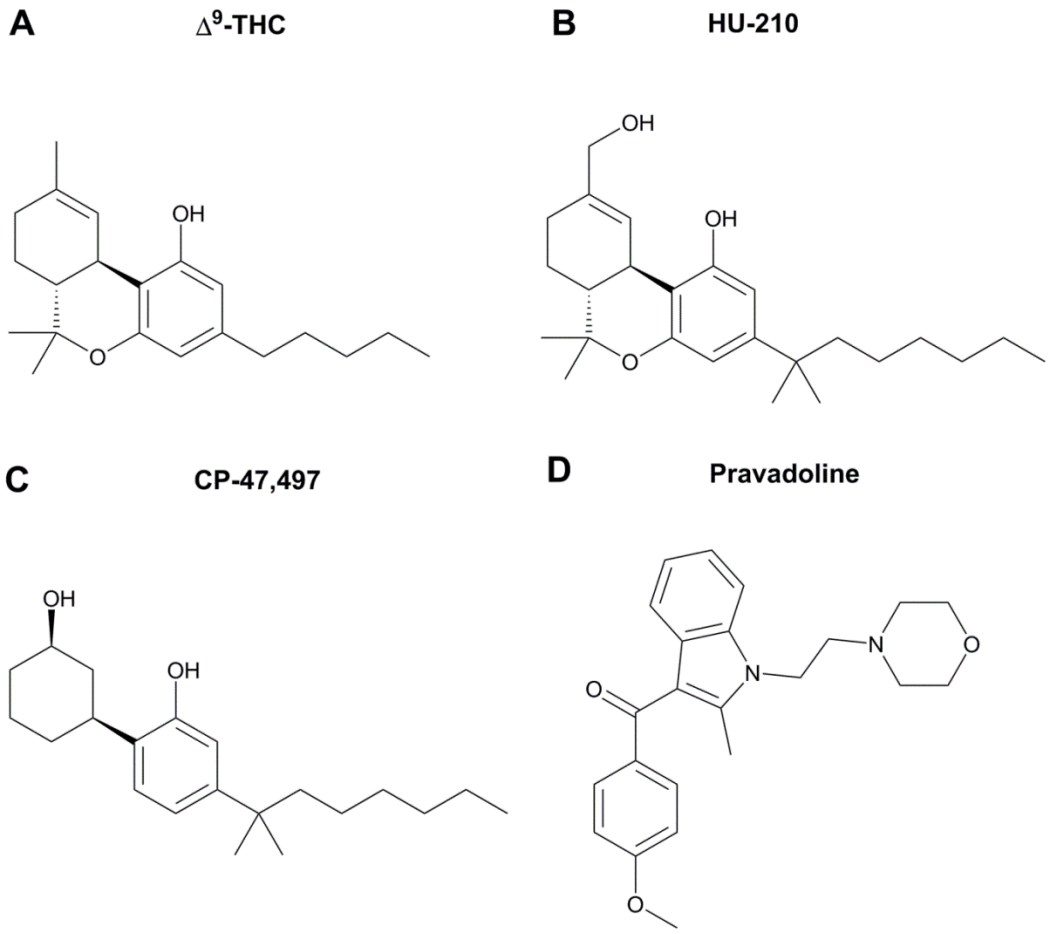

Figure 1. *Molecular structures of Δ^9-THC and early synthetic cannabinoids. Note the structurally similarities between (A) Δ^9-THC, (B) HU-210, and (C) CP-47,497, which each possess six-membered rings and hydrocarbon chains in similar configurations. Pravadoline (D) is also a cannabinoid receptor agonist, despite substantial structural differences from the early bicyclic synthetic cannabinoids. See Section 1.3.2 for further detail.*

1.3.2 Pravadoline and the aminoalkylindoles

The synthetic cannabinoid landscape diversified with the development of pravadoline (WIN-48,098; (4-methoxyphenyl)[2-methyl]-1-[2-(4-morpholinyl)ethyl]-1H-indol-3-yl]-methanone) in the 1980s. Pravadoline was developed as an anti-

inflammatory cyclooxygenase inhibitor, but unexpectedly produced strong analgesic effects at doses ten times below its effective anti-inflammatory dose. Antagonist studies with naloxone and opioid receptor binding studies demonstrated that this analgesic effect was not opioid dependent (Haubrich et al., 1990). Further research revealed that pravadoline was in fact a CB_1 receptor agonist (D'Ambra et al., 1992).

The chemical structure of pravadoline differs substantially from that of the phytocannabinoids and phytocannabinoid-based synthetic cannabinoids (Figure 1D). Pravadoline is an aminoalkylindole, and further experimentation with variants of this structure revealed that many compounds of this class act on cannabinoid receptors as agonists or antagonists (Aung et al., 2000; D'Ambra et al., 1992; Huffman et al., 1994). An early example of this class is WIN-55,212-2 ([(3*R*)-2,3-dihydro-5-methyl-3-(4-morpholinylmethyl)pyrrolo[1,2,3-de]-1,4-benzoxazin-6-yl]-1-naphthalenyl-methanone), an aminoalkylindole with strong cannabinoid receptor binding affinity (CB_1 K_i = 1.9 nM, CB_2 K_i = 0.28 nM) (Kuster et al., 1993). An important property of WIN-55,212-2 and many aminoalkylindole synthetic cannabinoids is that they are full agonists; that is, they have maximum efficacy at cannabinoid receptors (Fantegrossi et al., 2014). This is in contrast to Δ^9-THC, which is a partial agonist that cannot activate CB_1 receptors to the same extent regardless of concentration. It is therefore possible that aminoalkylindole synthetic cannabinoids may produce effects beyond or entirely different to that of Δ^9-THC.

This aminoalkylindole framework underwent extensive development in the 1990s. Of particular note is the development of the "JWH" and "AM" series of synthetic cannabinoids, named after their creators John W. Huffman and Alexandros Makriyannis respectively (Huffman et al., 1994; Makriyannis & Deng, 2005). Together,

these series are comprised of over 200 unique compounds with varying cannabinoid receptor binding affinity. Of these compounds, JWH-018 (1-pentyl-3-(1-naphthoyl)indole) possessed strong CB_1 receptor affinity and was relatively easy to synthesise, and became the most well-known synthetic cannabinoid in recreational products. However, it should be noted from the outset that synthetic cannabinoid products contain an enormous variety of synthetic cannabinoids with diverse yet related molecular structures.

1.3.3 Synthetic cannabinoids as recreational drugs

By the mid-2000s, a large collection of synthetic CB_1 agonists had been identified in scientific literature. Their syntheses were readily available, and were also straightforward for many aminoalkylindoles. Moreover, these compounds were largely unknown outside of the research community and were consequently legal, or at least not explicitly illegal, to possess or manufacture in most countries. In light of these factors, it is of little surprise that synthetic cannabinoids have been used recreationally as novel psychoactive substances.

Synthetic cannabinoids experienced a spike in popularity in 2004, when the product “Spice” commenced sale in European markets. Initially, synthetic cannabinoids were sold in online marketplaces, often under the guise of “research chemicals”. In this setting, compounds could be ordered in a powdered or crystalline form, albeit with little to no testing of purity or confirmation of chemical identity. Alternatively, products were packaged and sold as “natural”, “herbal”, or “legal highs”. These products proved to be immensely popular, and profitable – the first company to

commence sale in Europe, "The Psyche Deli", reportedly made profit of £700,000 between 2006 and 2007 (Schifano et al., 2009).

The packaging of early herbal products listed up to 14 different types of plants, two of which had potential psychoactive effects (Seely et al., 2011). However, the two plants - *Pedicularis densiflora* (indian warrior) and *Leonotis leonuris* (lion's ear) – were not known to be able to produce the intense highs described by users. This prompted researchers to analyse the products for additionally psychoactive ingredients. It was quickly discovered that in reality, these "herbal" products contained a number of synthetic cannabinoids, primarily JWH-018 (EMCDDA, 2009). These products were produced by dissolving synthetic cannabinoid compounds of unknown purity in a volatile solvent and then spraying the mixture onto largely inert plant material. This process was not mentioned on the product packaging, nor was there any mention of synthetic cannabinoids. Often products were labelled "not for human consumption" in an attempt to circumvent legislation (Figure 2).

After this discovery, recreational synthetic cannabinoid products were monitored by the European Monitoring Centre for Drugs and Drug Addiction (EMCDDA). However, synthetic cannabinoid products quickly spread to other markets and were found in the USA in 2008, containing the older, phytocannabinoid derived HU-210. Similarly synthetic cannabinoids were detected in Japan in 2008, and in Australia in 2011, although it is possible that synthetic cannabinoid use began several years before they were detected (Barratt, Cakic, & Lenton, 2012).

Figure 2. *Front and back of a typical synthetic cannabinoid product "Banana Cream Nuke", as published by Schneir, Cullen, and Ly (2011). Note that a variety of ingredients are listed, none of which are synthetic cannabinoids, and that it displays the warning "NOT FOR HUMAN CONSUMPTION". This particular product contained JWH-018 and JWH-073 ((1-butyl-1H-indol-3-yl)-1-naphthalenyl-methanone), and produced tachycardia and severe anxiety in two people admitted to an emergency department.*

During this time, the pharmacological and legal situation remained unclear, among both synthetic cannabinoid users and concerned members of the public. The pharmacology of synthetic cannabinoid use in humans was unknown until the publication of case studies focusing on acute toxicity, and some studies using animal models (reviewed in Section 1.3). The legislative and forensic responses to synthetic cannabinoid products varied widely between countries, and are reviewed in Section 1.4.

1.3.4 Common structures and modifications

Modern synthetic cannabinoids are comprised of a variety of chemical classes beyond the aminoalkylindoles. The complexity of synthetic cannabinoid nomenclature can be seen in their increasingly long abbreviations (for example, AB-CHMINACA is short for *N*-[(1*S*)-1-(aminocarbonyl)-2-methylpropyl]-1-(cyclohexylmethyl)-1*H*-indazole-3-carboxamide). However, the composition of most synthetic cannabinoids can be simplified, such that most structures can be decomposed into four broad components (EMCDDA, 2016; Figure 3):

1) A core, typically an indole or indazole moiety
2) A "bulky" structure that varies widely, often utilising ring structures, including but not limited to naphthyl, adamantyl, or cyclopropyl moieties
3) A linker or "bridge", often a carboxamide, carboxylate, or methanone moiety, connecting the core and bulky structure
4) A tail, extending from the core, often an *N*-pentyl chain, which is frequently terminally halogenated

These components can be combined in various configurations in order to generate large numbers of novel compounds. For example, JWH-018 is composed of an indole core, a naphthyl bulky structure, a methanone linker, and an *N*-pentyl tail (Figure 3A). Terminal fluorination of the *N*-pentyl chain yields AM-2201 (1-(5-fluoropentyl)-3-(1-naphthoyl)indole; Figure 3B). Alternatively, the indole moiety of JWH-018 could be replaced with an indazole to yield THJ-018 (1-naphthalenyl(1-pentyl-1*H*-indazol-3-yl)-methanone; Figure 3D), or the naphthyl moiety could be exchanged for an adamantyl group to give AB-001 (1-pentyl-3-(1-adamantoyl)indole; Figure 3C), a compound first detected in Irish recreational products in 2010

(Grigoryev, Kavanagh, & Melnik, 2012). Substitution of the methanone linker of AB-001 for a carboxamide results in SDB-001 (also known as APICA; *N*-(1-adamantyl)-1-pentyl-1*H*-indole-3-carboxamide; Figure 3E) found in Japan in 2012 (Uchiyama et al., 2013). SDB-001 can then be modified; for example, swapping the adamantyl moiety for an α,α-dimethylbenzyl group yields CUMYL-PICA (*N*-(1-methyl-1-phenylethyl)-1-pentyl-1*H*-indole-3-carboxamide; Figure 3F), which was detected in Europe in 2014 (EMCDDA, 2014).

Note that there are many alternate pathways and connections between the structures of these and other synthetic cannabinoids, and some exceptions to this general framework. For example, EG-018 (naphthalen-1-yl(9-pentyl-9*H*-carbazol-3-yl)methanone) is an analogue of JWH-018, with a benzene ring directly attached to the aminoalkylindole group. This modification is rarely seen elsewhere. However, for the majority of synthetic cannabinoids, the above framework is useful in the conceptualisation of the relationships between large numbers of compounds, and for understanding of various structure-activity relationships (SARs) that exist within the many classes of synthetic cannabinoids.

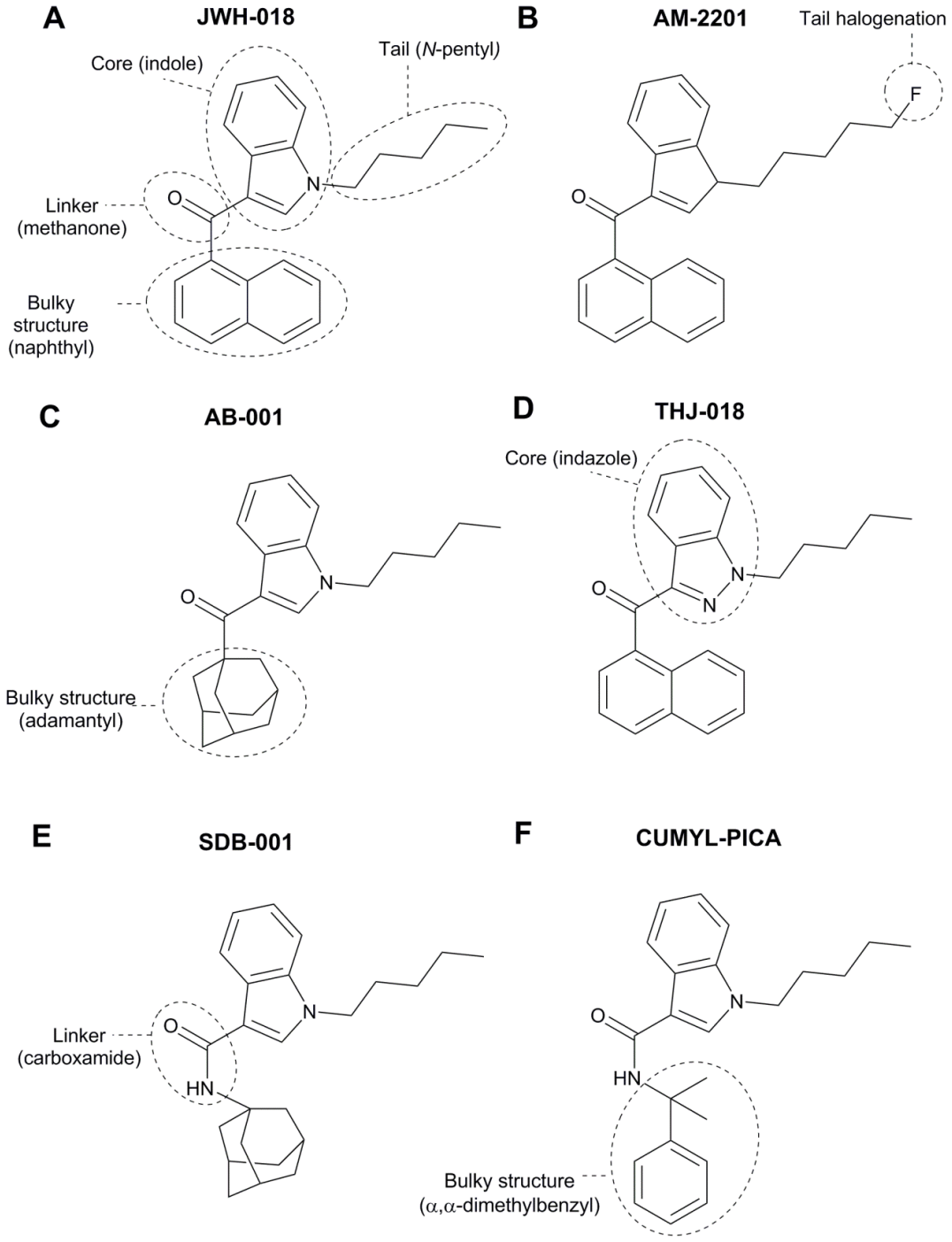

Figure 3. *Molecular structures of synthetic cannabinoids (A) JWH-018, (B) AM-2201, (C) AB-001, (D) THJ-018, (E) SDB-001, and (F) CUMYL-PICA. All structures have a core, linker, tail, and bulky structure, which can be altered to produce many diverse yet structurally related compounds (see text for further detail).*

1.3.5 Structure-activity relationships

The use of SARs to predict the pharmacological properties of novel synthetic cannabinoids is an important area of research. Rather than individually testing each and every novel compound, it may be possible to predict the pharmacology of novel synthetic cannabinoids by understanding the effects of common structural alterations. Specifically, understanding how certain components of synthetic cannabinoids (e.g. tail length, bulky group composition) impact cannabinoid receptor binding strength and *in vivo* responses is an important area of research.

Some SARs have been established within specific classes of cannabinoids. Bicyclic synthetic cannabinoids (e.g. CP-47,497 and the early Δ^9-THC –derived compounds) exhibit maximum binding affinity with a six or seven membered ring structure in place of the cyclohexyl ring of Δ^9-THC (Melvin et al., 1993). Alkyl extensions from the cyclohexyl ring do not affect binding, but hydroxyalkyl extensions of three or four carbons improve binding strength at CB_1 receptors (Figure 4). Additionally, bicyclic synthetic cannabinoids bind to cannabinoid receptors most strongly when their alkyl chains have seven or eight carbons (Melvin et al., 1993). In aminoalkylindoles, the length of the alkyl "tail" also profoundly affects cannabinoid receptor binding. A tail length of at least three carbons is necessary for high binding affinity at CB_1 and CB_2 receptors, and a length of five carbons is optimal (Aung et al., 2000). Extension of the tail to seven or more carbons results in a sharp decrease in binding affinity at both cannabinoid receptors.

Other SARs are at present partly characterised or uncharacterised. For example, many synthetic cannabinoids with *N*-pentyl tails are terminally fluorinated, forming pairs of fluorinated and non-fluorinated compounds. AM-2201 is the 5-fluoropentyl

analogue of JWH-018, XLR-11 (1-(5-fluoropentyl)-1*H*-indol-3-yl)(2,2,3,3-tetramethylcyclopropyl)methanone) is the 5-fluoropentyl analogue of UR-144 (1-(pentyl-1*H*-indol-3-yl)(2,2,3,3-tetramethylcyclopropyl)-methanone), and 5F-PB-22 (1-(5-fluoropentyl)-8-quinolinyl ester-1*H*-indole-3-carboxylic acid) is the 5-fluoropentyl analogue of PB-22 (1-pentyl-8-quinolinyl ester-1*H*-indole-3-carboxylic acid). Terminal bromination or iodination of the *N*-pentyl chain is known to increase cannabinoid receptor binding in Δ^9-THC analogues (*i.e.* early bicyclic synthetic cannabinoids), and fluorination produces a smaller increase in affinity (Compton et al., 1993). This is less well characterised in aminoalkylindoles and it is unknown whether any such increases in binding affinity carry through to improve *in vivo* efficacy. Similarly, the effect of modification of the "bulky" groups of synthetic cannabinoids is also yet to be fully characterised. For example, the *in vivo* pharmacological effect of the substitution of the naphthyl group in JWH-018 for the adamantyl group in SDB-001 is unknown. Further research is needed to establish the *in vivo* and *in vitro* consequences of such structural alterations.

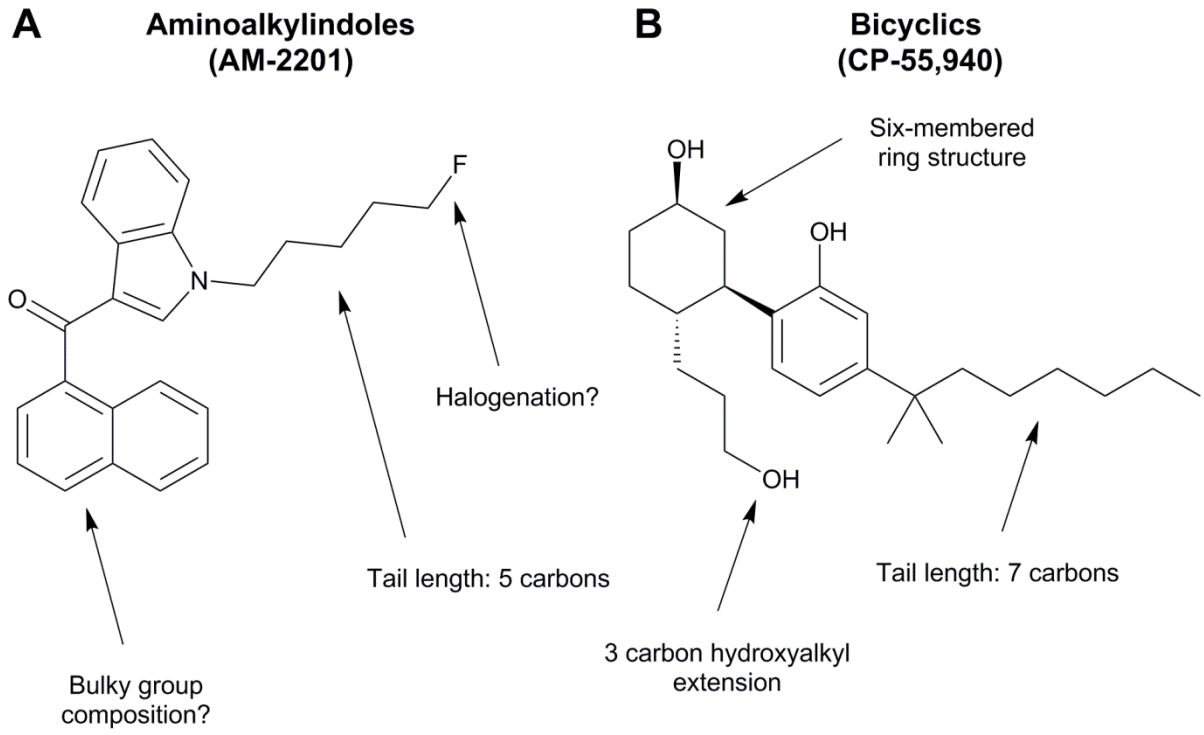

Figure 4. *Structure-activity relationships for (A) aminoalkylindoles, with AM-2201 as an example, and (B) bicyclic synthetic cannabinoids, with CP-55,940 as an example. Structural components that improve cannabinoid receptor binding affinity are labelled. The effects of aminoalkylindole halogenation and bulky group composition on in vivo pharmacology are presently uncharacterised.*

1.4 The psychopharmacology of synthetic cannabinoids

1.4.1 Acute effects

Recreationally used synthetic cannabinoids are usually strong CB_1 receptor agonists, so it would be expected that they would produce effects similar to, or possibly exceeding, that of Δ^9-THC. Indeed, the overall effects of synthetic cannabinoids in humans are typically described as being somewhat similar to that of cannabis, with additional, often negative, side effects (Winstock & Barratt, 2013). A global survey of synthetic cannabinoid users revealed that synthetic cannabinoid products reportedly had a shorter onset of effects as compared to cannabis (Winstock & Barratt, 2013). Moreover, users reported that synthetic cannabinoids produced more negative effects, hangover effects, and paranoia. Anecdotal online user reports describe similar effects, including anxiety and paranoia, vomiting, catalepsy, convulsions, agitation, and addiction. For example:

> *"After about 10 minutes and only about 3 hits of the 'Smiley Dog' herbal incense we are so high we cannot stand or walk... I lose motor control and can no longer stand after 20 minutes. My heart feels as if it is going to explode, I become convinced I could die at any moment. A tingling feeling starts at the tips of my fingers and slowly works its way up to my hands, then up my arm... At this point I lose it, and have my friend call an ambulance... I'm vomiting and the tingling feeling has moved terrifyingly close to my heart. When the ambulance arrives they cannot bring me under control and I cannot stop my body from convulsing, shaking, and screaming ... They had to strap me to a gurney and put me in an*

ambulance… They administered 10 milligrams of [lorazepam] to try to calm me down but nothing really works until I'm at the emergency room and they put me down with [ziprasidone]. I'm convinced JWH-018 triggered a full psychotic break in me." (Evilpoptart, 2011)

This user seems to describe motor function impairment and tachycardia followed by a panic attack produced by a synthetic cannabinoid (which the user assumes to be JWH-018). Similar case reports are abundant across various internet forums, and closely mirror symptoms described in emergency room case studies (Schneir et al., 2011; Schwartz et al., 2015).

In rodents, synthetic cannabinoids with high CB_1 affinity produce classic "tetrad" effects, the same as those produced by Δ^9-THC. Hypothermia can be reliably produced by JWH-018, SDB-001, UR-144, and XLR-11 in rodent models (Banister et al., 2013; Wiley et al., 2015). This effect is dose-dependent, blocked by rimonabant, and absent in CB_1 knockout mice. In general, recreationally abused synthetic cannabinoids are several times more potent than Δ^9-THC in rodent models, as would be expected given their strong binding affinity and full agonism at CB_1 receptors. The remaining three tetrad effects – analgesia, catalepsy, and hypomotility – are also observed in rodents following synthetic cannabinoid administration (Wiley et al., 2013). However, large numbers of synthetic cannabinoids have never been assessed for their *in vivo* effects.

Tetrad assessment is a widely used screening tool, but it is limited in some aspects. Importantly, CB_1 receptor agonism requires confirmation using antagonists or CB_1 genetic knockouts, because all four tetrad measures are non-specific – that is, they

can be produced by other pharmacological mechanisms. Additionally, tetrad effects do not necessarily reflect psychoactivity – *i.e.* the cannabis "high". To assess suspected psychoactive effects in rodents, drug discrimination paradigms have been utilised (Wiley et al., 2015; Wiley et al., 2013). In these paradigms, rodents are trained to respond in a certain way (e.g. lever press on a particular lever) when administered a drug (e.g. Δ^9-THC). Drugs that produce similar subjective effects (e.g. synthetic cannabinoids) should elicit the same response. UR-144, XLR-11, AB-CHMINACA, AB-PINACA ((*S*)-*N*-(1-amino-3-methyl-1-oxobutan-2-yl)-1-pentyl-1*H*-indazole-3-carboxamide), FUBIMINA ((1-(5-fluoropentyl)-1*H*-benzo[d]imidazol-2-yl)(naphthalen-1-yl)methanone), JWH-018, and several 1-pentyl-3-phenylacetylindoles substitute for Δ^9-THC in drug discrimination assessments (Wiley et al., 2015; Wiley et al., 2013; Wiley et al., 2012).

Another issue with the tetrad assessment is that measurement of each effect requires experimenter manipulation of the animal. For example, commonly used rectal temperature measurement can produce artifactual hyperthermic effects due to stress. In recent years, technological advancement in implantable radiotelemetric probes have permitted the measurement hypothermia in real time, allowing a high rate of sampling while avoid confounding effects from animal handling. Application of these radiotelemetric probes to synthetic cannabinoid screening has been demonstrated, and has shown that JWH-018 and SDB-001 produce hypothermic effects that last for at least 5 hours post-drug administration (Banister et al., 2013). Additionally, implantable radiotelemetric probes can measure heart-rate in real time. As reviewed in Section 1.2.3, the effect of cannabinoids on heart rate is undefined compared to standard tetrad effects. In humans, tachycardia is usually observed

following synthetic cannabinoid or Δ^9-THC administration (Lapoint et al., 2011; Renault et al., 1971; Schneir et al., 2011), yet in rodents, CB_1 receptor agonists produce bradycardia as measured via radiotelemetry probes (Banister et al., 2013). It is not clear whether this bradycardic effect is a direct action of CB_1 activation or instead a by-product of hypothermia or locomotor suppression. Nevertheless, these alternate measurement techniques are potentially useful for high throughput screening of the acute effects of novel synthetic cannabinoids *in vivo*.

1.4.2 Acute toxicity

In addition to the acute behavioural and physiological effects described in the previous section, severe toxicity has also been reported following synthetic cannabinoid administration. These include acute kidney injury, cardiotoxicity, cerebral ischemia, and seizures.

Multiple case reports detail acute kidney injury following use of synthetic cannabinoids (Bhanushali et al., 2012; Buser et al., 2014; Pendergraft et al., 2014; Thornton et al., 2013). Generally, these cases concern individuals who have been admitted to emergency wards following the use of one or more synthetic cannabinoid products, often in conjunction with other drugs or alcohol. Histological examination has revealed acute injury to tubules in the renal cortex and increased inflammation in the renal medulla (Buser et al., 2014). It should be noted, however, that no case study has been able to confirm whether these injuries are produced by a synthetic cannabinoid in isolation, or an interaction of one or more synthetic cannabinoids with each other or other substances, by the product medium, or contaminants.

Cardiovascular side effects have been reported in numerous case studies reporting synthetic cannabinoid effects (Hermanns-Clausen et al., 2012; Mir et al., 2011; Schwartz et al., 2015; Young et al., 2012). Tachycardia and hypertension seem particularly common, which might be expected given that Δ^9-THC reliably increases heart rate in humans (Ashton, 2001). Beyond tachycardia and hypertension, palpitations have been reported (Schneir et al., 2011). It is unclear whether these palpitations are a direct pharmacological effect or if they are more closely linked to the anxiogenic features of synthetic cannabinoids. Most alarmingly, there is also evidence that suggests the involvement of synthetic cannabinoids in cases of acute myocardial infarction (Mir et al., 2011; Schwartz et al., 2015).

Ischemic stroke following synthetic cannabinoid use has been reported on several occasions (Degirmenci, Kececi, & Olmez, 2016; Freeman et al., 2013; Inal et al., 2014). For example, Bernson-Leung, Leung, and Kumar (2014) reported cases of ischemic stroke in two women, aged 22 and 26. Similarly, Dogan et al. (2016) reported the occurrence of strokes in two men aged 28 and 35 while using synthetic cannabinoids. In some cases, the locations of strokes indicate an embolic aetiology, such that hypertension, tachycardia and arrhythmia could expose a pre-existing vulnerability in certain people (Degirmenci et al., 2016; Dogan et al., 2016).

Interestingly, to the author's knowledge, there are no published studies that report acute toxicity in animals following synthetic cannabinoid administration. Moreover, in humans, only 3.5 % of synthetic cannabinoid users experience acute toxic effects requiring urgent medical care, although this statistic rises to 12.5 % for regular (weekly or more) users (GDS, 2016). That is, synthetic cannabinoid products as a whole do not seem to produce toxicity in a reliable manner. Reasons for this

variability may include unique toxidromes for each compound, specific drug interactions, dosage, user vulnerability, and product contamination. In some cases, specific compounds have been implicated in a number of poisoning cases. For example, a recent cluster of toxicity in New York has been attributed to AMB-FUBINACA (methyl (1-(4-fluorobenzyl)-1*H*-indazole-3-carbonyl)-L-valinate), which was found in both the suspected product and blood of several patients (Adams et al., 2017). In other cases, contamination of a particular batch of products may be the root cause. Contamination of synthetic cannabinoid products with caffeine, *O*-desmethyltramadol (an opioid analgesic), eugenol, and nicotine has been documented (Dresen et al., 2010). In sum, the available evidence indicates that some synthetic cannabinoid compounds or products may be substantially more toxic than others. Identification of toxic compounds before they reach large numbers of users is therefore a crucial area of research.

1.4.3 Metabolism

Synthetic cannabinoid metabolism appears to proceed in a similar manner to phytocannabinoids – predominantly undergoing oxidative transformations (e.g. hydroxylations) before phase II glucuronidation. These hydroxylations occur in most reports of synthetic cannabinoid metabolism (Sobolevsky, Prasolov, & Rodchenkov, 2010; Takayama et al., 2014; Thomsen et al., 2014). Other phase II transformations (e.g. sulfation) are generally not observed.

For synthetic cannabinoids containing a carboxamide or ester bulky group, metabolic transformations other than hydroxylation appear to be favourable. Available studies suggest that in these cases, hydrolysis is a primary metabolic pathway. For

example, indazole carboxamides AB-PINACA and AB-FUBINACA are hydrolysed primarily by carboxylesterase 1 (Thomsen et al., 2014). A similar hydrolysis occurs for quinolinol synthetic cannabinoids PB-22 and 5F-PB-22 (Takayama et al., 2014; Thomsen et al., 2014). Hydroxylation then precedes on the hydrolysis products.

Importantly, minor metabolic transformations can produce metabolites that retain CB_1 binding affinity. For example, JWH-018 can be hydroxylated to form a metabolite that retains CB_1 binding affinity (Seely, Brents, et al., 2012). Glucuronidation then forms a metabolite which is an antagonist at CB_1 receptors. Thus, *in vitro* assessments of potency of the parent compound in isolation may not accurately reflect potency following metabolic transformations *in vivo*.

Closely structurally related synthetic cannabinoids (e.g. fluorinated analogues) may produce identical metabolites (Andersson et al., 2016). This has the potential to thwart forensic attempts to identify a unique compound in biological samples. This problem may be compounded if the metabolic pathways that produce such metabolites are highly favoured. Thus, careful choice of forensic targets may be required, but for many new synthetic cannabinoids, these metabolic pathways are uncharacterised.

Most studies that characterise synthetic cannabinoid metabolism do so using microsomal and hepatocyte incubations (Andersson et al., 2016; Takayama et al., 2014; Thomsen et al., 2014; Wohlfarth et al., 2014). Relatively few studies have been conducted using *in vivo* models (Carlier et al., 2016). Interestingly, metabolism often appears to be rapid in microsomal incubations, particularly for compounds possessing less stable functional groups like esters (Andersson et al., 2016; Takayama et al., 2014). Yet human case studies and radiotelemetric data indicate that the effects of synthetic

cannabinoids persist over several hours (Banister et al., 2013; Lapoint et al., 2011), and that in some cases, the parent compound remains detectible in adipose tissue for an extended period of time (Hasegawa et al., 2015). Therefore, there appears to be a discrepancy between *in vivo* and *in vitro* pharmacokinetic data. Future studies that directly compare *in vivo* and *in vitro* models of synthetic cannabinoid pharmacokinetics may prove valuable.

1.4.4 Thermal degradation

Smoking or vaporising synthetic cannabinoids involves heating to high temperatures. Burning a cigarette or joint produces temperatures of approximately 700 °C, which can increase up to 900 °C during puffs (Baker, 1974). At these temperatures, there is emerging evidence that some synthetic cannabinoids thermally decompose, forming a variety of thermolysis products. For example, UR-144 and XLR-11 contain a tetramethylcyclopropyl ring system that is sterically strained and opens when heated when burnt (Figure 5) (Adamowicz, Zuba, & Sekuła, 2013; Grigoryev et al., 2013). These ring-opened degradants retain affinity and efficacy at CB_1, and can substitute for Δ^9-THC in drug discrimination tests (Thomas et al., 2017). Thus, like synthetic cannabinoid metabolites, pyrolysis products may play a role in the total effect of synthetic cannabinoids.

There is also the possibility that some synthetic cannabinoids could form toxic thermal degradants. For example, a common constituent of synthetic cannabinoids is a naphthyl group, which in isolation (*i.e.* naphthalene) is a suspected human carcinogen. If that group is thermally liberated from the remaining structure and inhaled, it could theoretically produce toxicity over and above that of the parent

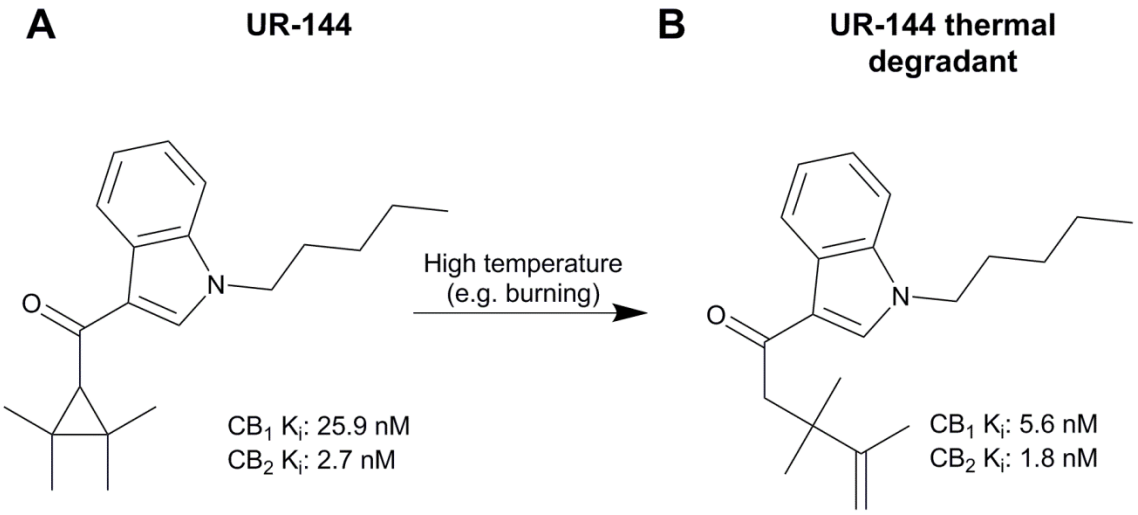

Figure 5. *(A) UR-144 and (B) UR-144 thermal degradant formed after heating to 800 °C. Note that the degradant not only retains cannabinoid receptor binding affinity, but binds more strongly to CB_1 and CB_2 receptors than the parent compound. Binding values determined via [^{3}H]CP-55,940 displacement (Thomas et al., 2017).*

compound. Similarly, carboxamide synthetic cannabinoids could thermally decompose into a range of amides and nitriles (Davidson & Karten, 1956; Metcalfe et al., 1983). Even fluorinated degradants, including hydrofluoric acid, could theoretically be liberated from fluorinated synthetic cannabinoids (Hutter et al., 2013).

Crucially, thermal degradants and their effects will not be detected in studies using other routes of administration (e.g. injections or infusions). If a synthetic cannabinoid produces thermal degradants that retain cannabinoid receptor affinity, as appears to be the case with UR-144 above, then the pharmacological impact of that compound may be under or overestimated. It is noteworthy that the thermal degradants of several classes of synthetic cannabinoids, such as the increasingly detected and potentially toxic carboxamides, are presently unknown.

1.4.5 Long-term effects and toxicity

As synthetic cannabinoid use is a relatively recent phenomenon, there are very few reports of the long-term effects of synthetic cannabinoid use in humans. Some users anecdotally report addiction, although a specific synthetic cannabinoid is rarely specified and multiple drug use is frequently reported, for example:

> *"I have been clean for 14 days now from the synthetic weed. I was addicted to it for a year. The only way I got clean was when all smoke shops here ... were raided and shut down. I was so angry when this happen cause the cravings were unbarable [sic]. This drug has turn [sic] me in to [sic] a depressed person with anxietx [sic]... I still get the urge every now and then to smoke but it usllay [sic] goes away within 10 min... I would say this addiction is up there in the crack addiction. I would know because I was addicted to crack from 2006 to 2007." (brittney_burch, 2013)*

Tolerance and withdrawal following repeated use of synthetic cannabinoid products has also been reported in scientific literature (Macfarlane & Christie, 2015; Zimmermann et al., 2009). Common symptoms of synthetic cannabinoid withdrawal are irritability, agitation, anxiety, depression, and mood swings. This symptomology appears to be similar to cannabis withdrawal syndrome, which as mentioned in Section 1.1.2, can also produce irritability, agitation, and anxiety (Allsop et al., 2012). However users (as above) describe synthetic cannabinoid withdrawal as more severe than for cannabis (Winstock & Barratt, 2013), sometimes comparing it to cocaine or opiate withdrawal.

Unfortunately, physiological and toxicological data are extremely limited beyond acute case reports. A very recent study has reported impairments to executive function in chronic synthetic cannabinoid users, compared to both cannabis and non-cannabis users (Cohen et al., 2017). However, the authors could not focus on any one specific synthetic cannabinoid, nor could they rule out additional drug or medication use or the impact of socioeconomic status. Unfortunately, to the author's knowledge, there are no controlled studies concerning long-term toxic outcomes of synthetic cannabinoid use using animal models.

1.5 Legislation, forensics, and treatments

1.5.1 Reasons for synthetic cannabinoid use/abuse

In spite of the apparent dangers discussed in the previous sections, people continue to use synthetic cannabinoids. Using products of unknown potency and composition with a number of negative side-effects, and a high possibility of toxicity or addiction, does not seem appealing. However, like other drugs of abuse, the use of synthetic cannabinoids appears to be mediated by a wide array of factors (Figure 6). Understanding these factors is important for the design of effective legislation and treatments.

User surveys have found that the most commonly stated reason for using synthetic cannabinoids is simple curiosity, or as an alternative to cannabis use (Vandrey et al., 2012; Winstock & Barratt, 2013). Nearly all surveyed synthetic cannabinoid users report having used cannabis previously (Winstock & Barratt, 2013). However, most users do report a preference for cannabis over synthetic cannabinoid products (Winstock & Barratt, 2013), citing adverse side-effects as a dissuading factor.

Workplace drug testing has been identified as a strong motivating factor for synthetic cannabinoid use (Gunderson et al., 2014). There is a delay between first detection of a novel synthetic cannabinoid, the development of forensic analyses, and the widespread implementation of these analyses. These delays create a period of time in which drug tests may fail to detect use of novel synthetic cannabinoids. These same tests are generally capable of detecting cannabis use, thereby encouraging synthetic cannabinoid use over cannabis, despite a higher risk of adverse side-effects. Although

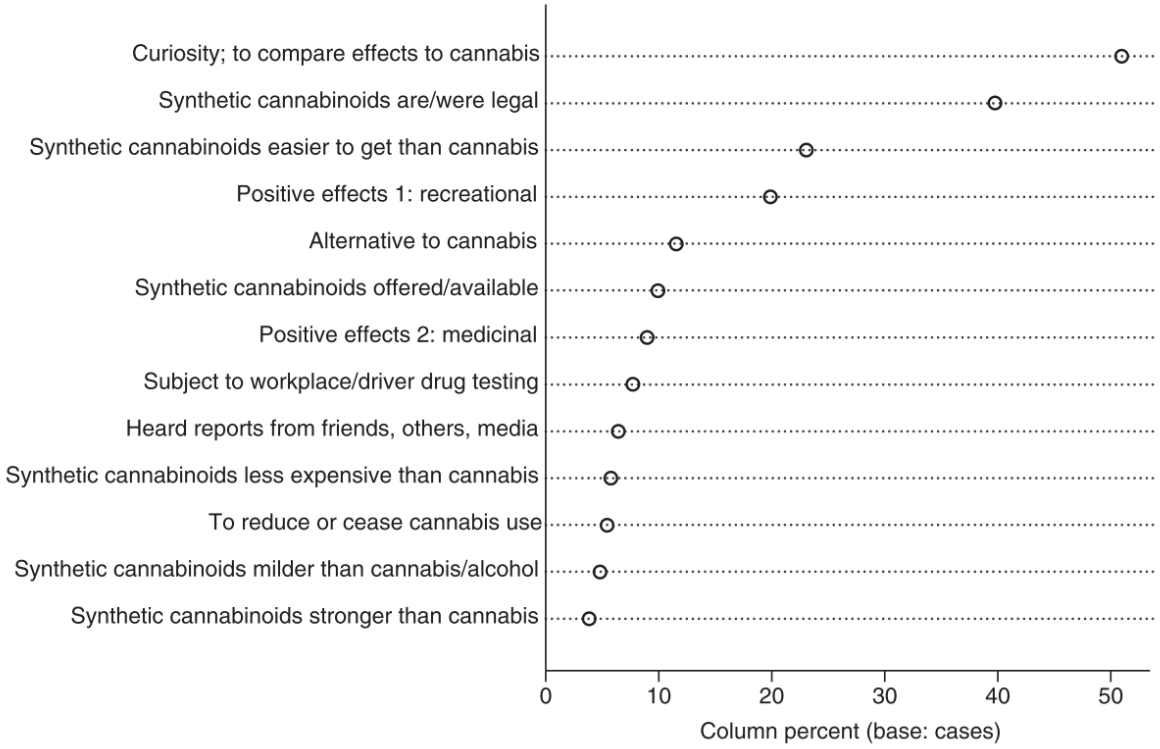

Figure 6. *Self-reported reasons for first using synthetic cannabinoids from 316 Australian synthetic cannabinoid users (Barratt et al., 2012).*

blood and urine screens for synthetic cannabinoids have developed in recent years in response to increasing data regarding synthetic cannabinoid pharmacokinetics and metabolism (Hutter et al., 2012; Marino et al., 2016), newly discovered synthetic cannabinoids can remain undetected in drug screens for a substantial period of time. This is discussed further in Section 1.5.3.

In places where synthetic cannabinoids are not yet banned, or where enforcement of legislation is lax or impractical, real or implied legality might be interpreted as a tacit guarantee of product safety. Products sold in physical "bricks and mortar" stores may be assumed to have met the product safety requirements of that jurisdiction. In reality, synthetic cannabinoid products have undergone no

toxicological testing. Additionally, in places where cannabis is illegal, so called "legal highs" provide an attractive alternate to illicit drug use. In a survey of Australian synthetic cannabinoid users, the second most common reason for use (behind curiosity) was that "synthetic cannabinoids are/were legal" (Barratt et al., 2012, p. 4). The legal status of synthetic cannabinoids is reviewed in Section 1.5.2.

The ease with which products can be obtained through stores and online marketplaces also contributes to the popularity of synthetic cannabinoid products (Barratt et al., 2012). Synthetic cannabinoids, along with some other designer and non-designer drugs of abuse, can be packaged and shipped discreetly, because most can be powdered, stored at room temperature, and do not possess a strong odour. Users have reported that synthetic cannabinoids are easier to obtain than cannabis (Barratt et al., 2012).

And finally, as reviewed in Section 1.4.5, addiction and withdrawal symptoms may contribute to the development of chronic synthetic cannabinoid use. This does not account for first use, but likely accounts for a substantial portion of total synthetic cannabinoid sales. Effective treatment of chronic users may therefore be particularly important for reducing the size of the synthetic cannabinoid market.

1.5.2 Legislation and the "chemical arms race"

In response to the psychoactive and potentially toxic effects reviewed in the previous sections, many countries have implemented legislation to curb the use of synthetic cannabinoids. International drug scheduling legislation (*i.e.* the UN Convention on Psychotropic Substances of 1971) contained no provisions concerning structural analogues of scheduled drugs, so the precise method of drug control fell to

individual jurisdictions. The scope and implementation of such legislation varies widely between and within countries. In many cases (e.g. Japan and the US) early legislation banned individual compounds, which triggered a "chemical arms race" that rapidly replaced banned compounds via structural alterations (Section 1.3.4). Subsequent laws attempted to ban substances based on chemical class (e.g. belonging to the aminoalkylindole class), effect (e.g. producing cannabimimetic effects), or action (e.g. binding to CB_1), in order to capture novel synthetic cannabinoid variants.

In Europe, a number of countries (Austria, Estonia, France, Germany, Lithuania, Luxembourg, Poland, Sweden, and the UK) implemented controls on synthetic cannabinoids in 2009, such that all synthetic cannabinoid products were banned from head shops and online stores (Seely, Lapoint, et al., 2012). Similar bans were expanded to Denmark, Ireland, Italy, Latvia, and Romania by 2011, and to Finland, Russia, and Switzerland by 2014 (Thomas et al., 2014).

In the United States in 2011, the DEA placed JWH-018, JWH-200 ([1-[2-(4-morpholinyl)ethyl]-1H-indol-3-yl]-1-naphthalenyl-methanone), JWH-073, CP-47,497, and cannabicyclohexanol into Schedule I for one year (Fattore & Fratta, 2011). This was followed by the Food and Drug Administration Safety and Innovation Act (2012) that banned substances via the placement of any CB_1 agonist into Schedule I. Canada implemented similar controls on all "synthetic preparations of cannabis" (CCENDU, 2014, p. 3).

In 2013, Australia implemented a 3 month interim ban on the possession or sale of synthetic drug products in response to high-profile cases of toxicity produced by a range of synthetic drugs beyond synthetic cannabinoids. Following expiration of the ban, most Australian states implemented legislation regulating synthetic products. In

particular, New South Wales enacted “analogue laws” that banned substances based on chemical class or cannabimimetic activity. Additionally, Queensland, New South Wales, and South Australia placed a blanket ban on possessing or selling any psychoactive substance other than alcohol, tobacco, and food (ADF, 2016). New Zealand originally allowed synthetic products to be sold if their safety could be demonstrated, but subsequently banned the sale and possession of designer drugs following concern about their addictive potential (The Guardian, 2014).

The use of analogue laws such as those present in Australia or the United States are intended to counter circumvention via structural alterations, however loopholes remain. For example, if a structure falls outside established classes of CB_1 agonists, binding studies must be performed to demonstrate CB_1 efficacy before that structure can be legislated against. This takes time, during which a particular synthetic cannabinoid can be technically legal, or at least not explicitly illegal. In some cases, cannabimimetic activity may also need to be established before prosecutions can take place, even if the compounds belong to a known cannabimimetic class. Consequently, cases of poisoning caused by synthetic cannabinoid products sold from stores have persisted even after legislation has been enacted, and structural alterations are still used to circumvent legislation (Brook, 2016). Surveys of synthetic cannabinoid products show that over the last decade popular synthetic cannabinoids have emerged in waves as a result of legislative bans (Schwartz et al., 2015). In 2010-2012, JWH-018 and AM-2201 were frequently detected in synthetic cannabinoid products, but their popularity declined sharply as they were specifically banned in several countries (NFILS, 2014). They were replaced by various indole carboxylates and indole or indazole carboxamides (Schwartz et al., 2015). Despite these legal difficulties, it should

be noted that legislation has been effective in reducing synthetic cannabinoid use. For example, synthetic cannabinoid use in New Zealand fell sharply following bans in 2014 (GDS, 2016).

1.5.3 Forensic detection and identification of synthetic cannabinoids

The frequently changing synthetic cannabinoid landscape has proven challenging for forensic chemists. Constantly emerging novel compounds necessitate the development of analytical methods that are broad, so as to detect as many compounds as possible, and adaptable, so that newly discovered compounds can be added to the method. Two common analytical approaches to the problem are immunoassay screens and mass spectrometric analysis (Thomas et al., 2014).

Immunoassay screens involve mixing samples with solutions of antibodies that react to a specific drug or a class of drug (Cone et al., 2002). These screens can be designed to detect large numbers of structurally-related compounds, including synthetic cannabinoids. However, immunoassays require frequent updating and can be non-specific. False positives can occur with closely related structures, even though they may not have any CB_1 affinity or produce any psychoactive effects. Therefore, confirmation with other methods and further testing for cannabimimetic activity is usually still required for enforcement of legislation (Mule & Casella, 1988).

Mass spectrometric testing is increasingly used to detect and confirm the identity of synthetic cannabinoids. Mass spectra and retention time measurements in chromatographic systems can provide more specific information regarding compound identity than immunoassay screens. Recent years have seen the publication of generic methods designed to detect as many synthetic cannabinoids as possible (Hess et al.,

2016; Scheidweiler, Jarvis, & Huestis, 2015). Both gas chromatography (GC)- and liquid chromatography (LC)-mass spectrometry (MS) have been implemented for the detection of synthetic cannabinoids and their metabolites in blood and urine (Hess et al., 2016; Paul & Bosy, 2015). However, analytical standards are still required to confirm compound identity.

Advanced mass spectrometric techniques may be useful for screening novel synthetic cannabinoids. For example, mass defect filtering has been somewhat successful as a screening tool for detecting a wide range of synthetic cannabinoids (Grabenauer et al., 2012). A mass defect is the difference between a compound's nominal mass and its exact mass; for example, PB-22 has a nominal mass of 358 Da and an exact mass of 358.1754 Da, yielding a mass defect of 0.1754 Da (Wohlfarth et al., 2014). This mass defect will tend to be similar to compounds of similar, but not necessarily identical, composition. Scanning a sample for compounds of similar mass defect to a known compound can potentially detect novel synthetic cannabinoids while excluding noise from irrelevant substances. This approach is particularly useful for analysing samples with complex biological matrices like blood or urine.

Additionally, non-targeted mass spectrometric techniques have been implemented for detection of novel compounds and for characterisation of metabolites. These techniques usually involve using high resolution and mass accurate time of flight (TOF) or orbitrap instruments (Thomas et al., 2014). High mass accuracy instruments can, in some cases, be used to distinguish between isomers, and the high resolution of orbitrap instruments can improve identification of compounds in complex biological matrices. Ultimately however, all analytical methods require

frequent updates based on new research as novel compounds continue to be developed.

1.5.4 Treatments for synthetic cannabinoid toxicity and dependence

While the acute effects of synthetic cannabinoid intoxication have been the subject of numerous reports, no specific antidotes for acute synthetic cannabinoid intoxication have been established. Theoretically, CB_1 antagonists/inverse agonists could be used to reverse acute symptoms. However, the preeminent CB_1 antagonist/inverse agonist rimonabant is well known for its deleterious psychiatric side-effects, including depressed mood disorders and anxiety (Moreira & Crippa, 2009; Sam, Salem, & Ghatei, 2011). Case studies report treatment of acute synthetic cannabinoid symptoms with close monitoring coupled with administration of fluids and sedatives as appropriate (Hermanns-Clausen et al., 2012; Lapoint et al., 2011; Schneir et al., 2011; Schwartz et al., 2015).

In case reports, withdrawal has been managed with benzodiazepines (diazepam) and antipsychotics (quetiapine) (Macfarlane & Christie, 2015). This approach is similar to treatment of cannabis withdrawal, which has been pharmacological treated with antidepressants, mood stabilizers, anticonvulsants, and anxiolytics (Allsop et al., 2015). However, these treatments produce minimal benefits in clinical populations (Marshall et al., 2014), and cannabis withdrawal symptoms are thought to increase the likelihood of relapse to cannabis use (Allsop et al., 2012). Similarly, it is conceivable that synthetic cannabinoid withdrawal, which appears to be more severe than cannabis withdrawal, may increase the likelihood of relapse to synthetic cannabinoid use.

An alternative to the aforementioned treatments is agonist replacement therapy. Agonist replacement therapy has been used successfully in the treatment of opiate withdrawal, and involves replacing a hazardous agonist (e.g. heroin) with a less hazardous one (e.g. methadone). The dose is gradually tapered downward until the user is free of both the drug and withdrawal symptoms. Alternatively, the agonist can be the same as the abused drug (e.g. nicotine patches or gum for treatment of nicotine addiction), and gradually reduced over time. This approach helps to control withdrawal symptoms and thereby reduces the likelihood of relapse caused by a desire to reduce withdrawal symptoms. In the case of cannabis dependence, Δ^9-THC and nabiximols (Sativex®; a buccal spray consisting of equal parts Δ^9-THC and CBD) have shown promise as an agonist substitution therapy (Allsop et al., 2015; Balter, Cooper, & Haney, 2014; Budney et al., 2007; Haney et al., 2013). Appropriate doses of nabiximols reduced withdrawal symptoms and rates of patient dropout in a double-blind, inpatient study of cannabis dependent users (Allsop et al., 2014).

A similar treatment might be viable for synthetic cannabinoid withdrawal symptoms. However, the viability of such an approach depends on being able to administer the treatment at appropriate concentrations, and being able to accurately monitor patient pharmacokinetics. Specifically, being able to accurately monitor concentrations of the replacement agonist (e.g. Δ^9-THC) and the previously abused drug (a given synthetic cannabinoid) is essential. If daily monitoring is required, then urinalysis is also desirable as a less invasive alternative to repeated blood draws. At present, the trajectory of Δ^9-THC concentrations during multiple days of agonist replacement therapy is uncharacterised. It is also unclear if urinalysis can be used as an accurate substitute for plasma analysis. These issues need clarification before the

widespread implementation of agonist replacement therapy for the treatment of cannabis withdrawal, and possibly synthetic cannabinoid withdrawal.

1.6 Thesis overview

This thesis is comprised of investigations that were designed to build knowledge and understanding in several keys areas reviewed in this chapter. Specifically, the studies presented in this thesis aimed to:

1. Characterise the *in vivo* potency and basic physiological effects of several synthetic cannabinoids that are in current use as recreational drugs (Chapter 2).

2. Identify structure-activity relationships for aminoalkylindoles and related synthetic cannabinoids using *in vivo* measures (Chapter 2).

3. Establish metabolic pathways and identify valid analytical targets among novel synthetic cannabinoids and their metabolites (Chapter 3).

4. Identify and discuss the discrepancy between *in vitro* and *in vivo* synthetic cannabinoid pharmacokinetic data, where, for example, *in vitro* data predicts rapid clearance while *in vivo* data describes long durations of action (Chapter 3).

5. Explore the long-term residual effects (e.g. cognitive effects, toxicological effects) arising from repeated synthetic cannabinoid exposure in rats (Chapter 4).

6. Establish accurate and practical urinalysis techniques to accompany agonist replacement therapies (involving Δ^9-THC) for cannabis and/or synthetic cannabinoid dependence and withdrawal (Chapter 5).

Accordingly, Chapter 2 features *in vivo* physiological assessment of twelve synthetic cannabinoids of varying structure via biotelemetry. Hypothermic and bradycardic effects are characterised *in vivo* for the first time, and structure-activity relationships are established, addressing points 1 and 2.

Chapter 3 examines the metabolism of two synthetic cannabinoids *in vitro* using rat and human liver microsomes and hepatocytes, in addition to *in vivo*

assessment in rats. Analytical methods for detecting these synthetic cannabinoids and their metabolites using LC-MS/MS are described. Relationships between compound structure and metabolism are identified, and *in vitro* and *in vivo* pharmacokinetic models are compared, addressing points 3 and 4.

Chapter 4 details the acute and chronic effects of two synthetic cannabinoids in adolescent rats, addressing point 5. Acute increases in anxiety-like behaviour coupled with decreases in locomotor activity are observed. Long term impairment of object recognition memory, and down-regulation of cytokines are described. The effects produced by these synthetic cannabinoids are compared directly to Δ^9-THC.

Chapter 5 explores urinary monitoring of cannabinoids in humans, following inpatient treatment of cannabinoid withdrawal with nabiximols. Although this work did not focus on a synthetic cannabinoid using population, it establishes the viability of urinary monitoring of cannabinoids in clinical settings, addressing point 6. A similar approach, monitoring both phytocannabinoids and synthetic cannabinoids (using the metabolic data established in Chapter 4 and by other research groups) may be useful in treating synthetic cannabinoid dependence and withdrawal in the future.

Finally, Chapter 6 contains a general discussion of the preceding work. The work presented in Chapters 2 – 5 is combined to illustrate the value of SARs and common metabolic pathways for predicting the crucial properties of novel synthetic cannabinoids, the potential impacts of chronic synthetic cannabinoid use, and the potential for agonist substitution therapy for treating synthetic cannabinoid dependence and withdrawal.

1.7 References

Adamowicz, P., Zuba, D., & Sekuła, K. (2013). Analysis of UR-144 and its pyrolysis product in blood and their metabolites in urine. *Forensic Science International, 233*(1), 320-327.

Adams, A. J., Banister, S. D., Irizarry, L., Trecki, J., Schwartz, M., & Gerona, R. (2017). "Zombie" outbreak caused by the synthetic cannabinoid AMB-FUBINACA in New York. *New England Journal of Medicine, 376*(3), 235-242.

ADF. (2016). *Drug law in Australia*. Retrieved from: http://www.druginfo.adf.org.au/topics/drug-law-in-australia

Allsop, D. J., Copeland, J., Lintzeris, N., Dunlop, A. J., Montebello, M., Sadler, C., et al. (2014). Nabiximols as an agonist replacement therapy during cannabis withdrawal: a randomized clinical trial. *JAMA Psychiatry, 71*(3), 281-291.

Allsop, D. J., Copeland, J., Norberg, M. M., Fu, S., Molnar, A., Lewis, J., et al. (2012). Quantifying the clinical significance of cannabis withdrawal. *PloS One, 7*(9), e44864.

Allsop, D. J., Lintzeris, N., Copeland, J., Dunlop, A., & McGregor, I. S. (2015). Cannabinoid replacement therapy (CRT): Nabiximols (Sativex) as a novel treatment for cannabis withdrawal. *Clinical Pharmacology and Therapeutics, 97*(6), 571-574.

Allsop, D. J., Norberg, M. M., Copeland, J., Fu, S., & Budney, A. J. (2011). The Cannabis Withdrawal Scale development: Patterns and predictors of cannabis withdrawal and distress. *Drug and Alcohol Dependence, 119*(1-2), 123-129.

Andersson, M., Diao, X., Wohlfarth, A., Scheidweiler, K. B., & Huestis, M. A. (2016). Metabolic profiling of new synthetic cannabinoids AMB and 5F-AMB by human hepatocyte and liver microsome incubations and high-resolution mass spectrometry. *Rapid Communications in Mass Spectrometry, 30*(8), 1067-1078.

Ashton, C. H. (2001). Pharmacology and effects of cannabis: A brief review. *The British Journal of Psychiatry, 178*(2), 101-106.

Aung, M. M., Griffin, G., Huffman, J. W., Wu, M.-J., Keel, C., Yang, B., et al. (2000). Influence of the N-1 alkyl chain length of cannabimimetic indoles upon CB_1 and CB_2 receptor binding. *Drug and Alcohol Dependence, 60*(2), 133-140.

Baker, R. R. (1974). Temperature distribution inside a burning cigarette. *Nature, 247*(5440), 405-406.

Balter, R. E., Cooper, Z. D., & Haney, M. (2014). Novel pharmacologic approaches to treating cannabis use disorder. *Current Addiction Reports, 1*(2), 137-143.

Balunas, M. J., & Kinghorn, A. D. (2005). Drug discovery from medicinal plants. *Life Sciences, 78*(5), 431-441.

Banister, S. D., Wilkinson, S. M., Longworth, M., Stuart, J., Apetz, N., English, K., et al. (2013). The synthesis and pharmacological evaluation of adamantane-derived indoles: Cannabimimetic drugs of abuse. *ACS Chemical Neuroscience, 4*(7), 1081-1092.

Barratt, M. J., Cakic, V., & Lenton, S. (2012). Patterns of synthetic cannabinoid use in Australia. *Drug and Alcohol Review, 32*(2), 141-146.

Bernson-Leung, M. E., Leung, L. Y., & Kumar, S. (2014). Synthetic cannabis and acute ischemic stroke. *Journal of Stroke and Cerebrovascular Diseases, 23*(5), 1239-1241.

Bhanushali, G. K., Jain, G., Fatima, H., Leisch, L. J., & Thornley-Brown, D. (2012). AKI associated with synthetic cannabinoids: A case series. *Clinical Journal of the American Society of Nephrology, 8*(4), 523-526.

Blessing, E. M., Steenkamp, M. M., Manzanares, J., & Marmar, C. R. (2015). Cannabidiol as a potential treatment for anxiety disorders. *Neurotherapeutics, 12*(4), 825-836.

Bornheim, L. M., & Correia, M. A. (1989). Effect of cannabidiol on cytochrome P-450 isozymes. *Biochemical Pharmacology, 38*(17), 2789-2794.

Bornheim, L. M., & Correia, M. A. (1990). Selective inactivation of mouse liver cytochrome P-450IIIA by cannabidiol. *Molecular Pharmacology, 38*(3), 319-326.

Bornheim, L. M., & Correia, M. A. (1991). Purification and characterization of the major hepatic cannabinoid hydroxylase in the mouse: A possible member of the cytochrome P-450IIC subfamily. *Molecular Pharmacology, 40*(2), 228-234.

Braida, D., Iosue, S., Pegorini, S., & Sala, M. (2004). Δ^9-Tetrahydrocannabinol-induced conditioned place preference and intracerebroventricular self-administration in rats. *European Journal of Pharmacology, 506*(1), 63-69.

Braida, D., Pozzi, M., Cavallini, R., & Sala, M. (2001). Conditioned place preference induced by the cannabinoid agonist CP 55,940: Interaction with the opioid system. *Neuroscience, 104*(4), 923-926.

brittney_burch. (2013). *Say no to synthetic weed*. Retrieved from: https://drugs-forum.com/forum/showthread.php?t=219448

Brook, B. (2016). Calls for action as teenager dies as synthetic cannabis crisis worsens. *news.com.au*. Retrieved from: http://www.news.com.au/lifestyle/health/health-problems/calls-for-action-as-teenager-dies-as-synthetic-cannabis-crisis-worsens/news-story/51fd93a2747add2e0a54518d7c83ca27

Bruci, Z., Papoutsis, I., Athanaselis, S., Nikolaou, P., Pazari, E., Spiliopoulou, C., et al. (2012). First systematic evaluation of the potency of *Cannabis sativa* plants grown in Albania. *Forensic Science International, 222*(1-3), 40-46.

Budney, A. J., Vandrey, R. G., Hughes, J. R., Moore, B. A., & Bahrenburg, B. (2007). Oral Δ^9-tetrahydrocannabinol suppresses cannabis withdrawal symptoms. *Drug and Alcohol Dependence, 86*(1), 22-29.

Burgdorf, J. R., Kilmer, B., & Pacula, R. L. (2011). Heterogeneity in the composition of marijuana seized in California. *Drug and Alcohol Dependence, 117*(1), 59-61.

Buser, G. L., Gerona, R. R., Horowitz, B. Z., Vian, K. P., Troxell, M. L., Hendrickson, R. G., et al. (2014). Acute kidney injury associated with smoking synthetic cannabinoid. *Clinical Toxicology, 52*(7), 664-673.

Caffarel, M. M., Andradas, C., Mira, E., Pérez-Gómez, E., Cerutti, C., Moreno-Bueno, G., et al. (2010). Cannabinoids reduce ErbB2-driven breast cancer progression through Akt inhibition. *Molecular Cancer, 9*(1), 196.

Carlier, J., Diao, X., Wohlfarth, A., Scheidweiler, K., & Huestis, M. A. (2016). In vitro metabolite profiling of ADB-FUBINACA, a new synthetic cannabinoid. *Current Neuropharmacology*.

Cascini, F., Aiello, C., & Di Tanna, G. (2012). Increasing delta-9-tetrahydrocannabinol (Δ^9-THC) content in herbal cannabis over time: Systematic review and meta-analysis. *Current drug abuse reviews, 5*(1), 32-40.

Cascio, M. G., & Pertwee, R. G. (2014). Known pharmacological actions of nine nonpsychotropic phytocannabinoids. In R. G. Pertwee (Ed.), *Handbook of Cannabis*. Oxford, UK: Oxford University Press.

CCENDU. (2014). *CCENDU Bulletin: Synthetic Cannabinoids in Canada*. Retrieved from: http://www.ccsa.ca/Resource%20Library/CCSA-CCENDU-Synthetic-Cannabis-Bulletin-2014-en.pdf

Chaperon, F., & Thiébot, M. H. (1999). Behavioral effects of cannabinoid agents in animals. *Critical Reviews in Neurobiology, 13*(3), 243-281.

Cohen, K., Kapitány-Fövény, M., Mama, Y., Arieli, M., Rosca, P., Demetrovics, Z., et al. (2017). The effects of synthetic cannabinoids on executive function. *Psychopharmacology, 234*(7), 1121-1134.

Colombo, G., Agabio, R., Diaz, G., Lobina, C., Reali, R., & Gessa, G. L. (1998). Appetite suppression and weight loss after the cannabinoid antagonist SR 141716. *Life Sciences, 63*(8), PL113-PL117.

Compton, D., Rice, K. C., De Costa, B. R., Razdan, R., Melvin, L. S., Johnson, M. R., et al. (1993). Cannabinoid structure-activity relationships: Correlation of receptor binding and in vivo activities. *Journal of Pharmacology and Experimental Therapeutics, 265*(1), 218-226.

Cone, E. J., Presley, L., Lehrer, M., Seiter, W., Smith, M., Kardos, K. W., et al. (2002). Oral fluid testing for drugs of abuse: Positive prevalence rates by Intercept™ immunoassay screening and GC-MS-MS confirmation and suggested cutoff concentrations. *Journal of Analytical Toxicology, 26*(8), 541-546.

Cox, M. L., Haller, V. L., & Welch, S. P. (2007). The antinociceptive effect of Δ^9-tetrahydrocannabinol in the arthritic rat involves the CB_2 cannabinoid receptor. *European Journal of Pharmacology, 570*(1), 50-56.

Crean, R. D., Crane, N. A., & Mason, B. J. (2011). An evidence based review of acute and long-term effects of cannabis use on executive cognitive functions. *Journal of Addiction Medicine, 5*(1), 1.

Curran, V. H., Brignell, C., Fletcher, S., Middleton, P., & Henry, J. (2002). Cognitive and subjective dose-response effects of acute oral Δ^9-tetrahydrocannabinol (THC) in infrequent cannabis users. *Psychopharmacology, 164*(1), 61-70.

D'Ambra, T. E., Estep, K. G., Bell, M. R., Eissenstat, M. A., Josef, K. A., Ward, S. J., et al. (1992). Conformationally restrained analogs of pravadoline: Nanomolar potent, enantioselective, (aminoalkyl)indole agonists of the cannabinoid receptor. *Journal of Medicinal Chemistry, 35*(1), 124-135.

Davidson, D., & Karten, M. (1956). The pyrolysis of amides. *Journal of the American Chemical Society, 78*(5), 1066-1068.

Degirmenci, Y., Kececi, H., & Olmez, N. (2016). A case of ischemic stroke after bonzai: Syntetic(sic) cannabinoid from Turkey. *Neurological Sciences, 37*(2), 299-300.

Deutsch, D. G., & Chin, S. A. (1993). Enzymatic synthesis and degradation of anandamide, a cannabinoid receptor agonist. *Biochemical Pharmacology, 46*(5), 791-796.

Devane, W. A., Hanus, L., Breuer, A., Pertwee, R. G., Stevenson, L. A., Griffin, G., et al. (1992). Isolation and structure of a brain constituent that binds to the cannabinoid receptor. *Science, 258*(5090), 1946-1949.

Di Marzo, V., & De Petrocellis, L. (2010). Endocannabinoids as regulators of transient receptor potential (TRP) channels: a further opportunity to develop new endocannabinoid-based therapeutic drugs. *Current Medicinal Chemistry, 17*(14), 1430-1449.

Dogan, B., Dogru, H., Gungor, L., & Balci, K. (2016). Stroke due to Bonzai use: Two patients. *World, 7*(4), 310-312.

Dresen, S., Ferreiros, N., Putz, M., Westphal, F., Zimmermann, R., & Auwarter, V. (2010). Monitoring of herbal mixtures potentially containing synthetic cannabinoids as psychoactive compounds. *Journal of Mass Spectrometry, 45*(10), 1186-1194.

ElSohly, M. A., & Gul, W. (2014). Constituents of Cannabis Sativa. In R. G. Pertwee (Ed.), *Handbook of Cannabis* (pp. 3-22). Oxford, UK: Oxford University Press.

ElSohly, M. A., & Slade, D. (2005). Chemical constituents of marijuana: The complex mixture of natural cannabinoids. *Life Sciences, 78*(5), 539-548.

EMCDDA. (2009). *Understanding the 'Spice' Phenomenon*. Retrieved from: http://www.emcdda.europa.eu/publications/thematic-papers/understanding-spice-phenomenon

EMCDDA. (2014). *Annual Report on the Implementation of the Council Decision 2005/387/JHA*. Retrieved from: http://www.emcdda.europa.eu/publications/implementation-reports/2015

EMCDDA. (2015). *European Drug Report 2015*. Retrieved from: http://www.emcdda.europa.eu/attachements.cfm/att_239505_EN_TDAT15001ENN.pdf

EMCDDA. (2016). *Synthetic cannabinoids in Europe*. Retrieved from: http://www.emcdda.europa.eu/attachements.cfm/att_212361_EN_EMCDDA_POD_2013_Synthetic

Evilpoptart. (2011). *Never again*. Retrieved from: https://erowid.org/experiences/exp.php?ID=88807

Fantegrossi, W. E., Moran, J. H., Radominska-Pandya, A., & Prather, P. L. (2014). Distinct pharmacology and metabolism of K2 synthetic cannabinoids compared to Δ^9-THC: Mechanism underlying greater toxicity? *Life Sciences, 97*(1), 45-54.

Farquhar-Smith, W. P., Egertová, M., Bradbury, E. J., McMahon, S. B., Rice, A. S., & Elphick, M. R. (2000). Cannabinoid CB_1 receptor expression in rat spinal cord. *Molecular and Cellular Neuroscience, 15*(6), 510-521.

Fattore, L., & Fratta, W. (2011). Beyond THC: The new generation of cannabinoid designer drugs. *Frontiers in Behavioral Neuroscience*, doi: 10.3389/fnbeh.2011.00060.

Ferrari, F., Ottani, A., Vivoli, R., & Giuliani, D. (1999). Learning impairment produced in rats by the cannabinoid agonist HU 210 in a Water-Maze task. *Pharmacology Biochemistry and Behavior, 64*(3), 555-561.

Fields, H. L., & Margolis, E. B. (2015). Understanding opioid reward. *Trends in Neurosciences, 38*(4), 217-225.

Flores-Sanchez, I. J., & Verpoorte, R. (2008). Secondary metabolism in cannabis. *Phytochemistry Reviews, 7*(3), 615-639.

Fox, A., Kesingland, A., Gentry, C., McNair, K., Patel, S., Urban, L., et al. (2001). The role of central and peripheral Cannabinoid$_1$ receptors in the antihyperalgesic activity of cannabinoids in a model of neuropathic pain. *Pain, 92*(1–2), 91-100.

Freeman, M. J., Rose, D. Z., Myers, M. A., Gooch, C. L., Bozeman, A. C., & Burgin, W. S. (2013). Ischemic stroke after use of the synthetic marijuana "spice". *Neurology, 81*(24), 2090-2093.

Freund, T. F., Katona, I., & Piomelli, D. (2003). Role of endogenous cannabinoids in synaptic signaling. *Physiological Reviews, 83*(3), 1017-1066.

Friedman, D., & Devinsky, O. (2015). Cannabinoids in the treatment of epilepsy. *New England Journal of Medicine, 373*(11), 1048-1058.

Gaoni, Y., & Mechoulam, R. (1964). Isolation, structure, and partial synthesis of an active constituent of hashish. *Journal of the American Chemical Society, 86*(8), 1646-1647.

Gardner, E. L. (2014). Cannabinoids and addiction. In R. Pertwee (Ed.), *Handbook of Cannabis*. Oxford, UK: Oxford University Press.

Gates, P. J., Albertella, L., & Copeland, J. (2014). The effects of cannabinoid administration on sleep: A systematic review of human studies. *Sleep Medicine Reviews, 18*(6), 477-487.

GDS. (2016). *Global Drug Survey 2016*. Retrieved from: https://www.globaldrugsurvey.com/

Giuliani, D., Ferrari, F., & Ottani, A. (2000). The cannabinoid agonist HU 210 modifies rat behavioural responses to novelty and stress. *Pharmacological Research, 41*(1), 47-53.

Glass, M., Faull, R., & Dragunow, M. (1997). Cannabinoid receptors in the human brain: A detailed anatomical and quantitative autoradiographic study in the fetal, neonatal and adult human brain. *Neuroscience, 77*(2), 299-318.

Gonsiorek, W., Lunn, C., Fan, X., Narula, S., Lundell, D., & Hipkin, R. W. (2000). Endocannabinoid 2-arachidonyl glycerol is a full agonist through human type 2 cannabinoid receptor: Antagonism by anandamide. *Molecular Pharmacology, 57*(5), 1045.

Grabenauer, M., Krol, W. L., Wiley, J. L., & Thomas, B. F. (2012). Analysis of synthetic cannabinoids using high-resolution mass spectrometry and mass defect filtering: Implications for nontargeted screening of designer drugs. *Analytical Chemistry, 84*(13), 5574-5581.

Grigoryev, A., Kavanagh, P., & Melnik, A. (2012). The detection of the urinary metabolites of 3-[(adamantan-1-yl)carbonyl]-1-pentylindole (AB-001), a novel cannabimimetic, by gas chromatography-mass spectrometry. *Drug Testing and Analysis, 4*(6), 519-524.

Grigoryev, A., Kavanagh, P., Melnik, A., Savchuk, S., & Simonov, A. (2013). Gas and liquid chromatography-mass spectrometry detection of the urinary metabolites

of UR-144 and its major pyrolysis product. *Journal of Analytical Toxicology, 37*(5), 265-276.

Guardian, T. (2014). *New Zealand in U-turn on designer drugs*. Retrieved from: https://www.theguardian.com/world/2014/may/07/new-zealand-u-turn-synthetic-designer-drugs

Guindon, J., & Hohmann, A. G. (2009). The endocannabinoid system and pain. *CNS & Neurological Disorders Drug Targets, 8*(6), 403-421.

Gunderson, E. W., Haughey, H. M., Ait-Daoud, N., Joshi, A. S., & Hart, C. L. (2014). A survey of synthetic cannabinoid consumption by current cannabis users. *Substance Abuse, 35*(2), 184-189.

Haney, M., Cooper, Z. D., Bedi, G., Vosburg, S. K., Comer, S. D., & Foltin, R. W. (2013). Nabilone decreases marijuana withdrawal and a laboratory measure of marijuana relapse. *Neuropsychopharmacology, 38*(8), 1557-1565.

Hasegawa, K., Wurita, A., Minakata, K., Gonmori, K., Nozawa, H., Yamagishi, I., et al. (2015). Postmortem distribution of AB-CHMINACA, 5-fluoro-AMB, and diphenidine in body fluids and solid tissues in a fatal poisoning case: usefulness of adipose tissue for detection of the drugs in unchanged forms. *Forensic Toxicology, 33*(1), 45-53.

Haubrich, D. R., Ward, S. J., Baizman, E., Bell, M. R., Bradford, J., Ferrari, R., et al. (1990). Pharmacology of pravadoline: A new analgesic agent. *Journal of Pharmacology and Experimental Therapeutics, 255*(2), 511-522.

Hayakawa, K., Mishima, K., Hazekawa, M., Sano, K., Irie, K., Orito, K., et al. (2008). Cannabidiol potentiates pharmacological effects of Δ^9-tetrahydrocannabinol via CB_1 receptor-dependent mechanism. *Brain Research, 1188*, 157-164.

Heishman, S. J., Huestis, M. A., Henningfield, J. E., & Cone, E. J. (1990). Acute and residual effects of marijuana: Profiles of plasma THC levels, physiological, subjective, and performance measures. *Pharmacology Biochemistry and Behavior, 37*(3), 561-565.

Herkenham, M., Lynn, A. B., Johnson, M. R., Melvin, L. S., de Costa, B. R., & Rice, K. C. (1991). Characterization and localization of cannabinoid receptors in rat brain: A quantitative in vitro autoradiographic study. *The Journal of Neuroscience, 11*(2), 563-583.

Herkenham, M., Lynn, A. B., Little, M. D., Johnson, M. R., Melvin, L. S., De Costa, B. R., et al. (1990). Cannabinoid receptor localization in brain. *Proceedings of the National Academy of Sciences, 87*(5), 1932-1936.

Hermanns-Clausen, M., Kneisel, S., Szabo, B., & Auwarter, V. (2012). Acute toxicity due to the confirmed consumption of synthetic cannabinoids: Clinical and laboratory findings. *Addiction, 108*(3), 534-544.

Hess, C., Murach, J., Krueger, L., Scharrenbroch, L., Unger, M., Madea, B., et al. (2016). Simultaneous detection of 93 synthetic cannabinoids by liquid chromatography-tandem mass spectrometry and retrospective application to real forensic samples. *Drug Testing and Analysis*, doi: 10.1002/dta.2030.

Higuera-Matas, A., Ucha, M., & Ambrosio, E. (2015). Long-term consequences of perinatal and adolescent cannabinoid exposure on neural and psychological processes. *Neuroscience & Biobehavioral Reviews, 55*, 119-146.

Hill, M. N., & Tasker, J. G. (2012). Endocannabinoid signaling, glucocorticoid-mediated negative feedback and regulation of the HPA axis. *Neuroscience, 204*, 5-16.

Hirvonen, J., Goodwin, R., Li, C.-T., Terry, G., Zoghbi, S., Morse, C., et al. (2012). Reversible and regionally selective downregulation of brain cannabinoid CB_1 receptors in chronic daily cannabis smokers. *Molecular Psychiatry, 17*(6), 642-649.

Hollister, L. E., & Gillespie, H. (1975). Interactions in man of Δ^9-tetrahydrocannabinol; II. Cannabinol and cannabidiol. *Clinical Pharmacology and Therapeutics, 18*(1), 80-83.

Hua, T., Vemuri, K., Pu, M., Qu, L., Han, Gye W., Wu, Y., et al. (2016). Crystal structure of the human cannabinoid receptor CB_1. *Cell, 167*(3), 750-762.e714.

Huestis, M. A. (2007). Human cannabinoid pharmacokinetics. *Chemistry & Biodiversity, 4*(8), 1770-1804.

Huestis, M. A., Gorelick, D. A., Heishman, S. J., Preston, K. L., Nelson, R. A., Moolchan, E. T., et al. (2001). Blockade of effects of smoked marijuana by the CB_1-selective cannabinoid receptor antagonist SR141716. *Archives of General Psychiatry, 58*(4), 322-328.

Huffman, J. W., Dai, D., Martin, B. R., & Compton, D. R. (1994). Design, synthesis and pharmacology of cannabimimetic indoles. *Bioorganic & Medicinal Chemistry Letters, 4*(4), 563-566.

Hutter, M., Broecker, S., Kneisel, S., & Auwarter, V. (2012). Identification of the major urinary metabolites in man of seven synthetic cannabinoids of the aminoalkylindole type present as adulterants in 'herbal mixtures' using LC-MS/MS techniques. *Journal of Mass Spectrometry, 47*(1), 54-65.

Hutter, M., Moosmann, B., Kneisel, S., & Auwärter, V. (2013). Characteristics of the designer drug and synthetic cannabinoid receptor agonist AM-2201 regarding its chemistry and metabolism. *Journal of Mass Spectrometry, 48*(7), 885-894.

Inal, T., Köse, A., Köksal, O., Armagan, E., Aydın, S. A., & Ozdemir, F. (2014). Acute temporal lobe infarction in a young patient associated with marijuana abuse: An unusual cause of stroke. *World J Emerg Med, 5*(1), 72-74.

Karniol, I. C., Shirakawa, I., Kasinaki, N., & Carlini, E. A. (1974). Cannabidiol interferes with the effects of Δ^9-tetrahydrocannabinol in man. *European Journal of Pharmacology, 28*, 172-177.

Karschner, E., Darwin, W., McMahon, R., Liu, F., Wright, S., Goodwin, R., et al. (2011). Subjective and physiological effects after controlled Sativex and oral THC administration. *Clinical Pharmacology and Therapeutics, 89*(3), 400-407.

Kathmann, M., Flau, K., Redmer, A., Tränkle, C., & Schlicker, E. (2006). Cannabidiol is an allosteric modulator at mu-and delta-opioid receptors. *Naunyn-Schmiedeberg's Archives of Pharmacology, 372*(5), 354-361.

Klein, C., Karanges, E., Spiro, A., Wong, A., Spencer, J., Huynh, T., et al. (2011). Cannabidiol potentiates Δ^9-tetrahydrocannabinol (THC) behavioural effects and alters THC pharmacokinetics during acute and chronic treatment in adolescent rats. *Psychopharmacology (Berl), 218*(2), 443-457.

Kuster, J. E., Stevenson, J. I., Ward, S. J., D'Ambra, T. E., & Haycock, D. A. (1993). Aminoalkylindole binding in rat cerebellum: Selective displacement by natural and synthetic cannabinoids. *Journal of Pharmacology and Experimental Therapeutics, 264*(3), 1352-1363.

Lapoint, J., James, L., Moran, C., Nelson, L., Hoffman, R., & Moran, J. (2011). Severe toxicity following synthetic cannabinoid ingestion. *Clinical Toxicology, 49*(8), 760-764.

Lemberger, L., Tamarkin, N. R., Axelrod, J., & Kopin, I. J. (1971). Δ^9-tetrahydrocannabinol: Metabolism and disposition in long-term marihuana smokers. *Science, 173*(3991), 72-74.

Louh, I. K., & Freeman, W. D. (2014). A 'spicy' encephalopathy: Synthetic cannabinoids as cause of encephalopathy and seizure. *Critical Care, 18*(5), 553.

Lupica, C. R., Riegel, A. C., & Hoffman, A. F. (2004). Marijuana and cannabinoid regulation of brain reward circuits. *British Journal of Pharmacology, 143*(2), 227-234.

Macfarlane, V., & Christie, G. (2015). Synthetic cannabinoid withdrawal: A new demand on detoxification services. *Drug and Alcohol Review*, doi: 10.1111/dar.12225.

Mackie, K. (2005). Distribution of cannabinoid receptors in the central and peripheral nervous system. In R. G. Pertwee (Ed.), *Cannabinoids* (pp. 299-325). Berlin, Heidelberg: Springer Berlin Heidelberg.

Makriyannis, A., & Deng, H. (2005). Cannabimimetic indole derivatives. US6900236 B1.

Malfitano, A. M., Basu, S., Maresz, K., Bifulco, M., & Dittel, B. N. (2014). What we know and do not know about the cannabinoid receptor 2 (CB_2). *Seminars in Immunology, 26*(5), 369-379.

Malone, D. T., Jongejan, D., & Taylor, D. A. (2009). Cannabidiol reverses the reduction in social interaction produced by low dose Δ^9-tetrahydrocannabinol in rats. *Pharmacology Biochemistry and Behavior, 93*(2), 91-96.

Maresz, K., Pryce, G., Ponomarev, E. D., Marsicano, G., Croxford, J. L., Shriver, L. P., et al. (2007). Direct suppression of CNS autoimmune inflammation via the cannabinoid receptor CB_1 on neurons and CB_2 on autoreactive T cells. *Nature Medicine, 13*(4), 492-497.

Marino, M. A., Voyer, B., Cody, R. B., Dane, A. J., Veltri, M., & Huang, L. (2016). Rapid identification of synthetic cannabinoids in herbal incenses with DART-MS and NMR. *Journal of Forensic Sciences, 61*(S1).

Marshall, K., Gowing, L., Ali, R., & Le Foll, B. (2014). Pharmacotherapies for cannabis dependence. *Cochrane Database Syst Rev, 12*, CD008940.

Marsicano, G., & Lafenetre, P. (2009). Roles of the endocannabinoid system in learning and memory. *Current Topics in Behavioral Neurosciences, 1*, 201-230.

Martin, B. R., Compton, D. R., Thomas, B. F., Prescott, W. R., Little, P. J., Razdan, R. K., et al. (1991). Behavioral, biochemical, and molecular modeling evaluations of cannabinoid analogs. *Pharmacology Biochemistry and Behavior, 40*(3), 471-478.

Matsuda, L. A., Lolait, S. J., Brownstein, M. J., Young, A. C., & Bonner, T. I. (1990). Structure of a cannabinoid receptor and functional expression of the cloned cDNA. *Nature, 346*(6284), 561-564.

Mattes, R. D., Engelman, K., Shaw, L. M., & Elsohly, M. A. (1994). Cannabinoids and appetite stimulation. *Pharmacology Biochemistry and Behavior, 49*(1), 187-195.

McGregor, I. S., Issakidis, C. N., & Prior, G. (1996). Aversive effects of the synthetic cannabinoid CP 55,940 in rats. *Pharmacology Biochemistry and Behavior, 53*(3), 657-664.

McPartland, J. M., Duncan, M., Di Marzo, V., & Pertwee, R. G. (2015). Are cannabidiol and Δ^9-tetrahydrocannabivarin negative modulators of the endocannabinoid system? A systematic review. *British Journal of Pharmacology, 172*(3), 737-753.

Mechoulam, R., Ben-Shabat, S., Hanus, L., Ligumsky, M., Kaminski, N. E., Schatz, A. R., et al. (1995). Identification of an endogenous 2-monoglyceride, present in canine gut, that binds to cannabinoid receptors. *Biochemical Pharmacology, 50*(1), 83-90.

Mechoulam, R., Fride, E., Hanu, L., Sheskin, T., Bisogno, T., Di Marzo, V., et al. (1997). Anandamide may mediate sleep induction. *Nature, 389*(6646), 25-26.

Mechoulam, R., & Gaoni, Y. (1967). Recent advances in the chemistry of hashish. In L. Zechmeister (Ed.), *Progress in the Chemistry of Organic Natural Products* (pp. 175-213). Vienna: Springer Vienna.

Mechoulam, R., Hanuš, L. O., Pertwee, R., & Howlett, A. C. (2014). Early phytocannabinoid chemistry to endocannabinoids and beyond. *Nature Reviews Neuroscience, 15*(11), 757-764.

Melvin, L. S., Milne, G. M., Johnson, M. R., Subramaniam, B., Wilken, G. H., & Howlett, A. C. (1993). Structure-activity relationships for cannabinoid receptor-

binding and analgesic activity: Studies of bicyclic cannabinoid analogs. *Molecular Pharmacology, 44*(5), 1008.

Metcalfe, E., Booth, D., McAndrew, H., & Wooley, W. (1983). The pyrolysis of organic nitriles. *Fire and Materials, 7*(4), 185-192.

Mir, A., Obafemi, A., Young, A., & Kane, C. (2011). Myocardial infarction associated with use of the synthetic cannabinoid K2. *Pediatrics, 128*(6), e1622-e1627.

Mittleman, M. A., Lewis, R. A., Maclure, M., Sherwood, J. B., & Muller, J. E. (2001). Triggering myocardial infarction by marijuana. *Circulation, 103*(23), 2805-2809.

Moreira, F. A., & Crippa, J. A. (2009). The psychiatric side-effects of rimonabant. *Rev Bras Psiquiatr, 31*(2), 145-153.

Morgan, C. J. A., Page, E., Schaefer, C., Chatten, K., Manocha, A., Gulati, S., et al. (2013). Cerebrospinal fluid anandamide levels, cannabis use and psychotic-like symptoms. *The British Journal of Psychiatry, 202*(5), 381-382.

Mule, S., & Casella, G. (1988). Confirmation of marijuana, cocaine, morphine, codeine, amphetamine, methamphetamine, phencyclidine by GC/MS in urine following immunoassay screening. *Journal of Analytical Toxicology, 12*(2), 102-107.

Munro, S., Thomas, K. L., & Abu-Shaar, M. (1993). Molecular characterization of a peripheral receptor for cannabinoids. *Nature, 365*(6441), 61-65.

NFILS. (2014). *Synthetic cannabinoids and synthetic cathinones reported in NFILS, 2010-2013*. Retrieved from: https://www.nflis.deadiversion.usdoj.gov/DesktopModules/ReportDownloads/Reports/NFLIS_SR_CathCan_508.pdf

Notcutt, W., Price, M., Miller, R., Newport, S., Phillips, C., Simmons, S., et al. (2004). Initial experiences with medicinal extracts of cannabis for chronic pain: results from 34 'N of I'studies. *Anaesthesia, 59*(5), 440-452.

O'Shea, M., Singh, M. E., McGregor, I. S., & Mallet, P. E. (2004). Chronic cannabinoid exposure produces lasting memory impairment and increased anxiety in adolescent but not adult rats. *Journal of Psychopharmacology, 18*(4), 502-508.

Onaivi, E. S. (2011). Commentary: Functional neuronal CB_2 cannabinoid receptors in the CNS. *Current Neuropharmacology, 9*(1), 205-208.

Ottani, A., & Giuliani, D. (2001). HU 210: A potent tool for investigations of the cannabinoid system. *CNS drug reviews, 7*(2), 131-145.

Paul, B. D., & Bosy, T. (2015). A sensitive GC-EIMS method for simultaneous detection and quantification of JWH-018 and JWH-073 carboxylic acid and hydroxy metabolites in urine. *Journal of Analytical Toxicology, 39*(3), 172-182.

Pendergraft, W. F., Herlitz, L. C., Thornley-Brown, D., Rosner, M., & Niles, J. L. (2014). Nephrotoxic effects of common and emerging drugs of abuse. *Clinical Journal of the American Society of Nephrology*, doi: 10.2215/CJN.00360114.

Pertwee, R. G. (1988). The central neuropharmacology of psychotropic cannabinoids. *Pharmacology and Therapeutics, 36*(2-3), 189-261.

Pertwee, R. G., & Cascio, M. G. (2014). Known pharmacological actions of Δ^9-tetrahydrocannabinol and four other chemical constituents of cannabis that activate cannabinoid receptors. In R. G. Pertwee (Ed.), *Handbook of Cannabis* (pp. 115-136). Oxford, UK: Oxford University Press.

Power, M. (2014). *Drugs 2.0: The web revolution that's changing how the world gets high*.

Quinn, H. R., Matsumoto, I., Callaghan, P. D., Long, L. E., Arnold, J. C., Gunasekaran, N., et al. (2008). Adolescent rats find repeated Δ^9-THC less aversive than adult rats but display greater residual cognitive deficits and changes in hippocampal protein expression following exposure. *Neuropsychopharmacology, 33*(5), 1113-1126.

Reggio, P. H. (2010). Endocannabinoid binding to the cannabinoid receptors: What is known and what remains unknown. *Current Medicinal Chemistry, 17*(14), 1468-1486.

Reid, M. J., & Bornheim, L. M. (2001). Cannabinoid-induced alterations in brain disposition of drugs of abuse. *Biochemical Pharmacology, 61*(11), 1357-1367.

Renault, P. F., Schuster, C. R., Heinrich, R., & Freeman, D. X. (1971). Marihuana: Standardized smoke administration and dose effect curves on heart rate in humans. *Science, 174*(4009), 589-591.

Rinaldi-Carmona, M., Barth, F., Heaulme, M., Alonso, R., Shire, D., Congy, C., et al. (1995). Biochemical and pharmacological characterisation of SR141716A, the

first potent and selective brain cannabinoid receptor antagonist. *Life Sciences, 56*(23-24), 1941-1947.

Rockwell, C. E., Snider, N. T., Thompson, J. T., Vanden Heuvel, J. P., & Kaminski, N. E. (2006). Interleukin-2 suppression by 2-arachidonyl glycerol is mediated through peroxisome proliferator-activated receptor γ independently of cannabinoid receptors 1 and 2. *Molecular Pharmacology, 70*(1), 101-111.

Ross, R. A., Gibson, T. M., Brockie, H. C., Leslie, M., Pashmi, G., Craib, S. J., et al. (2001). Structure-activity relationship for the endogenous cannabinoid, anandamide, and certain of its analogues at vanilloid receptors in transfected cells and vas deferens. *British Journal of Pharmacology, 132*(3), 631-640.

Russo, E. B. (2007). History of cannabis and its preparations in saga, science, and sobriquet. *Chemistry & Biodiversity, 4*(8), 1614-1648.

Russo, E. B. (2011). Taming THC: Potential cannabis synergy and phytocannabinoid-terpenoid entourage effects. *British Journal of Pharmacology, 163*(7), 1344-1364.

Russo, E. B., Burnett, A., Hall, B., & Parker, K. K. (2005). Agonistic properties of cannabidiol at 5-HT_{1A} receptors. *Neurochemical Research, 30*(8), 1037-1043.

Ryberg, E., Larsson, N., Sjögren, S., Hjorth, S., Hermansson, N. O., Leonova, J., et al. (2007). The orphan receptor GPR55 is a novel cannabinoid receptor. *British Journal of Pharmacology, 152*(7), 1092-1101.

Sam, A. H., Salem, V., & Ghatei, M. A. (2011). Rimonabant: From RIO to ban. *Journal of Obesity*, doi: 10.1155/2011/432607.

Scallet, A. C. (1991). Neurotoxicology of cannabis and THC: A review of chronic exposure studies in animals. *Pharmacology Biochemistry and Behavior, 40*(3), 671-676.

Scheidweiler, K. B., Jarvis, M. J., & Huestis, M. A. (2015). Nontargeted SWATH acquisition for identifying 47 synthetic cannabinoid metabolites in human urine by liquid chromatography-high-resolution tandem mass spectrometry. *Analytical and Bioanalytical Chemistry, 407*(3), 883-897.

Schifano, F., Corazza, O., Deluca, P., Davey, Z., Di Furia, L., Farre', M., et al. (2009). Psychoactive drug or mystical incense? Overview of the online available information on Spice products. *International Journal of Culture and Mental Health, 2*(2), 137-144.

Schneir, A. B., Cullen, J., & Ly, B. T. (2011). “Spice” girls: Synthetic cannabinoid intoxication. *The Journal of emergency medicine, 40*(3), 296-299.

Schwartz, M. D., Trecki, J., Edison, L. A., Steck, A. R., Arnold, J. K., & Gerona, R. R. (2015). A common source outbreak of severe delirium associated with exposure to the novel synthetic cannabinoid ADB-PINACA. *Journal of Emergency Medicine, 48*(5), 573-580.

Seely, K. A., Brents, L. K., Radominska-Pandya, A., Endres, G. W., Keyes, G. S., Moran, J. H., et al. (2012). A major glucuronidated metabolite of JWH-018 is a neutral antagonist at CB1 receptors. *Chemical Research in Toxicology, 25*(4), 825-827.

Seely, K. A., Lapoint, J., Moran, J. H., & Fattore, L. (2012). Spice drugs are more than harmless herbal blends: a review of the pharmacology and toxicology of synthetic cannabinoids. *Progress in Neuro-Psychopharmacology and Biological Psychiatry, 39*(2), 234-243.

Seely, K. A., Prather, P. L., James, L. P., & Moran, J. H. (2011). Marijuana-based drugs: Innovative therapeutics or designer drugs of abuse? *Molecular Interventions, 11*(1), 36.

Sim-Selley, L. J., Schechter, N. S., Rorrer, W. K., Dalton, G. D., Hernandez, J., Martin, B. R., et al. (2006). Prolonged recovery rate of CB_1 receptor adaptation after cessation of long-term cannabinoid administration. *Molecular Pharmacology, 70*(3), 986-996.

Sobolevsky, T., Prasolov, I., & Rodchenkov, G. (2010). Detection of JWH-018 metabolites in smoking mixture post-administration urine. *Forensic Science International, 200*(1), 141-147.

Stella, N., Schweitzer, P., & Piomelli, D. (1997). A second endogenous cannabinoid that modulates long-term potentiation. *Nature, 388*(6644), 773-778.

Stempel, A. V., Stumpf, A., Zhang, H.-Y., Özdoğan, T., Pannasch, U., Theis, A.-K., et al. (2016). Cannabinoid type 2 receptors mediate a cell type-specific plasticity in the hippocampus. *Neuron, 90*(4), 795-809.

Stern, E., & Lambert, D. M. (2007). Medicinal chemistry endeavors around the phytocannabinoids. *Chemistry & Biodiversity, 4*(8), 1707-1728.

Sugiura, T., Kondo, S., Sukagawa, A., Nakane, S., Shinoda, A., Itoh, K., et al. (1995). 2-arachidonoylgylcerol: A possible endogenous cannabinoid receptor ligand in brain. *Biochemical and Biophysical Research Communications, 215*(1), 89-97.

Svizenska, I., Dubovy, P., & Sulcova, A. (2008). Cannabinoid receptors 1 and 2 (CB_1 and CB_2), their distribution, ligands and functional involvement in nervous system structures--a short review. *Pharmacology, Biochemistry and Behavior, 90*(4), 501-511.

Swift, W., Wong, A., Li, K. M., Arnold, J. C., & McGregor, I. S. (2013). Analysis of cannabis seizures in NSW, Australia: Cannabis potency and cannabinoid profile. *PloS One, 8*(7), e70052.

Takayama, T., Suzuki, M., Todoroki, K., Inoue, K., Min, J. Z., Kikura-Hanajiri, R., et al. (2014). UPLC/ESI-MS/MS-based determination of metabolism of several new illicit drugs, ADB-FUBINACA, AB-FUBINACA, AB-PINACA, QUPIC, 5F-QUPIC and α-PVT, by human liver microsome. *Biomedical Chromatography, 28*(6), 831-838.

Tanda, G., Munzar, P., & Goldberg, S. R. (2000). Self-administration behavior is maintained by the psychoactive ingredient of marijuana in squirrel monkeys. *Nature Neuroscience, 3*(11), 1073-1074.

Tanda, G., Pontieri, F. E., & Chiara, G. D. (1997). Cannabinoid and heroin activation of mesolimbic dopamine transmission by a common μ_1 opioid receptor mechanism. *Science, 276*(5321), 2048.

Taura, F., Sirikantaramas, S., Shoyama, Y., Shoyama, Y., & Morimoto, S. (2007). Phytocannabinoids in *Cannabis sativa*: Recent studies on biosynthetic enzymes. *Chemistry & Biodiversity, 4*(8), 1649-1663.

Thomas, B. F., Gilliam, A. F., Burch, D. F., Roche, M. J., & Seltzman, H. H. (1998). Comparative receptor binding analyses of cannabinoid agonists and antagonists. *Journal of Pharmacology and Experimental Therapeutics, 285*(1), 285-292.

Thomas, B. F., Lefever, T. W., Cortes, R. A., Kovach, A. L., Anderson, C. O., Patel, P. R., et al. (2017). Thermolytic degradation of synthetic cannabinoids: Chemical exposures and pharmacological consequences. *Journal of Pharmacology and Experimental Therapeutics, 361*(1), 162-171.

Thomas, B. F., Wiley, J. L., Pollard, G. T., & Grabenauer, M. (2014). Cannabinoid designer drugs: Effects and forensics. *Handbook of cannabis. Oxford University Press, Oxford*, 710-729.

Thomsen, R., Nielsen, L. M., Holm, N. B., Rasmussen, H. B., Linnet, K., & Consortium, T. I. (2014). Synthetic cannabimimetic agents metabolized by carboxylesterases. *Drug Testing and Analysis, 7*(7), 565-576.

Thornton, S. L., Wood, C., Friesen, M. W., & Gerona, R. R. (2013). Synthetic cannabinoid use associated with acute kidney injury. *Clinical Toxicology, 51*(3), 189-190.

Titishov, N., Mechoulam, R., & Zimmerman, A. M. (1989). Stereospecific effects of (–)- and (+)-7-Hydroxy-Δ^6-tetrahydrocannabinol-dimethylheptyl on the immune system of mice. *Pharmacology, 39*(6), 337-349.

Trecki, J., Gerona, R. R., & Schwartz, M. D. (2015). Synthetic cannabinoid–related illnesses and deaths. *New England Journal of Medicine, 373*(2), 103-107.

Tsou, K., Brown, S., Sanudo-Pena, M. C., Mackie, K., & Walker, J. M. (1998). Immunohistochemical distribution of cannabinoid CB_1 receptors in the rat central nervous system. *Neuroscience, 83*(2), 393-411.

Uchiyama, N., Matsuda, S., Wakana, D., Kikura-Hanajiri, R., & Goda, Y. (2013). New cannabimimetic indazole derivatives, N-(1-amino-3-methyl-1-oxobutan-2-yl)-1-pentyl-1H-indazole-3-carboxamide (AB-PINACA) and N-(1-amino-3-methyl-1-oxobutan-2-yl)-1-(4-fluorobenzyl)-1H-indazole-3-carboxamide (AB-FUBINACA) identified as designer drugs in illegal products. *Forensic Toxicology, 31*(1), 93-100.

Vandrey, R., Dunn, K. E., Fry, J. A., & Girling, E. R. (2012). A survey study to characterize use of Spice products (synthetic cannabinoids). *Drug and Alcohol Dependence, 120*(1), 238-241.

Vann, R. E., Gamage, T. F., Warner, J. A., Marshall, E. M., Taylor, N. L., Martin, B. R., et al. (2008). Divergent effects of cannabidiol on the discriminative stimulus and place conditioning effects of Δ^9-tetrahydrocannabinol. *Drug and Alcohol Dependence, 94*(1), 191-198.

Volkow, N. D., Baler, R. D., Compton, W. M., & Weiss, S. R. B. (2014). Adverse health effects of marijuana use. *New England Journal of Medicine, 370*(23), 2219-2227.

Wachtel, S., ElSohly, M., Ross, S., Ambre, J., & de Wit, H. (2002). Comparison of the subjective effects of Δ9-tetrahydrocannabinol and marijuana in humans. *Psychopharmacology, 161*(4), 331-339.

Watanabe, K., Kijima, T., Narimatsu, S., Nishikami, J., Yamamoto, I., & Yoshimura, H. (1990). Comparison of pharmacological effects of tetrahydrocannabinols and their 11-hydroxy-metabolites in mice. *Chemical & Pharmaceutical Bulletin, 38*(8), 2317-2319.

Watanabe, K., Yamaori, S., Funahashi, T., Kimura, T., & Yamamoto, I. (2007). Cytochrome P450 enzymes involved in the metabolism of tetrahydrocannabinols and cannabinol by human hepatic microsomes. *Life Sciences, 80*(15), 1415-1419.

Weiss, J. L., Watanabe, A. M., Lemberger, L., Tamarkin, N. R., & Cardon, P. V. (1972). Cardiovascular effects of Δ^9-tetrahydrocannabinol in man. *Clinical Pharmacology and Therapeutics, 13*(5), 671-684.

Weissman, A., Milne, G. M., & Melvin, L. (1982). Cannabimimetic activity from CP-47,497, a derivative of 3-phenylcyclohexanol. *Journal of Pharmacology and Experimental Therapeutics, 223*(2), 516-523.

Westlake, T., Howlett, A., Bonner, T., Matsuda, L., & Herkenham, M. (1994). Cannabinoid receptor binding and messenger RNA expression in human brain: An in vitro receptor autoradiography and in situ hybridization histochemistry study of normal aged and Alzheimer's brains. *Neuroscience, 63*(3), 637-652.

Wiley, J. L., Marusich, J. A., Lefever, T. W., Antonazzo, K. R., Wallgren, M. T., Cortes, R. A., et al. (2015). AB-CHMINACA, AB-PINACA, and FUBIMINA: Affinity and potency of novel synthetic cannabinoids in producing Δ^9-tetrahydrocannabinol-like effects in mice. *Journal of Pharmacology and Experimental Therapeutics, 354*(3), 328-339.

Wiley, J. L., Marusich, J. A., Lefever, T. W., Grabenauer, M., Moore, K. N., & Thomas, B. F. (2013). Cannabinoids in disguise: Δ^9-tetrahydrocannabinol-like effects of tetramethylcyclopropyl ketone indoles. *Neuropharmacology, 75*, 145-154.

Wiley, J. L., Marusich, J. A., Martin, B. R., & Huffman, J. W. (2012). 1-Pentyl-3-phenylacetylindoles and JWH-018 share in vivo cannabinoid profiles in mice. *Drug and Alcohol Dependence, 123*(1-3), 148-153.

Wiley, J. L., O'Connell, M. M., Tokarz, M. E., & Wright, M. J. (2007). Pharmacological effects of acute and repeated administration of Δ^9-tetrahydrocannabinol in adolescent and adult rats. *Journal of Pharmacology and Experimental Therapeutics, 320*(3), 1097-1105.

Wilson, R. I., & Nicoll, R. A. (2001). Endogenous cannabinoids mediate retrograde signalling at hippocampal synapses. *Nature, 410*(6828), 588-592.

Winstock, A. R., & Barratt, M. J. (2013). Synthetic cannabis: A comparison of patterns of use and effect profile with natural cannabis in a large global sample. *Drug and Alcohol Dependence, 131*, 106-111.

Witkin, J. M., Tzavara, E. T., & Nomikos, G. G. (2005). A role for cannabinoid CB_1 receptors in mood and anxiety disorders. *Behavioural Pharmacology, 16*(5-6), 315-331.

Wohlfarth, A., Gandhi, A. S., Pang, S., Zhu, M., Scheidweiler, K. B., & Huestis, M. A. (2014). Metabolism of synthetic cannabinoids PB-22 and its 5-fluoro analog, 5F-PB-22, by human hepatocyte incubation and high-resolution mass spectrometry. *Analytical and Bioanalytical Chemistry, 406*(6), 1763-1780.

Wollner, H. J., Matchett, J. R., Levine, J., & Loewe, S. (1942). Isolation of a physiologically active tetrahydrocannabinol from *Cannabis sativa* resin. *Journal of the American Chemical Society, 64*(1), 26-29.

Young, A. C., Schwarz, E., Medina, G., Obafemi, A., Feng, S.-Y., Kane, C., et al. (2012). Cardiotoxicity associated with the synthetic cannabinoid, K9, with laboratory confirmation. *The American Journal of Emergency Medicine, 30*(7), 1320.e1325-1320.e1327.

Zhang, M., Martin, B. R., Adler, M. W., Razdan, R. K., Jallo, J. I., & Tuma, R. F. (2007). Cannabinoid CB_2 receptor activation decreases cerebral infarction in a mouse focal ischemia/reperfusion model. *Journal of Cerebral Blood Flow and Metabolism, 27*(7), 1387-1396.

Zimmer, A., Zimmer, A. M., Hohmann, A. G., Herkenham, M., & Bonner, T. I. (1999). Increased mortality, hypoactivity, and hypoalgesia in cannabinoid CB_1 receptor knockout mice. *Proceedings of the National Academy of Sciences of the United States of America, 96*(10), 5780-5785.

Zimmermann, U. S., Winkelmann, P. R., Pilhatsch, M., Nees, J. A., Spanagel, R., & Schulz, K. (2009). Withdrawal phenomena and dependence syndrome after the consumption of "spice gold". *Deutsches Ärzteblatt International, 106*(27), 464-467.

Zuardi, A. W. (2006). History of cannabis as a medicine: A review. *Revista Brasileira de Psiquiatria, 28*, 153-157.

Zuardi, A. W., Crippa, J. A., Hallak, J. E., Bhattacharyya, S., Atakan, Z., Martin-Santos, R., et al. (2012). A critical review of the antipsychotic effects of cannabidiol: 30 years of a translational investigation. *Current Pharmaceutical Design, 18*(32), 5131-5140.

Zuardi, A. W., Finkelfarb, E., Bueno, O. F., Musty, R. E., & Karniol, I. G. (1981). Characteristics of the stimulus produced by the mixture of cannabidiol with Δ^9-tetrahydrocannabinol. *Archives internationales de pharmacodynamie et de therapie, 249*(1), 137-146.

Zuardi, A. W., Shirakawa, I., Finkelfarb, E., & Karniol, I. G. (1982). Action of cannabidiol on the anxiety and other effects produced by Δ^9-THC in normal subjects. *Psychopharmacology, 76*(3), 245-250.

Chapter 2. Physiological effects of synthetic cannabinoids as measured by biotelemetry

NOTE: The supporting information referred to by the publications in this chapter can be found in Appendix 1

ACS Chemical Neuroscience
Research Article
pubs.acs.org/chemneuro

Effects of Bioisosteric Fluorine in Synthetic Cannabinoid Designer Drugs JWH-018, AM-2201, UR-144, XLR-11, PB-22, 5F-PB-22, APICA, and STS-135

Samuel D. Banister,[†,‡] Jordyn Stuart,[§] Richard C. Kevin,[∥] Amelia Edington,[§] Mitchell Longworth,[‡] Shane M. Wilkinson,[‡] Corinne Beinat,[†,‡] Alexandra S. Buchanan,[⊥,#] David E. Hibbs,[▽] Michelle Glass,[¶] Mark Connor,[§] Iain S. McGregor,[∥] and Michael Kassiou*[,‡,◆]

[†]Department of Radiology, Stanford University School of Medicine, Stanford, California 94305, United States
[‡]School of Chemistry, The University of Sydney, Sydney, New South Wales 2006, Australia
[§]Faculty of Medicine and Health Sciences, Macquarie University, Sydney, New South Wales 2109, Australia
[∥]School of Psychology, The University of Sydney, Sydney, New South Wales 2006, Australia
[⊥]Center for Immersive and Simulation-based Learning, Stanford University School of Medicine, Stanford, California 94305, United States
[#]Department of Anaesthesia, Prince of Wales Hospital, Randwick, New South Wales 2031, Australia
[▽]Faculty of Pharmacy, The University of Sydney, Sydney, New South Wales 2006, Australia
[¶]School of Medical Sciences, The University of Auckland, Auckland 1142, New Zealand
[◆]Discipline of Medical Radiation Sciences, The University of Sydney, Sydney, New South Wales 2006, Australia

Supporting Information

ABSTRACT: Synthetic cannabinoid (SC) designer drugs featuring bioisosteric fluorine substitution are identified by forensic chemists and toxicologists with increasing frequency. Although terminal fluorination of *N*-pentyl indole SCs is sometimes known to improve cannabinoid type 1 (CB_1) receptor binding affinity, little is known of the effects of fluorination on functional activity of SCs. This study explores the *in vitro* functional activities of SC designer drugs JWH-018, UR-144, PB-22, and APICA, and their respective terminally fluorinated analogues AM-2201, XLR-11, 5F-PB-22, and STS-135 at human CB_1 and CB_2 receptors using a FLIPR membrane potential assay. All compounds demonstrated agonist activity at CB_1 (EC_{50} = 2.8−1959 nM) and CB_2 (EC_{50} = 6.5−206 nM) receptors, with the fluorinated analogues generally showing increased CB_1 receptor potency (~2−5 times). Additionally, the cannabimimetic activities and relative potencies of JWH-018, AM-2201, UR-144, XLR-11, PB-22, 5F-PB-22, APICA, and STS-135 *in vivo* were evaluated in rats using biotelemetry. All SCs dose-dependently induced hypothermia and reduced heart rate at doses of 0.3−10 mg/kg. There was no consistent trend for increased potency of fluorinated SCs over the corresponding des-fluoro SCs *in vivo*. Based on magnitude and duration of hypothermia, the SCs were ranked for potency (PB-22 > 5F-PB-22 = JWH-018 > AM-2201 > APICA = STS-135 = XLR-11 > UR-144).

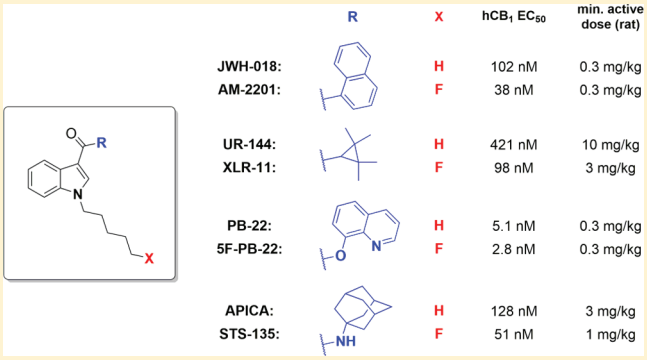

KEYWORDS: *Cannabinoid, THC, JWH-018, AM-2201, XLR-11, PB-22*

Synthetic cannabinoids (SCs) are the most rapidly growing class of recreational "designer drugs". The European Monitoring Centre for Drugs and Drug Addiction (EMCDDA) reports that, as of March 2015, 134 new SCs have been identified in the European Union (EU) since 2008, with 30 novel SCs formally notified in 2014 alone.[1] In the United States (US) in 2010, the Drug Enforcement Administration's National Forensic Laboratory Information System (NFLIS) reported 19 distinct SCs across 3286 samples, but by 2012, there were 61 SC variants identified in 41 458 cases.[2] In the EU in 2013, there were over 21 000 seizures of SCs, a more than 200-fold increase since 2008.[1] Many SCs have no precedent in the scientific literature yet bear hallmarks of rational design.

Like Δ^9-tetrahydrocannabinol (Δ^9-THC, **1**; Figure 1), the principal bioactive component of cannabis, SCs typically exert agonist activity at both cannabinoid receptor subtypes, namely,

Received: April 2, 2015
Accepted: April 28, 2015
Published: April 28, 2015

DOI: 10.1021/acschemneuro.5b00107
ACS Chem. Neurosci. 2015, 6, 1445−1458

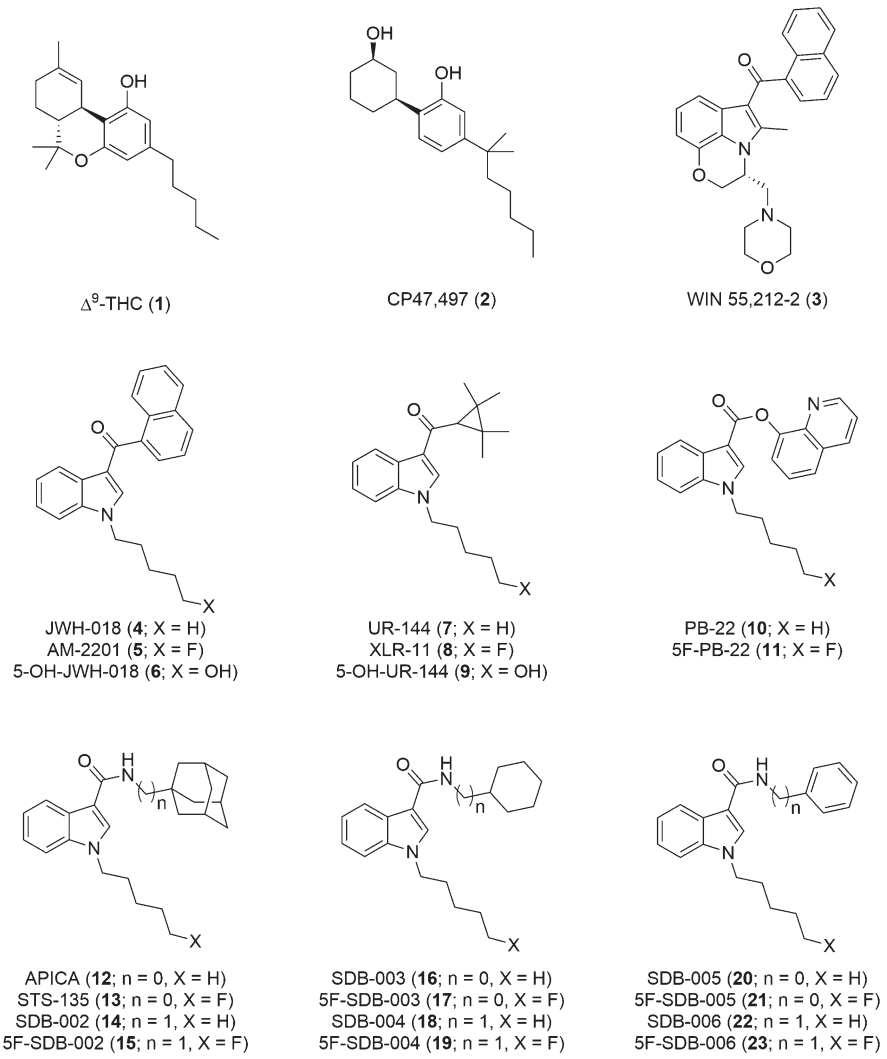

Figure 1. Selected natural and synthetic cannabinoids.

CB_1 and CB_2 receptors, with psychoactivity attributed to activation of the former.[3] Generally, SCs are found as adulterants in smoking mixtures of otherwise nonpsychoactive herbal blends and are intended to substitute for the intoxicating effects of Δ^9-THC. Although these products are disingenuously marketed as incense and labeled "not for human consumption", consumers are aware of the psychoactivity of such products and use them as technically legal cannabis substitutes. One of the earliest SC products, branded "Spice", was analyzed in 2008 and found to contain the C8-homologue of CP 47,497 (CP 47,497-C8, **2**) and an (aminoalkyl)indole analogue of WIN 55,212-2 (**3**)[4] known as JWH-018 (**4**), thereby accounting for the anecdotal cannabimimetic effects of this product.[5] After the active ingredients of Spice were identified, many governments prohibited CP 47,497-C8 and JWH-018, forcing manufacturers of Spice to circumvent restriction by substituting the active constituents with other unregulated SCs. The iterative cycle of SC identification, prohibition, and substitution has produced hundreds of differently branded products, with names like "Kronic", and "K2", containing one or more SCs.

A popular design trend in the SC market currently is the incorporation of a terminal fluorine atom in variously substituted *N*-pentylindoles.[6] The terminally fluorinated analogue of JWH-018, AM-2201 (**5**), was one of several nanomolar affinity SCs (CB_1 K_i = 1.0 nM; CB_2 K_i = 2.6 nM) reported by Makriyannis and colleagues in 2001,[7] and was identified in consumer products by forensic researchers in several countries in 2011.[8,9] Anecdotal reports that AM-2201 possesses psychoactivity at submilligram doses in humans likely instigated the trend of bioisosteric fluorine substitution in other structurally related SC designer drugs. For example, South Korea's National Forensic Service reported no fluorinated SCs in 2010, but 90% of all seized SCs were fluorinated by 2013.[10] Several dozen terminally fluorinated SCs have been reported by forensic laboratories worldwide, and the rate of emergence appears to be increasing.[6]

The SC sold as UR-144 (**7**, CB_1 K_i = 150 nM; CB_2 K_i = 1.8 nM) was first reported by Abbott Laboratories in 2010 during their exploration of CB_2-selective ligands[11,12] and has since been identified in numerous forensic samples.[9,13−15] The 5-fluoro analogue of UR-144, sold as XLR-11 (**8**), has also been identified in consumer products, despite no prior reports of its structure in the scientific literature.[16−19] In Korea, XLR-11 first appeared in 2012 and was the most frequently encountered SC by 2013.[10] XLR-11 use is associated with adverse health effects, including acute kidney injury (AKI)[20,21] and cerebral ischemia.[22] Wiley and colleagues recently showed that XLR-11 (CB_1 K_i = 24 nM; CB_2 K_i = 2.1 nM) has binding affinities

DOI: 10.1021/acschemneuro.5b00107
ACS Chem. Neurosci. 2015, 6, 1445−1458

Scheme 1. Synthesis of Synthetic Cannabinoids 7−23[a]

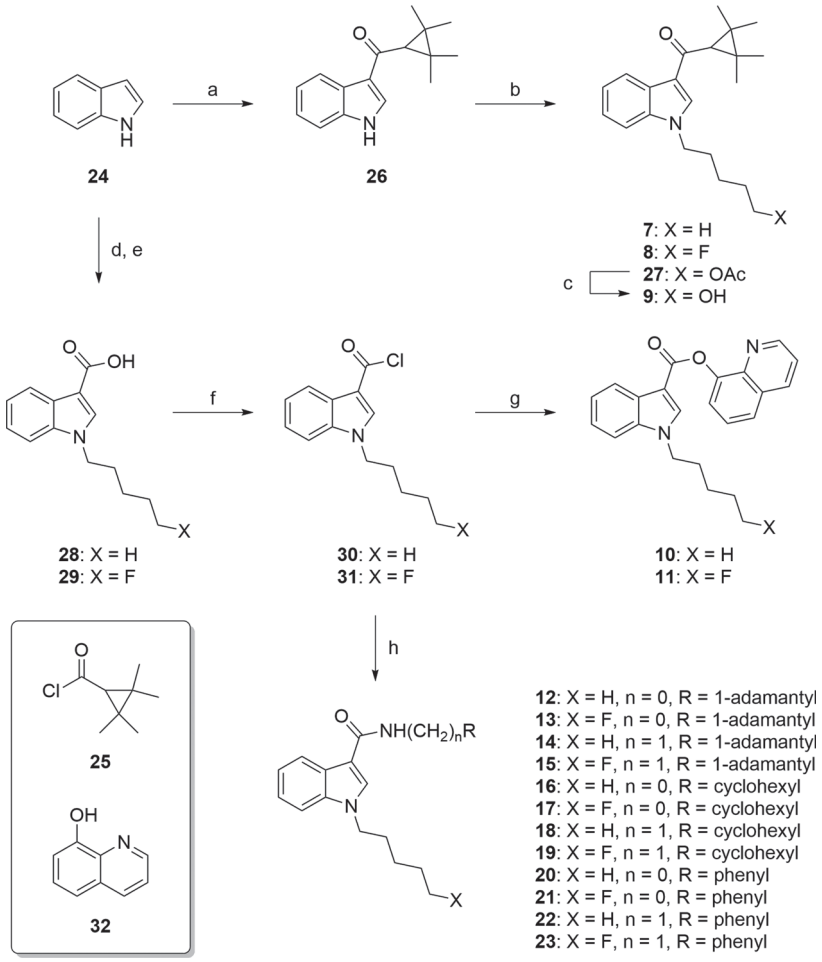

[a]Reagents and conditions: (a) **25**, Me_2AlCl, CH_2Cl_2, 0 °C to rt, 3 h, 82%; (b) NaH, $Br(CH_2)_4X$, DMF, 0 °C to rt, 1 h, 67−91%; (c) aq. NaOH, MeOH,-THF, rt, 16 h, 94%; (d) NaH (2.0 equiv), $Br(CH_2)_4X$, DMF, 0 °C to rt, then $(CF_3CO)_2O$, 0 °Cto rt, 1 h; (e) KOH, MeOH, PhMe, reflux, 2 h, 79−88% (over 2 steps); (f) $(COCl)_2$, DMF (cat.), CH_2Cl_2, rt, 1 h, quant.; (g) **32**, Et_3N, CH_2Cl_2, rt, 24 h, 78−86%; (h) $R(CH_2)_nNH_2$, Et_3N, CH_2Cl_2, rt, 14 h, 73−90%.

and functional activities at cannabinoid receptors that are comparable to UR-144 (CB_1 K_i = 29 nM; CB_2 K_i = 4.5 nM) and that both compounds show a preference for CB_2 receptors.[23] UR-144 and XLR-11 also showed similar cannabimimetic potencies, greater than Δ^9-THC, in mice.[23]

The indole-3-carboxylate derivative PB-22 (QUPIC, **10**) and its 5-fluoropentyl analogue, 5F-PB-22 (**11**), were similarly unprecedented when discovered by forensic scientists in 2013.[24−26] Like AM-2201,[27] PB-22 and 5F-PB-22 were implicated in clinical reports of seizure,[28,29] and the latter was detected in several fatal intoxications in the USA.[30] The metabolism of PB-22 and 5F-PB-22 has been investigated, but little else is known about the effects of these SCs.[31−33] The adamantane-derived indole-3-carboxamide APICA (2NE1, SDB-001, **12**) was also unprecedented when discovered in SC products,[34] and 5-fluoro-APICA (sold as STS-135, **13**) was identified shortly thereafter.[26] The phase I metabolism of APICA and STS-135 was recently published,[35] and the pharmacology of APICA was explored (CB_1 IC_{50} = 175 nM; CB_2 IC_{50} = 176 nM),[17,36] but like PB-22 and 5F-PB-22, there are no scientific reports regarding the activity of STS-135.

The increasing popularity of *N*-(5-fluoropentyl)indole SCs is concerning because of the limited information regarding their pharmacology and toxicity, as well as those of their metabolites. Oxidation of JWH-018 produces several bioactive hydroxylated metabolites, some of which exhibit cannabinoid activity as potent as the parent compound, raising concerns about their toxicity and ultimate fate in the human body.[37−40] Many terminally fluorinated *N*-pentylindole SCs undergo thermolytic defluorination due to the route of administration (smoking), as well as metabolic oxidative defluorination *in vivo*.[33,41−44] For example, the 5-hydroxylated metabolite **6** is common to both JWH-018 and AM-2201.[9,38,43,45] Similarly, UR-144 and XLR-11 share a common 5-hydroxylated metabolite (**9**).[9,42] There is also justifiable concern regarding the fate of N-dealkylated metabolites of fluorinated SCs, given their potential for metabolism to toxic fluorinated metabolites like fluoroacetic acid.

RESULTS AND DISCUSSION

The aim of the present study was to address the paucity of data in the scientific literature regarding the pharmacology of fluorinated SCs. To this end, JWH-018, UR-144, PB-22, and APICA were compared to the corresponding 5-fluoropentyl analogues AM-2201, XLR-11, 5F-PB-22, and STS-135, respectively. The cannabinoid activity of 5-OH-UR-144, a

DOI: 10.1021/acschemneuro.5b00107
ACS Chem. Neurosci. 2015, 6, 1445−1458

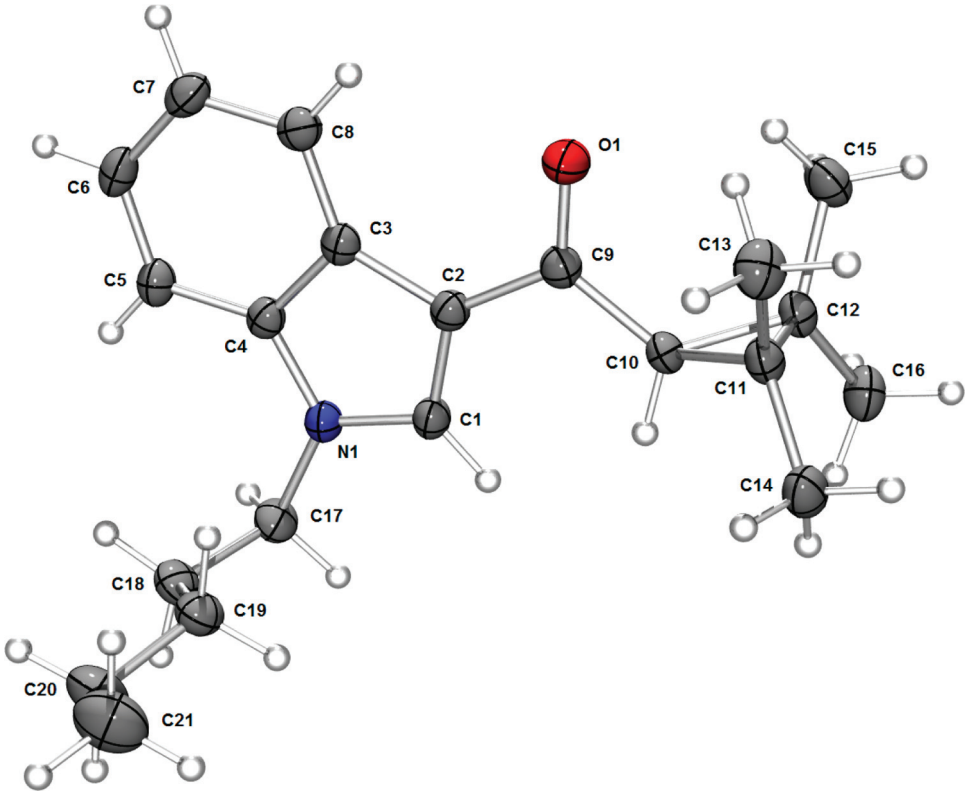

Figure 2. ORTEP diagram of the crystal structure of UR-144 (**7**) with thermal ellipsoids at the 50% probability level.

Table 1. Functional Activity of Δ^9-THC and Indole SCs 4, 5, and 7−23 at CB_1 and CB_2 Receptors

	hCB$_1$		hCB$_2$		
compound	pEC$_{50}$ ± SEM (EC$_{50}$, nM)	max ± SEM (% WIN 55,212-2)	pEC$_{50}$ ± SEM (EC$_{50}$, nM)	max ± SEM (% WIN 55,212-2)	CB$_1$ selectivity[a]
1 (Δ^9-THC)	6.60 ± 0.11 (250)	51 ± 3	5.94 ± 0.57 (1157)	13 (at 10 μM)	4.6
3 (WIN 55,212-2)	6.55 ± 0.06 (284)		7.21 ± 0.09 (62)		0.2
4 (JWH-018)	6.99 ± 0.09 (102)	107 ± 6	6.88 ± 0.06 (133)	95 ± 5	1.3
5 (AM-2201)	7.43 ± 0.09 (38)	111 ± 6	7.23 ± 0.10 (58)	102 ± 7	1.5
7 (UR-144)	6.38 ± 0.06 (421)	94 ± 4	7.15 ± 0.05 (72)	104 ± 3	0.2
8 (XLR-11)	7.01 ± 0.07 (98)	110 ± 4	7.08 ± 0.15 (83)	117 ± 10	0.8
9 (5-OH-UR-144)	5.71 ± 0.12 (1959)	159 ± 11	8.18 ± 0.11 (6.5)	102 ± 5	0.003
10 (PB-22)	8.30 ± 0.06 (5.1)	114 ± 3	7.43 ± 0.08 (37)	101 ± 5	7.3
11 (5F-PB-22)	8.55 ± 0.10 (2.8)	108 ± 5	7.97 ± 0.07 (11)	101 ± 3	3.9
12 (APICA)	6.89 ± 0.11 (128)	100 ± 6	7.54 ± 0.11 (29)	91 ± 5	0.2
13 (STS-135)	7.29 ± 0.12 (51)	123 ± 8	7.88 ± 0.26 (13)	114 ± 13	0.3
14 (SDB-002)	6.58 ± 0.08 (264)	53 ± 3	7.24 ± 0.26 (57)	23 ± 4	0.2
15 (5F-SDB-002)	6.56 ± 0.16 (273)	87 ± 8	6.69 ± 0.12 (206)	39 ± 3	0.8
16 (SDB-003)	6.78 ± 0.06 (166)	82 ± 3	6.99 ± 0.08 (102)	95 ± 5	0.6
17 (5F-SDB-003)	7.13 ± 0.12 (75)	104 ± 7	7.53 ± 0.06 (29)	84 ± 3	0.4
18 (SDB-004)	6.68 ± 0.05 (207)	104 ± 3	6.67 ± 0.09 (216)	71 ± 5	1.0
19 (5F-SDB-004)	7.39 ± 0.06 (41)	107 ± 4	7.20 ± 0.12 (63)	62 ± 4	1.5
20 (SDB-005)	6.94 ± 0.07 (116)	99 ± 4	6.86 ± 0.12 (140)	74 ± 6	1.2
21 (5F-SDB-005)	6.83 ± 0.13 (148)	92 ± 7	6.87 ± 0.09 (136)	69 ± 4	0.9
22, SDB-006)	6.94 ± 0.09 (115)	96 ± 5	6.88 ± 0.22 (134)	68 ± 9	1.2
23, 5F-SDB-006	7.30 ± 0.09 (50)	87 ± 4	6.91 ± 0.11 (123)	61 ± 4	2.5

[a]CB_1 selectivity expressed as CB_2 EC_{50} divided by CB_1 EC_{50}.

common metabolite of UR-144 and XLR-11, was also assessed. To more fully examine the effects of terminal fluorination on the cannabinoid activity of SCs, the 5-fluoropentyl congeners of previously described APICA analogues SDB-002 (**14**), -003 (**16**), -004 (**18**), -005 (**20**), and -006 (**22**) were also synthesized and subjected to pharmacological evaluation. Although there are no literature reports of the identification of 5F-SDB-002 (**15**), -003 (**17**), -004 (**19**), or -005 (**21**), both SDB-006 and 5F-SDB-006 (**23**) were recently identified in Finland.[46]

DOI: 10.1021/acschemneuro.5b00107
ACS Chem. Neurosci. 2015, 6, 1445−1458

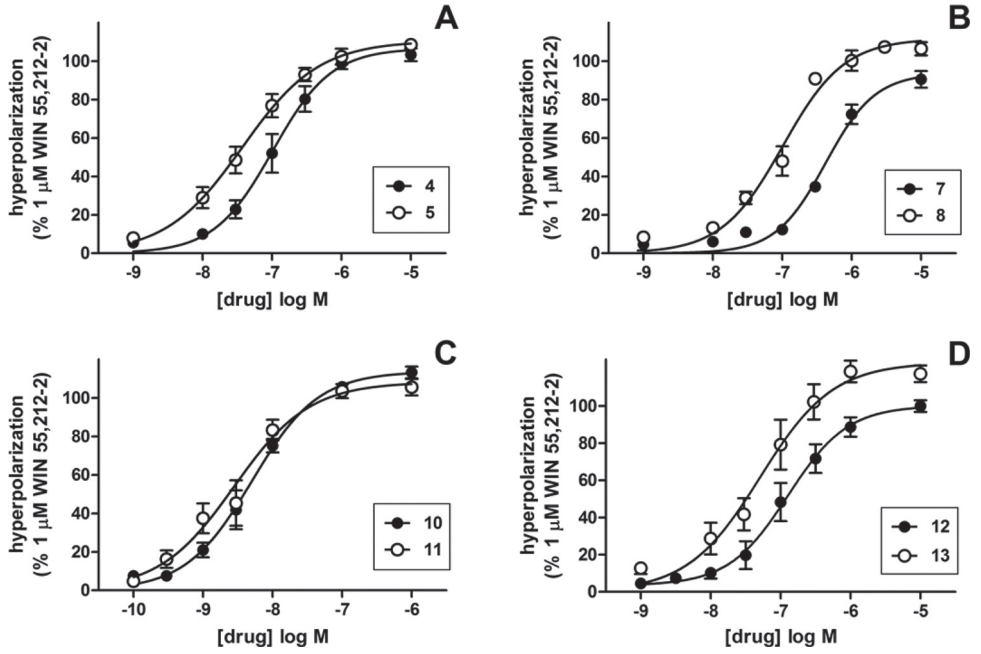

Figure 3. Hyperpolarization of CB_1 receptors induced by (A) JWH-018 (**4**) and AM-2201 (**5**), (B) UR-144 (**7**) and XLR-11 (**8**), (C) PB-22 (**10**) and 5F-PB-22 (**11**), and (D) APICA (**12**) and STS-135 (**13**) as a proportion of that produced by 1 μM WIN 55,212-2. Membrane potential was measured using a fluorescent dye, as outlined in the Methods. Each point represents the mean ± SEM of at least five independent determinations, each performed in duplicate. Data was fitted with a four parameter logistic equation in Graphpad Prism.

JWH-018 and AM-2201 were purchased from the National Measurement Institute (NMI), Australia. The synthesis of **7** to **23** is shown in Scheme 1. The synthesis of **7**−**9** started from indole (**24**), which was acylated with 2,2,3,3-tetramethylcyclopropyl-1-carbonyl chloride (**25**, freshly prepared from the corresponding carboxylic acid) under Okauchi conditions[47] to give **26** in 82% yield. Alkylation of **26** with 1-bromopentane or 1-bromo-5-fluoropentane gave **7** or **8**, respectively. Attempts to reverse the order of operations by performing the alkylation and then acylation were successful for the preparation of **7** but not **8**, due to incompatibility of the fluoroalkyl group with Lewis acids. Alkylation of **26** with the 5-bromopentyl acetate under the same conditions gave **27**, and saponification of the ester cleanly furnished **9**.

The synthesis of PB-22 and 5F-PB-22 started from indole, which was alkylated with either 1-bromopentane or 5-fluoro-1-bromopentane in the presence of excess sodium hydride and treated with trifluoroacetic anhydride to generate the intermediate N-alkylated 3-(trifluoroacetyl)indole in one pot, the hydrolysis of which provided either carboxylic acid **28** or **29**, respectively. Treating **28** or **29** with oxalyl chloride gave acid chlorides **30** and **31**, respectively, each of which was treated with 8-hydroxyquinoline (**32**) to yield esters **10** and **11**. Alternative, treating **30** and **31** with the appropriate amines gave the desired carboxamides **12**−**23** in yields of 73−90%.

Several of these novel SCs formed large prismatic crystals during recrystallization, especially the 2,2,3,3-tetramethylcyclopropanone derivatives **7** and **8**. A single crystal of **7** was obtained by slow evaporation of an isopropanol−water mixture, and an X-ray crystal structure was obtained. An ORTEP diagram of the crystal structure of **7** is shown in Figure 2. All bond lengths and angles were as expected, with the pentyl chain in a fully extended conformation. Full details of X-ray data collection and tables of bond lengths and angles are available in the Supporting Information.

All synthesized SCs were screened against CB_1 and CB_2 receptors in a fluorometric imaging plate reader (FLIPR) membrane potential assay to provide basic structure−activity relationships for agonist activity at each CB receptor subtype (see Table S8 of the Supporting Information for comparisons to available binding affinity data). Additionally, selected fluoro/des-fluoro-SC pairs were evaluated *in vivo* to allow direct comparison of the relative potency of JWH-018, AM-2201, UR-144, XLR-11, PB-22, 5F-PB-22, APICA, and STS-135.

The cannabimimetic activity of indoles **4**, **5**, and **7**−**23** at CB_1 and CB_2 receptors was compared with the activity of established agonist Δ^9-THC, and the results are shown in Table 1. Mouse AtT20 neuroblastoma cells were stably transfected with human CB_1 or CB_2 receptors, and activities of Δ^9-THC and **7**−**23** were evaluated using a FLIPR membrane potential assay whereby endogenously expressed G protein-gated inwardly rectifying K^+ channels (GIRKs) are activated by agonists at the coexpressed CB_1 or CB_2 receptors.[48,49] The maximum effects of **4**, **5**, and **7**−**23** were compared with the high efficacy CB_1/CB_2 receptor full agonist WIN 55,212-2, which produced a maximal decrease in fluorescence, corresponding to cellular hyperpolarization, of 29% ± 2% in AtT20-CB_1 cells and 31% ± 3% in AtT20-CB_2 cells. None of the compounds produced a significant change in the membrane potential of wild-type AtT-20 cells, which do not express CB1 or CB2 receptors.

All SCs activated CB_1 and CB_2 receptors and, with few exceptions, did so with greater potency than Δ^9-THC (250 nM) for CB_1 receptor-mediated activation of GIRK (Table 1). The psychoactivity of cannabinoid ligands is largely attributed to activation of the CB_1 receptor,[3] focusing our attention to structure−activity relationships (SAR) for this series of SCs around the CB_1 receptor-mediated activation of GIRK. Δ^9-THC is a low efficacy CB_2 agonist, and in the assay of GIRK activation in AtT20-CB_2, its effects at 10 μM were only 13% of

DOI: 10.1021/acschemneuro.5b00107
ACS Chem. Neurosci. 2015, 6, 1445−1458

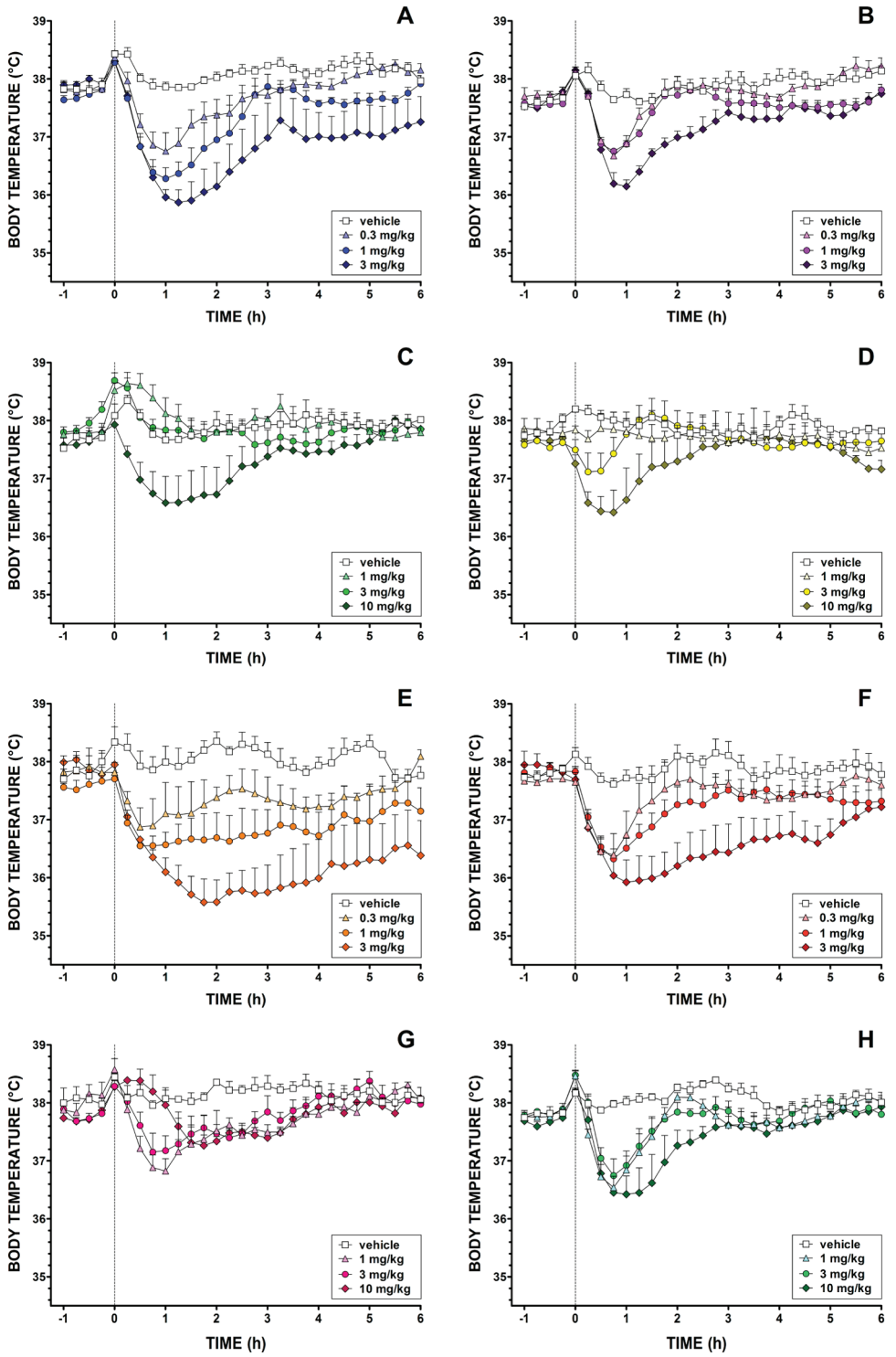

Figure 4. Effects of (A) JWH-018, (B) AM-2201, (C) UR-144, (D) XLR-11, (E) PB-22, (F) 5F-PB-22, (G) APICA, and (H) STS-135 on rat body temperature. Dashed line denotes time of intraperitoneal injection. Each point represents the mean ± SEM for three animals.

CB_1/CB_2 agonist WIN 55,212-2. WIN 55,212-2 showed an approximately 4-fold preference for stimulating a cellular hyperpolarization in AtT-20-CB2 compared with AtT-20-CB1 cells.

The most potent compounds in the series were PB-22 (CB_1 EC_{50} = 5.1 nM; CB_2 EC_{50} = 37 nM) and 5F-PB-22 (CB_1 EC_{50} = 2.8 nM; CB_2 EC_{50} = 11 nM), both possessing nanomolar potency at CB_1 receptors. PB-22 and 5F-PB-22 were an order of magnitude more potent at CB_1 receptors than the next most potent SCs AM-2201 (CB_1 EC_{50} = 38 nM), STS-135 (CB_1 EC_{50} = 51 nM), 5F-SDB-004 (CB_1 EC_{50} = 41 nM), and 5F-SDB-006 (CB_1 EC_{50} = 50 nM). Most SCs in the series demonstrated little selectivity for either CB receptor subtype, with the exception of 5-OH-UR-144, a UR-144 metabolite, which was a potent and selective CB_2 receptor agonist (EC_{50} = 6.5 nM, 300-fold selectivity).

Excluding two des-fluoro/fluoro analogue pairs (**14**/**15** and **20**/**21**), for which there was little change, terminal fluorination

DOI: 10.1021/acschemneuro.5b00107
ACS Chem. Neurosci. 2015, 6, 1445−1458

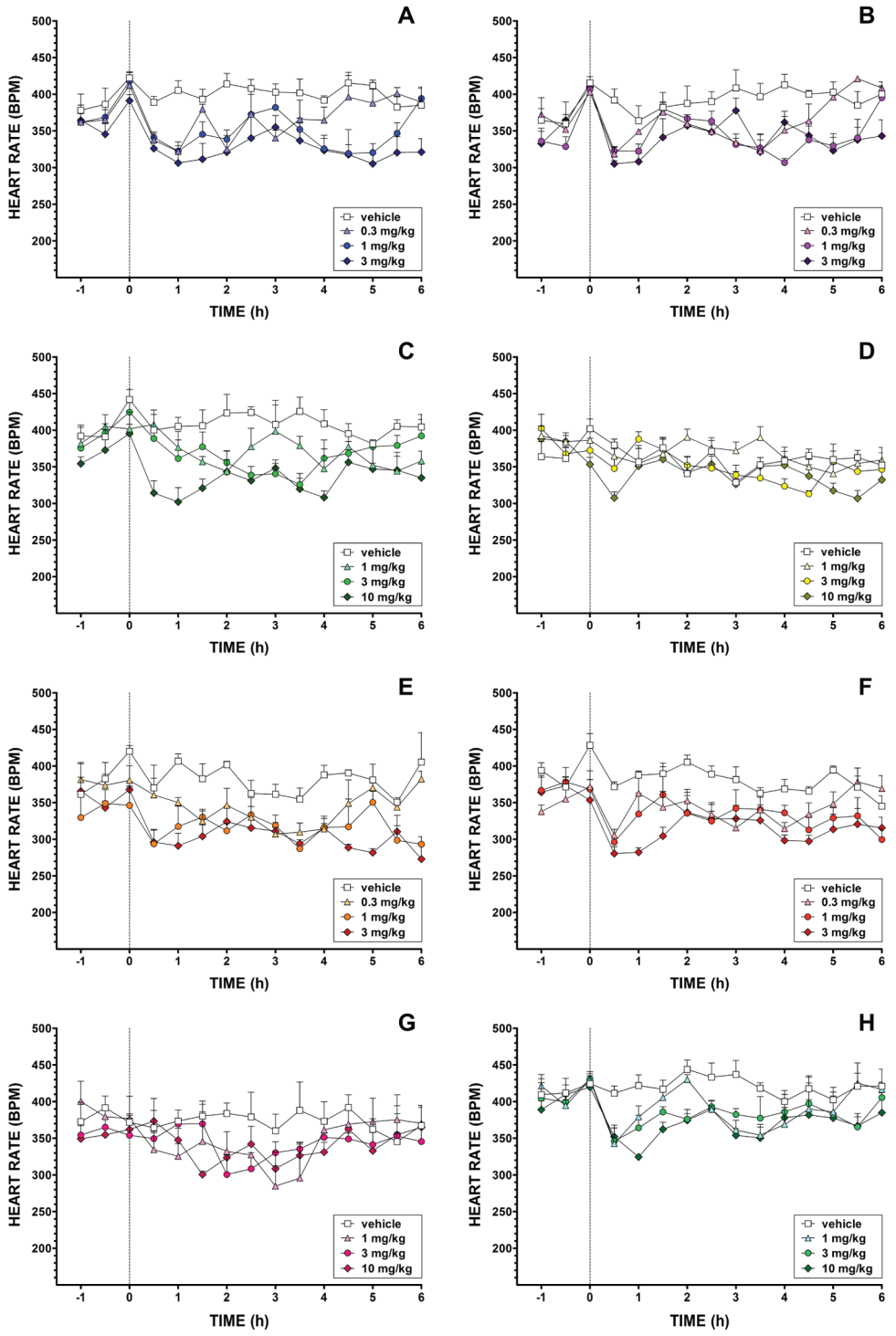

Figure 5. Effects of (A) JWH-018, (B) AM-2201, (C) UR-144, (D) XLR-11, (E) PB-22, (F) 5F-PB-22, (G) APICA, and (H) STS-135 on rat heart rate. Dashed line denotes time of intraperitoneal injection. Each point represents the mean ± SEM for three animals.

produced a roughly 2−5-fold increase in CB_1 receptor potency. This was most pronounced moving from UR-144 (EC_{50} = 421 nM) to XLR-11 (EC_{50} = 98 nM) and from **18** (EC_{50} = 207 nM) to **19** (EC_{50} = 41 nM). Interestingly, **14** possessed the lowest efficacy at CB_1 and CB_2 receptors in the series, and while fluorination to give **15** did not improve potency, it did increase efficacy at CB_1 and CB_2 receptors. The relative potency change for des-fluoro/fluoro pairs JWH-018/AM-2201, UR-144/XLR-11, PB-22/5F-PB-22, and APICA/STS-135 is depicted in Figure 3.

Our results with UR-144, XLR-11, and common metabolite 5-OH-UR-144 are broadly consistent with previous studies. In an assay of GTPγS binding in HEK 293 cell membranes, Wiley and colleagues found that UR-144 showed a preference for CB_1, in contrast to our findings of a CB_2 preference for UR-144.[23] Wiley and colleagues found that XLR-11 had a similar potency at CB_1 and CB_2 receptors, consistent with XLR-11 in our assay.[23] A definitive explanation for these differences is not possible, but it should be noted that HEK 293 cells are thought to express a significantly different complement of G proteins

DOI: 10.1021/acschemneuro.5b00107
ACS Chem. Neurosci. 2015, 6, 1445−1458

from AtT-20 cells,[50] and any signaling differences between ligands might be magnified by the cumulative nature of the GTPγS binding assay when compared with the acute, peak effect measurements made for GIRK activation. Consistent with our data from the GIRK assay, UR-144/XLR-11 common metabolite 5-OH-UR-144 was previously reported to be highly CB_2 preferring in binding assays, significantly more so than UR-144 and XLR-11.[12,23]

Although the potency of any drug effect depends on the number of receptors expressed in the system under study, and we have not directly measured the number of receptors in our AtT-20-CB_1 and -CB_2 cells at the time of these assays, WIN 55,212-2 is recognized as having a higher affinity for CB_2 receptors than CB_1 receptors in binding assays,[11,12] so it is likely that CB_2 preference of the SCs is genuine and not an artifact of our expression systems.

Various Internet drug forums contain anecdotal reports by SC consumers regarding the potency and psychoactivity of these compounds. For more well-studied SCs, like JWH-018, cross-substitution with Δ^9-THC has been demonstrated.[51−53] However, for the majority of SCs, there are little to no pharmacological data or formal *in vivo* evaluations available. The ability to induce hypothermia and bradycardia in rats is common to phytocannabinoid Δ^9-THC and newer, non-classical synthetic cannabinoids such as JWH-018.[23,36,54,55] The cannabimimetic activities of des-fluoro/fluoro SC pairs JWH-018/AM-2201, UR-144/XLR-11, PB-22/5F-PB-22, and APICA/STS-135 were therefore evaluated using biotelemetry in male Wistar rats, and the effects of various doses of JWH-018/AM-2201, UR-144/XLR-11, PB-22/5F-PB-22, and APICA/STS-135 on body temperature (Figure 4) and heart rate (Figure 5) are presented.

Body temperature 1 h prior to intraperitoneal (ip) injection and 6 h postinjection of JWH-018, AM-2201, UR-144, XLR-11, PB-22, 5F-PB-22, APICA, and STS-135 are presented in 15 min bins in Figure 4. The dashed line on the figures represents the time of SC injection. Doses were escalated from 0 (baseline) to 3 mg/kg for all compounds. If a large magnitude effect on body temperature was not evident at a 3 mg/kg dose (defined as an approximate mean maximal drop in body temperature of 1.5 °C) then a further 10 mg/kg dose was tested. Each SC was investigated in an ascending dose sequence using a single cohort of three or four rats, with a new cohort of rats used for each SC.

Results showed a dose-dependent hypothermia for all SCs, with statistically significant treatment or treatment by time effects at the specified doses (ANOVA, planned contrasts, SC dose versus vehicle, $P < 0.05$). A large hypothermic effect (mean >1.5 °C) was evoked by 3 mg/kg of JWH-018, AM-2201, PB-22, and 5F-PB-22. However, doses of 10 mg/kg of APICA, STS-135, UR-144, and XLR-11 were required to induce more modest hypothermia, indicating lower *in vivo* potency of these compounds. Terminal fluorination had no obvious effect on *in vivo* potency in any of the pairs of SCs examined. This can be clearly seen in Figure S5, Supporting Information, which displays the mean maximal decrease in body temperature induced by different doses of each compound, and Figure S6, Supporting Information, which shows the area under the curve (AUC) for body temperature for each dose of each compound relative to baseline. Formal statistical comparison of each pair of fluorinated versus nonfluorinated compounds showed no significant statistical difference between any of these pairs.

On the basis of the mean maximal hypothermia and AUC obtained with a 3 mg/kg dose of each compound (Figures S5 and S6, Supporting Information), it is possible to rank SCs in decreasing order of potency: PB-22 > 5F-PB-22 = JWH-018 > AM-2201 > APICA = STS-135 = XLR-11 > UR-144.

Results for heart rate are presented in 30 min bins in Figure 5 with the dashed line on the figures again representing the time of ip injection of each SC. Results were generally consistent with body temperature data, although data were generally more variable than with body temperature data, reflecting the multiple determinants of heart rate including locomotor activity, stress, and direct cardiovascular pharmacological effects. All doses shown produced a significant decrease in heart rate, with statistically significant treatment or treatment by time effects at these doses (ANOVA, planned contrasts, SC dose versus vehicle, $P < 0.05$).

There is variability in the duration of effects for each SC, as determined by hypothermic and bradycardic responses. A point of interest is the potential two-stage hypothermic and bradycardic response demonstrated by JWH-018 and AM-2201. Given their several common metabolites, it is possible that the second hypothermic and bradycardic reponse oberserved for JWH-018 and AM-2201 around 4−5 h postinjection may be due to the combination of active parent compounds and active metabolites.

■ CONCLUSION

This study is the first to pharmacologically characterize the effect of terminal fluorination across structurally diverse classes of 3-subsituted *N*-pentylindole SC designer drugs, exemplified by JWH-018/AM-2201, UR-144/XLR-11, PB-22/5F-PB-22, and APICA/STS-135. A synthetic route to UR-144, XLR-11, and their common metabolite 5-OH-UR-144 was established. The synthesis of PB-22, 5F-PB-22, APICA, STS-135, and several analogues of the latter was achieved. These routes may prove useful to forensic chemists and pharmacologists interested in the cannabinoid activity of novel *N*-alkyl-3-acylindoles, *N*-alkylindole-3-carboxylates, and *N*-alkylindole-3-carboxamides. All synthesized SCs acted as agonists of CB_1 and CB_2 receptors in a FLIPR membrane potential assay and thus are cannabinoids.

Preliminary structure−activity relationships suggest that terminal fluorination of the *N*-pentyl substituent of these SCs generally enhances potency of CB_1 receptor activation, consistent with previously demonstrated improvements to binding affinity conferred by such a change, as well as anecdotal reports of the potent psychoactive effects of fluorinated SCs. However, in rats, although JWH-018/AM-2201, UR-144/XLR-11, PB-22/5F-PB-22, and APICA/STS-135 were able to dose-dependently decrease body temperature and heart rate at doses of 0.3−10 mg/kg, depending on the SC, there was no obvious effect of fluorination on *in vivo* potency. The reasons for the discrepancy between *in vitro* and *in vivo* results is not entirely clear but may reflect pharmacokinetic factors, species-related differences in ligand affinity and efficacy, or an inability of body temperature and heart rate measures to detect subtle differences in overall potency. Nonetheless, the *in vivo* results confirm that all of the SCs explored have cannabimimetic effects that parallel those of Δ^9-THC, albeit with a wide range of differing potencies across compounds.

DOI: 10.1021/acschemneuro.5b00107
ACS Chem. Neurosci. 2015, 6, 1445−1458

ACS Chemical Neuroscience Research Article

METHODS

General Chemical Synthesis Details. All reactions were performed under an atmosphere of nitrogen or argon unless otherwise specified. Toluene was dried over sodium wire and distilled from sodium benzophenone ketyl. Dichloromethane and methanol were distilled from calcium hydride. Anhydrous DMF (Sigma-Aldrich) was used as purchased. Commercially available chemicals (Sigma-Aldrich) were used as purchased. Analytical thin layer chromatography (TLC) was performed using Merck aluminum-backed silica gel 60 F254 (0.2 mm) plates, which were visualized using shortwave (254 nm) ultraviolet fluorescence. Flash chromatography was performed using Merck Kieselgel 60 (230−400 mesh) silica gel. Melting points were measured in open capillaries using a Stuart SMP10 melting point apparatus and are uncorrected. Nuclear magnetic resonance spectra were recorded at 300 K using either a Bruker AVANCE DRX400 (400.1 MHz) or AVANCE III 500 Ascend (500.1 MHz) spectrometer. The data are reported as chemical shift (δ ppm) relative to the residual protonated solvent resonance, relative integral, multiplicity (s = singlet, br s = broad singlet, d = doublet, t = triplet, q = quartet, sep = septet, m = multiplet), coupling constants (J, Hz), and assignment. Assignment of signals was assisted by COSY, DEPT, HSQC, and HMBC experiments where necessary. Low resolution mass spectra (LRMS) were recorded using electrospray ionization (ESI) on a Finnigan LCQ ion trap spectrometer. Elemental analysis was obtained from the Chemical Analysis Facility in the Department of Chemistry and Biomolecular Sciences, Macquarie University, Australia.

General Procedure A: N-Alkylation of 1H-Indole-3-yl(2,2,3,3-tetramethylcyclopropyl)methanone. A cooled (0 °C) solution of **26** (241 mg, 1.0 mmol) in DMF (2 mL) was treated portionwise with sodium hydride (60% dispersion in mineral oil, 80 mg, 2.0 mmol, 2.0 equiv), stirred for 10 min, allowed to warm to ambient temperature, and stirred for 1 h. The mixture was cooled to 0 °C and treated with the appropriate bromoalkane (1.05 mmol, 1.05 equiv) in a single portion, allowed to warm to ambient temperature, and stirred for 1 h. The mixture was poured portionwise onto cooled (0 °C) half-saturated aq. NH_4Cl (40 mL) and extracted with EtOAc (3 × 10 mL). The combined organic layers were washed with H_2O (20 mL) and brine (20 mL) and dried ($MgSO_4$), and the solvent was evaporated under reduced pressure to give crude products. The crude products were purified using flash chromatography or recrystallization.

(1-Pentyl-1H-indol-3-yl)(2,2,3,3-tetramethylcyclopropyl)-methanone (7). Treating **26** (241 mg, 1.0 mmol) with 1-bromopentane (130 μL, 1.05 mmol) according to general procedure A gave, following recrystallization from isopropanol, **7** (283 mg, 91%) as prismatic colorless crystals. R_f 0.41 (hexane−EtOAc, 65:35); mp (*i*-PrOH−H_2O) 72−74 °C. ^{1}H NMR (500 MHz, $CDCl_3$): δ 8.42−8.40 (1H, m, ArH), 7.66 (1H, s, ArH), 7.35−7.33 (1H, m, ArH), 7.29−7.24 (2H, m, ArH), 4.14 (2H, t, J = 7.5 Hz, NCH_2), 1.95 (1H, s, CH), 1.89 (2H, quin., J = 7.5 Hz, CH_2), 1.40−1.33 (10H, m, 2 × CH_2, 2 × CH_3), 1.31 (6H, s, 2 × CH_3), 0.91 (3H, t, J = 7.0 Hz, CH_3). ^{13}C NMR (125 MHz, $CDCl_3$): δ 194.7 (CO), 136.8 (quat.), 133.6 (CH), 126.5 (quat.), 123.0 (CH), 122.8 (CH), 122.2 (CH), 119.8 (quat.), 109.8 (CH), 47.1 (NCH_2), 41.8 (CH), 31.6 ($C_{quat.}$), 29.8 (CH_2), 29.2 (CH_2), 24.2 (CH_3), 22.4 (CH_2), 17.2 (CH_3), 14.0 (CH_3). LRMS (+ESI) m/z 644.80 ([2M + Na]$^+$, 80%), 622.40 ([2M]$^+$, 55%), 312.07 ([M + H]$^+$, 100%). Anal. ($C_{21}H_{29}NO$) Calcd: C 80.98, H 9.38, N 4.50. Found: C 80.99, H 9.54, N 4.49.

(1-(5-Fluoropentyl)-1H-indol-3-yl)(2,2,3,3-tetramethylcyclopropyl)methanone (8). Treating **26** (241 mg, 1.0 mmol) with 1-bromo-5-fluoropentane (177 mg, 1.05 mmol) according to general procedure A, followed by purification using flash chromatography (hexane−EtOAc, 90:10), gave **8** (287 mg, 87%) as a white crystalline solid. R_f 0.47 (hexane−EtOAc, 80:20); mp (*i*-PrOH−H_2O) 76−77 °C. ^{1}H NMR (500 MHz, $CDCl_3$): δ 8.41−8.39 (1H, m, ArH), 7.65 (1H, s, ArH), 7.33−7.32 (1H, m, ArH), 7.29−7.24 (2H, m, ArH), 4.43 (2H, dt, $^2J_{H-F}$ = 47.0 Hz, $^3J_{H-H}$ = 6.0 Hz, CH_2F), 4.17 (2H, t, J = 7.3 Hz, NCH_2), 1.97−1.91 (3H, m, $NCH_2C\underline{H}_2$, CH), 1.77−1.69 (2H, m, $C\underline{H}_2CH_2F$), 1.52−1.47 (2H, m, $NCH_2CH_2C\underline{H}_2$), 1.35 (6H, s, CH_3), 1.30 (6H, s, CH_3). ^{13}C NMR (125 MHz, $CDCl_3$): δ 194.8 (CO), 136.7 (quat.), 133.5 (CH), 126.5 (quat.), 123.1 (CH), 122.9 (CH), 122.3 (CH), 119.9 (quat.), 109.7 (CH), 83.8 (d, $^1J_{C-F}$ = 165.0 Hz, CH_2F), 47.0 (NCH_2), 41.8 (CH), 31.8 ($C_{quat.}$), 30.1 (d, $^2J_{C-F}$ = 19.7 Hz, CH_2), 29.8 (CH_2) 24.2 (CH_3), 23.0 (d, $^3J_{C-F}$ = 4.8 Hz, CH_2), 17.2 (CH_3). LRMS (+ESI) m/z 680.73 ([2M + Na]$^+$, 100%), 658.53 ([2M]$^+$, 42%), 330.20 ([M + H]$^+$, 98%). Anal. ($C_{21}H_{28}NOF$) Calcd: C 76.56, H 8.57, N 4.25. Found: C 76.65, H 8.58, N 4.31.

(1-(5-Hydroxypentyl)-1H-indol-3-yl)(2,2,3,3-tetramethylcyclopropyl)methanone (9). A solution of **27** (185 mg, 0.5 mmol) in THF (2.5 mL) was treated dropwise with a solution of NaOH (40 mg, 1.0 mmol, 2.0 equiv) in MeOH−H_2O (80:20, 2.5 mL), and the mixture was stirred for 16 h. The solvent was evaporated under reduced pressure, and the residue was partitioned between half-saturated aq. $NaHCO_3$ (10 mL) and CH_2Cl_2 (10 mL). The layers were separated, and the aqueous layer was washed with CH_2Cl_2 (2 × 5 mL). The combined organic phases were washed with brine (10 mL) and dried ($MgSO_4$), and the solvent was evaporated. The crude product was purified using flash chromatography (hexane−EtOAc, 50:50, R_f 0.22) from **8** (154 mg, 94%) to give **9** as a white crystalline solid. Mp 80−81 °C. ^{1}H NMR (500 MHz, $CDCl_3$): δ 8.41−8.39 (1H, m, ArH), 7.66 (1H, s, ArH), 7.34−7.33 (1H, m, ArH), 7.28−7.24 (2H, m, ArH), 4.16 (2H, t, J = 7.5 Hz, NCH_2), 3.64 (2H, t, J = 6.5 Hz, $C\underline{H}_2OH$), 1.95 (1H, s, CH), 1.92 (2H, quin., J = 7.5 Hz, CH_2), 1.64−1.58 (2H, m, CH_2), 1.55 (1H, br s, OH), 1.47−1.43 (2H, m, CH_2), 1.35 (6H, s, 2 × CH_3), 1.31 (6H, s, 2 × CH_3). ^{13}C NMR (125 MHz, $CDCl_3$): δ 194.8 (CO), 136.7 (quat.), 133.6 (CH), 126.5 (quat.), 123.1 (CH), 122.8 (CH), 122.2 (CH), 119.8 (quat.), 109.7 (CH), 62.6 (CH_2OH), 47.1 (NCH_2), 41.8 (CH), 32.3 (CH_2), 31.8 ($C_{quat.}$), 29.9 (CH_2), 24.2 (CH_3), 23.4 (CH_2), 17.2 (CH_3). LRMS (+ESI) m/z 676.73 ([2M + Na]$^+$, 89%), 654.47 ([2M]$^+$, 79%), 350.00 ([M + Na]$^+$, 32%), 328.00 ([M + H]$^+$, 100%). Anal. ($C_{21}H_{29}NO_2$) Calcd: C 77.02, H 8.93, N 4.28. Found: C 76.64, H 9.27, N 4.32.

General Procedure B: Esterification of 1-Alkylindole-3-carboxylic Acids. A suspension of the appropriate 1-alkylindole-3-carboxylic acid (**28** or **29**, 1.0 mmol) in CH_2Cl_2 (2 mL) was treated with oxalyl chloride (170 μL, 2.0 mmol, 2.0 equiv) followed by DMF (1 drop). After stirring for 1 h, the solution was evaporated *in vacuo*. A solution of the crude acid chloride and Et_3N (490 μL, 3.5 mmol, 3.5 equiv) in CH_2Cl_2 (5 mL) was slowly treated with a solution of 8-hydroxyquinoline (**32**, 174 mg, 1.2 mmol, 1.2 equiv) in CH_2Cl_2 (5 mL). The mixture was stirred for 24 h, the solvent was evaporated, and the residue was partitioned between EtOAc (75 mL) and H_2O (25 mL). The layers were separated, and the organic phase was washed with sat. aq. $NaHCO_3$ (3 × 25 mL) and brine (25 mL) and dried ($MgSO_4$), and the solvent was evaporated under reduced pressure. The crude products were purified using flash chromatography.

Quinolin-8-yl 1-Pentyl-1H-indole-3-carboxylate (10). Treating **28** (230 mg, 1.0 mmol) with 8-hydroxyquinoline (174 mg, 1.2 mmol, 1.2 equiv) according to general procedure B gave, following purification by flash chromatography (hexane−EtOAc, 50:50, R_f 0.50), **10** (280 mg, 78%) as an off-white crystalline solid. Mp 111−112 °C. ^{1}H NMR (500 MHz, $CDCl_3$): δ 8.92 (1H, dd, J = 4.1, 1.3 Hz), 8.33 (1H, dd, J = 7.7, 1.4 Hz), 8.19 (1H, dd, J = 8.4, 1.3 Hz), 8.17 (1H, s) 7.75 (1H, dd, J = 7.8, 1.3 Hz) 7.63−7.57 (2H, m), 7.43−7.40 (2H, m) 7.34−7.29 (2H, m), 4.20 (2H, t, J = 7.3 Hz), 1.94 (2H, quin., J = 7.1 Hz), 1.40−1.37 (4H, m), 0.93 (3H, t, J = 6.7 Hz). ^{13}C NMR (125 MHz, $CDCl_3$): δ 163.4 (COO), 150.7 (CH), 147.8 ($C_{quat.}$), 142.2 ($C_{quat.}$), 136.9 ($C_{quat.}$), 136.1 (CH), 135.6 (CH), 129.7 ($C_{quat.}$), 127.5 ($C_{quat.}$), 126.4 (CH), 125.7 (CH), 123.0 (CH), 122.21 (CH), 122.19 (CH), 122.16 (CH), 121.7 (CH), 110.2 (CH), 106.1 ($C_{quat.}$), 47.3 (CH_2), 29.8 (CH_2), 29.2 (CH_2), 22.4 (CH_2), 14.0 (CH_3). LRMS (+ESI) m/z 738.73 ([2M + Na]$^+$, 53%), 716.73 ([2M]$^+$, 100%), 358.93 ([M + H]$^+$, 60%), 214.07 (M − C_9H_7N − OH, 17%). Anal. ($C_{23}H_{22}N_2O_2$) Calcd: C 77.07, H 6.19, N 7.82. Found: C 77.29, H 6.19, N 7.89.

Quinolin-8-yl 1-(5-Fluoropentyl)-1H-indole-3-carboxylate (11). Treating **29** (249 mg, 1.0 mmol) with 8-hydroxyquinoline (174 mg, 1.2 mmol, 1.2 equiv) according to general procedure B gave, following purification by flash chromatography (hexane−EtOAc, 50:50, R_f 0.38), **11** (324 mg, 86%) as an off-white/tan crystalline solid. Mp 116−117 °C. ^{1}H NMR (500 MHz, $CDCl_3$): δ 8.91 (1H, dd, J = 4.1, 1.5 Hz),

DOI: 10.1021/acschemneuro.5b00107
ACS Chem. Neurosci. 2015, 6, 1445−1458

8.33 (1H, dd, J = 6.9, 1.7 Hz), 8.19 (1H, dd, J = 8.3, 1.4 Hz), 8.17 (1H, s) 7.75 (1H, dd, J = 7.8, 1.5 Hz), 7.63−7.57 (2H, m), 7.43−7.40 (2H, m), 7.34−7.29 (2H, m), 4.45 (2H, dt, $^2J_{CF}$ = 47.3, $^3J_{HH}$ = 5.9 Hz, CH_2F), 4.22 (2H, t, J = 7.2 Hz), 1.99 (2H, quin., J = 7.5 Hz), 1.80−1.70 (2H, m), 1.56−1.49 (2H, m). ^{13}C NMR (125 MHz, $CDCl_3$): δ 163.4 (COO), 150.7 (CH), 147.8 ($C_{quat.}$), 142.1 ($C_{quat.}$), 136.8 ($C_{quat.}$), 136.1 (CH), 135.5 (CH), 129.7 ($C_{quat.}$), 127.5 ($C_{quat.}$), 126.4 (CH), 125.7 (CH), 123.1 (CH), 122.29 (CH), 122.25 (CH), 122.16 (CH), 122.7 (CH), 110.1 (CH), 106.3 ($C_{quat.}$), 83.8 (d, $^1J_{CF}$ = 166.0 Hz, CH_2F), 47.2 (CH_2), 30.1 (d, $^2J_{CF}$ = 18.9 Hz, $\underline{C}H_2CH_2F$), 29.8 (CH_2), 23.0 (d, $^3J_{CF}$ = 5.0 Hz, $\underline{C}H_2CH_2CH_2F$). LRMS (+ESI) m/z 774.73 ([2M + Na]$^+$, 66%), 752.60 ([2M]$^+$, 100%), 399.00 ([M + Na]$^+$, 33%), 376.87 ([M + H]$^+$, 99%), 232.00 (M − C_9H_7N − OH, 23%). Anal. ($C_{23}H_{21}N_2O_2F$) Calcd: C 73.39, H 5.62, N 7.44. Found: C 73.46, H 5.46, N 7.37.

General Procedure C: Amidation of 1-Alkylindole-3-carboxylic Acids. A suspension of the appropriate 1-alkylindole-3-carboxylic acid (**28** or **29**, 2.0 mmol) in CH_2Cl_2 (5 mL) was treated with oxalyl chloride (420 μL, 5.0 mmol, 2.0 equiv) followed by DMF (1 drop). After stirring for 1 h, the solution was evaporated *in vacuo*. A solution of the crude acid chloride in CH_2Cl_2 (5 mL) was added dropwise to a solution of the appropriate amine (2.4 mmol, 1.2 equiv) and Et_3N (700 μL, 5.0 mmol, 2.5 equiv) in CH_2Cl_2 (20 mL). The mixture was stirred for 14 h, the solvent was evaporated, and the residue was partitioned between EtOAc (200 mL) and 1 M aq. HCl (50 mL). The layers were separated, and the organic phase was washed with 1 M aq. HCl (2 × 50 mL), sat. aq. $NaHCO_3$ (3 × 50 mL), and brine (50 mL) and dried ($MgSO_4$), and the solvent was evaporated under reduced pressure. The crude products were recrystallized from *i*-PrOH or *i*-PrOH−H_2O. The preparation of **12**, **14**, **16**, **18**, **20**, and **22** was described previously.[36]

*N-(Adamantan-1-yl)-1-(5-fluoropentyl)-1H-indole-3-carboxamide (**13**).* Treating (5-fluoropentyl)indole-3-carboxylic acid (499 mg, 2.0 mmol, 1.0 equiv) with 1-aminoadamantane (363 mg, 2.4 mmol, 1.2 equiv) according to general procedure C gave **13** (663 mg, 87%) as fine white needles. Mp (*i*-PrOH−H_2O) 138−140 °C. ^{1}H NMR (500 MHz, $CDCl_3$): δ 7.88 (1H, d, J = 7.5 Hz), 7.64 (1H, s), 7.36 (1H, d, J = 7.5 Hz), 7.28−7.22 (2H, m), 5.69 (1H, br s, NH), 4.41 (2H, dt, $^2J_{CF}$ = 47.0, $^3J_{HH}$ = 6.0 Hz, CH_2F), 4.14 (2H, t, J = 7.2 Hz), 2.19 (6H, br s), 2.14 (3H, br s), 1.90 (2H, quin., J = 7.8 Hz), 1.78−1.62 (8H, m), 1.48−1.41 (2H, m). ^{13}C NMR (125 MHz, $CDCl_3$): δ 164.5 (CO), 136.7 (quat.), 131.3 (CH), 125.4 (quat.), 122.4 (CH), 121.3 (CH), 120.1 (CH), 112.6 (quat.), 110.3 (CH), 83.8 (d, $^1J_{CF}$ = 165.0 Hz, CH_2F), 52.2 (quat.), 46.7 (CH_2), 42.4 (CH_2), 36.7 (CH_2), 30.1 (d, $^2J_{CF}$ = 19.9 Hz, $\underline{C}H_2CH_2F$), 29.8 (CH_2), 29.7 (CH), 23.0 (d, $^3J_{CF}$ = 5.0 Hz, $\underline{C}H_2CH_2CH_2F$). LRMS (+ESI) m/z 764.80 ([2M]$^+$, 100%), 383.13 ([M + H]$^+$, 41%). Anal. ($C_{24}H_{31}N_2OF$) Calcd: C 75.36, H 8.17, N 7.32. Found: C 75.37, H 8.43, N 7.42.

*N-(Adamantan-1-ylmethyl)-1-(5-fluoropentyl)-1H-indole-3-carboxamide (**15**).* Treating (5-fluoropentyl)indole-3-carboxylic acid (499 mg, 2.0 mmol, 1.0 equiv) with 1-(aminomethyl)adamantane (397 mg, 2.4 mmol, 1.2 equiv) according to general procedure C gave **15** (579 mg, 73%) as a white crystalline solid. Mp (*i*-PrOH−H_2O) 148−150 °C. ^{1}H NMR (500 MHz, $CDCl_3$): δ 7.88 (1H, d, J = 7.5 Hz), 7.74 (1H, s), 7.39 (1H, d, J = 7.5 Hz), 7.29−7.26 (2H, m), 6.01 (1H, br s, NH), 4.42 (2H, dt, $^2J_{CF}$ = 47.5, $^3J_{HH}$ = 5.5 Hz, CH_2F), 4.16 (2H, t, J = 7.0 Hz), 3.22 (2H, d, J = 6.0 Hz), 2.02 (3H, br s), 1.92 (2H, quin., J = 7.0 Hz), 1.75−1.62 (14H, m), 1.49−1.43 (2H, m). ^{13}C NMR (125 MHz, $CDCl_3$): δ 164.5 (CO), 136.8 (quat.), 131.8 (CH), 125.3 (quat.), 122.5 (CH), 121.5 (CH), 120.0 (CH), 111.6 (quat.), 110.5 (CH), 83.8 (d, $^1J_{CF}$ = 165.0 Hz, CH_2F), 51.0 (CH_2), 46.8 (CH_2), 40.6 (CH_2), 37.2 (CH_2), 34.1 (quat.), 30.1 (d, $^2J_{CF}$ = 19.9 Hz, $\underline{C}H_2CH_2F$), 29.8 (CH_2), 28.5 (CH), 23.0 (d, $^3J_{CF}$ = 5.0 Hz, $\underline{C}H_2CH_2CH_2F$). LRMS (+ESI) m/z 793.00 ([2M]$^+$, 100%), 397.13 ([M + H]$^+$, 60%). Anal. ($C_{25}H_{33}N_2OF$) Calcd: C 75.72, H 8.39, N 7.06. Found: C 75.46, H 8.69, N 7.09.

*N-Cyclohexyl-1-(5-fluoropentyl)-1H-indole-3-carboxamide (**17**).* Treating (5-fluoropentyl)indole-3-carboxylic acid (499 mg, 2.0 mmol, 1.0 equiv) with cyclohexylamine (275 μL, 2.4 mmol, 1.2 equiv) according to general procedure C gave **17** (488 mg, 74%) as fine white needles. Mp (*i*-PrOH) 145−147 °C. ^{1}H NMR (500 MHz, $CDCl_3$): δ 7.89 (1H, d, J = 7.0 Hz), 7.69 (1H, s), 7.37 (1H, d, J = 7.0 Hz), 7.29−7.23 (2H, m), 5.82 (1H, d, J = 7.5 Hz, NH), 4.42 (2H, dt, $^2J_{CF}$ = 47.0, $^3J_{HH}$ = 6.0 Hz, CH_2F), 4.15 (2H, t, J = 7.0 Hz), 4.10−4.02 (1H, m), 2.10−2.07 (2H, m), 1.91 (2H, quin., J = 7.6 Hz), 1.78−1.67 (5H, m), 1.50−1.42 (4H, m), 1.33−1.20 (3H, m). ^{13}C NMR (125 MHz, $CDCl_3$): δ 164.4 (CO), 136.7 (quat.), 131.4 (CH), 125.5 (quat.), 122.5 (CH), 121.4 (CH), 120.1 (CH), 111.6 (quat.), 110.4 (CH), 83.8 (d, $^1J_{CF}$ = 165.0 Hz, CH_2F), 48.1 (CH), 46.8 (CH_2), 33.7 (CH_2), 30.1 (d, $^2J_{CF}$ = 19.7 Hz, $\underline{C}H_2CH_2F$), 29.8 (CH_2), 25.9 (CH_2), 25.1 (CH_2), 23.0 (d, $^3J_{CF}$ = 4.9 Hz, $\underline{C}H_2CH_2CH_2F$). LRMS (+ESI) m/z 660.73 ([2M]$^+$, 100%), 331.13 ([M + H]$^+$, 78%). Anal. ($C_{20}H_{27}N_2OF$) Calcd: C 72.70, H 8.24, N 8.48. Found: C 72.38, H 8.46, N 8.42.

*N-(Cyclohexylmethyl)-1-(5-fluoropentyl)-1H-indole-3-carboxamide (**19**).* Treating (5-fluoropentyl)indole-3-carboxylic acid (499 mg, 2.0 mmol, 1.0 equiv) with (aminomethyl)cyclohexane (310 μL, 2.4 mmol, 1.2 equiv) according to general procedure C gave **19** (578 mg, 84%) as fine white crystals. Mp (*i*-PrOH) 114−116 °C. ^{1}H NMR (500 MHz, $CDCl_3$): δ 7.89 (1H, d, J = 7.0 Hz), 7.71 (1H, s), 7.38 (1H, d, J = 7.0 Hz), 7.30−7.24 (2H, m), 6.00 (1H, br s, NH), 4.42 (2H, dt, $^2J_{CF}$ = 47.0, $^3J_{HH}$ = 6.0 Hz, CH_2F), 4.15 (2H, t, J = 7.0 Hz), 3.36 (2H, t, J = 6.5 Hz), 1.91 (2H, quin., J = 7.8 Hz), 1.85−1.82 (2H, m), 1.78−1.60 (6H, m), 1.48−1.42 (2H, m), 1.31−1.17 (3H, m), 1.04 (2H, ddd, J = 24.3, 12.3, 3.0 Hz). ^{13}C NMR (125 MHz, $CDCl_3$): δ 165.4 (CO), 136.7 (quat.), 131.6 (CH), 125.4 (quat.), 122.5 (CH), 121.5 (CH), 120.1 (CH), 111.5 (quat.), 110.4 (CH), 83.8 (d, $^1J_{CF}$ = 165.0 Hz, CH_2F), 46.8 (CH_2), 45.8 (CH_2), 38.4 (CH), 31.2 (CH_2), 30.1 (d, $^2J_{CF}$ = 19.9 Hz, $\underline{C}H_2CH_2F$), 29.8 (CH_2), 26.6 (CH_2), 26.1 (CH_2), 23.0 (d, $^3J_{CF}$ = 4.9 Hz, $\underline{C}H_2CH_2CH_2F$). LRMS (+ESI) m/z 710.93 ([2M + Na]$^+$, 95%), 688.73 ([2M]$^+$, 100%), 345.07 ([M + H]$^+$, 48). Anal. ($C_{21}H_{29}N_2OF$) Calcd: C 73.22, H 8.49, N 8.13. Found: C 72.97, H 8.62, N 8.01.

*N-Phenyl-1-(5-fluoropentyl)-1H-indole-3-carboxamide (**21**).* Treating (5-fluoropentyl)indole-3-carboxylic acid (499 mg, 2.0 mmol, 1.0 equiv) with aniline (220 μL, 2.4 mmol, 1.2 equiv) according to general procedure C gave **21** (584 mg, 90%) as a white powder. Mp (*i*-PrOH) 116−119 °C. ^{1}H NMR (500 MHz, $CDCl_3$): δ 8.07−8.05 (1H, m), 7.79 (1H, s), 7.71 (1H, br s, NH) 7.67 (2H, d, J = 8.0 Hz), 7.42−7.36 (3H, m), 7.34−7.29 (2H, m), 7.13 (1H, t, J = 7.5 Hz), 4.42 (2H, dt, $^2J_{CF}$ = 47.0, $^3J_{HH}$ = 6.0 Hz, CH_2F), 4.18 (2H, t, J = 7.0 Hz), 1.93 (2H, quin., J = 7.5 Hz), 1.76−1.68 (2H, m), 1.50−1.44 (2H, m). ^{13}C NMR (125 MHz, $CDCl_3$): δ 163.3 (CO), 138.6 (quat.), 136.8 (quat.), 131.8 (CH), 129.2 (CH), 125.6 (quat.), 124.0 (CH), 122.9 (CH), 121.9 (CH), 120.4 (CH), 120.2 (CH), 111.4 (quat.), 110.5 (CH), 83.8 (d, $^1J_{CF}$ = 165.0 Hz, CH_2F), 46.9 (CH_2), 30.1 (d, $^2J_{CF}$ = 19.9 Hz, $\underline{C}H_2CH_2F$), 29.7 (CH_2), 23.0 (d, $^3J_{CF}$ = 4.9 Hz, $\underline{C}H_2CH_2CH_2F$). LRMS (+ESI) m/z 670.73 ([2M + Na]$^+$, 90%), 648.67 ([2M]$^+$, 89%), 325.00 ([M + H]$^+$, 100). Anal. ($C_{20}H_{21}N_2OF$) Calcd: C 74.05, H 6.53, N 8.64. Found: C 74.20, H 6.69, N 8.65.

*N-Benzyl-1-(5-fluoropentyl)-1H-indole-3-carboxamide (**23**).* Treating (5-fluoropentyl)indole-3-carboxylic acid (499 mg, 2.0 mmol, 1.0 equiv) with benzylamine (260 μL, 2.4 mmol, 1.2 equiv) according to general procedure C gave **23** (549 mg, 81%) as fine white needles. Mp (*i*-PrOH) 128−130 °C. ^{1}H NMR (500 MHz, $CDCl_3$): δ 7.94 (1H, d, J = 8.0 Hz), 7.72 (1H, s), 7.42−7.34 (5H, m), 7.31−7.22 (3H, m), 6.25 (1H, br s, NH), 4.71 (2H, d, J = 5.5 Hz), 4.41 (2H, dt, $^2J_{CF}$ = 47.5 Hz, $^3J_{HH}$ = 6.0 Hz, CH_2F), 4.14 (2H, t, J = 7.5 Hz), 1.91 (2H, quin., J = 8.0 Hz), 1.76−1.64 (2H, m), 1.48−1.41 (2H, m). ^{13}C NMR (125 MHz, $CDCl_3$): δ 165.2 (CO), 139.0 (quat.), 136.7 (quat.), 131.5 (CH), 128.9 (CH), 128.0 (CH), 127.6 (CH), 125.6 (quat.), 122.6 (CH), 121.6 (CH), 120.4 (CH), 111.0 (quat.), 110.3 (CH), 83.8 (d, $^1J_{CF}$ = 165.0 Hz, CH_2F), 46.8 (CH_2), 43.7 (CH_2), 30.1 (d, $^2J_{CF}$ = 19.9 Hz, $\underline{C}H_2CH_2F$), 29.8 (CH_2), 23.0 (d, $^3J_{CF}$ = 4.9 Hz, $\underline{C}H_2CH_2CH_2F$). LRMS (+ESI) m/z 698.73 ([2M + Na]$^+$, 100%), 676.87 ([2M]$^+$, 31%), 339.13 ([M + H]$^+$, 29). Anal. ($C_{21}H_{23}N_2OF$) Calcd: C 74.53, H 6.85, N 8.28. Found: C 74.59, H 6.94, N 8.36.

*1H-Indole-3-yl(2,2,3,3-tetramethylcyclopropyl)methanone (**26**).* A solution of 2,2,3,3-tetramethylcyclopropanecarboxylic acid (**25**,

DOI: 10.1021/acschemneuro.5b00107
ACS Chem. Neurosci. 2015, 6, 1445−1458

1.19 g, 8.4 mmol) in CH_2Cl_2 (20 mL) was treated with $(COCl)_2$ (1.4 mL, 2.4 mmol, 2.0 equiv) followed by DMF (1 drop). After stirring for 1 h, the solution was evaporated *in vacuo*, and the crude acid chloride was used immediately in the following step.

A cooled (0 °C) solution of **24** (820 mg, 7.0 mmol) in CH_2Cl_2 (15 mL) was treated dropwise with a solution of 1 M Me_2AlCl in hexane (10.5 mL, 10.5 mmol, 1.5 equiv) and stirred for 30 min. To this solution was added dropwise a solution of the freshly prepared acid chloride in CH_2Cl_2 (15 mL), and the reaction was stirred for 3 h. The reaction was quenched by dropwise addition to a solution of 1 M aq. HCl (30 mL), the layers were separated, and the aqueous phase was extracted with CH_2Cl_2 (2 × 30 mL). The combined organic layers were washed with sat. aq. $NaHCO_3$ (2 × 30 mL) and dried ($MgSO_4$), and the solvent was evaporated under reduced pressure. The crude product was purified by flash chromatography ($CHCl_3$, R_f 0.26), to give **26** as a pale yellow solid (1.38 g, 82%). ^{1}H NMR (500 MHz, $CDCl_3$): δ 9.51 (1H, br s, NH), 8.44−8.41 (1H, m, ArH), 7.75 (1H, d, J = 2.5 Hz, ArH), 7.39−7.37 (1H, m, ArH), 7.25−7.22 (2H, m, ArH), 1.97 (1H, s, CH), 1.37 (6H, s, CH_3), 1.30 (6H, s, CH_3). ^{13}C NMR (125 MHz, $CDCl_3$): δ 196.1 (CO), 136.6 (quat.), 131.2 (CH), 125.5 (quat.), 123.4 (CH), 122.4 (CH), 122.2 (CH), 120.9 (quat.), 111.7 (CH), 41.9 (CH), 32.0 (quat.), 24.1 (CH_3), 17.2 (CH_3). All spectral data were consistent with those published previously.[11,12]

*(1-(5-Acetoxypentyl)-1H-indol-3-yl)(2,2,3,3-tetramethylcyclopropyl)methanone (**27**).* Treating **26** (362 mg, 1.5 mmol) with 5-bromopentyl acetate (275 μL, 1.65 mmol, 1.1 equiv) according to the general procedure gave, following purification by flash chromatography (hexane−EtOAc, 65:35, R_f 0.30), **27** (371 mg, 67%) as a white crystalline solid. Mp (*i*-PrOH−H_2O) 57−59 °C. ^{1}H NMR (400 MHz, $CDCl_3$): δ 8.42−8.39 (1H, m, ArH), 7.65 (1H, s, ArH), 7.35−7.31 (1H, m, ArH), 7.29−7.24 (2H, m, ArH), 4.17 (2H, t, J = 7.2 Hz, NCH_2), 4.05 (2H, t, J = 6.6 Hz, CH_2OAc), 2.02 (3H, s, Ac), 1.97−1.89 (3H, m, CH, CH_2), 1.71-.164 (2H, m, CH_2), 1.46−1.40 (2H, m, CH_2), 1.35 (6H, s, 2 × CH_3), 1.31 (6H, s, 2 × CH_3). ^{13}C NMR (100 MHz, $CDCl_3$): δ 194.7 (CO), 171.2 ($\underline{C}(O)OCH_3$) 136.7 (quat.), 133.4 (CH), 126.5 (quat.), 123.1 (CH), 122.9 (CH), 122.3 (CH), 119.9 (quat.), 109.7 (CH), 64.1 ($\underline{C}H_2OAc$), 47.0 (NCH_2) 41.8 (CH), 31.8 ($C_{quat.}$), 29.8 (CH_2), 28.3 (CH_2), 24.2 (CH_3), 23.5 (CH_2), 21.1 (CH_3), 17.2 (CH_3). LRMS (+ESI) m/z 760.67 ($[2M + Na]^+$, 72%), 370.07 ($[M + H]^+$, 100%). Anal. ($C_{23}H_{31}NO_3$) Calcd: C 74.76, H 8.46, N 3.79. Found: C 74.43, H 8.58, N 3.93.

General Procedure D: Synthesis of 1-Alkylindole-3-carboxylic Acids. A cooled (0 °C) mixture of sodium hydride (60% dispersion in mineral oil, 2.00 g, 50.0 mmol, 2.0 equiv) in DMF (30 mL) was treated slowly with a solution of indole (2.93 g, 25 mmol) in DMF (3 mL), warmed to ambient temperature, and stirred for 10 min. The mixture was cooled in an ice−water bath and then treated slowly with the appropriate bromoalkane (26.3 mmol, 1.05 equiv). The mixture was warmed to ambient temperature and stirred for 1 h, at which point TLC analysis indicated complete consumption of indole. The solution was cooled to 0 °C and treated slowly with trifluoroacetic anhydride (8.70 mL, 62.5 mmol, 2.5 equiv). The resultant clear, red solution was warmed to ambient temperature and stirred for 1 h, at which point TLC analysis indicated the complete conversion of the 1-alkylindole to 1-alkyl-3-trifluoroacetylindole. The reaction was poured portionwise onto stirred ice−water (500 mL), and the mixture was vigorously stirred at 0 °C until complete solidification of the oil layer had occurred. The precipitate was collected by filtration and air-dried to give crude 1-alkyl-1*H*-3-trifluoroacetylindoles as pink solids.

A solution of crude 1-alkyl-1*H*-3-trifluoroacetylindole (25.0 mmol) in toluene (22 mL) was slowly added to a refluxing solution of KOH (4.63 g, 82.5 mmol, 3.3 equiv) in MeOH (8 mL), and the mixture was heated at reflux for 2 h. The mixture was cooled to ambient temperature, and H_2O (80 mL) was added. The layers were separated, and the organic layer was extracted with 1 M aq. NaOH (25 mL). The combined aqueous phases were acidified to pH 1 with 10 M aq. HCl, extracted with Et_2O (3 × 50 mL) or CH_2Cl_2 (3 × 50 mL), and dried ($MgSO_4$), and the solvent was evaporated. The crude products were recrystallized from isopropanol to give analytically pure materials.

*1-Pentylindole-3-carboxylic Acid (**28**).* Treating indole with 1-bromopentane according to general procedure D gave, after recrystallization from *i*-PrOH, **28** as colorless crystals (4.57 g, 19.8 mmol, 79%). Mp (i-PrOH) 106−108 °C. ^{1}H NMR (500 MHz, CDCl3): δ 8.27−8.24 (1H, m), 7.93 (1H, s), 7.40−7.38 (1H, m), 7.33−7.29 (2H, m), 4.17 (2H, t, J = 7.2 Hz), 1.90 (2H, quin., J = 7.2 Hz), 1.39−1.32 (4H, m), 0.91 (3H, t, J = 7.0 Hz). ^{13}C NMR (125 MHz, CDCl3): δ 170.7 (COOH), 136.9 (quat.), 135.6, 127.2 (quat.), 123.0, 122.3, 122.1, 110.2, 106.4 (quat.), 47.3 (CH_2), 29.7 (CH_2), 29.1 (CH_2), 22.4 (CH2), 14.0. Anal. (C14H17NO2) Calcd: C 72.70, H 7.41, N 6.06. Found: C 72.67, H 7.77, N 5.93

*1-(5-Fluoropentyl)indole-3-carboxylic Acid (**29**).* Treating indole with 1-bromo-5-fluoropentane according to general procedure D gave, after recrystallization from *i*-PrOH (twice), **29** as colorless crystals (5.28 g, 21.2 mmol, 85%). Mp (*i*-PrOH−H_2O) 120−122 °C. ^{1}H NMR (500 MHz, $CDCl_3$): δ 8.29−8.25 (1H, m), 7.93 (1H, s), 7.40−7.37 (1H, m), 7.34−7.30 (2H, m), 4.43 (2H, dt, $^2J_{CF}$ = 47.3, $^3J_{HH}$ = 5.9 Hz, CH_2F), 4.18 (2H, t, J = 7.1 Hz), 1.98−1.92 (2H, m, CH_2), 1.78−1.68 (2H, m, CH_2), 1.51−1.45 (2H, m, CH_2). ^{13}C NMR (125 MHz, $CDCl_3$): δ 170.9 (CO), 136.8 (quat.), 135.5 (CH), 127.1 (quat.), 123.1 (CH), 122.3 (CH), 122.1 (CH), 110.1 (CH), 106.6 (quat.), 83.8 (d, $^1J_{CF}$ = 166.0 Hz, CH_2F), 47.1 (CH_2), 30.0 (d, $^2J_{CF}$ = 20.1 Hz, $\underline{C}H_2CH_2F$), 29.6 (CH_2), 22.9 (d, $^3J_{CF}$ = 5.0 Hz, $\underline{C}H_2CH_2CH_2F$). Anal. ($C_{14}H_{16}FNO_2$) Calcd: C 67.45, H 6.47, N 5.62. Found: C 67.31, H 6.60, N 5.46.

X-ray Data Collection. The solid was crystallized from *i*-PrOH−H_2O to give colorless crystals by slow evaporation at ambient temperature.

The single-crystal X-ray diffraction experiments were carried out at the Faculty of Pharmacy, University of Sydney, using a Bruker APEX-II CCD-based diffractometer with an X-ray wavelength of 0.71073 Å (Mo Kα) and at an experimental temperature of 150 K. The single crystal of **7** was mounted on the tip of a thin glass fiber with a minimum amount of Paratone N oil, which acted as both an adhesive and a cryoprotectant, and inserted in the cold N_2 stream of an Oxford Cryosystem COBRA cooler. X-ray diffraction data were collected using 0.3° $\Delta\omega$-scans, maintaining the crystal-to-detector distance at 6.0 cm. A total of 1588 frames were collected. The diffraction data were integrated using SAINT+,[56] which included corrections for Lorentz, polarization, and absorption effects. Unit cell parameters for **7** at 150 K were refined from 999 reflections.

The structure was solved using direct methods (SHELX-S)[57] and refined using full-matrix least-squares (SHELXL).[57] All non-hydrogen atoms were treated as anisotropic, while hydrogen atoms were placed in idealized positions, with U_{eq} set at 1.5 times that of the parent atom.

empirical formula	$C_{21}H_{29}NO$
formula wt	311.45
temp (K)	150.15
cryst syst	monoclinic
space group	$P2_1/n$
unit cell dimensions	
a (Å)	12.112
α (deg)	90
b (Å)	10.799
β (deg)	93.69
c (Å)	13.920
γ (deg)	90
Z	4
GOF on F^2	1.050
final R indices $[I > 2\sigma(I)]$	
R_1	0.0398
wR_2	0.1019
R indices (all data)	
R_1	0.0478
wR_2	0.1077

***In Vitro* Pharmacological Assessment of SCs.** Mouse AtT-20 neuroblastoma cells stably transfected with human CB_1 or human CB_2

DOI: 10.1021/acschemneuro.5b00107
ACS Chem. Neurosci. 2015, 6, 1445−1458

have been previously described[36] and were cultured in Dulbecco's modified Eagle's medium (DMEM) containing 10% fetal bovine serum (FBS), 100 U of penicillin/streptomycin, and 300 μg/mL G418. Cells were passaged at 80% confluency as required. Cells for assays were grown in 75 cm^2 flasks and used at 90% confluence. The day before the assay, cells were detached from the flask with trypsin/EDTA (Sigma) and resuspended in 10 mL of Leibovitz's L-15 media supplemented with 1% FBS, 100 U of penicillin/streptomycin, and 15 mM glucose (membrane potential assay and Ca5 calcium assay). The cells were plated in volume of 90 μL in black-walled, clear bottomed 96-well microplates (Corning), which had been precoated with poly(L-lysine) (Sigma, Australia). Cells were incubated overnight at 37 °C in ambient CO_2.

Membrane potential was measured using a FLIPR membrane potential assay kit (blue) from Molecular Devices, as described previously.[49] The dye was reconstituted with assay buffer of composition (mM): NaCl 145, 4-(2-hydroxyethyl)-1-piperazineethanesulfonic acid (HEPES) 22, Na_2HPO_4 0.338, $NaHCO_3$ 4.17, KH_2PO_4 0.441, $MgSO_4$ 0.407, $MgCl_2$ 0.493, $CaCl_2$ 1.26, glucose 5.56 (pH 7.4, osmolarity 315 ± 5). Prior to the assay, cells were loaded with 90 μL/well of the dye solution without removal of the L-15, giving an initial assay volume of 180 μL/well. Plates were then incubated at 37 °C at ambient CO_2 for 45 min. Fluorescence was measured using a FlexStation 3 (Molecular Devices) microplate reader with cells excited at a wavelength of 530 nm and emission measured at 565 nm. Baseline readings were taken every 2 s for at least 2 min, at which time either drug or vehicle was added in a volume of 20 μL. The background fluorescence of cells without dye or dye without cells was negligible. Changes in fluorescence were expressed as a percentage of baseline fluorescence after subtraction of the changes produced by vehicle addition, which was less than 2% for drugs dissolved in assay buffer or DMSO. The final concentration of DMSO was not more than 0.1%.

Data were analyzed with PRISM (GraphPad Software Inc., San Diego, CA), using four-parameter nonlinear regression to fit concentration−response curves. In all plates, a maximally effective concentration of WIN 55,212-2 was added to allow for normalization between assays.

***In Vivo* Pharmacological Assessment of SCs.** Eight cohorts of three or four adult male Wistar rats (Animal Resources Centre, Perth, Australia) initially weighing between 200 and 230 g were used for biotelemetric assessment of each compound. The rats were singly housed in an air-conditioned testing room (22 ± 1 °C) on a 12 h reverse light/dark cycle (lights on from 21:00 to 09:00). Standard rodent chow and water were provided *ad libitum*. All experiments were approved by The University of Sydney Animal Ethics Committee.

Biotelemetry transmitters (TA11CTA-F40, Data Sciences International, St. Paul, MN) were implanted as previously described.[36] Briefly, following anaesthetization (isoflurane, 3% induction, 2% maintenance), a rostro-caudal incision was made along the midline of the abdomen, and a biotelemetry transmitter (TA11CTA-F40, Data Sciences International, St. Paul, MN) was placed in the peritoneal cavity according to the manufacturers protocol. The wound was sutured closed, and the rats were allowed 1 week of recovery before data collection.

The rats were habituated over multiple days to injections of vehicle (5% EtOH, 5% Tween 80, 90% physiological saline) at a set time of day (11:00 am). Each cohort then received intraperitoneal injections of each compound at the same time of day in an ascending dose sequence (0.1, 0.3, 1, 3 mg/kg). This ascending sequence reduces the risk posed to the animals in assessing hitherto untested compounds, and the use of multiple cohorts limits the potential development of tolerance to the compound. Two washout days were given between each dose. If only a modest or negligible hypothermic response was seen at 3 mg/kg, then a further 10 mg/kg dose of the compound was given. Two washout days were given between each dose.

Data for heart rate and body temperature was gathered continuously at 1000 Hz, organized into 15 or 30 min bins using Dataquest A.R.T. software (version 4.3, Data Sciences International, St. Paul, MN), and analyzed using PRISM (Graphpad Software Inc., San Diego, CA).

■ ASSOCIATED CONTENT

Ⓢ Supporting Information

X-ray crystallographic data, selected ^1H and ^{13}C NMR spectra, and area under curve (AUC) plots for biotelemetry. The Supporting Information is available free of charge on the ACS Publications website at DOI: 10.1021/acschemneuro.5b00107.

■ AUTHOR INFORMATION

Corresponding Author

*E-mail: michael.kassiou@sydney.edu.au.

Author Contributions

S.D.B., M.L., S.M.W., C.B., and A.S.B. performed the synthesis, purification, and chemical characterization of compounds **7**−**23** with guidance from M.K. J.S. and A.E. conducted all *in vitro* pharmacological evaluation under the supervision of M.C., with data analysis performed by J.S., S.D.B., A.S.B., and M.C. R.C.K. carried out all behavioral pharmacology with direction from I.S.M. D.E.H. provided X-ray crystallographic analysis of UR-144 (**7**). M.G. assisted the creation of stably transfected cells expressing hCB_2R. The manuscript was prepared by S.D.B., A.S.B., M.C., I.S.M., and M.K. All authors have given approval to the final version of the manuscript.

Funding

Work performed at The University of Sydney and presented herein was supported in part by the European Union's Seventh Framework Programme [FP7/2007-2013] INMiND (Grant Agreement No. HEALTH-F2-2011-278850). Work performed at Macquarie University and presented herein was supported by NHMRC Project Grant 1002680 awarded to M.C. and M.K., and J.S. is the recipient of an International Research Scholarship from Macquarie University.

Notes

The authors declare no competing financial interest.

■ ABBREVIATIONS

CB, cannabinoid; FLIPR, fluorometric imaging plate reader; GIRK, G-protein-gated inwardly rectifying K^+ channels; ip, intraperitoneal; NMR, nuclear magnetic resonance; pi, post-injection; SAR, structure−activity relationship; SC, synthetic cannabinoid; Δ^9-THC, Δ^9-tetrahydrocannabinol; TLC, thin layer chromatography

■ REFERENCES

(1) European Monitoring Centre for Drugs and Drug Addiction (2015), New psychoactive substances in Europe. An update from the EU Early Warning System (March 2015), Publications Office of the European Union, Luxembourg.

(2) Maxwell, J. C. (2014) Psychoactive substances-Some new, some old: A scan of the situation in the U.S. *Drug Alcohol Depend. 134*, 71−77.

(3) Huestis, M. A., Gorelick, D. A., Heishman, S. J., Preston, K. L., Nelson, R. A., Moolchan, E. T., and Frank, R. A. (2001) Blockade of effects of smoked marijuana by the CB1-selective cannabinoid receptor antagonist SR141716. *Arch. Gen. Psychiatry 58*, 322−328.

(4) D'Ambra, T. E., Estep, K. G., Bell, M. R., Eissenstat, M. A., Josef, K. A., Ward, S. J., Haycock, D. A., Baizman, E. R., and Casiano, F. M. (1992) Conformationally restrained analogs of pravadoline: Nanomolar potent, enantioselective, (aminoalkyl)indole agonists of the cannabinoid receptor. *J. Med. Chem. 35*, 124−135.

(5) Auwarter, V., Dresen, S., Weinmann, W., Muller, M., Putz, M., and Ferreiros, N. (2009) 'Spice' and other herbal blends: Harmless incense or cannabinoid designer drugs? *J. Mass Spectrom. 44*, 832−837.

DOI: 10.1021/acschemneuro.5b00107
ACS Chem. Neurosci. 2015, 6, 1445−1458

(6) Wilkinson, S. M., Banister, S. D., and Kassiou, M. (2015) Bioisosteric Fluorine in the Clandestine Design of Synthetic Cannabinoids. *Aust. J. Chem. 68*, 4−8.
(7) Makriyannis, A.; Deng, H. Preparation of cannabimimetic indole derivatives with cannabinoid CB1 or CB2 receptor binding affinity. World patent WO 2001/028557, 26 April, 2001.
(8) Nakajima, J.i., Takahashi, M., Nonaka, R., Seto, T., Suzuki, J., Yoshida, M., Kanai, C., and Hamano, T. (2011) Identification and quantitation of a benzoylindole (2-methoxyphenyl)(1-pentyl-1*H*-indol-3-yl)methanone and a naphthoylindole 1-(5-fluoropentyl-1*H*-indol-3-yl)-(naphthalene-1-yl)methanone (AM-2201) found in illegal products obtained via the Internet and their cannabimimetic effects evaluated by in vitro [^{35}S]GTPγS binding assays. *Forensic Toxicol. 29*, 132−141.
(9) Sobolevsky, T., Prasolov, I., and Rodchenkov, G. (2012) Detection of urinary metabolites of AM-2201 and UR-144, two novel synthetic cannabinoids. *Drug Test. Anal. 4*, 745−753.
(10) Chung, H., Choi, H., Heo, S., Kim, E., and Lee, J. (2014) Synthetic cannabinoids abused in South Korea: Drug identifications by the National Forensic Service from 2009 to June 2013. *Forensic Toxicol. 32*, 82−88.
(11) Frost, J. M., Dart, M. J., Tietje, K. R., Garrison, T. R., Grayson, G. K., Daza, A. V., El-Kouhen, O. F., Miller, L. N., Li, L., Yao, B. B., Hsieh, G. C., Pai, M., Zhu, C. Z., Chandran, P., and Meyer, M. D. (2008) Indol-3-yl-tetramethylcyclopropyl ketones: Effects of indole ring substitution on CB2 cannabinoid receptor activity. *J. Med. Chem. 51*, 1904−1912.
(12) Frost, J. M., Dart, M. J., Tietje, K. R., Garrison, T. R., Grayson, G. K., Daza, A. V., El-Kouhen, O. F., Yao, B. B., Hsieh, G. C., Pai, M., Zhu, C. Z., Chandran, P., and Meyer, M. D. (2010) Indol-3-ylcycloalkyl ketones: Effects of N1 substituted indole side chain variations on CB(2) cannabinoid receptor activity. *J. Med. Chem. 53*, 295−315.
(13) Kavanagh, P., Grigoryev, A., Savchuk, S., Mikhura, I., and Formanovsky, A. (2013) UR-144 in products sold via the Internet: Identification of related compounds and characterization of pyrolysis products. *Drug Test. Anal. 5*, 683−692.
(14) Shevyrin, V., Melkozerov, V., Nevero, A., Eltsov, O., Morzherin, Y., and Shafran, Y. (2013) Identification and analytical properties of new synthetic cannabimimetics bearing 2,2,3,3-tetramethylcyclopropanecarbonyl moiety. *Forensic Sci. Int. 226*, 62−73.
(15) Zuba, D., and Byrska, B. (2013) Analysis of the prevalence and coexistence of synthetic cannabinoids in "herbal high" products in Poland. *Forensic Toxicol. 31*, 21−30.
(16) Seely, K. A., Patton, A. L., Moran, C. L., Womack, M. L., Prather, P. L., Fantegrossi, W. E., Radominska-Pandya, A., Endres, G. W., Channell, K. B., Smith, N. H., McCain, K. R., James, L. P., and Moran, J. H. (2013) Forensic investigation of K2, Spice, and "bath salt" commercial preparations: A three-year study of new designer drug products containing synthetic cannabinoid, stimulant, and hallucinogenic compounds. *Forensic Sci. Int. 233*, 416−422.
(17) Uchiyama, N., Kawamura, M., Kikura-Hanajiri, R., and Goda, Y. (2013) URB-754: A new class of designer drug and 12 synthetic cannabinoids detected in illegal products. *Forensic Sci. Int. 227*, 21−32.
(18) Choi, H., Heo, S., Kim, E., Hwang, B. Y., Lee, C., and Lee, J. (2013) Identification of (1-pentylindol-3-yl)-(2,2,3,3-tetramethylcyclopropyl)methanone and its 5-pentyl fluorinated analog in herbal incense seized for drug trafficking. *Forensic Toxicol. 31*, 86−92.
(19) Langer, N., Lindigkeit, R., Schiebel, H. M., Ernst, L., and Beuerle, T. (2014) Identification and quantification of synthetic cannabinoids in 'spice-like' herbal mixtures: a snapshot of the German situation in the autumn of 2012. *Drug Test. Anal. 6*, 59−71.
(20) Thornton, S. L., Wood, C., Friesen, M. W., and Gerona, R. R. (2013) Synthetic cannabinoid use associated with acute kidney injury. *Clin. Toxicol. 51*, 189−190.
(21) Buser, G. L., Gerona, R. R., Horowitz, B. Z., Vian, K. P., Troxell, M. L., Hendrickson, R. G., Houghton, D. C., Rozansky, D., Su, S. W., and Leman, R. F. (2014) Acute kidney injury associated with smoking synthetic cannabinoid. *Clin. Toxicol. 52*, 664−673.
(22) Takematsu, M., Hoffman, R. S., Nelson, L. S., Schechter, J. M., Moran, J. H., and Wiener, S. W. (2014) A case of acute cerebral ischemia following inhalation of a synthetic cannabinoid. *Clin. Toxicol. 52*, 973−975.
(23) Wiley, J. L., Marusich, J. A., Lefever, T. W., Grabenauer, M., Moore, K. N., and Thomas, B. F. (2013) Cannabinoids in disguise: Δ^9-Tetrahydrocannabinol-like effects of tetramethylcyclopropyl ketone indoles. *Neuropharmacology 75*, 145−154.
(24) Shevyrin, V., Melkozerov, V., Nevero, A., Eltsov, O., and Shafran, Y. (2013) Analytical characterization of some synthetic cannabinoids, derivatives of indole-3-carboxylic acid. *Forensic Sci. Int. 232*, 1−10.
(25) Uchiyama, N., Matsuda, S., Kawamura, M., Kikura-Hanajiri, R., and Goda, Y. (2014) Identification of two new-type designer drugs, piperazine derivative MT-45 (I-C6) and synthetic peptide Noopept (GVS-111), with synthetic cannabinoid A-834735, cathinone derivative 4-methoxy-α-PVP, and phenethylamine derivative 4-methylbuphedrine from illegal products. *Forensic Toxicol. 32*, 9−18.
(26) Uchiyama, N., Matsuda, S., Kawamura, M., Kikura-Hanajiri, R., and Goda, Y. (2013) Two new-type cannabimimetic quinolinyl carboxylates, QUPIC and QUCHIC, two new cannabimimetic carboxamide derivatives, ADB-FUBINACA and ADBICA, and five synthetic cannabinoids detected with a thiophene derivative α-PVT and an opioid receptor agonist AH-7921 identified in illegal products. *Forensic Toxicol. 31*, 223−240.
(27) McQuade, D., Hudson, S., Dargan, P. I., and Wood, D. M. (2013) First European case of convulsions related to analytically confirmed use of the synthetic cannabinoid receptor agonist AM-2201. *Eur. J. Clin. Pharmacol. 69*, 373−376.
(28) Gugelmann, H., Gerona, R., Li, C., Tsutaoka, B., Olson, K. R., and Lung, D. (2014) 'Crazy Monkey' poisons man and dog: Human and canine seizures due to PB-22, a novel synthetic cannabinoid. *Clin. Toxicol. 52*, 635−638.
(29) Schep, L., Slaughter, R., Hudson, S., Place, R., and Watts, M. (2014) Delayed seizure-like activity following analytically confirmed use of previously unreported synthetic cannabinoid analogues. *Hum. Exp. Toxicol.*, DOI: 10.1177/0960327114550886.
(30) Behonick, G., Shanks, K. G., Firchau, D. J., Mathur, G., Lynch, C. F., Nashelsky, M., Jaskierny, D. J., and Meroueh, C. (2014) Four Postmortem Case Reports with Quantitative Detection of the Synthetic Cannabinoid, 5F-PB-22. *J. Anal. Toxicol. 38*, 559−562.
(31) Takayama, T., Suzuki, M., Todoroki, K., Inoue, K., Min, J. Z., Kikura-Hanajiri, R., Goda, Y., and Toyo'oka, T. (2014) UPLC/ESI-MS/MS-based determination of metabolism of several new illicit drugs, ADB-FUBINACA, AB-FUBINACA, AB-PINACA, QUPIC, 5F-QUPIC and alpha-PVT, by human liver microsome. *Biomed. Chromatogr. 28*, 831−838.
(32) Thomsen, R., Nielsen, L. M., Holm, N. B., Rasmussen, H. B., Linnet, K., and INDICES Consortium (2014) Synthetic cannabimimetic agents metabolized by carboxylesterases. *Drug Test. Anal.*, DOI: 10.1002/dta.1731.
(33) Wohlfarth, A., Gandhi, A. S., Pang, S., Zhu, M., Scheidweiler, K. B., and Huestis, M. A. (2014) Metabolism of synthetic cannabinoids PB-22 and its 5-fluoro analog, 5F-PB-22, by human hepatocyte incubation and high-resolution mass spectrometry. *Anal. Bioanal. Chem. 406*, 1763−1780.
(34) Uchiyama, N., Kawamura, M., Kikura-Hanajiri, R., and Goda, Y. (2012) Identification of two new-type synthetic cannabinoids, N-(1-adamantyl)-1-pentyl-1*H*-indole-3-carboxamide (APICA) and N-(1-adamantyl)-1-pentyl-1*H*-indazole-3-carboxamide (APINACA), and detection of five synthetic cannabinoids, AM-1220, AM-2233, AM-1241, CB-13 (CRA-13), and AM-1248, as designer drugs in illegal products. *Forensic Toxicol. 30*, 114−125.
(35) Sobolevsky, T., Prasolov, I., and Rodchenkov, G. (2015) Study on the phase I metabolism of novel synthetic cannabinoids, APICA and its fluorinated analogue. *Drug Test. Anal. 7*, 131−142.

DOI: 10.1021/acschemneuro.5b00107
ACS Chem. Neurosci. 2015, 6, 1445−1458

(36) Banister, S. D., Wilkinson, S. M., Longworth, M., Stuart, J., Apetz, N., English, K., Brooker, L., Goebel, C., Hibbs, D. E., Glass, M., Connor, M., McGregor, I. S., and Kassiou, M. (2013) The synthesis and pharmacological evaluation of adamantane-derived indoles: cannabimimetic drugs of abuse. *ACS Chem. Neurosci. 4*, 1081−1092.
(37) Brents, L. K., Reichard, E. E., Zimmerman, S. M., Moran, J. H., Fantegrossi, W. E., and Prather, P. L. (2011) Phase I hydroxylated metabolites of the K2 synthetic cannabinoid JWH-018 retain *in vitro* and *in vivo* cannabinoid 1 receptor affinity and activity. *PLoS One 6*, No. e21917.
(38) Chimalakonda, K. C., Seely, K. A., Bratton, S. M., Brents, L. K., Moran, C. L., Endres, G. W., James, L. P., Hollenberg, P. F., Prather, P. L., Radominska-Pandya, A., and Moran, J. H. (2012) Cytochrome P450-mediated oxidative metabolism of abused synthetic cannabinoids found in K2/Spice: identification of novel cannabinoid receptor ligands. *Drug Metab. Dispos. 40*, 2174−2184.
(39) Rajasekaran, M., Brents, L. K., Franks, L. N., Moran, J. H., and Prather, P. L. (2013) Human metabolites of synthetic cannabinoids JWH-018 and JWH-073 bind with high affinity and act as potent agonists at cannabinoid type-2 receptors. *Toxicol. Appl. Pharmacol. 269*, 100−108.
(40) Fantegrossi, W. E., Moran, J. H., Radominska-Pandya, A., and Prather, P. L. (2014) Distinct pharmacology and metabolism of K2 synthetic cannabinoids compared to Delta(9)-THC: Mechanism underlying greater toxicity? *Life Sci. 97*, 45−54.
(41) Grigoryev, A., Kavanagh, P., and Melnik, A. (2013) The detection of the urinary metabolites of 1-[(5-fluoropentyl)-1H-indol-3-yl]-(2-iodophenyl)methanone (AM-694), a high affinity cannabimimetic, by gas chromatography - mass spectrometry. *Drug Test. Anal. 5*, 110−115.
(42) Wohlfarth, A., Pang, S., Zhu, M., Gandhi, A. S., Scheidweiler, K. B., Liu, H. F., and Huestis, M. A. (2013) First metabolic profile of XLR-11, a novel synthetic cannabinoid, obtained by using human hepatocytes and high-resolution mass spectrometry. *Clin. Chem. 59*, 1638−1648.
(43) Jang, M., Yang, W., Shin, I., Choi, H., Chang, H., and Kim, E. (2014) Determination of AM-2201 metabolites in urine and comparison with JWH-018 abuse. *Int. J. Leg. Med. 128*, 285−294.
(44) Kanamori, T., Kanda, K., Yamamuro, T., Kuwayama, K., Tsujikawa, K., Iwata, Y. T., and Inoue, H. (2015) Detection of main metabolites of XLR-11 and its thermal degradation product in human hepatoma HepaRG cells and human urine. *Drug Test. Anal.*, DOI: 10.1002/dta.1765.
(45) Hutter, M., Moosmann, B., Kneisel, S., and Auwärter, V. (2013) Characteristics of the designer drug and synthetic cannabinoid receptor agonist AM-2201 regarding its chemistry and metabolism. *J. Mass Spectrom. 48*, 885−894.
(46) European Monitoring Centre for Drugs and Drug Addiction (2014), EMCDDA−Europol 2013 Annual Report on the implementation of Council Decision 2005/387/JHA, Implementation reports, Publications Office of the European Union, Luxembourg.
(47) Okauchi, T., Itonaga, M., Minami, T., Owa, T., Kitoh, K., and Yoshino, H. (2000) A general method for acylation of indoles at the 3-position with acyl chlorides in the presence of dialkylaluminum chloride. *Org. Lett. 2*, 1485−1487.
(48) Grimsey, N. L., Graham, E. S., Dragunow, M., and Glass, M. (2010) Cannabinoid Receptor 1 trafficking and the role of the intracellular pool: Implications for therapeutics. *Biochem. Pharmacol. 80*, 1050−1062.
(49) Knapman, A., Santiago, M., Du, Y. P., Bennallack, P. R., Christie, M. J., and Connor, M. (2013) A continuous, fluorescence-based assay of μ-opioid receptor activation in AtT-20 cells. *J. Biomol. Screening 18*, 269−276.
(50) Atwood, B. K., Lopez, J., Wager-Miller, J., Mackie, K., and Straiker, A. (2011) Expression of G protein-coupled receptors and related proteins in HEK293, AtT20, BV2, and N18 cell lines as revealed by microarray analysis. *BMC Genomics 12*, No. 14.
(51) Wiley, J. L., Compton, D. R., Dai, D., Lainton, J. A. H., Phillips, M., Huffman, J. W., and Martin, B. R. (1998) Structure-activity relationships of indole- and pyrrole-derived cannabinoids. *J. Pharmacol. Exp. Ther. 285*, 995−1004.
(52) Wiley, J. L., Marusich, J. A., and Huffman, J. W. (2014) Moving around the molecule: Relationship between chemical structure and in vivo activity of synthetic cannabinoids. *Life Sci. 97*, 55−63.
(53) Wiley, J. L., Lefever, T. W., Cortes, R. A., and Marusich, J. A. (2014) Cross-substitution of Δ^9-tetrahydrocannabinol and JWH-018 in drug discrimination in rats. *Pharmacol., Biochem. Behav. 124*, 123−128.
(54) Hine, B., Torrelio, M., and Gershon, S. (1977) Analgesic, heart rate, and temperature effects of Δ^8-THC during acute and chronic administration to conscious rats. *Pharmacology 15*, 65−72.
(55) Wiley, J. L., Marusich, J. A., Martin, B. R., and Huffman, J. W. (2012) 1-Pentyl-3-phenylacetylindoles and JWH-018 share in vivo cannabinoid profiles in mice. *Drug Alcohol Depend. 123*, 148−153.
(56) Bruker (2011) *Apex2 suite of programs*, Bruker AXS Inc., Madison, Wisconsin, USA.
(57) Sheldrick, G. M. (2008) A short history of SHELX. *Acta Crystallogr. A64*, 112−122.

DOI: 10.1021/acschemneuro.5b00107
ACS Chem. Neurosci. 2015, 6, 1445−1458

ACS Chemical Neuroscience
Research Article
pubs.acs.org/chemneuro

Pharmacology of Indole and Indazole Synthetic Cannabinoid Designer Drugs AB-FUBINACA, ADB-FUBINACA, AB-PINACA, ADB-PINACA, 5F-AB-PINACA, 5F-ADB-PINACA, ADBICA, and 5F-ADBICA

Samuel D. Banister,[†,‡] Michael Moir,[‡] Jordyn Stuart,[§] Richard C. Kevin,[∥] Katie E. Wood,[∥] Mitchell Longworth,[‡] Shane M. Wilkinson,[‡] Corinne Beinat,[†,‡] Alexandra S. Buchanan,[⊥,#] Michelle Glass,[○] Mark Connor,[§] Iain S. McGregor,[∥] and Michael Kassiou*[,‡,▽]

[†]Department of Radiology, [⊥]Center for Immersive and Simulation-Based Learning, Stanford University School of Medicine, Stanford, California 94305, United States

[‡]School of Chemistry, [∥]School of Psychology, [▽]Faculty of Health Sciences, The University of Sydney, Sydney, NSW 2006, Australia

[§]Faculty of Medicine and Health Sciences, Macquarie University, Sydney, NSW 2109, Australia

[#]Department of Anaesthesia, Prince of Wales Hospital, Randwick, NSW 2031, Australia

[○]School of Medical Sciences, The University of Auckland, Auckland 1142, New Zealand

S *Supporting Information*

ABSTRACT: Synthetic cannabinoid (SC) designer drugs based on indole and indazole scaffolds and featuring L-valinamide or L-*tert*-leucinamide side chains are encountered with increasing frequency by forensic researchers and law enforcement agencies and are associated with serious adverse health effects. However, many of these novel SCs are unprecedented in the scientific literature at the time of their discovery, and little is known of their pharmacology. Here, we report the synthesis and pharmacological characterization of AB-FUBINACA, ADB-FUBINACA, AB-PINACA, ADB-PINACA, 5F-AB-PINACA, 5F-ADB-PINACA, ADBICA, 5F-ADBICA, and several analogues. All synthesized SCs acted as high potency agonists of CB_1 (EC_{50} = 0.24−21 nM) and CB_2 (EC_{50} = 0.88−15 nM) receptors in a fluorometric assay of membrane potential, with 5F-ADB-PINACA showing the greatest potency at CB_1 receptors. The cannabimimetic activities of AB-FUBINACA and AB-PINACA *in vivo* were evaluated in rats using biotelemetry. AB-FUBINACA and AB-PINACA dose-dependently induced hypothermia and bradycardia at doses of 0.3−3 mg/kg, and hypothermia was reversed by pretreatment with a CB_1 (but not CB_2) antagonist, indicating that these SCs are cannabimimetic *in vivo*, consistent with anecdotal reports of psychoactivity in humans.

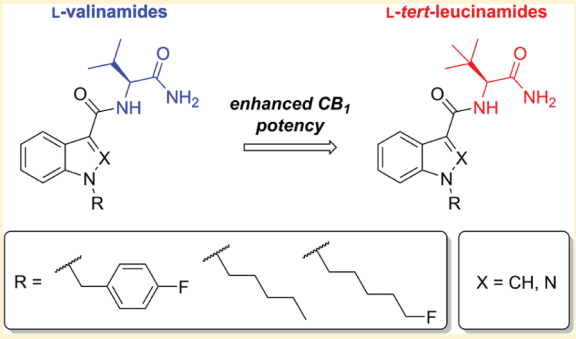

KEYWORDS: *Cannabinoid, THC, JWH-018, FUBINACA, PINACA*

Synthetic cannabinoids (SCs) are the most rapidly growing class of recreational designer drugs. Since the identification of the first SC designer drugs in 2008, more than 130 SCs have been reported to the European Monitoring Centre for Drugs and Drug Addiction (EMCDDA).[1] Of the 101 new psychoactive substances notified by the EMCDDA during 2014, 30 were SCs.[1] Although these products are often mislabeled as research chemicals or incense and include disclaimers stating that the products are not for human consumption, SCs are recreational designer drugs intended to mimic the effects of Δ^9-tetrahydrocannabinol (Δ^9-THC, **1**, Figure 1) while circumventing the law.

The phytocannabinoid Δ^9-THC is the principal bioactive component of marijuana (*Cannabis sativa*), the most widely used illicit substance in the world. Δ^9-THC exerts its psychoactive effects by acting as a partial agonist at cannabinoid type-1 (CB_1) receptors,[2] although it is also a partial agonist at type-2 (CB_2) receptors. CB_1 and CB_2 receptors are classical G protein-coupled receptors (GPCRs). While CB_1 receptors are found primarily at the terminals of central and peripheral neurons, where they inhibit neurotransmitter release, CB_2 receptors are mainly located in immune cells within and outside the central nervous system (CNS).[3,4] Due to the role of the CB receptor system in numerous diseases, early pharmaceutical drug discovery programs explored many phytocannabinoid analogues like CP 47,497 (**2**) and CP 55,940 (**3**), disclosed by Pfizer in the 1970s and 1980s.[5,6] Following structural leads from the pharmaceutical industry, Huffman and co-workers at Clemson University have

Received: April 8, 2015
Revised: June 9, 2015
Published: July 2, 2015

DOI: 10.1021/acschemneuro.5b00112
ACS Chem. Neurosci. 2015, 6, 1546−1559

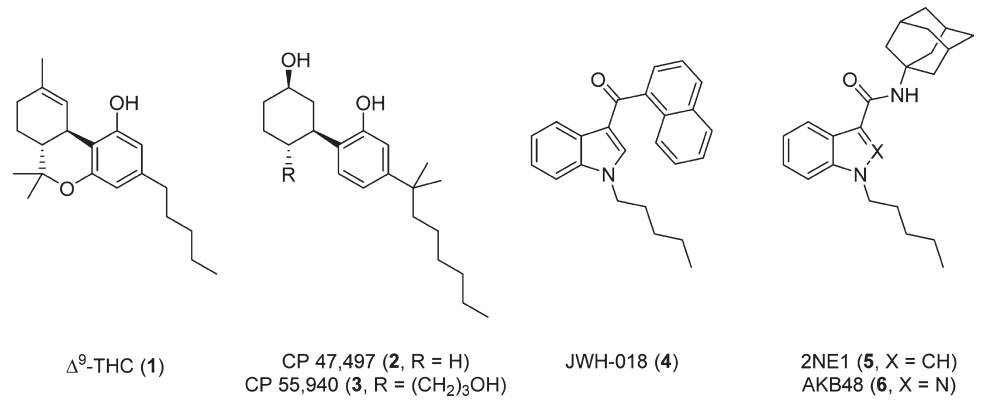

Δ^9-THC (**1**) CP 47,497 (**2**, R = H) CP 55,940 (**3**, R = $(CH_2)_3OH$) JWH-018 (**4**) 2NE1 (**5**, X = CH) AKB48 (**6**, X = N)

Figure 1. Selected phytocannabinoids and synthetic cannabinoids.

discovered many indole SCs with potent cannabimimetic activity, including JWH-018 (**4**).

In 2008, a recreational herbal blend was found to contain the C8 homologue of CP 47,497 and JWH-018.[7] Following the prohibition of CP 47,497-C8 and JWH-018 by many governments, other structurally diverse indole SCs began to appear.[8−11] Recently, numerous SCs with clandestine design origins and no precedent in the scientific literature have been detected in forensic samples. For example, indole-3-carboxamide SC 2NE1 (APICA, SDB-001, **5**) was identified along with its indazole analogue AKB48 (APINACA, **6**).[12] Presumably intended to mimic the alphanumeric format of compound codes used throughout the pharmaceutical industry, 2NE1 and AKB48 were named after Japanese and Korean female pop music groups, respectively, by their clandestine designers. Current popular design trends for modification of the *N*-pentyl group include terminal fluorination and replacement with cyclohexylmethyl or 4-fluorobenzylic moieties.[13,14]

In 2013, novel indazole SCs AB-FUBINACA (**7**, Figure 2) and ADB-FUBINACA (**8**) were identified in recreational products by Japanese forensic scientists.[10,15,16] Although many recent SCs have no precedent in the scientific literature prior to their identification as designer drugs, **7** and **8** were both described by Pfizer in a 2009 patent claiming CB_1 ligands as potential therapeutic agents.[17] The binding affinity and functional activity in a GTPγS binding assay of **7** (K_i = 0.9 nM, EC_{50} = 23.2 nM) and **8** (K_i = 0.36 nM, EC_{50} = 0.98 nM) at hCB_1 receptors was reported, indicating that both compounds are potent CB_1 agonists, but no further pharmacology was described. The stereochemistry of the isopropyl and *tert*-butyl side chains of illicit **7** and **8**, respectively, is unresolved. However, the Pfizer patent reports activity exclusively for the (*S*)-enantiomers, and it is likely that the Pfizer compounds and the illicit SCs are (*S*)-enantiomers derived from the abundant and inexpensive L-amino acids L-valine and L-*tert*-leucine.

AB-PINACA (**9**) was identified alongside **7**, representing a hybrid of **7** and *N*-pentyl SCs like **4** and **6**.[10,15] Although previously unreported in the scientific literature, ADB-PINACA (**10**) exposure was associated with severe adverse reactions, including neurotoxicity and cardiotoxicity in the USA in late 2013,[18−20] and was recently linked to a cluster of cases of severe delirium.[21] The 5-fluorinated analogues of **9** and **10**, 5F-AB-PINACA (**11**) and 5F-ADB-PINACA (**12**), respectively, have also been identified on the Japanese market.[22,23] By 2014, **7**−**11** and **16** had been formally notified by the EMCDDA as a result of seizures in Belgium, Germany, Turkey, the United Kingdom, and Sweden.[24]

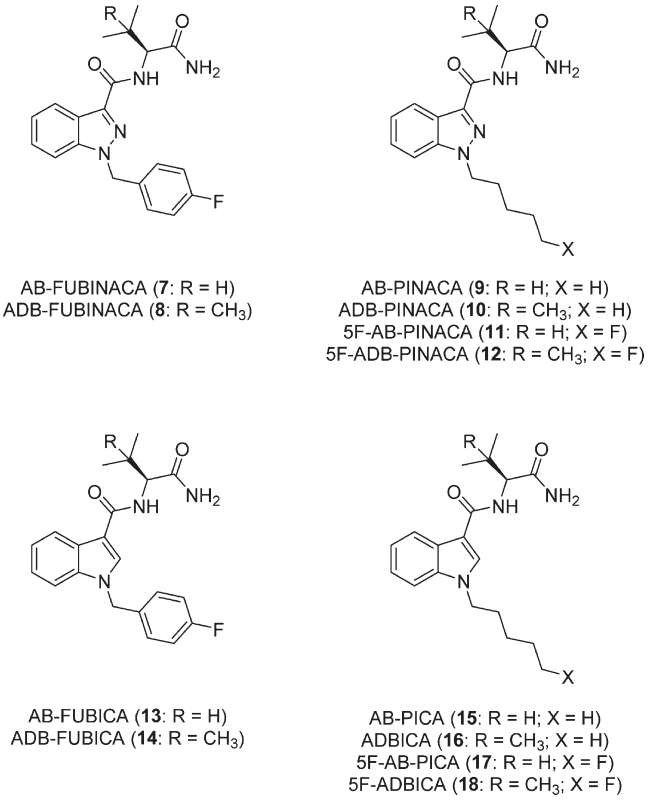

AB-FUBINACA (**7**: R = H) ADB-FUBINACA (**8**: R = CH_3) AB-PINACA (**9**: R = H; X = H) ADB-PINACA (**10**: R = CH_3; X = H) 5F-AB-PINACA (**11**: R = H; X = F) 5F-ADB-PINACA (**12**: R = CH_3; X = F)

AB-FUBICA (**13**: R = H) ADB-FUBICA (**14**: R = CH_3) AB-PICA (**15**: R = H; X = H) ADBICA (**16**: R = CH_3; X = H) 5F-AB-PICA (**17**: R = H; X = F) 5F-ADBICA (**18**: R = CH_3; X = F)

Figure 2. Indole- and indazole-3-carboxamide synthetic cannabinoid designer drugs.

AB-FUBICA (**13**), ADB-FUBICA (**14**), AB-PICA (**15**), and 5F-AB-PICA (**17**) represent the indole analogues of indazoles **7**, **8**, **9**, and **11** and have not appeared in the scientific literature. However, the indole analogue of **10**, ADBICA (**16**) was identified in Japan,[16] and its 5-fluoro analogue, 5F-ADBICA (**18**), was notified by the EMCDDA after law enforcement agencies in the U.S. implicated **18** in a series of non-fatal intoxications.[24]

Despite their widespread use and frequency of adverse reactions requiring hospitalization, very little is known about the activity of indole and indazole SCs comprising an L-valinamide or L-*tert*-leucinamide subunit. In addition to reports of the detection of SCs **7**−**11**, **16**, and **18** by forensic researchers, the metabolic profiles of **7**−**9** and **11** were recently published.[25−28]

DOI: 10.1021/acschemneuro.5b00112
ACS Chem. Neurosci. 2015, 6, 1546−1559

The aim of the present study was to address the paucity of data regarding the pharmacology of indole and indazole SCs by synthesizing **7**−**18**, evaluating their activity at human CB_1 and CB_2 receptors, and assessing the behavioral pharmacology of these novel SCs in rats using biotelemetry.

RESULTS AND DISCUSSION

The original patent by Pfizer describing AB-FUBINACA and ADB-FUBINACA utilized enantiopure amino acids L-valinamide (**19**, Figure 3) and L-*tert*-leucinamide (**20**) to give products with (*S*) stereocenters.

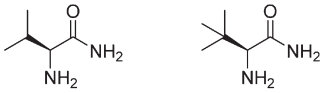

19 **20**

Figure 3. Amino acid derivatives L-valinamide (**19**) and L-*tert*-leucinamide (**20**).

While L-valinamide is available from numerous commercial sources as its hydrochloride salt, L-*tert*-leucinamide is derived from a non-natural amino acid, and the synthesis of **20** is shown in Scheme 1. Treatment of L-*tert*-leucine (**21**) with benzyl chloroformate gave Cbz-protected amine **22**. The free acid of **22** was converted to the corresponding amide (**23**) using the coupling reagents EDC and HOBt, and subsequent deprotection by catalytic hydrogenation afforded **20**. The three-step procedure proved to be operationally convenient, and analytically pure L-*tert*-leucinamide was obtained on a multigram scale following recrystallization.

The synthesis of indazole SCs **7**−**12** is shown in Scheme 2. Fischer esterification of indazole-3-carboxylic acid (**24**) gave **25**, which was deprotonated with potassium *tert*-butoxide and alkylated with either 4-fluorobenzyl bromide, 1-bromopentane, or 1-bromo-5-fluoropentane to afford the corresponding *N*-alkylindazole-3-carboxylic acid methyl esters **26**−**28**. Alkylation proceeded regioselectively to give 1-substituted 1*H*-indazoles as the major products; however, small quantities of 2-alkylated indazoles were obtained as minor products and separated by flash chromatography. Saponification of the methyl ester of **26**−**28** to give free acids **29**−**31** was followed by amide coupling with EDC-HOBt and either L-valinamide or L-*tert*-leucinamide to give **7**−**12**.

Access to the corresponding indole SCs (**13**−**18**) required an alternative synthetic route, shown in Scheme 3. Excess sodium hydride was added to indole (**33**), which was subsequently alkylated with the appropriate bromoalkane and then treated with trifluoroacetic anhydride to give the corresponding *N*-alkyl-3-(trifluoroacetyl)indole (**34**−**36**) in a one-pot process. Alkaline hydrolysis induced fluoroform elimination[29] and furnished, upon workup and recrystallization, the corresponding *N*-alkylindole-3-carboxylic acids (**37**−**39**) of analytical purity. Coupling of **37**−**39** with **19** or **20** using EDC-HOBt yielded **13**−**18**. Indole SCs derived from L-valinamide (**13**, **15**, **17**) were recrystallized from isopropanol to analytical purity, whereas those comprising L-*tert*-leucinamide (**14**, **16**, **18**) were purified by flash chromatography owing to their superior solubility in a range of alcoholic solvents.

The activity of synthesized indazole (**7**−**12**) and corresponding indole (**13**−**18**) SCs at CB_1 and CB_2 receptors was evaluated using a fluorometric imaging plate reader (FLIPR) assay to provide structure−activity relationship (SAR) data regarding the choice of heteroaromatic core, amino acid side-chain, and alkyl substituent within this class of SCs. Additionally, the *in vivo* activity of **7** and **9** was compared using biotelemetry in rats to provide information regarding the increasingly common 4-fluorobenzyl motif in SCs.

The cannabimimetic activities of **7**−**18** were compared to those of phytocannabinoid Δ^9-THC (a partial agonist at CB_1 and CB_2) and indole SC JWH-018 (a full agonist at CB_1 and CB_2), and the data is presented in Table 1. Murine AtT-20 neuroblastoma cells were stably transfected with human CB_1 or CB_2 receptors, and activities of Δ^9-THC, JWH-018, and **7**−**18** were evaluated using a FLIPR membrane potential assay whereby endogenously expressed G protein-gated inwardly rectifying K^+ channels (GIRKs) are activated by agonists at the expressed CB_1 or CB_2 receptors. The maximum effects of Δ^9-THC, JWH-018, and **7**−**18** were compared to high efficacy CB_1/CB_2 receptor agonist CP 55,490, which produced a maximal decrease in fluorescence, corresponding to cellular hyperpolarization, at a concentration of 1 μM in AtT-20-CB_1 and AtT-20-CB_2 cells. None of the compounds produced a significant change in the membrane potential of wild-type AtT-20 cells, which do not express CB_1 or CB_2 receptors.

All indole and indazole SCs activated CB_1 and CB_2 receptors. All compounds had greater potency (0.24−21 nM) than Δ^9-THC (172 nM) for CB_1 receptor-mediated activation of GIRK. Δ^9-THC is a low-efficacy CB_2 agonist, and in the assay of GIRK activation in AtT-20-CB_2, its effects at 30 μM were only 32 ± 1% of that mediated by CP 55,940. CP 55,940 was more potent at stimulating a cellular hyperpolarization in AtT-20-CB_2 cells than AtT-20-CB_1 cells, displaying an approximately 2-fold CB_2 preference. All indazole and indole SCs had a similar maximal effect to CP 55,940 at CB_1 and CB_2 receptors, suggesting that these SCs are also high efficacy agonists. With the exception of **13**, all novel SCs showed a mild preference for CB_1 receptors, and it is activation of CB_1 receptors that is associated with the psychoactive effects of cannabinoids.[2]

The least potent compound in the series (indole **13**) was 11-fold more potent than Δ^9-THC at CB_1 receptors, and the most potent compound (indazole **12**) showed more than 1000 times

Scheme 1. Synthesis of L-*tert*-Leucinamide[a]

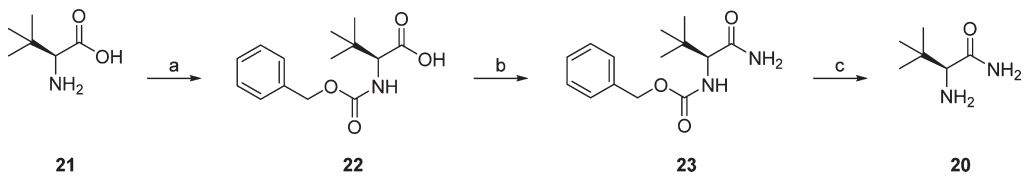

21 **22** **23** **20**

[a]Reagents and conditions: (a) NaOH, BnOC(O)Cl, 0 °C to rt, 2 h, 99%; (b) NH_4Cl, Et_3N, HOBt, EDCI, DMF, rt, 16 h, 84%; (c) 10% Pd/C, THF, 48%.

DOI: 10.1021/acschemneuro.5b00112
ACS Chem. Neurosci. 2015, 6, 1546−1559

Scheme 2. Synthesis of Indazole SCs 7−12[a]

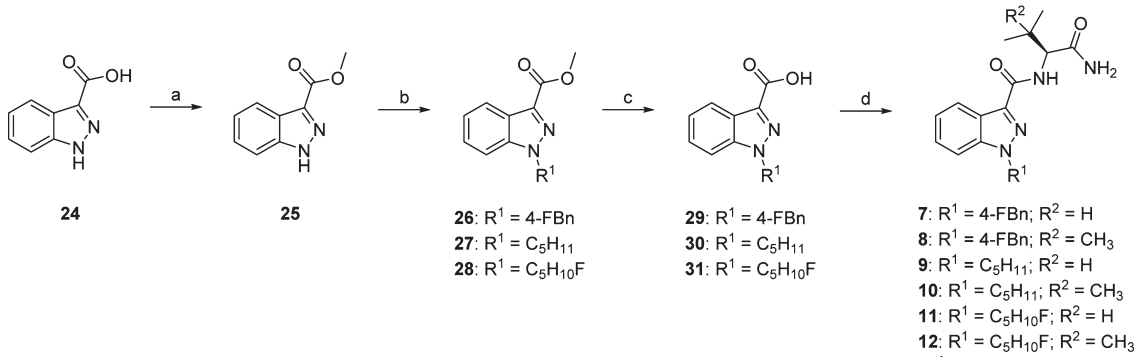

[a]Reagents and conditions: (a) conc. H_2SO_4, MeOH, reflux, 4 h, 76%; (b) BrR^1, *t*-BuOK, THF, 0 °C to rt, 48 h, 67−77%; (c) NaOH, MeOH, rt, 24 h, 76−96%; (d) EDC·HCl, HOBt, DIPEA, **19** or **20**, DMF, rt, 24 h, 31−63%.

Scheme 3. Synthesis of Indole SCs 13−18[a]

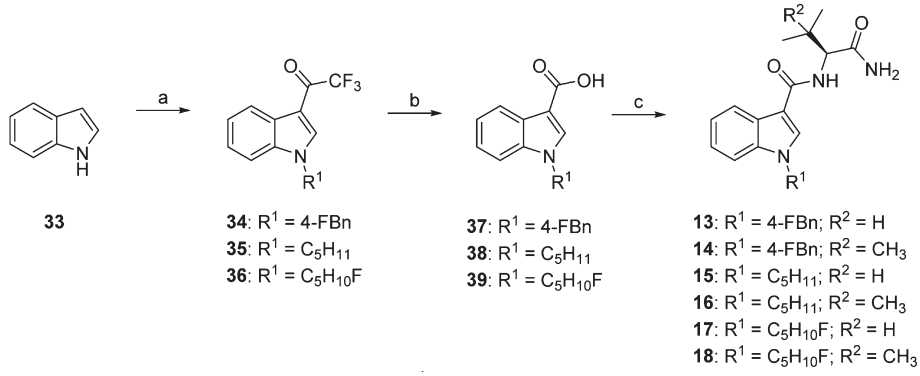

[a]Reagents and conditions: (a) (i) NaH, BrR^1, DMF, 0 °C to rt, 1 h, (ii) $(CF_3CO)_2O$, DMF, 0 °C to rt, 1 h; (b) KOH, MeOH, PhMe, reflux, 2 h 54−68% (over two steps); (d) EDC·HCl, HOBt, DIPEA, **19** or **20**, DMF, rt, 24 h, 65−86%.

Table 1. Functional Activity of Δ^9-THC, CP 55,940, JWH-018, and Novel SCs 7−18 at CB_1 and CB_2 Receptors

	hCB_1	hCB_1	hCB_2	hCB_2	
compound	pEC_{50} ± SEM (EC_{50}, nM)	nax ± SEM (% CP 55,940)	pEC_{50} ± SEM (EC_{50}, nM)	nax ± SEM (% CP 55,940)	CB_1 sel.[a]
Δ^9-THC (**1**)	6.76 ± 0.09 (172)	58 ± 3		32 ± 1 at 30 μM	
CP 55,490 (**3**)	7.63 ± 0.09 (24)		7.88 ± 0.08 (13)		0.5
JWH-018 (**4**)	7.74 ± 0.16 (18)	116 ± 9	7.66 ± 0.16 (22)	87 ± 7	1.2
AB-FUBINACA (**7**)	8.76 ± 0.10 (1.8)	108 ± 7	8.50 ± 0.20 (3.2)	95 ± 12	1.8
ADB-FUBINACA (**8**)	8.92 ± 0.16 (1.2)	152 ± 11	8.46 ± 0.13 (3.5)	104 ± 7	2.9
AB-PINACA (**9**)	8.91 ± 0.09 (1.2)	103 ± 4	8.60 ± 0.16 (2.5)	104 ± 8	2.1
ADB-PINACA (**10**)	9.28 ± 0.08 (0.52)	117 ± 6	9.06 ± 0.31 (0.88)	107 ± 16	1.7
5F-AB-PINACA (**11**)	9.32 ± 0.10 (0.48)	94 ± 6	8.59 ± 0.25 (2.6)	110 ± 13	5.4
5F-ADB-PINACA (**12**)	9.61 ± 0.19 (0.24)	91 ± 7	8.68 ± 0.11 (2.1)	94 ± 5	8.8
AB-FUBICA (**13**)	7.67 ± 0.14 (21)	115 ± 7	7.84 ± 0.27 (15)	99 ± 10	0.7
ADB-FUBICA (**14**)	8.58 ± 0.15 (2.6)	113 ± 8	8.52 ± 0.16 (3.0)	96 ± 7	1.2
AB-PICA (**15**)	7.92 ± 0.07 (12)	99 ± 3	7.92 ± 0.21 (12)	94 ± 9	1.0
ADBICA (**16**)	9.16 ± 0.16 (0.69)	98 ± 7	8.75 ± 0.18 (1.8)	94 ± 7	2.6
5F-AB-PICA (**17**)	8.28 ± 0.21 (5.2)	123 ± 13	8.05 ± 0.53 (8.9)	121 ± 24	1.7
5F-ADBICA (**18**)	9.12 ± 0.14 (0.77)	110 ± 7	8.91 ± 14 (1.2)	92 ± 6	1.6

[a]CB_1 selectivity expressed as the ratio of CB_1 EC_{50} to CB_2 EC_{50}.

the potency of Δ^9-THC, making 5F-ADB-PINACA one of the most potent SC designer drugs reported to date. Excluding **7** and **8**, indazoles and indoles containing the L-*tert*-leucinamide group were more potent at both CB_1 and CB_2 receptors than the corresponding SC featuring an L-valinamide substituent. In the most dramatic example, the additional methyl group of **16** (EC_{50} = 0.68 nM) conferred a 17-fold increase in potency over **15** (EC_{50} = 12 nM) at CB_1 receptors. The same trend was observed for CB_2 receptors, but potency enhancement was more moderate, with **18** (EC_{50} = 1.2 nM) showing a 7-fold improvement over **17** (EC_{50} = 1.2 nM).

Surprisingly, there were no clear trends for differences of potency or efficacy between indazole SCs **7−12** and the corresponding indoles **13−18**. Similarly, choice of *N*-alkyl

DOI: 10.1021/acschemneuro.5b00112
ACS Chem. Neurosci. 2015, 6, 1546−1559

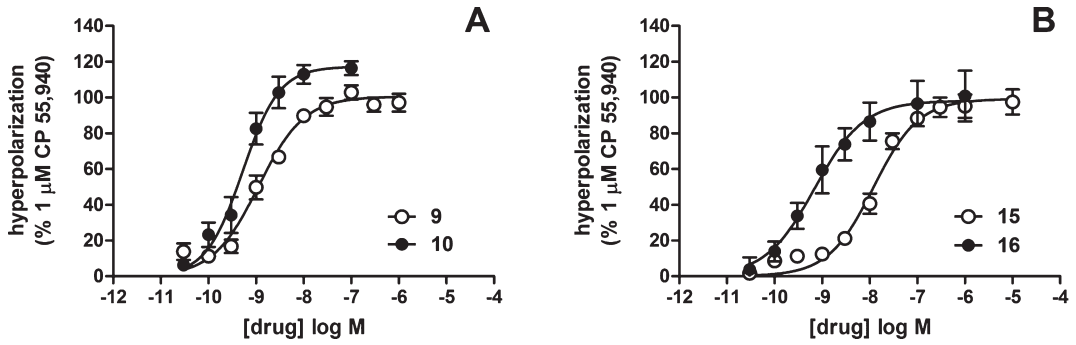

Figure 4. Hyperpolarization of CB_1 receptors induced by (A) AB-PINACA (**9**) and ADB-PINACA (**10**) and (B) AB-PICA (**15**) and ADBICA (**16**) as a proportion of that produced by 1 μM CP 55,940. Membrane potential was measured using a fluorescent dye, as outlined in the Methods. Each point represents the mean ± SEM of at least five independent determinations, each performed in duplicate. Data was fitted with a four-parameter logistic equation in GraphPad Prism.

group had little effect on potency. However, indoles containing the L-valinamide group (**13**, **15**, **17**), the least potent SCs identified in this series, were each less potent than the corresponding indazoles (**7**, **9**, **11**). Taken together, these results suggest that the heteroaromatic core and indole nitrogen substituent of these SCs contribute less to the activity of these compounds than the pendant amide group. The difference in CB_1 activity between L-valinamide and L-*tert*-leucinamide derivatives featuring a 1-pentyl group and containing an indazole core (**9** and **10**, respectively) or an indole core (**15** and **16**, respectively) is depicted in Figure 4.

Very little is known about the potency and psychoactivity of newer SCs in humans. Having demonstrated that **7**−**18** are potent and efficacious cannabimimetic agents *in vitro*, we sought to demonstrate activity of some of these SCs *in vivo*. Cross-substitution of older SCs, like JWH-018, with Δ^9-THC has been demonstrated.[30−32] Cannabinoids are known to induce hypothermia and bradycardia in rats, effects that are common to phytocannabinoids like Δ^9-THC and heteroaromatic SCs such as JWH-018.[33−35] We have previously evaluated the hypothermic and bradycardic potencies of Δ^9-THC and numerous structurally diverse SCs including JWH-018, AM-2201, UR-144, XLR-11, PB-22, 5F-PB-22, APICA, and STS-135.[14,36] The cannabimimetic activities AB-FUBINACA and AB-PINACA were evaluated using radiotelemetry in male Wistar rats, and the effects of these SCs on body temperature (Figure 5) and heart rate (Figure 6) are presented below.

Rat body temperature 1 h prior to intraperitoneal (i.p.) injection and 6 h postinjection of AB-FUBINACA and AB-PINACA are presented in 15 min bins in Figure 5. For each drug, these data are presented for 1 h before (baseline) and 6 h after injection of various doses. The dashed line on the figures represents the time of SC injection. Each SC was investigated using a cohort of 3−4 rats, with a different cohort used for the two compounds. Doses were escalated from 0 mg/kg (baseline) to 0.1, 0.3, 1, and 3 mg/kg for each compound, with at least two washout days between each dose. The 0.1 mg/kg doses of each compound were without significant effects on body temperature and heart rate, so data for these doses are not presented.

A substantial hypothermic effect was evoked by 0.3−3 mg/kg of both drugs, with the peak reduction in body temperature generally greater with AB-FUBINACA (>2 °C) than AB-PINACA (>1.5 °C). As Figure 5 shows, the 4-fluorobenzyl-substituted AB-FUBINACA appeared to confer a hypothermic effect of greater magnitude and duration (∼4 h) than that observed for the pentyl-substituted AB-PINACA (∼2 h) at the same dose (3 mg/kg). This was verified by a statistical analysis showing a significantly greater area under the curve for body temperature (relative to vehicle baseline) for AB-FUBINACA doses compared to that for AB-PINACA at 3 mg/kg ($P < 0.05$).

Results for heart rate are presented in 30 min bins in Figure 6, with the dashed line on the figures again representing the time of SC injection. Results were consistent with body temperature data, although data were generally more variable than they were with body temperature data, reflecting the multiple determinants of heart rate including locomotor activity, stress, and direct cardiovascular pharmacological effects. All doses shown produced a significant decrease in heart rate, with statistically significant treatment or treatment by time effects at these doses (ANOVA, planned contrasts, SC dose versus vehicle, $P < 0.05$).

To confirm that the observed effects were mediated through CB_1 or CB_2 receptors, the reversibility of the effects of AB-PINACA and AB-FUBINACA on body temperature and heart rate in rats following pretreatment with either CB_1 receptor antagonist rimonabant (SR141176, **40**, Figure 7) or CB_2 receptor antagonist SR144528 (**41**) was assessed. Rimonabant is a potent, selective, CB_1 receptor neutral antagonist that reverses CB_1-mediated cannabinoid agonist effects in rodents and humans,[2,37,38] whereas SR144528 is selective CB_2 antagonist/inverse agonist.[39,40]

Rat body temperatures after injection (i.p.) with vehicle, CB_1 antagonist (rimonabant, 3 mg/kg), or CB_2 antagonist (SR144528, 3 mg/kg) 30 min prior to treatment with either AB-FUBINACA (3 mg/kg) or AB-PINACA (3 mg/kg) are presented in 15 min bins in Figure 8. For each treatment condition, these data are presented for 1 h before (baseline) and 6 h after injection of various doses. The first dashed line on the figure represents the time of vehicle/antagonist injection, and the second dashed line represents time of SC injection. Each SC was investigated using a cohort of 3−4 rats, with a different cohort used for the two compounds. The dose of each antagonist was 3 mg/kg, and the dose of each SC was also 3 mg/kg.

Pretreatment with rimonabant was able to completely reverse the hypothermic effects of AB-FUBINACA, whereas pretreatment with SR144528 had no effect on the body temperature decrease induced by AB-FUBINACA (Figure 8A). Similarly, rimonabant partially reversed the decreased body temperature effected by AB-PINACA, but SR144528 had negligible effect on

DOI: 10.1021/acschemneuro.5b00112
ACS Chem. Neurosci. 2015, 6, 1546−1559

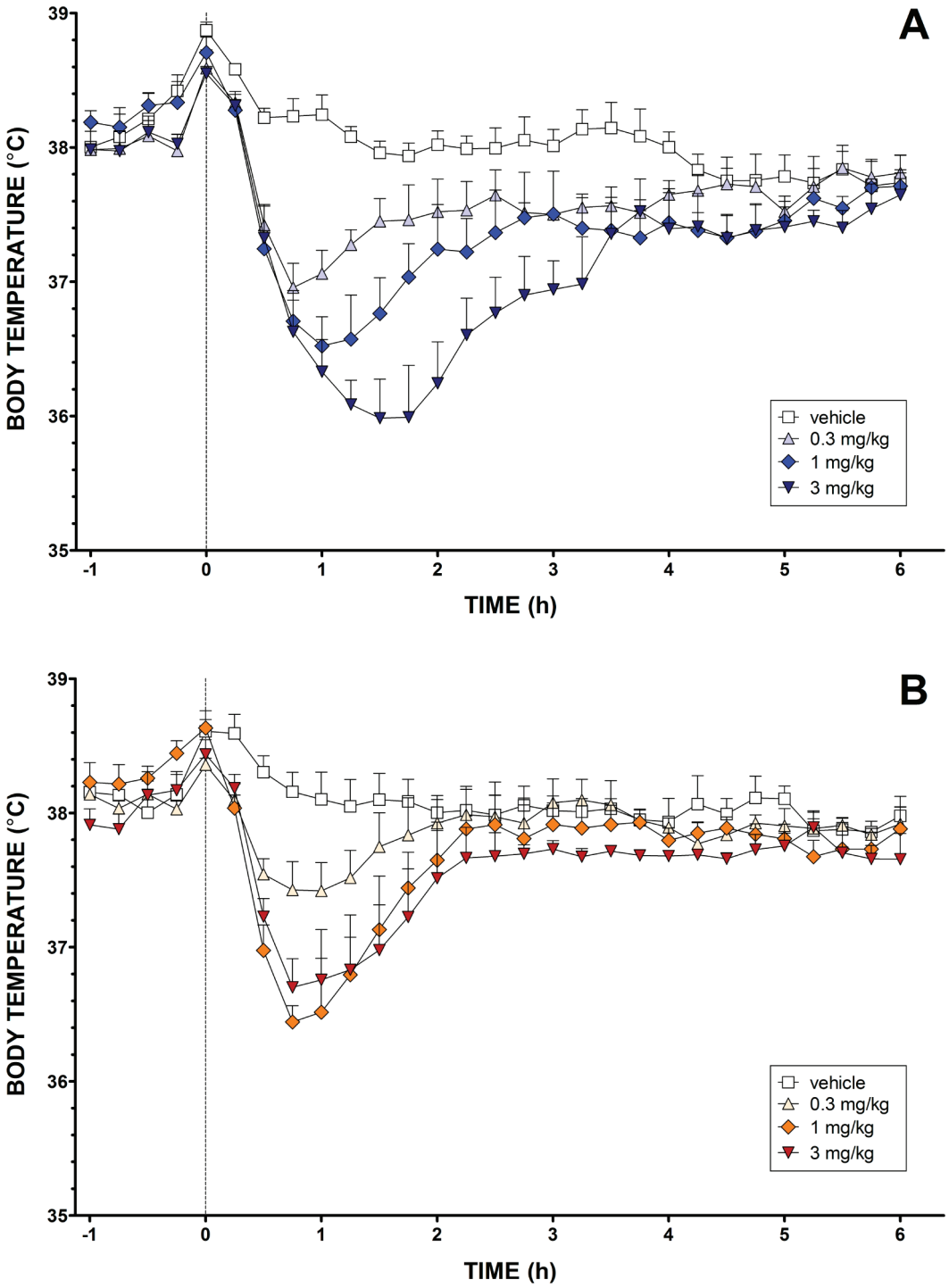

Figure 5. Effects of (A) AB-FUBINACA and (B) AB-PINACA on rat body temperature. Dashed line denotes time of intraperitoneal injection. Each point represents the mean ± SEM for three animals.

AB-PINACA-induced hypothermia (Figure 8B). These interpretations are confirmed by a statistical analysis of the areas between each drug treatment and baseline (Figure S13, Supporting Information). This suggests a CB_1-mediated hypothermic mechanism. Similar trends were observed for the reversal of AB-FUBINACA- or AB-PINACA-induced bradycardia by rimonabant but not SR144528; however, these differences did not reach significance (data not shown). This is likely due to a combination of the relatively smaller magnitude of SC-induced bradycardic effects and high variability of the heart rate data.

CONCLUSIONS

This study is the first to pharmacologically characterize the emergent class of recreational SC designer drugs based on indole and indazole scaffolds and featuring L-valinamide or L-*tert*-leucinamide side chains. Synthetic routes to identified SCs of forensic interest (AB-FUBINACA, ADB-FUBINACA, AB-PINACA, ADB-PINACA, 5F-AB-PINACA, 5F-ADB-PINACA,

DOI: 10.1021/acschemneuro.5b00112
ACS Chem. Neurosci. 2015, 6, 1546−1559

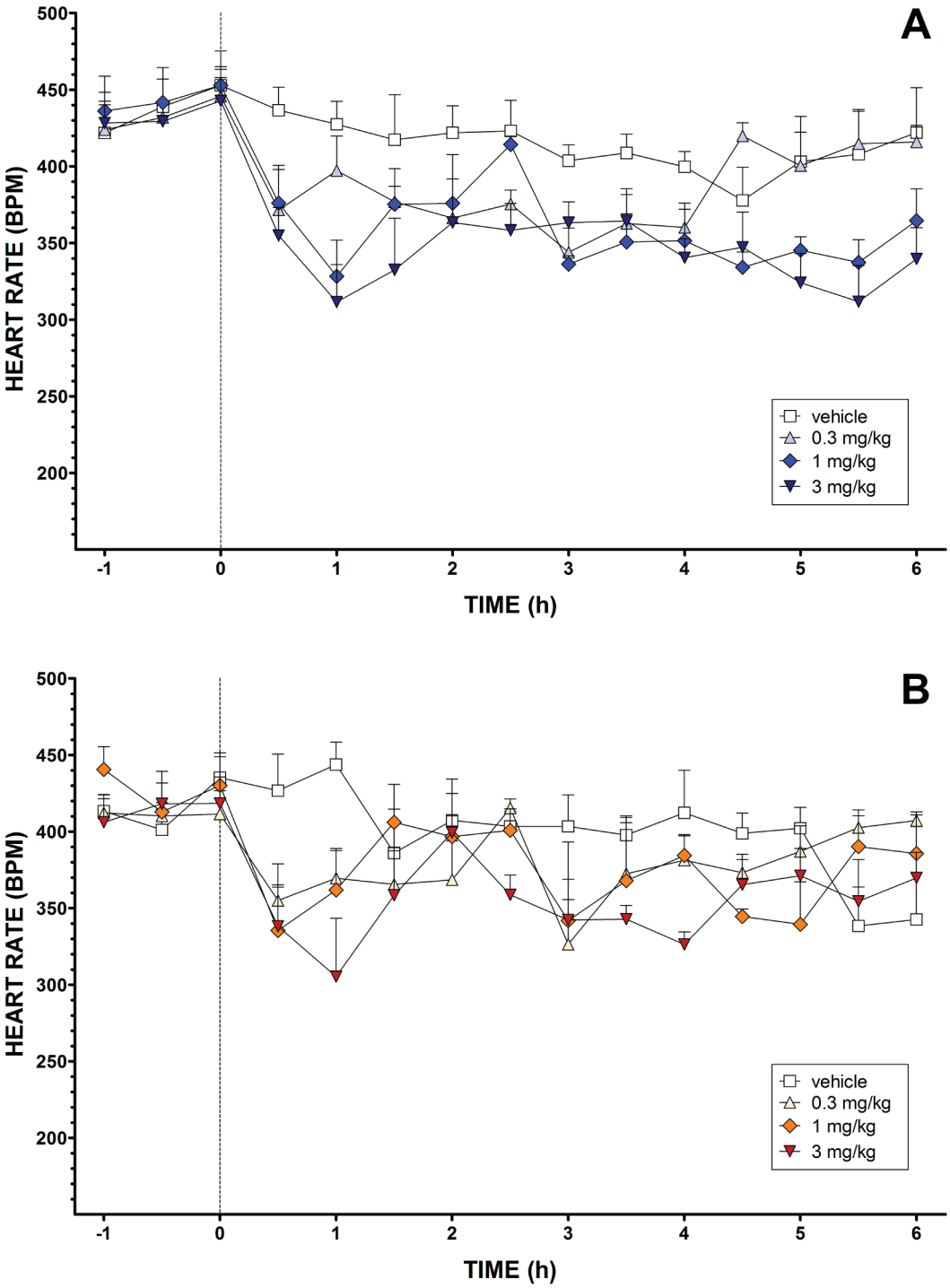

Figure 6. Effects of (A) AB-FUBINACA and (B) AB-PINACA on rat heart rate. Dashed line denotes time of intraperitoneal injection. Each point represents the mean ± SEM for three animals.

ADBICA, 5F-ADBICA), as well as several undetected analogues, were developed. These synthetic routes are general for 1-alkyl-1*H*-indazole-3-carboxamides and 1-alkyl-1*H*-indole-3-carboxamides and enable forensic chemists to proactively develop reference standards for structurally related SCs expected to appear in the future. All synthesized SCs acted as agonists of CB_1 and CB_2 receptors in a FLIPR membrane potential assay and thus are functional cannabinoids. Preliminary SARs suggest that L-*tert*-leucinamide derivatives possess greater potency at CB_1 receptors *in vitro* than the corresponding L-valinamide analogues. The most potent of these was 5F-ADB-PINACA. In rats, AB-FUBINACA and AB-PINACA were able to dose-dependently decrease body temperature and heart rate at doses of 0.3−3 mg/kg, indicating that these SCs are also cannabimimetic *in vivo*. AB-FUBINACA had more potent effects on body temperature than AB-PINACA. The hypothermic effects of AB-FUBINACA and AB-PINACA appear to be mediated through CB_1 receptors and could be reversed by pretreatment with CB_1 antagonist rimonabant but not CB_2 antagonist SR144528. Both *in vitro* and *in vivo* results confirm that all of the SCs explored have

DOI: 10.1021/acschemneuro.5b00112
ACS Chem. Neurosci. 2015, 6, 1546−1559

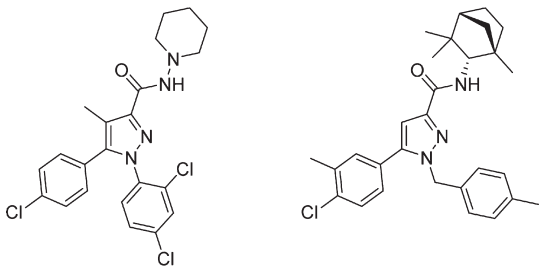

40 41

Figure 7. Structures of selective CB_1 receptor antagonist rimonabant (SR141176, **40**) and selective CB_2 receptor antagonist SR144528 (**41**).

cannabimimetic effects that parallel those of Δ^9-THC, but with greater potency.

METHODS

General Chemical Synthesis Details. All reactions were performed under an atmosphere of nitrogen unless otherwise specified. Commercially available chemicals were used as purchased. Flash column chromatography was performed using Merck Kieselgel 60 (230−400 mesh) silica gel. Melting points were measured in open capillaries using a Gallenkamp 5A 6797 melting point apparatus and are uncorrected. Nuclear magnetic resonance spectra were recorded at 300 K using a Bruker 300, 400, or 500 MHz spectrometer. The data are reported as chemical shift (δ ppm) relative to the residual protonated solvent resonance, relative integral, multiplicity (s = singlet, bs = broad singlet, d = doublet, t = triplet, q = quartet, quin. = quintet, m = multiplet, dd = doublet of doublets, dt = doublet of triplets, qd = quartet of doublets), coupling constants (J Hz), and assignment. Low-resolution mass spectra (LRMS) were recorded using electrospray ionization (ESI) recorded on a Finnigan LCQ ion trap spectrometer. HPLC analysis of the organic purity of the compounds submitted for *in vivo* testing (**4**−**7**) was conducted on a Waters e2695 separations module using a Waters Sunfire C18 5 μm, 2.1 × 150 mm column and detected using a Waters 2489 UV/vis detector set at 254 nm. Separation was achieved using water with 0.1% formic acid (solvent A) and acetonitrile with 0.1% formic acid (solvent B) at a flow rate of 0.2 mL/min and a gradient of 5% B for 1 min, then 5−100% B over 30 min. Elemental analysis was obtained from the Chemical Analysis Facility in the Department of Chemistry and Biomolecular Sciences, Macquarie University, Australia.

General Procedure A: Amidation of 1-Alkyl-1*H*-indazole-3-carboxylic Acids and 1-Alkylindole-3-carboxylic Acids. A solution of the appropriate carboxylic acid **29**, **30**, **31**, **37**, **38**, or **39** (7.5 mmol, 1.5 equiv) in DMF (50 mL) was treated with EDC (7.5 mmol, 1.5 equiv), HOBt (7.5 mmol, 1.5 equiv), DIPEA (25.5 mmol, 5.1 equiv), **19**·HCl, or **20** (5 mmol) and stirred for 24 h. The mixture was partitioned between and H_2O (100 mL) and EtOAc (50 mL), the layers were separated, and the aqueous layer was extracted with EtOAc (2 × 50 mL). The combined organic phases were dried ($MgSO_4$), and the solvent was evaporated under reduced pressure. The crude products were purified by flash chromatography and/or recrystallization.

*(S)-N-(1-Amino-3-methyl-1-oxobutan-2-yl)-1-(4-fluorobenzyl)-1H-indazole-3-carboxamide (AB-FUBINACA, **7**).* Treating **29** (1.20 g, 4.4 mmol) with **19** (1.04 g, 6.8 mmol) according to general procedure A gave, following purification by flash chromatography (hexane−EtOAc, 10:90), **7** (0.94 g, 57%) as a white solid. Recrystallization from *i*-PrOH−H_2O yielded material of analytical purity. mp 151−152 °C; ^{1}H NMR (500 MHz, $CDCl_3$): δ 8.33 (1H, d), 7.54 (1H, d, J = 8.9 Hz), 7.37 (1H, m), 7.32 (1H, m), 7.27 (1H, m), 6.39 (1H, bs), 5.69 (1H, bs), 5.57 (2H, s), 4.58 (1H, dd, J = 8.9 Hz, 6.8 Hz), 2.35 (1H, dq., J = 13.6 Hz, 6.8 Hz), 1.09 (6H, dd, J = 7.2 Hz, 5.1 Hz); ^{13}C NMR (125 MHz, $CDCl_3$): δ 173.7 (CO), 162.9 (CO), 162.6 (d, $^1J_{C-F}$ = 249.1 Hz, quat.), 140.9 (quat.), 137.3 (quat.), 131.7 (d, $^4J_{C-F}$ = 3.4 Hz, quat.), 129.2 (d, $^3J_{C-F}$ = 8.3 Hz, CH), 127.3 (CH), 123.4 (quat.), 123.1 (CH), 122.8 (CH), 116.0 (d, $^2J_{C-F}$ = 21.6 Hz, CH), 109.7 (CH), 58.0 (CH), 53.1 (CH_2), 30.8 (CH), 19.6 (CH_3), 18.4 (CH_3); ^{19}F NMR (470 MHz, $CDCl_3$): δ −113.9 ppm; LRMS (+ESI): m/z 323.9 ([M − $CONH_3$]$^+$, 100%), 351.8 ([M − NH_3]$^+$, 50%), 368.8 ([M + H]$^+$, 20%); Anal. Calcd for $C_{20}H_{21}N_4O_2F$: C, 65.20; H, 5.75; N, 15.21. Found: C, 65.28; H, 5.73; N, 15.21; HPLC purity: 99.2%.

*(S)-N-(1-Amino-3,3-dimethyl-1-oxobutan-2-yl)-1-(4-fluorobenzyl)-1H-indazole-3-carboxamide (ADB-FUBINACA, **8**).* Treating **29** (0.51 g, 1.9 mmol) with **20** (0.37 g, 2.8 mmol) according to general procedure A gave, following purification by flash chromatography (hexane−EtOAc, 10:90), **8** (0.22 g, 31%) as a white solid. mp 135−137 °C; NMR (500 MHz, $CDCl_3$): δ 8.21 (1H, d, J = 8.0 Hz), 7.72 (1H, d, J = 9.7 Hz), 7.27 (1H, m), 7.19 (1H, m), 7.14 (2H, dd, J = 8.3 Hz, 5.4 Hz), 6.99 (1H, bs), 6.93 (2H, t, J = 8.6 Hz), 6.16 (1H, bs), 5.52 (2H, s), 4.74 (1H, d, 9.6 Hz), 1.15 (1H, s), 1.11 (9H, s); ^{13}C NMR (125 Hz, $CDCl_3$): δ 173.5 (CO), 162.6 (CO), 162.6 (d, $^1J_{C-F}$ = 245.8 Hz, quat.), 140.9 (quat.), 137.3 (quat.), 131.8 (d, $^4J_{C-F}$ = 3.1 Hz, quat.), 129.1 (d, $^3J_{C-F}$ = 8.3 Hz, CH), 127.1 (CH), 123.4 (quat.), 123.0 (CH), 122.6 (CH), 115.9 (d, $^2J_{C-F}$ = 21.6 Hz, CH), 109.7 (CH), 59.7 (CH), 53.1 (CH_2), 34.8 (quat.), 26.9 (CH_3); ^{19}F NMR (470 MHz, $CDCl_3$): δ −113.9; LRMS (+ESI): m/z 337.9 ([M − $CONH_3$]$^+$, 100%), 365.8 ([M − NH_3]$^+$, 50%), 382.7 ([M + H]$^+$, 21%); Anal. Calcd for $C_{21}H_{23}N_4O_2F$: C, 65.95; H, 6.06; N, 14.65. Found: C, 65.38; H, 6.08; N, 14.38.

*(S)-N-(1-Amino-3-methyl-1-oxobutan-2-yl)-1-pentyl-1H-indazole-3-carboxamide (AB-PINACA, **9**).* Treating **30** (0.50 g, 2.2 mmol) with **19** (0.50 g, 3.3 mmol) according to general procedure A gave, following purification by flash chromatography (hexane−EtOAc, 50:50), **9** (0.44 g, 62%) as a white solid. Recrystallization from EtOAc−hexane yielded material of analytical purity. mp 125−126 °C; ^{1}H NMR (500 MHz, $CDCl_3$): δ 8.30 (1H, d, J = 8.3 Hz), 7.51 (1H, d, J = 8.8 Hz), 7.45−7.37 (2H, m), 7.26 (1H, m), 6.51 (1H, bs), 5.75 (1H, bs), 4.86 (1H, m), 4.38 (2H, t, J = 7.2 Hz), 2.36 (1H, dq., J = 13.6 Hz, 6.9 Hz), 1.94 (2H, quin., J = 7.4 Hz), 1.43−1.25 (4H, m), 1.08 (6H, m), 0.89 (3H, t, J = 7.1 Hz); ^{13}C NMR (125 MHz, $CDCl_3$): δ 173.9 (CO), 163.2 (CO), 141.0 (quat.), 136.5 (quat.), 126.8 (CH), 123.0 (quat.), 122.8 (CH), 122.7 (CH), 109.5 (CH), 57.9 (CH), 49.7 (CH_2), 30.7 (CH), 29.5 (CH_2), 29.1 (CH_2), 22.4 (CH_2), 19.6 (CH_3), 18.3 (CH_3), 14.0 (CH_3); LRMS (+ESI): m/z 258.9 ([M − $CONH_3$]$^+$, 100%), 313.9 ([M − NH_3]$^+$, 88%), 330.8 ([M + H]$^+$, 46%) ; Anal. Calcd for $C_{18}H_{26}N_4O_2$: C, 65.43; H, 7.93; N, 16.96. Found: C, 65.75; H, 8.11; N, 16.98; HPLC purity: 97.6%.

*(S)-N-(1-Amino-3,3-dimethyl-1-oxobutan-2-yl)-1-pentyl-1H-indazole-3-carboxamide (ADB-PINACA, **10**).* Treating **30** (0.50 g, 2.2 mmol) with **20** (0.43 g, 3.3 mmol) according to general procedure A gave, following purification by flash chromatography (hexane−EtOAc, 50:50), **10** (0.46 g, 63%) as a white solid. mp 135−137 °C; NMR (400 MHz, $CDCl_3$): δ 8.27 (1H, m), 7.71 (1H, d, J = 9.5 Hz), 7.45−7.36 (2H, m), 7.29−7.22 (1H, m), 6.65 (1H, bs), 5.80 (1H, bs), 4.69 (1H, d, J = 9.5 Hz), 4.38 (2H, t, J = 7.2 Hz), 1.95 (2H, quin., J = 7.2 Hz), 1.45−1.25 (4H, m), 1.16 (9H, s), 0.89 (3H, t, J = 7.0 Hz); ^{13}C NMR (100 MHz, $CDCl_3$): δ 173.2 (CO), 162.8 (CO), 141.0 (quat.), 136.5 (quat.), 126.7 (CH), 123.0 (quat.), 122.7 (CH), 122.5 (CH), 109.5 (CH), 59.7 (CH), 49.6 (CH_2), 34.8 (quat.), 29.5 (CH_2), 29.0 (CH_2), 26.9 (CH_3), 22.3 (CH_2), 14.0 (CH_3); LRMS (+ESI): m/z 299.9 ([M − $CONH_3$]$^+$, 100%), 327.9 ([M − NH_3]$^+$, 59%), 344.8 ([M + H]$^+$, 19%) ; Anal. Calcd for $C_{19}H_{28}N_4O_2$: C, 66.25; H, 8.19; N, 16.27. Found: C, 66.45; H, 8.40; N, 16.29.

*(S)-N-(1-Amino-3-methyl-1-oxobutan-2-yl)-1-(5-fluoropentyl)-1H-indazole-3-carboxamide (5F-AB-PINACA, **11**).* Treating **31** (1.10 g, 4.4 mmol) with **19** (1.00 g, 6.7 mmol) according to general procedure A gave, following purification by flash chromatography (hexane−EtOAc, 10:90), **11** (0.56 g, 37%). Recrystallization from EtOAc−hexane yielded material of analytical purity. mp 110−111 °C; ^{1}H NMR (500 MHz, $CDCl_3$): δ 8.30 (1H, m), 7.51 (1H, d, J = 8.9 Hz), 7.45−7.39 (2H, m), 7.27 (1H, m), 6.48 (1H, bs), 5.74 (1H, bs), 4.58 (1H, dd, J = 9.1 Hz, 6.7 Hz), 4.47 (1H, t, J = 6.0 Hz), 4.43−4.36 (3H, m), 2.35 (1H, dq, J = 13.6 Hz, 6.8 Hz), 2.00 (2H, m), 1.80−1.66 (2H, m), 1.51−1.41 (2H, m), 1.08 (6H, dd, J = 7.1 Hz, 5.2 Hz); ^{13}C

DOI: 10.1021/acschemneuro.5b00112
ACS Chem. Neurosci. 2015, 6, 1546−1559

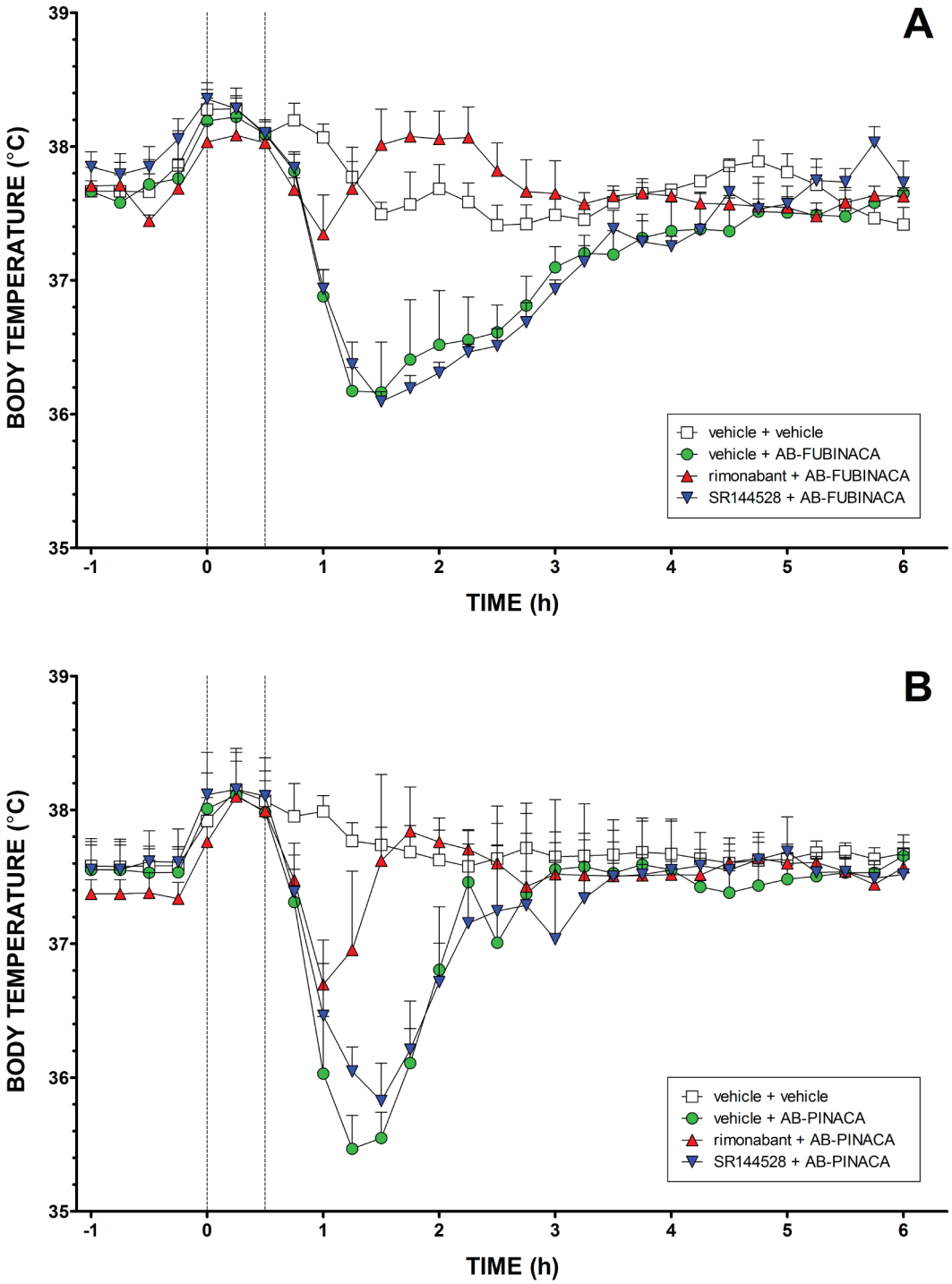

Figure 8. Effects of 3 mg/kg of (A) AB-FUBINACA or (B) AB-PINACA on rat body temperature following pretreatment (30 min prior) with vehicle, 3 mg/kg rimonabant (CB_1 antagonist), or 3 mg/kg SR144528 (CB_2 antagonist). The first dashed line denotes time of intraperitoneal injection of vehicle or antagonist. Second dashed line represents time of intraperitoneal injection of SC. Each point represents the mean ± SEM for three animals.

NMR (125 MHz, $CDCl_3$): δ 173.8 (CO), 163.0 (CO), 141.0 (quat.), 136.6 (quat.), 126.9 (CH), 122.99 (quat.), 122.91 (CH), 122.7 (CH), 109.4 (CH), 83.8 (CH_2, d, $^1J_{C-F}$ = 164.0 Hz), 57.9 (CH), 49.3 (CH_2), 30.7 (CH), 30.0 (CH_2, d, $^2J_{C-F}$ = 20.1 Hz), 29.4 (CH_2), 22.8 (CH_2, d, $^3J_{C-F}$ = 5.1 Hz), 19.6 (CH_3), 18.3 (CH_3); ^{19}F NMR (470 MHz, $CDCl_3$): δ −218.6; LRMS (ESI): *m/z* 303.9 ($[M - CONH_3]^+$, 100%), 331.9 ($[M - NH_3]^+$, 59%), 348.9 ($[M + H]^+$, 48%); Anal. Calcd for $C_{18}H_{25}N_4O_2F$: C, 62.05; H, 7.23; N, 16.08. Found: C, 61.96; H, 7.26; N, 15.83.

*(S)-N-(1-Amino-3,3-dimethyl-1-oxobutan-2-yl)-1-(5-fluoropentyl)-1H-indazole-3-carboxamide (5F-ADB-PINACA, **12**).* Treating **31** (0.40 g, 1.6 mmol) with **20** (0.32 g, 2.4 mmol) according to general procedure A gave, following purification by flash chromatography (hexane−EtOAc, 10:90), **12** (0.27 g, 47%) as a white solid. mp 135−137 °C; ^{1}H NMR (400 MHz, $CDCl_3$): δ 8.28 (1H, d, *J* = 8.2 Hz), 7.70 (1H, 9.4 Hz), 7.45−7.38 (2H, m), 7.30−7.23 (1H, m), 6.53 (1H, bs), 5.75 (1H, bs), 4.66 (1H, d, *J* = 9.6 Hz), 4.45−4.33 (3H, m), 2.18 (1H, bs), 2.00 (2H, quin., *J* = 7.7 Hz), 1.84−1.64 (2H, m), 1.48 (2H, m), 1.16 (9H, s); ^{13}C NMR (100 MHz, $CDCl_3$): δ 173.1 (CO), 162.8

DOI: 10.1021/acschemneuro.5b00112
ACS Chem. Neurosci. 2015, 6, 1546−1559

(CO), 141.0 (quat.), 136.8 (quat.), 126.9 (CH), 123.0 (quat.), 122.8 (CH), 122.7 (CH), 109.4 (CH), 83.9 (d, $^{1}J_{C-F}$ = 164.6, CH_2), 59.8 (CH), 49.4 (CH_2), 34.8 (quat.), 30.0 (d, $^{2}J_{C-F}$ = 19.7 Hz, CH_2), 29.4 (CH_2), 26.9 (CH_3), 22.8 (d, $^{3}J_{C-F}$ = 5.1 Hz, CH_2); ^{19}F NMR (376 MHz, $CDCl_3$): δ −218.3; LRMS (+ESI): m/z 317.9 ([M − $CONH_3$]$^+$, 100%), 345.9 ([M − NH_3]$^+$, 50%), 362.8 ([M + H]$^+$, 17%); Anal. Calcd for $C_{19}H_{27}N_4O_2F$: C, 62.96; H, 7.51; N, 15.46. Found: C, 63.12; H, 7.57; N, 15.29.

*(S)-N-(1-Amino-3-methyl-1-oxobutan-2-yl)-1-(4-fluorobenzyl)-1H-indole-3-carboxamide (AB-FUBICA, **13**).* Treating **37** (1.20 g, 4.5 mmol) with **19** (1.03 g, 6.7 mmol) according to general procedure A gave, following recrystallization from *i*-PrOH, **13** (1.28 g, 82%) as a white solid. mp 212−214 °C; ^{1}H NMR (300 MHz, DMSO-d_6): δ 8.53 (1H, bs), 8.11 (1H, m), 7.64−7.50 (2H, m), 7.48 (1H, bs), 7.41−7.27 (2H, m), 7.24−7.10 (4H, m), 7.07 (1H, bs), 5.45 (2H, m), 4.36 (1H, m), 2.09 (1H, m), 0.94 (6H, dd, J = 6.7 Hz, 2.7 Hz); ^{13}C NMR (75 MHz, DMSO-d_6): δ 173.5 (CO), 164.0 (CO), 161.6 (quat., d, $^{1}J_{C-F}$ = 243.18 Hz), 136.0 (CH), 133.7 (quat., d, $^{4}J_{C-F}$ = 2.87 Hz), 131.6 (quat.), 129.3 (d, $^{3}J_{C-F}$ = 8.1 Hz, CH), 126.7 (CH), 122.1 (CH), 121.1 (CH), 120.8 (CH), 115.5 (d, $^{2}J_{C-F}$ = 21.4 Hz, CH), 110.6 (quat.), 110.0 (CH), 57.4 (CH), 48.7 (CH_2), 30.4 (CH), 19.5 (CH_3), 18.5 (CH_3); ^{19}F NMR (282 MHz, DMSO-d_6): δ −114.9 (m); LRMS (+ESI): m/z 350.9 ([M − NH_3]$^+$, 100%), 367.8 ([M + H]$^+$, 70%); Anal. Calcd for $C_{21}H_{22}N_3O_2F$: C, 68.65; H, 6.04; N, 11.44. Found: C, 68.88; H, 6.15; N, 11.37; HPLC purity: 99.4%.

*(S)-N-(1-Amino-3,3-dimethyl-1-oxobutan-2-yl)-1-(4-fluorobenzyl)-1H-indole-3-carboxamide (ADB-FUBICA, **14**).* Treating **37** (0.63 g, 2.3 mmol) with **20** (0.46 g, 3.5 mmol) according to general procedure A gave, following purification by flash chromatography (hexane−EtOAc, 10:90), **14** (0.76 g, 86%) as a white solid. mp 107−108 °C; ^{1}H NMR (400 MHz, $CDCl_3$): δ 8.03 (1H, d, J = 7.7 Hz), 7.73 (1H, s), 7.31−7.20 (4H, m), 7.14−7.06 (2H, m), 6.99 (2H, t, J = 8.6 Hz), 6.77 (1H, d, J = 9.2 Hz), 6.54 (1H, bs), 5.71 (1H, bs), 5.27 (2H, s), 4.71 (1H, d, J = 9.2 Hz), 1.14 (9H, s); ^{13}C NMR (100 MHz, $CDCl_3$): δ 173.4 (CO), 165.0 (CO), 162.6 (d, $^{1}J_{C-F}$ = 247.2 Hz, quat.), 136.8 (CH), 132.0 (d, $^{4}J_{C-F}$ = 3.2 Hz, quat.), 131.8 (quat.), 128.8 (d, $^{3}J_{C-F}$ = 8.1 Hz, CH), 125.8 (quat.), 123.1 (CH), 122.1 (CH), 120.5 (CH), 116.6 (d, $^{2}J_{C-F}$= 21.6 Hz, CH), 111.4 (quat.), 110.7 (CH), 59.9 (CH), 50.1 (CH_2), 34.9 (quat.), 27.0 (CH_3); ^{19}F NMR (376 MHz, $CDCl_3$): δ −113.9; LRMS (+ESI): m/z 363.9 ([M − NH_3]$^+$, 100%), 381.8 ([M + H]$^+$, 42%); Anal. Calcd $C_{22}H_{24}N_3O_2F$: C, 69.27; H, 6.34; N, 11.02. Found: C, 69.68; H, 6.02; N, 10.95.

*(S)-N-(1-Amino-3-methyl-1-oxobutan-2-yl)-1-pentyl-1H-indole-3-carboxamide (AB-PICA, **15**).* Treating **38** (0.50 g, 2.2 mmol) with **19** (0.50, 3.3 mmol) according to general procedure A gave, following purification by flash chromatography (hexane−EtOAc, 10:90), **15** (0.58 g, 81%) as a white solid. mp 214−215 °C; ^{1}H NMR (400 MHz, DMSO-d_6): δ 8.25 (1H, s), 8.11 (1H, d, J = 7.7 Hz), 7.61−7.39 (3H, m), 7.20 (1H, m), 7.13 (1H, t, J = 7.6 Hz), 7.06 (1H, bs), 4.35 (1H, m), 4.19 (2H, m), 2.09 (1H, dq, J = 13.5 Hz, 6.8 Hz), 1.08 (2H, quin., J = 7.3 Hz), 1.39−1.19 (4H, m), 0.94 (6H, dd, J = 6.6 Hz, 3.1 Hz), 0.85 (3H, t, J = 7.0 Hz); ^{13}C NMR (100 MHz, DMSO-d_6): δ 173.6 (CO), 164.0 (CO), 136.1 (CH), 131.2 (quat.), 126.5 (quat.), 121.8 (CH), 121.0 (CH), 120.6 (CH), 110.3 (quat.), 109.3 (CH), 57.3 (CH), 45.8 (CH_2), 30.3 (CH), 29.3 (CH_2), 28.4 (CH_2), 21.7 (CH_2), 19.5 (CH_2), 18.5 (CH_3), 13.8 (CH_3); LRMS (+ESI): m/z 312.87 ([M − NH_2]$^+$, 100%), 329.80 ([M + H]$^+$, 60%); Anal. Calcd for $C_{19}H_{27}N_3O_2$: C, 69.27; H, 8.26; N, 12.76. Found: C, 69.21; H, 8.66; N, 12.55; HPLC purity: 99.1%.

*(S)-N-(1-Amino-3,3-dimethyl-1-oxobutan-2-yl)-1-pentyl-1H-indole-3-carboxamide (ADBICA, **16**).* Treating **38** (0.57 g, 2.5 mmol) with **20** (0.49 g, 3.7 mmol) according to general procedure A gave, following purification by flash chromatography (hexane−EtOAc, 10:90), **16** (0.64 g, 75%) as a white solid. mp 138−139 °C; ^{1}H NMR (400 MHz,$CDCl_3$): δ 8.01 (1H, m), 7.72 (1H, s), 7.38 (1H, m), 7.33−7.22 (2H, m), 6.74 (1H, d, J = 8.9 Hz), 6.60 (1H, bs), 5.71 (1H, bs), 4.73 (1H, d, J = 8.9 Hz), 4.11 (2H, t, J = 7.2 Hz), 1.85 (2H, m), 1.42−1.25 (4H, m), 1,15 (9H, s), 0.89 (3H, t, J = 7.0 Hz); ^{13}C NMR (100 MHz, $CDCl_3$): δ 173.5 (CO), 165.2 (CO), 136.8 (CH), 131.6 (quat.), 125.6 (quat.), 122.6 (CH), 121.8 (CH), 120.4 (CH), 110.6 (quat.), 110.4 (CH), 59.9 (CH), 47.1 (CH_2), 34.9 (quat.), 29.8 (CH_2), 29.1 (CH_2), 27.0 (CH_2), 22.4 (CH_3), 14.0 (CH_3); LRMS (+ESI): m/z 326.9 ([M − NH_3]$^+$, 100%), 343.9 ([M + H]$^+$, 31%); Anal. Calcd for $C_{20}H_{29}N_3O_2$: C, 69.94; H, 8.51; N, 12.23. Found: C, 70.23; H, 8.65; N, 12.17.

*(S)-N-(1-Amino-3-methyl-1-oxobutan-2-yl)-1-(5-fluoropentyl)-1H-indole-3-carboxamide (5F-AB-PICA, **17**).* Treating **39** (1.53 g, 6.5 mmol) with **19** (1.50 g, 9.8 mmol) according to general procedure A gave, following recrystallization from *i*-PrOH, **17** (1.56 g, 69%) as a white solid. mp 210−211 °C; ^{1}H NMR (400 MHz, DMSO-d_6): δ 8.25, (1H, s), 8.11, (1H, d, J = 7.8 Hz), 7.61−7.39 (3H, m), 7.25−7.10 (2H, m), 7.07 (1H, bs), 4.47 (1H, t, J = 6.0 Hz), 4.35 (2H, m), 4.21 (2H, m), 2.09 (1H, dq, J = 13.5 Hz, 6.8 Hz), 1.84 (2H, m), 1.67 (2H, m), 1.35 (2H, m), 0.93 (6H, dd, J = 6.5 Hz, 2.9 Hz); ^{13}C NMR (100 MHz, DMSO-d_6): δ 173.7 (CO), 164.1 (CO), 136.1 (CH), 131.3 (quat.), 126.5 (quat.), 121.9 (CH), 121.0 (CH), 120.7 (CH), 110.4 (quat.), 109.4 (CH), 83.7 (d, $^{1}J_{C-F}$ = 161.7 Hz, CH_2), 57.4 (CH), 45.78 (CH_2), 30.5 (CH), 29.5 (CH_2), 29.3 (d, $^{3}J_{C-F}$ = 3.8 Hz, CH_2), 22.2 (d, $^{2}J_{C-F}$ = 5.3 Hz, CH_2), 19.5 (CH_3), 18.5 (CH_3); ^{19}F NMR (376 MHz, DMSO-d_6): δ −216.86; LRMS (+ESI): m/z 330.9 ([M − NH_3]$^+$, 100%), 347.8 ([M + H]$^+$, 67%); Anal. Calcd for $C_{19}H_{26}N_3O_2F$: C, 65.68; H, 7.54; N, 12.09. Found: C, 65.83; H, 7.66; N, 11.99.

*(S)-N-(1-Amino-3,3-dimethyl-1-oxobutan-2-yl)-1-(5-fluoropentyl)-1H-indole-3-carboxamide (5F-ADBICA, **18**).* Treating **39** (1.14 g, 4.9 mmol) with **20** (0.95 g, 7.3 mmol) according to general procedure A gave, following purification by flash chromatography (hexane−EtOAc, 90:10), **18** (1.14 g, 65%) as a white solid. mp 130−131 °C; ^{1}H NMR (400 MHz, $CDCl_3$): δ 8.02 (1H, m), 7.71 (1H, s), 7.37 (1H, m), 7.32−7.23 (2H, m), 6.76 (1H, d, J = 9.2 Hz), 6.67 (1H, bs), 5.74 (1H, bs), 4.74 (1H, d, J = 9.2 Hz), 4.47 (2H, dt, $^{2}J_{H-F}$ = 48, $^{3}J_{H-H}$ = 6.0 Hz), 4.13 (2H, t, J = 7.1 Hz), 1.90 (2H, m), 1.70 (2H, m), 1.45 (2H, m), 1.15 (9H, s) ppm; ^{13}C NMR (100 MHz, $CDCl_3$): δ 173.5 (CO), 165.1 (CO), 136.7 (CH), 131.5 (quat.), 125.7 (quat.), 122.7 (CH), 121.8 (CH), 120.5 (CH), 110.8 (quat.), 110.3 (CH), 83.8 (d, $^{1}J_{C-F}$ = 164.8 Hz, CH_2), 59.9 (CH), 46.9 (CH_2), 34.9 (quat.), 30.1 (d, $^{2}J_{C-F}$ = 19.9 Hz, CH_2), 29.8 (CH_2), 27.0 (CH_3), 23.0 (d, $^{3}J_{C-F}$ = 5.1 Hz, CH_2); ^{19}F NMR (376 MHz, $CDCl_3$): δ −218.53; LRMS (+ESI): m/z 344.9 ([M − NH_3]$^+$, 100%), 361.8 ([M + H]$^+$, 26%); Anal. Calcd for $C_{20}H_{28}N_3O_2F$: C, 66.46; H, 7.81; N, 11.63. Found: C, 66.20; H, 7.94; N, 11.19.

*L-tert-Leucinamide (**20**).* To a solution of **23** (15.6 g, 59 mmol) in THF (150 mL) was added 10% Pd/C (3.0 g), and the mixture was stirred under an atmosphere of H_2 for 12 h. The suspension was filtered through a pad of Celite, and the filtrate was evaporated under reduced pressure. The resulting solid was recrystallized from EtOAc−hexane to yield **20** (4.74 g, 48%) as a white solid. mp 105−106 °C; ^{1}H NMR (500 MHz, DMSO-d_6): δ 7.17 (1H, bs), 6.81 (1H, bs), 3.35 (1H, bs), 2.79 (1H, s), 1.5 (2H, bs), 0.88 (9H, s); ^{13}C NMR (125 MHz, DMSO-d_6): δ 176.17 (CO), 62.83 (CH), 33.56 (quat.), 26.53 (CH_3); LRMS (+ESI): m/z 130.9 ([M + H]$^+$, 100%).

*N-Cbz-L-tert-leucine (**22**).* A cooled (0 °C) solution of L-*tert*-leucine (**21**, 10.0 g, 76 mmol) and 5 M aq. NaOH (15 mL, 75 mmol, 1.0 equiv) in H_2O (25 mL) was treated dropwise with benzyl chloroformate (12 mL, 84 mmol, 1.1 equiv) and 2 M aq. NaOH (42 mL, 84 mmol, 1.1 equiv), simultaneously. The mixture was warmed to rt and stirred for 2 h, and the pH was adjusted to 10 by the addition of sat. aq. $NaHCO_3$. The aqueous layer was washed with Et_2O (3 × 50 mL), acidified to pH 3 with 2 M aq. HCl, and extracted with Et_2O (4 × 50 mL). The combined organic phases were dried ($MgSO_4$), and the solvent was evaporated under reduced pressure to give a **22** (20 g, 99%) as a colorless oil. ^{1}H NMR (400 MHz, $CDCl_3$): δ 7.43−7.29 (5H, m), 5.78 (1H, bs), 5.36 (1H, d, J = 9.5 Hz), 5.12 (2H, m), 4.21 (1H, d, J = 9.5 Hz), 1.02 (9H, s); ^{13}C NMR (100 MHz, $CDCl_3$): δ 176.0 (CO), 156.4 (CO), 136.3 (quat.), 128.7 (CH), 128.4 (CH), 128.3 (CH), 67.4 (CH), 62.3 (CH_2), 34.7 (quat.), 26.6 (CH_3); LRMS (−ESI): m/z 528.9 ([2M − H]$^-$, 100%), 263.9 ([M − H]$^-$, 76%).

*N-Cbz-L-tert-leucinamide (**23**).* To a solution of **22** (20.2 g, 76 mmol) in DMF (400 mL) were added NH_4Cl (4.95 g, 93 mmol, 1.2 equiv), Et_3N (32 mL, 229 mmol, 3.0 equiv), HOBt (13.2 g, 98 mmol,

DOI: 10.1021/acschemneuro.5b00112
ACS Chem. Neurosci. 2015, 6, 1546−1559

1.3 equiv), and EDC·HCl (18.8 g, 98 mmol, 1.3 equiv). After stirring for 16 h, the reaction was quenched with sat. aq. $NaHCO_3$ (100 mL), and the aqueous phase was extracted with EtOAc (3 × 200 mL). The combined organic phases were washed with H_2O (3 × 200 mL) and brine (100 mL) and dried ($MgSO_4$), and the solvent removed under reduced pressure. The obtained crude solid was recrystallized from EtOAc−hexane to give **23** (16.9 g, 84%) as a white solid. mp 138−140 °C; ^{1}H NMR (300 MHz, $CDCl_3$): δ 7.40−7.29 (5H, m), 6.11 (1H, bs), 5.75 (1H, bs), 5.62 (1H, d, J = 9.5 Hz), 5.08 (2H, m), 4.03 (1H, d, J = 9.5 Hz), 1.01 (9H, s); ^{13}C NMR (75 MHz, $CDCl_3$): δ 175.1 (CO), 156.7 (CO), 136.4 (quat.), 128.7 (CH), 128.3 (CH), 128.1 (CH), 67.2 (CH), 62.4 (CH_2), 34.4 (quat.), 26.6 (CH_3); LRMS (+ESI): m/z 264.8 ([M + H]$^+$, 100%).

*Methyl 1H-Indazole-3-carboxylate (**25**).* A solution of indazole-3-carboxylic acid (**24**, 2.00 g, 12.3 mmol) in MeOH (30 mL) was treated with conc. H_2SO_4 (2 mL) and heated at reflux for 4 h. The mixture was concentrated *in vacuo* and dissolved in EtOAc (50 mL). The organic phase was washed with sat. aq. $NaHCO_3$ (20 mL), H_2O (20 mL), and brine (20 mL) and dried ($MgSO_4$), and the solvent was evaporated under reduced pressure. The crude solid was recrystallized from EtOAc−hexane to give **25** (1.65 g, 76%) as a white solid. mp 168−170 °C; ^{1}H NMR (300 MHz, $CDCl_3$): δ 8.23 (1H, m), 7.77 (1H, m), 7.49 (1H, m), 7.35 (1H, m), 4.08 (3H, s); ^{13}C NMR (75 MHz, $CDCl_3$): δ 163.41 (CO), 141.42 (quat.), 136.27 (quat.), 127.73 (CH), 123.60 (quat,), 122.50 (CH), 121.92 (CH), 111.35 (CH), 52.31 (CH_3); LRMS (ESI): m/z 176.8 ([M + H]$^+$, 100%).

General Procedure B: Alkylation of Methyl 1*H*-Indazole-3-carboxylate. To a cooled (0 °C) solution of **25** (2.17 g, 12.3 mmol) in THF (60 mL) was added *t*-BuOK (1.52 g, 13.5 mmol, 1.1 equiv). The mixture was warmed to rt, stirred for 1 h, and cooled (0 °C), and the appropriate bromoalkane (19.7 mmol, 1.6 equiv) was added dropwise. The mixture was warmed to rt and stirred for 48 h, and H_2O (60 mL) was added. The layers were separated, the aqueous layer was extracted with EtOAc (2 × 50 mL), and the combined organic phases were washed with H_2O (3 × 50 mL) and brine (20 mL) and dried ($MgSO_4$), and the solvent was evaporated under reduced pressure.

*Methyl 1-(4-Fluorobenzyl)-1H-indazole-3-carboxylate (**26**).* Treating **25** (2.30 g, 13.1 mmol) with 4-fluorobenzyl bromide (1.78 mL, 14.3 mmol) according to general procedure B gave, following purification by flash chromatography (hexane−EtOAc 70:30), **26** (2.50 g, 67%) as a clear glass-like solid. ^{1}H NMR (300 MHz, $CDCl_3$): δ 8.24 (1H, dt, J = 8.1 Hz, 1.1 Hz), 7.44−7.27 (3H, m), 7.25−7.16 (2H, m), 7.03−6.93 (2H, m), 5.67 (2H, s), 4.05 (3H, s); ^{13}C NMR (75 MHz, $CDCl_3$): δ 163.1 (CO), 162.6 (d, $^1J_{C-F}$ = 247.3 Hz, quat.), 140.6 (quat.), 135.3 (quat.), 131.6 (d, $^4J_{C-F}$ = 3.0 Hz, quat.), 129.2 (d, $^3J_{C-F}$ = 8.1 Hz, CH), 127.3 (CH), 124.3 (CH), 123.5 (quat.), 122.5 (CH), 116.0 (d, $^2J_{C-F}$ = 22.1 Hz, CH), 110.0 (CH), 53.5 (CH_2), 52.3 (CH_3); ^{19}F NMR (282 MHz, $CDCl_3$): δ −113.8 (m); LRMS (+ESI): m/z 284.8 ([M + H]$^+$, 100%).

*Methyl 1-Pentyl-1H-indazole-3-carboxylate (**27**).* Treating **25** (1.57 g, 8.9 mmol) with 1-bromopentane (1.75 mL, 14.1 mmol) according to general procedure B gave, following purification by flash chromatography (hexane−EtOAc 70:30), **26** (1.46 g, 77%) as a clear glass-like solid. ^{1}H NMR (400 MHz, $CDCl_3$): δ 8.22 (1H, m), 7.50−7.39 (2H, m), 7.30 (1H, m), 4.47 (2H, t, J = 7.4 Hz), 4.04 (3H, s), 1.97 (2H, quin., J = 7.2 Hz), 1.40−1.25 (4H, m), 0.88 (3H, m); ^{13}C NMR (100 MHz, $CDCl_3$): δ 163.0 (CO), 140.7 (quat.), 134.9 (quat.), 126.8 (CH), 123.9 (quat.), 123.1 (CH), 122.5 (CH), 109.8 (CH), 61.1 (CH_2), 50.1 (CH_3), 29.7 (CH_2), 29.1 (CH_2), 22.4 (CH_2), 14.0 (CH_3); LRMS (+ESI): m/z 246.9 ([M + H]$^+$, 100%).

*Methyl 1-(5-Fluoropentyl)-1H-indazole-3-carboxylate (**28**).* Treating **25** (2.30 g, 13.1 mmol) with 1-bromo-5-fluoropentane (2.42 g, 14.3 mmol) according to general procedure B gave, following purification by flash chromatography (hexane−EtOAc 70:30), **28** (2.39 g, 69%) as a colorless glass-like solid. ^{1}H NMR (400 MHz, $CDCl_3$): δ 8.24 (1H, m), 7.50−7.41 (2H, m), 7.32 (1H, m), 4.54−4.43 (3H, m), 4.35 (1H, t, J = 5.9 Hz), 4.04 (3H, s), 2.03 (2H, quin., J = 7.6 Hz), 1.80- 1.64 (2H, m), 1.52−1.41 (2H, m); ^{13}C NMR (100 MHz, $CDCl_3$): δ 163.2 (CO), 140.7 (quat.), 134.8 (quat.), 127.0 (CH), 123.9 (CH), 123.3 (quat.), 122.5 (CH), 109.7 (CH), 83.8 (d, $^1J_{C-F}$ = 165.1 Hz, quat.), 52.2 (CH_2), 49.9 (CH_3), 30.1 (d, $^2J_{C-F}$ = 19.7, CH_2), 29.6 (CH_2), 22.9 (d, $^3J_{C-F}$ = 5.1 Hz, CH_2); ^{19}F NMR (376 MHz, $CDCl_3$): δ −218.7; LRMS (+ESI): m/z 264.8 ([M + H]$^+$, 100%).

General Procedure C: Hydrolysis of Methyl 1-Alkyl-1*H*-indazole-3-carboxylates. A solution of the appropriate methyl 1-alkyl-1*H*-indazole-3-carboxylate (12.3 mmol) in MeOH (100 mL) was treated with 1 M aq. NaOH (18.5 mL, 18.5 mmol, 1.5 equiv) and stirred for 24 h. The solvent was reduced *in vacuo*, and the residue was dissolved in H_2O, acidified with 1 M aq. HCl, and extracted with EtOAc (2 × 50 mL). The organic phase was dried ($MgSO_4$), and the solvent was evaporated under reduced pressure to afford the free acid, which was used in the subsequent coupling step without further purification.

*1-(4-Fluorobenzyl)-1H-indazole-3-carboxylic Acid (**29**).* Subjecting **26** (2.30 g, 8.1 mmol) to general procedure C gave **29** (2.10 g, 96%) as a white solid. mp 200−203 °C; ^{1}H NMR (300 MHz, DMSO-d_6): δ 13.02 (1H, bs), 8.09 (1H, m), 8.47 (1H, m), 7.47 (1H, m), 7.39−7.27 (3H, m), 7.16 (2H, m), 5.76 (2H, s); ^{13}C NMR (75 MHz, DMSO-d_6): δ 163.4 (CO), 161.7 (d, $^1J_{C-F}$ = 244.8 Hz, quat.), 140.4 (quat.), 135.1 (quat.), 132.9 (d, $^4J_{C-F}$ = 2.8 Hz, quat.), 129.7 (d, $^3J_{C-F}$ = 8.3 Hz, CH), 126.9, 123.2, 123.0, 121.6, 115.5 (d, $^2J_{C-F}$ = 21.3 Hz, CH), 110.7 (CH), 51.8 (CH_2); ^{19}F NMR (282 MHz, $CDCl_3$): δ −114.6; LRMS (+ESI): m/z 270.9 ([M + H]$^+$, 100%).

*1-Pentyl-1H-indazole-3-carboxylic Acid (**30**).* Subjecting **27** (0.96 g, 3.9 mmol) to general procedure C gave **30** (0.65 g, 72%) as a white solid. mp 81−82 °C; ^{1}H NMR (300 MHz, $CDCl_3$): δ 9.85 (1H, bs), 8.26 (1H, m), 7.56−7.41 (2H, m), 7.34 (1H, m), 4.49 (2H, t, J = 7.3 Hz), 1.99 (2H, m), 1.45−1.25 (4H, m), 0.88 (3H, t, J = 6.9 Hz); ^{13}C NMR (75 MHz, $CDCl_3$): δ 167.3 (CO), 140.9 (quat.), 134.0 (quat.), 127.0 (CH), 124.0 (quat.), 123.6 (CH), 122.5 (CH), 109.9 (CH), 50.2 (CH_2), 29.6 (CH_2), 29.0 (CH_2), 22.4 (CH_2), 14.0 (CH_3); LRMS (+ESI): m/z 323.9 ([M + H]$^+$, 100%).

*1-(5-Fluoropentyl)-1H-indazole-3-carboxylic Acid (**31**).* Subjecting **28** (2.2 g, 8.3 mmol) to general procedure C gave **31** (1.9 g, 91%) as a white solid. mp 80−82 °C; ^{1}H NMR (300 MHz, $CDCl_3$): δ 9.88 (1H, bs), 8.27 (1H, m), 7.55−7.43 (2H, m), 7.36 (1H, m), 4.60−4.45 (3H, m), 4.34 (1H, t, J = 5.9 Hz), 2.06 (2H, m), 1.86−1.62 (2H, m), 1.58−1.39 (2H, m); ^{13}C NMR (75 MHz, $CDCl_3$): δ 167.4 (CO), 140.2 (quat.), 134.2 (quat.), 127.2 (CH), 124.0 (CH), 123.7 (CH), 122.5 (quat.), 109.8 (CH), 83.8 (d, $^1J_{C-F}$ = 165.1 Hz, CH_2), 50.0 (CH_2), 30.1 (d, $^2J_{C-F}$ = 19.8 Hz, CH_2), 29.5 (CH_2), 22.8 (d, $^3J_{C-F}$ = 4.9 Hz, CH_2); ^{19}F NMR (282 MHz, $CDCl_3$): δ −218.6; LRMS (+ESI): m/z 187.1 (100%), 250.9 ([M]$^+$, 49%).

General Procedure D: One-Pot Synthesis of 1-Alkyl-3-(trifluoroacetyl)indoles. A cooled (0 °C) suspension of NaH (60% dispersion in mineral oil, 0.68 g, 17.1 mmol, 2.0 equiv) in DMF (10 mL) was treated with a solution of indole (**33**, 1.00 g, 8.5 mmol) in DMF (2 mL), warmed to rt, and stirred for 10 min. The mixture was cooled to 0 °C, treated slowly with the appropriate bromoalkane (1.05 equiv), warmed to rt, and stirred for 1 h. The solution was cooled to 0 °C, treated with $(CF_3CO)_2O$ (3.00 mL, 21.3 mmol, 2.5 equiv), warmed to rt, and stirred for 1 h. The mixture was poured onto ice−water (120 mL) and stirred vigorously. The mixture was filtered, and the precipitate was dried to give the crude product as a red solid, which was used in the following step without purification.

*1-(4-Fluorobenzyl)-3-(trifluoroacetyl)indole (**34**).* Subjecting 4-fluorobenzyl bromide (1.13 mL, 9.0 mmol) to general procedure D gave **34** as a red crystalline solid (2.72 g, 100%). mp 83−86 °C; ^{1}H NMR (400 MHz, $CDCl_3$): δ 8.43 (1H, m), 7.96 (1H, m), 7.38 (1H, m), 7.43−7.29 (2H, m), 7.22−7.12 (2H, m), 7.11−7.00 (2H, m), 5.38 (2H, s); ^{13}C NMR (100 MHz, $CDCl_3$): δ 175.1 (q, $^2J_{C-F}$ = 34.9 Hz, CO), 162.9 (d, $^1J_{C-F}$ = 247.5 Hz, quat.), 137.5 (q, $^3J_{C-F}$ = 4.9 Hz, CH), 136.9 (quat.), 130.7 (d, $^3J_{C-F}$ = 3.4 Hz, quat.), 129.7 (d, $^2J_{C-F}$ = 8.1 Hz, CH), 127.3 (quat.), 125.0 (quat.), 124.3 (CH), 123.0 (CH), 117.1 (q, $^1J_{C-F}$ = 291.8 Hz, quat.), 116.4 (d, $^2J_{C-F}$ = 22.2 Hz, CH), 110.8 (CH), 110.2 (CH), 50.8 (CH_2); ^{19}F NMR (282 MHz, $CDCl_3$): δ −112.9 (m), −72.3; LRMS (+ESI): m/z 321.9 ([M + H]$^+$, 100%).

*1-Pentyl-3-(trifluoroacetyl)indole (**35**).* Subjecting 1-bromopentane (1.11 mL, 8.96 mmol) to general procedure D gave **35** as a red

DOI: 10.1021/acschemneuro.5b00112
ACS Chem. Neurosci. 2015, 6, 1546−1559

crystalline solid (2.41 g, 100%). mp 56−57 °C; ^{1}H NMR (400 MHz, $CDCl_3$): δ 8.42 (1H, m), 7.93 (1H, d, J = 1.5 Hz), 7.47−7.33 (3H, m), 4.20 (2H, t, J = 7.21), 1.93 (2H, quin., J = 7.16 Hz), 1.46−1.31 (4H, m), 0.92 (3H, t, J = 7.02 Hz); ^{13}C NMR (75 MHz, $CDCl_3$): δ 174.9 (q, $^2J_{C-F}$ = 34.7 Hz, CO), 137.4 (q, $^3J_{C-F}$ = 4.9 Hz, CH), 136.8 (quat.), 127.3 (quat.), 124.6 (quat.), 124.0 (CH), 122.9 (CH), 117.3 (q, $^1J_{C-F}$ = 291.5 Hz, quat.), 110.5 (CH), 109.6 (CH), 47.8 (CH_2), 29.6 (CH_2), 29.0 (CH_2), 22.3 (CH_2), 14.0 (CH_3); ^{19}F NMR (376 MHz, $CDCl_3$): δ −72.2; LRMS (ESI): m/z 284.0 ([M + H]$^+$, 100%).

*1-(5-Fluoropentyl)-3-(trifluoroacetyl)indole (**36**).* Subjecting 1-bromo-5-fluoropentane (1.51 g, 9.0 mmol) to general procedure D gave **36** as a red solid (2.59 g, 100%). mp 55−57 °C; ^{1}H NMR (500 MHz, $CDCl_3$): δ 8.41 (1H, m), 7.93 (1H, m), 7.46−7.32 (3H, m), 4.45 (2H, dt, $^2J_{H-F}$ = 45, $^3J_{H-H}$ = 5.8 Hz), 4.23 (2H, t, J = 7.2 Hz), 1.99 (2H, m), 1.75 (2H, m), 1.52 (2H, m); ^{13}C NMR (125 MHz, $CDCl_3$): δ 174.9 (q, $^2J_{C-F}$ = 34.8 Hz, CO), 137.4 (q, $^3J_{C-F}$ = 5.0 Hz, CH), 136.7 (quat.), 127.3 (quat.), 124.7 (CH), 124.1 (CH), 122.9 (CH), 117.2 (q, $^1J_{C-F}$ = 291.3 Hz, quat.), 110.4 (CH), 109.7 (quat.), 83.7 (d, $^1J_{C-F}$ = 165.1 Hz, CH_2), 47.7 (CH_2), 30.0 (d, $^2J_{C-F}$ 19.9 Hz, CH_2), 29.5 (CH_2), 23.0 (d, $^3J_{C-F}$ = 4.5 Hz, CH_2); ^{19}F NMR (470 MHz, $CDCl_3$): δ −72.2, −218.9; LRMS (+ESI): m/z 302.0 ([M + H]$^+$, 100%).

General Procedure E: Synthesis of 1-Alkylindole-3-carboxylic Acids. To a refluxing solution of KOH (1.57 g, 28.1 mmol, 3.3 equiv) in MeOH (3 mL) was added, portionwise, a solution of the appropriate crude 1-alkyl-3-trifluoroacetylindole (8.5 mmol) in toluene (7 mL). After heating at reflux for 2 h, the mixture was cooled to ambient temperature, and H_2O (30 mL) was added. The layers were separated, and the organic layer was extracted with 1 M aq. NaOH (8 mL). The combined aqueous phases were acidified to pH 1 with 10 M aq. HCl, extracted with Et_2O (3 × 10 mL), and dried ($MgSO_4$), and the solvent was removed under reduced pressure. The crude solid was recrystallized from *i*-PrOH to give the appropriate 1-alkylindole-3-carboxylic acid as colorless crystals.

*1-(4-Fluorobenzyl)indole-3-carboxylic Acid (**37**).* Subjecting **34** (2.74 g, 8.5 mmol) to general procedure E gave **37** (1.51 g, 66%) as a colorless crystalline solid. mp 205−208 °C; ^{1}H NMR (400 MHz, DMSO-d_6): δ 8.22 (1H, s), 8.02 (1H, m), 7.54 (1H, m), 7.40−7.31 (2H, m), 7.24−7.11 (4H, m), 5.48 (2H, s); ^{13}C NMR (100 MHz, DMSO-d_6): δ 165.5 (CO), 161.6 (d, $^1J_{C-F}$ = 243.3 Hz, quat.), 136.2 (CH), 135.4 (quat.), 133.4 (d, $^3J_{C-F}$ = 3.2 Hz, quat.), 129.5 (d, $^3J_{C-F}$ = 8.3 Hz, CH), 126.6 (quat.), 122.4 (CH), 121.4 (CH), 120.9 (CH), 115.4 (CH, d, $^2J_{C-F}$ = 21.7), 111.0 (CH), 107.0 (quat.), 48.7 (CH_2) ppm; ^{19}F NMR (282 MHz, DMSO-d_6) δ −114.80 (m) ppm; LRMS (+ESI): m/z 283.9 (100%), 269.9 ([M + H]$^+$, 10%).

*1-Pentylindole-3-carboxylic Acid (**38**).* Subjecting **35** (2.00 g, 7.1 mmol) to general procedure E gave **38** (0.88 g, 54%) as a colorless crystalline solid. mp 101−102 °C (lit mp 106−108 °C);[28] ^{1}H NMR (300 MHz, $CDCl_3$): δ 9.87 (1H, bs), 8.26 (1H, m), 7.93 (1H, s), 7.39 (1H, m). 7.35−7.27 (2H, m), 4.17 (2H, t, J = 7.1 Hz), 1.90 (2H, quin., J = 7.1 Hz), 1.46−1.25 (4H, m), 0.91 (3H, t, J = 6.8 Hz); ^{13}C NMR (75 MHz, $CDCl_3$): δ 170.7 (CO), 136.9 (CH), 135.6 (quat.), 127.2 (quat.), 123.0 (quat.), 122.3 (CH), 122.1 (CH), 110.2 (CH), 106.4 (CH), 47.3 (CH_2), 29.7 (CH_2), 29.1 (CH_2), 22.4 (CH_2), 14.0 (CH_3); LRMS (+ESI): m/z 245.9 (100%), 231.9 ([M + H]$^+$, 16%).

*1-(5-Fluoropentyl)indol-3-carboxylic Acid (**39**).* Subjecting **36** (2.57 g, 8.5 mmol) to general procedure E gave **39** (1.36 g, 68%) as a colorless crystalline solid. mp 117−118 °C; ^{1}H NMR (400 MHz, $CDCl_3$): δ 8.26 (1H, m), 7.93 (1H, s), 7.38 (1H, m), 7.35−7.28 (2H, m), 4.43 (2H, dt, $^2J_{H-F}$ = 48, $^3J_{H-H}$ = 5.9 Hz), 4.19 (2H, t, J = 7.1 Hz), 1.95 (2H, m), 1.73 (2H, m), 1.48 (2H, m); ^{13}C NMR (100 MHz, $CDCl_3$): δ 170.8 (CO), 136.8 (CH), 135.5 (quat.), 127.2 (quat.), 123.1 (CH), 122.3 (CH), 122.1 (CH), 110.1 (CH), 106.6 (quat.), 83.8 (d, $^1J_{C-F}$ = 164.9 Hz, CH_2), 47.2 (CH_2), 30.1 (d, $^2J_{C-F}$ = 20.0 Hz, CH_2), 29.7 (CH_2), 23.0 (d, $^3J_{C-F}$ = 5.0 Hz, CH_2); ^{19}F NMR (376 MHz, $CDCl_3$): δ −218.6; LRMS (+ESI): m/z 263.9 (100%), 249.9 ([M + H]$^+$, 18%).

***In Vitro* Pharmacological Assessment of SCs.** Mouse AtT-20 neuroblastoma cells stably transfected with human CB_1 or human CB_2 have been previously described[14,36,41] and were cultured in Dulbecco's modified Eagle's medium (DMEM) containing 10% fetal bovine serum (FBS), 100 U penicillin/streptomycin, and 300 μg/mL G418. Cells were passaged at 80% confluence, as required. Cells for assays were grown in 75 cm^2 flasks and used at 90% confluence. The day before the assay, cells were detached from the flask with trypsin/EDTA (Sigma) and resuspended in 10 mL of Leibovitz's L-15 media supplemented with 1% FBS, 100 U penicillin/streptomycin, and 15 mM glucose (membrane potential assay and Ca5 calcium assay). The cells were plated in a volume of 90 μL in black-walled, clear-bottomed 96-well microplates (Corning) that had been precoated with poly-L-lysine (Sigma, Australia). Cells were incubated overnight at 37 °C in ambient CO_2.

Membrane potential was measured using a FLIPR membrane potential assay kit (blue) from Molecular Devices, as described previously.[42] The dye was reconstituted with assay buffer of the following composition (mM): NaCl 145, HEPES 22, Na_2HPO_4 0.338, $NaHCO_3$ 4.17, KH_2PO_4 0.441, $MgSO_4$ 0.407, $MgCl_2$ 0.493, $CaCl_2$ 1.26, and glucose 5.56 (pH 7.4, osmolarity 315 ± 5). Prior to the assay, cells were loaded with 90 μL/well of the dye solution without removal of the L-15, giving an initial assay volume of 180 μL/well. Plates were then incubated at 37 °C at ambient CO_2 for 45 min. Fluorescence was measured using a FlexStation 3 (Molecular Devices) microplate reader, with cells excited at a wavelength of 530 nm and emission measured at 565 nm. Baseline readings were taken every 2 s for at least 2 min, at which time either drug or vehicle was added in a volume of 20 μL. The background fluorescence of cells without dye or dye without cells was negligible. Changes in fluorescence were expressed as a percentage of baseline fluorescence after subtraction of the changes produced by vehicle addition, which was less than 2% for drugs dissolved in assay buffer or DMSO. The final concentration of DMSO was not more than 0.1%.

Data were analyzed with PRISM (GraphPad Software Inc., San Diego, CA), using four-parameter nonlinear regression to fit concentration−response curves. In all plates, a maximally effective concentration of CP 55,940 was added to allow for normalization between assays.

***In Vivo* Pharmacological Assessment of SCs.** Four cohorts of 3−4 adult male Wistar rats (Animal Resources Centre, Perth, Australia) initially weighing between 168 and 186 g were used for biotelemetric assessment of body temperature and heart rate changes following each compound or following either compound administered with a CB_1 and CB_2 antagonist. The rats were singly housed in an air-conditioned testing room (22 ± 1 °C) on a 12 h reverse light/dark cycle (lights on from 21:00 to 09:00). Standard rodent chow and water were provided *ad libitum*. All experiments were approved by The University of Sydney Animal Ethics Committee.

Biotelemetry transmitters (TA11CTA-F40, Data Sciences International, St. Paul, MN) were implanted as previously described.[14,36] Briefly, following anesthetization (isoflurane, 3% induction, 2% maintenance), a rostro-caudal incision was made along the midline of the abdomen, and a biotelemetry transmitter (TA11CTA-F40, Data Sciences International, St. Paul, MN) was placed in the peritoneal cavity according to the manufacturer's protocol. The wound was sutured, and the rats were allowed 1 week of recovery before data collection.

The rats were habituated over multiple days to injections of vehicle (5% EtOH, 5% Tween 80, 90% physiological saline) at a set time of day (11:00 am). The first two cohorts then received injections of each compound at the same time of day in an ascending dose sequence (0.1, 0.3, 1, 3 mg/kg). This ascending sequence reduces the risk posed to the animals in assessing hitherto untested compounds, and the use of multiple cohorts limits the potential development of tolerance to the compound. Two washout days were given between each dose. If only a modest or negligible hypothermic response was seen at 3 mg/kg, then a further 10 mg/kg dose of the compound was given. At least two washout days were given between each dose.

For the antagonist studies (Figure 8), the third and fourth cohorts of drug-naïve rats were used for each compound, with a 48 h washout period between each dose. Each cohort received injections of either vehicle, CB_1 antagonist (rimonabant, 3 mg/kg), or CB_2 antagonist

DOI: 10.1021/acschemneuro.5b00112
ACS Chem. Neurosci. 2015, 6, 1546−1559

(SR144528, 3 mg/kg), followed by AB-FUBINACA (3 mg/kg) or AB-PINACA (3 mg/kg). The vehicle or antagonist injections were given to rats 30 min prior to the AB-FUBINACA or AB-PINACA injection.

Data for heart rate and body temperature was gathered continuously at 1000 Hz, organized into 15 or 30 min bins using Dataquest A.R.T. software (version 4.3, Data Sciences International, St. Paul, MN), and analyzed using Prism (GraphPad Software Inc., San Diego, CA).

We calculated the area between baseline and drug-treatment body temperature curves for each rat as a measure of compound potency. Briefly, for any time point, the area between baseline data points (B_t) and drug-treatment data points (D_t) and the subsequent time points (B_{t+1} and D_{t+1}) forms a trapezoid, the area of which can be calculated via the formula

$$\text{area} = \frac{(B_t - D_t) + (B_{t+1} - D_{t+1})}{2}$$

These areas were summed from the time of injection to 6 h postinjection. This data was analyzed using a two-way mixed model ANOVA with Bonferroni corrected contrasts comparing the compounds at each dose.

For the antagonist studies, the area between the vehicle−vehicle baseline and the vehicle−SC (i.e., vehicle−AB-FUBINACA or vehicle−AB-PINACA), rimonabant−SC, and SR144528−SC treatments was calculated over a 3 h time period postinjection of SC. These areas were analyzed using a one-way repeated measures ANOVA with planned Dunnet's contrasts comparing the antagonist areas to the vehicle−drug area.

■ ASSOCIATED CONTENT

Supporting Information

Table of compound names, CAS numbers, and relevant references. Selected ^{1}H and ^{13}C NMR spectra. Additional representations of biotelemetry data. The Supporting Information is available free of charge on the ACS Publications website at DOI: 10.1021/acschemneuro.5b00112.

■ AUTHOR INFORMATION

Corresponding Author

*E-mail: michael.kassiou@sydney.edu.au.

Author Contributions

S.D.B., M.M., S.M.W., M.L., C.B., and A.S.B. performed the synthesis, purification, and chemical characterization of compounds **7**−**18** with guidance from M.K. J.S. conducted all *in vitro* pharmacological evaluation under the supervision of M.C., and data analysis was performed by J.S., S.D.B., and M.C. K.E.W. and R.C.K carried out all behavioral pharmacology with direction from I.S.M. M.G. assisted the creation of stably transfected cells expressing hCB_2R. The manuscript was prepared by S.D.B., M.C., I.S.M., and M.K. All authors have given approval to the final version of the manuscript.

Funding

Work performed at The University of Sydney and presented herein was supported in part by the European Union's Seventh Framework Programme [FP7/2007-2013] INMiND (grant agreement no. HEALTH-F2-2011-278850). Work performed at Macquarie University and presented herein was supported by NHMRC project grant 1002680 awarded to M.C. and M.K.; J.S. is the recipient of an International Research Scholarship from Macquarie University

Notes

The authors declare no competing financial interest.

■ ABBREVIATIONS

ANOVA, analysis of variance; CB, cannabinoid; EDC, 1-ethyl-3-(3-dimethylaminopropyl)carbodiimide; EMCDDA, European Centre for Drugs and Drug Addiction; FLIPR, fluorometric imaging plate reader; GIRK, G protein-gated inwardly rectifying K^+ channels; GTPγS, guanosine 5′-O-[gamma-thio]-triphosphate; HOBt, hydroxybenzotriazole; i.p., intraperitoneal; NMR, nuclear magnetic resonance; p.i., postinjection; SAR, structure−activity relationship; SC, synthetic cannabinoid; Δ^9-THC, Δ^9-tetrahydrocannabinol; TLC, thin-layer chromatography

■ REFERENCES

(1) (2015) *New Psychoactive Substances in Europe: An Update from the EU Early Warning System*, European Monitoring Centre for Drugs and Drug Addiction, Luxembourg.

(2) Huestis, M. A., Gorelick, D. A., Heishman, S. J., Preston, K. L., Nelson, R. A., Moolchan, E. T., and Frank, R. A. (2001) Blockade of effects of smoked marijuana by the CB1-selective cannabinoid receptor antagonist SR141716. *Arch. Gen. Psychiatry 58*, 322−328.

(3) Howlett, A. C., Barth, F., Bonner, T. I., Cabral, G., Casellas, P., Devane, W. A., Felder, C. C., Herkenham, M., Mackie, K., Martin, B. R., Mechoulam, R., and Pertwee, R. G. (2002) International Union of Pharmacology. XXVII. Classification of cannabinoid receptors. *Pharmacol. Rev. 54*, 161−202.

(4) Pertwee, R. G., Howlett, A. C., Abood, M. E., Alexander, S. P. H., Di Marzo, V., Elphick, M. R., Greasley, P. J., Hansen, H. S., Kunos, G., Mackie, K., Mechoulam, R., and Ross, R. A. (2010) International Union of Basic and Clinical Pharmacology. LXXIX. Cannabinoid receptors and their ligands: Beyond CB1 and CB2. *Pharmacol. Rev. 62*, 588−631.

(5) Weissman, A., Milne, G. M., and Melvin, L. S. (1982) Cannabimimetic activity from CP-47,497, a derivative of 3-phenylcyclohexanol. *J. Pharmacol. Exp. Ther. 223*, 516−523.

(6) Wiley, J. L., Barrett, R. L., Lowe, J., Balster, R. L., and Martin, B. R. (1995) Discriminative stimulus effects of CP 55,940 and structurally dissimilar cannabinoids in rats. *Neuropharmacology 34*, 669−676.

(7) Auwärter, V., Dresen, S., Weinmann, W., Muller, M., Putz, M., and Ferreiros, N. (2009) 'Spice' and other herbal blends: harmless incense or cannabinoid designer drugs? *J. Mass Spectrom. 44*, 832−837.

(8) Seely, K. A., Patton, A. L., Moran, C. L., Womack, M. L., Prather, P. L., Fantegrossi, W. E., Radominska-Pandya, A., Endres, G. W., Channell, K. B., Smith, N. H., McCain, K. R., James, L. P., and Moran, J. H. (2013) Forensic investigation of K2, Spice, and "bath salt" commercial preparations: a three-year study of new designer drug products containing synthetic cannabinoid, stimulant, and hallucinogenic compounds. *Forensic Sci. Int. 233*, 416−422.

(9) Zuba, D., and Byrska, B. (2013) Analysis of the prevalence and coexistence of synthetic cannabinoids in "herbal high" products in Poland. *Forensic Toxicol. 31*, 21−30.

(10) Chung, H., Choi, H., Heo, S., Kim, E., and Lee, J. (2014) Synthetic cannabinoids abused in South Korea: drug identifications by the National Forensic Service from 2009 to June 2013. *Forensic Toxicol. 32*, 82−88.

(11) Langer, N., Lindigkeit, R., Schiebel, H. M., Ernst, L., and Beuerle, T. (2014) Identification and quantification of synthetic cannabinoids in 'spice-like' herbal mixtures: a snapshot of the German situation in the autumn of 2012. *Drug Test. Anal. 6*, 59−71.

(12) Uchiyama, N., Kawamura, M., Kikura-Hanajiri, R., and Goda, Y. (2012) Identification of two new-type synthetic cannabinoids, N-(1-adamantyl)-1-pentyl-1*H*-indole-3-carboxamide (APICA) and N-(1-adamantyl)-1-pentyl-1*H*-indazole-3-carboxamide (APINACA), and detection of five synthetic cannabinoids, AM-1220, AM-2233, AM-1241, CB-13 (CRA-13), and AM-1248, as designer drugs in illegal products. *Forensic Toxicol. 30*, 114−125.

DOI: 10.1021/acschemneuro.5b00112
ACS Chem. Neurosci. 2015, 6, 1546−1559

(13) Wilkinson, S. M., Banister, S. D., and Kassiou, M. (2015) Bioisosteric Fluorine in the Clandestine Design of Synthetic Cannabinoids. *Aust. J. Chem. 68*, 4−8.
(14) Banister, S. D., Stuart, J., Kevin, R. C., Edington, A., Longworth, M., Wilkinson, S. M., Beinat, C., Buchanan, A. S., Hibbs, D. E., Glass, M., Connor, M., McGregor, I. S., and Kassiou, M. (2015) Effects of Bioisosteric Fluorine in Synthetic Cannabinoid Designer Drugs JWH-018, AM-2201, UR-144, XLR-11, PB-22, 5F-PB-22, APICA, and STS-135. *ACS Chem. Neurosci.*, DOI: 10.1021/acschemneuro.5b00107.
(15) Uchiyama, N., Matsuda, S., Wakana, D., Kikura-Hanajiri, R., and Goda, Y. (2013) New cannabimimetic indazole derivatives, N-(1-amino-3-methyl-1-oxobutan-2-yl)-1-pentyl-1H-indazole-3-carboxamide (AB-PINACA) and N-(1-amino-3-methyl-1-oxobutan-2-yl)-1-(4-fluorobenzyl)-1H-indazole-3-carboxamide (AB-FUBINACA) identified as designer drugs in illegal products. *Forensic Toxicol. 31*, 93−100.
(16) Uchiyama, N., Matsuda, S., Kawamura, M., Kikura-Hanajiri, R., and Goda, Y. (2013) Two new-type cannabimimetic quinolinyl carboxylates, QUPIC and QUCHIC, two new cannabimimetic carboxamide derivatives, ADB-FUBINACA and ADBICA, and five synthetic cannabinoids detected with a thiophene derivative α-PVT and an opioid receptor agonist AH-7921 identified in illegal products. *Forensic Toxicol. 31*, 223−240.
(17) Buchler, I. P., Hayes, M. J., Hedge, S. G., Hockerman, S. L., Jones, D. E., Kortum, S. W., Rico, J. G., Tenbrink, R. E., and Wu, K. K. (2009) Indazole derivatives as CB1 receptor modulators and their preparation and use in the treatment of CB1-mediated diseases. Patent WO 2009/106982.
(18) Centers for Disease Control and Prevention (2013) Notes from the field: Severe Illness Associated with Synthetic Cannabinoid Use — Brunswick, Georgia, 2013. *Morb. Mortal. Wkly Rep. 62*, 939.
(19) Centers for Disease Control and Prevention (2013) Notes from the field: Severe Illness Associated with Reported Use of Synthetic Marijuana — Colorado, August−September 2013. *Morb. Mortal. Wkly Rep. 62*, 1016−1017.
(20) Monte, A. A., Bronstein, A. C., Cao, D. J., Heard, K. J., Hoppe, J. A., Hoyte, C. O., Iwanicki, J. L., and Lavonas, E. J. (2014) An outbreak of exposure to a novel synthetic cannabinoid. *N. Engl. J. Med. 370*, 389−90.
(21) Schwartz, M. D., Trecki, J., Edison, L. A., Steck, A. R., Arnold, J. K., and Gerona, R. R. (2015) A Common Source Outbreak of Severe Delirium Associated with Exposure to the Novel Synthetic Cannabinoid ADB-PINACA. *J. Emerg. Med. 48*, 573−580.
(22) Uchiyama, N., Shimokawa, Y., Kawamura, M., Kikura-Hanajiri, R., and Hakamatsuka, T. (2014) Chemical analysis of a benzofuran derivative, 2-(2-ethylaminopropyl)benzofuran (2-EAPB), eight synthetic cannabinoids, five cathinone derivatives, and five other designer drugs newly detected in illegal products. *Forensic Toxicol. 32*, 266−281.
(23) Wurita, A., Hasegawa, K., Minakata, K., Gonmori, K., Nozawa, H., Yamagishi, I., Watanabe, K., and Suzuki, O. (2015) Identification and quantitation of 5-fluoro-ADB-PINACA and MAB-CHMINACA in dubious herbal products. *Forensic Toxicol.*, DOI: 10.1007/s11419-015-0264-y.
(24) (2014) *EMCDDA−Europol 2013 Annual Report on the implementation of Council Decision 2005/387/JHA*, Implementation reports, European Monitoring Centre for Drugs and Drug Addiction, Luxembourg.
(25) Takayama, T., Suzuki, M., Todoroki, K., Inoue, K., Min, J. Z., Kikura-Hanajiri, R., Goda, Y., and Toyo'oka, T. (2014) UPLC/ESI-MS/MS-based determination of metabolism of several new illicit drugs, ADB-FUBINACA, AB-FUBINACA, AB-PINACA, QUPIC, 5F-QUPIC and alpha-PVT, by human liver microsome. *Biomed. Chromatogr. 28*, 831−838.
(26) Thomsen, R., Nielsen, L. M., Holm, N. B., Rasmussen, H. B., and Linnet, K. (2014) Synthetic cannabimimetic agents metabolized by carboxylesterases. *Drug Test. Anal.*, DOI: 10.1002/dta.1731.
(27) Wohlfarth, A., Castaneto, M. S., Zhu, M., Pang, S., Scheidweiler, K. B., Kronstrand, R., and Huestis, M. A. (2015) Pentylindole/Pentylindazole Synthetic Cannabinoids and Their 5-Fluoro Analogs Produce Different Primary Metabolites: Metabolite Profiling for AB-PINACA and 5F-AB-PINACA. *AAPS J. 17*, 660−677.
(28) Castaneto, M. S., Wohlfarth, A., Pang, S., Zhu, M., Scheidweiler, K. B., Kronstrand, R., and Huestis, M. A. (2015) Identification of AB-FUBINACA metabolites in human hepatocytes and urine using high-resolution mass spectrometry. *Forensic Toxicol.*, DOI: 10.1007/s11419-015-0275-8.
(29) Liang, G., Choi-Sledeski, Y. M., Poli, G., Chen, X., Shum, P., Minnich, A., Wang, Q., Tsay, J., Sides, K., Cairns, J., Stoklosa, G., Nieduzak, T., Zhao, Z., Wang, J., and Vaz, R. J. (2010) A conformationally constrained inhibitor with an enhanced potency for β-tryptase and stability against semicarbazide-sensitive amine oxidase (SSAO). *Bioorg. Med. Chem. Lett. 20*, 6721−6724.
(30) Wiley, J. L., Compton, D. R., Dai, D., Lainton, J. A. H., Phillips, M., Huffman, J. W., and Martin, B. R. (1998) Structure-activity relationships of indole- and pyrrole-derived cannabinoids. *J. Pharmacol. Exp. Ther. 285*, 995−1004.
(31) Wiley, J. L., Marusich, J. A., and Huffman, J. W. (2014) Moving around the molecule: Relationship between chemical structure and in vivo activity of synthetic cannabinoids. *Life Sci. 97*, 55−63.
(32) Wiley, J. L., Lefever, T. W., Cortes, R. A., and Marusich, J. A. (2014) Cross-substitution of Delta-tetrahydrocannabinol and JWH-018 in drug discrimination in rats. *Pharmacol., Biochem. Behav. 124*, 123−128.
(33) Hine, B., Torrelio, M., and Gershon, S. (1977) Analgesic, Heart Rate, and Temperature Effects of Delta^8-THC during Acute and Chronic Administration to Conscious Rats. *Pharmacology 15*, 65−72.
(34) Wiley, J. L., Marusich, J. A., Martin, B. R., and Huffman, J. W. (2012) 1-Pentyl-3-phenylacetylindoles and JWH-018 share in vivo cannabinoid profiles in mice. *Drug Alcohol Depend. 123*, 148−153.
(35) Wiley, J. L., Marusich, J. A., Lefever, T. W., Grabenauer, M., Moore, K. N., and Thomas, B. F. (2013) Cannabinoids in disguise: Delta9-tetrahydrocannabinol-like effects of tetramethylcyclopropyl ketone indoles. *Neuropharmacology 75*, 145−154.
(36) Banister, S. D., Wilkinson, S. M., Longworth, M., Stuart, J., Apetz, N., English, K., Brooker, L., Goebel, C., Hibbs, D. E., Glass, M., Connor, M., McGregor, I. S., and Kassiou, M. (2013) The synthesis and pharmacological evaluation of adamantane-derived indoles: cannabimimetic drugs of abuse. *ACS Chem. Neurosci. 4*, 1081−1092.
(37) Rinaldi-Carmona, M., Barth, F., Heaulme, M., Shire, D., Calandra, B., Congy, C., Martinez, S., Maruani, J., Neliat, G., Caput, D., Ferrara, P., Soubrié, P., Brelière, J. C., and Le Fura, G. (1994) SR141716A, a potent and selective antagonist of the brain cannabinoid receptor. *FEBS Lett. 350*, 240−244.
(38) Rinaldi-Carmona, M., Barth, F., Heaulme, M., Alonso, R., Shire, D., Congy, C., Soubrié, P., Brelière, J. C., and Le Fur, G. (1995) Biochemical and pharmacological characterisation of SR141716A, the first potent and selective brain cannabinoid receptor antagonist. *Life Sci. 56*, 1941−1947.
(39) Rinaldi-Carmona, M., Barth, F., Millan, J., Derocq, J. M., Casellas, P., Congy, C., Oustric, D., Sarran, M., Bouaboula, M., Calandra, B., Portier, M., Shire, D., Brelière, J. C., and Le Fur, G. L. (1998) SR 144528, the first potent and selective antagonist of the CB2 cannabinoid receptor. *J. Pharmacol. Exp. Ther. 284*, 644−650.
(40) Portier, M., Rinaldi-Carmona, M., Pecceu, F., Combes, T., Poinot-Chazel, C., Calandra, B., Barth, F., le Fur, G., and Casellas, P. (1999) SR 144528, an antagonist for the peripheral cannabinoid receptor that behaves as an inverse agonist. *J. Pharmacol. Exp. Ther. 288*, 582−589.
(41) Banister, S. D., Stuart, J., Conroy, T., Longworth, M., Manohar, M., Beinat, C., Wilkinson, S. M., Kevin, R. C., Hibbs, D. E., Glass, M., Connor, M., McGregor, I. S., and Kassiou, M. (2015) Structure−activity relationships of synthetic cannabinoid designer drug RCS-4 and its regioisomers and C4 homologues. *Forensic Toxicol.*, DOI: 10.1007/s11419-015-0282-9.
(42) Knapman, A., Santiago, M., Du, Y. P., Bennallack, P. R., Christie, M. J., and Connor, M. (2013) A continuous, fluorescence-based assay of μ-opioid receptor activation in AtT-20 cells. *J. Biomol. Screening 18*, 269−276.

DOI: 10.1021/acschemneuro.5b00112
ACS Chem. Neurosci. 2015, 6, 1546−1559

ACS Chemical Neuroscience
Research Article
pubs.acs.org/chemneuro

Pharmacology of Valinate and *tert*-Leucinate Synthetic Cannabinoids 5F-AMBICA, 5F-AMB, 5F-ADB, AMB-FUBINACA, MDMB-FUBINACA, MDMB-CHMICA, and Their Analogues

Samuel D. Banister,[†,∥,○] Mitchell Longworth,[†,○] Richard Kevin,[‡] Shivani Sachdev,[⊥] Marina Santiago,[⊥] Jordyn Stuart,[⊥] James B. C. Mack,[#] Michelle Glass,[▽] Iain S. McGregor,[‡] Mark Connor,[⊥] and Michael Kassiou*[,†,§]

[†]School of Chemistry, [‡]School of Psychology, and [§]Faculty of Health Sciences, The University of Sydney, Sydney, NSW 2006, Australia

[∥]Department of Radiation Oncology, Stanford University School of Medicine, Stanford, California 94305, United States

[⊥]Department of Biomedical Sciences, Macquarie University, Sydney, NSW 2109, Australia

[#]Department of Chemistry, Stanford University, Stanford, California 94304, United States

[▽]School of Medical Sciences, The University of Auckland, Auckland 1142, New Zealand

Supporting Information

ABSTRACT: Indole and indazole synthetic cannabinoids (SCs) featuring L-valinate or L-*tert*-leucinate pendant group have recently emerged as prevalent recreational drugs, and their use has been associated with serious adverse health effects. Due to the limited pharmacological data available for these compounds, 5F-AMBICA, 5F-AMB, 5F-ADB, AMB-FUBINACA, MDMB-FUBINACA, MDMB-CHMICA, and their analogues were synthesized and assessed for cannabimimetic activity in vitro and in vivo. All SCs acted as potent, highly efficacious agonists at CB_1 (EC_{50} = 0.45−36 nM) and CB_2 (EC_{50} = 4.6−128 nM) receptors in a fluorometric assay of membrane potential, with a general preference for CB_1 activation. The cannabimimetic properties of two prevalent compounds with confirmed toxicity in humans, 5F-AMB and MDMB-FUBINACA, were demonstrated in vivo using biotelemetry in rats. Bradycardia and hypothermia were induced by 5F-AMB and MDMB-FUBINACA doses of 0.1−1 mg/kg (and 3 mg/kg for 5F-AMB), with MDMB-FUBINACA showing the most dramatic hypothermic response recorded in our laboratory for any SC (>3 °C at 0.3 mg/kg). Reversal of hypothermia by pretreatment with a CB_1, but not CB_2, antagonist was demonstrated for 5F-AMB and MDMB-FUBINACA, consistent with CB_1-mediated effects in vivo. The in vitro and in vivo data indicate that these SCs act as highly efficacious CB receptor agonists with greater potency than Δ^9-THC and earlier generations of SCs.

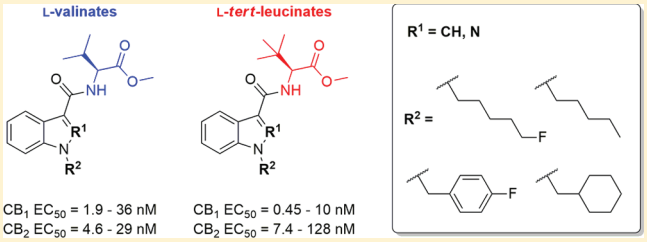

KEYWORDS: *Cannabinoid, THC, JWH-018, AMB, MDMB*

Synthetic cannabinoids (SCs) are the most rapidly growing class of "designer drugs", or new psychoactive substances (NPSs).[1] Consumer products available since about 2004 and intended as "legal cannabis substitutes" were found in 2008 to contain JWH-018 (**1**, Figure 1) and CP 47,497-C8 (**2**).[2,3] In 2014, 177 different SCs were reported to the United Nations Office on Drugs and Crime (UNODC) Early Warning Advisory (EWA).[4] Many novel SCs have already been discovered in 2016, and the structural diversity of these substances is increasing.[5−14]

SCs are typically found to function as agonists of cannabinoid receptor type 1 (CB_1) and type-2 (CB_2), with activation of the former accounting for the psychoactivity of these substances.[15] However, many SCs are unknown prior to first detection by forensic chemists, and nothing is known of their activity in humans. The scarcity of data regarding the pharmacological and toxicological properties of emergent SCs poses an ongoing challenge for scientists, healthcare workers, and lawmakers across the globe.[16−26]

We have previously described the in vitro and in vivo pharmacology of SCs based on 3-benzoylindoles (e.g., RCS-4, **3**), 3-naphthoylindoles (e.g., AM-2201, **4**), 3-alkanoylindoles (e.g., XLR-11, **5**), indole-3-carboxylates (e.g., 5F-PB-22, **6**), and indole-3-carboxamides (e.g., STS-135, **7**).[27−32] One of the most prevalent, recent groups of SCs are 1-alkyl-1*H*-indazole-3-carboxamides featuring pendant valinamide and *tert*-leucinamide groups, exemplified by AB-FUBINACA (**8**) and ADB-PINACA (**9**), respectively. Following the designation of several members of this class as Schedule I substances by the Drug Enforcement Administration (DEA) in the United States

Received: May 18, 2016
Accepted: July 15, 2016
Published: July 15, 2016

DOI: 10.1021/acschemneuro.6b00137
ACS Chem. Neurosci. 2016, 7, 1241−1254

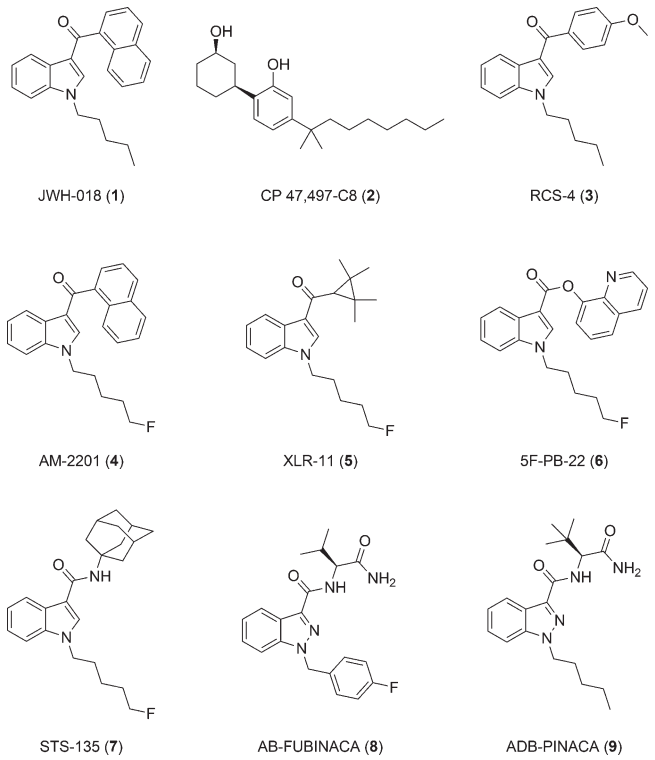

Figure 1. Selected synthetic cannabinoids.

(US),[33,34] newer indole- and indazole-3-carboxamide variants have appeared featuring currently popular 5-fluoropentyl, 4-fluorobenzyl, cyclohexylmethyl, or pentyl substituents at the 1-position, and valinate and *tert*-leucinate methyl ester side chains (**10**–**25**, Figure 2).

5F-AMB-PICA (MMB-2201, 5F-AMBICA, **10**) was reported to the European Monitoring Centre for Drugs and Drug

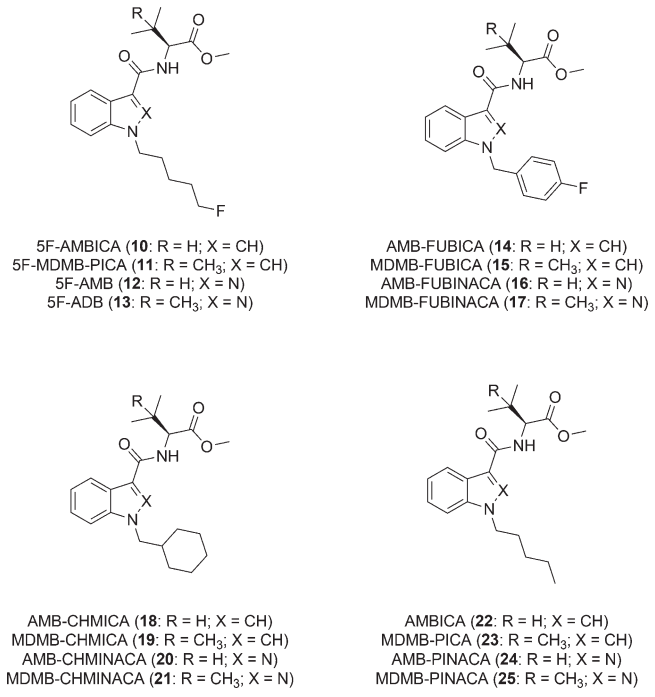

Figure 2. Emergent indole and indazole SCs featuring pendant methyl valinate and methyl *tert*-leucinate functional groups.

Addiction (EMCDDA) following its identification in Hungary and Sweden in 2014, and its indazole analogue, 5F-AMB-PINACA (5F-AMB, **12**), was found in Hungary contemporaneously.[35] The *tert*-leucinate analogue of **12**, 5F-MDMB-PINACA (5F-ADB, **13**), was notified to the UNODC EWA in Hungary and Japan in 2015. The indole derivative MDMB-FUBICA (**15**) was discovered in Hungary and Sweden in 2015, according to UNODC EWA, and AMB-FUBINACA (**16**) was reported to the EMCDDA in Sweden around the same time.[35] MDMB-FUBINACA (**17**) was identified following media monitoring by EMCDDA after it was responsible for dozens of deaths and hundreds of hospitalizations in the Russian Federation in 2015.[35,36] MDMB-CHMICA was first identified in Hungary in 2014, but has since been reported to the EWA in France, Mauritius, Serbia, Turkey, and the UK.[35]

SC use is associated with serious adverse reactions,[37−53] and the most recent SCs appear to possess greater dependence liabilities[54−57] and toxicities[58−64] than earlier examples. AMB-FUBINACA was clinically confirmed in a case of rhabdomolysis,[65] and fatal intoxications have been attributed to consumption of 5F-AMB,[44,66,67] 5F-ADB,[68] and MDMB-CHMICA.[69−71]

Aspects of the spectral properties of selected members of this class of SCs have been reported,[72−76] and details of the metabolism of AMB-PICA and 5F-AMB were recently published,[77] but little is known about the pharmacology of these compounds in vitro or in vivo.

A systematic library of indole and indazole SCs featuring a valinate or *tert*-leucinate functional group was prepared and screened for cannabinoid activity in vitro and in vivo, in order to elucidate the hitherto unknown structure−activity relationships within this class.

RESULTS AND DISCUSSION

The synthesis of indole and indazole SCs required a different strategy for each heteroaromatic core. The synthesis of indole SCs **10**, **11**, **14**, **15**, **18**, **19**, **22**, and **23** is shown in Scheme 1, and the synthesis of indazole SCs **12**, **13**, **16**, **17**, **20**, **21**, **24**, and **25** is shown in Scheme 2.

As shown in Scheme 1, indole was subjected to a one-pot procedure in the presence of excess base whereby *N*-alkylation with the appropriate alkyl bromide was followed treatment with trifluoroacetic anhydride and gave trifluoroacetylindoles **27**−**30**. Base-mediated hydrolysis of the trifluoroacetyl groups of **27**−**30** gave the corresponding carboxylic acids **31**−**34**. Finally, amide bond formation was achieved by subjecting **31**−**34** to HOBt/EDC coupling with methyl L-valinate or methyl *tert*-L-leucinate to afford **10**, **11**, **14**, **15**, **18**, **19**, **22**, and **23**.

As depicted in Scheme 2, the synthesis of indazole analogues started from methyl 1*H*-indazole-3-carboxylate (**35**), which was regioselectively alkylated with the suitable bromoalkane to give the 1-alkyl-1*H*-indazole-3-carboxylate methyl esters **36**−**39**. Saponification of esters **36**−**39** afforded the corresponding acids **40**−**43**, which were coupled to methyl L-valinate or methyl *tert*-L-leucinate using the HOBt/EDC method described above, to furnish 1-alkyl-1*H*-indazole-3-carboxamides **12**, **13**, **16**, **17**, **20**, **21**, **24**, and **25**.

The activity of synthesized indole and indazole SCs **10**−**25** at CB_1 and CB_2 receptors was assessed in a fluorometric imaging plate reader (FLIPR) assay to elucidate structure−activity relationships (SARs) for this class. The activities of **10**−**25** at CB_1 and CB_2 were compared to phytocannabinoid Δ^9-THC (a low efficacy agonist at CB_1 and CB_2), and CP 55,940 (an

DOI: 10.1021/acschemneuro.6b00137
ACS Chem. Neurosci. 2016, 7, 1241−1254

ACS Chemical Neuroscience Research Article

Scheme 1. Synthesis of Indole SCs 10, 11, 14, 15, 18, 19, 22, and 23[a]

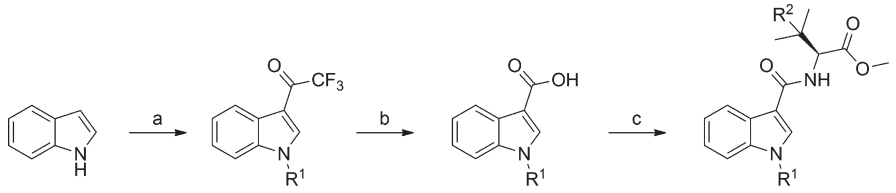

[a]Reagents and conditions: (a) (i) NaH, BrR^1, DMF, 0 °C−rt, 1 h; (ii) $(CF_3CO)_2O$, DMF, 0 °C−rt, 1 h, 72−94%; (b) 1 M aq. NaOH, MeOH, reflux, 24 h, 67−92%; (c) methyl L-valinate or methyl L-*tert*-leucinate, EDC·HCl, HOBt, DIPEA, DMSO, rt, 24 h, 63−81%.

Scheme 2. Synthesis of Indazole SCs 12, 13, 16, 17, 20, 21, 24, and 25[a]

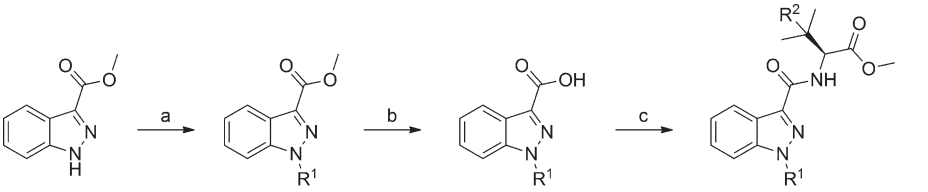

[a]Reagents and conditions: (a) *t*-BuOK, BrR^1, THF, 0 °C−rt, 48 h; 65−84%; (b) 1 M aq. NaOH, MeOH, reflux, 24 h, 76−91%; (c) methyl L-valinate or methyl L-*tert*-leucinate, EDC·HCl, HOBt, DIPEA, DMSO, rt, 24 h, 60−77%.

Table 1. Functional Activity of Δ^9-THC, CP 55,940, and Novel SCs 10−25 at CB_1 and CB_2 Receptors

	hCB$_1$		hCB$_2$		
compd	pEC$_{50}$ ± SEM (EC$_{50}$, nM)	max ± SEM (% CP 55,940)	pEC$_{50}$ ± SEM (EC$_{50}$, nM)	max ± SEM (%CP 55,940)	CB$_1$ sel.[a]
Δ^9-THC	6.77 ± 0.05 (171)	50 ± 11		20 ± 3 at 10 μM	
CP 55,490	7.47 ± 0.05 (42)		7.17 ± 0.07 (68)		1.6
5F-AMBICA (**10**)	8.62 ± 0.06(2.4)	107 ± 4	8.34 ± 0.07 (4.6)	94 ± 3	1.9
5F-MDMB-PICA (**11**)	9.35 ± 0.07(0.45)	110 ± 4	8.13 ± 0.05 (7.4)	94 ± 3	16.4
5F-AMB (**12**)	8.71 ± 0.04(1.9)	109 ± 3	7.99 ± 0.13 (10)	103 ± 7	5.3
5F-ADB (**13**)	9.23 ± 0.11(0.59)	108 ± 5	8.12 ± 0.06 (7.5)	94 ± 3	12.7
AMB-FUBICA (**14**)	7.45 ± 0.05(36)	106 ± 3	7.85 ± 0.09 (14)	86 ± 4	0.4
MDMB-FUBICA (**15**)	8.57 ± 0.05(2.7)	109 ± 3	7.60 ± 0.12 (25)	92 ± 6	9.3
AMB-FUBINACA (**16**)	8.71 ± 0.10(2.0)	103 ± 5	7.75 ± 0.05 (18)	92 ± 3	9.0
MDMB-FUBINACA (**17**)	8.41 ± 0.04 (3.9)	108 ± 3	7.26 ± 0.14 (55)	101 ± 9	14.1
AMB-CHMICA (**18**)	8.45 ± 0.08(3.5)	114 ± 4	7.93 ± 0.07 (12)	88 ± 4	3.4
MDMB-CHMICA (**19**)	8.00 ± 0.05 (10)	112 ± 3	7.15 ± 0.05 (71)	103 ± 3	7.1
AMB-CHMINACA (**20**)	8.29 ± 0.07(5.1)	109 ± 4	7.54 ± 0.13 (29)	92 ± 7	5.7
MDMB-CHMINACA (**21**)	7.99 ± 0.04 (10)	111 ± 2	6.89 ± 0.04 (128)	96 ± 3	12.8
AMBICA (**22**)	7.74 ± 0.10(18)	111 ± 6	7.63 ± 0.08 (23)	90 ± 4	1.3
MDMB-PICA (**23**)	8.77 ± 0.06 (1.7)	109 ± 4	7.78 ± 0.13 (17)	90 ± 5	10
AMB-PINACA (**24**)	8.48 ± 0.05 (3.3)	110 ± 3	7.79 ± 0.11 (16)	96 ± 5	4.8
MDMB-PINACA (**25**)	8.84 ± 0.06 (1.4)	112 ± 4	7.56 ± 0.06 (28)	91 ± 4	20

[a]CB_1 selectivity expressed as the ratio of CB_1 EC_{50} to CB_2 EC_{50}.

DOI: 10.1021/acschemneuro.6b00137
ACS Chem. Neurosci. 2016, 7, 1241−1254

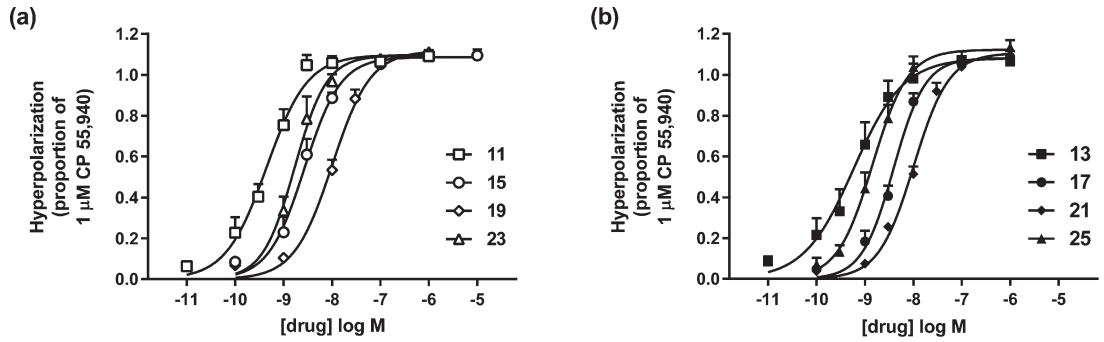

Figure 3. Hyperpolarization mediated by CB_1 receptors induced by differently 1-substituted (a) indoles **11**, **15**, **19**, and **23**, and the corresponding (b) indazoles **13**, **17**, **21**, and **25** as a proportion of that produced by 1 μM CP 55,940. Membrane potential was measured using a fluorescent dye, as outlined in the Methods. Each point represents the mean ± SEM of at least five independent determinations, each performed in duplicate. Data was fitted with a four-parameter logistic equation in GraphPad Prism.

efficacious agonist at CB_1 and CB_2), in an assay of CB receptor-dependent membrane hyperpolarization (Table 1). The assay used murine AtT20-FlpIn neuroblastoma cells stably expressing human CB_1 or CB_2 receptors. Activation of CB receptors resulted in opening of endogenous G protein-gated inwardly rectifying potassium channels (GIRKs) that produced a hyperpolarization of the cells which was reflected in a decrease in the fluorescence of a proprietary membrane potential dye. The maximum effects of Δ^9-THC and **10**–**25** were compared to the high efficacy CB_1/CB_2 agonist CP 55,490. Data for each experiment were normalized to the change in fluorescence produced by a maximally effective concentration of CP 55,940 (1 μM). CP 55,940 (1 μM) decreased fluorescence by 31 ± 1% in CB1-expressing cells, and 26 ± 1% in CB2 expressing cells (n = 18 each). None of **10**–**25** produced a significant change in the membrane potential of wild type AtT-20 cells (n = 5 each, data not shown), which do not express CB_1 or CB_2 receptors. Consistent with a predominant coupling of CB_1 and CB_2 receptors to G_i/G_o family G proteins, the effects of **10**–**25** were abolished by overnight treatment of the cells with pertussis toxin (200 ng/mL), which blocks the coupling of GPCR to G_i/G_o family G proteins (n = 3 each, data not shown).

All indole and indazole SCs **10**–**25** activated CB_1 and CB_2 receptors. All compounds had greater potency (0.45–36 nM) than either Δ^9-THC (171 nM) or CP 55,940 (42 nM) for CB_1 receptor-mediated activation of GIRK. Consistent with our previous studies using this assay, Δ^9-THC was found to be a low efficacy agonist at CB_2 receptors, and its effects on GIRK activation in AtT20-CB_2 at 10 μM were only 20 ± 3% of that mediated by a maximally effective concentration of CP 55,940 (1 μM). Compounds **10**–**25** had a similar maximal effect to CP 55,940 at CB_1 and CB_2 receptors, suggesting that these SCs are also high efficacy agonists. Excluding **14**, all SCs showed a preference for CB_1 receptors over CB_2 receptors, ranging from low (e.g., **22**; 1.3 times) to moderate (e.g., **25**; 20 times). The psychoactivity of cannabinoids is attributed to activation of CB_1 receptors,[15] and our data are consistent the anecdotally reported psychoactive effects of members of this class of SCs.

With the exception of several pairs of nearly equal potency (**16** and **17**; **20** and **21**), all *tert*-leucinate-functionalized SCs were more potent CB_1 agonists than the corresponding valinate analogues, a trend that was also observed for *tert*-leucinimde and valinamide analogues in our previous work.[30]

CB_1 EC_{50} values for **10**–**25** ranged from 0.45 to 36 nM, but only two of the 16 SCs had EC_{50} values greater than 10 nM (**14** and **22**), and two demonstrated subnanomolar potencies (**11** and **13**). The least potent SC in this class (AMB-FUBICA; **14**) was roughly 4 times more potent than Δ^9-THC at CB_1 receptors, while the most potent compound (5F-MDMB-PICA; **11**) was 380 times more potent than Δ^9-THC.

Consistent with our previous work on other indole and indazole SCs, there were no obvious trends for differences in potency or efficacy when moving between these heteroaromatic cores for corresponding pairs of compounds. However, within the *tert*-leucinate-flunctionalized compounds, the nature of *N*-alkyl substituent had a consistent effect on CB_1 potency for compounds containing either an indole or indazole core.

For the *tert*-leucinate functionalized indoles, CB_1 potency decreased as a function of *N*-alkyl substituent in the order of 5-fluoropentyl (**11**), pentyl (**23**), 4-fluorobenzyl (**15**), and cyclohexylmethyl (**19**), and this trend is depicted in Figure 3a. The same trend was found for corresponding indazoles **13**, **25**, **17**, and **21**, respectively (Figure 3b). Although no such clear trend was evident for valinate-containing SCs, it is notable that three of the five least potent SCs contained a cyclohexylmethyl group at the 1-position (**19**, **20**, and **21**), and three of the five most potent SCs contained a 5-fluoropentyl substituent (**11**, **12**, and **13**) regardless of heteroaromatic core or amino acid ester side-chain.

Having demonstrated that **10**–**25** are potent and efficacious cannabimimetic agents in vitro, we sought to demonstrate activity of several of the most prevalent and toxic SCs in vivo. Both 5F-AMB and MDMB-FUBINACA have been linked with numerous incidents of adverse effects, including death, in humans.[35,36,44,66,67] The in vivo activity of 5F-AMB (**12**) and MDMB-FUBINACA (**17**) were compared using biotelemetry in rats to provide information regarding the activity of these newer SCs in a living system. Biotelemetry provides a high resolution, high fidelity alternative to the classical cannabinoid tetrad, and has the capacity to show both the magnitude and time-course of cannabinoid effects on rodent physiology.

In rodents, cross-substitution of older SCs, like JWH-018, and Δ^9-THC has been demonstrated, indicating that these classes produce similar pharmacological effects despite structural dissimilarity.[78−81] Cannabinoids induce hypothermia and bradycardia in rats, and these physiological changes are common to phytocannabinoids like Δ^9-THC and structurally distinct indole and indazole SCs.[82−84] We have previously determined the hypothermic and bradycardic potencies of Δ^9-THC and numerous structurally diverse SCs, including JWH-018, AM-2201, UR-144, XLR-11, APICA, STS-135, PB-22, 5F-

DOI: 10.1021/acschemneuro.6b00137
ACS Chem. Neurosci. 2016, 7, 1241−1254

PB-22, AB-PINACA, and AB-FUBINACA in rats.[27,28,30] The cannabimimetic activities of 5F-AMB and MDMB-FUBINACA were assessed using radiotelemetry in male Long Evans rats, and the effects of these SCs on body temperature (Figure 4) and heart rate (Figure 5) are presented below.

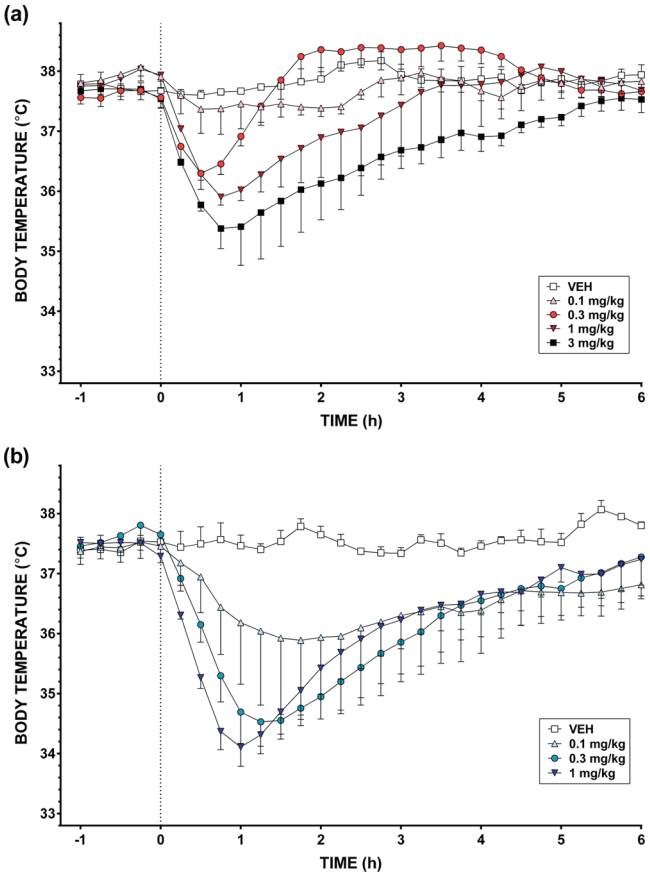

Figure 4. Effects of (a) 5F-AMB and (b) MDMB-FUBINACA on rat body temperature. Dashed line denotes time of intraperitoneal injection. Each point represents the mean ± SEM for four animals.

Rat body temperatures 1 h prior to intraperitoneal (i.p.) injection and 6 h post injection of 5F-AMB and MDMB-FUBINACA are presented in 15 min bins in Figure 4. For each drug, these data are presented for 1 h before (baseline) and 6 h after injection of various doses. The dashed line on the figures represents the time of SC injection. Each SC was investigated using a cohort of 3−4 rats, with a different cohort used for the two compounds. Doses were escalated from 0 mg/kg (baseline) to 0.1, 0.3, 1, and 3 mg/kg for each compound with at least 2 washout days with no injections between each dose.

Both 5F-AMB and MDMB-FUBINACA evoked a substantial hypothermic effect at doses of 0.1−1 mg/kg, and up to 3 mg/kg in the case of 5F-AMB (Figure 4). The peak reduction in body temperature was generally greater with MDMB-FUBINACA (>3 °C) than 5F-AMB (>2 °C). The hypothermic effects of MDMB-FUBINACA were so dramatic at a dose of 0.3 mg/kg, and differed so little from the increased dose of 1 mg/kg, that no higher doses were explored. These data indicate that MDMB-FUBINACA is one of the most potent SCs evaluated in rats in our laboratories thus far. Interestingly, the 0.1 mg/kg dose of MDMB-FUBINACA produced a strong hypothermic response (>3 °C) in two of the four rats tested,

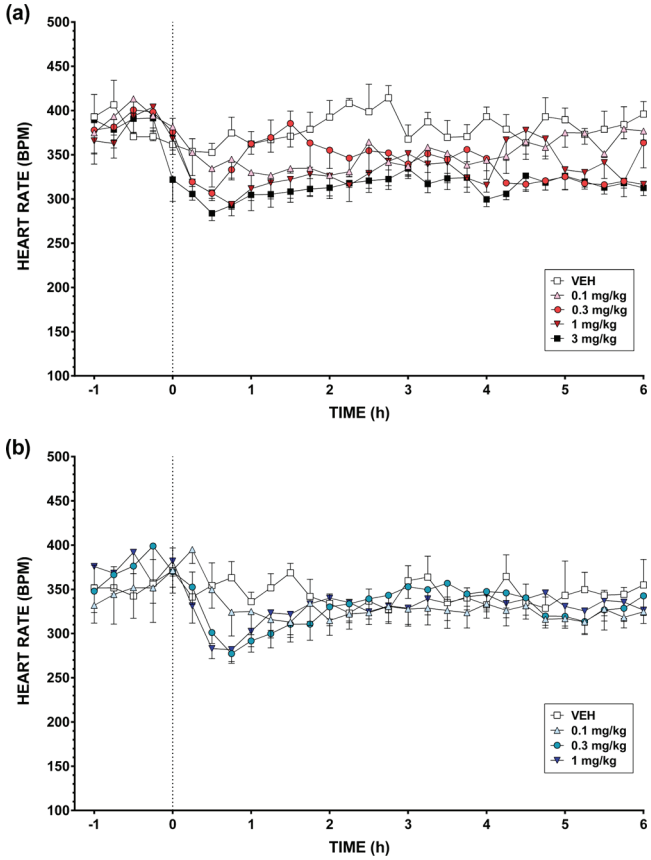

Figure 5. Effects of (a) 5F-AMB and (b) MDMB-FUBINACA on rat heart rate. Dashed line denotes time of intraperitoneal injection. Each point represents the mean ± SEM for four animals.

while the remaining pair did not respond. At higher doses, all four rats responded consistently. When compared to 5F-AMB, MDMB-FUBINACA induced a prolonged hypothermia at all doses, with mean core body temperature returning to baseline after more than 8 h at the smallest dose tested (0.1 mg/kg, data shown in SI). This was verified by a statistical analysis showing a significantly greater area under the curve for body temperature (relative to vehicle baseline) for MDMB-FUBINACA doses compared to 5F-AMB at 0.3 mg/kg ($P < 0.05$) and 1 mg/kg ($P < 0.05$) (see Figure S33, Supporting Information).

Data for heart rate changes effected by 5F-AMB and MDMB-FUBINACA are presented in 15 min bins in Figure 5, with the dashed line on the figures representing time of SC injection. A two-way mixed-model ANOVA with planned contrasts revealed that 5F-AMB produced a significant decrease in heart rate over the 6 h immediately following dosing at 0.3 mg/kg ($P < 0.05$), 1 mg/kg ($P < 0.05$), and 3 mg/kg ($P < 0.01$) compared to vehicle. MDMB-FUBINACA did not significantly reduce heart rate compared to vehicle at any dose over the same time period. However, heart rate was reduced in the first 2 h following injection with 0.3 mg/kg MDMB-FUBINACA ($P < 0.05$). It should be noted that heart rate data were generally more variable than those for body temperature. Variability in heart rate data is expected due to multiple determinants; locomotor activity, stress, and direct pharmacological cardiovascular effects.

To confirm that the observed effects were mediated through CB_1 or CB_2 receptors, the reversibility of the effects of 5F-AMB

DOI: 10.1021/acschemneuro.6b00137
ACS Chem. Neurosci. 2016, 7, 1241−1254

and MDMB-FUBINACA on body temperature and heart rate in rats following pretreatment with either CB_1 receptor antagonist rimonabant or CB_2 receptor antagonist SR144528 was assessed. Rimonabant is a potent and selective CB_1 receptor antagonist, and reverses CB_1-mediated cannabinoid agonist effects in rodents[85] and humans,[15] while SR144528 is a selective CB_2 functional antagonist.[86]

Rat body temperatures after injection (i.p.) with vehicle, CB_1 antagonist (rimonabant, 3 mg/kg), or CB_2 antagonist (SR144528, 3 mg/kg) 30 min prior to treatment with either 5F-AMB (3 mg/kg) or MDMB-FUBINACA (1 mg/kg) are presented in 15 min bins in Figure 6. For each treatment

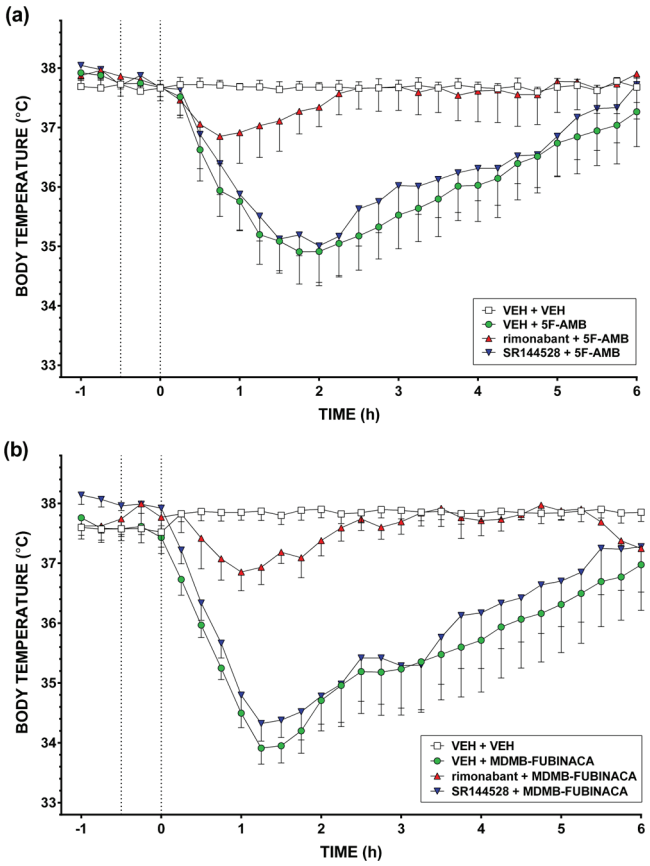

Figure 6. Effects of (a) 3 mg/kg 5F-AMB or (b) 1 mg/kg MDMB-FUBINACA on rat body temperature following pretreatment (30 min prior) with vehicle (VEH), 3 mg/kg rimonabant (CB_1 antagonist), or 3 mg/kg SR144528 (CB_2 antagonist). The first dashed line denotes time of intraperitoneal injection of vehicle or antagonist. Second dashed line represents time of intraperitoneal injection of SC. Each point represents the mean ± SEM for three animals.

condition, the data are presented for 1 h before (baseline) and 6 h after injection of various doses. The first dashed line on the figure represents the time of vehicle/antagonist injection, and the second dashed line represents time of SC injection. Each SC was investigated using a cohort of 3−4 rats, with a different cohort used for the two compounds.

Rimonabant pretreatment completely reversed the body temperature decrease induced by 5F-AMB or MDMB-FUBINACA, while pretreatment with SR144528 had no effect on the hypothermic effects of 5F-AMB or MDMB-FUBINACA (Figure 6a). These interpretations are confirmed by a statistical analysis of the areas between each drug treatment and baseline (Figure S35, Supporting Information), and suggest a CB_1-mediated hypothermic mechanism. Similar trends were observed for the reversal of 5F-AMB- or MDMB-FUBINACA-induced bradycardia by rimonabant but not SR144528, however, these differences did not reach significance (data not shown). This is likely due to a combination of the relatively smaller magnitude of SC-induced bradycardic effects and high variability of the heart rate data.

CONCLUSION

The proactive pharmacological evaluation of emergent SCs is essential to harm minimization and law enforcement efforts targeting these compounds. This study is the first to pharmacologically characterize the most recent, prevalent class of SC designer drugs based on 1-alkylindole-3-carboxamide and 1-alkyl-1*H*-indazole-3-carboxamide scaffolds featuring pendant methyl L-valinate or methyl L-*tert*-leucinate functional groups. Synthetic routes to identified SCs of forensic interest (5F-AMBICA, 5F-AMB, AMB-FUBINACA, MDMB-FUBINACA, MDMB-CHMICA), as well as several anticipated but hitherto undetected analogues, were developed. These synthetic routes are general for 1-alkyl-1*H*-indole-3-carboxamides and 1-alkyl-1*H*-indazole-3-carboxamides and facilitate the proactive development of reference standards for SCs expected to appear in future. All synthesized SCs acted as agonists of CB_1 and CB_2 receptors in the nanomolar range in a FLIPR membrane potential assay, and are potent, functional cannabinoids. In rats, 5F-AMB and MDMB-FUBINACA dose-dependently effected hypothermia and bradycardia at doses of 0.1−1 mg/kg (and up to 3 mg/kg in the case of the former), demonstrating that these SCs are potently cannabimimetic in vivo. The dramatic reduction of body temperature induced by MDMB-FUBINACA at doses as low as 0.1 mg/kg positions this compounds as one of the most potent SCs explored in our laboratories. The hypothermic effects of 5F-AMB (3 mg/kg) and MDMB-FUBNACA (1 mg/kg) could be reversed by pretreatment with CB_1 antagonist rimonabant (3 mg/kg), but not CB_2 antagonist SR144528 (3 mg/kg), and appear to be mediated through CB_1 receptors. Taken together, in vitro and in vivo data confirm that SCs **10**−**25** are cannabimimetic agents of greater potency than Δ^9-THC and earlier SCs.

METHODS

General Chemical Synthesis Details. All reactions were performed under an atmosphere of nitrogen or argon unless otherwise specified. Commercially available chemicals were used as purchased. Analytical thin-layer chromatography was performed using Merck aluminum-backed silica gel 60 F254 (0.2 mm) plates (Merck, Darmstadt, Germany), which were visualized using shortwave (254 nm) UV fluorescence. Flash chromatography was performed using Merck Kieselgel 60 (230−400 mesh) silica gel. Melting point ranges (m.p.) were measured in open capillaries using a Stuart SMP10 melting point apparatus (Bibby Scientific, Staffordshire, UK) and are uncorrected. Nuclear magnetic resonance spectra were recorded at 300 K using either a Bruker AVANCE DRX400 (400.1 MHz) or AVANCE III 500 Ascend (500.1 MHz) spectrometer (Bruker, Bremen, Germany). The data are reported as chemical shift (δ ppm) relative to the residual protonated solvent resonance, relative integral, multiplicity (s = singlet, br s = broad singlet, d = doublet, t = triplet, quart. = quartet, quin. = quintet, m = multiplet), coupling constants (J Hz), and assignment. Assignment of signals was assisted by correlation spectroscopy (COSY), distortionless enhancement by polarization transfer (DEPT), heteronuclear single quantum coherence (HSQC), and heteronuclear multiple-bond correlation (HMBC) experiments where necessary. Low-resolution mass spectra (LRMS) was recorded

DOI: 10.1021/acschemneuro.6b00137
ACS Chem. Neurosci. 2016, 7, 1241−1254

using electrospray ionization (ESI) recorded on a Finnigan LCQ ion trap mass spectrometer (ThermoFisher Scientific, Waltham, MA). High-resolution mass spectra (HRMS) were run on a Bruker 7T Apex Qe Fourier Transform Ion Cyclotron resonance mass spectrometer equipped with an Apollo II ESI/APCI/MALDI Dual source by the Mass Spectrometry Facility of the School of Chemistry at the University of Sydney. IR absorption spectra were recorded on a Bruker ALPHA FT-IR spectrometer as solid or thin film from ethanol, and the data are reported as vibrational frequencies (cm^{-1}). Please see the Supporting Information for ^{1}H and ^{13}C NMR spectra and Fourier transform infrared (FTIR) spectra of all final compounds.

General Procedure A: Amidation of 1-Alkylindole-3-carboxylic Acids and 1-Alkyl-1*H*-indazole-3-carboxylic Acids. To a solution of the appropriate 1-alkylindole-3-carboxylic acid or 1-alkyl-1*H*-indazole-3-carboxylic acid (0.39 mmol), methyl L-valinate hydrochloride (69 mg, 0.41 mmol, 1.05 equiv) or methyl L-*tert*-leucinate hydrochloride (75 mg, 0.41 mmol, 1.05 equiv), EDC·HCl (150 mg, 0.78 mmol, 2.0 equiv), and HOBt (119 mg, 0.78 mmol, 2.0 equiv) in DMSO (5 mL) was added DIPEA (340 μL, 1.95 mmol, 5.0 equiv) dropwise and the mixture was stirred for 14 h. The reaction was quenched by the addition of sat. aq. $NaHCO_3$ (75 mL) and extracted with EtOAc (3 × 75 mL). The combined organic layers were washed with brine (100 mL), dried ($MgSO_4$), and evaporated under reduced pressure. The pure amides were obtained following purification by flash chromatography.

*Methyl (S)-2-(1-(5-Fluoropentyl)-1H-indole-3-carboxamido)-3-methylbutanoate (5F-AMB-PICA, **10**).* Subjecting **31** (100 mg, 0.40 mmol) and methyl L-valinate hydrochloride (70 mg, 0.42 mmol, 1.05 equiv) to general procedure A gave, following purification by flash chromatography (hexane-EtOAc, 80:20), **10** (92 mg, 63%) as a white solid. mp 146−148 °C; R_f 0.30 (hexane/EtOAc, 80:20); ^{1}H NMR (300 MHz, $CDCl_3$): δ 7.96 (1H, d, J = 8.1 Hz), 7.70 (1H, s), 7.34 (1H, d, J = 8.7 Hz), 7.25−7.22 (2H, m), 6.44 (1H, d, J = 8.7 Hz), 4.83 (1H, dd, J = 8.7, 4.8 Hz), 4.46 (1H, t, J = 5.7 Hz), 4.30 (1H, t, J = 6.0 Hz), 4.12 (2H, t, J = 6.9 Hz), 3.75 (3H, s), 2.27 (1H, m), 1.88 (2H, quin., J = 7.5 Hz), 1.80−1.62 (2H, m), 1.42 (2H, quin., J = 8.4 Hz), 1.00 (6H, t, J = 6.9 Hz); ^{13}C NMR (75 MHz, $CDCl_3$): δ 173.3 (CO), 165.0 (CO), 136.7 (quat.), 131.8 (CH), 125.5 (quat.), 122.7 (CH), 121.8 (CH), 120.3 (CH), 110.8 (quat.), 110.4 (CH), 83.8 (CH_2F, d, $^{1}J_{CF}$ = 163.5 Hz), 57.1 (CH), 52.3 (CH_2), 46.9 (CH_3), 31.9 (CH), 30.1 (CH_2, d, $^{2}J_{CF}$ = 20.3 Hz), 29.8 (CH_2), 23.0 (CH_2, d, $^{3}J_{CF}$ = 5.3 Hz), 19.2 (CH_3), 18.2 (CH_3); ^{19}F NMR (282 MHz, $CDCl_3$): − 218.6 (1F, m); LRMS (+ESI): m/z 385.14 ([M + Na]$^+$, 100%); HRMS (+ESI): m/z calculated [M + Na]$^+$ 399.2060, found 399.2054; IR (diamond cell, thin film) 3343 (w), 2977 (m), 2962 (m), 2877 (w), 1736 (s), 1625 (s), 1509 (s), 1465 (s), 1225 (s), 1198 (s), 1167 (s), 1147 (s), 751 (s).

*Methyl (S)-2-(1-(5-Fluoropentyl)-1H-indole-3-carboxamido)-3,3-dimethylbutanoate (5F-MDMB-PICA, **11**).* Subjecting **31** (100 mg, 0.40 mmol) and methyl L-*tert*-leucinate hydrochloride (76 mg, 0.42 mmol, 1.05 equiv) to general procedure A gave, following purification by flash chromatography (hexane-EtOAc, 80:20), **10** (112 mg, 74%) as a white solid. mp 82−84 °C; R_f 0.35 (hexane/EtOAc, 80:20); ^{1}H NMR (300 MHz, $CDCl_3$): δ 7.99 (1H, m), 7.74 (1H, s), 7.38 (1H, m), 7.31−7.27 (2H, m), 7.52 (1H, d, J = 9.3 Hz), 4.78 (1H, d, J = 9.3 Hz), 4.40 (2H, dt, J = 41.4 Hz, 6.0 Hz), 4.15 (2H, t, J = 7.2 Hz), 3.76 (3H, s), 1.91 (2H, quin., J = 7.2 Hz), 1.81−1.62 (2H, m), 1.46 (2H, quin., J = 6.3 Hz), 0.93 (9H, s); ^{13}C NMR (75 MHz, $CDCl_3$): δ 172.8 (CO), 164.8 (CO), 136.7 (quat.), 131.9 (CH), 125.4 (quat.), 122.6 (CH), 121.8 (CH), 120.1 (CH), 110.8 (quat.), 110.4 (CH), 83.7 (CH_2F, d, $^{1}J_{CF}$ = 164.3 Hz), 59.9 (CH), 51.9 (CH_2), 46.8 (CH_3), 35.2 (quat.), 30.1 (CH_2, d, $^{2}J_{CF}$ = 19.5 Hz), 29.7 (CH_2), 26.9 (CH_3), 22.9 (CH_2, d, $^{3}J_{CF}$ = 5.3 Hz); ^{19}F NMR (282 MHz, $CDCl_3$): δ − 218.5 (1F, m); LRMS (+ESI): m/z 399.14 ([M + Na]$^+$, 100%); HRMS (+ESI): m/z calculated [M + Na]$^+$ 399.2060, found 399.2056; IR (diamond cell, thin film) 3437 (w), 2971 (m), 2959 (m), 1730 (s), 1639 (s), 1499 (s), 1234 (s), 1186 (s), 773 (m), 751 (s).

*Methyl (S)-2-(1-(5-Fluoropentyl)-1H-indazole-3-carboxamido)-3-methylbutanoate (5F-AMB-PINACA, **12**).* Subjecting **40** (100 mg, 0.42 mmol) and methyl L-valinate hydrochloride (75 mg, 0.45 mmol, 1.1 equiv) to general procedure A gave, following purification by flash chromatography (hexane/EtOAc, 80:20), **12** (105 mg, 69%) as a white solid. mp 68−70 °C; R_f 0.50 (hexane/EtOAc, 60:40); ^{1}H NMR (300 MHz, $CDCl_3$): δ 8.35 (1H, d, J = 8.1 Hz), 7.47 (1H, d, J = 9.0 Hz), 7.42−7.39 (2H, m), 4.80 (1H, dd, J = 8.7, 5.1 Hz), 4.51 (1H, t, J = 5.7 Hz), 4.42 (2H, t, J = 6.9 Hz), 4.36 (1H, t, J = 5.7 Hz), 3.78 (3H, s), 2.30 (1H, m, J = 6.6 Hz), 2.05 (2H, quin., J = 7.5 Hz), 1.83−1.62 (2H, m), 1.48 (2H, quin., J = 7.5 Hz), 1.04 (6H, t, J = 6.0 Hz); ^{13}C NMR (75 MHz, $CDCl_3$): δ 172.8 (CO), 162.6 (CO), 141.0 (quat.), 136.9 (quat.), 126.9 (CH), 123.1 (quat.), 123.0 (CH), 122.8 (CH), 109.3 (CH), 84.0 (CH_2, d, $^{1}J_{CF}$ = 149.3 Hz), 56.9 (CH), 52.3 (CH_2), 49.3 (CH_3), 31.7 (CH), 30.0 (CH_2, d, $^{2}J_{CF}$ = 19.9 Hz), 29.5 (CH_2), 22.8 (CH_2, d, $^{3}J_{CF}$ = 5.0 Hz), 19.3 (CH_3), 18.2 (CH_3); ^{19}F NMR (282 MHz, CDCl3): δ − 218.5 (1F, m); LRMS (+ESI): m/z 386.11 ([M + Na]$^+$, 100%); HRMS (+ESI): m/z calculated [M + Na]$^+$ 386.1856, found 386.1849; IR (diamond cell, thin film): 3415 (w), 2960 (m), 1740 (s), 1667 (s), 1526 (s), 1491 (s), 1710 (m), 752 (m).

*Methyl (S)-2-(1-(5-Fluoropentyl)-1H-indazole-3-carboxamido)-3,3-dimethylbutanoate (5F-MDMB-PINACA, **13**).* Subjecting **40** (150 mg, 0.63 mmol) and methyl L-*tert*-leucinate hydrochloride (97 mg, 0.67 mmol, 1.05 equiv) to general procedure A gave, following purification by flash chromatography (hexane-EtOAc, 80:20), **13** (151 mg, 63%) as a white solid. mp 64−66 °C; R_f 0.60 (hexane/EtOAc, 60:40); ^{1}H NMR (300 MHz, $CDCl_3$): δ 8.35 (1H, d, J = 8.1 Hz), 7.54 (1H, d, J = 9.6 Hz), 7.42−7.39 (2H, m), 4.73 (1H, d, J = 9.6 Hz), 4.52 (1H, t, J = 5.7 Hz), 4.42 (2H, t, J = 7.2 Hz), 4.36 (1H, t, J = 6.0 Hz), 3.76 (3H, s), 1.99 (2H, quin., J = 7.8 Hz), 1.84−1.67 (2H, m), 1.48 (2H, quin., J = 8.1 Hz), 1.09 (9H, s); ^{13}C NMR (300 MHz, $CDCl_3$): δ 172.3 (CO), 162.5 (CO), 141.0 (quat.), 137.0 (quat.), 126.9 (CH), 123.1 (quat.), 123.0 (CH), 122.8 (CH), 109.3 (CH), 83.9 (CH_2, d, $^{1}J_{CF}$ = 163.5 Hz,), 59.6 (quat.), 51.9 (CH_2), 49.3 (CH_3), 35.2 (quat.), 30.3 (CH_2, d, $^{2}J_{CF}$ = 19.5 Hz), 29.5 (CH_2), 26.8 (CH_3), 22.8 (CH_2, d, $^{3}J_{CF}$ = 4.5 Hz); ^{19}F NMR (282 MHz, $CDCl_3$): δ − 218.5 (1F, m); LRMS (+ESI): m/z 400.14 ([M + Na]$^+$, 100%); HRMS (+ESI): m/z calculated [M + Na]$^+$ 400.2012, found 400.2007; IR (diamond cell, thin film): 3420 (w), 2960 (m), 2870 (w), 1737 (s), 1671 (s), 1524 (s), 1491 (s), 1262 (m), 1216 (s), 752 (m).

*Methyl (S)-2-(1-(4-Fluorobenzyl)-1H-indole-3-carboxamido)-3-methylbutanoate (AMB-FUBICA, **14**).* Subjecting **32** (100 mg, 0.37 mmol) and methyl L-valinate hydrochloride (65 mg, 0.39 mmol, 1.05 equiv) to general procedure A gave, following purification by flash chromatography (hexane/EtOAc, 80:20), **14** (110 mg, 78%) as a white solid. mp 151−153 °C; R_f 0.30 (hexane/EtOAc, 80:20); ^{1}H NMR (300 MHz, $CDCl_3$): δ 8.05 (1H, d, J = 7.8 Hz), 7.78 (1H, s), 7.35−7.28 (3H, m), 7.15 (2H, t, J = 5.4 Hz), 7.03 (2H, t, J = 7.5 Hz), 5.33 (2H, s), 4.90 (1H, dd, J = 8.7, 4.8 Hz), 3.82 (3H, s), 2.33 (1H, m, J = 6.0 Hz), 1.07 (6H, t, J = 7.2 Hz); ^{13}C NMR (75 MHz, $CDCl_3$): δ 173.3 (CO), 164.9 (CO), 162.6 (quat., d, $^{1}J_{CF}$ = 247.2 Hz), 136.9 (quat.), 132.0 (CH), 131.9 (quat., d, $^{4}J_{CF}$ = 3.1 Hz), 129.0 (CH, d, $^{3}J_{CF}$ = 8.3 Hz), 125.7 (quat.), 123.0 (CH), 122.1 (CH), 120.4 (CH), 116.1 (CH, d, $^{2}J_{CF}$ = 21.9 Hz), 111.5 (quat.), 110.7 (CH), 57.1 (CH_2), 52.3 (CH_3), 50.1 (CH), 31.8 (CH), 19.2 (CH_3), 18.2 (CH_3); ^{19}F NMR (282 MHz, CDCl3): δ − 113.9 (1F, m); LRMS (+ESI): m/z 405.11 ([M + Na]$^+$, 100%); HRMS (+ESI): m/z 405.1590, found 405.1583; IR (diamond cell, thin film): 3327 (m), 2944 (m), 2875 (w), 1738 (s), 1630 (s), 1510 (s), 1125 (s), 766 (s), 566 (m).

*Methyl (S)-2-(1-(4-Fluorobenzyl)-1H-indole-3-carboxamido)-3,3-dimethylbutanoate (MDMB-FUBICA, **15**).* Subjecting **32** (50 mg, 0.19 mmol) and methyl L-*tert*-leucinate hydrochloride (42 mg, 0.23 mmol, 1.2 equiv) to general procedure A gave, following purification by flash chromatography (hexane/EtOAc, 80:20), **15** (58 mg, 77%) as a white solid. mp 132−134 °C; R_f 0.40 (hexane/EtOAc, 80:20); ^{1}H NMR (300 MHz, $CDCl_3$): δ 8.02 (1H, d, J = 7.8 Hz), 7.77 (1H, s), 7.32−7.26 (3H, m), 7.14 (2H, t, J = 6.3 Hz), 7.01 (2H, t, J = 6.3 Hz), 6.55 (1H, d, J = 9.3 Hz), 5.32 (2H, s), 4.79 (1H, d, J = 9.6 Hz), 3.78 (3H, s), 1.10 (9H, s); ^{13}C NMR (75 MHz, $CDCl_3$): δ 172.8 (CO), 164.7 (CO), 162.6 (quat., d, $^{1}J_{CF}$ = 246.0 Hz), 136.9 (quat.), 132.2 (CH), 131.9 (quat., d, $^{4}J_{CF}$ = 3.0 Hz), 128.9 (CH, d, $^{3}J_{CF}$ = 8.3 Hz), 125.6 (quat.), 123.0 (CH), 122.1 (CH), 120.2 (CH), 116.1 (CH, d, $^{2}J_{CF}$ = 21.8 Hz), 111.5 (quat.), 110.8 (CH), 59.9 (CH_2), 52.0 (CH_3), 50.1

DOI: 10.1021/acschemneuro.6b00137
ACS Chem. Neurosci. 2016, 7, 1241−1254

(CH), 35.2 (quat.), 26.9 (CH_3); ^{19}F NMR (282 MHz, $CDCl_3$): δ − 113.9 (1F, m); LRMS (+ESI): m/z 419.13 ([M + Na]$^+$, 100%); HRMS (+ESI): m/z calculated [M + Na]$^+$ 419.1747, found 419.1740; IR (diamond cell, thin film): 3440 (w), 2961 (w), 1725 (s), 1637 (s), 1537 (s), 1327 (s), 815 (m).

*Methyl (S)-2-(1-(4-Fluorobenzyl)-1H-indazole-3-carboxamido)-3-methylbutanoate (AMB-FUBINACA, **16**).* Subjecting **41** (100 mg, 0.37 mmol) and methyl L-valinate hydrochloride (65 mg, 0.39 /EtOAc, 90:10), **16** (85 mg, 60%) as a colorless oil. R_f. 0.65 (hexane/EtOAc, 80:20); ^1H NMR (300 MHz, $CDCl_3$): δ 8.36 (1H, d, J = 7.8 Hz), 7.50 (1H, d, J = 9.0 Hz), 7.42−7.27 (2H, m), 7.23−7.19 (2H, t, J = 6.9 Hz), 7.01 (2H, t, J = 7.8 Hz), 5.61 (2H, s), 4.83 (1H, dd, J = 8.7, 5.1 Hz), 3.78 (3H, s), 2.30 (1H, m, J = 6.6 Hz), 1.05 (6H, t, J = 5.4 Hz); ^{13}C NMR (75 MHz, $CDCl_3$): δ 172.7 (CO), 162.6 (quat., $^1J_{CF}$ = 245.3 Hz), 162.5 (CO), 140.9 (quat.), 137.5 (quat.), 131.9 (quat., d, $^4J_{CF}$ = 3.1 Hz), 129.1 (CH, d, $^3J_{CF}$ = 8.3 Hz), 127.2 (CH), 123.5 (quat.), 123.1 (CH), 123.0 (CH), 116.0 (CH, d, $^2J_{CF}$ = 21.8 Hz), 109.6 (CH), 56.9 (CH), 53.1 (CH_2), 52.3 (CH_3), 31.8 (CH), 19.3 (CH_3), 18.2 (CH_3); ^{19}F NMR (282 MHz, CDCl3): δ − 114.0 (1F, m); LRMS (+ESI): m/z 406.08 ([M + Na]$^+$, 100%); HRMS (+ESI): m/z calculated [M + Na]$^+$ 406.1543, found 406.1537; IR (diamond cell, thin film): 3415 (w), 2964 (m), 1740 (s), 1667 (s), 1527 (s), 1511 (s), 1492 (s), 1261 (s), 1172 (s), 1158 (s), 750 (m).

*Methyl (S)-2-(1-(4-Fluorobenzyl)-1H-indazole-3-carboxamido)-3,3-dimethylbutanoate (MDMB-FUBINACA, **17**).* Subjecting **41** (100 mg, 0.37 mmol) and methyl L-*tert*-leucinate hydrochloride (81 mg, 0.41 mmol, 1.1 equiv) to general procedure A gave, following purification by flash chromatography (hexane/EtOAc, 80:20), **17** (96 mg, 65%) as a white crystalline solid. mp 120−122 °C; R_f. 0.60 (hexane/EtOAc, 60:40); ^1H NMR (300 MHz, $CDCl_3$): δ 8.21 (1H, d, J = 7.8 Hz), 7.59 (1H, d, J = 8.4 Hz), 7.44 (1H, t, J = 7.8 Hz), 7.33−7.27 (3H, m), 7.06 (2H, t, J = 8.4 Hz), 5.72 (2H, s), 4.61 (1H, s), 3.77 (3H, s), 1.09 (9H, s); ^{13}C NMR (75 MHz, $CDCl_3$): δ 172.3 (CO), 162.6 (quat., d, $^1J_{CF}$ = 245.3 Hz), 162.3 (CO), 140.9 (quat.), 137.5 (quat.), 131.9 (quat., d, $^4J_{CF}$ = 3.3 Hz), 129.1 (CH, d, $^3J_{CF}$ = 8.3 Hz), 127.2 (CH), 123.5 (quat.), 123.1 (CH), 123.0 (CH), 116.0 (CH, d, $^2J_{CF}$ = 21.8 Hz), 109.6 (CH), 59.7 (CH), 53.1 (CH_2), 51.95 (CH_3), 35.2 (quat.), 26.8 (CH_3); ^{19}F NMR (282 MHz, $CDCl_3$): δ − 114.00 (1F, m); LRMS (+ESI): m/z 419.12 ([M + Na]$^+$, 100%); HRMS (+ESI): m/z calculated [M + Na]$^+$ 420.1699, found 420.1694; IR (diamond cell, thin film): 3419 (w), 2966 (m), 1737 (s), 1670 (s), 1526 (s), 1511 (s), 1222 (s), 1166 (s), 749 (m).

*Methyl (S)-2-(1-(Cyclohexylmethyl)-1H-indole-3-carboxamido)-3-methylbutanoate (AMB-CHMICA, **18**).* Subjecting **33** (50 mg, 0.20 mmol) and methyl L-valinate hydrochloride (35 mg, 0.21 mmol, 1.05 equiv) to general procedure A gave, following purification by flash chromatography (hexane/EtOAc, 90:10), **18** (60 mg, 81%) as a white solid. mp 137−139 °C; R_f. 0.55 (hexane/EtOAc, 80:20); ^1H NMR (300 MHz, $CDCl_3$): δ 7.99 (1H, m), 7.70 (1H, s), 7.38 (1H, m), 7.31−7.27 (2H, m), 6.47 (1H, d, J = 8.7 Hz), 4.87 (1H, dd, J = 8.7, 4.8 Hz), 3.96 (2H, d, J = 7.2 Hz), 3.77 (3H, s), 2.31 (1H, m, J = 5.1 Hz), 1.88 (1H, m), 1.74−1.60 (5H, m), 1.25−1.18 (3H, m), 1.06−0.98 (8H, m); ^{13}C NMR (75 MHz, $CDCl_3$): δ 173.3 (CO), 165.1 (CO), 137.1 (quat.), 132.7 (CH), 125.4 (quat.), 122.5 (CH), 121.6 (CH), 120.1 (CH), 110.8 (CH), 110.5 (quat.), 57.0 (CH), 53.5 (CH_2), 52.3 (CH_3), 38.7 (CH), 31.9 (CH), 31.2 (CH_2), 26.3 (CH_2), 25.8 (CH_2), 19.3 (CH_3), 18.3 (CH_3); LRMS (+ESI): m/z 393.16 ([M + Na]$^+$, 100%); HRMS (+ESI): m/z calculated [M + Na]$^+$ 393.2154, found 393.2147; IR (diamond cell, thin film): 3327 (w), 2929 (m), 2849 (w), 1735 (s), 1618 (s), 1539 (s), 1518 (s), 1257 (s), 735 (s).

*Methyl (S)-2-(1-(Cyclohexylmethyl)-1H-indole-3-carboxamido)-3,3-dimethylbutanoate (MDMB-CHMICA, **19**).* Subjecting **33** (50 mg, 0.20 mmol) and methyl L-*tert*-leucinate hydrochloride (40 mg, 0.21 mmol, 1.05 equiv) to general procedure A gave, following purification by flash chromatography (hexane/EtOAc, 90:10), **19** (55 mg, 72%) as a white solid. mp 136−138 °C; R_f. 0.70 (hexane/EtOAc, 80:20); ^1H NMR (300 MHz, $CDCl_3$): δ 8.09 (1H, d, J = 5.7 Hz), 8.00 (1H, s), 7.46 (1H, d, J = 8.1 Hz), 7.27−7.16 (2H, m), 4.64 (1H, s), 4.04 (2H, d, J = 6.9 Hz), 3.75 (3H, s), 1.89 (1H, m), 1.71−1.57 (5H, m), 1.28−1.02 (14H, m); ^{13}C NMR (75 MHz, $CDCl_3$): δ 172.9 (CO), 164.9 (CO), 137.1 (quat.), 132.8 (CH), 125.3 (quat.), 122.5 (CH), 121.7 (CH), 120.0 (CH), 110.8 (CH), 110.5 (quat.), 59.8 (CH), 53.5 (CH_2), 52.0 (CH_3), 38.7 (quat.), 35.2 (CH), 31.1 (CH_2), 26.9 (CH_3), 26.3 (CH_2), 25.8 (CH_2); LRMS (+ESI): m/z ([M + Na]$^+$, 100%); HRMS (+ESI): m/z calculated [M + Na]$^+$ 407.2311, found 407.2304; IR (diamond cell, thin film): 3320 (w), 2928 (m), 2851 (w), 1738 (s), 1614 (s), 1536 (s), 1512 (s), 1141 (s), 739 (s).

*Methyl (S)-2-(1-(Cyclohexylmethyl)-1H-indazole-3-carboxamido)-3-methylbutanoate (AMB-CHMINACA, **20**).* Subjecting **42** (75 mg, 0.29 mmol) and methyl L-valinate hydrochloride (56 mg, 0.31 mmol, 1.05 equiv) to general procedure A gave, following purification by flash chromatography (hexane/EtOAc, 80:20), **20** (83 mg, 77%) as a colorless oil. R_f. 0.75 (hexane/EtOAc, 60:40); ^1H NMR (300 MHz, $CDCl_3$): δ 8.34 (1H, d, J = 8.1 Hz), 7.47 (1H, d, J = 9 Hz), 7.42−7.36 (2H, m), 4.80 (1H, dd, J = 9.1 Hz, 5.7 Hz), 4.22 (2H, d, J = 7.2 Hz), 3.78 (3H, s), 2.31 (1H, m), 2.04 (1H, m), 1.72−1.58 (5H, m), 1.30−0.97 (11H, m); ^{13}C NMR (300 MHz, $CDCl_3$): δ 172.7 (CO), 162.7 (CO), 141.5 (quat.), 136.7 (quat.), 126.6 (CH), 122.83 (quat.), 122.77 (CH), 122.6 (CH), 109.6 (CH), 56.8 (CH), 55.8 (CH_2), 52.2 (CH_3), 38.8 (CH), 31.7 (CH), 31.0 (CH_2), 26.3 (CH_2), 25.7 (CH_2), 19.2 (CH_3), 18.2 (CH_3); LRMS (+ESI): m/z 394.15 ([M + Na]$^+$, 100%); HRMS (+ESI): m/z calculated [M + Na]$^+$ 394.2107, found 394.2100; IR (diamond cell, thin film): 3411 (w), 2927 (s), 2852 (m), 1741 (s), 1670 (s), 1525 (s), 1491 (s), 1176 (m), 751 (m).

*Methyl (S)-2-(1-(Cyclohexylmethyl)-1H-indazole-3-carboxamido)-3,3-dimethylbutanoate (MDMB-CHMINACA, **21**).* Subjecting **42** (100 mg, 0.39 mmol) and methyl L-*tert*-leucinate hydrochloride (69 mg, 0.41 mmol, 1.05 equiv) to general procedure A gave, following purification by flash chromatography (hexane/EtOAc, 80:20), **21** (110 mg, 73%) as a colorless oil. R_f. 0.85 (hexane/EtOAc, 60:40); ^1H NMR (300 MHz, $CDCl_3$): δ 8.34 (1H, d, J = 8.1 Hz), 7.55 (1H, d, J = 9.6 Hz), 7.40−7.36 (2H, m), 4.73 (1H, d, J = 9.9 Hz), 4.22 (2H, d, J = 7.2 Hz), 3.76 (3H, s), 2.03 (1H, m), 1.75−1.58 (5H, m), 1.30−1.04 (14H, m); ^{13}C NMR (300 MHz, $CDCl_3$): δ 172.4 (CO), 162.6 (CO), 141.5 (quat.), 136.8 (quat.), 126.7 (CH), 122.91 (quat.), 122.87 (CH), 122.6 (CH), 109.6 (CH), 59.6 (CH), 55.8 (CH_2), 51.9 (CH_3), 38.9 (quat.), 35.2 (CH), 31.1 (CH_2), 26.8 (CH_3), 26.4 (CH_2), 25.8 (CH_2); LRMS (+ESI): m/z 408.17 ([M + Na]$^+$, 100%); HRMS (+ESI): m/z calculated [M + Na]$^+$ 408.2263, found 408.2257; IR (diamond cell, thin film): 3417 (w), 2927 (s), 2852 (m), 1738 (s), 1672 (s), 1524 (s), 1491 (m), 1164 (m), 1134 (m), 751 (m).

*Methyl (S)-2-(1-(Pentyl)-1H-indole-3-carboxamido)-3-methylbutanoate (AMB-PICA, **22**).* Subjecting **34** (100 mg, 0.43 mmol) and methyl L-valinate hydrochloride (76 mg, 0.45 mmol, 1.1 equiv) to general procedure A gave, following purification by flash chromatography (hexane/ethyl acetate, 85:15), **22** (98 mg, 66%) as a white solid. mp 148−150 °C; R_f. 0.50 (hexane/ethyl acetate, 80:20); ^1H NMR (300 MHz, $CDCl_3$): δ 7.99 (1H, d, J = 6 Hz), 7.74 (1H, s), 7.38 (1H, d, J = 8.7 Hz), 7.29−7.26 (2H, m), 6.48 (1H, d, J = 8.4 Hz), 4.86 (1H, dd, J = 8.7, 4.8 Hz), 4.13 (2H, t, J = 6.9 Hz), 3.78 (3H, s), 2.31 (1H, m), 1.86 (2H, quin., J = 6.9 Hz), 1.33 (4H, m), 1.04 (6H, t, J = 6.9 Hz), 0.89 (3H, t, J = 6.9 Hz); ^{13}C NMR (75 MHz, $CDCl_3$): δ 173.3 (CO), 165.1 (CO), 136.8 (quat.), 132.0 (CH), 125.5 (quat.), 122.6 (CH), 121.7 (CH), 120.2 (CH), 110.6 (quat.), 110.5 (CH), 57.0 (CH), 52.3 (CH_3), 47.0 (CH_2), 31.9 (CH), 29.8 (CH_2), 29.1 (CH_2), 22.4 (CH_2), 19.2 (CH_3), 18.2 (CH_3), 14.0 (CH_3); LRMS (+ESI): m/z 367.14 ([M + Na]$^+$, 100); HRMS (+ESI): m/z calculated [M + Na]$^+$ 367.1998, found 367.1992; IR (diamond cell, thin film) 3338 (w), 2952 (m), 2928 (m), 2868 (w), 1739 (s), 1630 (s), 1508 (s), 1195 (s), 1157 (s), 751 (s).

*Methyl (S)-2-(1-(Pentyl)-1H-indole-3-carboxamido)-3,3-dimethylbutanoate (MDMB-PICA, **23**).* Subjecting **34** (75 mg, 0.32 mmol) and methyl L-*tert*-leucinate hydrochloride (61 mg, 0.39 mmol, 1.2 equiv) to general procedure A gave, following purification by flash chromatography (hexane/EtOAc, 90:10), **21** (82 mg, 71%) as a white solid. mp 70−72 °C; R_f. 0.60 (hexane/EtOAc 80:20); ^1H NMR (300 MHz, $CDCl_3$): δ 8.00−7.95 (2H, m), 7.75 (1H, s), 7.42−7.37 (1H, m), 7.31−7.26 (2H, m), 6.53 (1H, d, J = 9.3 Hz), 4.79 (1H, d, J = 9.4 Hz), 4.13 (2H, t, J = 7.2 Hz), 3.76 (3H, s), 1.86 (2H, quin., J = 7.1 Hz), 1.39−1.26 (4H, m), 1.09 (9H, s), 0.89 (3H, t, J = 6.8 Hz); ^{13}C NMR

DOI: 10.1021/acschemneuro.6b00137
ACS Chem. Neurosci. 2016, 7, 1241−1254

(75 MHz, $CDCl_3$): δ 172.9 (CO), 164.9 (CO), 136.8 (quat.), 132.1 (CH), 125.4 (quat.), 122.5 (CH), 121.7 (CH), 120.1 (CH), 110.6 (quat.), 110.5 (CH), 59.8 (CH), 51.9 (CH_3), 47.0 (CH_2), 35.2 (quat.), 29.8 (CH_2), 29.1 (CH_2), 26.9 (CH_3), 22.4 (CH_2), 14.0 (CH_3); LRMS (+ESI): *m/z* 381.15 ($[M + Na]^+$, 100%); HRMS (+ESI): *m/z* calculated $[M + Na]^+$ 381.2154, found 381.2149; IR (diamond cell, thin film): 3434 (w), 2952 (m), 2927 (m), 2868 (w), 1732 (s), 1641 (s), 1530 (s), 1498 (s), 1214 (s), 1185 (s), 1157 (s), 1129 (s), 751 (s).

*Methyl (S)-2-(1-(Pentyl)-1H-indazole-3-carboxamido)-3-methylbutanoate (AMB-PINACA, **24**).* Subjecting **43** (100 mg, 0.46 mmol) and methyl L-valinate hydrochloride (80 mg, 0.48 mmol, 1.05 equiv) to general procedure A gave, following purification by flash chromatography (hexane/EtOAc, 85:15), **24** (108 mg, 68%) as a colorless oil. R_f 0.75 (hexane/EtOAc, 60:40); ^{1}H NMR (300 MHz, $CDCl_3$): δ 8.35 (1H, d, *J* = 8.1 Hz), 7.47 (1H, d, *J* = 8.7 Hz), 7.44−7.37 (2H, m), 4.81 (1H, dd, *J* = 9.0, 5.1 Hz), 4.39 (2H, t, *J* = 7.5 Hz), 3.78 (3H, s), 2.31 (1H, m), 1.40−1.26 (4H, m), 1.04 (6H, t, *J* = 6.0 Hz), 0.90 (3H, t, *J* = 6.0 Hz); ^{13}C NMR (300 MHz, $CDCl_3$): δ 172.8 (CO), 162.7 (CO), 141.0 (quat.), 136.7 (quat.), 126.7 (CH), 123.1 (quat.), 122.9 (CH), 122.7 (CH), 109.4 (CH), 56.9 (CH), 52.3 (CH_3), 49.6 (CH_2), 31.7 (CH), 29.6 (CH_2), 29.1 (CH_2), 22.4 (CH_2), 19.3 (CH_3), 18.2 (CH_3), 14.1 (CH_3); LRMS (+ESI): *m/z* 368.12 ($[M + Na]^+$, 100%); HRMS (+ESI): *m/z* calculated $[M + Na]^+$ 368.1950, found 368.1944; IR (diamond cell, thin film): 3419 (w), 2959 (m), 2932 (m), 2873 (w), 1742 (s), 1670 (s), 1526 (s), 1491 (s), 1181 (s), 752 (m).

*Methyl (S)-2-(1-(Pentyl)-1H-indazole-3-carboxamido)-3,3-dimethylbutanoate (MDMB-PINACA, **25**).* Subjecting **43** (100 mg, 0.46 mmol) and methyl L-*tert*-leucinate hydrochloride (71 87 mg, 0.48 mmol, 1.05 equiv) to general procedure A gave, following purification by flash chromatography (hexane/EtOAc, 85:15), **25** (125 mg, 76%) as a colorless oil. R_f 0.85 (hexane/EtOAc, 60:40); ^{1}H NMR (300 MHz, $CDCl_3$): δ 8.34 (1H, d, *J* = 8.1 Hz), 7.55 (1H, d, *J* = 9.6 Hz), 7.41−7.36 (2H, m), 4.73 (1H, d, *J* = 9.9 Hz), 4.39 (2H, t, *J* = 7.5 Hz), 3.76 (3H, s), 1.95 (2H, quin., *J* = 6.9 Hz), 1.41−1.30 (4H, m), 1.09 (9H, s), 0.90 (3H, t, *J* = 7.2 Hz); ^{13}C NMR (300 MHz, $CDCl_3$): δ 172.3 (CO), 162.5 (CO), 141.0 (quat.), 136.7 (quat.), 126.7 (CH), 123.1 (quat.), 122.9 (CH), 122.7 (CH), 109.4 (CH), 59.6 (CH), 51.9 (CH_3), 49.6 (CH_2), 35.2 (quat.), 29.6 (CH_2), 29.1 (CH_2), 26.8 (CH_3), 22.4 (CH_2), 14.1 (CH_3); LRMS (+ESI): *m/z* 382.07 ($[M + Na]^+$, 100%); HRMS (+ESI): *m/z* calculated $[M + Na]^+$ 382.2107, found 382.2101; IR (diamond cell, thin film): 3419 (bs), 2960 (m), 2873 (w), 1738 (s), 1672 (s), 1525 (s), 1492 (m), 1163 (m), 751 (m).

General Procedure B: Synthesis of 1-Alkyl-3-(trifluoroacetyl)indoles. To a cooled (0 °C) suspension of sodium hydride (60% dispersion in mineral oil, 137 mg, 3.42 mmol, 2.0 equiv) in DMF (6 mL) was added indole (200 mg, 1.71 mmol) portionwise and the mixture stirred for 10 min. The mixture was treated dropwise with the appropriate bromoalkane (1.80 mmol, 1.05 equiv) and stirred at ambient temperature for 1 h. The cooled (0 °C) mixture was treated dropwise with trifluoroacetic anhydride (600 μL, 4.28 mmol, 2.5 equiv) and stirred at ambient temperature for 1 h. The reaction was poured into ice water (75 mL) and extracted with CH_2Cl_2 (3 × 75 mL). The combined organic extracts were washed with H_2O (100 mL), brine (100 mL), dried ($MgSO_4$) and the solvent evaporated under reduced pressure. The pure 1-alkyl-3-trifluoroacetylindoles were obtained following purification by flash chromatography.

*2,2,2-Trifluoro-1-(1-(5-fluoropentyl)-1H-indol-3-yl)ethanone (**27**).* Subjecting indole (500 mg, 4.27 mmol) and 1-bromo-5-fluoropentane (560 μL, 4.48 mmol, 1.05 equiv) to general prcoedure B gave, following purification by flash chromatography (hexane/EtOAc, 90:10), **27** as a red solid (920 mg, 72%). mp 42−44 °C; R_f 0.53 (hexane/EtOAc, 80:20); ^{1}H NMR (300 MHz, $CDCl_3$): δ 8.42−8.39 (1H, m), 7.93 (1H, s), 7.42−7.33 (3H, m), 4.43 (2H, dt, *J* = 47.1, 5.8 Hz), 4.21 (2H, t, *J* = 6.6 Hz), 1.97 (2H, quin., *J* = 6.0 Hz), 1.74 (2H, dquin., *J* = 26.1 Hz, 5.2 Hz), 1.50 (2H, quin., *J* = 6.6 Hz); ^{13}C NMR (75 MHz, $CDCl_3$): δ 174.8 (q, $^2J_{CF}$ = 34.5 Hz, quat.), 137.4 (q, $^3J_{CF}$ = 4.9 Hz, CH), 136.7 (quat.), 127.2 (quat.), 124.7 (CH), 124.0 (CH), 122.8 (CH), 117.2 (q, $^1J_{CF}$ = 289.5 Hz, CF_3), 110.4 (CH), 109.6 (quat.), 83.7 (d, $^1J_{CF}$ = 164.3 Hz, CH_2), 47.6 (CH_2), 29.9 (d, $^2J_{CF}$ = 19.5 Hz, CH_2), 29.5 (CH_2), 22.9 (d, $^3J_{CF}$ = 4.5 Hz, CH_2); ^{19}F NMR (282 MHz, $CDCl_3$): δ − 72.2 (3F, s), − 218.7 (1F, m); LRMS (+ESI): *m/z* 324.00 ($[M + Na]^+$, 100%); IR (diamond cell, thin film): 3154 (w), 2956 (m), 2922 (m), 2862 (w), 1658 (s), 1526 (s), 1280 (s), 1176 (s), 1133 (s), 876 (s), 759 (s), 726 (s).

*2,2,2-Trifluoro-1-(1-(4-fluorobenzyl)-1H-indol-3-yl)ethanone (**28**).* Subjecting indole (250 mg, 2.13 mmol) and 4-fluorobenzyl bromide (290 μL, 2.35 mmol, 1.1 equiv) to general prcoedure B gave, following purification by flash chromatography (hexane/EtOAc, 90:10), **28** as a red solid (518 mg, 76%). mp 82−84 °C; R_f 0.57 (hexane/EtOAc, 80:20); ^{1}H NMR (300 MHz, $CDCl_3$): δ 8.40 (1H, d, *J* = 7.7 Hz), 7.95 (1H, s), 7.38−7.29 (3H, m), 7.17−7.06 (2H, m), 7.06−7.00 (2H, m), 5.35 (2H, s); ^{13}C NMR (75 MHz, $CDCl_3$): δ 175.1 (q, $^2J_{CF}$ = 35.3 Hz, CO), 162.8 (d, $^1J_{CF}$ = 246.8 Hz, quat.), 137.6 (q, $^4J_{CF}$ = 4.9 Hz, CH), 136.8 (quat.), 130.7 (d, $^4J_{CF}$ = 3.2 Hz, quat.), 128.9 (d, $^3J_{CF}$ = 8.2 Hz, CH), 127.3 (quat.), 125.0 (CH), 124.3 (CH), 122.8 (CH), 117.1 (q, $^1J_{CF}$ = 291.1 Hz, quat.), 110.8 (CH), 110.1 (quat.), 50.8 (CH_2); ^{19}F NMR (282 MHz, $CDCl_3$): δ − 72.3 (3F, s), − 113.0 (1F, m); LRMS (+ESI): *m/z* 344.01 ($[M + Na]^+$, 100%); IR (diamond cell, thin film): 3130 (w), 3080 (w), 2943 (w), 2866 (w), 1654 (s), 1525 (s), 1509 (s), 1392 (s), 1281 (m), 1157 (s), 1131 (s), 1046 (s), 876 (s), 747 (s), 728 (s).

*2,2,2-Trifluoro-1-(1-(cyclohexylmethyl)-1H-indol-3-yl)ethanone (**29**).* Subjecting indole (200 mg, 1.71 mmol) and (cyclohexyl)methyl bromide (250 μL, 1.80 mmol, 1.05 equiv) to general prcoedure B gave, following purification by flash chromatography (hexane/EtOAc, 93:7), **29** as a pale brown solid (425 mg, 80%). mp 87−89 °C; R_f 0.79 (hexane/EtOAc, 80:20); ^{1}H NMR (300 MHz, $CDCl_3$): δ 8.42 (1H, d, *J* = 4.1 Hz), 7.89 (1H, s), 7.45−7.32 (3H, m), 4.02 (2H, d, *J* = 6.9 Hz), 1.90 (1H, m), 1.74−1.62 (5H, m), 1.24−1.00 (5H, m); ^{13}C NMR (75 MHz, $CDCl_3$): δ 174.8 (q, $^2J_{CF}$ = 34.5 Hz, CO), 138.1 (CH), 137.1 (quat.), 127.1 (quat.), 124.5 (CH), 123.9 (CH), 122.7 (CH), 117.2 (quat.), 110.7 (CH), 109.3 (quat.), 54.2 (CH_2), 38.3 (CH), 30.9 (CH_2), 26.1 (CH_2), 25.6 (CH_2); ^{19}F NMR (282 MHz, $CDCl_3$): δ − 72.2 (3F, s); LRMS (+ESI): *m/z* 332.06 ($[M + Na]^+$, 100%); IR (diamond cell, thin film): 3118 (w), 2925 (m), 2854 (w), 1650 (s), 1531 (s), 1397 (m), 1284 (m), 1179 (s), 1130 (s), 1048 (m), 875 (s), 748 (s), 725 (s).

*2,2,2-Trifluoro-1-(1-(pentyl)-1H-indol-3-yl)ethanone (**30**).* Subjecting indole (200 mg, 1.71 mmol) and 1-bromopentane (225 μL, 1.80 mmol, 1.05 equiv) to general prcoedure B gave, following purification by flash chromatography (hexane/ethyl acetate 94:6), **30** as a yellow oil (450 mg, 94%). R_f 0.81 (hexane-ethyl acetate 80:20); ^{1}H NMR (300 MHz, $CDCl_3$): δ 8.43 (1H, d, *J* = 8.7 Hz), 7.93 (1H, s), 7.42−7.36 (3H, m), 4.21 (2H, t, *J* = 6.9 Hz), 1.95 (2H, quin., *J* = 7.2 Hz), 1.43−1.32 (4H, m), 0.92 (3H, t, *J* = 6.6 Hz); ^{13}C NMR (75 MHz, $CDCl_3$): δ 174.8 (q, CO, $^2J_{CF}$ = 34.5 Hz), 137.5 (d, CH, $^4J_{CF}$ = 4.5 Hz), 136.8 (quat.), 127.3 (quat.), 124.6 (CH), 124.0 (CH), 122.8 (CH), 117.3 (q, CF_3, $^1J_{CF}$ = 289.5 Hz), 110.5 (CH), 109.5 (quat.), 47.8 (CH_2), 29.5 (CH_2), 29.0 (CH_2), 22.3 (CH_2), 14.0 (CH_3); ^{19}F NMR (282 MHz, $CDCl_3$): δ − 72.2 (3F, s); LRMS (+ESI): *m/z* 306.03 ($[M + Na]^+$, 100%); IR (diamond cell, thin film): 3124 (w), 2959 (m), 2933 (m), 2863 (w), 1662 (s), 1527 (s), 1397 (m), 1286 (m), 1181 (s), 1132 (s), 878 (m), 751 (m).

General Procedure C: Synthesis of 1-Alkyl-1*H*-indole-3-carboxylic Acids and 1-Alkyl-1*H*-indazole-3-carboxylic Acids. To a solution of the appropriate 1-alkyl-3-(trifluoroacetyl)indole or methyl 1-alkyl-1*H*-indazole-3-carboxylate (2.58 mmol) in MeOH (20 mL) was added 1 M aq. NaOH (3.87 mL, 3.87 mmol, 1.5 equiv) and the solution heated at reflux for 18 h. The mixture was cooled to ambient temperature, solvent was evaporated in vacuo, and the mixture was poured onto sat. aq. $NaHCO_3$ (75 mL). The aqueous phase was washed with Et_2O (75 mL) and the pH adjusted to 2 with 1 M aq. HCl. The aquoeus phase was extracted with Et_2O (3 × 75 mL) and the combined organic layers were washed with brine (150 mL), dried ($MgSO_4$) and concentrated in vacuo to give the crude products. Analytical purity for 1-alkyl-1*H*-indazole-3-carboxylic acids was achieved by recrystallization from *i*-PrOH.

DOI: 10.1021/acschemneuro.6b00137
ACS Chem. Neurosci. 2016, 7, 1241−1254

*1-(5-Fluoropentyl)-1H-indole-3-carboxylic Acid (**31**).* Subjecting **27** (500 mg, 1.66 mmol) to general procedure C gave **31** (338 mg, 82%) as a white solid. mp 120−122 °C; ^{1}H NMR (75 MHz, CD_3OD): δ 8.08 (1H, d, J = 7.8 Hz), 7.96 (1H, s), 7.48 (1H, d, J = 7.8 Hz), 7.28−7.17 (2H, m), 4.38 (2H, dt, J = 47.4, 6.0 Hz), 4.25 (2H, t, J = 6.9 Hz), 1.91 (2H, quin., J = 7.8 Hz), 1.77−1.63 (2H, dquin., J = 25.8, 7.2 Hz), 1.42 (2H, quin., J = 7.8 Hz); ^{13}C NMR (75 MHz, CD_3OD): δ 168.8 (CO), 138.1 (quat.), 136.3 (CH), 128.3 (quat.), 123.6 (CH), 122.6 (CH), 122.5 (CH), 111.4 (CH), 107.8 (quat.), 84.6 (d, $^2J_{CF}$ = 162.8 Hz, CH_2), 47.6 (CH_2), 31.1 (d, $^3J_{CF}$ = 9.5 Hz, CH_2), 30.7 (CH_2), 23.7 (CH_2); ^{19}F NMR (282 MHz, CD_3OD): δ − 221.8 (1F, m); LRMS (−ESI): m/z 248.29 ([M − H]$^-$, 100%); IR (diamond cell, thin film): 3043 (w), 2962 (m), 2895 (w), 2704 (w), 2585 (w), 1635 (s), 1523 (s), 1467 (s), 1397 (s), 1272 (s), 1170 (s), 920 (s), 742 (s), 618 (s), 427 (s).

*1-(4-Fluorobenzyl)-1H-indole-3-carboxylic Acid (**32**).* Subjecting **28** (500 mg, 1.56 mmol) to general procedure C gave **32** (282 mg, 67%) as a white solid. mp 207−209 °C; ^{1}H NMR (300 MHz, CD_3OD): δ 8.10 (1H, dd, J = 6.3, 3.3 Hz), 8.03 (1H, s), 7.39 (1H, dd, J = 5.7, 2.1 Hz), 7.26−7.19 (4H, m), 7.05 (2H, t, J = 8.4 Hz), 5.43 (2H, s); ^{13}C NMR (75 MHz, CD_3OD): δ 168.7 (CO), 163.8 (d, $^1J_{CF}$ = 243.8 Hz, quat.), 138.2 (quat.), 136.5 (CH), 134.2 (quat.), 130.2 (d, $^3J_{CF}$ = 8.3 Hz, CH), 128.5 (quat.), 123.8 (CH), 122.8 (CH), 122.5 (CH), 116.6 (d, $^2J_{CF}$ = 21.8 Hz, CH), 111.7 (CH), 108.5 (quat.), 50.6 (CH_2); ^{19}F NMR (282 MHz, CD_3OD): δ − 118.3 (1F, m); LRMS (−ESI): 268.22 ([M − H]$^-$, 100%); IR (diamond cell, thin film): 3108 (w), 2938 (w), 2587 (bs), 1652 (s), 1525 (m), 1508 (m), 1277 (m), 1225 (s), 1185 (s), 830 (s), 753 (s), 744 (s), 428 (s).

*1-(Cyclohexylmethyl)-1H-indole-3-carboxylic Acid (**33**).* Subjecting **29** (400 mg, 1.29 mmol) to general procedure C gave **33** (305 mg, 92%) as a white solid. mp 180−182 °C; ^{1}H NMR (400 MHz, $CDCl_3$): δ 8.19−8.16 (1H, m), 7.81 (1H, s), 7.32−7.28 (1H, m), 7.25−7.20 (2H, m), 3.92 (2H, d, J = 7.2 Hz), 1.87−1.76 (1H, m), 1.68−1.56 (5H, m), 1.19−1.03 (3H, m), 1.00−0.90 (2H, m); ^{13}C NMR (100 MHz, $CDCl_3$): δ 170.6 (CO), 137.1 (quat.), 136.3 (CH), 127.1 (quat.), 122.9 (CH), 122.2 (CH), 122.0 (CH), 110.5 (CH), 106.2 (quat.), 53.8 (CH_2), 38.5 (CH), 31.1 (CH_2), 26.3 (CH_2), 25.8 (CH_2); LRMS (−ESI): m/z 256.52 ([M − H]$^-$, 100%); IR (diamond cell, thin film): 2926 (w), 2852 (w), 1652 (s), 1523 (m), 1467 (m), 1395 (m), 1236 (s), 754 (s), 744 (s).

*1-(Pentyl)-1H-indole-3-carboxylic Acid (**34**).* Subjecting **30** (450 mg, 1.59 mmol) to general procedure C gave **33** (323 mg, 88%) as a white solid. mp 106−108 °C; ^{1}H NMR (300 MHz, CD_3OD): δ 8.09 (1H, dd, J = 6.5, 1.9 Hz), 7.93 (1H, s), 7.42−7.28 (3H, m), 4.17 (2H, t, J = 7.2 Hz), 1.90 (2H, quin., J = 7 Hz), 1.40−1.32 (4H, m), 0.90 (3H, t, J = 6.6 Hz); ^{13}C NMR (75 MHz, CD_3OD): δ 168.8 (CO), 138.1 (quat.), 136.3 (CH), 128.3 (quat.), 123.6 (CH), 122.6 (CH), 122.4 (CH), 111.3 (CH), 107.7 (quat.), 47.7 (CH_2), 30.7 (CH_2), 30.0 (CH_2), 23.3 (CH_2), 14.2 (CH_3); LRMS (−ESI): m/z 230.32 ([M − H]$^-$, 100%); IR (diamond cell, thin film): 3106 (w), 2925 (m), 2856 (w), 2525 (bs), 1649 (s), 1526 (s), 1461 (m), 1273 (m), 1204 (s), 1117 (m), 940 (m), 731 (s).

*1-(5-Fluoropentyl)-1H-indazole-3-carboxylic Acid (**40**).* Subjecting **36** (750 mg, 2.84 mmol) to general procedure C gave **40** (580 mg, 81%) as a white solid. mp 89−91 °C; ^{1}H NMR (300 MHz, CD_3OD): δ 8.36 (1H, d, J = 7.8 Hz), 7.52 (2H, m), 7.33 (1H, t, J = 7.5 Hz), 4.53−4.49 (3H, m), 4.34 (1H, t, J = 5.7 Hz), 2.03 (2H, quin., J = 7.2 Hz), 1.82−1.65 (2H, m), 1.50 (2H, quin., J = 6.9 Hz); ^{13}C NMR (75 MHz, CD_3OD): δ 165.5 (CO), 142.2 (quat.), 136.1 (quat.), 128.1 (CH), 124.7 (quat.), 124.2 (CH), 123.0 (CH), 111.2 (CH), 84.6 (d, $^1J_{CF}$ = 162.8 Hz, CH_2), 50.3 (CH_2), 31.0 (d, $^2J_{CF}$ = 20.3 Hz, CH_2), 30.4 (CH_2), 23.6 (d, $^3J_{CF}$ = 5.3 Hz, CH_2); ^{19}F NMR (282 MHz, CD_3OD): δ − 221.8 (1F, m); LRMS (−ESI): m/z 249.12 ([M − H]$^-$, 100%); IR (diamond cell, thin film): 3052 (bs), 2941 (m), 2866 (w), 1685 (s), 1480 (s), 1167 (s), 1120 (s), 751 (s).

*1-(4-Fluorobenzyl)-1H-indazole-3-carboxylic Acid (**41**).* Subjecting **37** (560 mg, 1.97 mmol) to general procedure C gave **41** (480 mg, 91%) as a white solid. mp 203−205 °C; ^{1}H NMR (300 MHz, CD_3OD): δ 8.17 (1H, d, J = 8.1 Hz), 7.62 (1H, d, J = 8.7 Hz), 7.44 (1H, t, J = 7.5 Hz), 7.31 (3H, m), 7.04 (2H, t, J = 8.4 Hz), 5.71 (2H, s); ^{13}C NMR (75 MHz, CD_3OD): δ 165.5 (CO), 163.9 (d, $^1J_{CF}$ = 244.5 Hz, quat.), 142.1 (quat.), 136.7 (quat.), 133.7 (d, $^4J_{CF}$ = 3 Hz, quat.), 130.6 (d, $^3J_{CF}$ = 8.3 Hz, CH), 128.3 (CH), 125.0 (quat.), 124.3 (CH), 123.1 (CH), 116.5 (d, $^2J_{CF}$ = 21.8 Hz, CH), 111.4 (CH), 53.6 (CH_2); ^{19}F NMR (285 MHz, CD_3OD): δ − 118.0 (1F, m); LRMS (−ESI): m/z 269.07 ([M − H]$^-$, 100%); IR (diamond cell, thin film): 3058 (bs), 2926 (w), 1696 (s), 1510 (s), 1481 (s), 1224 (s), 1170 (s), 1157 (s), 749 (s).

*1-(Cyclohexylmethyl)-1H-indazole-3-carboxylic Acid (**42**).* Subjecting **38** (475 mg, 1.74 mmol) to general procedure C gave **42** (388 mg, 86%) as a white solid. mp 124−126 °C; ^{1}H NMR (300 MHz, CD_3OD): δ 8.16 (1H, d, J = 8.1 Hz), 7.66 (1H, d, J = 8.4 Hz), 7.47 (1H, t, J = 7.2 Hz), 7.31 (1H, t, J = 7.8 Hz), 4.34 (2H, d, J = 7.2 Hz), 2.05 (1H, m), 1.72−1.66 (3H, m), 1.56 (2H, d, J = 12.9 Hz), 1.26−1.02 (5H, m); ^{13}C NMR (75 MHz, CD_3OD): δ 165.5 (CO), 142.6 (quat.), 135.9 (quat.), 128.0 (CH), 124.5 (quat.), 124.1 (CH), 123.0 (CH), 111.4 (CH), 56.5 (CH_2), 40.0 (CH), 31.7 (CH_2), 27.7 (CH), 26.7 (CH_2); LRMS (−ESI): m/z 257.16 ([M − H]$^-$, 100%); IR (diamond cell, thin film): 3060 (bs), 2926 (s), 2851 (m), 1707 (s), 1479 (s), 1230 (s), 1174 (s), 752 (s).

*1-(Pentyl)-1H-indazole-3-carboxylic Acid (**43**).* Subjecting **39** (600 mg, 2.58 mmol) to general procedure C gave **43** (510 mg, 85%) as a white solid. mp 76−78 °C; ^{1}H NMR (300 MHz, CD_3OD): δ 8.26 (1H, d, J = 8.1 Hz), 7.52−7.44 (2H, m), 7.35 (1H, t, J = 7.8 Hz), 4.48 (2H, t, J = 7.2 Hz), 1.99 (2H, quin., J = 7.2 Hz), 1.34 (4H, m), 0.89 (3H, t, J = 6.0 Hz); ^{13}C NMR (75 MHz, CD_3OD): δ 165.4 (CO), 142.0 (quat.), 135.9 (quat.), 127.9 (CH), 124.5 (quat.), 124.0 (CH), 122.9 (CH), 111.0 (CH), 49.7 (CH_2), 30.4 (CH_2), 29.8 (CH_2), 23.1 (CH_2), 14.1 (CH_3); LRMS (−ESI): m/z 231.12 ([M − H]$^-$, 100%); IR (diamond cell, thin film): 3053 (bs), 2956 (m), 2931 (m), 2860 (w), 1687 (s), 1503 (s), 1218 (s), 1176 (s), 1121 (s), 752 (s).

General Procedure D: Synthesis of Methyl 1-Alkyl-1*H*-indazole-3-carboxylates. To a cooled (0 °C) solution of methyl 1*H*-indazole-3-carboxylate (**35**, 500 mg, 2.84 mmol) in THF (15 mL) was added potassium *tert*-butoxide (350 mg, 3.12 mmol, 1.1 equiv), and the mixture warmed to ambient temperature and stirred for 1 h. The cooled (0 °C) mixture was treated dropwise with the appropriate bromoalkane (2.98 mmol, 1.05 equiv) and stirred for 48 h. The reaction was quenched by pouring onto H_2O (100 mL) and the layers separated. The aqueous phase was extracted with EtOAc (3 × 100 mL), and the combined organic layers were washed with brine (150 mL), dried ($MgSO_4$), and the solvent evaporated under reduced pressure. The crude materials were purified by flash chromatography.

*Methyl 1-(5-Fluoropentyl)-1H-indazole-3-carboxylate (**36**).* Subjecting **35** (500 mg, 2.84 mmol) and 1-bromo-5-fluoropentane (370 μL, 2.98 mmol, 1.05 equiv) to general procedure D gave, following purification by flash chromatography (hexane/EtOAc, 80:20), **36** (560 mg, 75%) as a colorless oil. R_f 0.30 (hexane/EtOAc, 80:20); ^{1}H NMR (300 MHz, $CDCl_3$): δ 8.24 (1H, d, J = 8.1 Hz), 7.49−7.45 (2H, m), 7.32 (1H, t, J = 6.3 Hz), 4.52−4.47 (3H, m), 4.33 (1H, t, J = 5.7 Hz), 4.04 (3H, s), 2.03 (2H, quin., J = 7.2 Hz), 2.00−1.63 (2H, m), 1.46 (2H, quin., J = 12.0 Hz); ^{13}C NMR (75 MHz, $CDCl_3$): δ 163.2 (CO), 140.6 (quat.), 134.8 (quat.), 127.0 (CH), 123.9 (quat.), 123.2 (CH), 122.4 (CH), 109.6 (CH), 83.8 (d, $^1J_{CF}$ = 163.5 Hz, CH_2F), 52.1 (CH_2), 49.8 (CH_3), 30.0 (d, $^2J_{CF}$ = 19.5 Hz, CH_2), 29.6 (CH_2), 22.8 (d, $^3J_{CF}$ = 4.5 Hz, CH_2); ^{19}F NMR (282 MHz, $CDCl_3$): δ − 218.6 (1F, m); LRMS (+ESI): m/z 287.03 ([M + Na]$^+$, 100%); IR (diamond cell, thin film): 2950 (m), 2867 (w), 1729 (s), 1710 (s), 1478 (s), 1163 (s), 1118 (s), 752 (s).

*Methyl 1-(4-Fluorobenzyl)-1H-indazole-3-carboxylate (**37**).* Subjecting **35** (500 mg, 2.84 mmol) and 4-fluorobenzyl bromide (371 μL, 2.98 mmol, 1.05 equiv) to general procedure D gave, following purification by flash chromatography (hexane/EtOAc, 80:20), **37** (570 mg, 71%) as a white solid. mp 83−84 °C; R_f 0.35 (hexane/EtOAc, 80:20); ^{1}H NMR (300 MHz, $CDCl_3$): δ 8.25 (1H, d, J = 7.8 Hz), 7.42−7.29 (3H, m), 7.21 (2H, t, J = 6.9 Hz), 6.99 (2H, t, J = 8.1 Hz), 5.67 (2H, s), 4.06 (3H, s); ^{13}C NMR (75 MHz, $CDCl_3$): δ 163.1 (CO), 162.6 (d, $^1J_{C-F}$ = 245.3 Hz, quat.), 140.6 (quat.), 135.3 (quat.), 131.6 (d, $^4J_{CF}$ = 3.8 Hz, quat.), 129.2 (d, $^3J_{CF}$ = 8.3 Hz, CH), 127.3 (CH), 124.3 (quat.), 123.5 (CH), 122.5 (CH), 116.0 (d, $^2J_{CF}$ = 21.8

DOI: 10.1021/acschemneuro.6b00137
ACS Chem. Neurosci. 2016, 7, 1241−1254

Hz, CH), 53.5 (CH_2), 52.2 (CH_3); ^{19}F NMR (282 MHz, $CDCl_3$): δ −113.8 (1F, s); LRMS (+ESI): m/z 307.00 ([M+ Na]$^+$, 100%). IR (diamond cell, thin film): 3071 (w), 2952 (w), 1712 (s), 1510 (s), 1479 (s), 1268 (s), 1157 (s), 749 (s).

*Methyl 1-(Cyclohexylmethyl)-1H-indazole-3-carboxylate (**38**).* Subjecting **35** (500 mg, 2.84 mmol) and (bromomethyl)cyclohexane (415 μL, 2.98 mmol, 1.05 equiv) to general procedure D gave, following purification by flash chromatography (hexane/EtOAc, 80:20), **38** (505 mg, 65%) as a colorless oil. R_f 0.60 (hexane/EtOAc, 80:20); ^1H NMR (300 MHz, $CDCl_3$): δ 8.22 (1H, dt, J = 8.1, 0.9 Hz), 7.48−7.39 (2H, m), 7.33−7.28 (1H, m), 4.28 (2H, d, J = 7.5 Hz), 4.03 (3H, s), 2.08 (1H, m), 1.74−1.52 (5H, m), 1.32−0.98 (5H, m); ^{13}C NMR (75 MHz, $CDCl_3$): δ 163.3 (CO), 141.3 (quat.), 134.6 (quat.), 126.8 (CH), 123.7 (quat.), 123.1 (CH), 122.3 (CH), 110.0 (CH), 56.1 (CH_2), 52.1 (CH_3), 38.9 (CH_2), 31.7 (CH), 26.3 (CH_2), 25.7 (CH_2); LRMS (+ESI) m/z 295.05 ([M + Na]$^+$, 100%); IR (diamond cell, thin film): 2925 (s), 2851 (m), 1710 (s), 1477 (s), 1441 (m), 1224 (s), 1161 (s), 1121 (s), 751 (s).

*Methyl 1-(Pentyl)-1H-indazole-3-carboxylate (**39**).* Subjecting **35** (500 mg, 2.84 mmol) and 1-bromopentane (370 μL, 2.98 mmol, 1.05 equiv) to general procedure D gave, following purification by flash chromatography (hexane/EtOAc, 80:20), **39** (585 mg, 84%) as a colorless oil. R_f 0.50 (hexane-EtOAc, 80:20); ^1H NMR (300 MHz, $CDCl_3$): δ 8.24 (1H, d, J = 8.0 Hz), 7.50−7.44 (2H, m), 7.35−7.27 (1H, m), 4.47 (2H, t, J = 7.4 Hz), 4.04 (3H, s), 1.97 (2H, quin., J = 7.0 Hz), 1.32 (4H, m), 0.87 (3H, t, J = 6.6 Hz); ^{13}C NMR (75 MHz, $CDCl_3$): δ 163.3 (CO), 140.6 (quat.), 134.6 (quat.), 126.8 (CH), 123.9 (quat.), 123.1 (CH), 122.3 (CH), 109.7 (CH), 52.1 (CH_3), 50.1 (CH_2), 29.7 (CH_2), 29.0 (CH_2), 22.4 (CH_2), 14.0 (CH_3); LRMS (+ESI): m/z 269.03 ([M + Na]$^+$, 60%), 515.16 ([2 M + Na]$^+$, 100%); IR (diamond cell, thin film): 2954 (m), 2932 (m), 2860 (w), 1709 (s), 1477 (s), 1215 (s), 1159 (s), 1117 (s), 751 (s).

In Vitro Pharmacological Assessment of SCs. Mouse AtT-20 pituitary tumor cells engineered to express a FLP recombination site were transfected with HA-tagged human CB_1 or human CB_2 receptors (Genscript, Piscataway, NJ) as previously described for opioid receptors in the same cells.[87] Cells were cultured in Dulbecco's modified Eagle's medium (DMEM) containing 10% fetal bovine serum (FBS), 100 U penicillin/streptomycin ml^{-1}, and 80 μg/mL hygromycin. Wild type AtT-20 FlpIn cells were grown without hygromycin. Cells were passaged at 80% confluency as required. Cells for assays were grown in 75 cm^2 flasks and used at 90% confluence. The day before the assay cells were detached from the flask with trypsin/EDTA (Sigma-Aldrich) and resuspended in 10 mL of Leibovitz's L-15 media supplemented with 1% FBS, 100 U penicillin/streptomycin ml^{-1} and 15 mM glucose. The cells were plated in volume of 90 μL in black walled, clear bottomed 96-well microplates (Corning, Oneonta, NY). For experiments where cells were treated with pertussis toxin (PTX), the cells were plated as normal and PTX (200 ng/mL final concentration, List Biological Laboratories, Campbell, California) was added to the wells immediately afterward. Cells were incubated overnight at 37 °C in ambient CO_2.

Membrane potential was measured using a FLIPR membrane potential assay kit (blue) from Molecular Devices (Sunnyvale, CA), as described previously.[88] The dye was reconstituted with assay buffer of composition (mM): NaCl 145, HEPES 22, Na_2HPO_4 0.338, $NaHCO_3$ 4.17, KH_2PO_4 0.441, $MgSO_4$ 0.407, $MgCl_2$ 0.493, $CaCl_2$ 1.26, glucose 5.56 (pH 7.4, osmolarity 315 ± 5). Prior to the assay, cells were loaded with 90 μL/well of the dye solution without removal of the L-15, giving an initial assay volume of 180 μL/well. Plates were then incubated at 37 °C at ambient CO_2 for 60 min. Fluorescence was measured using a FlexStation 3 (Molecular Devices) microplate reader with cells excited at a wavelength of 530 nm and emission measured at 565 nm. Baseline readings were taken every 2 s for 60−120 s, after which either drug or vehicle was added in a volume of 20 μL. The background fluorescence of cells without dye or dye without cells was negligible. Changes in fluorescence were expressed as a percentage of baseline fluorescence after subtraction of the changes produced by vehicle addition. Drug solutions were made up in assay buffer containing 0.01% BSA (Sigma) and 1% DMSO, thus the final concentration of dimethyl sulfoxide was always 0.1%.

Data were analyzed with PRISM (GraphPad Software Inc., San Diego, CA), using four-parameter nonlinear regression to fit concentration−response curves. In all plates, a maximally effective concentration of CP 55,940 (1 μM, Cayman Chemical, Ann Arbor, MI) was added to allow for normalization between assays.

In Vivo Pharmacological Assessment of SCs. Two cohorts of four adult male Long Evans rats (Animal Resources Centre, Perth, Australia) initially weighing between 168 and 186 g were used for biotelemetric assessment of body temperature and heart rate changes following each compound. The rats were singly housed in an air-conditioned testing room (22 ± 1 °C) on a 12 h reverse light/dark cycle (lights on from 21:00 to 09:00). Standard rodent chow and water were provided ad libitum. All experiments were approved by The University of Sydney Animal Ethics Committee.

Biotelemetry transmitters (TA11CTA-F40, Data Sciences International, St. Paul, MN) were implanted as previously described.[27] Briefly, following anesthetization (isoflurane, 3% induction, 2% maintenance) a rostro-caudal incision was made along the midline of the abdomen, and a biotelemetry transmitter (TA11CTA-F40, Data Sciences International, St. Paul, MN) was placed in the peritoneal cavity according to the manufacturers protocol. The wound was sutured closed and the rats were allowed 1 week of recovery before data collection.

The rats were habituated over multiple days to injections of vehicle (5% EtOH, 5% Tween 80, 90% physiological saline) at a set time of day (11:00 am). Each cohort then received injections of each compound at the same time of day in an ascending dose sequence (0.1, 0.3, 1, mg/kg). This ascending sequence reduces the risk posed to the animals in assessing hitherto untested compounds, and the use of multiple cohorts limits the potential development of tolerance to the compound. Two washout days were given between each dose. If only a modest or negligible hypothermic response was seen at 1 mg/kg, then a further 3 mg/kg dose of the compound was given. At least two washout days were given between each dose.

For the antagonist studies (Figure 6), the third and fourth cohort of drug-naïve rats were used for each compound, with a 48 h washout period between each dose. Each cohort received injections of either vehicle, CB_1 antagonist (rimonabant, 3 mg/kg), or CB_2 antagonist (SR144528, 3 mg/kg), followed by 5F-AMB (3 mg/kg) or MDMB-FUBINACA (1 mg/kg). The vehicle or antagonist injections were given to rats 30 min prior to the 5F-AMB or MDMB-FUBINACA injections.

Data for heart rate and body temperature was gathered continuously at 1000 Hz and organized into 15 min bins using Dataquest A.R.T. software (version 4.3, Data Sciences International, St. Paul, MN), and analyzed using PRISM (Graphpad Software Inc., San Diego, CA).

We calculated the area between baseline and drug-treatment body temperature curves for each rat as a measure of compound potency. Briefly, for any time point, the area between baseline data points (B_t) and drug-treatment data points (D_t) and the subsequent time points (B_{t+1} and D_{t+1}) forms a trapezoid, the area of which can be calculated via the formula:

$$\text{area} = \frac{(B_t - D_t) + (B_{t+1} - D_{t+1})}{2}$$

These areas were summed from the time of injection to 6 h postinjection. MDMB-FUBINACA and 5F-AMB AUC data were compared at each dose level with independent samples t tests.

For the antagonist studies, the area between the vehicle−vehicle baseline and the vehicle−SC (i.e., vehicle−5F-AMB or vehicle−MDMB-FUBINACA), rimonabant-SC, and SR144528-SC treatments was calculated over a 3 h time period postinjection of SC. These areas were analyzed using a one-way repeated measures ANOVA with planned Dunnet's contrasts comparing the antagonist areas to the vehicle-drug area.

DOI: 10.1021/acschemneuro.6b00137
ACS Chem. Neurosci. 2016, 7, 1241−1254

■ ASSOCIATED CONTENT

Supporting Information

The Supporting Information is available free of charge on the ACS Publications website at DOI: 10.1021/acschemneuro.6b00137.

Table of compound names, CAS numbers, and relevant references; selected ^{1}H and ^{13}C NMR spectra (PDF)

■ AUTHOR INFORMATION

Corresponding Author

*E-mail: michael.kassiou@sydney.edu.au.

Author Contributions

○S.D.B. and M.L. contributed equally.

Author Contributions

The synthesis, purification, and chemical characterization of compounds **10**−**25** was carried out by S.D.B., M.L., and J.B.C.M., and overseen by M.K. M.C. and S.S. designed and conducted all in vitro pharmacological studies, and data analysis was performed by M.C., S.S., S.D.B., M.G., and J.S. M.S. made and characterized the CB_1 and CB_2 cells. All behavioral pharmacology was performed by R.K. with direction from I.S.M. The manuscript was drafted by S.D.B. with contributions from M.L., J.S. R.C.K., M.G., M.C., I.S.M., and M.K. All authors have given approval to the final version of the manuscript.

Funding

Work performed at The University of Sydney and presented herein was supported in part by the European Union's Seventh Framework Programme [FP7/2007-2013] INMiND (Grant Agreement No. HEALTH-F2-2011-278850). Work was also supported by NHMRC Project Grant 1107088 awarded to M.K., I.S.M., and M.C.

Notes

The authors declare no competing financial interest.

■ ABBREVIATIONS

CB, cannabinoid; FLIPR, fluorometric imaging plate reader; GIRK, G-protein-gated inwardly rectifying K^+ channels; ip, intraperitoneal; NMR, nuclear magnetic resonance; pi, post-injection; SAR, structure−activity relationship; SC, synthetic cannabinoid; Δ^9-THC, Δ^9-tetrahydrocannabinol; TLC, thin layer chromatography

■ REFERENCES

(1) Brandt, S. D., King, L. A., and Evans-Brown, M. (2014) The new drug phenomenon. *Drug Test. Anal. 6*, 587−597.

(2) Auwarter, V., Dresen, S., Weinmann, W., Muller, M., Putz, M., and Ferreiros, N. (2009) 'Spice' and other herbal blends: harmless incense or cannabinoid designer drugs? *J. Mass Spectrom. 44*, 832−837.

(3) Uchiyama, N., Kikura-Hanajiri, R., Kawahara, N., and Goda, Y. (2009) Identification of a cannabimimetic indole as a designer drug in a herbal product. *Forensic Toxicol. 27*, 61−66.

(4) United Nations Office on Drugs and Crime, World Drug Report 2015 (United Nations publication, Sales No. E.15.XI.6).

(5) Blakey, K., Boyd, S., Atkinson, S., Wolf, J., Slottje, P. M., Goodchild, K., and McGowan, J. (2016) Identification of the novel synthetic cannabimimetic 8-quinolinyl 4-methyl-3-(1-piperidinylsulfonyl)benzoate (QMPSB) and other designer drugs in herbal incense. *Forensic Sci. Int. 260*, 40−53.

(6) Carlsson, A., Lindberg, S., Wu, X., Dunne, S., Josefsson, M., Astot, C., and Dahlen, J. (2015) Prediction of designer drugs: synthesis and spectroscopic analysis of synthetic cannabinoid analogues of 1H-indol-3-yl(2,2,3,3-tetramethylcyclopropyl)methanone and 1H-indol-3-yl-(adamantan-1-yl)methanone. *Drug Test. Anal.*, DOI: 10.1002/dta.1904.

(7) Kondrasenko, A. A., Goncharov, E. V., Dugaev, K. P., and Rubaylo, A. I. (2015) CBL-2201. Report on a new designer drug: Napht-1-yl 1-(5-fluoropentyl)-1H-indole-3-carboxylate. *Forensic Sci. Int. 257*, 209−213.

(8) McLaughlin, G., Morris, N., Kavanagh, P. V., Power, J. D., Twamley, B., O'Brien, J., Talbot, B., Dowling, G., and Brandt, S. D. (2015) The synthesis and characterization of the 'research chemical' *N*-(1-amino-3-methyl-1-oxobutan-2-yl)-1-(cyclohexylmethyl)-3-(4-fluorophenyl)-1*H*-pyrazole-5-carboxamide (3,5-AB-CHMFUPPYCA) and differentiation from its 5,3-regioisomer. *Drug Test. Anal.*, DOI: 10.1002/dta.1864.

(9) Uchiyama, N., Asakawa, K., Kikura-Hanajiri, R., Tsutsumi, T., and Hakamatsuka, T. (2015) A new pyrazole-carboxamide type synthetic cannabinoid AB-CHFUPYCA [*N*-(1-amino-3-methyl-1-oxobutan-2-yl)-1-(cyclohexylmethyl)-3-(4-fluorophenyl)-1*H*-pyrazole-5-carboxamide] identified in illegal products. *Forensic Toxicol. 33*, 367−373.

(10) Uchiyama, N., Shimokawa, Y., Kikura-Hanajiri, R., Demizu, Y., Goda, Y., and Hakamatsuka, T. (2015) A synthetic cannabinoid FDU-NNEI, two 2-indazole isomers of synthetic cannabinoids AB-CHMINACA and NNEI indazole analog (MN-18), a phenethylamine derivative OH-EDMA, and a cathinone derivative dimethoxy-alpha-PHP, newly identified in illegal products. *Forensic Toxicol. 33*, 244−259.

(11) Westphal, F., Sonnichsen, F. D., Knecht, S., Auwarter, V., and Huppertz, L. (2015) Two thiazolylindoles and a benzimidazole: Novel compounds on the designer drug market with potential cannabinoid receptor activity. *Forensic Sci. Int. 249*, 133−147.

(12) Jia, W., Meng, X., Qian, Z., Hua, Z., Li, T., and Liu, C. (2016) Identification of three cannabimimetic indazole and pyrazole derivatives, APINACA 2*H*-indazole analogue, AMPPPCA, and 5F-AMPPPCA. *Drug Test. Anal.*, DOI: 10.1002/dta.1967.

(13) Qian, Z., Hua, Z., Liu, C., and Jia, W. (2016) Four types of cannabimimetic indazole and indole derivatives, ADB-BINACA, AB-FUBICA, ADB-FUBICA, and AB-BICA, identified as new psychoactive substances. *Forensic Toxicol. 34*, 133−143.

(14) Shevyrin, V., Melkozerov, V., Eltsov, O., Shafran, Y., and Morzherin, Y. (2016) Synthetic cannabinoid 3-benzyl-5-[1-(2-pyrrolidin-1-ylethyl)-1H-indol-3-yl]-1,2,4-oxadiazole. The first detection in illicit market of new psychoactive substances. *Forensic Sci. Int. 259*, 95−100.

(15) Huestis, M. A., Gorelick, D. A., Heishman, S. J., Preston, K. L., Nelson, R. A., Moolchan, E. T., and Frank, R. A. (2001) Blockade of effects of smoked marijuana by the CB1-selective cannabinoid receptor antagonist SR141716. *Arch. Gen. Psychiatry 58*, 322−328.

(16) Castaneto, M. S., Gorelick, D. A., Desrosiers, N. A., Hartman, R. L., Pirard, S., and Huestis, M. A. (2014) Synthetic cannabinoids: epidemiology, pharmacodynamics, and clinical implications. *Drug Alcohol Depend. 144*, 12−41.

(17) Tuv, S. S., Krabseth, H., Karinen, R., Olsen, K. M., Oiestad, E. L., and Vindenes, V. (2014) Prevalence of synthetic cannabinoids in blood samples from Norwegian drivers suspected of impaired driving during a seven weeks period. *Accid. Anal. Prev. 62*, 26−31.

(18) Andreeva-Gateva, P. A., Nankova, V. H., Angelova, V. T., and Gatev, T. N. (2015) Synthetic cannabimimetics in Bulgaria 2010−2013. *Drug Alcohol Depend. 157*, 200−204.

(19) Zawilska, J. B., and Andrzejczak, D. (2015) Next generation of novel psychoactive substances on the horizon - A complex problem to face. *Drug Alcohol Depend. 157*, 1−17.

(20) Langer, N., Lindigkeit, R., Schiebel, H.-M., Papke, U., Ernst, L., and Beuerle, T. (2016) Identification and quantification of synthetic cannabinoids in "spice-like" herbal mixtures: update of the German situation for the spring of 2015. *Forensic Toxicol. 34*, 94−107.

(21) Schifano, F., Orsolini, L., Duccio Papanti, G., and Corkery, J. M. (2015) Novel psychoactive substances of interest for psychiatry. *World Psychiatry. 14*, 15−26.

(22) Costain, W. J., Tauskela, J. S., Rasquinha, I., Comas, T., Hewitt, M., Marleau, V., and Soo, E. C. (2016) Pharmacological character-

DOI: 10.1021/acschemneuro.6b00137
ACS Chem. Neurosci. 2016, 7, 1241−1254

ization of emerging synthetic cannabinoids in HEK293T cells and hippocampal neurons. *Eur. J. Pharmacol. 786*, 234−245.
(23) Frinculescu, A., Lyall, C. L., Ramsey, J., and Miserez, B. (2016) Variation in commercial smoking mixtures containing third-generation synthetic cannabinoids. *Drug Test. Anal.*, DOI: 10.1002/dta.1975.
(24) Gerostamoulos, D., Elliott, S., Walls, H. C., Peters, F. T., Lynch, M., and Drummer, O. H. (2016) To Measure or Not to Measure? That is the NPS Question. *J. Anal. Toxicol. 40*, 318−320.
(25) Hess, C., Schoeder, C. T., Pillaiyar, T., Madea, B., and Müller, C. E. (2016) Pharmacological evaluation of synthetic cannabinoids identified as constituents of spice. *Forensic Toxicol. 34*, 329.
(26) Odoardi, S., Romolo, F. S., and Strano-Rossi, S. (2016) A snapshot on NPS in Italy: Distribution of drugs in seized materials analysed in an Italian forensic laboratory in the period 2013−2015. *Forensic Sci. Int. 265*, 116−120.
(27) Banister, S. D., Wilkinson, S. M., Longworth, M., Stuart, J., Apetz, N., English, K., Brooker, L., Goebel, C., Hibbs, D. E., Glass, M., Connor, M., McGregor, I. S., and Kassiou, M. (2013) The synthesis and pharmacological evaluation of adamantane-derived indoles: cannabimimetic drugs of abuse. *ACS Chem. Neurosci. 4*, 1081−1092.
(28) Banister, S. D., Stuart, J., Kevin, R. C., Edington, A., Longworth, M., Wilkinson, S. M., Beinat, C., Buchanan, A. S., Hibbs, D. E., Glass, M., Connor, M., McGregor, I. S., and Kassiou, M. (2015) Effects of Bioisosteric Fluorine in Synthetic Cannabinoid Designer Drugs JWH-018, AM-2201, UR-144, XLR-11, PB-22, 5F-PB-22, APICA, and STS-135. *ACS Chem. Neurosci. 6*, 1445−1458.
(29) Banister, S. D., Stuart, J., Conroy, T., Longworth, M., Manohar, M., Beinat, C., Wilkinson, S. M., Kevin, R. C., Hibbs, D. E., Glass, M., Connor, M., McGregor, I. S., and Kassiou, M. (2015) Structure−activity relationships of synthetic cannabinoid designer drug RCS-4 and its regioisomers and C4 homologues. *Forensic Toxicol. 33*, 355−366.
(30) Banister, S. D., Moir, M., Stuart, J., Kevin, R. C., Wood, K. E., Longworth, M., Wilkinson, S. M., Beinat, C., Buchanan, A. S., Glass, M., Connor, M., McGregor, I. S., and Kassiou, M. (2015) Pharmacology of Indole and Indazole Synthetic Cannabinoid Designer Drugs AB-FUBINACA, ADB-FUBINACA, AB-PINACA, ADB-PINACA, 5F-AB-PINACA, 5F-ADB-PINACA, ADBICA, and 5F-ADBICA. *ACS Chem. Neurosci. 6*, 1546−1559.
(31) Wilkinson, S. M., Banister, S. D., and Kassiou, M. (2015) Bioisosteric Fluorine in the Clandestine Design of Synthetic Cannabinoids. *Aust. J. Chem. 68*, 4−8.
(32) Longworth, M., Banister, S. D., Mack, J. B. C., Glass, M., Connor, M., and Kassiou, M. (2016) The 2-alkyl-2*H*-indazole regioisomers of synthetic cannabinoids AB-CHMINACA, AB-FUBINACA, AB-PINACA, and 5F-AB-PINACA are possible manufacturing impurities with cannabimimetic activities. *Forensic Toxicol. 34*, 286.
(33) Drug Enforcement Administration, Department of Justice (2014) Schedules of controlled substances: temporary placement of four synthetic cannabinoids into Schedule I. Final order. *Fed. Reg. 79*, 7577−7582.
(34) Drug Enforcement Administration, Department of Justice (2015) Schedules of controlled substances: temporary placement of three synthetic cannabinoids into schedule I. Final order. *Fed. Reg. 80*, 5042−5047.
(35) European Monitoring Centre for Drugs and Drug Addiction (2015), EMCDDA−Europol 2014 Annual Report on the implementation of Council Decision 2005/387/JHA, Implementation reports, Publications Office of the European Union, Luxembourg.
(36) European Monitoring Centre for Drugs and Drug Addiction (2015), New psychoactive substances in Europe. An update from the EU Early Warning System (March 2015), Publications Office of the European Union, Luxembourg.
(37) Von Der Haar, J., Talebi, S., Ghobadi, F., Singh, S., Chirurgi, R., Rajeswari, P., Kalantari, H., and Hassen, G. W. (2016) Synthetic Cannabinoids and Their Effects on the Cardiovascular System. *J. Emerg. Med. 50*, 258−262.
(38) Louh, I. K., and Freeman, W. D. (2014) A 'spicy' encephalopathy: synthetic cannabinoids as cause of encephalopathy and seizure. *Crit. Care. 18*, 553.
(39) Besli, G. E., Ikiz, M. A., Yildirim, S., and Saltik, S. (2015) Synthetic Cannabinoid Abuse in Adolescents: A Case Series. *J. Emerg. Med. 49*, 644−650.
(40) Gerostamoulos, D., Drummer, O. H., and Woodford, N. W. (2015) Deaths linked to synthetic cannabinoids. *Forensic Sci., Med., Pathol. 11*, 478.
(41) Hermanns-Clausen, M., Kneisel, S., Szabo, B., and Auwarter, V. (2013) Acute toxicity due to the confirmed consumption of synthetic cannabinoids: clinical and laboratory findings. *Addiction. 108*, 534−544.
(42) Hermanns-Clausen, M., Kneisel, S., Hutter, M., Szabo, B., and Auwarter, V. (2013) Acute intoxication by synthetic cannabinoids–four case reports. *Drug Test. Anal. 5*, 790−794.
(43) Hermanns-Clausen, M., Kithinji, J., Spehl, M., Angerer, V., Franz, F., Eyer, F., and Auwarter, V. (2016) Adverse effects after the use of JWH-210 - a case series from the EU Spice II plus project. *Drug Test. Anal.*, DOI: 10.1002/dta.1936.
(44) Hess, C., Stockhausen, S., Kernbach-Wighton, G., and Madea, B. (2015) Death due to diabetic ketoacidosis: Induction by the consumption of synthetic cannabinoids? *Forensic Sci. Int. 257*, e6−e11.
(45) Lovett, C., Wood, D. M., and Dargan, P. I. (2015) Pharmacology and toxicology of the synthetic cannabinoid receptor agonists. *Réanimation. 24*, 527−541.
(46) Mills, B., Yepes, A., and Nugent, K. (2015) Synthetic Cannabinoids. *Am. J. Med. Sci. 350*, 59−62.
(47) Muller, H. H., Kornhuber, J., and Sperling, W. (2015) The behavioral profile of spice and synthetic cannabinoids in humans. *Brain Res. Bull.*, DOI: 10.1016/j.brainresbull.2015.10.013.
(48) Obafemi, A. I., Kleinschmidt, K., Goto, C., and Fout, D. (2015) Cluster of Acute Toxicity from Ingestion of Synthetic Cannabinoid-Laced Brownies. *J. Med. Toxicol. 11*, 426−429.
(49) van Amsterdam, J., Brunt, T., and van den Brink, W. (2015) The adverse health effects of synthetic cannabinoids with emphasis on psychosis-like effects. *J. Psychopharmacol. 29*, 254−263.
(50) Winstock, A., Lynskey, M., Borschmann, R., and Waldron, J. (2015) Risk of emergency medical treatment following consumption of cannabis or synthetic cannabinoids in a large global sample. *J. Psychopharmacol. 29*, 698−703.
(51) Castellanos, D., and Gralnik, L. M. (2016) Synthetic cannabinoids 2015: An update for pediatricians in clinical practice. *World J. Clin. Pediatr. 5*, 16−24.
(52) Tait, R. J., Caldicott, D., Mountain, D., Hill, S. L., and Lenton, S. (2016) A systematic review of adverse events arising from the use of synthetic cannabinoids and their associated treatment. *Clin. Toxicol. 54*, 1−13.
(53) Schifano, F., Orsolini, L., Papanti, D., and Corkery, J. (2016) NPS: Medical Consequences Associated with Their Intake. In *Current Topics in Behavioral Neurosciences*, pp 1−30, Springer International Publishing, Berlin.
(54) Nacca, N., Vatti, D., Sullivan, R., Sud, P., Su, M., and Marraffa, J. (2013) The synthetic cannabinoid withdrawal syndrome. *J. Addict. Med. 7*, 296−298.
(55) Macfarlane, V., and Christie, G. (2015) Synthetic cannabinoid withdrawal: a new demand on detoxification services. *Drug Alcohol Rev. 34*, 147−153.
(56) Cooper, Z. D. (2016) Adverse Effects of Synthetic Cannabinoids: Management of Acute Toxicity and Withdrawal. *Curr. Psychiatry Rep. 18*, 52.
(57) Van Hout, M. C., and Hearne, E. (2016) User Experiences of Development of Dependence on the Synthetic Cannabinoids, 5f-AKB48 and 5F-PB-22, and Subsequent Withdrawal Syndromes. *Int. J. Ment. Health Addict.*, DOI: 10.1007/s11469-016-9650-x.
(58) Sasaki, C., Saito, T., Shinozuka, T., Irie, W., Murakami, C., Maeda, K., Nakamaru, N., Oishi, M., Nakamura, S., and Kurihara, K. (2015) A case of death caused by abuse of a synthetic cannabinoid N-

DOI: 10.1021/acschemneuro.6b00137
ACS Chem. Neurosci. 2016, 7, 1241−1254

1-naphthalenyl-1-pentyl-1H-indole-3-carboxamide. *Forensic Toxicol. 33*, 165−169.
(59) Chung, H., Lee, J., and Kim, E. (2016) Trends of novel psychoactive substances (NPSs) and their fatal cases. *Forensic Toxicol. 34*, 1−11.
(60) Kasper, A. M., Ridpath, A. D., Morrison, M., Olayinka, O., Parker, C., Galli, R., Cox, R., Preacely, N., Anderson, J., Kyle, P. B., Gerona, R., Martin, C., Schier, J., Wolkin, A., Dobbs, T., Arnold, J. K., and Chatham-Stephens, K. (2015) Notes from the Field: Severe Illness Associated with Reported Use of Synthetic Cannabinoids — Mississippi, April 2015 *MMWR Morb. Mortal. Wkly Rep. 64*, 1121−1122.
(61) Law, R., Schier, J., Martin, C., Chang, A., and Wolkin, A. (2015) Increase in Reported Adverse Health Effects Related to Synthetic Cannabinoid Use — United States, January−May 2015. *MMWR Morb. Mortal. Wkly. Rep. 64*, 618−619.
(62) Trecki, J., Gerona, R. R., and Schwartz, M. D. (2015) Synthetic Cannabinoid-Related Illnesses and Deaths. *N. Engl. J. Med. 373*, 103−107.
(63) Labay, L. M., Caruso, J. L., Gilson, T. P., Phipps, R. J., Knight, L. D., Lemos, N. P., McIntyre, I. M., Stoppacher, R., Tormos, L. M., Wiens, A. L., Williams, E., and Logan, B. K. (2016) Synthetic cannabinoid drug use as a cause or contributory cause of death. *Forensic Sci. Int. 260*, 31−39.
(64) Klavž, J., Gorenjak, M., and Marinšek, M. (2016) Suicide attempt with a mix of synthetic cannabinoids and synthetic cathinones: Case report of non-fatal intoxication with AB-CHMINACA, AB-FUBINACA, alpha-PHP, alpha-PVP and 4-CMC. *Forensic Sci. Int. 265*, 121−124.
(65) Thornton, S. L., Bram, D., Milligan, D., and Gerona, R. (2015) Rhabdomyolysis associated with laboratory confirmed FUB-AMB use. *Clin. Toxicol. 53*, 650−651.
(66) Hasegawa, K., Wurita, A., Minakata, K., Gonmori, K., Nozawa, H., Yamagishi, I., Watanabe, K., and Suzuki, O. (2015) Postmortem distribution of AB-CHMINACA, 5-fluoro-AMB, and diphenidine in body fluids and solid tissues in a fatal poisoning case: usefulness of adipose tissue for detection of the drugs in unchanged forms. *Forensic Toxicol. 33*, 45−53.
(67) Shanks, K. G., and Behonick, G. S. (2016) Death after use of the synthetic cannabinoid 5F-AMB. *Forensic Sci. Int. 262*, e21−4.
(68) Hasegawa, K., Wurita, A., Minakata, K., Gonmori, K., Yamagishi, I., Nozawa, H., Watanabe, K., and Suzuki, O. (2015) Identification and quantitation of 5-fluoro-ADB, one of the most dangerous synthetic cannabinoids, in the stomach contents and solid tissues of a human cadaver and in some herbal products. *Forensic Toxicol. 33*, 112−121.
(69) Adamowicz, P. (2016) Fatal intoxication with synthetic cannabinoid MDMB-CHMICA. *Forensic Sci. Int. 261*, e5−e10.
(70) Angerer, V., Franz, F., Schwarze, B., Moosmann, B., and Auwarter, V. (2016) Reply to 'Sudden Cardiac Death Following Use of the Synthetic Cannabinoid MDMB-CHMICA'. *J. Anal. Toxicol. 40*, 240−242.
(71) Westin, A. A., Frost, J., Brede, W. R., Gundersen, P. O., Einvik, S., Aarset, H., and Slordal, L. (2016) Sudden Cardiac Death Following Use of the Synthetic Cannabinoid MDMB-CHMICA. *J. Anal. Toxicol. 40*, 86−87.
(72) Shevyrin, V. A., Morzherin, Y. Y., Melkozerov, V. P., and Nevero, A. S. (2014) New Synthetic Cannabinoid − Methyl 2-{[1-(5-Fluoro-Pentyl)-3-Methyl-1H-Indol-3-Ylcarbonyl]-Amino}Butyrate − as a Designer Drug. *Chem. Heterocycl. Compd. 50*, 583−586.
(73) Shevyrin, V., Melkozerov, V., Nevero, A., Eltsov, O., Shafran, Y., Morzherin, Y., and Lebedev, A. T. (2015) Identification and analytical characteristics of synthetic cannabinoids with an indazole-3-carboxamide structure bearing a N-1-methoxycarbonylalkyl group. *Anal. Bioanal. Chem. 407*, 6301−6315.
(74) Akamatsu, S., and Yoshida, M. (2016) Fragmentation of synthetic cannabinoids with an isopropyl group or a tert-butyl group ionized by electron impact and electrospray. *J. Mass Spectrom. 51*, 28−32.
(75) Andernach, L., Pusch, S., Weber, C., Schollmeyer, D., Münster-Müller, S., Pütz, M., and Opatz, T. (2016) Absolute configuration of the synthetic cannabinoid MDMB-CHMICA with its chemical characteristics in illegal products. *Forensic Toxicol. 34*, 344.
(76) Lobo Vicente, J., Chassaigne, H., Holland, M. V., Reniero, F., Kolar, K., Tirendi, S., Vandecasteele, I., Vinckier, I., and Guillou, C. (2016) Systematic analytical characterization of new psychoactive substances: A case study. *Forensic Sci. Int. 265*, 107−115.
(77) Andersson, M., Diao, X., Wohlfarth, A., Scheidweiler, K. B., and Huestis, M. A. (2016) Metabolic profiling of new synthetic cannabinoids AMB and 5F-AMB by human hepatocyte and liver microsome incubations and high-resolution mass spectrometry. *Rapid Commun. Mass Spectrom. 30*, 1067−1078.
(78) Wiley, J. L., Compton, D. R., Dai, D., Lainton, J. A. H., Phillips, M., Huffman, J. W., and Martin, B. R. (1998) Structure-activity relationships of indole- and pyrrole-derived cannabinoids. *J. Pharmacol. Exp. Ther. 285*, 995−1004.
(79) Wiley, J. L., Marusich, J. A., and Huffman, J. W. (2014) Moving around the molecule: Relationship between chemical structure and in vivo activity of synthetic cannabinoids. *Life Sci. 97*, 55−63.
(80) Wiley, J. L., Lefever, T. W., Cortes, R. A., and Marusich, J. A. (2014) Cross-substitution of Delta9-tetrahydrocannabinol and JWH-018 in drug discrimination in rats. *Pharmacol., Biochem. Behav. 124*, 123−128.
(81) Jarbe, T. U., Gifford, R. S., Zvonok, A., and Makriyannis, A. (2016) 9-Tetrahydrocannabinol discriminative stimulus effects of AM2201 and related aminoalkylindole analogs in rats. *Behav. Pharmacol. 27*, 211−214.
(82) Hine, B., Torrelio, M., and Gershon, S. (1977) Analgesic, Heart Rate, and Temperature Effects of Δ^8-THC during Acute and Chronic Administration to Conscious Rats. *Pharmacology 15*, 65−72.
(83) Wiley, J. L., Marusich, J. A., Martin, B. R., and Huffman, J. W. (2012) 1-Pentyl-3-phenylacetylindoles and JWH-018 share in vivo cannabinoid profiles in mice. *Drug Alcohol Depend. 123*, 148−153.
(84) Wiley, J. L., Marusich, J. A., Lefever, T. W., Grabenauer, M., Moore, K. N., and Thomas, B. F. (2013) Cannabinoids in disguise: Delta9-tetrahydrocannabinol-like effects of tetramethylcyclopropyl ketone indoles. *Neuropharmacology 75*, 145−154.
(85) Rinaldi-Carmona, M., Barth, F., Heaulme, M., Shire, D., Calandra, B., Congy, C., Martinez, S., Maruani, J., Neliat, G., Caput, D., Ferrara, P., Soubrié, P., Brelière, J. C., and Le Fur, G. (1994) SR141716A, a potent and selective antagonist of the brain cannabinoid receptor. *FEBS Lett. 350*, 240−244.
(86) Rinaldi-Carmona, M., Barth, F., Millan, J., Derocq, J. M., Casellas, P., Congy, C., Oustric, D., Sarran, M., Bouaboula, M., Calandra, B., Portier, M., Shire, D., Breliere, J. C., and Le Fur, G. L. (1998) SR 144528, the first potent and selective antagonist of the CB2 cannabinoid receptor. *J. Pharmacol. Exp. Ther. 284*, 644−650.
(87) Knapman, A., Santiago, M., and Connor, M. (2014) Buprenorphine signalling is compromised at the N40D polymorphism of the human mu opioid receptor in vitro. *Br. J. Pharmacol. 171*, 4273−4288.
(88) Knapman, A., Santiago, M., Du, Y. P., Bennallack, P. R., Christie, M. J., and Connor, M. (2013) A continuous, fluorescence-based assay of mu-opioid receptor activation in AtT-20 cells. *J. Biomol. Screening 18*, 269−276.

DOI: 10.1021/acschemneuro.6b00137
ACS Chem. Neurosci. 2016, 7, 1241−1254

Chapter 3. *In vitro* and *in vivo* pharmacokinetics and metabolism of synthetic cannabinoids CUMYL-PICA and 5F-CUMYL-PICA

Forensic Toxicol
DOI 10.1007/s11419-017-0361-1

ORIGINAL ARTICLE

In vitro and in vivo pharmacokinetics and metabolism of synthetic cannabinoids CUMYL-PICA and 5F-CUMYL-PICA

Richard C. Kevin[1,2] · Timothy W. Lefever[3] · Rodney W. Snyder[3] · Purvi R. Patel[3] · Timothy R. Fennell[3] · Jenny L. Wiley[3] · Iain S. McGregor[1,2] · Brian F. Thomas[3]

Received: 23 January 2017 / Accepted: 28 February 2017

Abstract CUMYL-PICA [1-pentyl-*N*-(2-phenylpropan-2-yl)-1*H*-indole-3-carboxamide] and 5F-CUMYL-PICA [1-(5-fluoropentyl)-*N*-(2-phenylpropan-2-yl)-1*H*-indole-3-carboxamide] are recently identified recreationally used/abused synthetic cannabinoids, but have uncharacterized pharmacokinetic profiles and metabolic processes. This study characterized clearance and metabolism of these compounds by human and rat liver microsomes and hepatocytes, and then compared these parameters with in vivo rat plasma and urine sampling. It also evaluated hypothermia, a characteristic cannabimimetic effect. Incubation of CUMYL-PICA and 5F-CUMYL-PICA with rat and human liver microsomes suggested rapid metabolic clearance, but in vivo metabolism was prolonged, such that parent compounds remained detectable in rat plasma 24 h post-dosing. At 3 mg/kg (intraperitoneally), both compounds produced moderate hypothermic effects. Twenty-eight metabolites were tentatively identified for CUMYL-PICA and, coincidentally, 28 metabolites for 5F-CUMYL-PICA, primarily consisting of phase I oxidative transformations and phase II glucuronidation. The primary metabolic pathways for both compounds resulted in the formation of identical metabolites following terminal hydroxylation or dealkylation of the *N*-pentyl chain for CUMYL-PICA or of the 5-fluoropentyl chain for 5F-CUMYL-PICA. These data provide evidence that in vivo elimination of CUMYL-PICA, 5F-CUMYL-PICA and other synthetic cannabinoids is delayed compared to in vitro modeling, possibly due to sequestration into adipose tissue. Additionally, the present data underscore the need for careful selection of metabolites as analytical targets to distinguish between closely related synthetic cannabinoids in forensic settings.

Keywords Synthetic cannabinoid · Pharmacokinetics · Metabolism · CUMYL-PICA · 5F-CUMYL-PICA · Delayed clearance in vivo

Introduction

Synthetic cannabinoid receptor 1 (CB_1) agonists comprise a large and growing class of recreationally used novel psychoactive substances. These synthetic chemicals produce psychoactive "cannabimimetic" effects in humans and rodents [1–5], and their use as recreational drugs has been linked to a number of adverse health effects [6–9]. The molecular structures of these compounds are regularly altered in an attempt to evade drug detection and legislation [10], and consequently users of synthetic cannabinoids are frequently exposed to novel substances with unknown pharmacokinetic and pharmacodynamic properties.

Two such novel synthetic cannabinoids are CUMYL-PICA [1-pentyl-*N*-(2-phenylpropan-2-yl)-1*H*-indole-3-carboxamide] and its fluorinated analogue 5F-CUMYL-PICA [1-(5-fluoropentyl)-*N*-(2-phenylpropan-2-yl)-1*H*-indole-3-carboxamide]. These synthetic cannabinoids are α,α-dimethylbenzyl analogues of SDB-006 and 5F-SDB-006, which are in turn analogues of SDB-001 (APICA) and STS-135 (Fig. 1). They are also structurally related to a

✉ Richard C. Kevin
richard.kevin@sydney.edu.au

[1] School of Psychology, The University of Sydney, A18, Sydney, NSW 2006, Australia

[2] The Lambert Initiative for Cannabinoid Therapeutics, The University of Sydney, Sydney, NSW 2050, Australia

[3] RTI International, 3040 Cornwallis Road, Research Triangle Park, Durham, NC 27709, USA

Published online: 10 March 2017

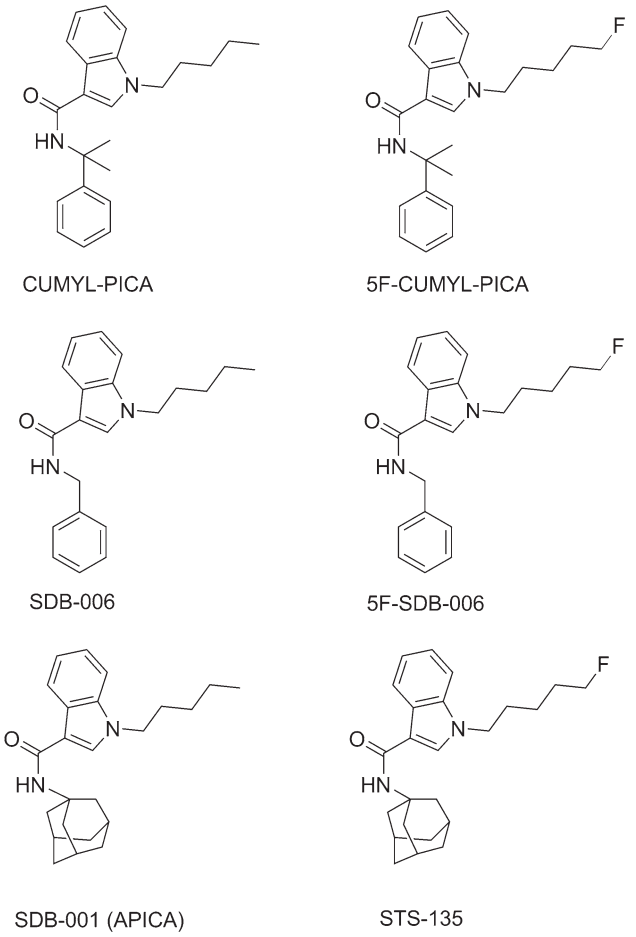

Fig. 1 Structures of CUMYL-PICA and 5F-CUMYL-PICA compared to benzyl analogues SDB-006 and 5F-SDB-006 and to adamantyl analogues SDB-001 and STS-135

number of other carboxamide synthetic cannabinoids such as AMB and 5F-AMB. CUMYL-PICA was detected first in European synthetic cannabinoid products in 2014 [11], and 5F-CUMYL-PICA was recently detected in toxicological analyses of blood samples in Germany [12].

To our knowledge, the pharmacokinetics of CUMYL-PICA and 5F-CUMYL-PICA have not been characterized. A thorough understanding of these processes is important for determining drug toxicology and for identifying these compounds in biological matrices where they are likely extensively metabolized [13–15]. A precise understanding of metabolic pathways is necessary, because closely structurally related synthetic cannabinoids can produce identical metabolites, which can increase the difficulty of forensic identification of a unique compound [13, 15]. In addition, some synthetic cannabinoid metabolites retain cannabinoid receptor efficacy and therefore may be relevant to the overall pharmacological profile following drug administration [16, 17].

Thus, the present study aimed to characterize the pharmacokinetics related to metabolism and clearance of CUMYL-PICA and 5F-CUMYL-PICA. First, these compounds were assessed in vitro using rat and human liver microsomes and hepatocytes, in order to measure clearance and to establish metabolic pathways. These assays were followed by in vivo kinetic assessment in rat blood and urine sampled at several time points following drug administration and measurement of body temperature. These data were used to propose metabolic pathways for CUMYL-PICA and 5F-CUMYL-PICA in rats and humans, to examine the predictive utility of in vitro approaches to synthetic cannabinoid metabolic studies, and to suggest viable analytical targets for forensic analysis.

Materials and methods

Chemicals and reagents

CUMYL-PICA and 5F-CUMYL-PICA were obtained from Cayman Chemicals (Ann Arbor, MI, USA). Acetonitrile and formic acid were purchased from Fisher Scientific (Raleigh, NC, USA). Rat and human liver microsomes and hepatocytes were obtained from XenoTech (Kansas City, KS, USA). Polysorbate 80 was purchased from Fisher Scientific (Pittsburgh, PA, USA) and saline from Patterson Veterinary Supply (Devens, MA, USA). All chemicals and solvents were at least ACS or high-performance liquid chromatography grade, respectively.

In vitro incubations

Rat and human liver microsomes

CUMYL-PICA and 5F-CUMYL-PICA were incubated at 1 μM with male human (pooled) or rat (pooled IGS Sprague–Dawley) liver microsomes at 37 °C, in triplicate, with gentle shaking. A solution of each compound was prepared in acetonitrile at a concentration of 0.1 mM. An assay mixture containing microsomes (1 mg protein/mL final concentration), nicotinamide adenine dinucleotide phosphate reduced form (NADPH; 1 mM final) and a buffer consisting of 50 mM potassium phosphate buffer, pH 7.4, with 3 mM $MgCl_2$ was prepared and pre-incubated at 37 °C for 5 min. Ten microliters of the 0.1 mM drug solutions was added to 990 μL of assay mixture in a glass test tube in a 37 °C water bath to initiate the assay; 100-μL samples were removed at 0, 5, 10, 30, and 60 min and added to 100 μL acetonitrile. Samples were centrifuged and stored at −80 °C until analysis.

Rat and human hepatocytes

Incubation of CUMYL-PICA and 5F-CUMYL-PICA at 10 μM with male human or rat hepatocytes was performed in triplicate, with 1 mL cell suspension (rat: 0.86×10^6 cells/mL, 80% viability; human: 0.80×10^6 cells/mL, 81.6% viability) in 24-well polystyrene cell culture plates in a 37 °C incubator with 5% CO_2 atmosphere. Both compounds were formulated in acetonitrile at 10 mM and further diluted to 1 mM in acetonitrile so that the final concentration of acetonitrile in the incubation was 1% after the addition of 10 μL drug solution to 990 μL of hepatocyte suspension. Incubation was conducted simultaneously using 1 mL incubation cell blank containing live cells and solvent blank; this incubation was treated exactly as the cell incubations. At 0, 10, 60, and 180 min, a 100-μL sample was removed and terminated with 100 μL acetonitrile, vortexed (11,000 *g* for 1 min) and stored at −80 °C until analysis.

In vivo dosing and sampling in rats

Animals

Twelve 49-day-old male Long–Evans rats (226.8–286.7 g) with jugular vein catheters were purchased from Charles River Laboratories (Raleigh, NC, USA). Different groups of rats ($n = 4$ per group) were used to test each compound and vehicle control. Prior to testing, all animals were kept in a temperature-controlled environment (20–22 °C) on a 12-h light–dark cycle (lights on at 6 a.m.), with access to food and water ad libitum. All in vivo work was carried out in accordance with guidelines published in the Guide for the Care and Use of Laboratory Animals (National Research Council 2011), and were approved by the RTI International Institutional Animal Care and Use Committee.

Procedures

The animals were placed individually into glass metabolic cages (Prism Research Glass, Raleigh, NC, USA). Animals were administered intraperitoneal injections, in case of 3 mg/mL CUMYL-PICA or 3 mg/mL 5F-CUMYL-PICA dissolved in vehicle solution comprising 7.8% polysorbate 80 NF (Fisher Scientific, Pittsburgh, PA, USA) and 92.2% saline USP (Patterson Veterinary Supply, Devens, MA, USA), with an injection volume of 1 mL/kg of rat body weight. Blood samples (200 μL) were drawn 15 min pre-injection and 15 min, 30 min, 1 h, 2 h, 4 h, 8 h, and 24 h post-injection, put into chilled K_3EDTA collection tubes, and centrifuged at 2800 *g* for 10 min at 4 °C. The plasma supernatant was decanted and stored at −80 °C until further analysis. Rectal temperature was also recorded at these time points using a digital thermometer (Physitemp Instruments Inc., Clifton, NJ, USA). Urine was collected at 8 and 24 h post-injection. At 24 h post-injection, rats were euthanized via CO_2 asphyxiation, and blood was rapidly collected and stored as specified above.

Analyte extraction

Extractions of all analytes (parent compounds and metabolites) from all matrices (microsomes, hepatocytes, plasma, and urine) was performed as follows. Acetonitrile was added in a 3:1 ratio to the sample volume (microsomes/hepatocytes sample volume 50 μL; plasma 25 μL; urine 100 μL) and centrifuged at 4000 *g* for 15 min at 4 °C. Supernatants were transferred to vials for immediate analysis via liquid chromatography–tandem mass spectroscopy (LC–MS/MS).

LC–MS/MS analyses

Parent compounds CUMYL-PICA and 5F-CUMYL-PICA in the media following incubation with rat and human liver microsomes and in rat plasma were quantified using LC–MS/MS. The LC–MS/MS system consisted of a Waters Acquity UPLC system, equipped with a Waters BEH C18 column (100 mm × 2.1 mm i.d., particle size 1.7 μm; Waters Corp., Milford, MA, USA), coupled to an API 5000 tandem mass spectrometer (AB Sciex, Framingham, MA, USA). Gradient elution was used with mobile phase solutions 0.1% formic acid in water (A) and acetonitrile (B), which started at 10% B for 0.5 min and was then ramped to 95% B over 10 min, held until 12.5 min and then returned to 10% B for 2.5 min, with a total run time of 15 min. The mass spectrometer was operated in positive electrospray ionization mode with multiple reaction monitoring. The monitored transitions were *m/z* 349.1 → 231.1 for CUMYL-PICA and *m/z* 367.1 → 249.1 for 5F-CUMYL-PICA.

Metabolites were also identified using LC–MS/MS, with a Thermo Fisher LTQ Orbitrap Velos mass spectrometer (Thermo Fisher Scientific, Waltham, MA, USA) coupled to a Waters Acquity UPLC system (Waters Corp.). Chromatographic conditions were identical to those specified above. The mass spectrometer was operated in positive electrospray ionization mode, with scan range of *m/z* 100–910 and capillary temperature of 250 °C. Because during method development, poor fragmentation was observed across a range of collision energies, higher-energy collisional dissociation was implemented, with a collision energy at 35 eV.

Data analysis

Hypothermic effects were statistically analyzed using a two-factor mixed ANOVA with drug treatment (vehicle, 3 mg/kg CUMYL-PICA, or 3 mg/kg 5F-CUMYL-PICA) as the between-subject factor and time (pre-dose, 15 min, 30 min, 1 h, 2 h, 4 h, 8 h, and 24 h) as the within-subject factor. Simple effects of drug treatment were then analyzed using Dunnett's tests ($\alpha = 0.05$), which compared the CUMYL-PICA or 5F-CUMYL-PICA cohort to the vehicle cohort at each time point.

Microsomal intrinsic clearance ($CL_{int,micr}$) and half-life were calculated from plots of chromatographic peak areas against time. Intrinsic clearance (CL_{int}) was calculated by scaling $CL_{int,micr}$ to whole-liver dimensions for rats and humans [18, 19]. Hepatic clearance (CL_H) and extraction ratios (ER) were estimated based on the corresponding rat and human CL_{int} values and estimates of liver blood flow rate (rat 13.8 mL/min; human 1400 mL/min) [20]. Plasma concentrations of CUMYL-PICA and 5F-CUMYL-PICA were calculated via a standard curve of the corresponding calibrator samples using a reference standard. Plasma kinetic parameters were then computed from plasma concentrations of each compound via non-compartmental analysis performed with WinNonlin® (Certara, Princeton, NJ, USA).

Metabolites were identified in hepatocyte incubations, rat plasma, and rat urine using Compound Discoverer 2.0 software (Thermo Fisher Scientific) and manual inspection and interpretation of mass spectra.

Results

Body temperature

Compared to vehicle injection, 3 mg/kg CUMYL-PICA and 5F-CUMYL-PICA produced hypothermic effects in rats (Fig. 2). The mean rectal body temperature was significantly reduced following treatment with CUMYL-PICA at 15 and 30 min and 1, 2, and 4 h post-injection. Similarly, significant hypothermic effects were observed following 5F-CUMYL-PICA treatment at 15 and 30 min and 1, 2, and 4 h post-injection.

Liver microsome clearance

Clearance of CUMYL-PICA and 5F-CUMYL-PICA was rapid in rat and human liver microsome incubations (Fig. 3a–d; Table 1). However, both compounds were still detectible after 3 h incubations. Kinetic parameters were similar across all incubations except for CUMYL-PICA in human liver microsomes, which had a substantially longer half-life and correspondingly reduced extraction ratio.

Plasma kinetics

Following intraperitoneal administration of 3 mg/kg CUMYL-PICA or 5F-CUMYL-PICA, plasma concentrations of the parent compounds rose quickly, followed by gradual and incomplete elimination over the following 24 h (Fig. 3e, f). Table 1 contains parameters generated from non-compartmental analysis of the pharmacokinetic data. Overall, the pharmacokinetics of both compounds in rat plasma were similar, although the maximum concentration of CUMYL-PICA was greater and occurred earlier than that of 5F-CUMYL-PICA. CUMYL-PICA had a shorter half-life than 5F-CUMYL-PICA, and the apparent clearance (CL/F) values for both compounds were lower than clearance values predicted by microsome preparations.

CUMYL-PICA metabolism

Phase I metabolites

Phase I metabolism of CUMYL-PICA was extensive, with oxidation occurring at numerous sites (Figs. 4a, 5; Table 2). Parent CUMYL-PICA eluted at 8.94 min, and was confirmed by matching fragmentation and retention times with an analytical standard (Fig. 4a). The $[M+H]^+$ molecular ion of CUMYL-PICA was *m/z* 349.2258, and produced product ions at *m/z* 231.1472, 214.1220, and 188.1449, corresponding to fragmentation along the carboxamide linking group, and 119.0848 and 91.0542, corresponding to fragmentation of the α,α-dimethylbenzyl moiety and subsequent formation of a tropylium ion.

Six monohydroxylated metabolites (C21, C22, C24–C27) with *m/z* 365.2210 were identified in rat hepatocytes. Metabolites C26 and C27 were likely hydroxylated on the benzene ring of the α,α-dimethylbenzyl moiety, as they produced product ions at *m/z* 135.0791 and 107.0493, 15.99 Da higher than product ions at *m/z* 119.0848 and 91.0542 of the parent molecule, respectively. However, C26 and C27 were not observed in human hepatocyte incubations. Metabolites C21 and C22 produced an ion at *m/z* 161.0707, suggesting that hydroxylation did not occur on the indole moiety, and also produced a product ion at *m/z* 119.0848, excluding the α,α-dimethylbenzyl moiety, leaving the *N*-pentyl chain as the likely hydroxylation location. C24 and C25 lacked the ion at *m/z* 161; thus hydroxylation may have occurred on the indole moiety for these metabolites, although the expected product ions at *m/z* 160 and 177 (144 + 16 and 161 + 16) were not observed.

Although fragmentation was insufficient to localize each hydroxylation to the exact molecular site, corresponding data from 5F-CUMYL-PICA incubations were informative. A metabolite (F22) with retention time and fragmentation identical to that of C21 was also formed

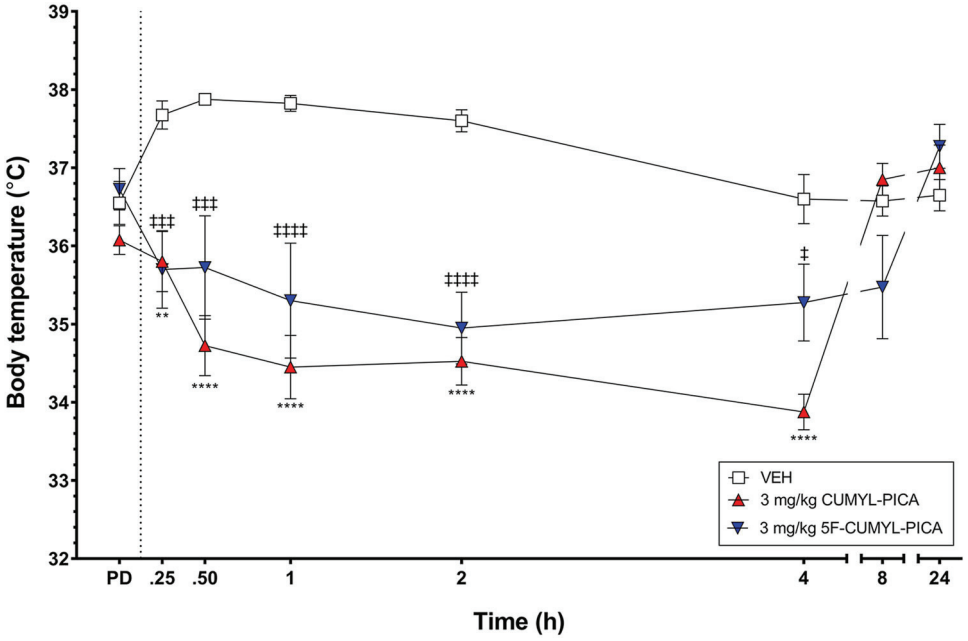

Fig. 2 Mean rectal body temperature of male rats following administration of vehicle solution or 3 mg/kg CUMYL-PICA or 5F-CUMYL-PICA ($n = 4$ per group). *Dashed line* denotes time of intraperitoneal (i.p.) injection. The *error bars* represent standard error of the mean (SEM). *$P < 0.05$, **$P < 0.01$, ***$P < 0.001$, ****$P < 0.0001$, comparing CUMYL-PICA to vehicle at each time point. ‡$P < 0.05$, ‡‡$P < 0.01$, ‡‡‡$P < 0.001$, ‡‡‡‡$P < 0.0001$, comparing 5F-CUMYL-PICA to vehicle at each time point. *PD* pre-dose, 15 min before injection; *VEH* vehicle

following hepatocyte incubation or rat dosing with 5F-CUMYL-PICA. Because this metabolite could only occur following oxidative defluorination of 5F-CUMYL-PICA, we conclude that metabolite C21 is hydroxylated at the terminal position of the *N*-pentyl chain. C21 was further oxidized to form a carboxylic acid metabolite C20 ($[M+H]^+$ *m/z* 379.2005). Product ions at *m/z* 200.1076 and 119.0848 exclude this transformation from the indole and α,α-dimethylbenzyl moieties, strongly suggesting formation of the carboxylic acid on the *N*-pentyl chain. Similar hydroxylation and carboxylation has been reported for AMB, 5F-AMB, JWH-018, AM-2201, RCS-4, UR-144, JWH-073, JWH-210, and others [15, 16, 21–24].

The monohydroxylated metabolites underwent further hydroxylation to form two dihydroxylated metabolites (C11 and C13) with *m/z* 381.2261 (Fig. 5; Table 2). Similar to metabolites C26 and C27, metabolite C11 was hydroxylated once on the α,α-dimethylbenzyl moiety based on product ion at *m/z* 135.0791, while the ion at *m/z* 144.0444 suggests that the other hydroxylation occurred on the *N*-pentyl chain. C13 produced product ions at *m/z* 263.1379 and 246.1144, 32 Da higher than CUMYL-PICA product ions at *m/z* 231.1472 and 214.1220, respectively, and also produced a product ion at *m/z* 119.0848, but not at *m/z* 135.0791, indicating that both hydroxylations occurred on the indole and/or *N*-pentyl moieties. In 5F-CUMYL-PICA preparations, we observed a metabolite (F15) with retention time and mass identical to those of C13; however product ions differed substantially, suggesting formation of a similar but non-identical dihydroxylated metabolite.

CUMYL-PICA was also carbonylated, forming metabolite C23 with $[M+H]^+$ *m/z* 363.2056. The product ions at *m/z* 245.1312 and 228.1023 were 13.98 Da larger than the corresponding CUMYL-PICA product ions at *m/z* 231.1472 and 214.1220 (i.e., +O–2H). Ions at *m/z* 119.0848 and 144.0444 indicate that this carbonylation did not occur on the α,α-dimethylbenzyl or indole moieties, respectively, while the product ion at *m/z* 85.0646 localized this transformation to the *N*-pentyl chain. Metabolite C28 had a molecular ion at *m/z* 347.2103, 2.0155 Da less than CUMYL-PICA, suggesting a dehydrogenation. Product ions at *m/z* 229.1315, 212.1048, 186.1290, and 119.0848 indicate that dehydrogenation occurred on the indole or *N*-pentyl moieties; however, this likely occurred on the *N*-pentyl chain, given the lack of suitable sites for dehydrogenation on the indole moiety, and in light of similar reports of dehydrogenation on the *N*-pentyl chain for other synthetic cannabinoids [15].

Additionally, CUMYL-PICA appears to undergo dealkylation of the *N*-pentyl chain, producing metabolite C18 with *m/z* 279.1978. The product ions at *m/z* 161.0707, 144.0444, 119.0848, 118.0642, and 91.0542 are consistent with this interpretation. Similar dealkylation occurred in some synthetic cannabinoids containing an *N*-pentyl or *N*-fluoropentyl chain [23, 25]. Four monohydroxylations of this metabolite were identified (*m/z* 295.1429). Two of these (C9 and C10) occurred on the indole moiety, evidenced by product ions at *m/z* 177.0669 and 160.0407, 16 Da higher than 161.0707 and 144.0444, respectively. The other two hydroxylations (C7 and C8) lacked these ions, and instead produced a product ion at *m/z* 135.0791 while retaining ions at *m/z* 161.0707 and 144.0444, strongly indicating that hydroxylation occurred on the α,α-dimethylbenzyl moiety.

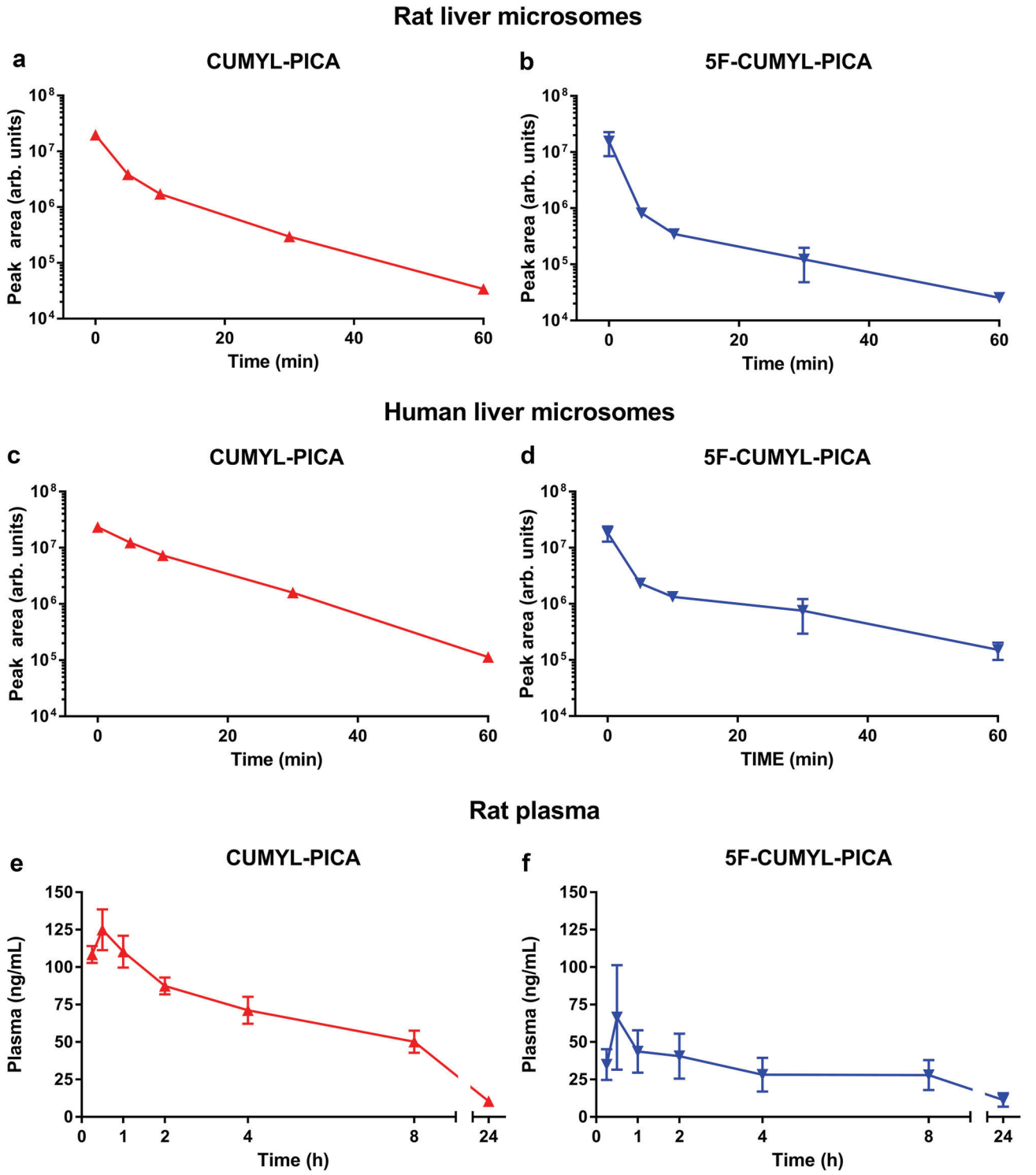

Fig. 3 Mean chromatographic peak areas of CUMYL-PICA and 5F-CUMYL-PICA following incubation with rat and human liver microsomes (panels **a**–**d**, $n = 3$), and mean plasma concentrations of CUMYL-PICA and 5F-CUMYL-PICA following a 3-mg/kg i.p. injection in male rats (panels **e** and **f**, $n = 4$). *Error bars* are SEM

Phase II metabolites

No direct phase II transformations of CUMYL-PICA were observed, but several phase I metabolites underwent glucuronidation. Five discrete peaks at *m/z* 541.2510 were identified in rat and human hepatocytes (C12, C14, C15, C17, and C19), 176 Da greater than monohydroxylated metabolites (*m/z* 365.2210), indicating glucuronidation. A

Table 1 Pharmacokinetic parameters of CUMYL-PICA and 5F-CUMYL-PICA incubated in rat and human liver microsomes in vitro and in rat plasma in vivo

Pharmacokinetic parameter	CUMYL-PICA	5F-CUMYL-PICA
Rat liver microsomes		
Half-life (min)	2.24	1.19
$CL_{int,micr}$ (mL/min/mg)	0.31	0.58
CL_{int} (mL/min/kg body wt.)	556.88	1048.24
CL_H (mL/min/kg body wt.)	50.22	52.44
ER	0.91	0.95
Human liver microsomes		
Half-life (min)	5.92	1.77
$CL_{int,micr}$ (mL/min/mg)	0.12	0.39
CL_{int} (mL/min/kg body wt.)	135.46	453.05
CL_H (mL/min/kg body wt.)	17.43	19.15
ER	0.87	0.96
Rat plasma		
Half-life (h)	7.26	12.00
CL/F (mL/min/kg body wt.)	43.31	147.88
C_{max} (ng/mL)	130.50	65.25
T_{max} (h)	0.50	0.50
AUC 0–24 h (h ng/mL)	1086.57	581.78
AUC 0–∞ (h ng/mL)	1214.85	843.28

AUC area under the curve, *CL/F* observed apparent clearance, CL_H estimated hepatic clearance, CL_{int} estimated intrinsic clearance, $CL_{int,\ micr}$ intrinsic microsome clearance, C_{max} mean maximum observed concentration, *ER* extraction ratio, T_{max} mean time of C_{max}

metabolite identical to C15 in mass, retention time, and product ions was observed in 5F-CUMYL-PICA incubations (F19), indicating that this metabolite is the glucuronide of C21. C19 was found following incubation with human hepatocytes, which likely excludes it as a glucuronide of the α,α-dimethylbenzyl hydroxylated metabolites (C26 and C27), because these metabolites were not found in human hepatocyte incubations (Table 2).

Dihydroxylated metabolites were glucuronidated to four identifiable glucuronides (C3–C5, C16). Mass spectral data were not sufficient to assign each glucuronide to a specific dihydroxylated metabolite. Interestingly, C16 was far more abundant and eluted much later than C3–C5 (Fig. 4a), indicating a substantially less polar structure. Carboxylic acid metabolite C20 formed glucuronide C6 (*m/z* 555.2334). Either C7 or C8 formed glucuronidated metabolite C1, which had a mass of *m/z* 471.1746 and product ions at *m/*z 161.0707, 144.0444, and 135.0791. Similarly, C9 or C10 was glucuronidated to C2 ($[M+H]^+$ *m/z* 471.1746, product ions at *m/z* 177.0669, 160.0407, and 119.0848). No sulfation or other phase II transformations were observed.

5F-CUMYL-PICA metabolism

Phase I metabolites

Similar to CUMYL-PICA, 5F-CUMYL-PICA was extensively oxidized and glucuronidated (Fig. 6; Table 3). The $[M+H]^+$ molecular ion was *m/z* 367.2161 for the unaltered compound, and major product ions were *m/z* 249.1417, 232.1116, and 206.1317, all 17.99 Da higher than corresponding CUMYL-PICA ions (i.e., +F−H), in addition to identical ions at *m/z* 119.0848 and 91.0542. Compound identity was also confirmed by matching retention time and fragmentation to the reference standard (retention time 8.11 min; Fig. 4b).

Six monohydroxylations of 5F-CUMYL-PICA were identified (F23–F28, *m/z* 383.2103, 15.99 Da larger than parent). Metabolites F23–F25 and F27 produced a product ion at *m/z* 119.0848, suggesting hydroxylation on the indole or *N*-fluoropentyl moiety, while metabolites F26 and F28 produced an ion at *m/z* 135.0791, indicating hydroxylation on the α,α-dimethylbenzyl moiety. Unfortunately, metabolites F23–F25 and F27 did not produce product ions that might be used to distinguish between indole or *N*-fluoropentyl chain oxidations (e.g., 144 vs 160, or 161 vs 177). However, we suggest that 5F-CUMYL-PICA hydroxylation likely proceeds in a manner similar to CUMYL-PICA, and that these metabolites are likely 5-fluoropentyl analogues of CUMYL-PICA metabolites C22, C24, and C25.

Dihydroxylated metabolites F14 and F17 were also detected. F14 produced a product ion at *m/z* 135.0791 suggesting that one hydroxylation occurred on the α,α-dimethylbenzyl moiety, while ions at *m/z* 265.1363 and 248.1018 indicate that the other hydroxylation occurred on the indole or *N*-fluoropentyl portion of the molecule. F17 produced ion at *m/z* 119.0848 instead of *m/z* 135.0791, suggesting both hydroxylations occurred on the indole or *N*-fluoropentyl portion of the molecule. This interpretation is supported by the presence of ions at *m/z* 281.1266 and 264.1018 (15.99 Da higher than ions at *m/z* 265.1363 and 248.1107, respectively).

Oxidative defluorination was a predominant metabolic pathway, forming metabolite F22 at *m/z* 365.2210 and product ions at *m/z* 247.1448, 230.1149, 204.1378, and 119.0848, identical to CUMYL-PICA metabolite C21. Similar dehalogenation has been reported as a major metabolic pathway for AM-2201, 5F-AMB, XLR-11, and AM-694 [15, 22, 26]. Additional hydroxylation of F22 produced dihydroxylated metabolite F15 ($[M+H]^+$ *m/*z 381.2169), which produced ions at *m/z* 263.1379, 246.1144, 202.1207, and 119.0848, indicating that the second hydroxylation occurred on the pentyl chain or indole moiety. Oxidation of F22 formed carboxylic acid

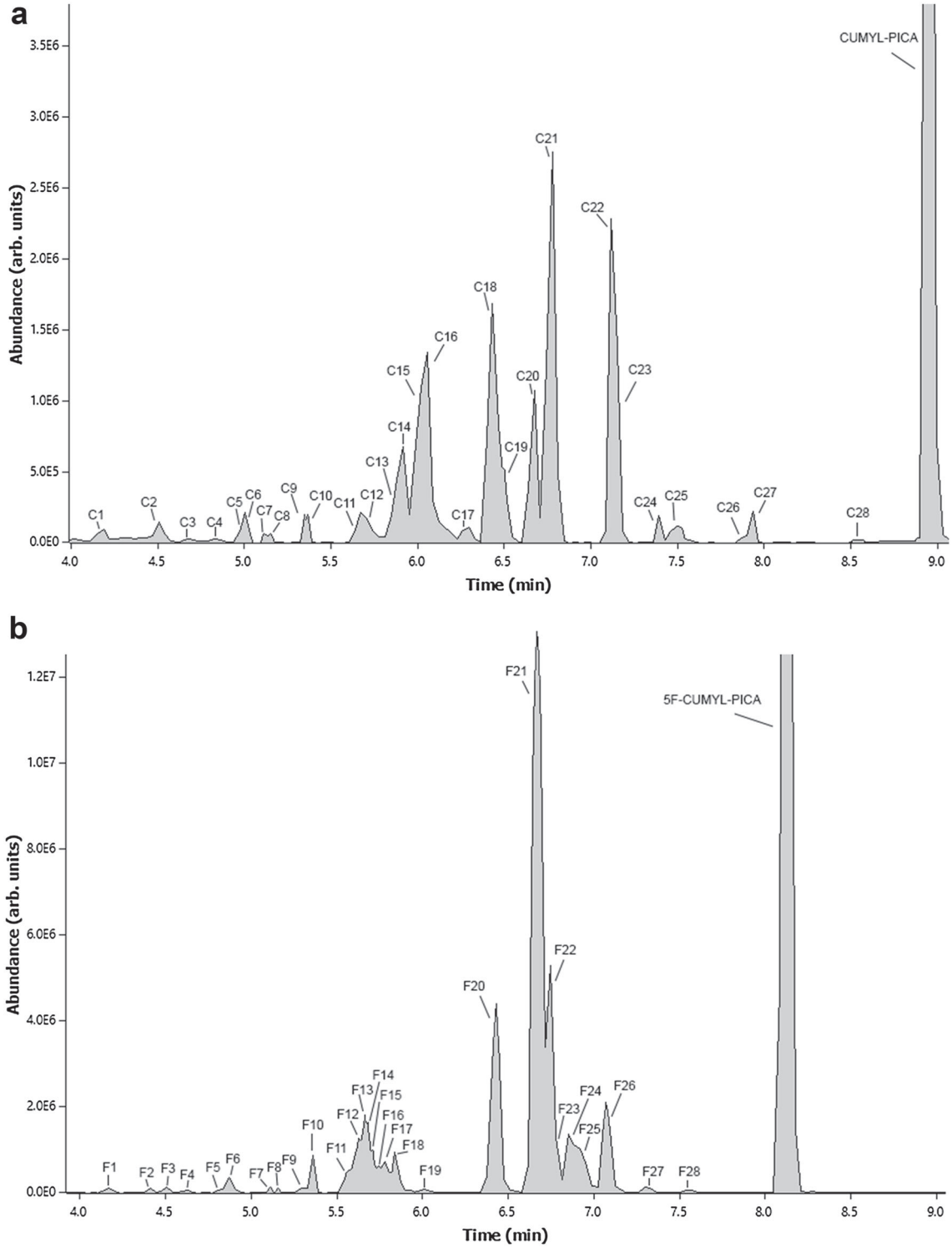

Fig. 4 Combined extracted ion chromatograms of **a** CUMYL-PICA and **b** 5F-CUMYL-PICA metabolites after 3-h incubation with rat hepatocytes, obtained by liquid chromatography–single-stage mass spectrometry

metabolite F21, identical to CUMYL-PICA metabolite C20. F21 was then hydroxylated, forming metabolites F11 and F13 ($[M+H]^+$ *m/z* 395.1937). F11 produced product ion at *m/z* 135.0791, indicating hydroxylation on the α,α-dimethylbenzyl moiety, and ion at *m/z* 200.1076 further localized this modification to the benzene ring. F13 produced ions at *m/z* 277.1163, 260.0936, 216.1009, and 119.0848, suggesting hydroxylation of the indole

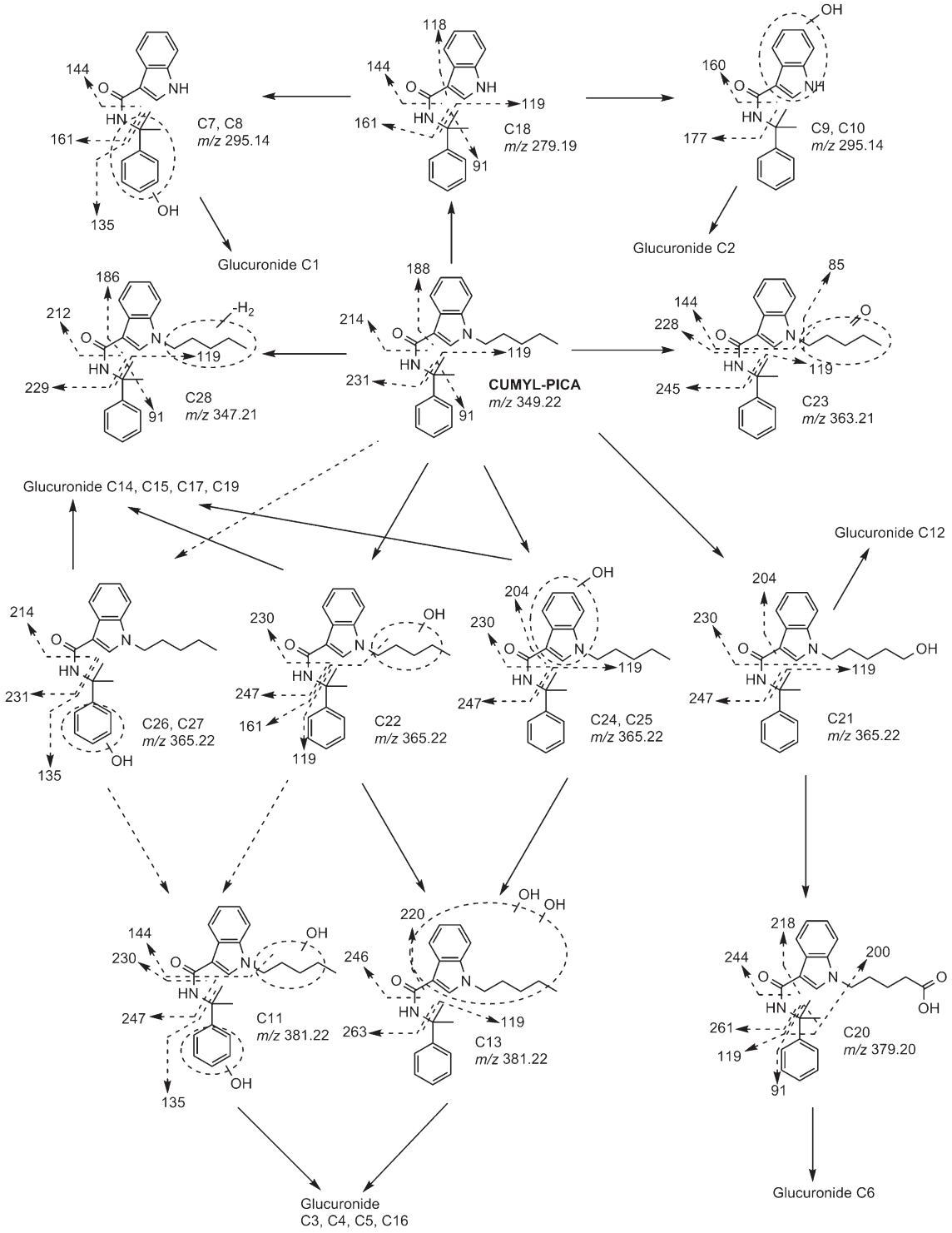

Fig. 5 Proposed CUMYL-PICA metabolic pathways in rats and humans. *Dashed arrows* between compounds denote formation of metabolites that were not observed in human hepatocyte incubations. Unlocalized transformations are shown as Markush structures

moiety. Interestingly, these hydroxylation reactions were not detected in CUMYL-PICA incubations. Oxidative defluorination may occur more readily than terminal hydroxylation of the *N*-pentyl chain, thereby increasing concentrations of subsequent metabolites. This is supported by our chromatographic data that show a larger extracted ion peak (*m/z* 365.2) for F22 compared to C21 (Fig. 4).

Table 2 CUMYL-PICA metabolites following incubation with rat and human hepatocytes, and their presence in rat plasma and urine following a 3-mg/kg intraperitoneal (i.p.) injection

Metabolite	RT (min)	Transformation	Molecular ion $[M+H]^+$ (*m/z*)	Major product ion(s) (*m/z*)	Rat hepatocyte	Human hepatocyte	Rat plasma	Rat urine
C1	4.15	*N*-Pentyl dealkylation + hydroxylation (α,α-dimethylbenzyl) + glucuronidation	471.17	177, 161, 135	✔			✔
C2	4.51	*N*-Pentyl dealkylation + hydroxylation (indole) + glucuronidation	471.17	177, 119	✔	✔		✔
C3	4.68	Dihydroxylation + glucuronidation	557.24	381, 263	✔	✔		
C4	4.83	Dihydroxylation + glucuronidation	557.24	381, 263	✔	✔		
C5	4.95	Dihydroxylation + glucuronidation	557.24	381, 263	✔	✔		
C6	5.01	Carboxylation + glucuronidation	555.23	379	✔	✔		✔
C7	5.11	*N*-Pentyl dealkylation + hydroxylation (α,α-dimethylbenzyl)	295.14	161, 144, 135	✔	✔	✔	
C8	5.17	*N*-Pentyl dealkylation + hydroxylation (α,α-dimethylbenzyl)	295.14	161, 144, 135	✔		✔	
C9	5.30	*N*-Pentyl dealkylation + hydroxylation (indole)	295.14	177, 160	✔	✔		
C10	5.34	*N*-Pentyl dealkylation + hydroxylation (indole)	295.14	177, 160	✔	✔	✔	
C11	5.65	Dihydroxylation (α,α-dimethylbenzyl, *N*-pentyl)	381.22	247, 230, 144, 135	✔		✔	
C12	5.78	Hydroxylation + glucuronidation	541.25	365, 230	✔	✔		
C13	5.87	Dihydroxylation (*N*-pentyl, indole)	381.22	263, 246, 220, 119	✔	✔	✔	
C14	5.92	Hydroxylation + glucuronidation	541.25	365, 230	✔			
C15	6.02	Hydroxylation (*N*-pentyl, terminal) + glucuronidation	541.25	423, 247, 230, 204, 119	✔	✔		✔
C16	6.12	Dihydroxylation + glucuronidation	557.24	381, 263	✔	✔		
C17	6.30	Hydroxylation + glucuronidation	541.25	365, 230	✔			
C18	6.41	*N*-Pentyl dealkylation	279.19	161, 144, 119, 118, 91	✔	✔		
C19	6.50	Hydroxylation + glucuronidation	541.25	365, 230	✔	✔	✔	
C20	6.68	Carboxylation	379.20	261, 244, 218, 200, 119, 91	✔	✔	✔	
C21	6.76	Hydroxylation (*N*-pentyl, terminal)	365.22	247, 230, 204, 119	✔	✔	✔	✔
C22	7.11	Hydroxylation (*N*-pentyl)	365.22	247, 230, 161, 119	✔	✔	✔	
C23	7.13	Carbonylation (*N*-pentyl)	363.21	245, 228, 144, 119, 85	✔	✔	✔	
C24	7.37	Hydroxylation (indole)	365.22	247, 230, 204, 119	✔	✔	✔	✔
C25	7.46	Hydroxylation (indole)	365.22	247, 230, 204, 119	✔	✔	✔	
C26	7.80	Hydroxylation (benzene ring)	365.22	231, 214, 135	✔			
C27	7.86	Hydroxylation (benzene ring)	365.22	231, 214, 135	✔		✔	
C28	8.52	Dehydrogenation (*N*-pentyl)	347.21	229, 212, 186, 119, 91	✔	✔	✔	
CUMYL-PICA	8.94	Parent compound	349.22	231, 214, 188, 119, 91	✔	✔	✔	

Ticks denote detection of compounds in a given matrix

RT retention time

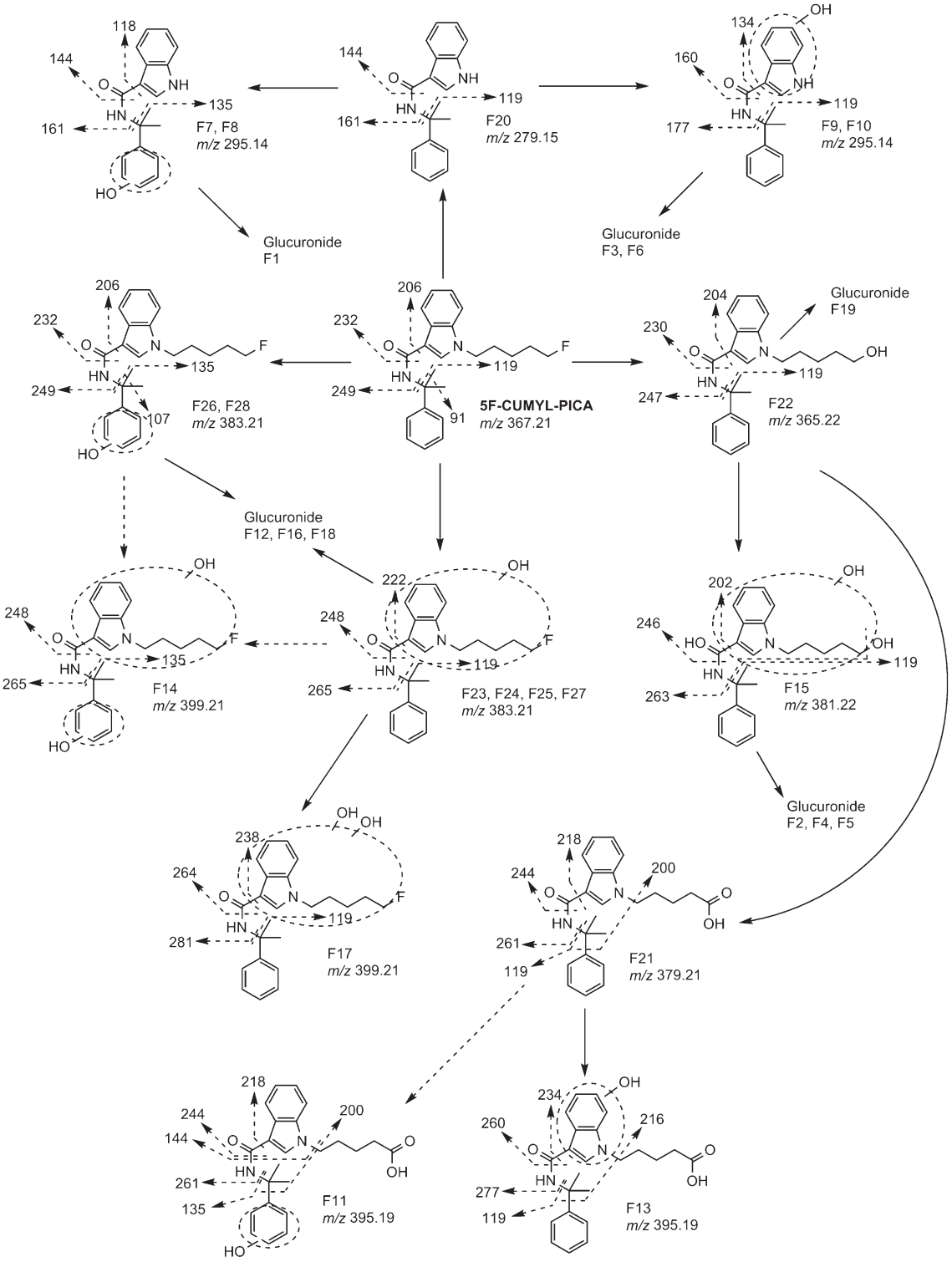

Fig. 6 Proposed 5F-CUMYL-PICA metabolic pathways in rats and humans. *Dashed arrows* between compounds denote formation of metabolites that were not observed in human hepatocyte incubations. Unlocalized transformations are shown as Markush structures

Similar to CUMYL-PICA, the *N*-fluoropentyl chain of 5F-CUMYL-PICA was eliminated, leaving metabolite F20, identical in retention time and fragmentation to CUMYL-PICA metabolite C18. As was the case for C18, F20 was further oxidized on the α,α-dimethylbenzyl moiety (F7 and F8, product ions at *m/z* 161.0707, 144.0444, 135.0791) or indole moiety (F9 and F10, product ions at *m/z* 177.0669, 160.0376, 119.0848).

Table 3 5F-CUMYL-PICA metabolites following incubation with rat and human hepatocytes, and in rat plasma and urine following a 3 mg/kg i.p. injection

Metabolite	RT (min)	Transformation	Molecular ion $[M+H]^+$ (*m/z*)	Major product ions (*m/z*)	Rat hepatocyte	Human hepatocyte	Rat plasma	Rat urine
F1	4.15	Fluoropentyl dealkylation + hydroxylation (α,α-dimethylbenzyl) + glucuronidation	471.17	177, 161, 135	✔			✔
F2	4.44	Oxidative defluorination + hydroxylation + glucuronidation	557.24	381, 263	✔			
F3	4.51	Fluoropentyl dealkylation + hydroxylation (indole) + glucuronidation	471.17	177, 119	✔	✔	✔	✔
F4	4.65	Oxidative defluorination + hydroxylation + glucuronidation	557.24	381, 263	✔	✔	✔	
F5	4.80	Oxidative defluorination + hydroxylation + glucuronidation	557.24	381, 263	✔	✔		
F6	4.87	Fluoropentyl dealkylation + hydroxylation (indole) + glucuronidation	471.17	177, 119	✔	✔		✔
F7	5.11	Fluoropentyl dealkylation + hydroxylation (α,α-dimethylbenzyl)	295.14	161, 144, 135, 118	✔	✔	✔	
F8	5.17	Fluoropentyl dealkylation + hydroxylation (α,α-dimethylbenzyl)	295.14	161, 144, 135, 118	✔	✔	✔	
F9	5.30	Fluoropentyl dealkylation + hydroxylation (indole)	295.14	177, 160, 134, 119	✔	✔	✔	
F10	5.34	Fluoropentyl dealkylation + hydroxylation (indole)	295.14	177, 160, 134, 119	✔	✔	✔	
F11	5.58	Oxidative defluorination + carboxylation + hydroxylation (α,α-dimethylbenzyl)	395.19	261, 244, 218, 200, 144, 135	✔		✔	
F12	5.61	Hydroxylation + glucuronidation	559.24	382, 248	✔			
F13	5.64	Oxidative defluorination + carboxylation + hydroxylation (indole)	395.19	277, 260, 234, 216, 119	✔	✔	✔	
F14	5.66	Dihydroxylation (α,α-dimethylbenzyl, indole/fluoropentyl)	399.21	265, 248, 135	✔		✔	
F15	5.68	Oxidative defluorination + oxidation	381.22	263, 246, 202, 119	✔	✔		
F16	5.70	Hydroxylation + glucuronidation	559.24	382, 248	✔	✔	✔	
F17	5.72	Dihydroxylation (indole/fluoropentyl)	399.21	281, 264, 238, 119	✔	✔	✔	
F18	5.78	Hydroxylation + glucuronidation	559.24	382, 248	✔	✔	✔	✔
F19	6.01	Oxidative defluorination + glucuronidation	541.25	247, 230, 204, 186, 119	✔			
F20	6.42	Fluoropentyl dealkylation	279.15	161, 144, 119	✔	✔	✔	
F21	6.68	Oxidative defluorination + carboxylation	379.21	261, 244, 218, 200, 119	✔	✔	✔	
F22	6.74	Oxidative defluorination	365.22	247, 230, 204, 119	✔	✔	✔	
F23	6.79	Hydroxylation (indole, fluoropentyl)	383.21	265, 248, 222, 119	✔	✔	✔	
F24	6.85	Hydroxylation (indole, fluoropentyl)	383.21	265, 248, 222, 119	✔	✔	✔	
F25	6.92	Hydroxylation (indole, fluoropentyl)	383.21	265, 248, 222, 119	✔		✔	
F26	7.03	Hydroxylation (benzene)	383.21	249, 232, 206, 135, 107	✔	✔	✔	
F27	7.31	Hydroxylation (indole, fluoropentyl)	383.21	265, 248, 222, 119	✔		✔	
F28	7.55	Hydroxylation (benzene)	383.21	249, 232, 206, 135, 107	✔			
5F-CUMYL-PICA	8.11	Parent compound	367.21	249, 232, 206, 119, 91	✔	✔	✔	

Ticks denote detection of compounds in a given matrix

Phase II metabolites

As was the case for CUMYL-PICA, 5F-CUMYL-PICA did not undergo direct phase II metabolism. Monohydroxylated metabolites formed three glucuronides of mass 559.2445 (F12, F16, and F18). Like monohydroxylated CUMYL-PICA glucuronides, mass spectra were not sufficient to localize each glucuronidation to a specific monohydroxylated metabolite.

Oxidatively defluorinated metabolite F22 was glucuronidated to F19, which was identical in retention time and fragmentation to CUMYL-PICA metabolite C12. F15, the hydroxylated metabolite of F22, was also glucuronidated. Interestingly, three distinct glucuronidations were identified (F2, F4, and F5). It is likely that glucuronidation occurred on either hydroxyl group of F15, which accounts for two glucuronides, but the presence of a third glucuronidated compound suggests that an additional dihydroxylated metabolite may have been formed but not detected.

F9 and F10 were glucuronidated to F3 and F6 ($[M+H]^+$ *m/z* 471.1746, product ions at *m/z* 177.0669, 160.0407, and 119.0848), while either F7 or F8 was glucuronidated to F1 ($[M+H]^+$ 471.1746, product ions at *m/z* 161.0707, 144.0444, and 135.0791). No sulfation or other phase II transformations were observed.

Discussion

This study examined the metabolism and clearance of synthetic cannabinoids CUMYL-PICA and 5F-CUMYL-PICA in rat and human liver microsomes and hepatocytes (in vitro), and in whole animals following administration of each compound in adult male rats. Both compounds produced moderate hypothermic effects at an intraperitoneal dose of 3 mg/kg. While rapid clearance for both compounds was predicted by in vitro data, actual elimination in vivo occurred slowly (Fig. 3). Both compounds were extensively metabolized via oxidative transformations and subsequent glucuronidation, and produced several identical metabolites.

CUMYL-PICA and 5F-CUMYL-PICA produced hypothermic effects of similar magnitude across a 4–8-h period (Fig. 2). For the most part, the magnitude of hypothermia was mirrored by blood drug concentration, although there was some delay between peak hypothermia and peak blood concentration. Rats dosed with CUMYL-PICA also returned to baseline body temperature more rapidly than might be expected from blood concentration. This could be the result of homeostatic mechanisms including rapid receptor internalization or down-regulation. Analogous hypothermic effects in rodents have been observed following administration of a wide variety of number of CB_1 agonists, including other synthetic cannabinoids [1, 2, 27–29] and phytocannabinoids [30]. These effects are blocked by the CB_1 antagonist rimonabant (SR141716), indicating a CB_1-dependent mechanism [2, 31]. Although we did not block hypothermia with rimonabant in this study, it is likely that CUMYL-PICA and 5F-CUMYL-PICA produce hypothermia via CB_1 given their structural similarity to several synthetic cannabinoids assessed in previous reports.

Although rapid clearance of CUMYL-PICA and 5F-CUMYL-PICA was observed in microsomal incubations, rat plasma half-lives were 7 and 12 h, respectively, and both untransformed compounds were detectible in plasma at 24 h post-dosing (Fig. 3; Table 1). In addition, apparent in vivo clearance was substantially slower than clearance values predicted by microsomal incubations. Several factors may account for this discrepancy; lipophilicity seems to be the most likely contributor. These compounds, including Δ^9-tetrahydrocannabinol (Δ^9-THC), are largely non-polar and dissolve poorly in aqueous solutions. In rats and humans, Δ^9-THC is sequestrated into adipose tissue and appears to passively and slowly diffuse back into blood during satiety [32, 33], or more rapidly during periods of food deprivation [34]. In a case of fatal poisoning involving synthetic cannabinoids AB-CHMINACA and 5F-AMB, unaltered parent compounds were found at higher levels in adipose tissue than in blood [35]. Thus it is plausible that similar sequestration of CUMYL-PICA and 5F-CUMYL-PICA in adipose tissue, followed by slow passive diffusion back into blood, could be at least partly responsible for the long half-lives of these compounds in vivo. Analysis of adipose tissue following synthetic cannabinoid administration may prove fruitful in future studies. It should also be noted that our in vitro calculations ignored protein binding, because it is presently uncharacterized for CUMYL-PICA and 5F-CUMYL-PICA. Regardless of the mechanisms, the rapid clearance of synthetic cannabinoids in microsomal incubations observed in this and similar studies should be interpreted with caution in light of rodent data and human case studies that point to long elimination periods in vivo.

A total of 28 metabolites of CUMYL-PICA and 28 metabolites of 5F-CUMYL-PICA were identified in hepatocyte preparations. However, some metabolites produced small peaks (Fig. 4), and subsets of 18 and 22 metabolites were detectable in rat plasma or urine for CUMYL-PICA and 5F-CUMYL-PICA, respectively (Tables 2, 3). CUMYL-PICA and 5F-CUMYL-PICA were generally metabolized similarly by rat and human hepatocytes, although a notable exception was that hydroxylation of the α,α-dimethylbenzyl moiety was rarely observed using human hepatocytes. Unsurprisingly, a greater number of phase I metabolites were detected in plasma than in urine, and most metabolites detected in urine were glucuronides. For urinalysis, glucuronide hydrolysis is recommended in

order to increase urinary metabolite concentrations to aid detection and identification. Extensive glucuronidation appears to be common in the metabolism of other synthetic cannabinoids [14, 15, 36] and phytocannabinoids [37, 38].

The terminally hydroxylated metabolite of CUMYL-PICA was abundant (as measured semi-quantitatively by peak area; Fig. 4), but it was identical to the oxidatively defluorinated metabolite of 5F-CUMYL-PICA. Similarly, the carboxylated metabolite of 5F-CUMYL-PICA was abundant but identical to the corresponding CUMYL-PICA metabolite. Consequently, CUMYL-PICA and 5F-CUMYL-PICA cannot be distinguished from each other using either of their most abundant metabolites. Additionally, elimination of the *N*-pentyl or 5-fluoropentyl chains of CUMYL-PICA and 5F-CUMYL-PICA, respectively, formed identical metabolites. Similar metabolic convergence has been observed with other pairs of structurally related compounds, including AMB and 5F-AMB, JWH-018 and AM-2201, and UR-144 and XLR-11 [15, 23].

Considering these data, analytical targets for forensic purposes must be selected with care. Long elimination periods in vivo suggest that screening for parent compounds in blood may be sufficient in cases of acute exposure. For less recent exposure, monohydroxylated metabolites are potentially useful analytical targets in these matrices, because they (or their glucuronides) were observed at levels well above detection thresholds. For CUMYL-PICA, a reasonable strategy would be to target monohydroxylations occurring on the indole moiety (considering that α,α-dimethylbenzyl hydroxylation was not observed in human hepatocyte preparations). Such hydroxylation was difficult to distinguish from the terminally hydroxylated metabolite, but the presence of more than one monohydroxylated metabolite at *m/z* 365 would be selective for CUMYL-PICA. For 5F-CUMYL-PICA, monohydroxylated metabolites retaining the terminal fluorine may be useful analytical targets.

Conclusions

CUMYL-PICA and 5F-CUMYL-PICA produced moderate hypothermic effects in male rats, and both compounds were metabolized primarily via oxidative transformations followed by glucuronidation in both rat and human models. In vivo clearance of CUMYL-PICA and 5F-CUMYL-PICA was substantially longer than predicted by in vitro incubations, possibly due to the high lipophilicity of these compounds or blood-protein binding. As is the case for other structurally related pairs of synthetic cannabinoids, formation of identical metabolites necessitates careful selection of analytical targets in order to differentiate between CUMYL-PICA and 5F-CUMYL-PICA.

Acknowledgements RCK was supported by an Australian Postgraduate Award. ISM was supported by a National Health and Medical Research Council fellowship. This work was supported by research grant funding to BFT from the National Institute on Drug Abuse (1R01DA-040460), to JLW from the National Institutes of Health (DA-03672), internal research and development funds provided by the Research Triangle Institute, NC, USA, and from the Lambert Initiative for Cannabinoid Therapeutics, NSW, Australia.

Compliance with ethical standards

Conflict of interest The authors have no conflict of interest to declare.

Ethical approval All applicable international, national, and/or institutional guidelines for the care and use of animals were followed. All procedures performed in studies involving animals were in accordance with the ethical standards of the institution at which the studies were conducted.

References

1. Wiley JL, Marusich JA, Lefever TW, Antonazzo KR, Wallgren MT, Cortes RA, Patel PR, Grabenauer M, Moore KN, Thomas BF (2015) AB-CHMINACA, AB-PINACA, and FUBIMINA: affinity and potency of novel synthetic cannabinoids in producing Δ^9-tetrahydrocannabinol-like effects in mice. J Pharmacol Exp Ther 354:328–339
2. Banister SD, Moir M, Stuart J, Kevin RC, Wood KE, Longworth M, Wilkinson SM, Beinat C, Buchanan AS, Glass M, Connor M, McGregor IS, Kassiou M (2015) The pharmacology of indole and indazole synthetic cannabinoid designer drugs AB-FUBINACA, ADB-FUBINACA, AB-PINACA, ADB-PINACA, 5F-AB-PINACA, 5F-ADB-PINACA, ADBICA and 5F-ADBICA. ACS Chem Neurosci 6:1546–1559
3. Wiebelhaus JM, Poklis JL, Poklis A, Vann RE, Lichtman AH, Wise LE (2012) Inhalation exposure to smoke from synthetic "marijuana" produces potent cannabimimetic effects in mice. Drug Alcohol Depend 126:316–323
4. Winstock AR, Barratt MJ (2013) Synthetic cannabis: a comparison of patterns of use and effect profile with natural cannabis in a large global sample. Drug Alcohol Depend 131:106–111
5. Kevin RC, Wood KE, Stuart J, Mitchell AJ, Moir M, Banister SD, Kassiou M, McGregor IS (2017) Acute and residual effects in adolescent rats resulting from exposure to the novel synthetic cannabinoids AB-PINACA and AB-FUBINACA. J Psychopharmacol. doi:10.1177/0269881116684336
6. Trecki J, Gerona RR, Schwartz MD (2015) Synthetic cannabinoid-related illnesses and deaths. N Engl J Med 373:103–107
7. Schwartz MD, Trecki J, Edison LA, Steck AR, Arnold JK, Gerona RR (2015) A common source outbreak of severe delirium associated with exposure to the novel synthetic cannabinoid ADB-PINACA. J Emerg Med 48:573–580
8. Khan M, Pace L, Truong A, Gordon M, Moukaddam N (2016) Catatonia secondary to synthetic cannabinoid use in two patients with no previous psychosis. Am J Addict 25:25–27
9. Louh IK, Freeman WD (2014) A 'spicy' encephalopathy: synthetic cannabinoids as cause of encephalopathy and seizure. Crit Care 18:553. doi:10.1186/s13054-014-0553-6
10. EMCDDA (2015) European drug report 2015. http://www.emcdda.europa.eu/attachements.cfm/att_239505_EN_TDAT15001ENN.pdf. Accessed 4 Oct 2015

11. EMCDDA (2014) Annual report on the implementation of the council decision 2005/387/JHA. http://www.emcdda.europa.eu/system/files/publications/1018/TDAN15001ENN.pdf. Accessed 5 Mar 2015
12. Hess C, Murach J, Krueger L, Scharrenbroch L, Unger M, Madea B, Sydow K (2016) Simultaneous detection of 93 synthetic cannabinoids by liquid chromatography-tandem mass spectrometry and retrospective application to real forensic samples. Drug Test Anal. doi:10.1002/dta.2030
13. Vikingsson S, Gréen H, Brinkhagen L, Mukhtar S, Josefsson M (2015) Identification of AB-FUBINACA metabolites in authentic urine samples suitable as urinary markers of drug intake using liquid chromatography quadrupole tandem time of flight mass spectrometry. Drug Test Anal 8:950–956
14. Thomsen R, Nielsen LM, Holm NB, Rasmussen HB, Linnet K, the IC (2015) Synthetic cannabimimetic agents metabolized by carboxylesterases. Drug Test Anal 7:565–576
15. Andersson M, Diao X, Wohlfarth A, Scheidweiler KB, Huestis MA (2016) Metabolic profiling of new synthetic cannabinoids AMB and 5F-AMB by human hepatocyte and liver microsome incubations and high-resolution mass spectrometry. Rapid Commun Mass Spectrom 30:1067–1078
16. Brents LK, Reichard EE, Zimmerman SM, Moran JH, Fantegrossi WE, Prather PL (2011) Phase I hydroxylated metabolites of the K2 synthetic cannabinoid JWH-018 retain in vitro and in vivo cannabinoid 1 receptor affinity and activity. PLoS One 6:e21917. doi:10.1371/journal.pone.0021917
17. Seely KA, Brents LK, Radominska-Pandya A, Endres GW, Keyes GS, Moran JH, Prather PL (2012) A major glucuronidated metabolite of JWH-018 is a neutral antagonist at CB1 receptors. Chem Res Toxicol 25:825–827
18. Davies B, Morris T (1993) Physiological parameters in laboratory animals and humans. Pharm Res 10:1093–1095
19. McNaney CA, Drexler DM, Hnatyshyn SY, Zvyaga TA, Knipe JO, Belcastro JV, Sanders M (2008) An automated liquid chromatography-mass spectrometry process to determine metabolic stability half-life and intrinsic clearance of drug candidates by substrate depletion. Assay Drug Dev Technol 6:121–129
20. Baranczewski P, Stanczak A, Sundberg K, Svensson R, Wallin A, Jansson J, Garberg P, Postlind H (2006) Introduction to in vitro estimation of metabolic stability and drug interactions of new chemical entities in drug discovery and development. Pharmacol Rep 58:453–472
21. Rajasekaran M, Brents LK, Franks LN, Moran JH, Prather PL (2013) Human metabolites of synthetic cannabinoids JWH-018 and JWH-073 bind with high affinity and act as potent agonists at cannabinoid type-2 receptors. Toxicol Appl Pharmacol 269:100–108
22. Knittel JL, Holler JM, Chmiel JD, Vorce SP, Magluilo J, Levine B, Ramos G, Bosy TZ (2016) Analysis of parent synthetic cannabinoids in blood and urinary metabolites by liquid chromatography tandem mass spectrometry. J Anal Toxicol 40:173–186
23. Sobolevsky T, Prasolov I, Rodchenkov G (2012) Detection of urinary metabolites of AM-2201 and UR-144, two novel synthetic cannabinoids. Drug Test Anal 4:745–753
24. Hutter M, Broecker S, Kneisel S, Auwärter V (2012) Identification of the major urinary metabolites in man of seven synthetic cannabinoids of the aminoalkylindole type present as adulterants in 'herbal mixtures' using LC-MS/MS techniques. J Mass Spectrom 47:54–65
25. Sobolevsky T, Prasolov I, Rodchenkov G (2010) Detection of JWH-018 metabolites in smoking mixture post-administration urine. Forensic Sci Int 200:141–147
26. Grigoryev A, Kavanagh P, Melnik A (2013) The detection of the urinary metabolites of 1-[(5-fluoropentyl)-1*H*-indol-3-yl]-(2-iodophenyl)methanone (AM-694), a high affinity cannabimimetic, by gas chromatography–mass spectrometry. Drug Test Anal 5:110–115
27. Banister SD, Stuart J, Kevin RC, Edington A, Longworth M, Wilkinson SM, Beinat C, Buchanan AS, Hibbs DE, Glass M, Connor M, McGregor IS, Kassiou M (2015) The effects of bioisosteric fluorine in synthetic cannabinoid designer drugs JWH-018, AM-2201, UR-144, XLR-11, PB-22, 5F-PB-22, APICA, and STS-135. ACS Chem Neurosci 6:1445–1458
28. Wiley JL, Marusich JA, Lefever TW, Grabenauer M, Moore KN, Thomas BF (2013) Cannabinoids in disguise: Δ^9-tetrahydrocannabinol-like effects of tetramethylcyclopropyl ketone indoles. Neuropharmacology 75:145–154
29. Wiley JL, Marusich JA, Martin BR, Huffman JW (2012) 1-Pentyl-3-phenylacetylindoles and JWH-018 share *in vivo* cannabinoid profiles in mice. Drug Alcohol Depend 123:148–153
30. Banister SD, Wilkinson SM, Longworth M, Stuart J, Apetz N, English K, Brooker L, Goebel C, Hibbs DE, Glass M, Connor M, McGregor IS, Kassiou M (2013) The synthesis and pharmacological evaluation of adamantane-derived indoles: cannabimimetic drugs of abuse. ACS Chem Neurosci 4:1081–1092
31. Marshall R, Kearney-Ramos T, Brents LK, Hyatt WS, Tai S, Prather PL, Fantegrossi WE (2014) In vivo effects of synthetic cannabinoids JWH-018 and JWH-073 and phytocannabinoid Δ^9-THC in mice: inhalation versus intraperitoneal injection. Pharmacol Biochem Behav 124:40–47
32. Johansson E, Norén K, Sjövall J, Halldin MM (1989) Determination of Δ^1-tetrahydrocannabinol in human fat biopsies from marihuana users by gas chromatography–mass spectrometry. Biomed Chromatogr 3:35–38
33. Kreuz DS, Axelrod J (1973) Δ^9-tetrahydrocannabinol: localization in body fat. Science 179:391–393
34. Gunasekaran N, Long LE, Dawson BL, Hansen GH, Richardson DP, Li KM, Arnold JC, McGregor IS (2009) Reintoxication: the release of fat-stored Δ^9-tetrahydrocannabinol (THC) into blood is enhanced by food deprivation or ACTH exposure. Br J Pharmacol 158:1330–1337
35. Hasegawa K, Wurita A, Minakata K, Gonmori K, Nozawa H, Yamagishi I, Watanabe K, Suzuki O (2015) Postmortem distribution of AB-CHMINACA, 5-fluoro-AMB, and diphenidine in body fluids and solid tissues in a fatal poisoning case: usefulness of adipose tissue for detection of the drugs in unchanged forms. Forensic Toxicol 33:45–53
36. Takayama T, Suzuki M, Todoroki K, Inoue K, Min JZ, Kikura-Hanajiri R, Goda Y, Toyo'oka T (2014) UPLC/ESI-MS/MS-based determination of metabolism of several new illicit drugs, ADB-FUBINACA, AB-FUBINACA, AB-PINACA, QUPIC, 5F-QUPIC and alpha-PVT, by human liver microsome. Biomed Chromatogr 28:831–838
37. Watanabe K, Yamaori S, Funahashi T, Kimura T, Yamamoto I (2007) Cytochrome P450 enzymes involved in the metabolism of tetrahydrocannabinols and cannabinol by human hepatic microsomes. Life Sci 80:1415–1419
38. Kevin RC, Allsop DJ, Lintzeris N, Dunlop AJ, Booth J, McGregor IS (2017) Urinary cannabinoid levels during nabiximols (Sativex®)-medicated inpatient cannabis withdrawal. Forensic Toxicol 35:33–44

Chapter 4. Acute and residual effects in adolescent rats resulting from exposure to the novel synthetic cannabinoids AB-PINACA and AB-FUBINACA

Original Paper

Psychopharm

Journal of Psychopharmacology
1–13

DOI: 10.1177/0269881116684336
jop.sagepub.com
SAGE

Acute and residual effects in adolescent rats resulting from exposure to the novel synthetic cannabinoids AB-PINACA and AB-FUBINACA

Richard C Kevin[1], Katie E Wood[1], Jordyn Stuart[1], Andrew J Mitchell[2], Michael Moir[3], Samuel D Banister[3], Michael Kassiou[3] and Iain S McGregor[1]

Abstract

Synthetic cannabinoids (SCs) have rapidly proliferated as recreational drugs, and may present a substantial health risk to vulnerable populations. However, information on possible effects of long-term use is sparse. This study compared acute and residual effects of the popular indazole carboxamide SC compounds AB-PINACA and AB-FUBINACA in adolescent rats with Δ^9-tetrahydrocannabinol (THC) and control treatments. Albino Wistar rats were injected (i.p.) with AB-PINACA or AB-FUBINACA every second day (beginning post-natal day (PND) 31), first at a low dose (0.2 mg/kg on 6 days) followed by a higher dose (1 mg/kg on a further 6 days). THC-treated rats received equivalent doses of 6 × 1 mg/kg and 6 × 5 mg/kg. During drug treatment, THC, AB-PINACA, and AB-FUBINACA decreased locomotor activity at high and low doses, increased anxiety-like behaviours and audible vocalisations, and reduced weight gain. Two weeks after dosing was completed, all cannabinoid pre-treated rats exhibited object recognition memory deficits. These were notably more severe in rats pre-treated with AB-FUBINACA. However, social interaction was reduced in the THC pre-treated group only. Six weeks post-dosing, plasma levels of cytokines interleukin (IL)-1α and IL-12 were reduced by AB-FUBINACA pre-treatment, while cerebellar endocannabinoids were reduced by THC and AB-PINACA pre-treatment. The acute effects of AB-PINACA and AB-FUBINACA were broadly similar to those of THC, suggesting that acute SC toxicity in humans may be modulated by dose factors, including inadvertent overdose and product contamination. However, some lasting residual effects of these different cannabinoid receptor agonists were subtly different, hinting at recruitment of different mechanisms of neuroadaptation.

Keywords

Cannabinoid, AB-FUBINACA, AB-PINACA, adolescent, memory, behaviour

Introduction

The emergence of synthetic cannabinoids (SCs) as recreational drugs over recent years is a significant health concern, with their increasing use linked to a variety of adverse health effects (Trecki et al., 2015). SCs comprise a large, growing family of compounds with efficacy for cannabinoid receptors (cannabinoid receptor 1 and 2; CB_1 and CB_2). Many different SCs have been detected in 'herbal' products sold worldwide (Seely et al., 2012b). These compounds produce psychoactive effects similar to cannabis use or Δ^9-tetrahydrocannabinol (THC) via actions at CB_1 (Wiley et al., 2012).

SC use has been associated with a toxidrome that in some ways resembles that of herbal cannabis itself, with features such as panic attacks, elevated blood pressure, and tachycardia (Schneir et al., 2011). Of greater concern are reports of severe toxic features that go beyond those of cannabis, including acute kidney injury, acute myocardial infarction, and generalised seizures (Brents and Prather, 2014). It is unclear at present whether such features reflect a more potent action of these compounds than THC at CB_1 or if there is some additional mechanism involved. Many SCs are also potent CB_2 agonists and this could also influence toxicity given the expression of the CB_2 receptor on immune and other cells (Malfitano et al., 2014). SCs may additionally act on G protein-coupled receptor 55 (GPR55) and transient receptor potential channels (Pertwee, 2010). Although actions on CB_1 and CB_2 vary widely between different SCs (Huffman et al., 1994; Rajasekaran et al., 2013), SCs generally tend to be full agonists with greater efficacy than the partial agonist THC (Spaderna et al., 2013).

Systematic research into the effects of SCs is complicated by their rapid evolution and the sheer number of compounds available (EMCDDA, 2016; UNODC, 2015). Identification of

[1]School of Psychology, The University of Sydney, NSW, Australia
[2]Centenary Institute of Cancer Medicine and Cell Biology, Sydney, NSW, Australia
[3]School of Chemistry, The University of Sydney, NSW, Australia

Corresponding author:
Iain S McGregor, School of Psychology, The University of Sydney, Badham Building (A16), NSW, 2006, Australia.
Email: iain.mcgregor@sydney.edu.au

specific SCs in illicit products leads to their prohibition, which in turn reduces their popularity and leads to replacement by novel uncharacterised compounds. Thus, over the past decade SC compounds have emerged in waves (Schwartz et al., 2015). For example, the naphthoylindole compounds JWH-018 and AM-2201 were popular from 2010 to 2012, but now appear in few SC products (NFILS, 2014). More recent waves of popular compounds include indole carboxylates and indazole carboxamides (Schwartz et al., 2015). It cannot be assumed that newly developed SCs will have the same effects as the older compounds in vivo, given substantial differences in chemical structure, cannabinoid receptor efficacy and metabolism (Takayama et al., 2014; Thomsen et al., 2014).

Existing reports of SC effects in humans mostly fall into three categories: case studies reporting acute toxicity, user self-reports, and large surveys of SC users (Castaneto et al., 2014). Such studies are useful for identifying usage trends and potential compounds or products of particular concern, but many reports do not include verification of chemical identity (e.g. via toxicological analysis of blood serum or urine), and those that do often reveal that multiple SC compounds have been used simultaneously (Musshoff et al., 2014). Use of SCs in conjunction with other types of recreational drugs and alcohol is also common (Barratt et al., 2012; Wilkins et al., 2016). Consequentially, the adverse effects observed in these reports cannot always be unambiguously attributed to any single compound.

A limited number of SCs have been examined in preclinical studies in rodents, using some or all of the classic 'tetrad' measures of CB_1 activation (decreased locomotor activity, catalepsy, hypothermia, antinociception). Such studies have revealed classic cannabimimetic effects of JWH-018 (Brents et al., 2012; Macri et al., 2013; Wiebelhaus et al., 2012), UR-144 and XLR-11 (Wiley et al., 2013), and recently AB-CHMINACA, AB-PINACA, and FUBIMINA (Wiley et al., 2015). Dose-dependent hypothermia and bradycardia have also been reported by our group with JWH-018, UR-144, PB-22, APICA and their fluorinated analogues (Banister et al., 2015b), as well as a variety of indazole SCs including AB-PINACA and AB-FUBINACA (Banister et al., 2015a).

More enriched studies of behavioural and physiological responses to novel SCs are sparse, with the exception of the large number of studies involving the very early SCs from the 1990s such as WIN-55,212-2, CP 55,940 and HU-210. A consistent finding among this research is the vulnerability of adolescent rats to lasting residual adverse effects of SCs and THC (for review see Higuera-Matas et al., 2015). Adolescent rats show greater residual memory deficits than adults following chronic THC administration (Quinn et al., 2008), and rats chronically treated with CP 55,940 during adolescence exhibit impaired working memory and social interaction compared with rats treated during adulthood (O'Shea et al., 2004). Similarly, chronic administration of WIN55,212-2 impaired recognition memory in adolescent but not adult rats (Schneider and Koch, 2003). These findings are of particular concern because adolescents constitute a substantial portion of SC users, with the median age of a global sample of users reported as 23 years (Winstock and Barratt, 2013) and recent studies showing that 10% of USA teenagers have tried SCs at least once (Palamar and Acosta, 2015). The dearth of behavioural and toxicological data regarding the effects of the most currently prevalent SCs means that potentially large numbers of people from a vulnerable population are being exposed to drugs with unknown long-term effects.

Therefore we sought here to examine in vivo data regarding the lasting residual effects of currently emerging SCs in adolescent animals. Two widely used indazole carboxamide SCs are *N*-(1-amino-3-methyl-1-oxobutan-2-yl)-1-pentyl-1*H*-indazole-3-carboxamide (AB-PINACA), and *N*-(1-amino-3-methyl-1-oxobutan-2-yl)-1-(4-fluorobenzyl)-1*H*-indazole-3-carboxamide (AB-FUBINACA; NFILS, 2015). These two compounds were first identified in herbal products in Japan (Uchiyama et al., 2013), have since been found in Sweden (Vikingsson et al., 2015), Germany (Langer et al., 2016), the United States (Monte et al., 2014), and elsewhere. Both AB-PINACA and AB-FUBINACA are highly potent CB_1 agonists, and also possess appreciable CB_2 potency (Banister et al., 2015a). Compounds in this class of have been implicated in recent poisonings causing intense anxiety, psychosis, and aggression (Schwartz et al., 2015; Trecki et al., 2015), resulting in their scheduling in the United States and elsewhere (DEA, 2015). We selected these compounds for this study on the basis of their prevalence and also their known dose-response relationship relative to THC and other cannabinoids in causing hypothermia and bradycardia in rats (Banister et al., 2015a; NFILS, 2015).

Here we examined the effects of these SCs in adolescent rats during and following repeated exposure relative to THC. Because the behavioural effects of most SCs are poorly characterised, we adopted an exploratory approach that utilised a variety of general behavioural measures. In line with human case reports and the known anxiogenic effects and memory deficits produced by other cannabinoid compounds in rats (e.g. THC, CP 55,940), we targeted anxiety-like behaviours and memory performance. Given user reports of unpleasant effects (e.g. physical discomfort, nausea, anxiety; Schwartz et al., 2015) we also tested for conditioned place aversion and measured vocalisations following drug administration. Social behaviours were also examined because these behaviours show lasting residual reductions in adolescent rats following THC or CP 55,940 administration (O'Shea et al., 2004; Quinn et al., 2008).

We also examined changes in a number of biomarkers after chronic administration, again adopting an exploratory approach. Plasma cytokines were assessed on the basis that cannabinoids have been shown to modulate cytokine production, typically decreasing levels of cytokines involved in pro-inflammatory processes while increasing levels of anti-inflammatory cytokines (Katchan et al., 2016; Klein et al., 2003). Corticosterone was analysed as a general marker of stress and immune response, with the hypothesis that this analyte might be elevated following SC treatment, based on reports of anxiety in addition to encephalopathy, acute kidney and cardiac injury (Bhanushali et al., 2012; Louh and Freeman, 2014; Mir et al., 2011). In addition we analysed plasma and cerebellar ethanolamides to examine any lasting modulation of endocannabinoid tone, which is thought to be generally decreased by chronic cannabinoid administration (Di Marzo et al., 2000; Rubino et al., 2015). The cerebellum was also targeted because human case reports have described impairment of movement sequences and disruption of fine motor skills following recreational use of a variety of SCs (Musshoff et al., 2014). Together, these measures provide a broad examination of systems which have previously shown sensitivity to cannabinoid receptor agonists. We also compared these effects with

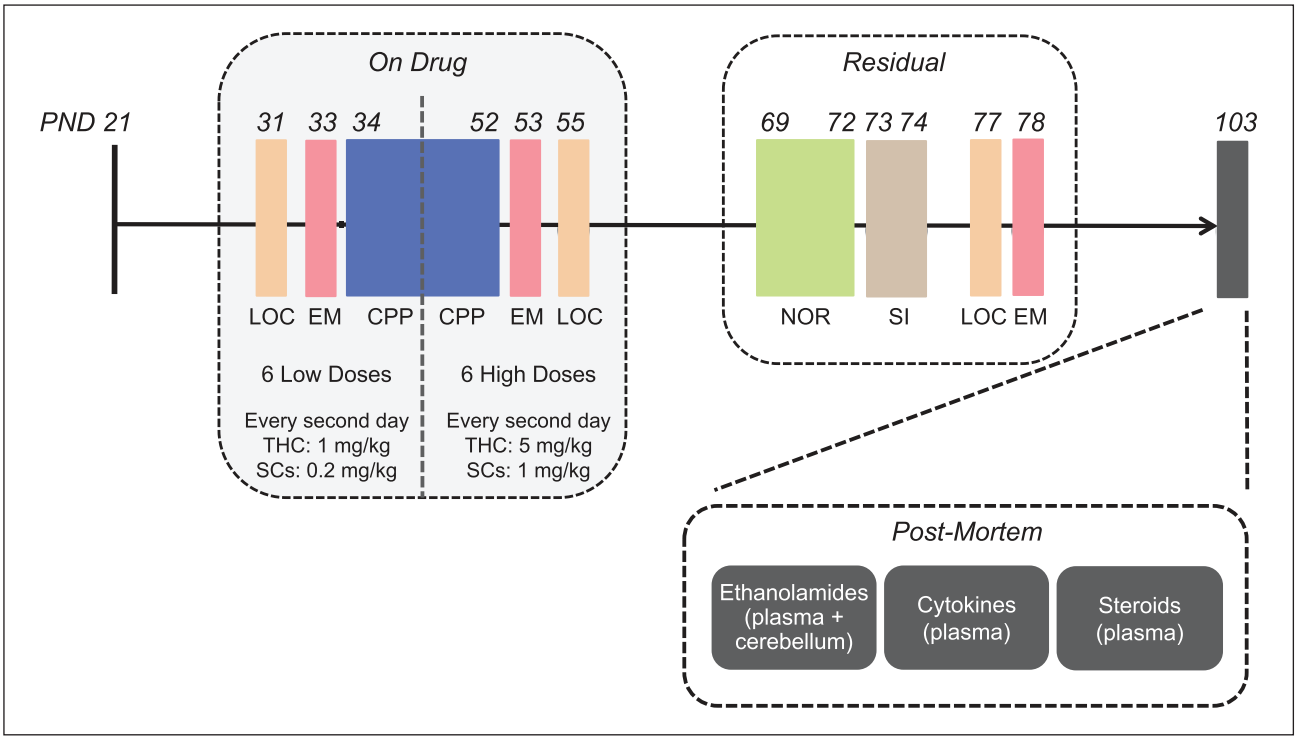

Figure 1. Schematic of behavioural assessment over the entire experiment.
CPP: conditioned place preference; LOC: locomotor; NOR: novel object recognition; EM: emergence test; PND: Post-natal day; SI: social interaction.

equivalent treatment with THC, anticipating that the SCs might produce more severe behavioural and biochemical effects.

Materials and methods

Subjects

A total of 64 experimentally naïve outbred male albino Wistar rats (*Rattus norvegicus*; Animal Resources Centre, Perth, Australia) were used for this experiment. Following their arrival at the laboratory, all rats were handled daily for 5 min each for 7 days before the commencement of testing on post-natal day (PND) 31, at which point they weighed an average of 147 g (range 130–178 g). Rats were housed in groups of four with food and water available ad libitum, on a 12 h reverse light cycle (lights off at 09:00) with temperature maintained at 21 ± 1°C. Rats were assigned to one of four drug-treatment conditions: vehicle, THC, AB-PINACA, or AB-FUBINACA ($n = 16$ per condition). One rat in the vehicle treatment condition was excluded from the experiment due to illness. All procedures were approved by the University of Sydney Animal Ethics committee in accordance with the Australian Code of Practice for the Care and Use of Animals for Scientific Purposes.

Dose selection and preparation

AB-PINACA and AB-FUBINACA were synthesised as previously reported (Banister et al. 2015a). A stock solution of 25 mg/mL THC in ethanol was obtained from Sigma Aldrich (Castle Hill, NSW, Australia).

Our dosing regimen consisted of six 'low' doses followed by six 'high' doses of each drug, with one drug dose administered every second day. This regimen was designed to mimic the escalation of dosage commonly observed during chronic drug use. All rats received vehicle injections on the days between drug treatments. We first selected THC doses used by Quinn et al. (2008), (1 and 5 mg/kg), and then selected approximately equivalent doses of AB-PINACA and AB-FUBINACA (0.2 and 1 mg/kg for both). These doses were selected based on in vivo biotelemetry data – specifically, the peak hypothermia and bradycardia following drug administration in adolescent rodents (Banister et al., 2013, 2015a).

Drugs were prepared in a vehicle solution consisting of ethanol, Tween 80, and physiological saline (5:5:90). For the low THC dose (1 mg/kg), ethanol was added to an appropriate amount of 25 mg/mL THC in ethanol stock solution before addition of the Tween 80 and saline. For the higher dose (5 mg/kg), the THC stock solution was first concentrated to 50 mg/mL by evaporation of excess ethanol under a stream of nitrogen then prepared as for the low dose. All drugs were injected intraperitoneally at a volume of 1 mL/kg.

Behavioural assessment

Behavioural assessment was conducted over two phases – an 'on-drug' phase during repeated drug administration during adolescence (PNDs 31–55), and a 'residual' phase following a 2-week washout during adulthood (PNDs 69–94). These ages are consistent with the adolescent ontogenetic window of 28–55 days for rats (Spear, 2000). A schematic of the assessment sequence is presented in Figure 1. All on-drug behavioural assessments commenced 15 min following injection.

On-drug measures

Locomotor activity (PNDs 31 and 53). Individual rats were placed into a dark chamber with acrylic walls and a grid floor measuring 600 × 250 × 350 mm (L × W × H) for 15 min where they could explore freely. An infrared camera was mounted above the chamber, and the distance travelled by each rat was recorded and scored using automated tracking software (TrackmatePro v1.01, Motion Mensura, NSW, Australia).

Emergence (PNDs 33 and 55). The emergence test, a test of anxiety-like behaviour (Crawley and Goodwin, 1980; Quinn et al., 2008), was conducted in a 1200 × 1200 × 900 mm wooden arena painted matte black. A black hide box (400 × 240 × 170 mm) with a red Perspex lid was positioned against the centre of one wall. The arena was illuminated by two floodlights (150 W white globes). Rats were tested individually for 5 min after being placed into the hide box. A camera mounted above the arena allowed recording of the test session that was scored offline by a blinded experimenter. The scored behaviours were (1) risk assessment (head protruding from the hide box while centre of mass remained inside the box), (2) latency to emerge (centre of mass outside the hide box), and (3) time spent in the open field (outside of the hide box). After each test the arena was cleaned with 50% ethanol.

Place conditioning (PNDs 34–52). Place conditioning was performed as previously described with minor modification (Quinn et al., 2008). The place conditioning chambers (Med Associates, St Albans, VT) consisted of two large side compartments (280 × 210 × 210 mm), separated by a smaller central compartment (120 × 210 × 210 mm). Each side compartment had different textural, visual, and olfactory cues. One had black and white striped walls, a grid mesh floor, and 1 mL white vinegar in the waste pan beneath the floor. The other side had black walls, a metal rod floor, and 1 mL vanilla essence beneath the floor. Compartments could be isolated with guillotine doors. Odours were refreshed between each session.

Testing consisted of five phases: Baseline (PND 34), low-dose conditioning (PNDs 35–42), low-dose test (PND 43), high-dose conditioning (PNDs 44–51), and high-dose test (PND 52). For the conditioning days, rats were given drug injections every second day (totalling four low-dose and four high-dose injections) and vehicle every other day (except for the vehicle group which always received vehicle injections). Rats were placed in alternate sides of the chamber for 15 min each day, such that one side (counterbalanced between and within drug conditions) was always paired with drug treatment and the other with vehicle treatment. For the baseline and test days, rats were placed in the central compartment and allowed to freely explore all compartments for 15 min and the time spent in each was recorded and scored via a camera mounted above the chamber. Preference scores were calculated as the amount of time spent in the drug-conditioned side minus the amount of time spent in the vehicle-conditioned side.

In addition, rat vocalisations were recorded as a supplementary measure of drug aversion (Giuliani et al., 2000; Henriksson and Jarbe, 1971; Quinn et al., 2008). Specifically, a blinded experimenter recorded the number of rats per group that emitted any audible vocalisation while being picked up and placed into the chambers during conditioning days (i.e. 15 min following drug administration). Each rat received a score of 0 for no vocalisations or 1 for any vocalisation, generating a total score ranging from 0 to 16 for each group on each day.

Residual measures

Novel object recognition (PNDs 69–72). The novel object recognition (NOR) testing occurred in a circular black plastic tub (diameter = 750 mm, height = 550 mm), in which two objects could be placed and secured with Velcro. Rats were first individually habituated to the arenas without objects for 10 min on PNDs 69 and 70. The following day, rats were placed in the arenas for 3 min before two identical objects (matte black painted spray bottles or sauce pourers) were placed in the arena and rats were allowed to explore for 3 min. Rats were removed from the arena for 2 min (the inter-trial interval, ITI) and returned to a holding cage while the one of the two identical objects was swapped for a novel one. Rats were then returned to the arena for 3 min and the time spent investigating each object was recorded. The short 2-min ITI was selected to minimise working memory demand in order to detect possible severe impairment to object recognition memory caused by drug exposure. The following day this test was repeated with a new set of objects (matte black painted salt shakers or blue egg-shaped object) using a longer 60-min ITI. This increased task difficulty allowed detection of more subtle impairments to object recognition memory, if present.

Social interaction (PNDs 73–74). The social interaction test was performed as previously described (Ramos et al., 2013). Briefly, rats were individually habituated for 20 min in a black plastic arena (780 × 520 × 470 mm) on PND 73. The following day, they were returned to the arena with a novel conspecific from the same drug-treatment group, and allowed to explore and interact freely. Anogenital sniffing (sniffing the anogenital region of the conspecific), general investigation (sniffing of non-anogenital regions of the conspecific), pinning (one rat lying on with its dorso-lateral surface to the floor with the other rat above it), and rearing (standing on hind legs, including leaning on the arena walls) was recorded via a camera mounted above the arena. These behaviours were selected because they are general behaviours that are frequently expressed by healthy animals, and are widely used in existing literature with similar social interaction tests including assessments of cannabinoid modulation of social behaviour (File and Seth, 2003; Trezza and Vanderschuren, 2008). Total interaction was calculated as the sum of anogenital sniffing, general investigation, and pinning. These behaviours were scored by an experimenter blinded to the experimental conditions.

Locomotor activity (PND 77). As described above, without any drug treatment.

Emergence (PND 78). As described above, without any drug treatment.

Post-mortem plasma and cerebellum analyses

Sample collection (PND 103). Individual rats from each treatment condition were taken to a separate room in a dark holding

box and killed by rapid decapitation without anaesthesia on PND 103. The rats were extensively habituated to the handling procedure up on the 3 days before decapitation to minimise any stress or novelty effects on steroid levels. Immediately following decapitation trunk blood was collected in a chilled EDTA-coated collection tube and immediately centrifuged at 4°C at 4000 *g* for 10 min. Plasma was collected in 1 mL aliquots while cerebellum was dissected with a razor blade and flash frozen with liquid nitrogen, prior to storage at −80°C until analysis.

Steroids. Plasma corticosterone, testosterone, and progesterone were analysed via liquid chromatography-tandem mass spectrometry (LC-MS/MS) as previously described (Bowen et al., 2014). Corticosterone was the primary analyte of interest, with testosterone and progesterone included because the method allows for simultaneous quantitation of these analytes. Briefly, steroids were extracted from 250 µL plasma (analysed in duplicate) into 1 mL methyl *tert*-butyl ether and dried under a gentle stream of nitrogen. Steroid residue was then reconstituted in initial mobile phase (0.1% formic acid in 10% methanol and 90% water) and analysed via LC-MS/MS.

Ethanolamides. Cerebellar and plasma ethanolamides were assessed as a measure of endocannabinoid tone, and also in light of reports of impaired movement sequences in humans following SC use (Di Marzo et al., 2000; Musshoff et al., 2014; Rubino et al., 2015). Ethanolamides (anandamide, AEA; palmitoylethanolamide, PEA; 2-arachidonoylglycerol, 2-AG; oleoylethanolamide, OEA; and linoleoyl ethanolamide, LEA) in cerebellum were extracted as follows, based on a previous method (Stuart et al., 2013). The right cerebellum was dissected from whole cerebellum and weighed, then 6 mL of MeOH and 10 µL of internal standard 1 µm deuterium labelled anandamide (d4-AEA) was added. Left cerebellum was preserved for possible future assays. Tissue was homogenised and centrifuged at 19,000 *g* for 20 min at 4°C. The resultant supernatant was decanted and 24 mL milli-Q water was added, forming a 20% organic final supernatant. Analytes were extracted from the supernatant using solid phase extraction (SPE) with 500 mg C18 columns preconditioned with 5 mL MeOH followed by 2.5 mL milli-Q water. Supernatant solution was loaded onto each column, washed with 2.5 mL milli-Q water, then 2 mL 40% MeOH, and analytes were washed with a final 1.5 mL 85% MeOH and eluted with 100% MeOH.

Plasma ethanolamides were also analysed. Briefly, 8 mL of 1:1 ice cold ACN/MeOH was added to 250 µL of plasma, 20 µL of d4-AEA was added, and samples were left covered in the dark for 2 h at 4°C. Following centrifugation, the supernatant was treated as described above for the cerebellar extraction, with washes of 2.5 mL milli-Q water, 2 mL 50% MeOH and 1.5 mL of 60% MeOH before the analytes were eluted from the SPE column with 100% MeOH. The SPE eluates for all samples were analysed via LC-MS/MS.

Cytokines. Plasma cytokine levels (granulocyte macrophage colony-stimulating factor, GM-CSF; interferon gamma, IFNγ; interleukins (IL)-1α, IL-1β, IL-2, IL-4, IL-6, IL-12, and tumour necrosis factor alpha, TNF-α) were measured using a commercially available multiplex bead immunoassay kit (Rat Cytokine 10-Plex Panel kit, Invitrogen, Camarillo, CA). The assay was performed according to the manufacturer's instructions, with minor modifications. In brief, all reagent and sample volumes were scaled down to 20% of recommended values, and washes were performed by centrifugation in a 96-well v-bottomed plate. The assay was read on an LSR Fortessa-X20 flow cytometer (Becton Dickinson, Sydney, NSW, Australia) and data were analysed using FlowJo software v9.8.5 (FlowJo, Ashland, OR).

Data analysis

Data were analysed using SPSS version 20 (IBM, Chicago, IL) with significance set at 0.05. Place conditioning was analysed using mixed-model ANOVA, with treatment group (vehicle-, THC-, AB-PINACA-, or AB-FUBINACA-treatment) as the between-subjects factor and dosing phase (baseline, low-dose test, and high-dose test) as the within-subjects factor. For the emergence test, latency to emerge data were not normally distributed as several rats remained inside the hidebox for the entire test duration. Similarly, vocalisation data were not normally distributed as it was a binary measure. In these cases, non-parametric Kruskal–Wallis H tests with Bonferroni-corrected Mann–Whitney tests were used in place of one-way ANOVAs. In all other cases, treatment groups were compared using a one-way ANOVA. In cases where the ANOVA reached statistical significance, the treatment groups were compared pairwise using Tukey's HSD tests.

Results

'On-drug' measures

Locomotor activity. There was a significant overall effect of low-dose drug treatment on locomotor activity ($F_{(3,59)} = 3.65$, $p < 0.05$). Tukey's HSD tests found that the distance travelled was reduced by AB-PINACA and AB-FUBINACA compared with vehicle (all $p < 0.05$), but not by THC ($p > 0.05$) although it produced a strong tendency towards reduced activity (Table 1). No other comparisons were significant (all $p > 0.05$).

Similarly, there was a significant overall effect of high-dose drug treatment on locomotor activity ($F_{(3,59)} = 12.16$, $p < 0.001$). Post-hoc tests found that all drugs reduced distance travelled compared with vehicle (all $p < 0.001$; Table 1), and no other pairwise comparisons reached significance (all $p > 0.05$).

Emergence. There was no overall significant effect of low-dose treatment on the latency to emerge ($\chi^2(3) = 6.05$, $p > 0.05$). High doses produced a significant overall effect ($\chi^2(3) = 30.47$, $p < 0.001$), with all drugs increasing latency relative to vehicle treatment (all $p < 0.05$).

There was a significant overall effect of treatment on time spent in the open field for high ($F_{(3,59)} = 5.16$, $p < 0.01$) but not low doses ($F_{(3,59)} = 0.97$, $p > 0.05$). Tukey's HSD tests showed that THC and AB-PINACA significantly reduced open field time at a high dose compared with vehicle (all $p < 0.05$).

Risk assessment was also significantly affected by low doses ($F_{(3,59)} = 10.76$, $p < 0.001$), such that all drug treatments significantly decreased risk assessment behaviour compared with vehicle (all $p < 0.05$) at a low dose. The same was true for high doses ($F_{(3,59)} = 24.26$, $p < 0.001$; all pairwise comparisons with vehicle $p < 0.001$). No other pairwise comparisons reached statistical significance.

Table 1. Locomotor and emergence results for all experimental phases.

	VEH	THC	AB-PINACA	AB-FUBINACA
Low-dose effects				
Locomotor (m)	27.5 (1.2)	20.2 (2.4)	19.5 (2.1)*	20.0 (1.9)*
LTE (s)	140.9 (35.5)	217.1 (32.2)	191.4 (36.3)	264.1 (24.5)*
Risk assessment (s)	52.2 (5.6)	30.9 (3.8)*	22.3 (6.2)***	15.7 (2.9)***
Open time (s)	48.8 (16.4)	30.4 (15.4)	34.8 (19.8)	11.0 (9.8)
High-dose effects				
Locomotor (m)	34.4 (1.5)	17.8 (3.2)***	19.5 (2.6)***	14.1 (2.4)***
LTE (s)	189.8 (23.4)	300.0 (0.0)***	287.5 (12.5)***	265.1 (23.7)*
Risk assessment (s)	62.2 (8.3)	4.4 (1.1)***	14.0 (7.0)***	6.4 (2.1)***
Open time (s)	57.5 (16.4)	0.0 (0.0)**	1.8 (1.8)**	22.9 (16.8)
Residual effects				
Locomotor (m)	44.4 (2.7)	39.9 (2.2)	41.2 (1.6)	41.1 (1.7)
LTE (s)	75.8 (24.5)	69.6 (18.7)	46.1 (11.6)	74.5 (20.7)
Risk assessment (s)	32.0 (4.5)	38.7 (6.7)	36.3 (4.6)	36.3 (5.0)
Open time (s)	160.7 (18.7)	161.1 (16.7)	165.6 (11.4)	158.3 (16.9)

Data represent means (SEM). LTE: Latency to emerge. *$p < .05$, **$p < .01$, ***$p < .001$ compared with vehicle. Locomotor data are given in metres (m); LTE, risk assessment, and open time are given in seconds (s).

Place conditioning. The results of the place conditioning test are presented in Figure 2. Overall, there was no main effect of drug treatment on preference scores (time in drug-conditioned side – time in vehicle-conditioned side; $F_{(3,59)} = 0.61$, $p > 0.05$) or dosing phase ($F_{(2,118)} = 1.51$, $p > 0.05$), nor was there a significant interaction effect ($F_{(6,118)} = 1.04$, $p > 0.05$). Although there was a strong trend towards a preference for the drug-conditioned side following low-dose AB-FUBINACA treatment compared with vehicle, this failed to reach statistical significance ($p = 0.06$). There was no significant baseline preference for striped compartments over blank ($t_{(62)} = 1.52$, $p > 0.05$), nor vanilla scented over vinegar scented ($t_{(62)} = 0.53$, $p > 0.05$).

Vocalisations on 'no drug' vehicle injection days of place preference testing did not differ between treatment groups ($\chi^2(3) = 2.82$, $p > 0.05$). There were overall treatment effects on vocalisations for low ($\chi^2(3) = 11.01$, $p < 0.01$) and high-dose phases ($\chi^2(3) = 13.02$, $p < 0.0001$). Post-hoc tests showed that significantly more rats vocalised following AB-FUBINACA low-dose treatment compared with vehicle ($p < 0.01$), as was the case for high-dose THC ($p < 0.001$), AB-PINACA ($p < 0.05$) and AB-FUBINACA ($p < 0.05$) compared with vehicle. No other pairwise comparisons reached statistical significance.

Residual measures

Novel object recognition. When tested with a 2-min ITI, there was an overall effect of drug pre-treatment ($F_{(3,59)} = 3.04$, $p < 0.05$), and AB-FUBINACA pre-treated rats spent a smaller percentage of time investigating the novel object compared with vehicle ($p < 0.05$). With a 60-min ITI there was a significant overall effect ($F_{(3,59)} = 9.43$, $p < 0.001$) and the percentage of time spent investigating the novel object was reduced by all three cannabinoid pre-treatments compared with vehicle (all $p < 0.01$; Figure 3). No other comparisons reached statistical significance (all $p > 0.05$).

Social interaction. For the social interaction test, there were significant overall effects of drug pre-treatment on rearing ($F_{(3,59)} = 3.03$, $p < 0.05$), general investigation ($F_{(3,59)} = 5.77$, $p < 0.05$), total interaction ($F_{(3,59)} = 3.50$, $p < 0.05$) but not for anogential sniffing ($F_{(3,59)} = 0.40$, $p > 0.05$) or pinning ($F_{(3,59)} = 2.52$, $p > 0.05$; Table 2). THC pre-treated rats showed less total social interaction with novel conspecifics compared with vehicle pre-treated rats ($p < 0.05$) and less general investigation than AB-FUBINACA pre-treated rats ($p < 0.05$). No other pairwise comparisons were statistically significant (all $p > 0.05$).

Locomotion. There were no significant residual effects on locomotor activity as a function of drug pre-treatment ($F_{(3,59)} = 0.82$, $p > 0.05$; Table 1).

Emergence. There were no significant differences in latency to emerge ($\chi^2(3) = 1.14$, $p > 0.05$), time spent in the open field ($F_{(3,59)} = 0.04$, $p > 0.05$), or risk assessment ($F_{(3,59)} = 0.85$, $p > 0.05$).

Body weight. Body weight data are summarised in Table 3. There were no significant differences between treatment conditions in weight at the beginning (PND 31) of the study ($F_{(3,59)} = 0.35$, $p > 0.05$). Over the dosing phase (PNDs 31–55), there was a significant overall treatment effect ($F_{(3,59)} = 8.97$, $p < 0.001$), and all cannabinoid treatment groups gained significantly less weight than vehicle-treated rats (all $p < 0.01$). No other pairwise comparisons reached significance (all $p > 0.05$). Over the residual testing phase (PNDs 56–103), there were no significant differences in weight gain ($F_{(3,59)} = 1.52$, $p > 0.05$), and at the end of residual testing (PND 103), there was no significant difference in weight ($F_{(3,59)} = 1.42$, $p > 0.05$).

Steroids. There were no significant effects of drug pre-treatment on plasma corticosterone ($F_{(3,44)} = 0.22$, $p > 0.05$), testosterone ($F_{(3,44)} = 0.20$, $p > 0.05$), or progesterone ($F_{(3,44)} = 0.02$, $p > 0.05$) levels (Table 4).

Cytokines. Levels of IL-1β, IL-4, GM-CSF, TFNα, and IFNg in all samples across all drug-treatment conditions fell below limits

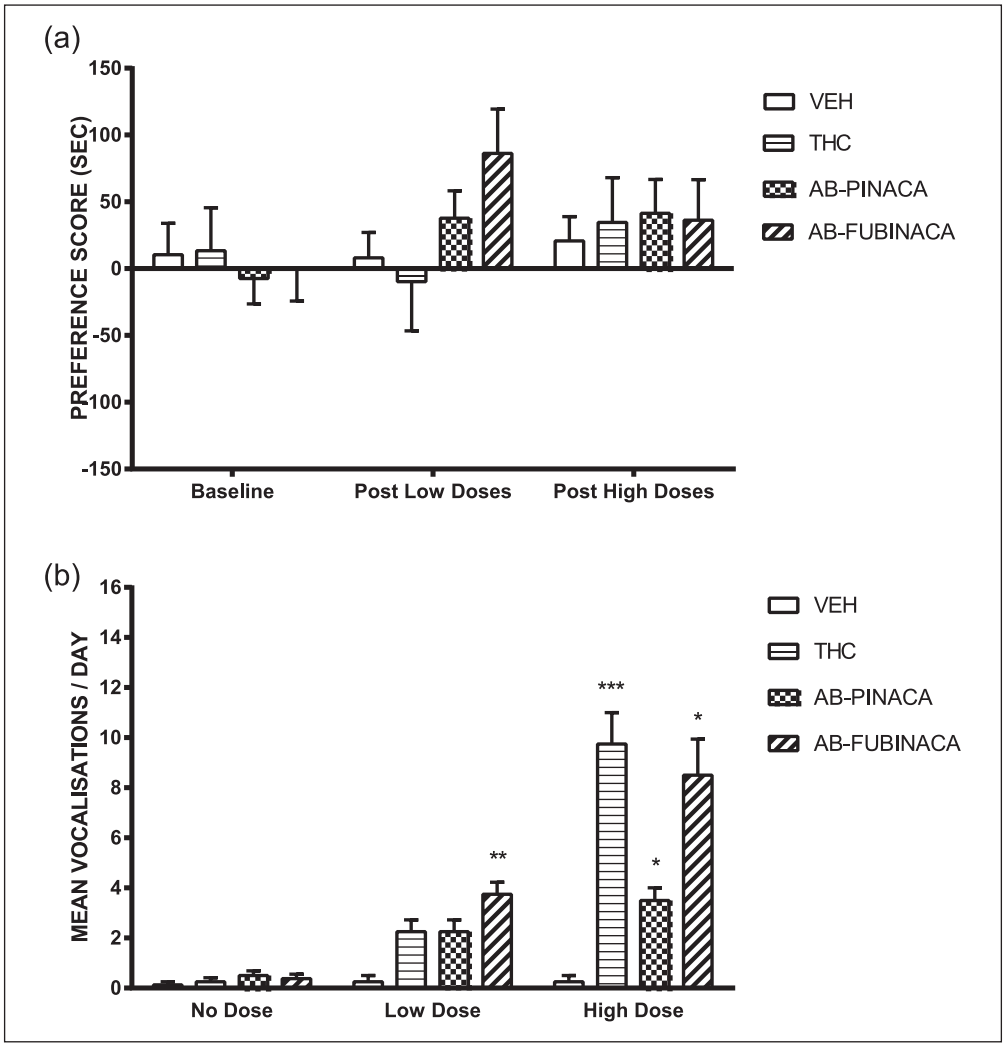

Figure 2. (a) Place conditioning following six low then six high doses of THC, AB-PINACA, and AB-FUBINACA. (b) Mean number of rats vocalising during placement in the CPP chambers during each training day. Vocalisations were significantly elevated following low doses of AB-FUBINACA and high doses of THC, AB-PINACA, and AB-FUBINACA compared with vehicle injections. Data are means ± SEM, $*p < 0.05$, $**p < 0.01$, $***p < 0.001$ compared with vehicle at the same dose level.

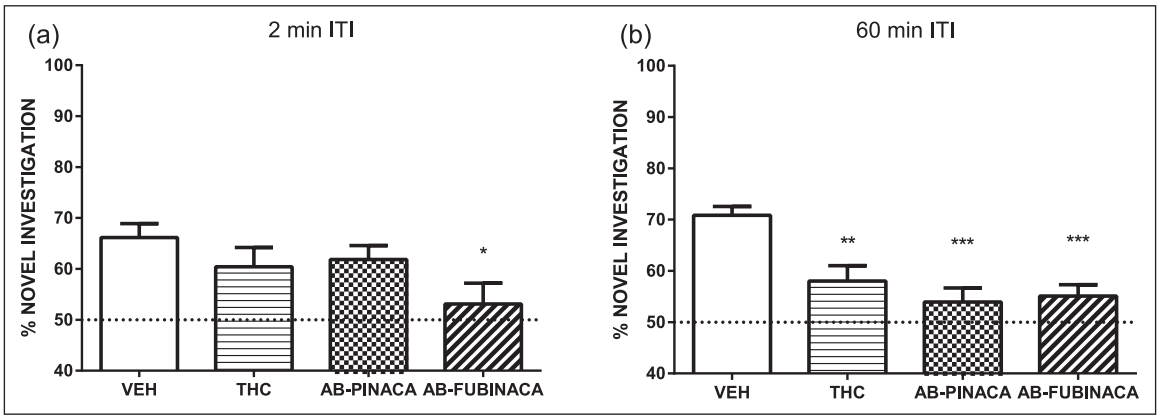

Figure 3. Mean ± SEM data for the novel object recognition test, 2 weeks post drug administration, with (a) a 2-min inter-trial interval (ITI) or (b) a 60-min ITI. AB-FUBINACA pre-treated rats spent significantly less time investigating the novel object compared with vehicle for the 2-min ITI test, and all cannabinoid treatments reduced novel investigation with a 60-min ITI. $*p < 0.05$, $**p < 0.01$, $***p < 0.001$ compared with vehicle.

Table 2. Behaviour in the social interaction test 19 days post drug administration.

Behaviour	Vehicle	THC	AB-PINACA	AB-FUBINACA
Exploratory behaviour				
Rearing	133.0 (10.4)	130.3 (10.0)	105.8 (7.9)	103.6 (7.2)
Social behaviour				
Anogenital sniffing	25.2 (5.2)	20.8 (2.3)	26.5 (3.9)	23.1 (4.3)
General investigation	37.6 (3.1)	27.1 (1.7)	38.1 (4.3)	46.6 (3.8)
Pinning	19.8 (4.2)	3.8 (1.6)	22.5 (9.0)	9.8 (4.1)
Total social interaction	82.6 (9.3)	51.8 (3.3)*†	87.0 (12.4)	79.5 (6.9)

Data are means (SEM) in seconds; *$p < 0.05$ compared with vehicle, †$p < 0.05$ compared with AB-FUBINACA.

Table 3. Effects of chronic administration of THC, AB-PINACA, and AB-FUBINACA on rat body weight.

	VEH	THC	AB-PINACA	AB-FUBINACA
Initial weight (g; PND 31)	148.8 (3.8)	147.4 (2.8)	149.3 (2.8)	145.6 (1.6)
Dosing phase weight gain (g; PNDs 31–55)[a]	186.1 (4.9)	155.2 (3.8)***	164.5 (5.3)**	162.9 (3.1)**
Residual phase weight gain (g; PNDs 56–103)[a]	122.7 (3.7)	131.0 (4.4)	118.8 (7.3)	133.4 (6.3)
Final weight (g; PND 103)	457.2 (8.9)	433.6 (8.5)	432.7 (11.4)	441.9 (8.6)

Data represent means (SEM). [a]Weight gain during the dosing phase was calculated by subtracting weights on PND 31 from PND 55, and weight gain during the residual phase was calculated by subtracting weights on PND 56 from PND 103. **$p < 0.01$, ***$p < 0.001$ compared with vehicle.

of detection (Table 4). There was no overall group difference in levels of IL-2 ($F_{(3,44)} = 1.62$, $p > 0.05$), IL-6 ($F_{(3,44)} = 0.40$, $p > 0.05$), or IL-10 ($F_{(3,44)} = 0.97$, $p > 0.05$). However, there were overall treatment effects for IL-1α ($F_{(3,44)} = 3.32$, $p < 0.05$) and IL-12 ($F_{(3,44)} = 4.91$, $p < 0.01$), with AB-FUBINACA treated rats showing significantly lower plasma levels of IL-1α compared with vehicle ($p < 0.05$) and IL-12 compared with both vehicle and AB-PINACA ($p < 0.05$).

Ethanolamides. There were significant overall effects of drug pre-treatment on most cerebellar ethanolamides: AEA, $F_{(3,44)} = 16.96$, $p < 0.0001$; PEA, $F_{(3,44)} = 9.91$, $p < 0.0001$; 2-AG, $F_{(3,44)} = 2.85$, $p < 0.05$; OEA, $F_{(3,44)} = 10.69$, $p < 0.0001$, but not LEA $F_{(3,44)} = 2.57$, $p > 0.05$.

Tukey's HSD tests showed that THC pre-treatment reduced AEA, PEA, 2-AG, and OEA when compared with vehicle (all $p < 0.05$), and reduced AEA, PEA, and OEA compared with AB-FUBINACA (all $p < 0.05$; Table 4). AEA, PEA, and OEA were reduced by AB-PINACA pre-treatment compared with vehicle (all $p < 0.05$) and AB-FUBINACA (all $p < 0.05$). No other comparisons were significant (all $p > 0.05$).

There were no significant differences in plasma ethanolamide levels as a function of treatment group (AEA, $F_{(3,44)} = 0.64$, $p < 0.05$; PEA, $F_{(3,44)} = 1.16$, $p < 0.05$; 2-AG, $F_{(3,44)} = 1.46$, $p < 0.05$; OEA, $F_{(3,44)} = 0.55$, $p < 0.05$; LEA, $F_{(3,44)} = 1.21$, $p < 0.05$).

Discussion

The present study examined various acute and long-lasting impacts of AB-PINACA and AB-FUBINACA relative to the prototypical cannabinoid THC in adolescent rats. During dosing, all three cannabinoids produced locomotor suppression, anxiogenic effects in the emergence test and inhibition of body weight gain. Following drug administration, a residual impairment of object recognition memory was detected with all three drug pre-treatments at a timepoint of 2 weeks. Six weeks post drug, a reduction in some cytokines was observed in the plasma of AB-FUBINACA pre-treated rats and a reduction in cerebellar ethanolamides in THC and AB-PINACA pre-treated rats. To our knowledge, this is the first investigation of long-term behavioural and biochemical effects of emerging SCs. Somewhat contrary to our expectations, THC administration produced similar acute effects, and only subtle differences in long-term effects, relative to the two SC compounds. Indeed, THC produced residual reductions in social interaction, an effect not seen with either SC.

Acute behavioural effects of chronic AB-PINACA and AB-FUBINACA

The acute responses to AB-PINACA and AB-FUBINACA were typical of those observed with other cannabinoid agonists such as THC, CP 55,940, and JWH-018. This included locomotor hypoactivity, inhibition of weight gain, and increased anxiety-like behaviours (Arevalo et al., 2001; O'Shea et al., 2004; Quinn et al., 2008). AB-PINACA, AB-FUBINACA and THC caused dose-dependent reductions in locomotor activity, consistent with previous reports of locomotor suppression in rodents administered indazole SC compounds including AB-PINACA (Wiley et al., 2015), and earlier SCs such as JWH-018 (Macri et al., 2013). There have also been observations of impairment of movement sequences and disruption of fine motor skills following human recreational use of SCs (Musshoff et al., 2014). Weight gain was inhibited by all three cannabinoid compounds in the present study, consistent with earlier reports involving

Table 4. Plasma steroid, cytokine, and ethanolamides with cerebellar ethanolamides 6 weeks post drug administration.

	VEH	THC	AB-PINACA	AB-FUBINACA
Plasma				
Steroids (ng/mL)				
Corticosterone	117.9 (13.6)	131.9 (16.2)	118.4 (13.5)	123.7 (11.7)
Testosterone	2.4 (0.3)	2.1 (0.4)	2.1 (0.3)	2.0 (0.3)
Progesterone	1.2 (0.2)	1.2 (0.1)	1.2 (0.1)	1.2 (0.2)
Cytokines (pg/mL)				
IL-1α	71.7 (13.0)	51.2 (7.5)	57.8 (7.3)	30.4 (8.9)*
IL-1β	–	–	–	–
IL-2	66.7 (7.1)	75.7 (9.6)	72.0 (5.8)	54.3 (6.4)
IL-4	–	–	–	–
IL-6	5.6 (0.7)	4.9 (0.4)	4.9 (0.4)	5.5 (0.8)
IL-10	21.2 (0.8)	21.8 (1.0)	20.5 (0.5)	20.3 (0.3)
IL-12	496.2 (58.8)	473.2 (41.2)	546.2 (38.9)	303.5 (48.8)*‡
IFNγ	–	–	–	–
GM-CSF	–	–	–	–
TNFα	–	–	–	–
Ethanolamides (ng/mL)				
AEA	0.33 (0.03)	0.39 (0.03)	0.34 (0.04)	0.36 (0.04)
PEA	13.4 (0.8)	13.2 (0.9)	14.0 (0.6)	15.1 (1.0)
2-AG	21.8 (4.4)	15.6 (4.7)	13.7 (2.6)	23.5 (3.6)
OEA	7.7 (0.8)	7.7 (0.5)	7.2 (0.5)	8.3 (0.7)
LEA	1.2 (0.1)	1.5 (0.1)	1.3 (0.1)	1.3 (0.1)
Cerebellum				
Ethanolamides (ng/g)				
AEA	46.6 (2.5)	32.8 (0.6)****††††	34.7 (1.1)****†††	45.0 (2.0)
PEA	330.3 (20.2)	238.9 (12.0)***††	258.1 (12.3)**†	320.1 (10.8)
2-AG	3316.7 (196.0)	2642.4 (156.3)*	2961.5 (163.9)	3144.0 (164.1)
OEA	351.1 (21.5)	246.3 (12.0)***†††	280.1 (13.2)*†	344.0 (13.4)
LEA	26.1 (1.3)	22.8 (0.7)	23.2 (0.6)	24.3 (0.8)

Data are means (SEM).
*$p < 0.05$, **$p < 0.01$, ***$p < 0.001$, ****$p < 0.0001$ compared with vehicle; ‡$p < 0.05$ compared with AB-PINACA; †$p < 0.05$, ††$p < 0.01$, †††$p < 0.001$, ††††$p < 0.0001$ compared with AB-FUBINACA; – all samples < limit of detection.
2-AG: 2-arachidonoylglycerol; AEA: anandamide; GM-CSF: granulocyte macrophage colony-stimulating factor; IFNγ: interferon gamma; IL: interleukin; LEA: linoleoyl ethanolamide; OEA: oleoylethanolamide; PEA: palmitoylethanolamide; TNFα: tumour necrosis factor alpha.

chronic administration of THC or CBD/ THC to adolescent rats (Klein et al., 2011), or chronic administration of HU-210 in adults rats (Dalton et al., 2009).

All three cannabinoids increased anxiety-like behaviours in the emergence test, similar to the effects of CP 55,940 (Arevalo et al., 2001; Marco et al., 2004) and THC Quinn et al. (2008). There were also large increases in audible vocalisations following drug administration, a measure previously used to index cannabinoid aversion (Giuliani et al., 2000; Henriksson and Jarbe, 1971). We previously showed that rat vocalisations during handling increases following administration of 5 mg/kg THC (Quinn et al., 2008), an effect replicated here. The acute anxiogenic and aversive effects of these compounds may be consistent with the anxiogenic effects of cannabinoids reported in some human case studies (Schwartz et al., 2015).

Despite these apparent increases in anxiety-like behaviours and vocalisations, neither SC nor THC produced conditioned place aversion. Quinn et al. (2008) found that only adult rats showed conditioned place aversion to THC, as has been described with other drugs such as nicotine (Wilmouth and Spear, 2004). These THC-treated adolescent rats also showed anxiety-like behaviours in the emergence test. Therefore adolescent rats may be less prone to acquiring conditioned aversion from cannabinoids even when they produce anxiety-like effects, and this could conceivably increase the abuse potential of SCs in adolescent populations. Adolescents appear to be more vulnerable to cannabinoid-induced memory impairments as compared with adults (Higuera-Matas et al., 2015; Quinn et al., 2008; Viveros and Marco, 2015), which may consequently impair the acquisition of place conditioning.

The development of preference and aversion to cannabinoids in the conditioned place preference paradigm depends to a large extent on dose (Tanda, 2016). Place preference data regarding recent SCs are limited, but JWH-073, JWH-81, and JWH-210 produce a place preference at low doses (0.5 mg/kg for JWH-073, and 0.1 mg/kg for JWH-81 and JWH-210) that is not present at 1 mg/kg (Cha et al., 2014). It is possible that our low doses were a little too high to demonstrate a place preference, although 0.2 mg/kg AB-FUBINACA pre-treatment trended towards producing such an effect. Future studies exploring a range of low doses may prove instructive in this regard.

Residual effects of chronic AB-PINACA and AB-FUBINACA administration

Residual recognition memory impairment was observed with all three cannabinoid pre-treatments 2 weeks following cessation of drug administration. Moreover, AB-FUBINACA pre-treated rats showed impaired NOR performance even with a short 2-min ITI, suggesting a more substantial impairment with this compound. Since SC compounds appear to be quickly metabolised (Paul and Bosy, 2015; Wohlfarth et al., 2015) and biotelemetry data demonstrates a return to baseline body temperature and heart rate approximately 3 and 5 h after drug administration for AB-PINACA and AB-FUBINACA, respectively (Banister et al., 2015a), it is unlikely that these residual effects are due to SCs persisting in the body. Residual impairment has been reported in previous studies of THC and CP 55,940 (O'Shea et al., 2004, 2006; Quinn et al., 2008). The underlying mechanism is unclear, but reduced NOR performance accompanies hippocampal (Barker and Warburton, 2011), and perirhinal cortex insult (Bussey et al., 1999; Norman and Eacott, 2004).

AB-PINACA and AB-FUBINACA had no residual effects on social interaction. In contrast, THC produced a lasting residual impairment, consistent with previous findings with chronic THC and CP 55,940 (O'Shea et al., 2004; Quinn et al., 2008). The absence of lasting social impairment with AB-PINACA and AB-FUBINACA treatment in the presence of a clear impairment with THC was unexpected, and suggests that mechanisms other than those arising from simple CB_1 activation may be involved. There is increasing evidence of an interaction between cannabinoids and oxytocin in social reward, which could play a role in the effects seen here. It is notable that chronic daily administration of 1.5 mg/kg THC to rats down-regulates expression of the prosocial neuropeptide oxytocin in nucleus accumbens and ventral tegmental areas (Butovsky et al., 2006). Further, social interaction or pharmacological activation of the oxytocin receptor (OTR) stimulates AEA mobilisation in the nucleus accumbens, which enhances social reward, while blockade of the OTR prevents this effect (Wei et al., 2015). Consequentially, a comparison of endocannabinoid or oxytocin levels in the nucleus accumbens following SC pre-treatment to THC pre-treatment may prove fruitful.

It was predicted that cytokines involved in pro-inflammatory processes (IL-1α, IL-1β, IL-2, IL-12, IFNγ, GM-CSF, TNFα; see Kopf et al. (2010) for review) might be decreased by SC pre-treatment, perhaps due to an influence on CB_2 receptors. This prediction was partially confirmed by reductions observed in plasma concentrations of cytokines IL-1α and IL-12 with AB-FUBINACA pre-treatment. CB_2 receptors are commonly expressed on immune cells and play a major role in inflammation (Galiegue et al., 1995; McPartland et al., 2015) and repeated stimulation with CB_2 agonists tends to reduce inflammation and related neuropathic pain (Guindon and Hohmann, 2008). Cytokines associated with anti-inflammatory processes (IL-4, IL-6, IL-10) were unaffected, although we note that the concentrations of most cytokines were low, or below limits of detection, as might be expected in healthy animals assessed a long time after drug administration (Cannon, 2000). Together with the lack of any long-term increase in corticosterone, these data indicate that the long-term impact of these SCs on immune or stress responses may be relatively minor, reflecting human case reports detailing acute injury followed by good recovery (Hermanns-Clausen et al., 2012; Schwartz et al., 2015). An analysis of plasma during acute dosing with SCs would be informative, particularly if combined with CB_2 inverse agonist SR144528 to isolate CB_2-mediated effects.

A lasting reduction of cerebellar ethanolamides following THC and AB-PINACA pre-treatment indicates some residual reduction in central endocannabinoid tone that is of potential concern. A similar reduction in AEA in the prefrontal cortex of female rats occurs following chronic THC administration in adolescence (Rubino et al., 2015), in the striatum of adult male THC-tolerant rats (Di Marzo et al., 2000), and in human cerebrospinal fluid following frequent cannabis use by schizophrenic patients (Leweke et al., 2007). The functional importance of such decreases are unclear but could potentially link to reported disruptions in fine motor skills reported in humans following SC use (Musshoff et al., 2014). Although the long-term effects of chronic cannabinoid treatment on the endocananbinoid system remain controversial (Higuera-Matas et al., 2015), a number of studies demonstrate a downregulation of CB_1 receptor expression in rodents (Breivogel et al., 2003; Sim-Selley et al., 2006) following chronic cannabinoid administration. The decreases in ethanolamides in the present and previous studies could be a consequence of a similar homeostatic compensation in endocannabinoid signalling that persists in the long term.

It was surprising that AB-FUBINACA pre-treatment failed to decrease cerebellar endocannabinoids given the otherwise strong effects produced by this compound. Similarly, it is unclear why AB-FUBINACA alone reduced plasma cytokine levels. At this time, the mechanisms underlying these idiosyncrasies are unknown, particularly while possible non-cannabinoid receptor targets of these compounds remain uncharacterised. AB-PINACA and AB-FUBINACA are known to differ markedly in metabolism despite their structural similarities. In human liver microsomes, hydroxylation occurs primarily at the 1-pentyl moiety for AB-PINACA, and at the *N*-(1-amino-alkyl-1-oxobutan) moiety for AB-FUBINACA (Takayama et al., 2014). Several metabolites of JWH-018, AM-2201, and JWH-073 retain cannabinoid receptor activity (Rajasekaran et al., 2013; Seely et al., 2012a). The cannabinoid receptor activity of AB-PINACA and AB-FUBINACA metabolites is presently uncharacterised, but it may be that some of these metabolites retain cannabinoid receptor activity. The potency of these metabolites could differ markedly given the difference in hydroxylation location. Ongoing studies in our laboratory are aimed at addressing this hypothesis.

Effects of AB-PINACA and AB-FUBINACA compared with THC

SC case reports generally describe adverse outcomes and toxicity that are more severe compared with cannabis use, yet in this study AB-PINACA and AB-FUBINACA produced effects very similar to THC on most measures. Overall differences between THC and the two SCs were only evident on two residual measures: social interaction (where THC alone produced an adverse

residual effect on social interaction), and in cerebellar ethanolamide levels (where THC and AB-PINACA reduced cerebellar AEA, PEA, and OEA but AB-FUBINACA did not). Moreover, we observed no obvious illness in any drug-treated rat at any point during the study.

This general failure to separate SCs from THC, despite numerous case reports of greater adverse effects of SCs, might reflect the fact that these case reports arise from persons seeking hospital treatment and consequentially reflect the most extreme cases (Khan et al., 2016; Trecki et al., 2015). Alternatively, there could be interspecies differences in SC pharmacokinetics, pharmacodynamics and toxicity. The co-use/abuse of other drugs with SCs is common; in particular tobacco, energy drinks, and alcohol could be relevant (Winstock and Barratt, 2013).

It is also possible that severe adverse reactions to SCs may be modulated by dose factors, with the high potency of SC compounds increasing the risk of accidental overdose and toxicity compared with cannabis. SC products have no established manufacturing standards, and dose may vary between batches or be unevenly distributed within the product (Musah et al., 2012). This makes it difficult for users to determine a safe dose, even if they have used that product previously. Moreover, contamination of SC products with other compounds including caffeine, nicotine, and eugenol has been reported (Dresen et al., 2010). Such contamination could account for some toxicity, particularly in the cases where toxicity is clustered around a specific batch of products (Monte et al., 2014; Schwartz et al., 2015). Finally, because many SCs are full cannabinoid receptor agonists, an overdose could produce more severe and qualitatively different effects to a similarly large dose of a partial agonist such as THC (Spaderna et al., 2013). With these factors in mind, it is perhaps not surprising that SC toxicity occurs in some but not all users, and often in clusters (Bhanushali et al., 2012).

Conclusion

In summary, the present study identifies both short-term and lasting residual behavioural impairments arising from chronic administration of AB-PINACA and AB-FUBINACA. Acute responses to both SCs resembled those observed with THC, but there were some subtle differences in the long term. AB-FUBINACA reduced some cytokine levels and produced more marked recognition memory impairments, THC alone produced lasting social impairment, while cerebellar endocannabinoids were reduced by THC and AB-PINACA, but not AB-FUBINACA. These results highlight that while acute responses to different cannabinoid agonists may be similar, the long-term behavioural or biochemical impacts effects may differ. This emphasises the need for ongoing assessment of long-term effects of emerging SCs, particularly in vulnerable adolescent populations where negative effects may be amplified.

Declaration of conflicting interest

The author(s) declared no potential conflicts of interest with respect to the research, authorship, and/or publication of this article.

Funding

The author(s) disclosed receipt of the following financial support for the research, authorship, and/or publication of this article: RCK is supported by an Australian Postgraduate Award. This research was supported by research grant funding to MK and ISM from the National Health and Medical Research Council (NHMRC).

References

Arevalo C, de Miguel R and Hernandez-Tristan R (2001) Cannabinoid effects on anxiety-related behaviours and hypothalamic neurotransmitters. *Pharmacol Biochem Behav* 70: 123–131.

Banister SD, Moir M, Stuart J, et al. (2015a) The pharmacology of indole and indazole synthetic cannabinoid designer drugs AB-FUBINACA, ADB-FUBINACA, AB-PINACA, ADB-PINACA, 5F-AB-PINACA, 5F-ADB-PINACA, ADBICA and 5F-ADBICA. *ACS Chem Neurosci* 6: 1546–1559.

Banister SD, Stuart J, Kevin RC, et al. (2015b) The effects of bioisosteric fluorine in synthetic cannabinoid designer drugs JWH-018, AM-2201, UR-144, XLR-11, PB-22, 5F-PB-22, APICA, and STS-135. *ACS Chem Neurosci* 6: 1445–1458.

Banister SD, Wilkinson SM, Longworth M, et al. (2013) The synthesis and pharmacological evaluation of adamantane-derived indoles: Cannabimimetic drugs of abuse. *ACS Chem Neurosci* 4: 1081–1092.

Barker GRI and Warburton EC (2011) When is the hippocampus involved in recognition memory? *J Neurosci* 31: 10721–10731.

Barratt MJ, Cakic V and Lenton S (2012) Patterns of synthetic cannabinoid use in Australia. *Drug Alcohol Rev* 32: 141–146.

Bhanushali GK, Jain G, Fatima H, et al. (2012) AKI associated with synthetic cannabinoids: A case series. *Clin J Am Soc Nephrol* 8: 523–526.

Bowen MT, Dass SA, Booth J, et al. (2014) Active coping toward predatory stress is associated with lower corticosterone and progesterone plasma levels and decreased methylation in the medial amygdala vasopressin system. *Horm Behav* 66: 561–566.

Breivogel CS, Scates SM, Beletskaya IO, et al. (2003) The effects of delta9-tetrahydrocannabinol physical dependence on brain cannabinoid receptors. *Eur J Pharmacol* 459: 139–150.

Brents LK, Gallus-Zawada A, Radominska-Pandya A, et al. (2012) Monohydroxylated metabolites of the K2 synthetic cannabinoid JWH-073 retain intermediate to high cannabinoid 1 receptor (CB1R) affinity and exhibit neutral antagonist to partial agonist activity. *Biochem Pharmacol* 83: 952–961.

Brents LK and Prather PL (2014) The K2/Spice Phenomenon: Emergence, identification, legislation and metabolic characterization of synthetic cannabinoids in herbal incense products. *Drug Metab Rev* 46: 72–85.

Bussey TJ, Muir JL and Aggleton JP (1999) Functionally dissociating aspects of event memory: The effects of combined perirhinal and postrhinal cortex lesions on object and place memory in the rat. *J Neurosci* 19: 495–502.

Butovsky E, Juknat A, Elbaz J, et al. (2006) Chronic exposure to Δ 9-tetrahydrocannabinol downregulates oxytocin and oxytocin-associated neurophysin in specific brain areas. *Mol Cell Neurosci* 31: 795–804.

Cannon JG (2000) Inflammatory cytokines in nonpathological States. *News Physiol Sci* 15: 298–303.

Castaneto MS, Gorelick DA, Desrosiers NA, et al. (2014) Synthetic cannabinoids: Epidemiology, pharmacodynamics, and clinical implications. *Drug Alcohol Depend* 144: 12–41.

Cha HJ, Lee KW, Song MJ, et al. (2014) Dependence potential of the synthetic cannabinoids JWH-073, JWH-081, and JWH-210: In vivo and in vitro approaches. *Biomol Ther (Seoul)*. 22: 363–369.

Crawley J and Goodwin FK (1980) Preliminary report of a simple animal behavior model for the anxiolytic effects of benzodiazepines. *Pharmacol Biochem Behav* 13: 167–170.

Dalton VS, Wang H and Zavitsanou K (2009) HU210-induced down-regulation in cannabinoid CB1 receptor binding strongly correlates with body weight loss in the adult rat. *Neurochem Res* 34: 1343–1353.

DEA (2015) Schedules of controlled substances: Temporary placement of three synthetic cannabinoids into schedule I. Final order. *Fed Regist* 80: 5042–5047.

Di Marzo V, Berrendero F, Bisogno T, et al. (2000) Enhancement of anandamide formation in the limbic forebrain and reduction of endocannabinoid contents in the striatum of Δ9-tetrahydrocannabinol-tolerant rats. *J Neurochem* 74: 1627–1635.

Dresen S, Ferreiros N, Putz M, et al. (2010) Monitoring of herbal mixtures potentially containing synthetic cannabinoids as psychoactive compounds. *J Mass Spectrom* 45: 1186–1194.

EMCDDA (2016) *EU Drug Markets Report*. Available at: http://www.emcdda.europa.eu/system/files/publications/2373/TD0216072ENN.PDF (accessed 16 May 2016).

File SE and Seth P (2003). A review of 25 years of the social interaction test. *Eur J Pharmacol* 463: 35–53.

Galiegue S, Mary S, Marchand J, et al. (1995) Expression of central and peripheral cannabinoid receptors in human immune tissues and leukocyte subpopulations. *Eur J Biochem* 232: 54–61.

Giuliani D, Ferrari F and Ottani A (2000) The cannabinoid agonist HU 210 modifies rat behavioural responses to novelty and stress. *Pharmacol Res* 41: 47–53.

Guindon J and Hohmann AG (2008) Cannabinoid CB2 receptors: A therapeutic target for the treatment of inflammatory and neuropathic pain. *Br J Pharmacol* 153: 319–334.

Henriksson BG and Jarbe T (1971) Cannabis-induced vocalization in the rat. *J Pharm Pharmacol* 23: 457–458.

Hermanns-Clausen M, Kneisel S, Szabo B, et al. (2012) Acute toxicity due to the confirmed consumption of synthetic cannabinoids: Clinical and laboratory findings. *Addiction* 108: 534–544.

Higuera-Matas A, Ucha M and Ambrosio E (2015) Long-term consequences of perinatal and adolescent cannabinoid exposure on neural and psychological processes. *Neurosci Biobehav Rev* 55: 119–146.

Huffman JW, Dai D, Martin BR, et al. (1994) Design, synthesis and pharmacology of cannabimimetic indoles. *Chem Pharm Bull (Tokyo)* 4: 563–566.

Katchan V, David P and Shoenfeld Y (2016) Cannabinoids and autoimmune diseases: A systematic review. *Autoimmun Rev* 15: 513–528.

Khan M, Pace L, Truong A, et al. (2016) Catatonia secondary to synthetic cannabinoid use in two patients with no previous psychosis. *Am J Addict* 25: 25–27.

Klein C, Karanges E, Spiro A, et al. (2011) Cannabidiol potentiates Delta (9)-tetrahydrocannabinol (THC) behavioural effects and alters THC pharmacokinetics during acute and chronic treatment in adolescent rats. *Psychopharmacology (Berl)* 218: 443–457.

Klein TW, Newton C, Larsen K, et al. (2003) The cannabinoid system and immune modulation. *J Leukoc Biol* 74: 486–496.

Kopf M, Bachmann MF and Marsland BJ (2010) Averting inflammation by targeting the cytokine environment. *Nat Rev Drug Discov* 9: 703–718.

Langer N, Lindigkeit R, Schiebel H-M, et al. (2016) Identification and quantification of synthetic cannabinoids in "spice-like" herbal mixtures: Update of the German situation for the spring of 2015. *Forensic Toxicology* 34: 94–107.

Leweke FM, Giuffrida A, Koethe D, et al. (2007) Anandamide levels in cerebrospinal fluid of first-episode schizophrenic patients: Impact of cannabis use. *Schizophr Res* 94: 29–36.

Louh IK and Freeman WD (2014) A 'spicy' encephalopathy: Synthetic cannabinoids as cause of encephalopathy and seizure. *Crit Care* 18: 553.

Macri S, Lanuzza L, Merola G, et al. (2013) Behavioral responses to acute and sub-chronic administration of the synthetic cannabinoid JWH-018 in adult mice prenatally exposed to corticosterone. *Neurotoxicity Research* 24: 15–28.

Malfitano AM, Basu S, Maresz K, et al. (2014) What we know and do not know about the cannabinoid receptor 2 (CB2). *Semin Immunol* 26: 369–379.

Marco EM, Perez-Alvarez L, Borcel E, et al. (2004) Involvement of 5-HT1A receptors in behavioural effects of the cannabinoid receptor agonist CP 55,940 in male rats. *Behav Pharmacol* 15: 21–27.

McPartland JM, Duncan M, Di Marzo V, et al. (2015) Are cannabidiol and Delta(9) -tetrahydrocannabivarin negative modulators of the endocannabinoid system? A systematic review. *Br J Pharmacol* 172: 737–753.

Mir A, Obafemi A, Young A, et al. (2011) Myocardial infarction associated with use of the synthetic cannabinoid K2. *Pediatrics* 128: e1622-e1627.

Monte AA, Bronstein AC, Cao DJ, et al. (2014) An outbreak of exposure to a novel synthetic cannabinoid. *N Engl J Med* 370: 389–390.

Musah RA, Domin MA, Walling MA, et al. (2012) Rapid identification of synthetic cannabinoids in herbal samples via direct analysis in real time mass spectrometry. *Rapid Commun Mass Spectrom* 26: 1109–1114.

Musshoff F, Madea B, Kernbach-Wighton G, et al. (2014) Driving under the influence of synthetic cannabinoids ("Spice"): A case series. *Int J Legal Med* 128: 59–64.

NFILS (2014) *Synthetic Cannabinoids and Synthetic Cathinones Reported in NFILS, 2010–2013*. Available at: https://www.nflis.deadiversion.usdoj.gov/DesktopModules/ReportDownloads/Reports/NFLIS_SR_CathCan_508.pdf (accessed 03 October 2015).

NFILS (2015) *2014 Midyear Report*. Available at: https://www.nflis.deadiversion.usdoj.gov/DesktopModules/ReportDownloads/Reports/NFLIS2014MY.pdf (accessed 20 December 2015).

Norman G and Eacott MJ (2004) Impaired object recognition with increasing levels of feature ambiguity in rats with perirhinal cortex lesions. *Behav Brain Res* 148: 79–91.

O'Shea M, McGregor IS and Mallet PE (2006) Repeated cannabinoid exposure during perinatal, adolescent or early adult ages produces similar longlasting deficits in object recognition and reduced social interaction in rats. *J Psychopharmacol* 20: 611–621.

O'Shea M, Singh ME, McGregor IS, et al. (2004) Chronic cannabinoid exposure produces lasting memory impairment and increased anxiety in adolescent but not adult rats. *J Psychopharmacol* 18: 502–508.

Palamar JJ and Acosta P (2015) Synthetic cannabinoid use in a nationally representative sample of US high school seniors. *Drug Alcohol Depend* 149: 194–202.

Paul BD and Bosy T (2015) A sensitive GC-EIMS method for simultaneous detection and quantification of JWH-018 and JWH-073 carboxylic acid and hydroxy metabolites in urine. *J Anal Toxicol* 39: 172–182.

Pertwee RG (2010) Receptors and channels targeted by synthetic cannabinoid receptor agonists and antagonists. *Curr Med Chem* 17: 1360–1381.

Quinn HR, Matsumoto I, Callaghan PD, et al. (2008) Adolescent rats find repeated Delta(9)-THC less aversive than adult rats but display greater residual cognitive deficits and changes in hippocampal protein expression following exposure. *Neuropsychopharmacology* 33: 1113–1126.

Rajasekaran M, Brents LK, Franks LN, et al. (2013) Human metabolites of synthetic cannabinoids JWH-018 and JWH-073 bind with high affinity and act as potent agonists at cannabinoid type-2 receptors. *Toxicology and Applied Pharmacology* 269: 100–108.

Ramos L, Hicks C, Kevin R, et al. (2013) Acute prosocial effects of oxytocin and vasopressin when given alone or in combination with 3,4-methylenedioxymethamphetamine in rats: Involvement of the V1A receptor. *Neuropsychopharmacology* 38: 2249–2259.

Rubino T, Prini P, Piscitelli F, et al. (2015) Adolescent exposure to THC in female rats disrupts developmental changes in the prefrontal cortex. *Neurobiol Dis* 73: 60–69.

Schneider M and Koch M (2003) Chronic pubertal, but not adult chronic cannabinoid treatment impairs sensorimotor gating, recognition

memory, and the performance in a progressive ratio task in adult rats. *Neuropsychopharmacology* 28: 1760–1769.

Schneir AB, Cullen J and Ly BT (2011) "Spice" girls: Synthetic cannabinoid intoxication. *J Emerg Med* 40: 296–299.

Schwartz MD, Trecki J, Edison LA, et al. (2015) A common source outbreak of severe delirium associated with exposure to the novel synthetic cannabinoid ADB-PINACA. *J Emerg Med* 48: 573–580.

Seely KA, Brents LK, Radominska-Pandya A, et al. (2012a) A major glucuronidated metabolite of JWH-018 is a neutral antagonist at CB1 receptors. *Chem Res Toxicol* 25: 825–827.

Seely KA, Lapoint J, Moran JH, et al. (2012b) Spice drugs are more than harmless herbal blends: A review of the pharmacology and toxicology of synthetic cannabinoids. *Prog Neuropsychopharmacol Biol Psychiatry* 39: 234–243.

Sim-Selley LJ, Schechter NS, Rorrer WK, et al. (2006) Prolonged recovery rate of CB1 receptor adaptation after cessation of long-term cannabinoid administration. *Mol Pharmacol* 70: 986–996.

Spaderna M, Addy PH and D'Souza DC (2013) Spicing things up: Synthetic cannabinoids. *Psychopharmacology (Berl)* 228: 525–540.

Spear LP (2000) The adolescent brain and age-related behavioral manifestations. *Neurosci Biobehav Rev* 24: 417–463.

Stuart JM, Paris JJ, Frye C, et al. (2013) Brain levels of prostaglandins, endocannabinoids, and related lipids are affected by mating strategies. *Int J Endocrinol* 2013: 436252.

Takayama T, Suzuki M, Todoroki K, et al. (2014) UPLC/ESI-MS/MS-based determination of metabolism of several new illicit drugs, ADB-FUBINACA, AB-FUBINACA, AB-PINACA, QUPIC, 5F-QUPIC and alpha-PVT, by human liver microsome. *Biomed Chromatogr* 28: 831–838.

Tanda G (2016) Preclinical studies on the reinforcing effects of cannabinoids. A tribute to the scientific research of Dr. Steve Goldberg. *Psychopharmacology (Berl)* 233: 1845–1866.

Thomsen R, Nielsen LM, Holm NB, et al. (2014) Synthetic cannabimimetic agents metabolized by carboxylesterases. *Drug Test Anal* 7: 565–576.

Trecki J, Gerona RR and Schwartz MD (2015) Synthetic cannabinoid–related illnesses and deaths. *N Engl J Med* 373: 103–107.

Trezza V and Vanderschuren LJ (2008) Bidirectional cannabinoid modulation of social behaviour in adolescent rats. *Psychopharmacology (Berl)* 197: 217–227.

Uchiyama N, Matsuda S, Wakana D, et al. (2013) New cannabimimetic indazole derivatives, N-(1-amino-3-methyl-1-oxobutan-2-yl)-1-pentyl-1H-indazole-3-carboxamide (AB-PINACA) and N-(1-amino-3-methyl-1-oxobutan-2-yl)-1-(4-fluorobenzyl)-1H-indazole-3-carboxamide (AB-FUBINACA) identified as designer drugs in illegal products. *Forensic Toxicology* 31: 93–100.

UNODC (2015) *World Drug Report*. Available at: http://www.unodc.org/documents/wdr2015/World_Drug_Report_2015.pdf (accessed 4 Oct 2015).

Vikingsson S, Green H, Brinkhagen L, et al. (2015) Identification of AB-FUBINACA metabolites in authentic urine samples suitable as urinary markers of drug intake using liquid chromatography quadrupole tandem time of flight mass spectrometry. *Drug Test Anal* 8: 950–956.

Viveros M and Marco ME (2015) Age-dependent effects of cannabinoids on neurophysiological, emotional, and motivational states. In: Fattore L and Campolongo P (eds) *Cannabinoid Modulation of Emotion, Memory, and Motivation*. New York: Springer, pp. 245–281.

Wiebelhaus JM, Poklis JL, Poklis A, et al. (2012) Inhalation exposure to smoke from synthetic "marijuana" produces potent cannabimimetic effects in mice. *Drug Alcohol Depend* 126: 316–323.

Wei D, Lee D, Cox CD, et al. (2015) Endocannabinoid signaling mediates oxytocin-driven social reward. *PNAS* 112: 14084–14089.

Wiley JL, Marusich JA, Lefever TW, et al. (2013) Cannabinoids in disguise: Delta9-tetrahydrocannabinol-like effects of tetramethylcyclopropyl ketone indoles. *Neuropharmacology* 75: 145–154.

Wiley JL, Marusich JA, Lefever TW, et al. (2015) AB-CHMINACA, AB-PINACA, and FUBIMINA: Affinity and potency of novel synthetic cannabinoids in producing delta9-tetrahydrocannabinol-like effects in mice. *J Pharmacol Exp Ther* 354: 328–339.

Wiley JL, Marusich JA, Martin BR, et al. (2012) 1-Pentyl-3-phenylacetylindoles and JWH-018 share in vivo cannabinoid profiles in mice. *Drug Alcohol Depend* 123: 148–153.

Wilkins C, Prasad J, Wong K, et al. (2016) An exploratory study of the health harms and utilisation of health services of frequent legal high users under the interim regulated legal high market in central Auckland. *N Z Med J* 129: 51–58.

Wilmouth CE and Spear LP (2004) Adolescent and adult rats' aversion to flavors previously paired with nicotine. *Ann N Y Acad Sci* 1021: 462–464.

Winstock AR and Barratt MJ (2013) Synthetic cannabis: A comparison of patterns of use and effect profile with natural cannabis in a large global sample. *Drug Alcohol Depend* 131: 106–111.

Wohlfarth A, Scheidweiler KB, Castaneto M, et al. (2015) Urinary prevalence, metabolite detection rates, temporal patterns and evaluation of suitable LC-MS/MS targets to document synthetic cannabinoid intake in US military urine specimens. *Clin Chem Lab Med* 53: 423–434.

Chapter 5. Urinary cannabinoid levels during nabiximols (Sativex®)-medicated inpatient cannabis withdrawal

NOTE: The supplementary material referred to by the publication in this chapter can be found in Appendix 2

Forensic Toxicol (2017) 35:33–44
DOI 10.1007/s11419-016-0330-0

ORIGINAL ARTICLE

Urinary cannabinoid levels during nabiximols (Sativex®)-medicated inpatient cannabis withdrawal

Richard C. Kevin[1] · David J. Allsop[1] · Nicholas Lintzeris[2,3] · Adrian J. Dunlop[4,5] · Jessica Booth[1] · Iain S. McGregor[1]

Received: 16 May 2016 / Accepted: 12 July 2016 / Published online: 4 August 2016

Abstract Nabiximols (Sativex®) is a buccal spray containing both Δ^9-tetrahydrocannabinol (THC) and cannabidiol (CBD). It has shown promise as an agonist substitution therapy for treating cannabis withdrawal and dependence. Monitoring urinary cannabinoid levels during treatment is important for determination of cannabinoid pharmacokinetics and for treatment adherence during clinical trials. Here, we use a recently described hydrolysis method to liberate urinary CBD from its glucuronide conjugate, and describe the trajectory of urinary CBD, THC, 11-nor-9-carboxy-THC (THC-COOH), and 11-hydroxy-THC (11-OH-THC) in patients receiving nabiximols treatment (or placebo) during cannabis withdrawal. Urine and plasma samples were taken before and during a 6-day inpatient treatment regime and during a 3-day drug-free washout. Urine was hydrolysed with red abalone β-glucuronidase, and CBD, THC, THC-COOH, and 11-OH-THC were quantified in daily urine using liquid chromatography-tandem mass spectrometry. Overall, urine and plasma cannabinoid levels followed similar trajectories and closely reflected the dosing schedule. During nabiximols treatment, CBD levels in urine and plasma rose markedly, while concentrations of THC and its metabolites remained at, or slightly above, pre-treatment levels. Following hydrolysis, urinary CBD was detected at levels 50 and 200 times as high as those in non-hydrolysed plasma and non-hydrolysed urine, respectively. THC, THC-COOH, and 11-OH-THC concentrations were also amplified by urinary hydrolysis. This method allows sensitive assessment of urinary CBD, and may prove useful in clinical studies involving nabiximols or other cannabinoid therapies.

Keywords Nabiximols · Sativex · Cannabinoid · Cannabidiol · Urine · Withdrawal

Introduction

Problems relating to cannabis dependence are a significant cause of drug and alcohol treatment episodes worldwide [1]. Cannabis dependence is thought to affect approximately 10 % of all cannabis users, amounting to roughly 13 million people globally [2]. Sudden abstinence from cannabis in dependent users can lead to a withdrawal syndrome with symptoms such as irritability, insomnia, restlessness, weight loss, tremors, depression, and anxiety [3, 4]. This can present a major obstacle to the reduction or cessation of cannabis use [5–7]. Attempts to manage these symptoms using conventional pharmacotherapies such as antidepressants and mood stabilisers have met with only limited success [8, 9]. However, the use of agonist replacement therapy involving a variety of cannabinoid receptor agonists shows considerable promise [10–13].

Nabiximols (Sativex®) is a buccal spray derived from *Cannabis sativa* plants which provides an approximate 1:1

Electronic supplementary material The online version of this article (doi:10.1007/s11419-016-0330-0) contains supplementary material, which is available to authorized users.

✉ Iain S. McGregor
iain.mcgregor@sydney.edu.au

[1] School of Psychology, The University of Sydney, A18, Sydney, NSW 2006, Australia

[2] Central Clinical School, The University of Sydney, Sydney, NSW 2006, Australia

[3] The Langton Centre, Sydney, NSW 2010, Australia

[4] Drug & Alcohol Clinical Services, Hunter New England Local Health District, Newcastle 2300, Australia

[5] School of Medicine and Public Health, Faculty of Health, University of Newcastle, Callaghan 2308, Australia

ratio of Δ^9-tetrahydrocannabinol (THC) and cannabidiol (CBD), with additional trace phytocannabinoids and terpenoids. It was developed primarily for the treatment of muscle spasticity and pain in multiple sclerosis [14]. Our group recently reported that nabiximols was efficacious in treating cannabis withdrawal [11]. The THC component of nabiximols provides an agonist substitution effect, while the addition of CBD may functionally minimise some of the negative effects of THC such as anxiety, cognitive impairments, and memory deficits, and provide intrinsic anxiolytic, hypnotic, and antipsychotic effects [15–17]. This could afford an advantage over pure THC preparations. Although CBD has poor affinity for cannabinoid receptors, it may act as an allosteric modulator at CB_1 receptors [18], can increase endocannabinoid levels [19] and may act at non-cannabinoid receptors such as 5-HT_{1A}, PPARγ, and TRP channels [20–22].

Measurement of CBD, THC, and THC metabolites during and following nabiximols administration is important for dose titration, safety, and for monitoring treatment adherence, particularly over an extended treatment period. THC is predominantly metabolised via cytochrome P450 2C9 and 2C19 isoenzymes to 11-hydroxyl-THC (11-OH-THC) and 11-nor-9-carboxy-THC (THC-COOH) [23, 24]. These metabolites can undergo phase II glucuronidation by various UDP-glucuronosyltransferases [25]. The metabolism of CBD is less well understood, but CBD appears to be a better substrate for human UDP-glucuronosyltransferases than THC, and is excreted both directly and in glucuronidated form in urine, together with 7-hydroxy-CBD (7-OH-CBD) and oxidised derivatives as major metabolites [26, 27].

These compounds can be measured in plasma, but urinalysis would provide easier and less invasive sampling in clinical studies. Until recently, sensitive and accurate analysis of CBD in urine has been challenging, due to uncharacterised phase II metabolites. A method optimised for analysing CBD and its secondary glucuronidated or sulfated metabolites using enzymatic hydrolysis with red abalone β-glucuronidase, followed by gas chromatography–mass spectrometry analysis, has been described, producing a 250-fold increase in urinary CBD levels compared to non-hydrolysed samples [28]. This method has the potential to greatly improve the viability of CBD urinalysis.

Here, we employed this method, adapted to liquid chromatography–tandem mass spectrometry (LC–MS/MS), in a clinical study involving cannabis withdrawal. It is unclear how well urine and plasma cannabinoid levels correlate during multiple days of nabiximols treatment, and how well this method detects THC and its metabolites; thus the method requires further validation in clinical settings. In addition, the levels of CBD, THC, and its metabolites during multiple days of nabiximols treatment are largely uncharacterised in terms of overall time course and peak concentration. Therefore, the present study demonstrates the trajectory of CBD levels, as well as THC and its primary metabolites, during treatment with nabiximols across an inpatient cannabis withdrawal episode in a clinical population of cannabis-dependent treatment-seekers [29]. We also examine the relationship between urine and plasma cannabinoid levels to validate the utility and sensitivity of urinary CBD monitoring in a clinical setting, using an enzymatic hydrolysis approach.

Materials and methods

Participants and dosing

Urine and blood samples were provided by 51 participants from a double-blind randomised clinical inpatient trial of nabiximols for cannabis withdrawal management (see Ref. [29]). Briefly, they were individuals aged 18–65 years who had a desire to reduce or halt cannabis use and had a history of cannabis withdrawal, but no current alcohol or other drug dependence except for nicotine or caffeine. Samples from 22 patients were selected for analysis based on the criterion that they had provided at least 5 daily urine samples across the 9 days of inpatient treatment. Of these, 11 were placebo-treated and 11 were nabiximols-treated. Patients were asked to abstain from cannabis use for at least 6 h before admission.

The first nabiximols dose was administered at 4 p.m. on day 1 (eight sprays, for a total of 21.6 mg THC and 20 mg CBD), and again at 10 p.m. (eight sprays). Maximal doses (eight sprays four times daily, for a total of 86.4 mg of THC and 80 mg CBD) were administered on days 2 and 3. The dose was tapered on subsequent days to six sprays four times daily on day 4 (64.8 mg THC and 60 mg CBD), four sprays four times daily on day 5 (43.2 mg THC, 40 mg CBD), and two sprays four times daily on day 6 (21.6 mg THC, 20 mg CBD). Days 7–9 were drug-free washout days. Placebo participants received a matched placebo (a spray with similar smell and taste) developed by GW Pharmaceuticals, Porton Down Science Park, UK. This research was approved by the Hunter New England Human Research Ethics Committee.

Plasma and urine sampling

Blood was taken on days 1 (pre-treatment), 3 (peak dose), and 7 (14.5 h after last nabiximols dose). Blood samples were was not taken daily, in order to limit the invasiveness of the study. Blood was drawn at 12:30 p.m. into an EDTA-

coated collection tube and centrifuged at 1500 *g* for 10 min. Plasma was stored at −20 °C until analysis. We obtained daily urine samples, collected at the first void of the day and stored at −20 °C until analysis. The urine sample on day 1 was taken before the first nabiximols dose.

Reagents

Cannabinoid standards and deuterated internal standards (THC, THC-d_3, CBD, CBD-d_3, 11-OH-THC, 11-OH-THC-d_3, THC-COOH, and THC-COOH-d_9) were obtained from Cerilliant® (Round Rock, TX, USA); methanol, acetonitrile, *n*-hexane, aqueous ammonia, and anhydrous sodium acetate from Merck Millipore (Bayswater, VIC, Australia); monobasic/dibasic potassium phosphate from Ajax Fine Chemicals (Sydney, NSW, Australia); glacial acetic acid from Fisher Scientific (Melbourne, VIC, Australia); and red abalone β-glucuronidase from PM Separations (Capalaba, QLD, Australia). All chemicals and solvents were at least ACS or HPLC grade, respectively.

Cannabinoid urinalysis

Urine samples (0.5 mL) were analysed in duplicate using a previously described method [28], adapted to LC–MS/MS as detailed in the following sections.

Enzyme hydrolysis

Following fortification with internal standard solutions, the samples were adjusted to pH 5 with 1 mL 0.2 M sodium acetate buffer, then hydrolysed with 25 µL red abalone β-glucuronidase (>100,000 units/mL) and incubated for 15 h at 37 °C. Calibrator and quality control samples, prepared using blank urine spiked with cannabinoid standards, were treated identically. Following incubation, protein precipitation was performed via addition of 1 mL ice-cold acetonitrile, followed by centrifugation and aspiration of the supernatant. Samples were adjusted to pH 6 with 2 mL 0.1 M phosphate buffer in preparation for solid-phase extraction.

Solid-phase extraction

Hydrolysed samples were directly loaded onto 3 mL UCT Styre Screen SSTHC063 SPE columns (United Chemical Technologies [UCT], Inc., Bristol, PA, USA), washed with 1 mL of water/acetonitrile/ammonia (84:15:1, v/v/v), and then dried under a vacuum for 20 min. Cannabinoid analytes were eluted from the columns with 3 mL of *n*-hexane/ethyl acetate/glacial acetic acid (49:49:2, v/v/v). Eluates were evaporated to dryness under a stream of high-purity nitrogen at 60 °C, and then reconstituted in 1 mL initial mobile phase (40 % methanol and 60 % 10 mM ammonium acetate) for LC–MS/MS analysis.

LC–MS/MS analysis

A Shimadzu Nexera® ultra-high-performance liquid chromatograph (Shimadzu Corp., Kyoto, Japan) with a Pinnacle DB Biphenyl column (100 × 2.1 mm i.d., particle size 1.9 µm; Restek Corp., Bellefonte, PA, USA) was used for chromatographic separation. This was performed via gradient elution with methanol and 10 mM ammonium acetate at a flow rate of 0.3 mL/min at 40 °C. A Shimadzu LCMS-8030 triple quadrupole mass spectrometer, operated in positive atmospheric pressure chemical ionisation mode with multiple reaction monitoring, was used for analyte identification and quantification.

Non-hydrolysed samples

To investigate the effect of hydrolysis with red abalone β-glucuronidase on all cannabinoid analytes, the urine samples of a single nabiximols-treated patient were analysed without the enzyme hydrolysis step. These results were compared to the analysis of the same samples using enzyme hydrolysis.

Validation

Although this hydrolysis method was validated previously for GC–MS [28], we determined selectivity, linearity, accuracy, precision, limits of quantification (LOQ), and limits of detection (LOD) for our LC–MS/MS adaptation. Selectivity was verified by analysing blank urine samples provided by an experimenter who had not used or been exposed to any cannabis in the last year. Linearity was assessed using calibrators at seven ascending concentration levels. Accuracy was determined using quality control (QC) samples at low and high concentrations relative to the calibration range, with bias calculated as percent deviation from the nominal analyte concentration. Precision was calculated using the same low and high QC samples, with percent relative standard deviation calculated from three runs on the same day (intraday) and on three separate days (interday). LOQ was selected on the basis of accuracy and precision of QC samples, while LOD was set as the lowest calibrator concentration, with a signal-to-noise ratio of ≥3.

Cannabinoid plasma analysis

Plasma was analysed as reported previously [29]. Briefly, cannabinoids were extracted from plasma using solid-phase extraction following protein precipitation with acetonitrile, dried under nitrogen, reconstituted in initial mobile phase,

and analysed with LC–MS/MS as specified in the previous section.

Data analysis

Raw chromatographic data were analysed using LabSolutions version 5.60 software (Shimadzu Corp., Kyoto, Japan). Quantified analytical data were analysed with SPSS version 22 software (IBM Corp., Armonk, NY, USA). The analysis considered the main effects of treatment (nabiximols or placebo) and time (days 1–9), and their interaction in a linear mixed model for repeated measures with first-order autoregressive covariance structure [30]. We examined significant effects with two sets of planned contrasts. The first set of contrasts compared the levels of each analyte between nabiximols and placebo patients on each day of the inpatient study (e.g., day 3 nabiximols urine compared to day 3 placebo urine). The second set compared the levels of analytes on each day to day 1 levels within each treatment group (e.g., day 3 nabiximols urine compared to day 1 nabiximols urine). All contrasts were adjusted for multiple comparisons using the Bonferroni method. Effect sizes were calculated using the bias-corrected Hedges *g* (raw difference between two means divided by standard deviation adjusted for population size [31]).

We also computed Pearson's correlations between plasma and hydrolysed urinary concentrations of each analyte to investigate whether urinalysis, a less invasive procedure, could be used as a proxy for plasma drug levels. All data across placebo and nabiximols treatment groups on days 1, 3, and 7 (plasma sampling days) were pooled to achieve sufficient statistical power. In addition, we computed correlations between plasma on days 1, 3, and 7 with urinary data on the days following plasma sampling (days 2, 4, and 8), in an attempt to account for any delay in analyte excretion. In all cases, data where either urine or plasma concentrations fell below the limits of quantification were excluded.

Finally, we calculated the ratios of hydrolysed urinary THC to CBD, THC-COOH to CBD, and 11-OH-THC to CBD at peak dosing (day 3) for nabiximols-treated participants, to investigate the consistency of analyte ratios during nabiximols treatment, theorising that deviation from a consistent ratio could be useful for identifying relapse to recreational cannabis use in outpatient settings.

Results

Patient demographics and prior substance use

Patient characteristics are presented in Table 1. Patients were on average 39 years of age, had used cannabis for an average of 24.4 years, and had used an average 19.3 g of cannabis per week in the month preceding treatment. There were no significant differences between nabiximols- and placebo-treated patients in demographics or substance use history. A greater number of urine and plasma samples were provided over the course of the study by nabiximols-treated participants, corresponding to greater treatment retention [29].

Table 1 Demographics and substance use history by treatment group

Characteristic	Nabiximols ($n = 11$)	Placebo ($n = 11$)	Total ($n = 22$)	*P* value[a]
Demographics, no. (%)				
Age, mean (SD)	38.4 (9.58)	39.6 (6.99)	39.0 (8.21)	0.73
Male	8 (72.7)	9 (81.8)	17 (77.2)	0.61
Aboriginal or Torres Strait Islander	0 (0)	1 (9.1)	1 (4.5)	0.31
Substance use history, mean (SD)				
Cannabis use g/week[b]	13.2 (6.92)	25.4 (32.2)	19.3 (23.6)	0.23
Years of cannabis use	23.7 (9.94)	25.0 (6.32)	24.4 (8.16)	0.72
Alcohol use, U/week[b]	4.60 (10.8)	5.83 (7.21)	5.21 (8.99)	0.76
Cigarettes/week[b]	69.8 (59.5)	50.8 (55.9)	60.3 (57.1)	0.29
Tobacco use g/week[b]	9.54 (2.37)	11.2 (2.83)	10.4 (8.48)	0.67
Samples, no.				
Urine samples provided	88	77	165	0.04
Plasma samples provided	31	24	55	<0.01
Remaining at day 9, no. (%)	7 (63.6)	5 (45.5)	12 (54.5)	0.41

SD standard deviation

[a] Statistical comparisons were independent samples *t*-tests for continuous variables, or χ^2 tests for categorical variables

[b] Weekly use in the month before entering the study, measured by modified timeline follow-back

Alcohol measured in units (1 U = 8 g ethanol)

Method validation

Validation and quantification parameters for the LC–MS/MS urinary hydrolysis method are presented in the supplementary material (Table S1). All analytes produced a linear response in the appropriate range, and precision and accuracy were within acceptable limits [32]. No interfering signals were detected in blank samples.

CBD

All but one placebo participant had undetectable CBD levels in plasma and urine for the duration of inpatient treatment. In contrast, in those patients receiving nabiximols treatment (Fig. 1a), plasma and urinary CBD appeared upon commencement of medication, rising to asymptote in urine on day 4. CBD levels decreased following reductions in dosing on day 4, and decreased towards zero over days 7, 8, and 9 (Fig. 1a), when nabiximols was withdrawn. Overall, CBD levels in hydrolysed urine were approximately 50 times those of plasma CBD.

In urine samples, levels of CBD were significantly higher in the nabiximols-treated group (treatment × time: $F_{8,102.93} = 3.285$, $P < 0.01$) across all 9 days, and contrasts demonstrated that CBD levels were higher in nabiximols patients on days 2–6, with maximal differences observed on day 4 (all $P < 0.05$; Hedges $g = 0.68$; Fig. 1a). On these days in nabiximols-treated patients, CBD levels were significantly elevated compared to pre-treatment levels (all $P < 0.05$), while no differences from pre-treatment were observed in placebo-treated patients.

Similarly, overall plasma CBD levels were significantly greater in nabiximols-treated patients than in those treated with placebo (treatment × time: $F_{2,40.68} = 38.42$, $P < 0.0001$), and contrasts revealed that CBD levels were higher in nabiximols-treated patients on days 3 and 7 (all $P < 0.05$; Fig. 1a), with the greatest difference occurring on day 3 (Hedges $g = 2.99$). Compared to day 1 levels, plasma CBD levels were elevated in nabiximols-treated patients on days 3 and 7 (all $P < 0.05$), while no differences from pre-treatment levels were found in placebo-treated patients. Day 1 adjusted data are presented in the supplementary material (Fig. S1).

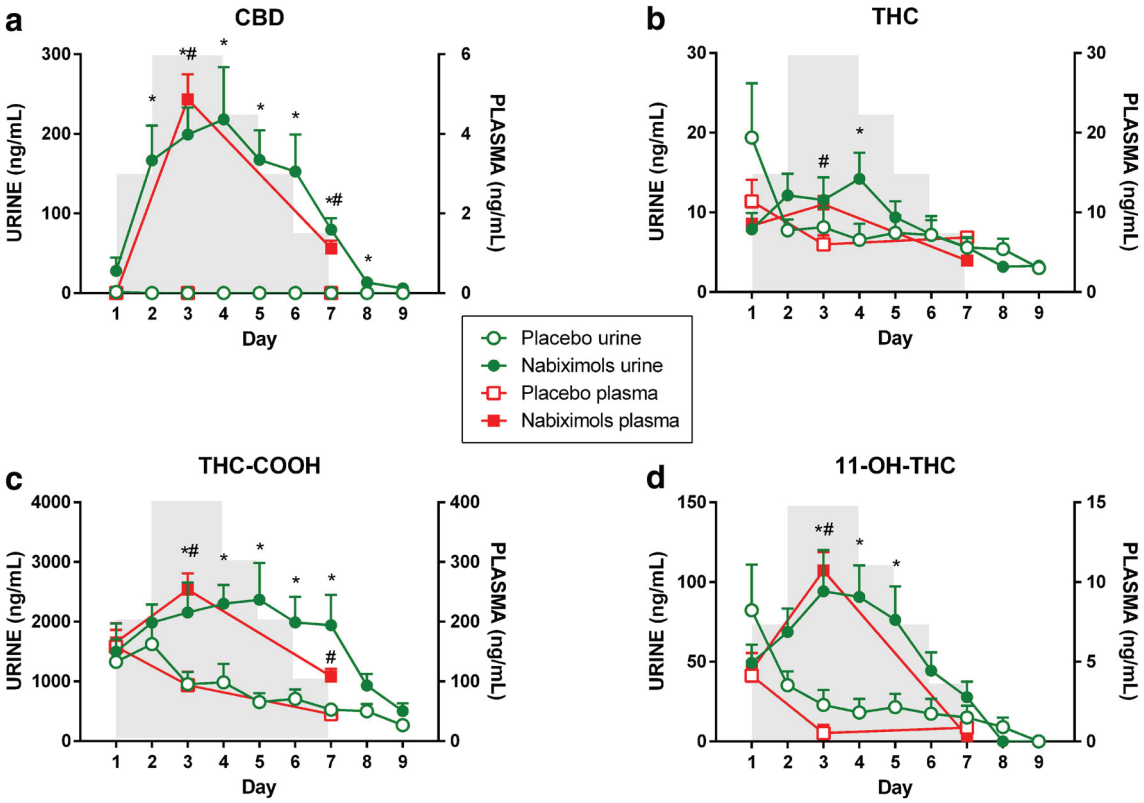

Fig. 1 Mean cannabidiol (CBD), Δ^9-tetrahydrocannabinol (THC), 11-nor-9-carboxy-THC (THC-COOH), and 11-hydroxy-THC (11-OH-THC) in plasma (non-hydrolysed) and urine of patients treated with placebo ($n = 11$) and nabiximols ($n = 11$). *Shaded background area* indicates the tapered nabiximols dosing schedule. Note that samples were taken in the morning and that day 1 samples were taken before the first nabiximols or placebo dose. Peak dosing occurred on days 2 and 3, and washout occurred on days 7–9. *Asterisk* (*) indicates nabiximols urine concentration significantly greater than placebo urine concentration. *Hash symbol* (#) indicates nabiximols plasma concentration significantly greater than placebo plasma concentration

THC

THC levels in urine were low compared to the other analytes, and were variable on day 1 (Fig. 1b). Overall, urinary THC was elevated across the inpatient period in nabiximols-treated patients (treatment × time: $F_{8,96.22} = 3.41$, $P < 0.01$), and contrasts showed higher urinary THC in patients treated with nabiximols compared to placebo on day 4 ($P < 0.05$; Hedges $g = 0.82$; Fig. 1b). Urinary THC did not significantly differ from day 1 levels on any day for nabiximols-treated patients, but THC levels for placebo-treated patients decreased below initial levels on all subsequent days (all $P < 0.05$).

Overall, plasma THC was elevated by nabiximols treatment compared to placebo (treatment × time: $F_{2,29.56} = 10.517$, $P < 0.001$), and contrasts showed higher THC in participants treated with nabiximols versus placebo on day 3 ($P < 0.05$; hedges $g = 1.41$; Fig. 1b). Compared to day 1 levels, THC decreased on day 7 for nabiximols-treated participants, and the THC levels for placebo-treated participants decreased on days 3 and 7 (all $P < 0.05$).

THC-COOH

THC-COOH urine levels rose steadily during nabiximols treatment, before declining rapidly as treatment ceased (Fig. 1c). In the placebo group, THC-COOH levels generally declined across all 9 days, but did not reach zero. Contrasts revealed that nabiximols treatment significantly increased THC-COOH levels on days 3–7, with the greatest difference occurring on day 5 (all $P < 0.05$; Fig. 1c; Hedges $g = 0.54$).

Plasma THC-COOH was higher in patients treated with nabiximols compared to placebo over the course of the study (treatment × time: $F_{2,32.50} = 17.36$, $P < 0.0001$), and contrasts showed that plasma THC-COOH was higher in nabiximols-treated patients on days 3 and 7 compared to those treated with placebo (all $P < 0.05$; Fig. 1c). This difference was greatest on day 3 (Hedges $g = 1.40$). Relative to day 1 levels, plasma THC-COOH increased on day 3 for nabiximols-treated patients, and THC-COOH in the placebo-treated group decreased on days 3 and 7 (all $P < 0.05$).

11-OH-THC

11-OH-THC levels followed a pattern similar to those of THC-COOH, albeit at lower concentrations (Fig. 1d). Urinary 11-OH-THC was higher in nabiximols-treated versus placebo-treated patients throughout the duration of the inpatient study (treatment × time: $F_{8,113.55} = 4.64$, $P < 0.0001$), and contrasts showed higher 11-OH-THC in patients treated with nabiximols compared to placebo on days 3–5 (all $P < 0.05$; Fig. 1d). The greatest increase occurred on day 4 (Hedges $g = 1.38$). Compared to day 1 levels, urinary 11-OH-THC levels were elevated on days 3 and 4 in nabiximols-treated patients, while placebo levels decreased relative to day 1 levels on all subsequent days (all $P < 0.05$).

Overall, plasma 11-OH-THC was significantly higher in nabiximols-treated compared to placebo-treated patients (treatment × time: $F_{2,33.63} = 31.79$, $P < 0.0001$). Contrasts revealed that on day 3, plasma 11-OH-THC was significantly greater in nabiximols-treated patients relative to those treated with placebo ($P < 0.05$; $g = 3.20$; Fig. 1d). Compared to pre-treatment levels, 11-OH-THC increased on day 3 for nabiximols-treated participants, and placebo levels decreased on days 3 and 7 (all $P < 0.05$).

β-Glucuronidase hydrolysis

Hydrolysis of urine samples with β-glucuronidase produced large increases in concentrations of all analytes (Fig. 2). CBD levels were approximately 200 times greater in hydrolysed urine, peaking at 245 ng/mL on day 3 in hydrolysed urine, compared to 1.2 ng/mL in non-hydrolysed urine on day 5. THC-COOH levels were several times higher in hydrolysed urine across the 9 days. Without hydrolysis, THC and 11-OH-THC levels fell below limits of quantification on all days.

Relationship between urine and plasma analyte concentrations

Scatter plots of urinary and plasma analyte concentrations are presented in Fig. 3. Urine–plasma Pearson correlations for pooled data from plasma sampling days 1, 3, and 7 were strong and statistically significant for CBD ($r = 0.87$, $P < 0.001$; Fig. 3) and THC ($r = 0.74$, $P < 0.001$), and moderate and statistically significant for THC-COOH ($r = 0.47$, $P < 0.001$) and 11-OH-THC ($r = 0.44$, $P < 0.05$). The urine–plasma correlation was improved for THC-COOH by using urinary data from the days following plasma sampling (i.e., days 2, 4, and 8; $r = 0.67$, $P < 0.001$), but CBD, THC, and 11-OH-THC correlations fell compared to same-day plasma and urine correlations (CBD: $r = 0.03$, $P > 0.05$; THC: $r = 0.30$, $P < 0.05$; 11-OH-THC: $r = 0.29$, $P > 0.05$).

Analyte ratios

Ratios of THC to CBD, THC-COOH to CBD, and 11-OH-THC to CBD for nabiximols-treated patients at peak dosing (day 3) are presented in Table 2. Relative standard deviations were high for all analyte ratios in both hydrolysed

Forensic Toxicol (2017) 35:33–44 39

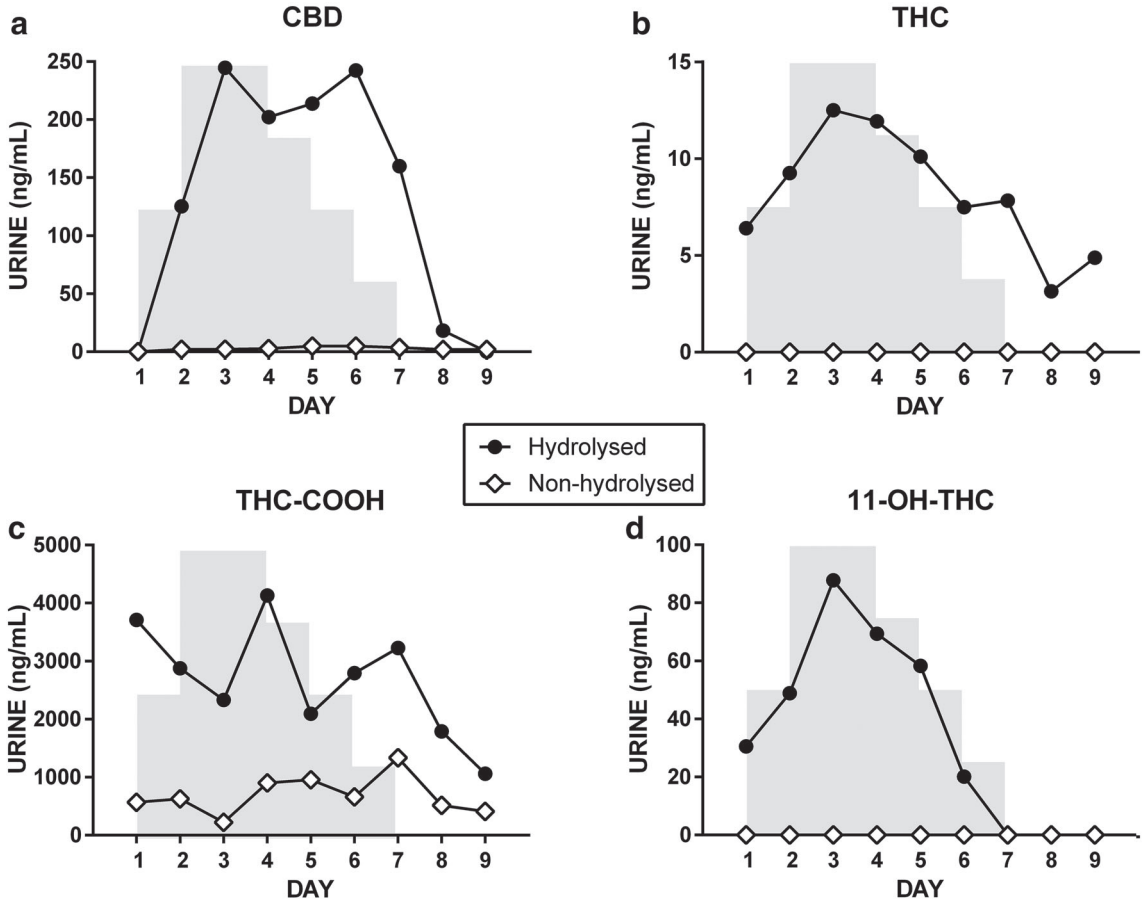

Fig. 2 Effect of hydrolysis with red abalone β-glucuronidase on urinary CBD, THC, THC-COOH, and 11-OH-THC in a single nabiximols-treated patient. The *background shaded area* indicates the tapered nabiximols dosing schedule. Note that samples were taken in the morning and that day 1 samples were taken before the first nabiximols or placebo dose

urine and non-hydrolysed plasma, indicating substantial variability in analyte ratios between individual patients.

Discussion

The current study examined urine and plasma cannabinoid concentrations during inpatient cannabis withdrawal, where participants received 6 days of nabiximols or placebo treatment followed by 3 washout days. All cannabinoid analytes of interest (THC, THC-COOH, 11-OH-THC, CBD) were detectable following β-glucuronidase hydrolysis. The hydrolysis method utilised was particularly effective in liberating urinary CBD.

CBD levels in urine were negligible before treatment, reflecting the low or non-existent CBD content of typical Australian street cannabis [33]. By contrast, THC, THC-COOH, and 11-OH-THC were readily detectible initially, although highly variable across individuals. Plasma THC-COOH was more abundant than its parent compound THC, consistent with cannabinoid pharmacokinetic studies following smoking or oral administration [34, 35]. Moreover, in day 2 placebo urine, THC and 11-OH-THC levels fell in comparison to day 1 levels, while THC-COOH did not, possibly reflecting the conversion of THC and/or 11-OH-THC to THC-COOH [34]. The concentrations of all cannabinoids in nabiximols-treated patients peaked shortly after peak dosing, and declined steadily over multiple days following cessation of dosing (Fig. 1), closely reflecting the tapered dosing schedule. However, urinary THC and THC-COOH was detectable in several patients on day 9, even in the placebo group, concordant with the long period of elimination of these analytes in heavy cannabis users [36]. Slow elimination of cannabinoids has been well characterised previously [37, 38], and may be partly due to the long-term sequestration of cannabinoids in fat tissue [36, 39, 40].

In participants receiving nabiximols treatment, CBD was detected at high levels in urine subsequent to hydrolysis of the urinary samples with red abalone β-glucuronidase. This produced urinary CBD at concentrations 50 times those seen in plasma, and approximately 200

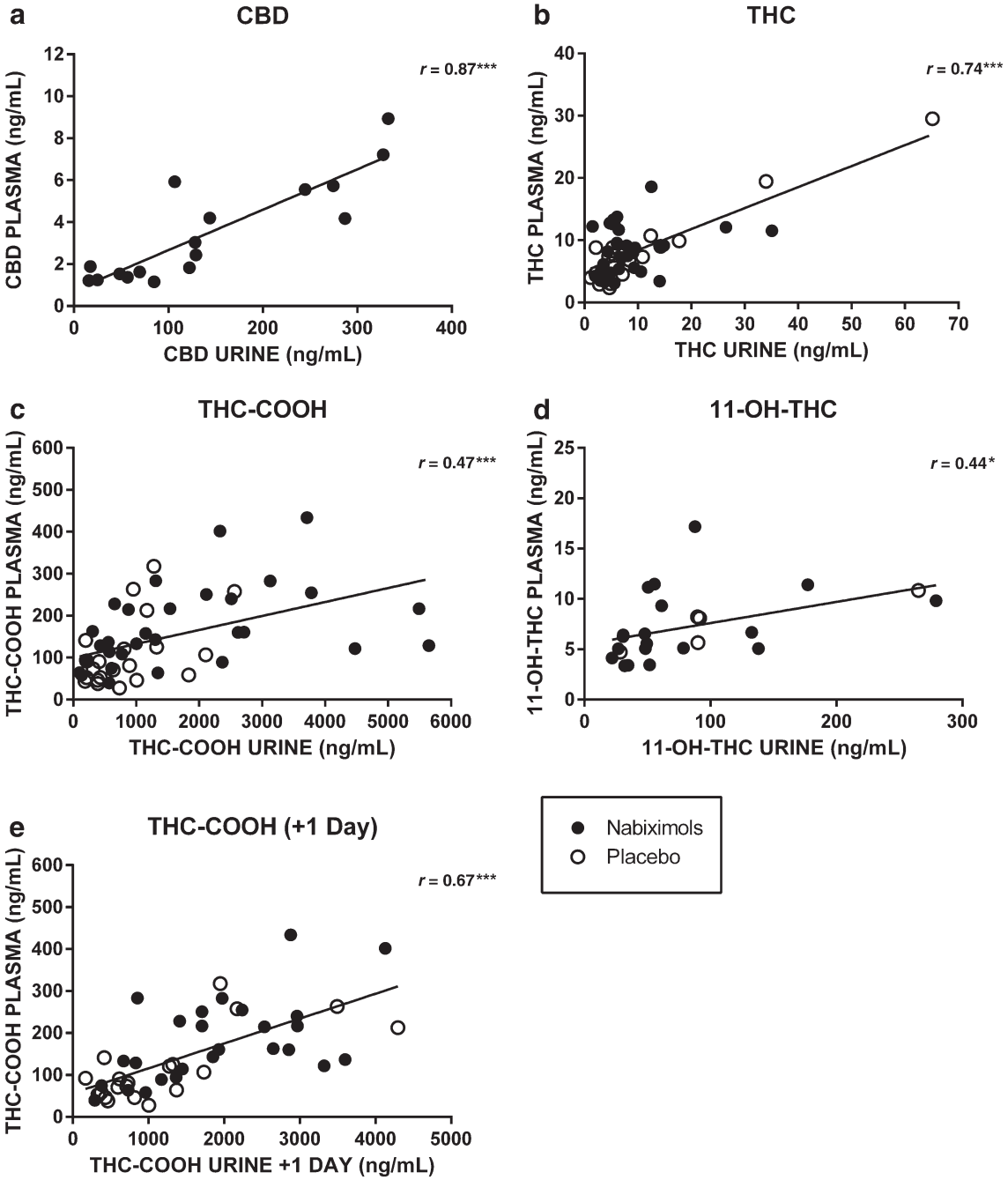

Fig. 3 *Scatter plots* of plasma (non-hydrolysed) and urine (hydrolysed) concentrations of **a** CBD ($n = 17$), **b** THC ($n = 51$), **c** THC-COOH ($n = 51$), and **d** 11-OH-THC ($n = 24$). Data were pooled across treatment groups and across days 1, 3, and 7 (plasma sampling days). *White dots* indicate data from placebo-treated patients; *solid black dots* indicate data from nabiximols-treated participants. The **e** is a THC-COOH *scatter plot* using urinary data from the days following plasma sampling (days 2, 4, and 8; $n = 47$). Only data points where both plasma and urine concentrations were above limits of quantification are included. *Lines* were fitted via linear regression. $^{*}P < 0.05$, $^{***}P < 0.001$

times those in non-hydrolysed urine, similar to the 250-fold increase reported previously [28]. Given that CBD is increasingly recognised as a potential treatment for a variety of conditions, including schizophrenia [17], epilepsy [41], and anxiety [42], this analytical technique could be useful across a range of situations in which CBD itself, or CBD-containing therapeutics such as nabiximols, are being administered.

THC, THC-COOH, and 11-OH-THC concentrations were also amplified by urinary hydrolysis (Fig. 2). We observed a fivefold increase in urinary THC-COOH following hydrolysis, and without the hydrolysis step, urinary

Table 2 Urinary and plasma analyte ratios in nabiximols-treated patients at peak dosing (on day 3)

Patient	THC : CBD		THC-COOH : CBD		11-OH-THC : CBD	
	Urine	Plasma	Urine	Plasma	Urine	Plasma
1	0.06	1.54	19.8	28.0	0.00	1.31
2	0.02	3.07	9.56	116	0.19	3.83
3	0.05	3.35	9.52	72.4	0.36	3.09
4	0.05	2.38	12.0	71.2	0.39	1.83
5	0.13	2.01	20.0	37.9	1.02	1.71
6	0.05	2.11	4.57	67.7	0.62	2.73
7	0.05	2.17	6.11	51.3	0.33	1.56
8	0.27	2.15	31.9	23.1	3.17	1.94
9	0.04	1.84	3.34	17.8	0.39	1.54
10	0.04	4.84	11.4	135	0.40	3.53
11	–[a]	2.13	–[a]	90.5	–[a]	3.83
Range	[0.02–0.27]	[1.54–4.84]	[3.34–31.9]	[17.8–135]	[0–3.17]	[1.31–3.83]
Mean	0.08	2.51	12.8	64.6	0.69	2.45
RSD	9.37	0.37	0.68	0.59	1.33	0.40

THC Δ^9-tetrahydrocannabinol, *CBD* cannabidiol, *THC-COOH* 11-nor-9-carboxy-THC, *11-OH-THC* 11-hydroxy-THC, *RSD* relative standard deviation, calculated as the standard deviation divided by the mean

[a] Urinary data for nabiximols-treated patient 11 on day 3 were unavailable

THC and 11-OH-THC concentrations fell below limits of quantification. Hydrolysed concentrations of both THC-COOH and 11-OH-THC in urine were approximately 10 times those in plasma (Fig. 1), potentially reflecting improved sensitivity for these analytes compared to the standard plasma assay. We also noted that THC-COOH was more concentrated even in non-hydrolysed urine than in plasma (Figs. 1c, 3c), as might be anticipated, given the polarity and long urinary half-life of this metabolite [43, 44]. Thus, although this method is optimised for CBD sensitivity, it also improves the analysis of other major cannabinoid analytes.

Importantly, urinary cannabinoid levels correlated with plasma levels for all analytes (Fig. 3). These correlations were stronger for CBD and THC than for metabolites THC-COOH and 11-OH-THC. Our plasma samples did not undergo hydrolysis; this variability in THC metabolites might arise from differences in the proportion of free and glucuronidated THC-COOH and 11-OH-THC in plasma and urine for some patients, or a delay in excretion of analytes from plasma into urine. Indeed, using urinary data from the days following plasma sampling improved the urine–plasma correlation for THC-COOH (Fig. 3e), although this correction reduced correlations for all other analytes. Creatinine normalisation might improve these correlations overall, but urinary dilution cannot account for the increased variability of THC metabolites compared to CBD and THC, since all analytes would be similarly impacted by dilution. Overall, these correlations suggest that, following suitable hydrolysis procedures, urinary cannabinoid measurement might find use as a proxy for plasma sampling in future clinical trials where CBD or THC are administered, although some correction for a delay in urinary excretion may be necessary for THC-COOH. This may prove useful for a variety of clinical trials where CBD and other cannabinoids are used, such as pediatric epilepsy [45].

There is increasing interest in the use of nabiximols as an agonist substitution therapy to treat persons who are cannabis-dependent [11, 29, 46]. An important technical issue thus arises as to whether any recreational use of smoked or vaporised cannabis (i.e., relapse) taken in addition to nabiximols treatment can be detected analytically, so that treatment efficacy can be accurately discerned. In oral fluid, analysis of cannabinoid ratios can distinguish nabiximols treatment from stand-alone smoked cannabis use via elevated CBD to THC ratios, but additional research is required to determine whether relapse to cannabis smoking in addition to nabiximols treatment can be accurately detected in oral fluid [47]. We have similarly considered the possibility of using urinary cannabinoid ratios to detect such relapse to recreational use during nabiximols treatment. In the current study, levels of CBD on day 1 and in the placebo group across all 9 days were low or negligible, reflecting the common lack of CBD in recreational cannabis consumed by users in multiple countries [33, 48–50]. Initiation of nabiximols therapy corresponds to a sustained increase in urinary CBD levels. It is possible that additional unsanctioned cannabis use during nabiximols treatment may produce a sudden

increase in THC and its metabolites THC-COOH and 11-OH-THC relative to CBD in urine.

However, computation of urinary THC to CBD on day 3 (peak dosing) for nabiximols-treated patients produced a large range of ratios, as was the case for ratios of THC-COOH to CBD and 11-OH-THC to CBD (Table 2). Similar variability was present to a smaller but still substantial extent in ratios calculated from plasma concentrations. These ranges may be too broad for detection of additional cannabis use, although longer-term treatment (i.e., constant nabiximols treatment over several additional days) might produce more consistent ratios. Ongoing studies by our group are aimed at addressing this hypothesis.

There are some caveats to consider. The lack of creatinine-corrected estimates of urinary analytes is a limitation, although the strong correlations between urinary and plasma levels of CBD and THC suggest that the impact of urinary dilution was minor. We were unable to collect plasma every day, due to the invasiveness of daily sampling; we could not calculate meaningful urine–plasma correlations for individual participants. Placebo data were impacted to a greater degree than nabiximols data by patient dropout (Table 1), and while this underscores the efficacy of nabiximols treatment for cannabis withdrawal, it reduced the reliability of placebo data and increased the difficulty in obtaining statistically significant results on later days. It should be noted that the dosing regimen in this study involved high doses of nabiximols, with peak doses at 32 sprays per day (86.4 mg THC, 80 mg CBD), several times higher than doses used in other clinical conditions (e.g., pain, multiple sclerosis) in non-cannabis dependent populations [51]. Replication of this study in patients using lower doses of nabiximols may be warranted. Finally, future studies could examine urinary levels of CBD metabolites (e.g., 7-OH-CBD) in addition to THC metabolites.

Conclusions

This study demonstrates a clinical application of urinary hydrolysis to determine urinary CBD, THC, and THC metabolites over multiple days of nabiximols treatment, which may be applicable to a wide range of emerging THC- and/or CBD-based treatments and clinical trials. Urinary concentrations of CBD, 11-OH-THC, and THC-COOH were greatly improved by hydrolysis with β-glucuronidase compared to the standard plasma assay and to non-hydrolysed urine. Urine and plasma concentrations of CBD, THC, THC-COOH and, to a lesser extent, 11-OH-THC followed similar trajectories that reflected the dosing schedule, suggesting that urine screening using this method may be an appropriate and less invasive proxy for blood testing.

Acknowledgments RCK is supported by an Australian Postgraduate Award. This research was supported by the National Health and Medical Research Council (NHMRC) Project Grant No. 1006036.

Compliance with ethical standards

Conflict of interest The authors declare that they have no conflict of interest.

Ethical approval All procedures performed in studies involving human participants were in accordance with the ethical standards of the institutional and/or national research committee and with the 1964 Declaration of Helsinki and its later amendments or comparable ethical standards.

References

1. Panlilio LV, Goldberg SR, Justinova Z (2015) Cannabinoid abuse and addiction: clinical and preclinical findings. Clin Pharmacol Ther 97:616–627
2. Degenhardt L, Ferrari AJ, Calabria B, Hall WD, Norman RE, McGrath J, Flaxman AD, Engell RE, Freedman GD, Whiteford HA, Vos T (2013) The global epidemiology and contribution of cannabis use and dependence to the global burden of disease: results from the GBD 2010 study. PLoS One 8:e76635. doi:10.1371/journal.pone.0076635
3. Budney AJ, Hughes JR (2006) The cannabis withdrawal syndrome. Curr Opin Psychiatry 19:233–238
4. Allsop DJ, Norberg MM, Copeland J, Fu S, Budney AJ (2011) The cannabis withdrawal scale development: patterns and predictors of cannabis withdrawal and distress. Drug Alcohol Depend 119:123–129
5. Levin KH, Copersino ML, Heishman SJ, Liu F, Kelly DL, Boggs DL, Gorelick DA (2010) Cannabis withdrawal symptoms in non-treatment-seeking adult cannabis smokers. Drug Alcohol Depend 111:120–127
6. Budney AJ, Vandrey RG, Hughes JR, Thostenson JD, Bursac Z (2008) Comparison of cannabis and tobacco withdrawal: severity and contribution to relapse. J Subst Abuse Treat 35:362–368
7. Allsop DJ, Copeland J, Norberg MM, Fu S, Molnar S, Lewis J, Budney AJ (2012) Quantifying the clinical significance of cannabis withdrawal. PLoS One 7:e44864. doi:10.1371/journal.pone.0044864
8. Haney M, Ward AS, Comer SD, Hart CL, Foltin RW, Fischman MW (2001) Bupropion SR worsens mood during marijuana withdrawal in humans. Psychopharmacology 155:171–179
9. Marshall K, Gowing L, Ali R, Le Foll B (2014) Pharmacotherapies for cannabis dependence. Cochrane Database Syst Rev 12:CD008940. doi:10.1002/14651858.CD008940.pub2
10. Balter RE, Cooper ZD, Haney M (2014) Novel pharmacologic approaches to treating cannabis use disorder. Curr Addict Rep 1:137–143
11. Allsop DJ, Lintzeris N, Copeland J, Dunlop A, McGregor IS (2015) Cannabinoid replacement therapy (CRT): nabiximols (Sativex) as a novel treatment for cannabis withdrawal. Clin Pharmacol Ther 97:571–574
12. Budney AJ, Vandrey RG, Hughes JR, Moore BA, Bahrenburg B (2007) Oral delta-9-tetrahydrocannabinol suppresses cannabis withdrawal symptoms. Drug Alcohol Depend 86:22–29

13. Haney M, Cooper ZD, Bedi G, Vosburg SK, Comer SD, Foltin RW (2013) Nabilone decreases marijuana withdrawal and a laboratory measure of marijuana relapse. Neuropsychopharmacology 38:1557–1565
14. Pertwee R (2007) Cannabinoids and multiple sclerosis. Mol Neurobiol 36:45–59
15. Fusar-Poli P, Crippa JA, Bhattacharyya S, Borgwardt SJ, Allen P, Martin-Santos R, Seal M, Surguladze SA, O'Carrol C, Atakan Z, Zuardi AW, McGuire PK (2009) Distinct effects of {delta}9-tetrahydrocannabinol and cannabidiol on neural activation during emotional processing. Arch Gen Psychiatry 66:95–105
16. Morgan CJ, Schafer G, Freeman TP, Curran HV (2010) Impact of cannabidiol on the acute memory and psychotomimetic effects of smoked cannabis: naturalistic study. Br J Psychiatry 197:285–290
17. Zuardi AW, Crippa JA, Hallak JE, Bhattacharyya S, Atakan Z, Martin-Santos R, McGuire PK, Guimaraes FS (2012) A critical review of the antipsychotic effects of cannabidiol: 30 years of a translational investigation. Curr Pharm Des 18:5131–5140
18. Laprairie RB, Bagher AM, Kelly ME, Denovan-Wright EM (2015) Cannabidiol is a negative allosteric modulator of the cannabinoid CB_1 receptor. Br J Pharmacol 172:4790–4805
19. Leweke FM, Piomelli D, Pahlisch F, Muhl D, Gerth CW, Hoyer C, Klosterkötter J, Hellmich M, Koethe D (2012) Cannabidiol enhances anandamide signaling and alleviates psychotic symptoms of schizophrenia. Transl Psychiatr 2:e94. doi:10.1038/tp.2012.15
20. O'Sullivan SE, Kendall DA (2010) Cannabinoid activation of peroxisome proliferator-activated receptors: potential for modulation of inflammatory disease. Immunobiology 215:611–616
21. Iannotti FA, Hill CL, Leo A, Alhusaini A, Soubrane C, Mazzarella E, Russo E, Whalley BJ, Di Marzo V, Stephens GJ (2014) Nonpsychotropic plant cannabinoids, cannabidivarin (CBDV) and cannabidiol (CBD), activate and desensitize transient receptor potential vanilloid 1 (TRPV1) channels in vitro: potential for the treatment of neuronal hyperexcitability. ACS Chem Neurosci 5:1131–1141
22. Hassan S, Eldeeb K, Millns PJ, Bennett AJ, Alexander SPH, Kendall DA (2014) Cannabidiol enhances microglial phagocytosis via transient receptor potential (TRP) channel activation. Br J Pharmacol 171:2426–2439
23. Stout SM, Cimino NM (2014) Exogenous cannabinoids as substrates, inhibitors, and inducers of human drug metabolizing enzymes: a systematic review. Drug Metab Rev 46:86–95
24. Watanabe K, Yamaori S, Funahashi T, Kimura T, Yamamoto I (2007) Cytochrome P450 enzymes involved in the metabolism of tetrahydrocannabinols and cannabinol by human hepatic microsomes. Life Sci 80:1415–1419
25. Williams PL, Moffat AC (1980) Identification in human urine of Δ^9-tetrahydrocannabinol-11-oic acid glucuronide: a tetrahydrocannabinol metabolite. J Pharm Pharmacol 32:445–448
26. Mazur A, Lichti CF, Prather PL, Zielinska AK, Bratton SM, Gallus-Zawada A, Finel M, Miller GP, Radominska-Pandya A, Moran JH (2009) Characterization of human hepatic and extrahepatic UDP-glucuronosyltransferase enzymes involved in the metabolism of classic cannabinoids. Drug Metab Dispos 37:1496–1504
27. Harvey DJ, Mechoulam R (1990) Metabolites of cannabidiol identified in human urine. Xenobiotica 20:303–320
28. Bergamaschi MM, Barnes A, Queiroz RH, Hurd YL, Huestis MA (2013) Impact of enzymatic and alkaline hydrolysis on CBD concentration in urine. Anal Bioanal Chem 405:4679–4689
29. Allsop DJ, Copeland J, Lintzeris N, Dunlop AJ, Montebello M, Sadler C, Rivas GR, Holland RM, Muhleisen P, Norberg MM, Booth J, McGregor IS (2014) Nabiximols as an agonist replacement therapy during cannabis withdrawal: a randomized clinical trial. JAMA Psychiatry 71:281–291
30. Bell ML, Fairclough DL (2014) Practical and statistical issues in missing data for longitudinal patient-reported outcomes. Stat Methods Med Res 23:440–459
31. Hedges LV (1981) Distribution theory for Glass's estimator of effect size and related estimators. J Educ Behav Stat 6:107–128
32. Peters FT, Drummer OH, Musshoff F (2007) Validation of new methods. Forensic Sci Int 165:216–224
33. Swift W, Wong A, Li KM, Arnold JC, McGregor IS (2013) Analysis of cannabis seizures in NSW, Australia: cannabis potency and cannabinoid profile. PLoS One 8:e70052. doi:10.1371/journal.pone.0070052
34. Desrosiers NA, Himes SK, Scheidweiler KB, Concheiro-Guisan M, Gorelick DA, Huestis MA (2014) Phase I and II cannabinoid disposition in blood and plasma of occasional and frequent smokers following controlled smoked cannabis. Clin Chem 60:631–643
35. Grauwiler SB, Scholer A, Drewe J (2007) Development of a LC/MS/MS method for the analysis of cannabinoids in human EDTA-plasma and urine after small doses of *Cannabis sativa* extracts. J Chromatogr B 850:515–522
36. Bergamaschi MM, Karschner EL, Goodwin RS, Scheidweiler KB, Hirvonen J, Queiroz RH, Huestis MA (2013) Impact of prolonged cannabinoid excretion in chronic daily cannabis smokers' blood on per se drugged driving laws. Clin Chem 59:519–526
37. Lemberger L, Tamarkin NR, Axelrod J, Kopin IJ (1971) Delta-9-tetrahydrocannabinol: metabolism and disposition in long-term marihuana smokers. Science 173:72–74
38. McGilveray IJ (2005) Pharmacokinetics of cannabinoids. Pain Res Manag 10(Suppl A):15A–22A
39. Wong A, Keats K, Rooney K, Hicks C, Allsop DJ, Arnold JC, McGregor IS (2014) Fasting and exercise increase plasma cannabinoid levels in THC pre-treated rats: an examination of behavioural consequences. Psychopharmacology 231:3987–3996
40. Johansson E, Noren K, Sjovall J, Halldin MM (1989) Determination of Δ^1-tetrahydrocannabinol in human fat biopsies from marihuana users by gas chromatography-mass spectrometry. Biomed Chromatogr 3:35–38
41. Rosenberg EC, Tsien RW, Whalley BJ, Devinsky O (2015) Cannabinoids and epilepsy. Neurotherapeutics 12:747–768
42. Blessing EM, Steenkamp MM, Manzanares J, Marmar CR (2015) Cannabidiol as a potential treatment for anxiety disorders. Neurotherapeutics 12:825–836
43. Scheidweiler KB, Desrosiers NA, Huestis MA (2012) Simultaneous quantification of free and glucuronidated cannabinoids in human urine by liquid chromatography tandem mass spectrometry. Clin Chim Acta 413:1839–1847
44. Huestis MA, Cone EJ (1998) Urinary excretion half-life of 11-nor-9-carboxy-Δ9-tetrahydrocannabinol in humans. Ther Drug Monit 20:570–576
45. Friedman D, Devinsky O (2015) Cannabinoids in the treatment of epilepsy. N Engl J Med 373:1048–1058
46. Trigo JM, Lagzdins D, Rehm J, Selby P, Gamaleddin I, Fischer B, Barnes AJ, Huestis MA, Le Foll B (2016) Effects of fixed or self-titrated dosages of Sativex on cannabis withdrawal and cravings. Drug Alcohol Depend 161:298–306
47. Lee D, Karschner EL, Milman G, Barnes AJ, Goodwin RS, Huestis MA (2013) Can oral fluid cannabinoid testing monitor medication compliance and/or cannabis smoking during oral THC and oromucosal Sativex administration? Drug Alcohol Depend 130:68–76
48. Bruci Z, Papoutsis I, Athanaselis S, Nikolaou P, Pazari E, Spiliopoulou C, Vyshka G (2012) First systematic evaluation of the potency of *Cannabis sativa* plants grown in Albania. Forensic Sci Int 222:40–46

49. Burgdorf JR, Kilmer B, Pacula RL (2011) Heterogeneity in the composition of marijuana seized in California. Drug Alcohol Depend 117:59–61
50. Tsumura Y, Aoki R, Tokieda Y, Akutsu M, Kawase Y, Kataoka T, Takagi T, Mizuno T, Fukada M, Fujii H, Kurahashi K (2012) A survey of the potency of Japanese illicit cannabis in fiscal year 2010. Forensic Sci Int 221:77–83
51. Novotna A, Mares J, Ratcliffe S, Novakova I, Vachova M, Zapletalova O, Gasperini C, Pozzilli C, Cefaro L, Comi G, Rossi P, Ambler Z, Stelmasiak Z, Erdmann A, Montalban X, Klimek A, Davies P, Sativex Spasticity Study Group (2011) A randomized, double-blind, placebo-controlled, parallel-group, enriched-design study of nabiximols (Sativex®), as add-on therapy, in subjects with refractory spasticity caused by multiple sclerosis. Eur J Neurol 18:1122–1131

Chapter 6. General Discussion

6.1 Chapter overview

The studies presented in this thesis were designed to build further knowledge and understanding in several key areas of cannabinoid research, as reviewed in Chapter 1. Specifically, these studies aimed to:

1. Characterise the *in vivo* potency and basic physiological effects of several synthetic cannabinoids that are in current use as recreational drugs (Chapter 2).

2. Identify structure-activity relationships for aminoalkylindoles and related synthetic cannabinoids using *in vivo* measures (Chapter 2).

3. Establish metabolic pathways and identify valid analytical targets among novel synthetic cannabinoids and their metabolites (Chapter 3).

4. Identify and discuss the discrepancy between *in vitro* and *in vivo* synthetic cannabinoid pharmacokinetic data, where, for example, *in vitro* data predicts rapid clearance while *in vivo* data describes long durations of action (Chapter 3).

5. Explore the long-term residual effects (e.g. cognitive effects, toxicological effects) arising from repeated synthetic cannabinoid exposure in rats (Chapter 4).

6. Establish accurate and practical urinalysis techniques to accompany agonist replacement therapies (involving Δ^9-THC) for cannabis and/or synthetic cannabinoid dependence and withdrawal (Chapter 5).

Overall, the studies presented in Chapters 2, 3, 4 and 5 successfully addressed these aims. The final chapter of the thesis provides a discussion of these studies, and is divided into two main sections. The first section provides a summary and discussion of the primary findings along with limitations and caveats from each experimental chapter. The latter section discusses the wider implications and significance of these findings and provides potential directions for future research.

6.2 Summary of findings

6.2.1 Chapter 2: Physiological dose-response effects of synthetic cannabinoids as measured by biotelemetry

The publications featured in Chapter 2 used adult male rats with surgically implanted radiotelemetric probes to measure the dose-response characteristics of twelve synthetic cannabinoids (JWH-018, AM-2201, UR-144, XLR-11, PB-22, 5F-PB-22, SDB-001, STS-135, AB-PINACA, AB-FUBINACA, 5F-AMB, and MDMB-FUBINACA) on body temperature and heart rate. The molecular structures of these compounds are diverse but interrelated; the list encompasses synthetic cannabinoids with fluorinated and non-fluorinated *N*-pentyl chains, indoles and indazoles, methanone, carboxylate and carboxamide linkers, and a variety of "bulky" groups (Section 1.3.4).

There were several interesting outcomes of this work. First, dose-dependent hypothermia and bradycardia were established for all twelve compounds when delivered via the intraperitoneal route of administration. The *in vivo* dose-response relationships established in Chapter 2 proved useful in choosing doses for subsequent experiments (e.g. Chapter 4). Second, it was observed that bradycardic effects and hypothermic effects occurred over similar timeframes, although bradycardic effects were more subtle and were potentially masked by inherently noisy heart rate data. For screening purposes, body temperature appears to be the superior measure. Finally it was demonstrated that the CB_1 receptor selective antagonist rimonabant, but not the CB_2 receptor selective antagonist SR144528, blocked hypothermia produced by the small subset of these compounds that were subjected to antagonist testing (AB-

PINACA, AB-FUBINACA, 5F-AMB, and MDMB-FUBINACA). This indicates a CB_1 receptor dependent mechanism of action in the hypothermic response.

More generally, these studies enabled preliminary structure-activity relationships (SARs) to be established *in vivo* (Table 1). Of the twelve compounds studied, eight contained an indole core while four contained an indazole core. Overall, the indazoles were more potent both *in vitro* and *in vivo*, suggesting that this structural element confers an increase in efficacy, at least in terms of the classic "tetrad" component of hypothermia. Alternatively, all four indazoles also contained a carboxamide linker, which could also potentially account for their superior potency. However, of the eight indoles, two also contained a carboxamide linker (SDB-001 and STS-135), but neither of these compounds were particularly potent *in vitro* and both required relatively high doses to produce threshold hypothermia *in vivo* (3 and 1 mg/kg, respectively). Thus, the carboxamide linker is probably not the key feature underpinning the greater potency of the indazole/carboxamide compounds *in vivo*. Instead, it is likely that the indazole substituent tends to increase potency compared to the indole moiety.

Interestingly, the effect of fluorination of the *N*-pentyl chain was minimal *in vivo*. Although fluorination increased CB_1 receptor binding activity *in vitro*, there were no consistent differences in elicited hypothermia for fluorinated *versus* non-fluorinated ligands. Although the fluorinated compound XLR-11 was active at lower doses than its non-fluorinated analogue UR-144 in producing hypothermia, as was STS-135 compared to SDB-001, this was not the case for pairings of AM-2201 *versus* JWH-018 or 5F-PB-22 *versus* PB-22. Moreover, the maximal magnitude of hypothermia tended to be similar for fluorinated and non-fluorinated pairs (e.g. JWH-

018 and AM-2201; Chapter 2). This indicates a discrepancy between predictions derived from *in vitro* binding studies and actual *in vivo* hypothermic responses.

Explanation of this discrepancy may require consideration of some of the metabolism results presented in Chapter 3. Specifically, this chapter, and other published studies, indicate that many 5-fluoropentyl synthetic cannabinoids undergo rapid and extensive oxidative defluorination (Chapter 3; Section 6.2.3; Andersson et al., 2016; Grigoryev, Kavanagh, & Melnik, 2013; Sobolevsky, Prasolov, & Rodchenkov, 2012; Wohlfarth et al., 2014). That is, while the 5-fluoropentyl compounds may bind more strongly to CB_1 receptors than their *N*-pentyl counterparts, they may also undergo rapid biotransformation into the corresponding 5-hydroxy metabolite. These metabolites may themselves possess CB_1 receptor binding activity greater than the parent compound (Seely et al., 2012), and are identical to the 5-hydroxy metabolites of the non-fluorinated *N*-pentyl analogues (Chapter 3). This metabolic convergence may contribute to the similarity in *in vivo* efficacy of fluorinated and non-fluorinated pairs. Direct assessment of the physiological effects of some of the 5-hydroxy metabolites using the biotelemetry paradigm could help to better substantiate this hypothesis.

In any case, the effect of fluorination was clearly of smaller magnitude relative to alterations in the "bulky" group, which appears to be a major determinant of potency (Table 1). For example, substitution of the naphthyl group of JWH-018 and AM-2201 for the 2,2,3,3-tetramethylcyclopropyl group of UR-144 and XLR-11 substantially reduced both *in vitro* and *in vivo* potency. Focusing on the indazole carboxamides, a (1*S*)-1-(aminocarbonyl)-2-methylpropyl group (present in AB-PINACA and AB-FUBINACA) confers a small potency increase compared to a methyl

Table 1. Comparison of *in vitro* receptor binding (hCB_1) and *in vivo* hypothermic effects produced by compounds assessed using biotelemetry in Chapter 2.

Compound	Bulky group	Tail	Core	Linker	hCB_1 EC_{50} (nM)	Min. active dose (rat; mg/kg)	Max. hypothermia at 1 mg/kg[#] (°C)
JWH-018[1]	Naphthyl	*N*-pentyl	Indole	Methanone	102	0.3	1.7
AM-2201[1]	Naphthyl	*N*-fluoropentyl	Indole	Methanone	38	0.3	1.0
UR-144[1]	2,2,3,3-tetramethylcyclopropyl	*N*-pentyl	Indole	Methanone	421	10	0.5
XLR-11[1]	2,2,3,3-tetramethylcyclopropyl	*N*-fluoropentyl	Indole	Methanone	98	3	1.0
PB-22[1]	8-quinolinyl	*N*-pentyl	Indole	Carboxylate	5.1	0.3	1.7
5F-PB-22[1]	8-quinolinyl	*N*-fluoropentyl	Indole	Carboxylate	2.8	0.3	1.4
SDB-001[1] (APICA)	Adamantyl	*N*-pentyl	Indole	Carboxamide	128	3	1.4
STS-135[1]	Adamantyl	*N*-fluoropentyl	Indole	Carboxamide	51	1	1.2
AB-PINACA[2]	(1*S*)-1-(aminocarbonyl)-2-methylpropyl	*N*-pentyl	Indazole	Carboxamide	1.2	0.3	1.1
AB-FUBINACA[2]	(1*S*)-1-(aminocarbonyl)-2-methylpropyl	N-(4-fluorobenzyl)	Indazole	Carboxamide	1.8	0.3	1.8
5F-AMB[3]	Methyl isovalerate	*N*-fluoropentyl	Indazole	Carboxamide	1.9	0.1	1.6
MDMB-FUBINACA[3]	Methyl isovalerate	N-(4-fluorobenzyl)	Indazole	Carboxamide	3.9	0.1	1.9

[1] Banister, Stuart, Kevin et al. (2015); [2] Banister, Moir, Stuart et al (2015); [3] Banister, Longworth, Kevin et al. (2016)

[#] 1 mg/kg selected for comparison because this dose was tested for all compounds.

isovalerate group (5F-AMB and MDMB-FUBINACA). Other relevant examples are provided in Table 1.

Interestingly, JWH-018 and AM-2201 were more potent *in vivo* than might be expected given their *in vitro* binding profile at CB_1 receptors. For example, JWH-018 acts on human CB_1 receptors with an EC_{50} of 102 nM, but only requires a dose of 0.3 mg/kg to produce hypothermia in rats, and produces very substantial hypothermia at higher doses (Chapter 2; Table 1). Consider that AB-PINACA, which is far more potent at human CB_1 (EC_{50} 1.2 nM), also required a dose of 0.3 mg/kg to elicit hypothermia and produced a lesser maximal hypothermic effect compared to JWH-018 at 1 mg/kg.

One possibility is that human CB_1 receptors could differ markedly from rat CB_1 receptors in terms of binding activity for JWH-018 and AM-2201. However, human and rat CB_1 receptors are 90% identical in terms of nucleotide sequence and are 98% identical in amino acid sequence (Gerard et al., 1990), indicating high receptor homology. Alternatively, JWH-018 metabolites are known to retain *in vitro* and *in vivo* affinity and activity at CB_1 receptors (Brents et al., 2011). AM-2201 can also form some of these metabolites via oxidative defluorination (Hutter et al., 2013). These CB_1 receptor active metabolites could potentially contribute to the unexpected *in vivo* potency of JWH-018 and AM-2201. However, it should be noted that some JWH-018 metabolites appear to be antagonists or neutral antagonists at CB_1 receptors (Seely et al., 2012). So, to the extent that metabolites are responsible for this effect, it probably occurs via a complex interaction between several metabolites.

The 2,2,3,3-tetramethylcyclopropyl bulky group of UR-144 and XLR-11 was associated with a smaller magnitude hypothermia than that obtained with close analogues. Similarly, the human CB_1 receptor potency of these two compounds was

low (UR-144 EC_{50}: 421 nM; XLR-11 EC_{50}: 98 nM), particularly for UR-144 which had an EC_{50} that was weaker than all of the other compounds tested in Chapter 2. This was surprising because UR-144 and XLR-11 have been very popular among users in recent years and are anecdotally reported as strongly efficacious (NFILS, 2015).

This discrepancy may be explained by consideration of active metabolites or thermal degradants formed during consumption of UR-144 and XLR-11 (Section 1.4.4). In our biotelemetric assessments, we injected UR-144 and XLR-11 intraperitoneally, but human consumption occurs via inhalation after these compounds are heated to high temperatures. UR-144 and XLR-11 form ring-opened thermal degradants upon heating, which possess human CB_1 binding 4.6– to 8-fold higher than the parent compounds, and substitute for JWH-018 as a discriminative stimulus in the drug discrimination paradigm in laboratory mice (Thomas et al., 2017). Therefore, future studies using intraperitoneal injection should consider thermal degradants before arriving at firm conclusions regarding the translation of results into human populations.

A caveat worth noting is that the hypothermic and bradycardic effects observed in Chapter 2 do not necessarily correspond to human psychoactive effects. It is assumed that the CB_1-mediated hypothermic effects in rats would strongly correlate with CB_1-mediated intoxication in humans, but this remains an assumption and is an inherent limitation of this experimental approach. It is therefore encouraging to note that drug discrimination studies have indicated that mice appear to experience the effects of synthetic cannabinoids as being similar to those of Δ^9-THC, or well-established psychoactive synthetic cannabinoids like JWH-018. For example, AB-PINACA substitutes for Δ^9-THC at 3 mg/kg (Wiley et al., 2015), a dose at which we observed substantial hypothermia. Similarly, as mentioned above, UR-144 and XLR-11

ring-opened thermal degradants substitute for JWH-018 (Thomas et al., 2017), indicating a similar subjective effect.

To summarise, the work presented in Chapter 2:

1. Established that a variety of modern synthetic cannabinoids are tolerated and efficacious in rats at an intraperitoneal dose between 0.1 and 3 mg/kg, but in some cases doses of up to 10 mg/kg are required for substantial hypothermia.

2. Found that terminal fluorination of the *N*-pentyl chain of indole or indazole synthetic cannabinoids will generally increase CB_1 receptor efficacy and potency *in vitro*. However, this is not always reflected in potency observed *in vivo*, at least in terms of hypothermic and bradycardic effects. This could be due to rapid and converging metabolic transformations, particularly oxidative defluorination.

3. Showed that indazole synthetic cannabinoids appear to be more potent both *in vitro* and *in vivo* than indole synthetic cannabinoids.

4. Established that the composition of the "bulky" group has a substantial influence on both *in vitro* and *in vivo* potency.

5. Suggests that in some cases, consideration of thermal degradants may be necessary before translation of results into human populations. For example, the potency of UR-144 and XLR-11 may be underestimated by using intraperitoneal injection as the route of administration as opposed to heating and inhalation, which can produce thermolytic products that may bind strongly to CB_1 receptors.

6.2.2 Chapter 3: *In vitro* and *in vivo* pharmacokinetics and metabolism of synthetic cannabinoids CUMYL-PICA and 5F-CUMYL-PICA

In Chapter 3, two carboxamide synthetic cannabinoids, CUMYL-PICA and 5F-CUMYL-PICA, were incubated with rat and human liver microsomes and hepatocytes *in vitro*. These microsome and hepatocyte incubations were used to generate basic pharmacokinetic parameters including half-life and clearance rate of the parent compound, and to establish metabolic pathways, respectively, through identification of metabolites. Additionally, CUMYL-PICA and 5F-CUMYL-PICA were administered to rats (at 3 mg/kg, i.p.) in order to compare the results obtained *in vitro* with pharmacokinetic and metabolic results obtained *in vivo*. Hypothermia was also quantified as a characteristic cannabinoid effect using rectal body temperature. This study was performed with the aim of establishing valid analytical targets to allow detection of consumption of CUMYL-PICA and 5F-CUMYL-PICA in humans. This could be of use in future studies (e.g. characterisation of metabolites in other matrices like hair or adipose tissue), in emergency medicine (e.g. identification of these compounds following episodes of toxicity), in the forensic context (e.g. in deaths associated with synthetic cannabinoid use), or for confirming cessation of drug use during treatment programmes, discussed further in Section 6.3.3.

Chapter 3 proposed specific metabolic pathways for CUMYL-PICA and 5F-CUMYL-PICA which involved extensive phase I oxidative transformations followed by phase II glucuronidation. In particular, CUMYL-PICA was terminally hydroxylated on the *N*-pentyl chain (nominally forming 5-OH-CUMYL-PICA), while 5F-CUMYL-PICA was oxidatively defluorinated to form the same metabolite. 5-OH-CUMYL-PICA was then further oxidised to a carboxylic acid metabolite. This metabolic convergence may

cause difficulty in differentiating CUMYL-PICA and 5F-CUMYL-PICA in biological samples, so other hydroxylated metabolites were identified as potentially useful analytical targets.

The metabolic transformations detailed in Chapter 3 are in agreement with metabolic data concerning other synthetic cannabinoids. For example, oxidative defluorination of the 5-fluoropentyl chain is also a major metabolic pathway for AM-2201, XLR-11, 5F-PB-22, 5F-AMB, and AM-694 (Andersson et al., 2016; Grigoryev et al., 2013; Sobolevsky et al., 2012; Wohlfarth et al., 2014). Additionally, it was noted that human and rat metabolic processes for CUMYL-PICA and 5F-CUMYL-PICA were similar, except that human hepatocytes generally failed to produce oxidations on the α,α-dimethylbenzyl moiety. Besides glucuronidation, no other phase II transformations, such as sulphation or acetylation, were observed in Chapter 3.

It is noteworthy, although quite possibly coincidental, that metabolism of phytocannabinoids occurs in much the same way. For example, Δ^9-THC is oxidised to 11-OH-THC and then to THC-COOH, which is subsequently glucuronidated. In contrast to Δ^9-THC metabolism, the specific metabolic enzymes responsible for synthetic cannabinoid metabolism remain largely uncharacterised. One exception is the case of the carboxamide synthetic cannabinoids (AB-PINACA, AB-FUBINACA, PB-22, and 5F-PB-22) which are primarily metabolised by carboxylesterase 1. This is very different to the cytochrome p450 (CYP)-dominated (e.g. CYP 2C9 and 2C19 isoenzymes) metabolism of Δ^9-THC (Thomsen et al., 2014).

The research presented in Chapter 3 focused on identification of metabolites in order to understand overall metabolic pathways and to identify useful analytical targets, rather than on identification of specific metabolic enzymes. Future studies

could focus on identifying relevant enzymes using specific microsomal isoforms. Such data could be used to better understand potential drug-drug interactions. For example, synthetic cannabinoids might inhibit or induce key enzymes responsible for the metabolism of other drugs (e.g. illicit drugs, prescription medications, natural products), potentially leading to toxicity in humans. In support of this hypothesis, a very recent study shows that AM-2201 can inhibit several CYP enzymes, specifically CYP 2C8, 2C9 and 3A4 (Kim et al., 2017), which are involved in the metabolism of a wide array of drugs and medications. Similar assessment of newer synthetic cannabinoids could prove valuable.

A key finding from Chapter 3 was that the clearance rates predicted by microsomal incubations were substantially more rapid than the results obtained from actual *in vivo* experiments in rats. Prior studies using microsomal incubation to generate kinetic parameters have also reported rapid clearance: for example, the half-lives of AMB and 5F-AMB were reported as 1.1 and 1.0 min, respectively (Andersson et al., 2016). As discussed in Chapter 3, sequestration of synthetic cannabinoids into adipose tissue and subsequent release into blood over time may delay elimination *in vivo* (Gunasekaran et al., 2009; Hasegawa et al., 2015; Johansson et al., 1989). Alternatively, or additionally, plasma protein binding may also account for this delay. Protein binding is presently uncharacterised for CUMYL-PICA, 5F-CUMYL-PICA, and most modern synthetic cannabinoids, and could be a key factor mediating long elimination times *in vivo*. Regardless of mechanism, these data highlight the need for careful comparisons of *in vivo* and *in vitro* pharmacokinetic data in ongoing studies with synthetic cannabinoids.

The hypothermic effects of CUMYL-PICA and 5F-CUMYL-PICA were largely as expected; a decrease of 2-3 °C and a return to baseline approximately 8 hours later. Compared to the biotelemetry data reported in Chapter 2, CUMYL-PICA and 5F-CUMYL-PICA were approximately as potent *in vivo* as AB-FUBINACA, PB-22, and 5F-PB-22. Further assessment of CUMYL-PICA and 5F-CUMYL-PICA at other doses (*i.e.* 0.3 mg/kg and 1 mg/kg) using the biotelemetry paradigm could prove informative.

In sum, the study presented in Chapter 3:

1. Identified the major and minor metabolic pathways for CUMYL-PICA and 5F-CUMYL-PICA.

2. Quantified the hypothermia produced by CUMYL-PICA and 5F-CUMYL-PICA in rats at a dose of 3 mg/kg i.p.

3. Established analytical methods for the measurement of CUMYL-PICA, 5F-CUMYL-PICA, and metabolites in blood and urine, and identified useful analytes for future clinical and forensic purposes.

4. Compared *in vitro* kinetic predictions with *in vivo* data, finding that *in vitro* data overestimated *in vivo* drug elimination, possibly due to sequestration of compounds in adipose tissue and/or due to protein binding.

6.2.3 Chapter 4: Acute and residual effects in adolescent rats resulting from exposure to the novel synthetic cannabinoids AB-PINACA and AB-FUBINACA

While Chapters 2 and 3 focused on the immediate physiological effects and metabolism of synthetic cannabinoids, Chapter 4 featured an exploratory study primarily concerned with identification of long-term (residual) effects produced by

repeated use of synthetic cannabinoids AB-PINACA and AB-FUBINACA. In this study, adolescent rats were employed in recognition of the predominance of the late adolescent/early adulthood age group among synthetic cannabinoid users (Winstock & Barratt, 2013). The rats were dosed every second day for two weeks to partially mimic patterns of chronic or sub-chronic use in humans.

The primary findings of this work were that AB-PINACA, AB-FUBINACA, and Δ^9-THC produced substantial and lasting recognition memory impairments. These impairments were most severe following AB-FUBINACA treatment. It was notable that a long-term residual deficit was seen in social interaction in rats following Δ^9-THC pre-treatment, but not with either of the two synthetic cannabinoids. Other findings included that AB-FUBINACA caused lasting changes in plasma cytokine concentrations, and that AB-PINACA and Δ^9-THC caused lasting residual changes in cerebellar endocannabinoids. Overall, it was notable that the three cannabinoid compounds produced similar acute effects, and, as with Chapters 2 and 3, no serious or unique toxicity was observed with synthetic cannabinoids.

AB-PINACA and AB-FUBINACA produced typical cannabimimetic effects during acute administration, including reduced locomotor activity, increased anxiety-like behaviour, and an inhibition of body weight gain. Similar effects have been observed following administration of Δ^9-THC, CP-55,940, and JWH-018 (Arevalo, de Miguel, & Hernandez-Tristan, 2001; Macri et al., 2013). Locomotor suppression has also been reported with AB-PINACA, AB-CHMINACA and FUBIMINA in mice (Wiley et al., 2015). Although these acute effects were expected given previous reports, observation of these effects following AB-PINACA and AB-FUBINACA served as

preliminary confirmation that these compounds were representative of the wide variety of synthetic cannabinoids used by humans.

During acute dosing with the cannabinoids, perhaps the most intriguing finding was that although AB-PINACA, AB-FUBINACA, and Δ^9-THC increased anxiety-like behaviours, none of the compounds produced conditioned place aversion. Several potential factors underlying this observation were identified in the discussion of Chapter 4 (Section 4.5). It is possible that adolescent rats are less sensitive to the aversive effects of cannabinoids, such that memory deficits could impair acquisition of conditioned place aversion, or that lower doses might have been more effective in producing aversion. Clearly, future studies that explore repeated synthetic cannabinoid administration using a more extensive dose range, or with adult rats for comparison with adolescents, could be enlightening.

Of the residual effects, of particular note were the lasting recognition memory impairments produced by AB-PINACA, AB-FUBINACA, and Δ^9-THC. These impairments were most severe for AB-FUBINACA. Similar lasting residual impairment to recognition memory has been previously reported for CP-55,940 and Δ^9-THC (O'Shea, McGregor, & Mallet, 2006; O'Shea et al., 2004; Quinn et al., 2008). Given that the hippocampus and perirhinal cortex have been implicated in recognition memory impairment (Barker & Warburton, 2011; Bussey, Muir, & Aggleton, 1999; Norman & Eacott, 2004), histological assessment of these areas following sub-chronic synthetic cannabinoid administration could prove instructive. Subtle endocannabinoid modulation was also observed following AB-PINACA and Δ^9-THC administration, which may point to long-term homeostatic compensations in the endocannabinoid system resulting from the repeated use synthetic cannabinoids.

Interestingly, neither AB-PINACA nor AB-FUBINACA produced any obvious toxicity in any animal. No animals showed signs of distress between drug doses (e.g. abnormal gait, coat abnormalities, seizures, etc). Indeed, no clear toxicity was observed in any animal tested with any of the compounds in Chapters 2, 3 or 4. This is in stark contrast with numerous case studies that detail toxicity arising from synthetic cannabinoid use (Adams et al., 2017; Bhanushali et al., 2012; Hermanns-Clausen et al., 2012; Khan et al., 2016; Lapoint et al., 2011; Louh & Freeman, 2014; Mir et al., 2011; Schneir, Cullen, & Ly, 2011; Schwartz et al., 2015; Thornton et al., 2013). In the case of the biotelemetry assessments, the dosing regimen was selected to minimise potential harms (e.g. the ascending dose sequence), which may have reduced the likelihood of observing any toxic outcomes. Conversely, human case studies may reflect only the most severe cases following admittance to emergency departments, representing only a tiny and perhaps atypical minority of synthetic cannabinoid users in the community. It is also possible that animal toxicity is very transient, much as is reported in case studies where adverse symptoms in users often quickly dissipate, or are too subtle and hidden to observe (for example, minor kidney damage). Accordingly, to deconvolute these potential factors, an experiment examining kidney damage and neurotoxicity following AB-PINACA and AB-FUBINACA is presently ongoing in our laboratory.

In sum, the study presented in Chapter 4:

1. Confirmed acute Δ^9-THC-like cannabimimetic effects following administration of AB-PINACA and AB-FUBINACA.

2. Identified lasting recognition memory deficits with all three cannabinoid pre-treatments, which were most severe for AB-FUBINACA pre-treated rats.

3. Identified subtle modulations in cytokine and endocannabinoid concentrations that persisted in the long-term (at least six weeks) and varied across treatments. The functional significance of these is unclear at present.

4. Noted that the psychopharmacological effects of dose-matched Δ^9-THC, AB-PINACA, and AB-FUBINACA were largely similar, and that contrary to human case-reports, no obvious toxicity was observed. A follow-up study concerning acute and residual toxic effects in brain and kidney may clarify this issue.

6.2.4 Chapter 5: Urinary cannabinoid levels during nabiximols (Sativex®)-medicated inpatient cannabis withdrawal

Chapter 5 presented an analysis of cannabinoid concentrations in the plasma and urine of twenty-two inpatients being treated for cannabis dependence and associated withdrawal symptoms with nabiximols (Sativex™) substitution therapy. Nabiximols comprises a 1:1 mix of Δ^9-THC and CBD, and is administered as a buccal spray. The dosing protocol used in the study involved relatively strong doses (peaking at daily doses of 86.4 mg THC and 80 mg CBD on days 2 and 3) before tapering to zero by treatment day 7. Blood was taken from patients on treatment days 1, 3 and 7, while urine was sampled daily (days 1 – 9). Importantly, the study was conducted in an inpatient setting to obviate unsanctioned use of cannabis or other drugs.

The primary outcome of Chapter 5 was the clinical validation of a cannabinoid urinalysis method involving β-glucuronidase hydrolysis. Plasma and urinary CBD, Δ^9-THC, THC-COOH, and 11-OH-THC concentrations closely reflected the dosing schedule and could be used to monitor or titrate dosing. Indeed, the results indicated that doses of nabiximols could probably be reduced slightly in future studies, given

that concentrations of Δ^9-THC and 11-OH-THC rose above initial values during the early stages of treatment (Appendix 2; Fig. S1). Additionally, the placebo group was useful for characterising elimination periods of analytes following heavy cannabis use, although elimination of Δ^9-THC and THC-COOH was incomplete over the course of the study. Blood and urine concentrations of these Δ^9-THC and THC-COOH remained above detection thresholds at the end of the inpatient period (day 9).

A key finding was that plasma concentrations of CBD and Δ^9-THC were positively and strongly correlated with urinary concentrations, providing evidence that cannabinoid urinalysis is a valid alternative to assays involving whole blood or plasma analysis. However, plasma and urinary Δ^9-THC metabolite concentrations were less well correlated, and it was necessary to adjust results and interpose a urinary delay of one day in order to achieve a moderate urine-plasma correlation for THC-COOH. Nevertheless, urine sampling is potentially advantageous as it is less invasive than blood sampling, and urinary concentrations of all analytes were greater than in plasma following hydrolysis. Urinary sampling could enable cannabinoid analysis using less sensitive instruments, or analysis of trace cannabinoids where plasma concentrations fall below limits of detection or quantitation.

The value of β-glucuronidase hydrolysis was also empirically demonstrated over several days of treatment. Without hydrolysis, concentrations of 11-OH-THC and Δ^9-THC often fell below limits of detection or quantitation. THC-COOH and CBD concentrations were also much lower. Given that synthetic cannabinoids are also extensively glucuronidated (Chapter 3; Andersson et al., 2016; Diao et al., 2016; Kavanagh, Grigoryev, & Krupina, 2017), this technique may prove valuable for

boosting detection of synthetic cannabinoids in urine. This possibility is discussed further in Section 6.3.3.

In sum, the study presented in Chapter 5:

1. Clinically validated a cannabinoid urinalysis method for monitoring nabiximols treatment of cannabis dependent inpatients

2. Validated cannabinoid urinalysis as an alternative to blood analysis in a clinical population and inpatient setting, which could be used in conjunction with the methodology presented in Chapter 3 for the monitoring of patients undergoing synthetic cannabinoid withdrawal (see Section 6.3.3).

3. Demonstrated that urinary cannabinoid concentrations (following hydrolysis) are substantially greater than plasma concentrations, such that urine may be useful for detecting trace concentrations of cannabinoids that may otherwise go undetected.

4. Demonstrated the utility of β-glucuronidase hydrolysis for increasing analyte concentrations, which may be a similarly useful technique to apply to detection and quantification of synthetic cannabinoids and their metabolites in urine.

6.3 Wider implications and future directions

6.3.1 Potency and metabolism prediction based on molecular structure

The rate at which novel psychoactive substances are being detected by monitoring agencies has arguably outstripped the rate at which regulators, researchers and forensic chemists can respond meaningfully to their threat. Between 2009 and 2015, 157 novel synthetic cannabinoids were detected in recreational products in Europe alone, in addition to 93 novel cathinones, 58 novel phenethylamines, and over 100 novel compounds belonging to several other drug classes (EMCDDA, 2016). The delay between when a compound is first discovered in recreational products and when that compound is characterised pharmacologically creates a window during which many people may be exposed to a compound with unknown potency, metabolism, and toxicity. Therefore, tools for predicting these key attributes may be of vital importance. Predictive tools could help to ease the burden of testing large numbers of newly discovered compounds, allowing researchers to focus on the most recent or the most toxic discoveries.

For example, it may be possible to use SARs to predict potency of novel synthetic cannabinoids. Based on the results presented in Chapter 2, pairs of 5-fluoropentyl and *N*-pentyl synthetic cannabinoids appear to produce similar physiological effects *in vivo*, at least in terms of body temperature and heart rate. In future, researchers could prioritise screening only one compound in each pair, predicting that *in vivo* efficacy will be similar for the remaining compound. Similarly, a newly discovered indazole synthetic cannabinoid could be predicted to possess somewhat higher potency *in vivo* compared to its indole analogue. Of course, in cases where a particular compound becomes popular in recreational products, or when a

compound appears anomalously potent compared to predictions, it could be prioritised for confirmatory screening.

The rate at which researchers can characterise the metabolites of novel synthetic cannabinoids also appears to be much slower than the rate of emergence of novel compounds. Therefore, predictive tools for synthetic cannabinoid metabolism and identification of likely metabolites of a parent molecule may be of value. Fortunately, metabolic pathways have already been identified for a variety of synthetic cannabinoids, as described in Chapter 3 and the broader literature (Table 2). Similar to the SARs identified in Chapter 2, structure-metabolism relationships (SMRs) are of potential future utility in clinical and forensic settings.

For example, the primary metabolic pathway for synthetic cannabinoids with an *N*-pentyl chain tends to be terminal hydroxylation of that chain (Table 2). Similarly, synthetic cannabinoids possessing a 5-fluoropentyl chain are usually oxidatively defluorinated, forming an identical metabolite to their non-fluorinated counterparts. It seems reasonable to predict that these metabolic patterns will continue for newly identified synthetic cannabinoids with *N*-pentyl or 5-fluoropentyl moieties. In this case, these compounds could be forensically identified (although not necessarily differentiated from each other) using 5-hydroxyl metabolites even before they are characterised via metabolic studies.

Similarly, synthetic cannabinoids with ester moieties are de-esterified to carboxylic acid metabolites (Table 2). This transformation is generally the predominant metabolic pathway, such that these carboxylic acid metabolites are potentially useful forensic markers. A practical example of this metabolite prediction can be found in a recent study that identified an AMB-FUBINACA metabolite in

Table 2. Proposed structure-metabolism relationships based on common structural elements found in synthetic cannabinoids

Structural element	Common metabolic transformation(s)	Example compounds	References
N-pentyl chain	Terminal hydroxylation + carboxylation; hydroxylation; dehydrogenation; dealkylation	AB-001, JWH-018, UR-144, PB-22, CUMYL-PICA, AMB, SDB-006	Chapter 3; Andersson et al. (2016); Grigoryev, Kavanagh, and Melnik (2012); Sobolevsky, Prasolov, and Rodchenkov (2010); Sobolevsky et al. (2012); Wohlfarth et al. (2014)
5-fluoropentyl chain	Oxidative fluorination; dealkylation	AM-2201, XLR-11, 5F-PB-22, 5F-CUMYL-PICA, 5F-AMB, AM-694	Chapter 3; Andersson et al. (2016); Grigoryev et al. (2013); Sobolevsky et al. (2012); Wohlfarth et al. (2014)
Indole core	Hydroxylation	JWH-018, AM-2201, CUMYL-PICA, 5F-CUMYL-PICA	Chapter 3; Sobolevsky et al. (2010)
Indazole core	Hydroxylation	AMB, 5F-AMB, AMB-FUBINACA, MDMB-FUBINACA	Andersson et al. (2016); Kavanagh et al. (2017)
Terminal carboxamide	Deamination to carboxylic acid	AB-PINACA, AB-FUBINACA	Thomsen et al. (2014); Vikingsson et al. (2015)
Linker carboxamide	Cleavage to amide OR no transformation (Figure 1)	AB-PINACA, AB-FUBINACA, MDMB-FUBINACA, CUMYL-PICA, 5F-CUMYL-PICA	Chapter 3; Diao et al. (2017); Thomsen et al. (2014); Vikingsson et al. (2015)
Ester	De-esterification to carboxylic acid	AMB, 5F-AMB, PB-22, 5F-PB-22, AMB-FUBINACA, MDMB-FUBINACA	Andersson et al. (2016); Kavanagh et al. (2017); Wohlfarth et al. (2014)
4-fluorobenzyl	Hydroxylation (benzene ring); no defluorination	AMB-FUBINACA, MDMB-FUBINACA, AB-FUBINACA	Kavanagh et al. (2017)

multiple blood and urine samples following a mass intoxication in New York City produced by a specific synthetic cannabinoid product (Adams et al., 2017). This study used the de-esterified carboxylic acid metabolite of AMB-FUBINACA as a forensic target. At the time, this metabolite had not been identified in the scientific literature, but similar de-esterified carboxylic acid metabolites were known for AMB and 5F-AMB (Andersson et al., 2016). In this way, SMR-based prediction of synthetic cannabinoid metabolism has the potential to speed detection of novel synthetic cannabinoids in forensic and clinical settings, providing important information regarding novel products associated with a distinctive and localised toxidrome.

However, in some cases complex interactions between structural elements may increase the difficulty of metabolite prediction. For example, when a carboxamide group is present as a linker (as in CUMYL-PICA and 5F-CUMYL-PICA, as opposed to when it is also located terminally, as in AB-PINACA), it is only converted to the corresponding amide in some circumstances (Figure 1). In Chapter 3, no such transformation was observed for CUMYL-PICA or 5F-CUMYL-PICA, nor has it been reported for AB-PINACA or AB-FUBINACA (Takayama et al., 2014; Thomsen et al., 2014). However this transformation is observed for SDB-006, ADB-FUBINACA, and MDMB-FUBINACA (Diao et al., 2017; Kavanagh et al., 2017). Given that SDB-006 only differs from CUMYL-PICA in “bulky” group composition, it seems that an interaction between the bulky group and catabolic enzymes determines whether this specific transformation occurs on the linking group. This is presently difficult to predict for novel compounds, but further research into the metabolism of carboxamide synthetic cannabinoids may reveal the mechanism behind this selective pattern of metabolic transformation.

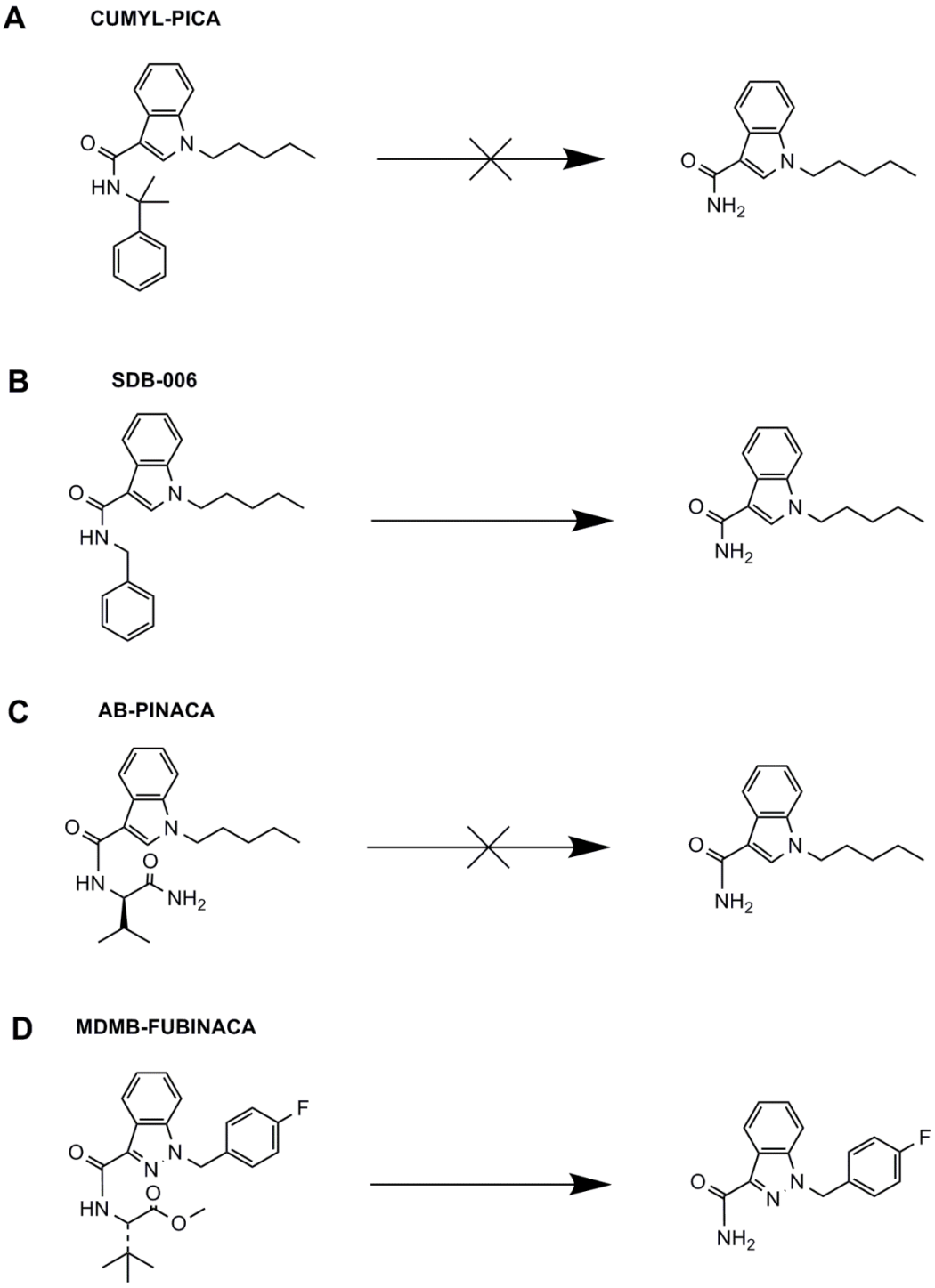

Figure 1. *In some cases, metabolic biotransformations can be difficult to predict. The linking carboxamide group in (B) SDB-006 and (D) MDMB-FUBINACA is converted to the corresponding amide, but this transformation is not observed for (A) CUMYL-PICA and (C) AB-PINACA. Interactions between the "bulky" group and catabolic enzymes presumably produce this pattern. See text for further detail.*

By combining the present understanding of SARs and SMRs, a simplified testing scheme can be proposed, as detailed in Figure 2. Under this scheme, rather than testing each and every novel compound, new compounds are first compared to existing ones. If SARs or SMRs are unknown, the new compound can be prioritised for testing. Otherwise, they are assumed to possess properties based on established SARs or SMRs and other more structurally unique or popular compounds can be prioritised. Further research that characterises or clarifies additional SARs/SMRs may be valuable in this regard. In cases where a compound is unexpectedly potent, has many thermolytic degradants, or presents potentially hazardous drug-drug interactions, it may require additional consideration.

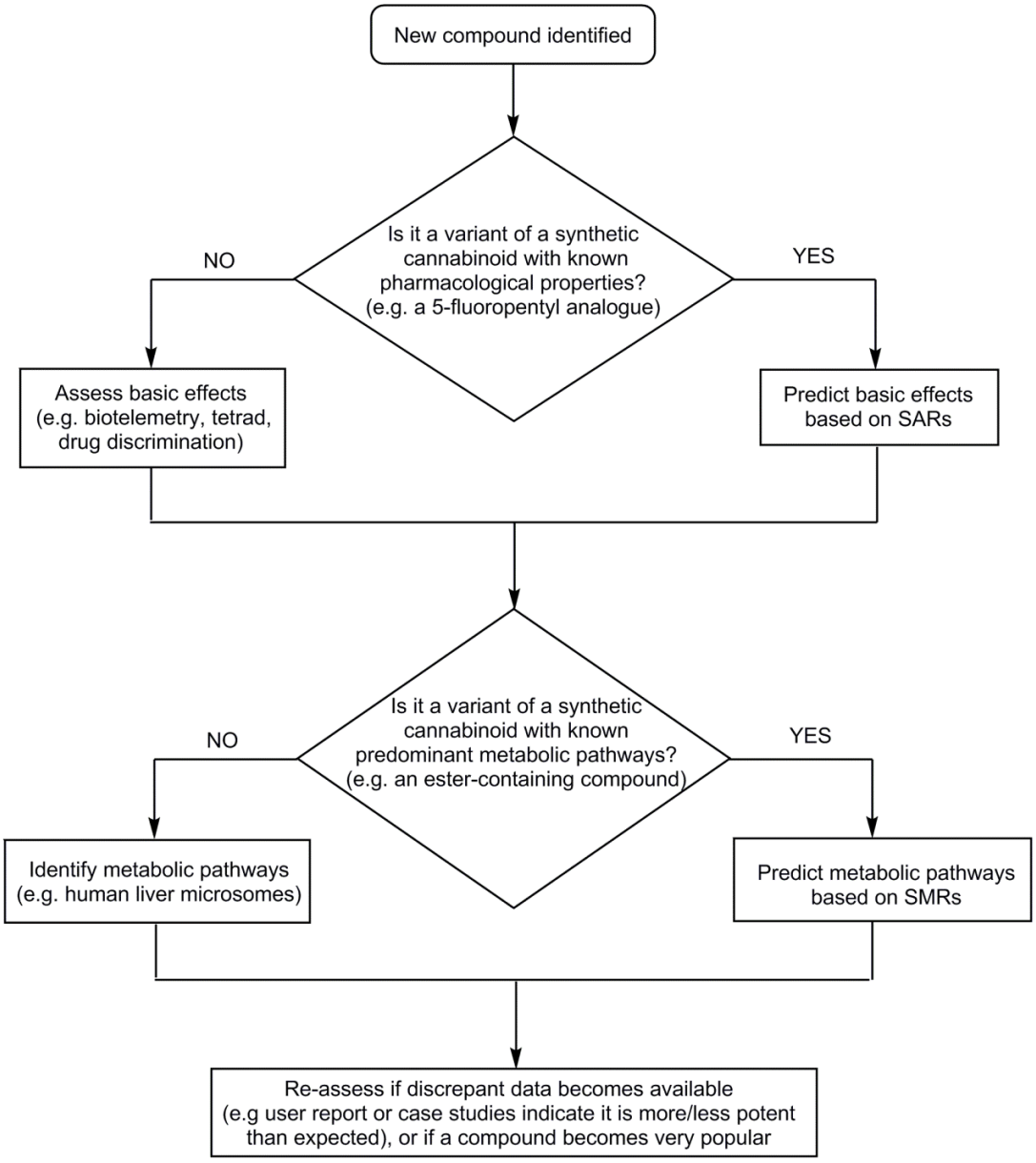

Figure 2. *Flow chart for the streamlined testing of novel synthetic cannabinoids. Under this scheme, the properties of new synthetic cannabinoids are predicted based on shared structural elements, unless discrepant data becomes available or a compound becomes particularly popular. Potential influences of thermolytic degradation or polydrug use may also require consideration.*

6.3.2 Implications of chronic use of synthetic cannabinoids

The long-term effects of synthetic cannabinoid administration identified in Chapter 4 persisted well beyond the period of drug administration. Therefore, treatment of chronic synthetic cannabinoid users may require consideration of lasting residual effects in addition to acute symptomology. Drug treatment and rehabilitation programs may need to consider the possibility that a person may test negative on drug screens (i.e. synthetic cannabinoids undetectable in blood or urine), yet suffer from lasting impairment or emotional disturbances resulting from prior use. Neuropsychological assessments during the treatment and rehabilitation of chronic synthetic cannabinoid users might determine whether cognitive function slowly improves with abstinence.

This of course assumes that the results of Chapter 4 will translate from rodent models into human populations. In this regard, it is worth noting that a very recent study found impaired executive function (assessed via the Stroop test, *n*-back task, and free-recall memory tasks) in synthetic cannabinoid users relative to both recreational cannabis users and non-users (Cohen et al., 2017). Thus, the preclinical findings concerning impaired recognition memory in Chapter 4 may well be an accurate portrait of impairments in human users.

A consistent finding from Chapter 4 and the wider cannabinoid literature is that adolescents are more vulnerable than adults to deleterious cognitive effects produced by synthetic cannabinoids and Δ^9-THC. For example, chronic CP-55,940 or Δ^9-THC administration during adolescence impairs social interaction and working memory to a greater degree than in rats treated during adulthood (O'Shea et al., 2004; Quinn et al., 2008). Future studies that specifically include adolescent human

populations of synthetic cannabinoid users could be particularly valuable in assessing potential long-term adverse effects of these drugs at this vulnerable developmental stage.

Additionally, the inhibitory effect of AB-FUBINACA (and possibly other synthetic cannabinoids) on pro-inflammatory cytokines uncovered in Chapter 4 is worthy of further investigation. In particular, it would be interesting to verify whether these cytokines are also elevated acutely, or whether a lasting downregulation is subsequent to acute upregulation following repeated drug administration. If cytokines are modulated acutely, then antagonist studies could quickly reveal systems (e.g. CB_2 receptors) that mediate the effect. Alternatively, transgenic rodents, specifically CB_1 and CB_2 receptor null mice, could be utilised to elucidate underlying mechanisms.

Future studies are also necessary to elucidate why AB-FUBINACA inhibited pro-inflammatory cytokines but the closely related AB-PINACA did not. AB-PINACA contains an *N*-pentyl chain in place of the *N*-(4-fluorobenzyl) group in AB-FUBINACA. It may be interesting to determine if this relationship holds for similar pairings, like AMB (which contains an *N*-pentyl group) and AMB-FUBINACA (which is identical except for an N-(4-fluorobenzyl) group).

Finally, it is important to acknowledge that some synthetic cannabinoids may have potential therapeutic applications. While the synthetic cannabinoids featured in this thesis were assessed with a view towards uncovering toxicological or deleterious effects, many early synthetic cannabinoids were developed by pharmaceutical companies as potential therapeutics. For example, the “CP” series of synthetic cannabinoids (e.g. CP-55,940) were developed by Pfizer as novel analgesics. The same

is true for both AB-PINACA and AB-FUBINACA, which were both developed by Pfizer and patented in 2009 (Buchler et al., 2009).

Moving forward, cytokine modulation and CB_2 receptor agonist effects have potential applications in areas where modulation of inflammatory or immune responses is desired. In addition to their action on CB_1 receptors, AB-PINACA and AB-FUBINACA are also potent CB_2 receptor agonists (Chapter 2). If these compounds were modified to reduce their CB_1 receptor affinity (and consequently their hypothermic and psychoactive effects), they could feasibly find use as therapeutic agents with reduced potential for recreational use. As reviewed in Chapter 1, some studies have shown therapeutic applications for CB_2 receptor selective agonists O-3853 and O-1966 in decreasing cerebral infarction following ischemic stroke in mice (Zhang et al., 2007). The clinical efficacy of other CB_2 receptor agonists in treatment of neuropathic pain is also being assessed, although in many cases encouraging preclinical findings have failed to translate into human populations (Dhopeshwarkar & Mackie, 2014). Continuing research using a variety of recently discovered CB_2 agonists, ranging from bicyclic-based molecular structures to indole-, benzimidazole-, γ-carboline-, and 1,4-diazepane carboxamide-based structures may fuel further research and development into CB_2 receptor mediated therapeutics (Nevalainen, 2014).

6.3.3 Agonist substitution therapy for synthetic cannabinoid withdrawal

Chronic synthetic cannabinoid users report a withdrawal syndrome similar to, but exceeding, that of cannabis withdrawal. For example, consider a user's self-report

of synthetic cannabinoid withdrawal that occurred after the user's daily supply was severed due to international travel:

> *"That week was a nightmare. During the first 3 days I didn't sleep at all, I had insane cravings ... and I thought I was going to die, on the 4th night I fell asleep from exhaustion only to dream about Spice for 2 hours and wake up with cold sweat and difficulty breathing, the worst thing was that I had nausea all the time, even when I made myself throw up the nausea would return in about 10 minutes to make me miserable, I couldn't talk to anyone ... I wasn't sure I could hold down my food anyway. By the 5th day I was smoking some random flowers I picked outside in a bong ... just to try and satisfy my cravings. Today I'm 2 months clean, I feel better than I did 2 months ago but still quite [bad]. I still get panic attacks, my stomach is still [expletive] and so I can't go outside my house, I still can't sleep properly and I still dream about Spice and crave it 24/7..." (MikePatton, 2011)*

As reviewed in Section 1.5.4, specific treatments for synthetic cannabinoid dependence and withdrawal are limited and often non-existent. Users are generally forced to cease drug use without specific supportive medical interventions for withdrawal symptoms and craving. This may well increase the likelihood of relapse to synthetic cannabinoid use. As mentioned in earlier sections, agonist replacement therapy for synthetic cannabinoid withdrawal using nabiximols could be an efficacious intervention to assist with withdrawal and craving. However, before such efficacy can be assessed in clinical settings, basic monitoring techniques need to be established,

such as the monitoring of synthetic cannabinoids, Δ^9-THC, CBD, and metabolites in biological samples to allow tracking of treatment adherence and optimal dose titration.

Chapter 5 primarily focused on urinalysis of phytocannabinoids and their metabolites in a clinical sample of treatment-seeking cannabis dependent users. However, synthetic cannabinoids could conceivably be analysed using a similar methodology. Certainly, synthetic cannabinoids can be measured in plasma, as was performed in Chapter 3, but for the same reasons that urinalysis is useful for monitoring agonist substitution therapy during cannabis withdrawal, urinalysis may be of use in monitoring synthetic cannabinoid withdrawal. Both synthetic cannabinoids and phytocannabinoids tend to be metabolised similarly via extensive oxidations and glucuronidations (Chapters 4, 5; Andersson et al., 2016; Williams & Moffat, 1980; Wohlfarth et al., 2014), so it follows that similar analytical methods can be applied to each cannabinoid class. Moreover, urinary synthetic cannabinoid metabolites have been detected in prior studies (Grigoryev et al., 2012, 2013), and some urinary metabolites of CUMYL-PICA and 5F-CUMYL-PICA were elucidated in Chapter 3.

Therefore, by combining techniques from Chapters 3 and 5, and from other relevant publications (Table 2), urinary and plasma synthetic cannabinoid and phytocannabinoid concentrations could be measured accurately and simultaneously, allowing verification of the cessation of synthetic cannabinoid use while monitoring and titrating concentrations of agonist replacement (*i.e.* Δ^9-THC and CBD). Application of glucuronidase hydrolysis using β-glucuronidase could also boost concentrations of key phase I metabolites for synthetic cannabinoids and

phytocannabinoids simultaneously, potentially improving detection rates (Chapters 4, 5; Wohlfarth et al., 2015).

Direct verification of the efficacy of agonist substitution therapy for synthetic cannabinoid dependence and withdrawal may be an important future step for progression of this area of research and treatment. A clinical validation focusing on synthetic cannabinoid dependent treatment-seeking inpatients would be an ideal follow-up study to the work presented in this thesis.

6.4 Conclusions

The research presented in this thesis commenced with the characterisation of *in vivo* physiological effects (hypothermia and bradycardia) of a wide range of contemporary synthetic cannabinoids in rats. For the first time, *in vivo* dose-response relationships of these compounds were elucidated and doses ranges with functional effects were established for future experiments. The use of radiotelemetric probes in rats enabled collection of body temperature and heart rate data in real time without experimental artefacts associated with the stress of animal handling. This work enabled the identification of *in vivo* SARs, which may be used to predict potency of future novel synthetic cannabinoids.

The thesis then moved to the characterisation of metabolic pathways for the recently detected synthetic cannabinoids CUMYL-PICA and 5F-CUMYL-PICA. This study identified dozens of metabolites, providing useful analytical targets for future forensic and scientific investigations. Additionally, this study found that *in vitro* predictions of kinetic parameters, which have also been reported to be rapid for several other synthetic cannabinoids, overestimated the rate of actual *in vivo* elimination in rats. *In vivo* synthetic cannabinoid sequestration in adipose tissue and blood protein binding may be important factors to consider when interpreting *in vitro* synthetic cannabinoid kinetic data.

The long-term effects of repeated administration of AB-PINACA, AB-FUBINACA and Δ^9-THC were then assessed in adolescent rats. This revealed several well-established acute impacts (e.g. increases in anxiety-like behaviours, decreases in locomotor activity), but also revealed subtle long-term alterations to several biochemical and cognitive systems. AB-PINACA and Δ^9-THC modulated

endocannabinoid concentrations while AB-FUBINACA decreased concentrations of some pro-inflammatory cytokines. AB-PINACA, AB-FUBINACA, and Δ^9-THC all produced recognition memory impairments in the long-term, which were notably more severe for AB-FUBINACA. These previously uncharacterised effects may have important implications in confronting the sequelae of synthetic cannabinoid use in humans, who may exhibit cognitive impairment even after cessation of drug use.

Finally, this thesis validated a cannabinoid urinalysis in a population of cannabis-dependent treatment-seeking users. It was found that cannabinoid urinalysis can substitute for plasma analysis, potentially reducing the invasiveness of sampling in future studies. Moreover, cannabinoid concentrations were greater in urine than in plasma, suggesting that cannabinoid urinalysis could be used for analysis of trace cannabinoids that may go undetected in blood. The utility of β-glucuronidase hydrolysis for increasing concentrations of phase I metabolites was demonstrated, which may also be useful for the analysis of urinary synthetic cannabinoid metabolites.

The work presented in this thesis culminated in the establishment of SARs and SMRs for the prediction of the pharmacological properties and metabolism of novel synthetic cannabinoids. It is hoped that a wider understanding of these processes will enable streamlined assessment of novel synthetic cannabinoids, allowing researchers, clinicians, and forensic chemists to prioritise the compounds that require the most attention from a public health perspective. Additionally, implications of chronic synthetic cannabinoid use for human users were identified - in particular, the lasting cognitive impact of synthetic cannabinoid use should be taken into account when designing treatments for chronic synthetic cannabinoid users. Finally, analytical methods were established for the future clinical validation of agonist replacement

therapy using Δ^9-THC and CBD for the treatment of synthetic cannabinoid withdrawal. Future studies are required to directly establish the efficacy of this approach, but it is hoped that the research presented here will constitute a first step towards the effective treatment of synthetic cannabinoid dependent populations.

6.5 References

Adams, A. J., Banister, S. D., Irizarry, L., Trecki, J., Schwartz, M., & Gerona, R. (2017). "Zombie" outbreak caused by the synthetic cannabinoid AMB-FUBINACA in New York. *New England Journal of Medicine, 376*(3), 235-242.

Andersson, M., Diao, X., Wohlfarth, A., Scheidweiler, K. B., & Huestis, M. A. (2016). Metabolic profiling of new synthetic cannabinoids AMB and 5F-AMB by human hepatocyte and liver microsome incubations and high-resolution mass spectrometry. *Rapid Communications in Mass Spectrometry, 30*(8), 1067-1078.

Arevalo, C., de Miguel, R., & Hernandez-Tristan, R. (2001). Cannabinoid effects on anxiety-related behaviours and hypothalamic neurotransmitters. *Pharmacology, Biochemistry and Behavior, 70*(1), 123-131.

Barker, G. R. I., & Warburton, E. C. (2011). When is the hippocampus involved in recognition memory? *The Journal of Neuroscience, 31*(29), 10721-10731.

Bhanushali, G. K., Jain, G., Fatima, H., Leisch, L. J., & Thornley-Brown, D. (2012). AKI associated with synthetic cannabinoids: A case series. *Clinical Journal of the American Society of Nephrology, 8*(4), 523-526.

Brents, L. K., Reichard, E. E., Zimmerman, S. M., Moran, J. H., Fantegrossi, W. E., & Prather, P. L. (2011). Phase I hydroxylated metabolites of the K2 synthetic cannabinoid JWH-018 retain in vitro and in vivo cannabinoid 1 receptor affinity and activity. *PloS One, 6*(7), e21917.

Buchler, I. P., Hayes, M. J., Hedge, S. G., Hockerman, S. L., Jones, D. E., Kortum, S. W., et al. (2009). Indazole derivatives. World patent WO2009106982.

Bussey, T. J., Muir, J. L., & Aggleton, J. P. (1999). Functionally dissociating aspects of event memory: the effects of combined perirhinal and postrhinal cortex lesions on object and place memory in the rat. *Journal of Neuroscience, 19*(1), 495-502.

Cohen, K., Kapitány-Fövény, M., Mama, Y., Arieli, M., Rosca, P., Demetrovics, Z., et al. (2017). The effects of synthetic cannabinoids on executive function. *Psychopharmacology, 234*(7), 1121-1134.

Dhopeshwarkar, A., & Mackie, K. (2014). CB_2 cannabinoid receptors as a therapeutic target—What does the future hold? *Molecular Pharmacology, 86*(4), 430-437.

Diao, X., Carlier, J., Scheidweiler, K. B., & Huestis, M. A. (2017). In vitro metabolism of new synthetic cannabinoid SDB-006 in human hepatocytes by high-resolution mass spectrometry. *Forensic Toxicology*, doi: 10.1007/s11419-016-0350-9.

Diao, X., Scheidweiler, K. B., Wohlfarth, A., Pang, S., Kronstrand, R., & Huestis, M. A. (2016). In vitro and in vivo human metabolism of synthetic cannabinoids FDU-PB-22 and FUB-PB-22. *The AAPS Journal, 18*(2), 455-464.

EMCDDA. (2016). *European Drug Report 2016*. Retrieved from: http://www.emcdda.europa.eu/edr2016

Gerard, C., Mollereau, C., Vassart, G., & Parmentier, M. (1990). Nucleotide sequence of a human cannabinoid receptor cDNA. *Nucleic Acids Research, 18*(23), 7142.

Grigoryev, A., Kavanagh, P., & Melnik, A. (2012). The detection of the urinary metabolites of 3-[(adamantan-1-yl)carbonyl]-1-pentylindole (AB-001), a novel cannabimimetic, by gas chromatography-mass spectrometry. *Drug Testing and Analysis, 4*(6), 519-524.

Grigoryev, A., Kavanagh, P., & Melnik, A. (2013). The detection of the urinary metabolites of 1-[(5-fluoropentyl)-1H-indol-3-yl]-(2-iodophenyl)methanone

(AM-694), a high affinity cannabimimetic, by gas chromatography – mass spectrometry. *Drug Testing and Analysis, 5*(2), 110-115.

Gunasekaran, N., Long, L. E., Dawson, B. L., Hansen, G. H., Richardson, D. P., Li, K. M., et al. (2009). Reintoxication: the release of fat-stored Δ9-tetrahydrocannabinol (THC) into blood is enhanced by food deprivation or ACTH exposure. *British Journal of Pharmacology, 158*(5), 1330-1337.

Hasegawa, K., Wurita, A., Minakata, K., Gonmori, K., Nozawa, H., Yamagishi, I., et al. (2015). Postmortem distribution of AB-CHMINACA, 5-fluoro-AMB, and diphenidine in body fluids and solid tissues in a fatal poisoning case: usefulness of adipose tissue for detection of the drugs in unchanged forms. *Forensic Toxicology, 33*(1), 45-53.

Hermanns-Clausen, M., Kneisel, S., Szabo, B., & Auwarter, V. (2012). Acute toxicity due to the confirmed consumption of synthetic cannabinoids: Clinical and laboratory findings. *Addiction, 108*(3), 534-544.

Hutter, M., Moosmann, B., Kneisel, S., & Auwarter, V. (2013). Characteristics of the designer drug and synthetic cannabinoid receptor agonist AM-2201 regarding its chemistry and metabolism. *Journal of Mass Spectrometry, 48*(7), 885-894.

Johansson, E., Norén, K., Sjövall, J., & Halldin, M. M. (1989). Determination of Δ1-tetrahydrocannabinol in human fat biopsies from marihuana users by gas chromatography–mass spectrometry. *Biomedical Chromatography, 3*(1), 35-38.

Kavanagh, P., Grigoryev, A., & Krupina, N. (2017). Detection of metabolites of two synthetic cannabimimetics, MDMB-FUBINACA and ADB-FUBINACA, in authentic human urine specimens by accurate mass LC–MS: a comparison of

intersecting metabolic patterns. *Forensic Toxicology*, doi: 10.1007/s11419-017-0356-y.

Khan, M., Pace, L., Truong, A., Gordon, M., & Moukaddam, N. (2016). Catatonia secondary to synthetic cannabinoid use in two patients with no previous psychosis. *The American Journal on Addictions, 25*(1), 25-27.

Kim, J.-H., Kwon, S.-S., Kong, T., Cheong, J., Kim, H., In, M., et al. (2017). AM-2201 inhibits multiple cytochrome P450 and uridine 5′-diphospho-glucuronosyltransferase enzyme activities in human liver microsomes. *Molecules, 22*(3), 443.

Lapoint, J., James, L., Moran, C., Nelson, L., Hoffman, R., & Moran, J. (2011). Severe toxicity following synthetic cannabinoid ingestion. *Clinical Toxicology, 49*(8), 760-764.

Louh, I. K., & Freeman, W. D. (2014). A 'spicy' encephalopathy: Synthetic cannabinoids as cause of encephalopathy and seizure. *Critical Care, 18*(5), 553.

Macri, S., Lanuzza, L., Merola, G., Ceci, C., Gentili, S., Valli, A., et al. (2013). Behavioral responses to acute and sub-chronic administration of the synthetic cannabinoid JWH-018 in adult mice prenatally exposed to corticosterone. *Neurotoxicity Research, 24*(1), 15-28.

MikePatton. (2011). *Terrible spice detox after a year of daily use*. Retrieved from: https://drugs-forum.com/threads/terrible-spice-detox-after-a-year-of-daily-use.166600/

Mir, A., Obafemi, A., Young, A., & Kane, C. (2011). Myocardial infarction associated with use of the synthetic cannabinoid K2. *Pediatrics, 128*(6), e1622-e1627.

Nevalainen, T. (2014). Recent development of CB2 selective and peripheral CB1/CB2 cannabinoid receptor ligands. *Current Medicinal Chemistry, 21*(2), 187-203.

NFILS. (2015). *2014 midyear report*. Retrieved from: https://www.nflis.deadiversion.usdoj.gov/DesktopModules/ReportDownloads/Reports/NFLIS2014MY.pdf

Norman, G., & Eacott, M. J. (2004). Impaired object recognition with increasing levels of feature ambiguity in rats with perirhinal cortex lesions. *Behavioural Brain Research, 148*(1-2), 79-91.

O'Shea, M., McGregor, I. S., & Mallet, P. E. (2006). Repeated cannabinoid exposure during perinatal, adolescent or early adult ages produces similar longlasting deficits in object recognition and reduced social interaction in rats. *Journal of Psychopharmacology, 20*(5), 611-621.

O'Shea, M., Singh, M. E., McGregor, I. S., & Mallet, P. E. (2004). Chronic cannabinoid exposure produces lasting memory impairment and increased anxiety in adolescent but not adult rats. *Journal of Psychopharmacology, 18*(4), 502-508.

Quinn, H. R., Matsumoto, I., Callaghan, P. D., Long, L. E., Arnold, J. C., Gunasekaran, N., et al. (2008). Adolescent rats find repeated Δ^9-THC less aversive than adult rats but display greater residual cognitive deficits and changes in hippocampal protein expression following exposure. *Neuropsychopharmacology, 33*(5), 1113-1126.

Schneir, A. B., Cullen, J., & Ly, B. T. (2011). “Spice” girls: Synthetic cannabinoid intoxication. *The Journal of emergency medicine, 40*(3), 296-299.

Schwartz, M. D., Trecki, J., Edison, L. A., Steck, A. R., Arnold, J. K., & Gerona, R. R. (2015). A common source outbreak of severe delirium associated with exposure

to the novel synthetic cannabinoid ADB-PINACA. *Journal of Emergency Medicine, 48*(5), 573-580.

Seely, K. A., Brents, L. K., Radominska-Pandya, A., Endres, G. W., Keyes, G. S., Moran, J. H., et al. (2012). A major glucuronidated metabolite of JWH-018 is a neutral antagonist at CB1 receptors. *Chemical Research in Toxicology, 25*(4), 825-827.

Sobolevsky, T., Prasolov, I., & Rodchenkov, G. (2010). Detection of JWH-018 metabolites in smoking mixture post-administration urine. *Forensic Science International, 200*(1), 141-147.

Sobolevsky, T., Prasolov, I., & Rodchenkov, G. (2012). Detection of urinary metabolites of AM-2201 and UR-144, two novel synthetic cannabinoids. *Drug Testing and Analysis, 4*(10), 745-753.

Takayama, T., Suzuki, M., Todoroki, K., Inoue, K., Min, J. Z., Kikura-Hanajiri, R., et al. (2014). UPLC/ESI-MS/MS-based determination of metabolism of several new illicit drugs, ADB-FUBINACA, AB-FUBINACA, AB-PINACA, QUPIC, 5F-QUPIC and α-PVT, by human liver microsome. *Biomedical Chromatography, 28*(6), 831-838.

Thomas, B. F., Lefever, T. W., Cortes, R. A., Kovach, A. L., Anderson, C. O., Patel, P. R., et al. (2017). Thermolytic degradation of synthetic cannabinoids: Chemical exposures and pharmacological consequences. *Journal of Pharmacology and Experimental Therapeutics, 361*(1), 162-171.

Thomsen, R., Nielsen, L. M., Holm, N. B., Rasmussen, H. B., Linnet, K., & Consortium, T. I. (2014). Synthetic cannabimimetic agents metabolized by carboxylesterases. *Drug Testing and Analysis, 7*(7), 565-576.

Thornton, S. L., Wood, C., Friesen, M. W., & Gerona, R. R. (2013). Synthetic cannabinoid use associated with acute kidney injury. *Clinical Toxicology, 51*(3), 189-190.

Vikingsson, S., Green, H., Brinkhagen, L., Mukhtar, S., & Josefsson, M. (2015). Identification of AB-FUBINACA metabolites in authentic urine samples suitable as urinary markers of drug intake using liquid chromatography quadrupole tandem time of flight mass spectrometry. *Drug Testing and Analysis, 8*(9), 950-956.

Wiley, J. L., Marusich, J. A., Lefever, T. W., Antonazzo, K. R., Wallgren, M. T., Cortes, R. A., et al. (2015). AB-CHMINACA, AB-PINACA, and FUBIMINA: Affinity and potency of novel synthetic cannabinoids in producing Δ^9-tetrahydrocannabinol-like effects in mice. *Journal of Pharmacology and Experimental Therapeutics, 354*(3), 328-339.

Williams, P. L., & Moffat, A. C. (1980). Identification in human urine of Δ^9-tetrahydrocannabinol-11-oic acid glucuronide: A tetrahydrocannabinol metabolite. *Journal of Pharmacy and Pharmacology, 32*(7), 445-448.

Winstock, A. R., & Barratt, M. J. (2013). Synthetic cannabis: A comparison of patterns of use and effect profile with natural cannabis in a large global sample. *Drug and Alcohol Dependence, 131*, 106-111.

Wohlfarth, A., Gandhi, A. S., Pang, S., Zhu, M., Scheidweiler, K. B., & Huestis, M. A. (2014). Metabolism of synthetic cannabinoids PB-22 and its 5-fluoro analog, 5F-PB-22, by human hepatocyte incubation and high-resolution mass spectrometry. *Analytical and Bioanalytical Chemistry, 406*(6), 1763-1780.

Wohlfarth, A., Scheidweiler, K. B., Castaneto, M., Gandhi, A. S., Desrosiers, N. A., Klette, K. L., et al. (2015). Urinary prevalence, metabolite detection rates, temporal patterns and evaluation of suitable LC-MS/MS targets to document synthetic cannabinoid intake in US military urine specimens. *Clinical Chemistry and Laboratory Medicine, 53*(3), 423-434.

Zhang, M., Martin, B. R., Adler, M. W., Razdan, R. K., Jallo, J. I., & Tuma, R. F. (2007). Cannabinoid CB_2 receptor activation decreases cerebral infarction in a mouse focal ischemia/reperfusion model. *Journal of Cerebral Blood Flow and Metabolism, 27*(7), 1387-1396.

Appendix 1. Supplementary information for Chapter 2

The effects of bioisosteric fluorine in synthetic cannabinoid designer drugs JWH-018, AM-2201, UR-144, XLR-11, PB-22, 5F-PB-22, APICA, and STS-135

Samuel D. Banister, Jordyn Stuart, Richard C. Kevin, Amelia Edington, Mitchell Longworth, Shane M. Wilkinson, Corinne Beinat, Alexandra S. Buchanan, David E. Hibbs, Michelle Glass, Mark Connor, Iain S. McGregor, Michael Kassiou

Contents:

Table S1. Crystal data and structure refinement for UR-144 (**7**).

Identification code	13sam001
Empirical formula	$C_{21}H_{29}NO$
Formula weight	311.45
Temperature/K	150.15
Crystal system	monoclinic
Space group	$P2_1/n$
a/Å	12.1123(8)
b/Å	10.7990(7)
c/Å	13.9200(9)
α/°	90.00
β/°	93.6870(10)
γ/°	90.00
Volume/Å^3	1817.0(2)
Z	4
ρ_{calc}mg/mm^3	1.139
m/mm^{-1}	0.069
F(000)	680.0
Crystal size/mm^3	0.15 × 0.15 × 0.1
2Θ range for data collection	4.32 to 56.5°
Index ranges	$-15 \leq h \leq 15$, $-14 \leq k \leq 12$, $-18 \leq l \leq 18$
Reflections collected	13869
Independent reflections	4170[R(int) = 0.0179]
Data/restraints/parameters	4170/0/213
Goodness-of-fit on F^2	1.050
Final R indexes [I>=2σ (I)]	R_1 = 0.0398, wR_2 = 0.1019
Final R indexes [all data]	R_1 = 0.0478, wR_2 = 0.1077
Largest diff. peak/hole / e Å^{-3}	0.26/-0.20

Table S2. Fractional Atomic Coordinates ($\times 10^4$) and Equivalent Isotropic Displacement Parameters ($Å^2 \times 10^3$) for UR-144 (**7**). U_{eq} is defined as 1/3 of of the trace of the orthogonalised U_{IJ} tensor.

Atom	**x**	**y**	**z**	**U_{eq}**
C1	11919.5(8)	1638.6(10)	2202.6(8)	23.7(2)
C2	11397.0(8)	2299.5(10)	1453.3(7)	22.7(2)
C3	12215.4(8)	3151.2(10)	1127.1(7)	22.4(2)
C4	13188.4(9)	2957.9(10)	1724.8(7)	22.8(2)
C5	14152.5(9)	3646.4(11)	1637.8(8)	26.2(2)
C6	14131.6(9)	4538.8(11)	927.6(8)	28.9(2)
C7	13181.9(10)	4735.9(11)	314.8(8)	29.7(3)
C8	12224.0(9)	4056(1)	402.3(8)	26.5(2)
C9	10242.0(9)	2202.4(10)	1073.1(8)	24.2(2)
C10	9547.6(8)	1249.8(10)	1517.4(8)	23.7(2)
C11	8620.4(8)	515.2(10)	959.5(8)	25.3(2)
C12	8318.1(8)	1442.5(11)	1706.8(8)	25.4(2)
C13	8361.6(10)	779.1(13)	-100.5(8)	34.5(3)
C14	8560.5(10)	-862.5(11)	1166.9(10)	33.0(3)
C15	7739.9(10)	2632.3(12)	1396.0(9)	33.4(3)
C16	7986.8(10)	1007.4(12)	2684.7(9)	33.0(3)
C17	13790.9(9)	1480.2(11)	3079.5(8)	28.3(2)
C18	14695.4(9)	744.0(11)	2618.3(9)	31.0(3)
C19	14273.7(10)	-156.0(11)	1838.3(9)	30.8(3)
C20	15187.5(11)	-962.6(13)	1475.6(10)	41.2(3)
C21	14809.3(14)	-1804.2(15)	646.8(12)	53.1(4)
N1	12982.9(7)	2027.3(9)	2374.1(6)	23.9(2)
O1	9888.8(7)	2895.1(8)	422.0(6)	34.0(2)

Table S3. Bond lengths [Å] for UR-144 (**7**).

Atom	**Atom**	**Length/Å**
C1	C2	1.3830(15)
C1	N1	1.3611(13)
C2	C3	1.4465(14)
C2	C9	1.4674(14)
C3	C4	1.4138(15)
C3	C8	1.4051(15)
C4	C5	1.3962(15)
C4	N1	1.3848(14)
C5	C6	1.3797(16)
C6	C7	1.4036(17)
C7	C8	1.3849(16)
C9	C10	1.4882(15)
C9	O1	1.2306(13)
C10	C11	1.5432(14)
C10	C12	1.5430(14)
C11	C12	1.5059(15)
C11	C13	1.5157(16)
C11	C14	1.5181(16)
C12	C15	1.5131(16)
C12	C16	1.5183(16)
C17	C18	1.5281(16)
C17	N1	1.4654(13)
C18	C19	1.5209(17)
C19	C20	1.5200(17)
C20	C21	1.516(2)

Table S4. Bond angles [deg] for UR-144 (**7**).

Atom	Atom	Atom	Angle/°
N1	C1	C2	110.80(9)
C1	C2	C3	105.98(9)
C1	C2	C9	127.92(10)
C3	C2	C9	126.08(10)
C4	C3	C2	106.47(9)
C8	C3	C2	134.79(10)
C8	C3	C4	118.74(10)
C5	C4	C3	122.72(10)
N1	C4	C3	108.25(9)
N1	C4	C5	129.02(10)
C6	C5	C4	117.21(10)
C5	C6	C7	121.19(10)
C8	C7	C6	121.65(10)
C7	C8	C3	118.47(10)
C2	C9	C10	116.79(9)
O1	C9	C2	120.03(10)
O1	C9	C10	123.18(10)
C9	C10	C11	123.97(9)
C9	C10	C12	123.72(9)
C12	C10	C11	58.41(7)
C12	C11	C10	60.79(7)
C12	C11	C13	120.21(10)
C12	C11	C14	120.24(10)
C13	C11	C10	119.44(9)
C13	C11	C14	111.10(10)
C14	C11	C10	116.76(9)
C11	C12	C10	60.80(7)
C11	C12	C15	119.72(10)
C11	C12	C16	120.23(10)
C15	C12	C10	119.98(10)
C15	C12	C16	112.02(10)
C16	C12	C10	115.16(9)
N1	C17	C18	113.22(9)
C19	C18	C17	114.55(9)
C20	C19	C18	112.64(10)
C21	C20	C19	113.92(12)
C1	N1	C4	108.49(9)
C1	N1	C17	125.23(9)
C4	N1	C17	126.12(9)

Table S5. Anisotropic Displacement Parameters ($Å^2 \times 10^3$) for UR-144 (**7**). The Anisotropic displacement factor exponent takes the form: $-2\pi^2[h^2a^{*2}U_{11}+...+2hka \times b \times U_{12}]$

Atom	U_{11}	U_{22}	U_{33}	U_{23}	U_{13}	U_{12}
C1	21.2(5)	23.5(5)	26.7(5)	-0.5(4)	3.3(4)	-2.4(4)
C2	22.3(5)	21.3(5)	24.6(5)	-0.8(4)	3.1(4)	-0.9(4)
C3	22.8(5)	20.9(5)	23.7(5)	-3.4(4)	3.9(4)	-0.4(4)
C4	23.6(5)	21.9(5)	23.4(5)	-1.9(4)	4.9(4)	-0.4(4)
C5	23.1(5)	28.1(6)	27.7(5)	-3.9(4)	3.5(4)	-3.7(4)
C6	28.3(6)	27.4(6)	32.0(6)	-3.3(4)	9.9(4)	-6.9(4)
C7	35.1(6)	26.1(6)	28.9(6)	2.7(4)	9.9(4)	-2.0(5)
C8	28.4(5)	25.6(6)	25.7(5)	0.3(4)	3.8(4)	1.4(4)
C9	22.7(5)	24.4(5)	25.6(5)	-0.8(4)	1.9(4)	0.4(4)
C10	18.4(5)	25.5(5)	27.0(5)	2.4(4)	-0.9(4)	0.1(4)
C11	18.9(5)	27.2(6)	29.6(5)	-2.3(4)	0.6(4)	-0.5(4)
C12	18.4(5)	28.5(6)	29.0(5)	-1.9(4)	0.6(4)	-0.6(4)
C13	33.0(6)	40.9(7)	29.2(6)	-3.8(5)	-1.2(5)	-4.9(5)
C14	26.2(6)	28.2(6)	44.7(7)	-2.5(5)	2.1(5)	-3.1(5)
C15	26.4(6)	31.8(6)	41.9(7)	-3.1(5)	0.5(5)	6.2(5)
C16	26.9(6)	40.9(7)	31.6(6)	-1.8(5)	5.6(4)	-4.7(5)
C17	25.1(5)	33.9(6)	25.2(5)	2.8(4)	-3.6(4)	-1.1(5)
C18	24.2(5)	33.8(6)	34.2(6)	1.8(5)	-4.3(4)	1.9(5)
C19	28.6(6)	29.1(6)	34.1(6)	2.4(5)	-2.5(4)	2.0(5)
C20	40.3(7)	39.7(7)	42.9(7)	-1.6(6)	-3.7(5)	13.2(6)
C21	62.4(10)	43.9(9)	52.5(9)	-10.3(7)	0.4(7)	11.6(7)
N1	20.7(4)	25.6(5)	25.4(4)	1.5(4)	1.3(3)	-1.5(3)
O1	28.5(4)	36.6(5)	36.2(4)	11.6(4)	-3.1(3)	-1.8(3)

Table S6. Hydrogen Atom Coordinates ($Å \times 10^4$) and Isotropic Displacement Parameters ($Å^2 \times 10^3$) for UR-144 (**7**).

Atom	x	y	z	U(eq)
H1	11582	1000	2550	28
H5	14796	3506	2050	31
H6	14772	5029	852	35
H7	13196	5351	-172	36
H8	11587	4198	-18	32
H10	9961	752	2028	28
H13A	8391	1674	-213	52
H13B	7619	471	-295	52
H13C	8906	363	-479	52
H14A	9105	-1301	802	50
H14B	7817	-1169	975	50
H14C	8721	-1007	1857	50
H15A	7850	3252	1908	50
H15B	6947	2474	1271	50
H15C	8049	2941	808	50
H16A	8453	306	2900	49
H16B	7209	750	2635	49
H16C	8085	1686	3150	49
H17A	13399	926	3511	34
H17B	14140	2150	3479	34
H18A	15211	1333	2337	37
H18B	15120	274	3128	37
H19A	13701	-694	2097	37
H19B	13923	318	1291	37
H20A	15786	-421	1267	49
H20B	15500	-1478	2015	49
H21A	14517	-1302	102	80
H21B	14229	-2359	851	80
H21C	15437	-2296	452	80

Table S7. Torsion angles [deg] for UR-144 (**7**).

A	B	C	D	Angle/°
C1	C2	C3	C4	-1.06(11)
C1	C2	C3	C8	179.50(12)
C1	C2	C9	C10	-2.38(16)
C1	C2	C9	O1	177.17(11)
C2	C1	N1	C4	-0.60(12)
C2	C1	N1	C17	-176.30(10)
C2	C3	C4	C5	-178.22(10)
C2	C3	C4	N1	0.73(11)
C2	C3	C8	C7	178.30(11)
C2	C9	C10	C11	-145.83(10)
C2	C9	C10	C12	142.21(10)
C3	C2	C9	C10	179.69(10)
C3	C2	C9	O1	-0.75(17)
C3	C4	C5	C6	-0.51(16)
C3	C4	N1	C1	-0.11(12)
C3	C4	N1	C17	175.54(10)
C4	C3	C8	C7	-1.08(15)
C4	C5	C6	C7	-0.51(16)
C5	C4	N1	C1	178.75(11)
C5	C4	N1	C17	-5.60(18)
C5	C6	C7	C8	0.73(17)
C6	C7	C8	C3	0.10(17)
C8	C3	C4	C5	1.33(16)
C8	C3	C4	N1	-179.73(9)
C9	C2	C3	C4	177.24(10)
C9	C2	C3	C8	-2.20(19)
C9	C10	C11	C12	-111.81(11)
C9	C10	C11	C13	-1.54(16)
C9	C10	C11	C14	136.82(11)
C9	C10	C12	C11	112.22(11)
C9	C10	C12	C15	2.74(16)
C9	C10	C12	C16	-135.77(11)
C10	C11	C12	C15	109.88(11)
C10	C11	C12	C16	-103.77(11)
C11	C10	C12	C15	-109.47(11)
C11	C10	C12	C16	112.01(11)
C12	C10	C11	C13	110.27(12)
C12	C10	C11	C14	-111.37(11)
C13	C11	C12	C10	-109.03(11)
C13	C11	C12	C15	0.86(15)
C13	C11	C12	C16	147.21(11)
C14	C11	C12	C10	105.73(11)

C14	C11	C12	C15	-144.39(11)
C14	C11	C12	C16	1.97(15)
C17	C18	C19	C20	-173.93(10)
C18	C17	N1	C1	108.19(12)
C18	C17	N1	C4	-66.76(14)
C18	C19	C20	C21	-175.75(12)
N1	C1	C2	C3	1.04(12)
N1	C1	C2	C9	-177.22(10)
N1	C4	C5	C6	-179.22(10)
N1	C17	C18	C19	-47.60(14)
O1	C9	C10	C11	34.63(16)
O1	C9	C10	C12	-37.32(16)

Figure S1. ^{1}H NMR spectrum (500 MHz, $CDCl_3$, 300 K) of XLR-11 (**8**).

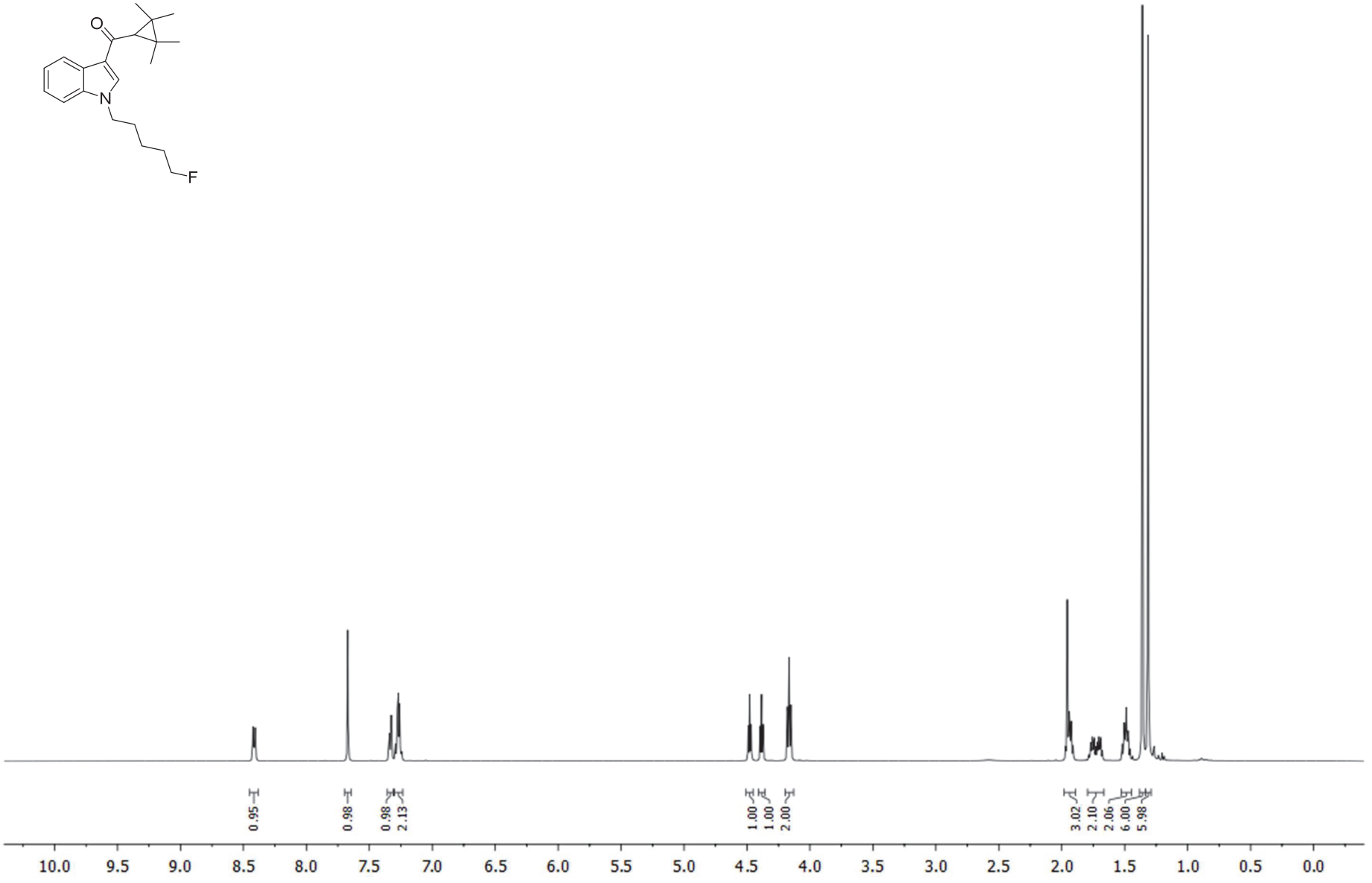

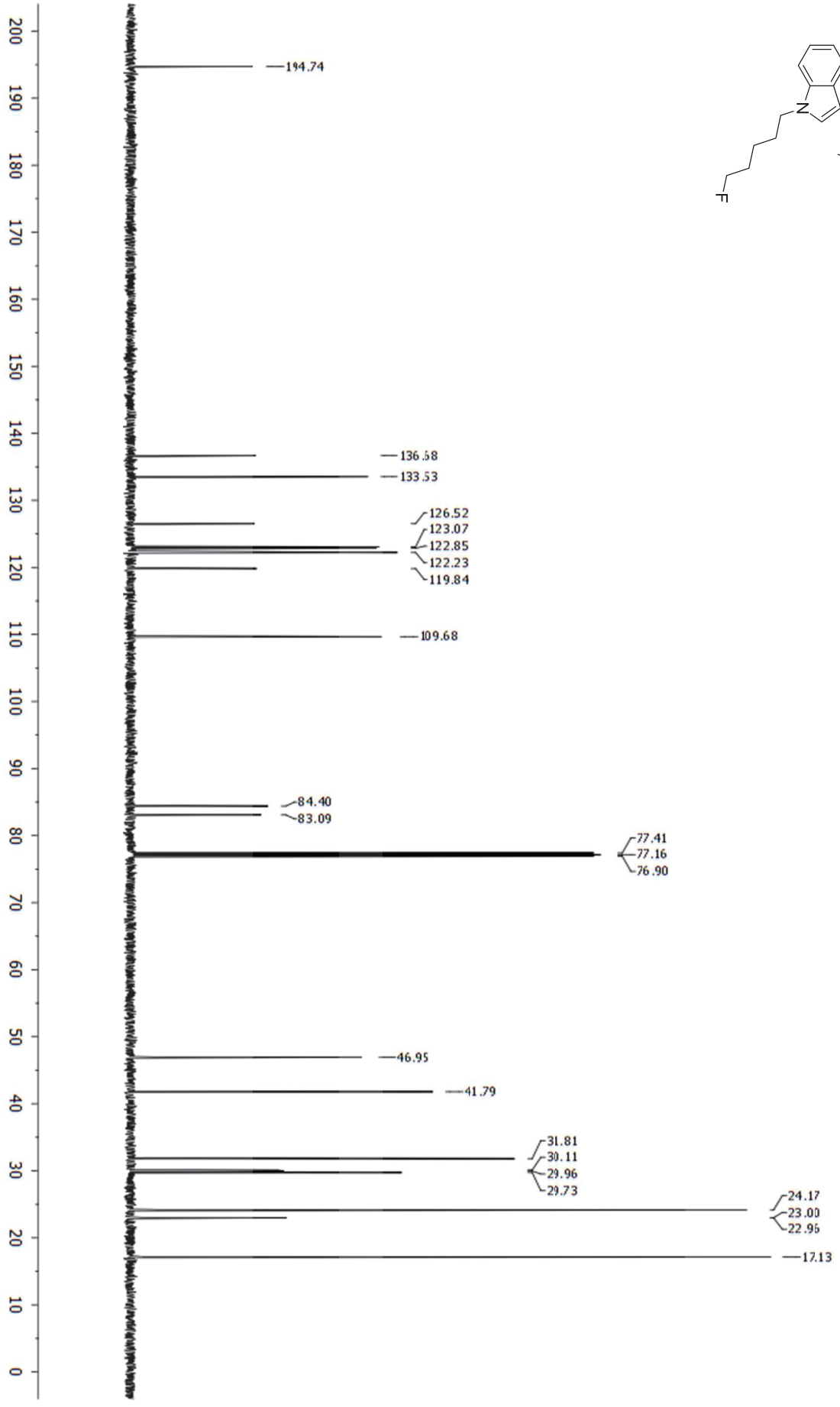

Figure S2. ^{13}C NMR spectrum (125 MHz, $CDCl_3$, 300 K) of XLR-11 (**8**).

Figure S3. ^{1}H NMR spectrum (500 MHz, $CDCl_3$, 300 K) of STS-135 (**13**).

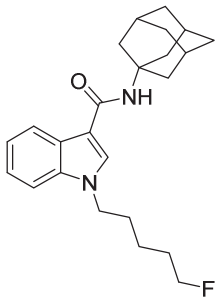

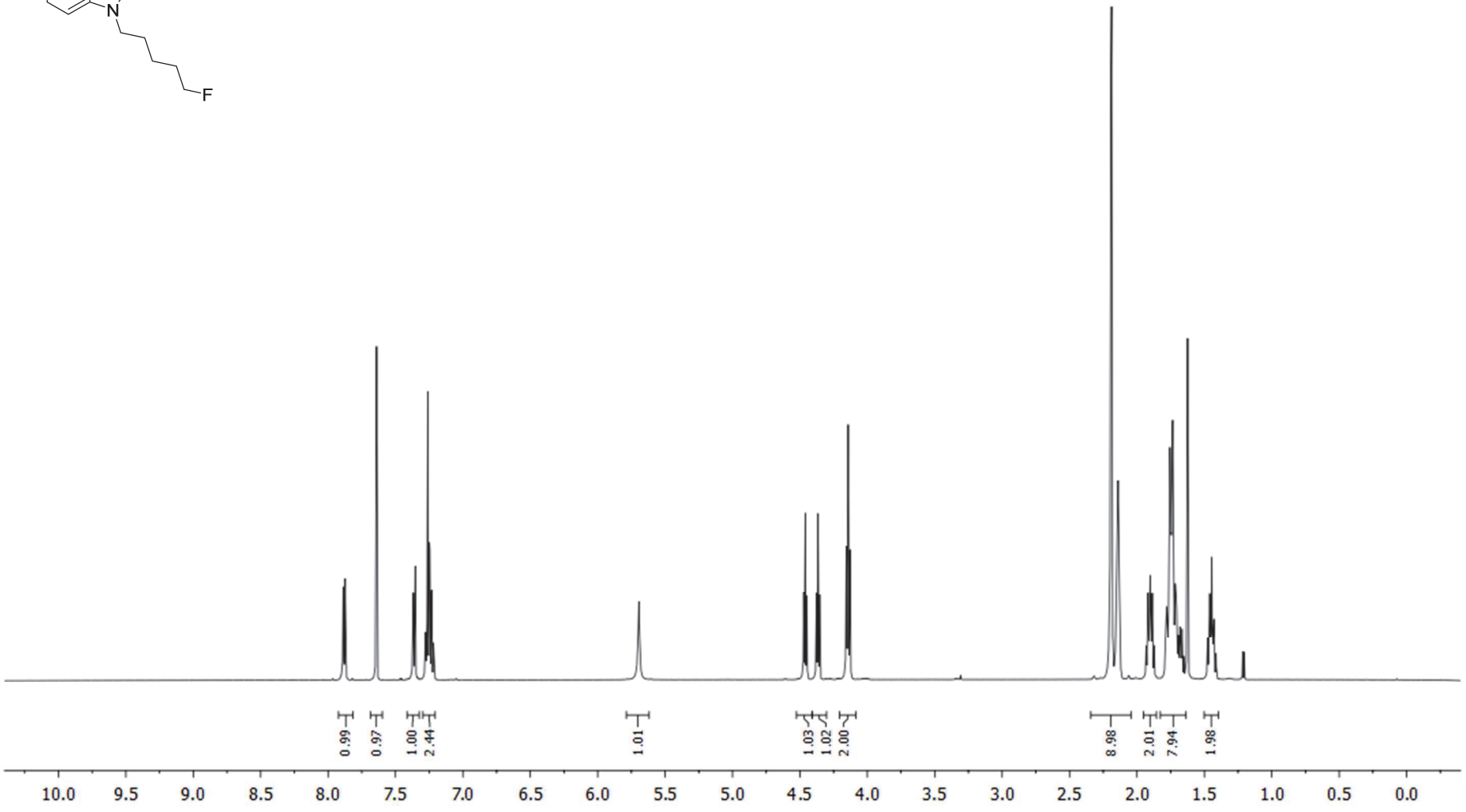

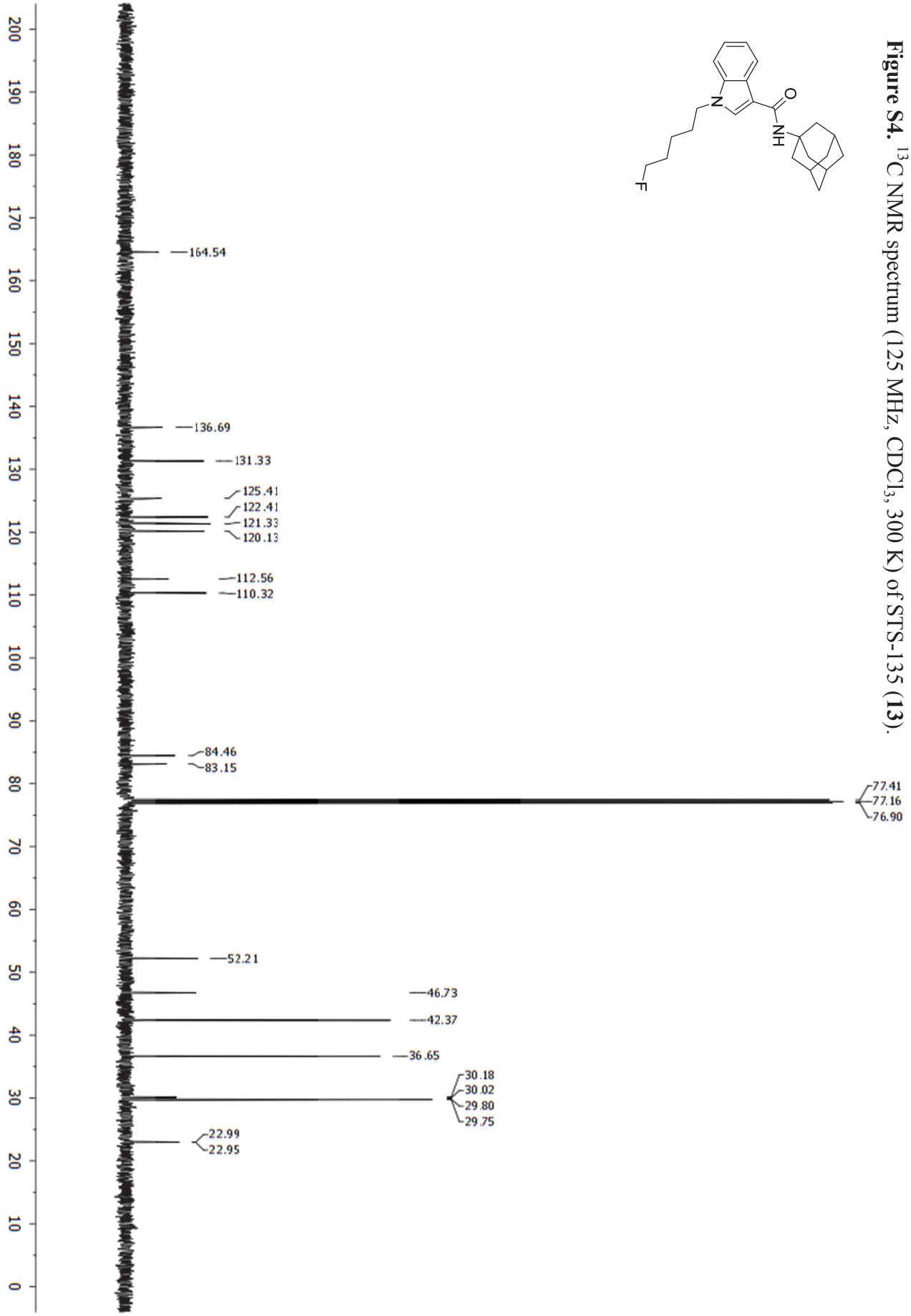

Figure S4. ^{13}C NMR spectrum (125 MHz, $CDCl_3$, 300 K) of STS-135 (**13**).

Figure S5. Mean maximal decrease in body temperature (+/- SEM) for all compounds tested *in vivo*

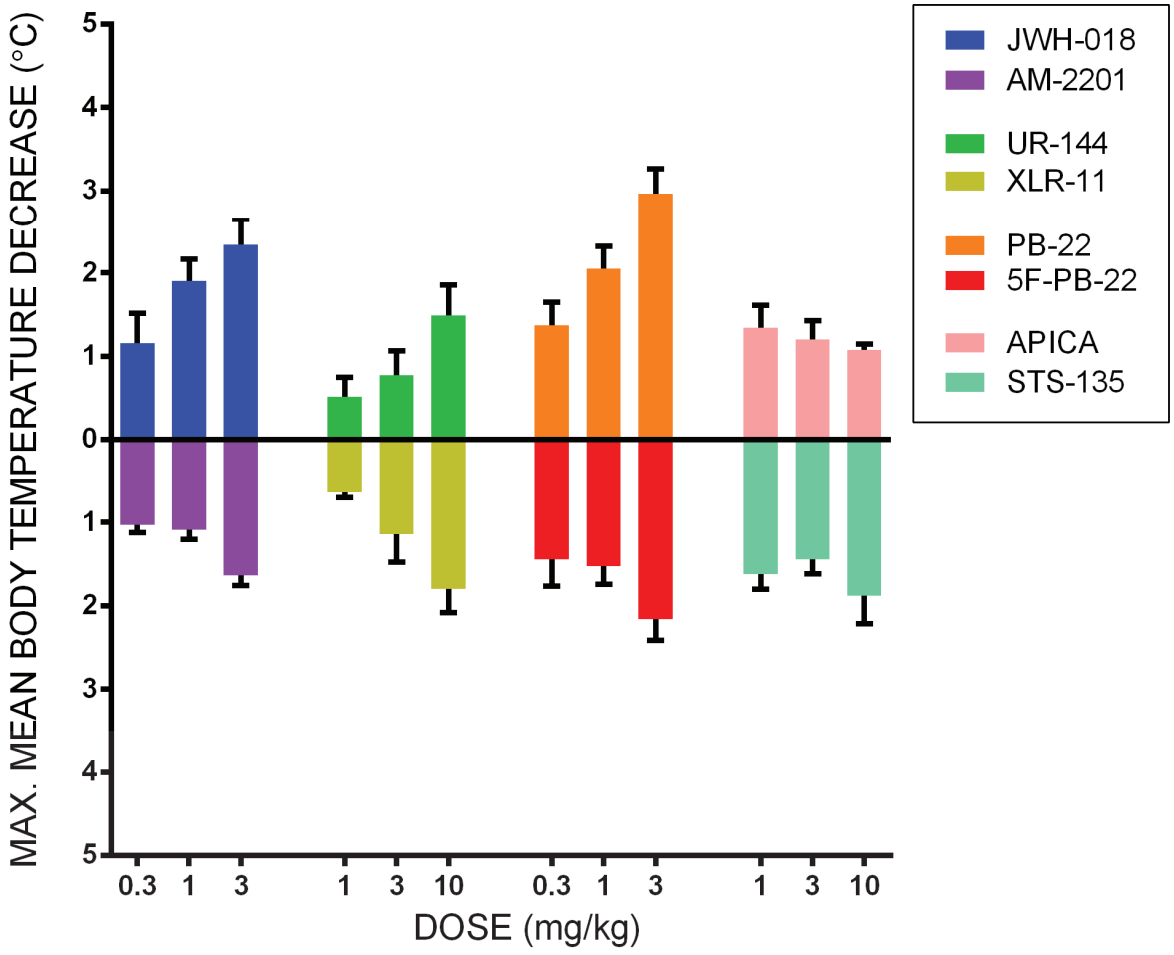

The body temperature data for individual rats during the 6 h post-drug was examined to determine the lowest body temperature datapoint recorded. The body temperature recorded during vehicle treatment at that same time point was then used to calculate body temperature change. This was averaged across all the rats receiving the same drug and dose to produce Figure 5. In this Figure compounds are presented in pairs, with the non-fluorinated compound extending upwards and the fluorinated compound downwards.

The data obtained for maximal body temperature change were compared between each drug pair using two-way mixed model ANOVAs, with drug-treatment as the between-subjects factor, and dose as the within-subjects factor. There was a significant main effect of dose for every drug pair (all $p < .05$). However there was no main effect of drug-treatment for any drug pair (all $p > .05$). Bonferroni contrasts comparing each dose for each pair (e.g. JWH-018 0.3 mg/kg – AM-2201 0.3 mg/kg) revealed no significant difference for any drug pair at any dose (all $p > .05$).

Figure S6. Mean area under the curve (AUC +/- SEM) for body temperature for each compound and dose tested, expressed as a percentage of that obtained with PB-22.

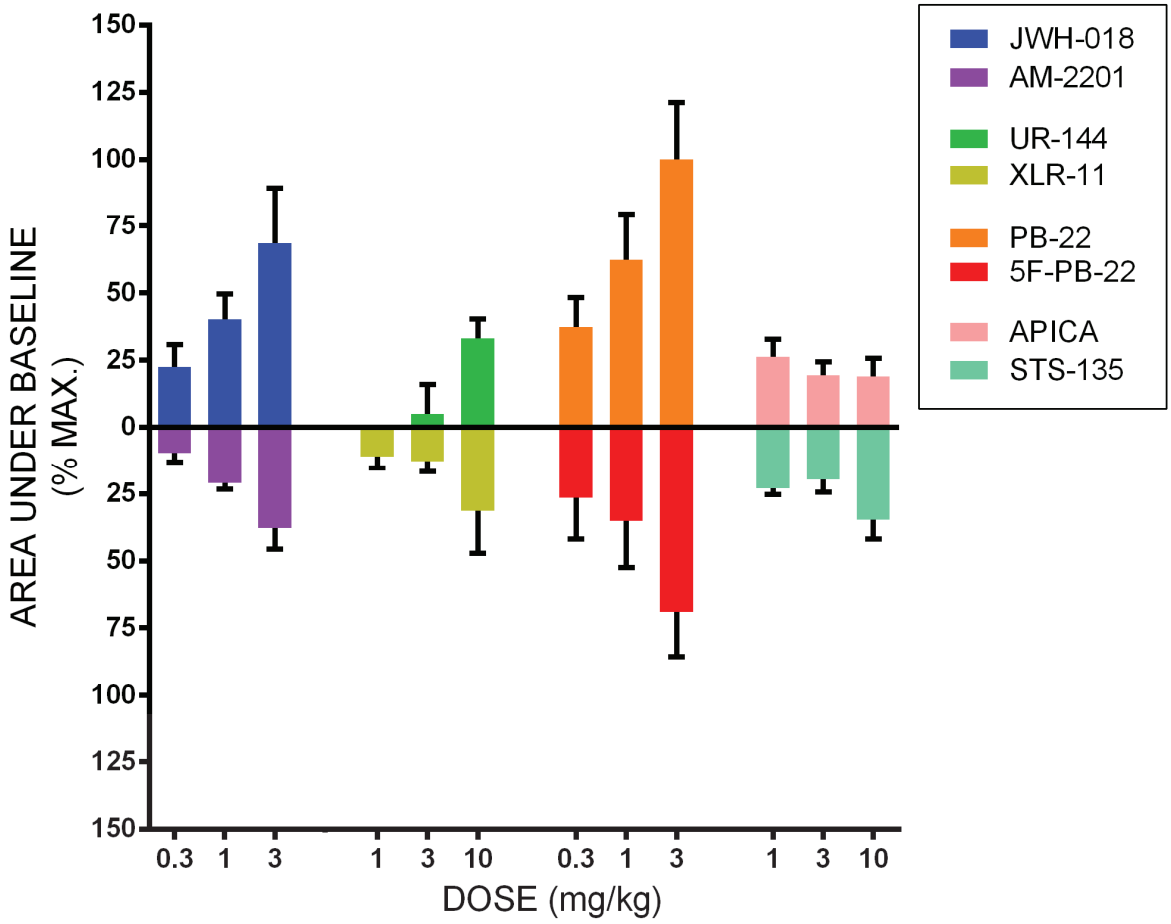

The mean area under each drug-treatment curve, relative to baseline under vehicle treatment, was calculated and normalized relative to the highest observed AUC (obtained with 3 mg/kg PB-22). Compounds are presented in pairs, with the fluorinated compound extending downwards.

These areas were calculated via the trapezoidal method. Briefly, for any time point, the area between baseline data points (B_t) and drug-treatment data points (D_t) and the next time points (B_{t+1} and D_{t+1}) forms a trapezoid, the area of which can be calculated via the formula:

$$Area = \frac{(B_t - D_t) + (B_{t+1} - D_{t+1})}{2}$$

These areas were summed from the time of injection to 6 hours post-injection.

The mean area for body temperature between baseline and drug-treatment for each drug pair was analysed using two-way mixed model ANOVAs, with drug-treatment as the between subjects factor, and dose as the within subjects factor. Similarly to peak body temperature decrease, there was a significant main effect of dose for every drug pair (all $p < .05$). However there was no main effect of drug-treatment for any drug pair (all $p > .05$). Bonferroni contrasts comparing

each dose for each pair revealed no significant difference for any drug pair at any dose (all $p > .05$).

These results suggest that terminal fluorination has no overall effect on potency as measured by body temperature. However, it remains possible that other measures (e.g. cognitive function, analgesia, appetite) may be differentially affected as a function of fluorination. Further behavioural testing is necessary to clarify this issue.

Ranking the AUCs for all eight compounds at the 3 mg/kg dose gave the following ranking: PB-22 > 5F-PB-22 = JWH-018 > AM-2201 > APICA = STS-135 = XLR-11 > UR-144.

Table S8. Binding affinities and functional activities of selected cannabinoids at CB_1 and CB_2 receptors.

Compound	CB_1 EC_{50} (nM)	CB_2 EC_{50} (nM)	CB_1 K_i (nM)	CB_2 K_i (nM)	Ref
1 (Δ^9-THC)	250	1157	35.3	3.9	1
			39.5	40	2
			40.7	36.4	3
			53.5	75.3	4
			80.3	32.2	5
3 (WIN 55,212-2)	284	62	1.89	0.28	3
			4.4	1.2	6
			9.94	16.2	1
			62.3	3.3	4
			123	4.1	7
4 (JWH-018)	102	133	9.00	2.94	8
5 (AM-2201)	38	58	1	2.6	9
7 (UR-144)	421	72	150	1.8	10
			29	4.5	11
8 (XLR-11)	98	83	24	2.1	11
9 (5-OH-UR-144)	1959	6.5	680	0.71	10
12 (APICA)	128	29	175[a]	176[a]	12

[a] IC_{50} (nM)

References

1. Rinaldi-Carmona, M.; Barth, F.; Héaulme, M.; Shire, D.; Calandra, B.; Congy, C.; Martinez, S.; Maruani, J.; Néliat, G.; Caput, D.; Ferrara, P.; Soubrié, P.; Brelière, J. C.; Le Fur, G. SR141716A, a potent and selective antagonist of the brain cannabinoid receptor. *FEBS Letters* **1994,** *350* (2–3), 240-244.

2. Bayewitch, M.; Rhee, M. H.; Avidor-Reiss, T.; Breuer, A.; Mechoulam, R.; Vogel, Z. (-)-Delta9-tetrahydrocannabinol antagonizes the peripheral cannabinoid receptor-mediated inhibition of adenylyl cyclase. *J. Biol. Chem.* **1996,** *271* (17), 9902-5.

3. Showalter, V. M.; Compton, D. R.; Martin, B. R.; Abood, M. E. Evaluation of binding in a transfected cell line expressing a peripheral cannabinoid receptor (CB2): identification of cannabinoid receptor subtype selective ligands. *J. Pharmacol. Exp. Ther.* **1996,** *278* (3), 989-99.

4. Felder, C. C.; Joyce, K. E.; Briley, E. M.; Mansouri, J.; Mackie, K.; Blond, O.; Lai, Y.; Ma, A. L.; Mitchell, R. L. Comparison of the pharmacology and signal transduction of the human cannabinoid CB1 and CB2 receptors. *Mol. Pharmacol.* **1995,** *48* (3), 443-50.

5. Rhee, M. H.; Vogel, Z.; Barg, J.; Bayewitch, M.; Levy, R.; Hanus, L.; Breuer, A.; Mechoulam, R. Cannabinol derivatives: binding to cannabinoid receptors and inhibition of adenylylcyclase. *J. Med. Chem.* **1997,** *40* (20), 3228-33.

6. Hillard, C. J.; Manna, S.; Greenberg, M. J.; DiCamelli, R.; Ross, R. A.; Stevenson, L. A.; Murphy, V.; Pertwee, R. G.; Campbell, W. B. Synthesis and Characterization of Potent and Selective Agonists of the Neuronal Cannabinoid Receptor (CB1). *J. Pharmacol. Exp. Ther.* **1999,** *289* (3), 1427-1433.

7. Shire, D.; Calandra, B.; Rinaldi-Carmona, M.; Oustric, D.; Pessegue, B.; Bonnin-Cabanne, O.; Le Fur, G.; Caput, D.; Ferrara, P. Molecular cloning, expression and function of the murine CB2 peripheral cannabinoid receptor. *Biochim. Biophys. Acta* **1996,** *1307* (2), 132-6.

8. Aung, M. M.; Griffin, G.; Huffman, J. W.; Wu, M. J.; Keel, C.; Yang, B.; Showalter, V. M.; Abood, M. E.; Martin, B. R. Influence of the N-1 alkyl chain length of cannabimimetic indoles upon CB1 and CB2 receptor binding. *Drug Alcohol Depen.* **2000,** *60* (2), 133-140.

9. Makriyannis, A.; Deng, H. Preparation of cannabimimetic indole derivatives with cannabinoid CB1 or CB2 receptor binding affinity. World patent WO 2001/028557, 26 April, 2001.

10. Frost, J. M.; Dart, M. J.; Tietje, K. R.; Garrison, T. R.; Grayson, G. K.; Daza, A. V.; El-Kouhen, O. F.; Yao, B. B.; Hsieh, G. C.; Pai, M.; Zhu, C. Z.; Chandran, P.; Meyer, M. D. Indol-3-ylcycloalkyl ketones: effects of N1 substituted indole side chain variations on CB(2) cannabinoid receptor activity. *J. Med. Chem.* **2010,** *53* (1), 295-315.

11. Wiley, J. L.; Marusich, J. A.; Lefever, T. W.; Grabenauer, M.; Moore, K. N.; Thomas, B. F. Cannabinoids in disguise: Delta9-tetrahydrocannabinol-like effects of tetramethylcyclopropyl ketone indoles. *Neuropharmacology* **2013,** *75*, 145-54.

12. Uchiyama, N.; Kawamura, M.; Kikura-Hanajiri, R.; Goda, Y. URB-754: A new class of designer drug and 12 synthetic cannabinoids detected in illegal products. *Forensic Sci. Int.* **2013,** *227* (1-3), 21-32.

The pharmacology of indole and indazole synthetic cannabinoid designer drugs AB-FUBINACA, ADB-FUBINACA, AB-PINACA, ADB-PINACA, 5F-AB-PINACA, 5F-ADB-PINACA, ADBICA and 5F-ADBICA

Samuel D. Banister, Michael Moir, Jordyn Stuart, Richard C. Kevin, Katie E. Wood, Mitchell Longworth, Shane M. Wilkinson, Corinne Beinat, Alexandra S. Buchanan, Michelle Glass, Mark Connor, Iain S. McGregor, Michael Kassiou

Contents:

Table S1. IUPAC names, CAS numbers, and literature references for valinamide- and *tert*-leucinamide-derived indole and indazole synthetic cannabinoids.

	IUPAC	CAS	Notified to EMCDDA	Refs
AB-FUBINACA (**7**)	*N*-(1-amino-3-methyl-1-oxobutan-2-yl)-1-(4-fluorobenzyl)-1*H*-indazole-3-carboxamide	1629062-56-1 (racemate) 1185282-01-2 (*S*)	4 July 2013, Belgium	1–5
ADB-FUBINACA (**8**)	*N*-(1-amino-3,3-dimethyl-1-oxobutan-2-yl)-1-(4-fluorobenzyl)-1*H*-indazole-3-carboxamide	1445583-51-6 (racemate) 1185282-00-1 (*S*)	28 November 2013, Turkey and Germany	1, 4, 6–8
AB-PINACA (**9**)	*N*-(1-amino-3-methyl-1-oxobutan-2-yl)-1-pentyl-1*H*-indazole-3-carboxamide	1445583-20-9 (racemate) 1445752-09-9 (*S*)	21 May 2013, Sweden	2, 4, 5, 7
ADB-PINACA (**10**)	*N*-(1-amino-3,3-dimethyl-1-oxobutan-2-yl)-1-pentyl-1*H*-indazole-3-carboxamide	1633766-73-0 (racemate)	3 December 2013, United Kingdom[a]	3, 8, 9
5F-AB-PINACA (**11**)	*N*-(1-amino-3-methyl-1-oxobutan-2-yl)-1-(5-fluoropentyl-1*H*-indazole-3-carboxamide	-	5 July 2013, Belgium	10
5F-ADB-PINACA (**12**)	*N*-(1-amino-3,3-dimethyl-1-oxobutan-2-yl)-1-(5-fluoropentyl-1*H*-indazole-3-carboxamide	-	-	11
AB-FUBICA (**13**)	*N*-(1-amino-3-methyl-1-oxobutan-2-yl)-1-(4-fluorobenzyl)-1*H*-indole-3-carboxamide	-	-	-
ADB-FUBICA (**14**)	*N*-(1-amino-3,3-dimethyl-1-oxobutan-2-yl)-1-(4-fluorobenzyl)-1*H*-indole-3-carboxamide	-	-	-
AB-PICA (**15**)	*N*-(1-amino-3-methyl-1-oxobutan-2-yl)-1-pentyl-1*H*-indole-3-carboxamide	-	-	-
ADBICA (**16**)	*N*-(1-amino-3,3-dimethyl-1-oxobutan-2-yl)-1-pentyl-1*H*-indole-3-carboxamide	1445583-48-1 (racemate)	11 October 2013, Sweden	6
5F-AB-PICA (**17**)	*N*-(1-amino-3-methyl-1-oxobutan-2-yl)-1-(5-fluoropentyl-1*H*-indole-3-carboxamide	-	-	-
5F-ADBICA (**18**)	*N*-(1-amino-3,3-dimethyl-1-oxobutan-2-yl)-1-(5-fluoropentyl-1*H*-indole-3-carboxamide	-	September 2013, USA[a]	8

[a]An advisory was issued in September 2013 after information provided by law enforcement agencies in the United States, supplemented by information from the EMCDDA's monitoring of open source information, identified a series of non-fatal

intoxications in the United States associated with ADB-PINACA and 5F-ADBICA. These substances are known to be present on the EU drug market and have been reported by several Member States.

References

1. Buchler, I.P.; Hayes, M.J.; Hedge, S.G.; Hockerman, S.L.; Jones, D.E.; Kortum, S.W.; Rico, J.G.; Tenbrink, R.E.; Wu, K.K. (Pfizer, USA). Indazole derivatives as CB1 receptor modulators and their preparation and use in the treatment of CB1-mediated diseases. World patent WO2009/106982 A1, September 3, 2009.
2. Uchiyama, N.; Matsuda, S.; Wakana, D.; Kikura-Hanajiri, R.Goda, Y. New cannabimimetic indazole derivatives, N-(1-amino-3-methyl-1-oxobutan-2-yl)-1-pentyl-1H-indazole-3-carboxamide (AB-PINACA) and N-(1-amino-3-methyl-1-oxobutan-2-yl)-1-(4-fluorobenzyl)-1H-indazole-3-carboxamide (AB-FUBINACA) identified as designer drugs in illegal products. *Forensic Toxicol.* **2013,** 31, 93-100.
3. Huang, L.; Marino, M. A.; Voyer, B. (Hofstra University, USA). Nuclear magnetic resonance implemanted synthetic indole and indazole cannabinoid detection, identification, and quantification. World patent WO2014/176542 A1, October 30, 2014.
4. Takayama, T.; Suzuki, M.; Todoroki, K.; Inoue, K.; Min, J.Z.; Kikura-Hanajiri, R.; Goda, Y.Toyo'oka, T. UPLC/ESI-MS/MS-based determination of metabolism of several new illicit drugs, ADB-FUBINACA, AB-FUBINACA, AB-PINACA, QUPIC, 5F-QUPIC and alpha-PVT, by human liver microsome. *Biomed. Chromatogr*. **2014,** 28, 831-838.
5. Thomsen, R.; Nielsen, L. M.; Holm, N. B.; Rasmussen, H. B.; Linnet, K.; the Indices Consortium. Synthetic cannabimimetic agents metabolized by carboxylesterases. *Drug Test. Anal.* Published online October 24, 2014. DOI: 10.1002/dta.1731.
6. Uchiyama, N.; Matsuda, S.; Kawamura, M.; Kikura-Hanajiri, R.Goda, Y. Two new-type cannabimimetic quinolinyl carboxylates, QUPIC and QUCHIC, two new cannabimimetic carboxamide derivatives, ADB-FUBINACA and ADBICA, and five synthetic cannabinoids detected with a thiophene derivative α-PVT and an opioid receptor agonist AH-7921 identified in illegal products. *Forensic Toxicol.* **2013,** 31, 223-240.
7. Chung, H.; Choi, H.; Heo, S.; Kim, E.Lee, J. Synthetic cannabinoids abused in South Korea: drug identifications by the National Forensic Service from 2009 to June 2013. *Forensic Toxicol.* **2014,** 32, 82-88.
8. European Monitoring Centre for Drugs and Drug Addiction (2014), *EMCDDA–Europol 2013 Annual Report on the implementation of Council Decision 2005/387/JHA,* Implementation reports, Publications Office of the European Union, Luxembourg.

9. Centers for Disease Control and Prevention. Notes from the field: Severe Illness Associated with Reported Use of Synthetic Marijuana — Colorado, August–September 2013. *Morb. Mortal. Wkly Rep.* **2013,** 62, 1016-1017.
10. Uchiyama, N.; Shimokawa, Y.; Kawamura, M.; Kikura-Hanajiri, R.; Hakamatsuka, T. Chemical analysis of a benzofuran derivative, 2-(2-ethylaminopropyl)benzofuran (2-EAPB), eight synthetic cannabinoids, five cathinone derivatives, and five other designer drugs newly detected in illegal products. *Forensic Toxicol.* **2014,** 32, 266-281.
11. Wurita, A.; Hasegawa, K.; Minakata, K.; Gonmori, K.; Nozawa, H.; Yamagishi, I.; Watanabe, K.Suzuki, O. Identification and quantitation of 5-fluoro-ADB-PINACA and MAB-CHMINACA in dubious herbal products. *Forensic Toxicol.* Published online Feb 3, 2015. DOI: 10.1007/s11419-015-0264-y.

Figure S1. ^{1}H NMR spectrum (500 MHz, $CDCl_3$, 300 K) of AB-FUBINACA (**7**).

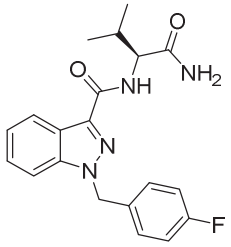

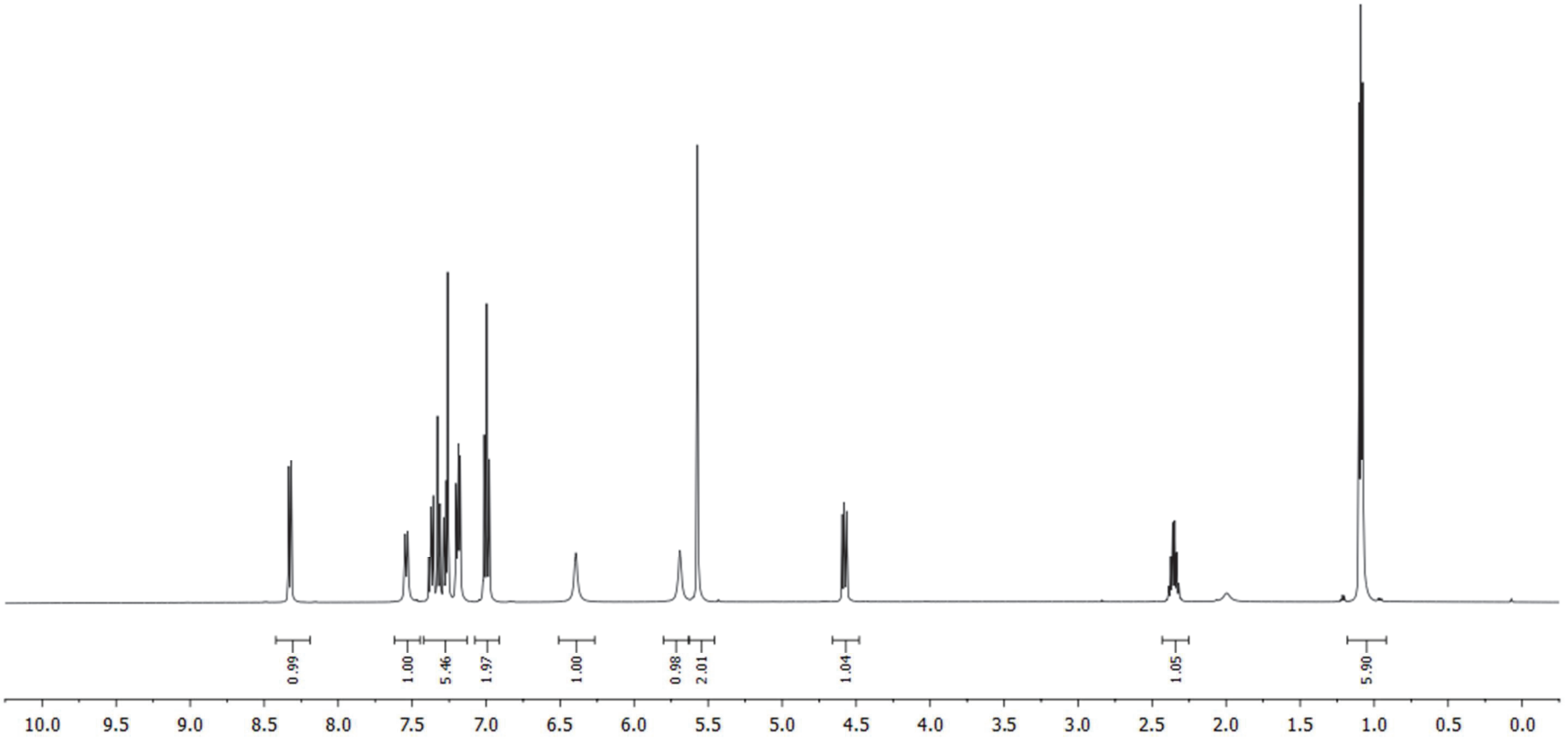

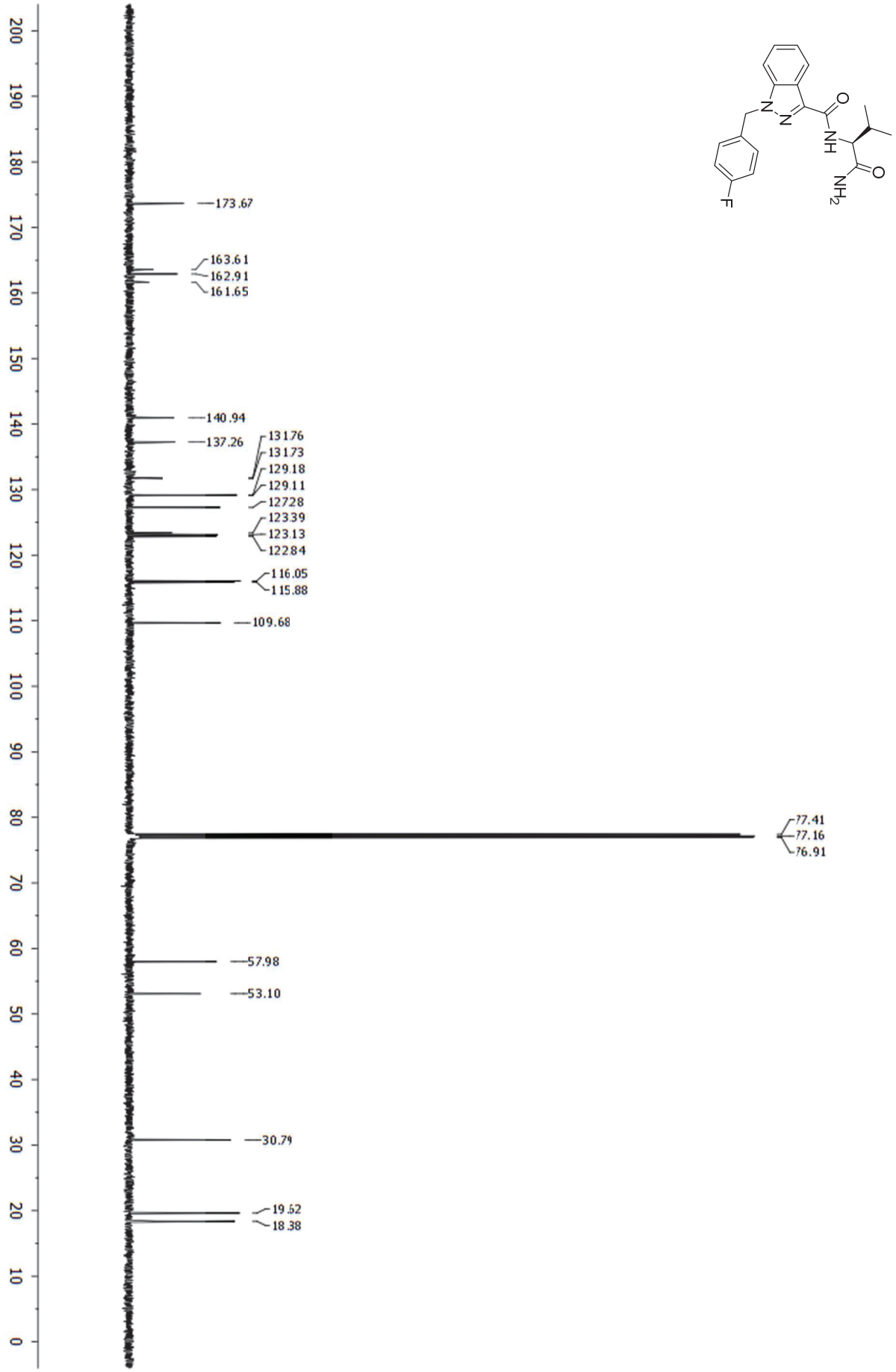

Figure S2. ^{13}C NMR spectrum (125 MHz, $CDCl_3$, 300 K) of AB-FUBINACA (**7**).

Figure S3. ^{1}H NMR spectrum (500 MHz, $CDCl_3$, 300 K) of AB-PINACA (**9**).

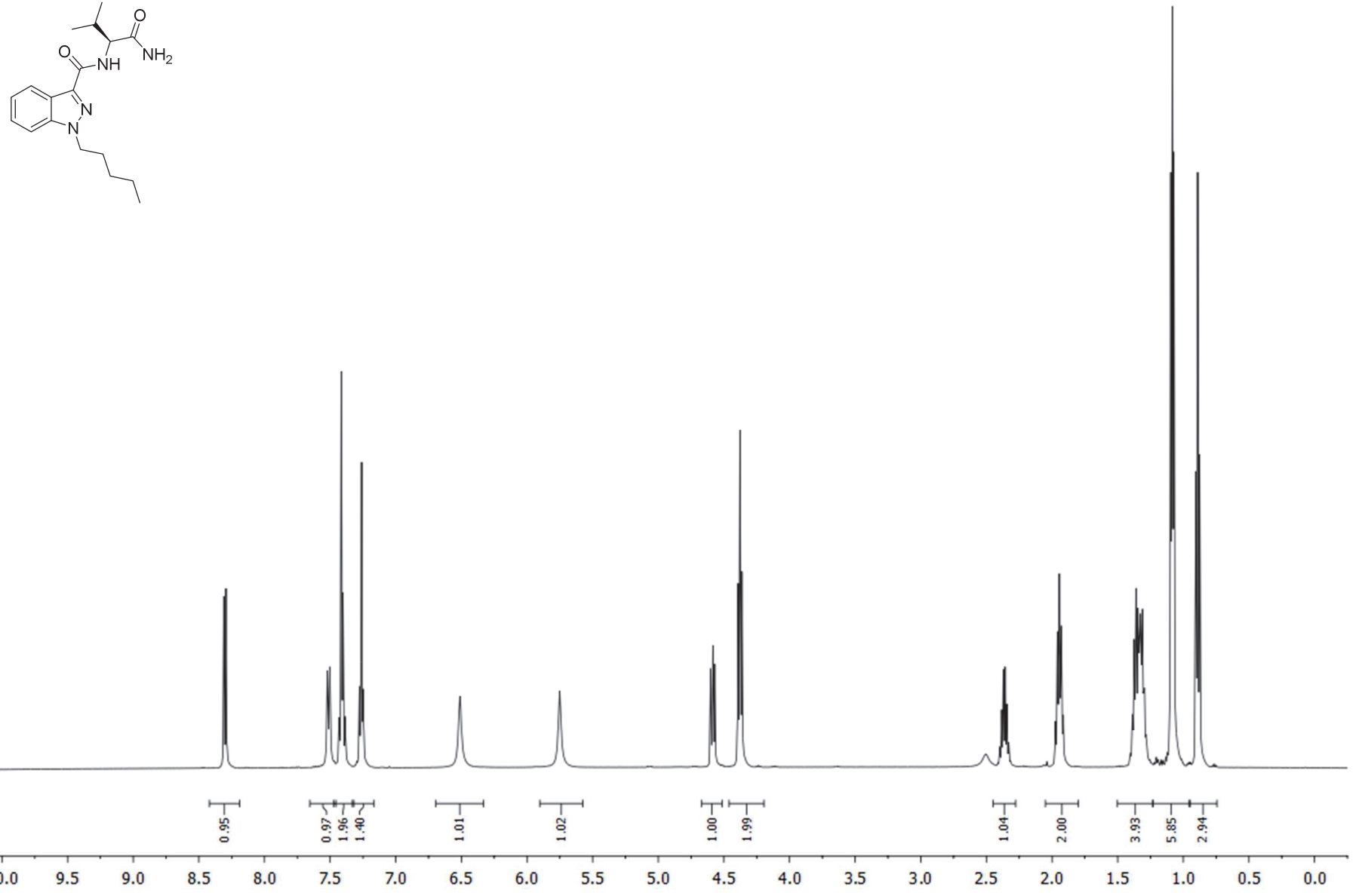

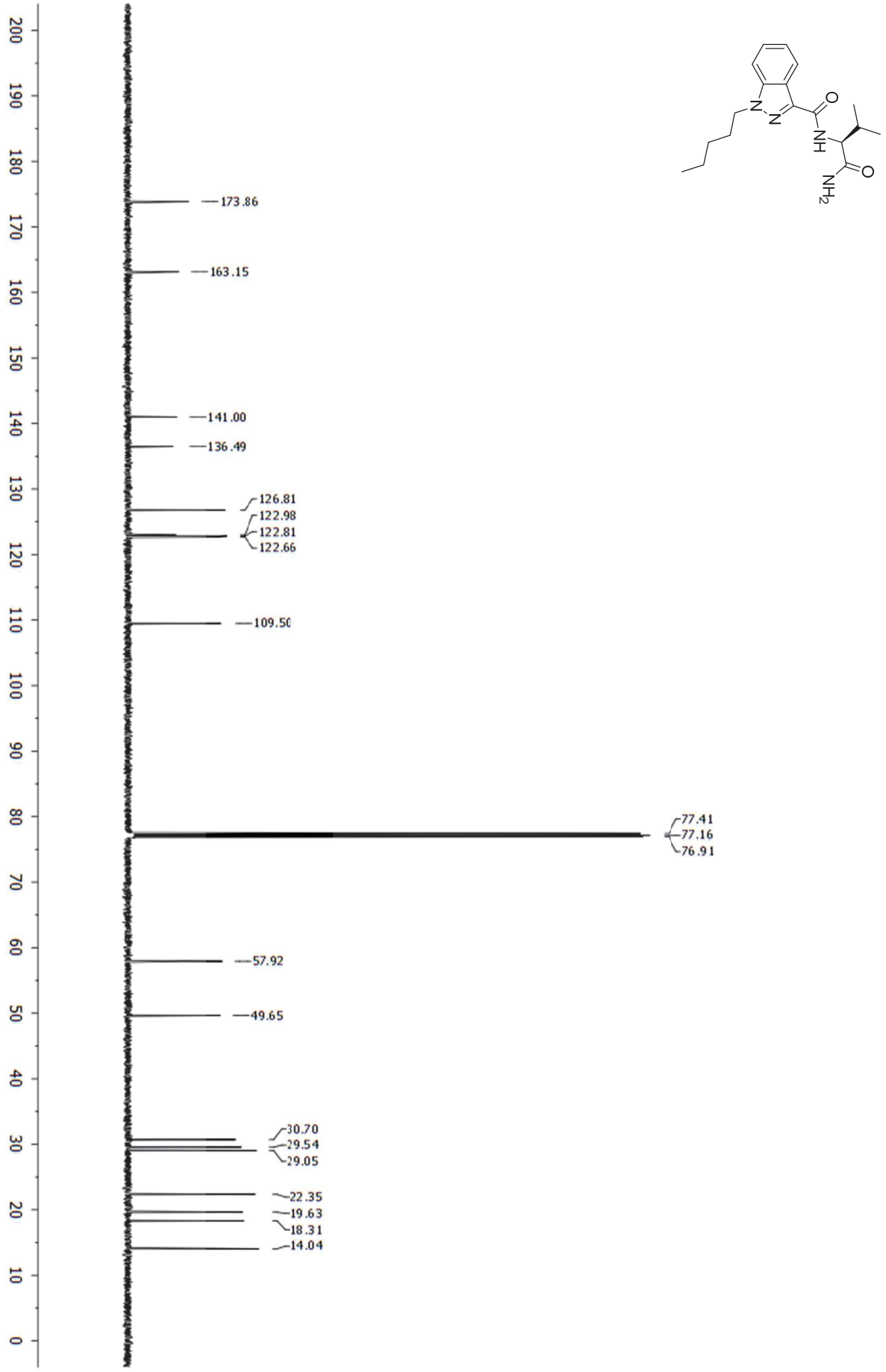

Figure S4. ^{13}C NMR spectrum (125 MHz, $CDCl_3$, 300 K) of AB-PINACA (**9**).

Figure S5. ^{1}H NMR spectrum (400 MHz, $CDCl_3$, 300 K) of ADB-PINACA (**10**).

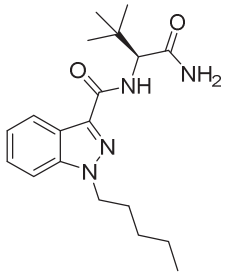

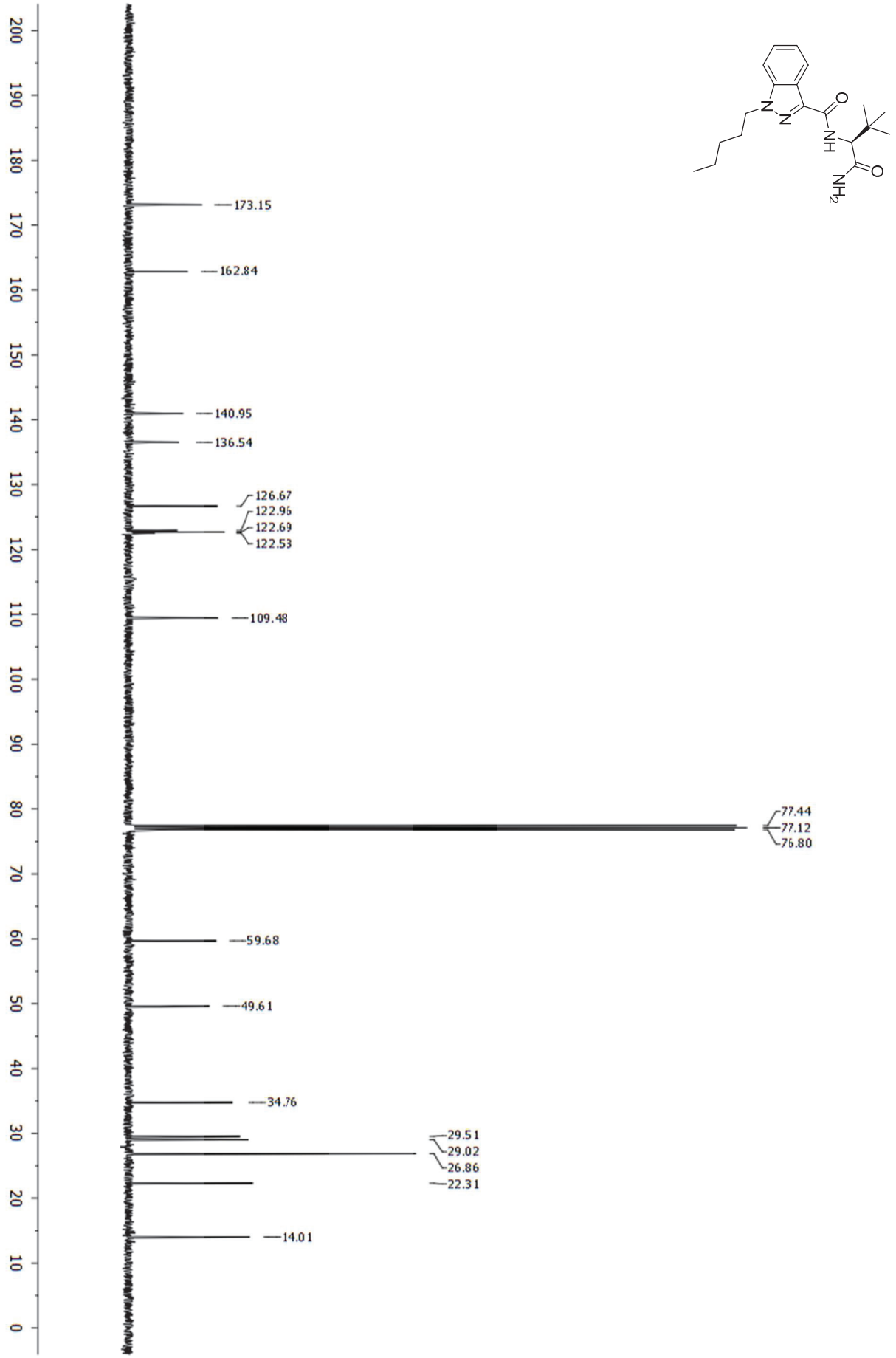

Figure S6. ^{13}C NMR spectrum (100 MHz, $CDCl_3$, 300 K) of ADB-PINACA (**10**).

Figure S7. ^{1}H NMR spectrum (400 MHz, DMSO-d_6, 300 K) of AB-PICA (**15**).

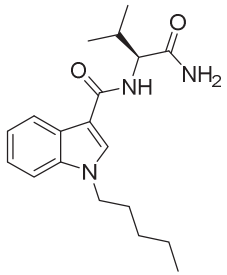

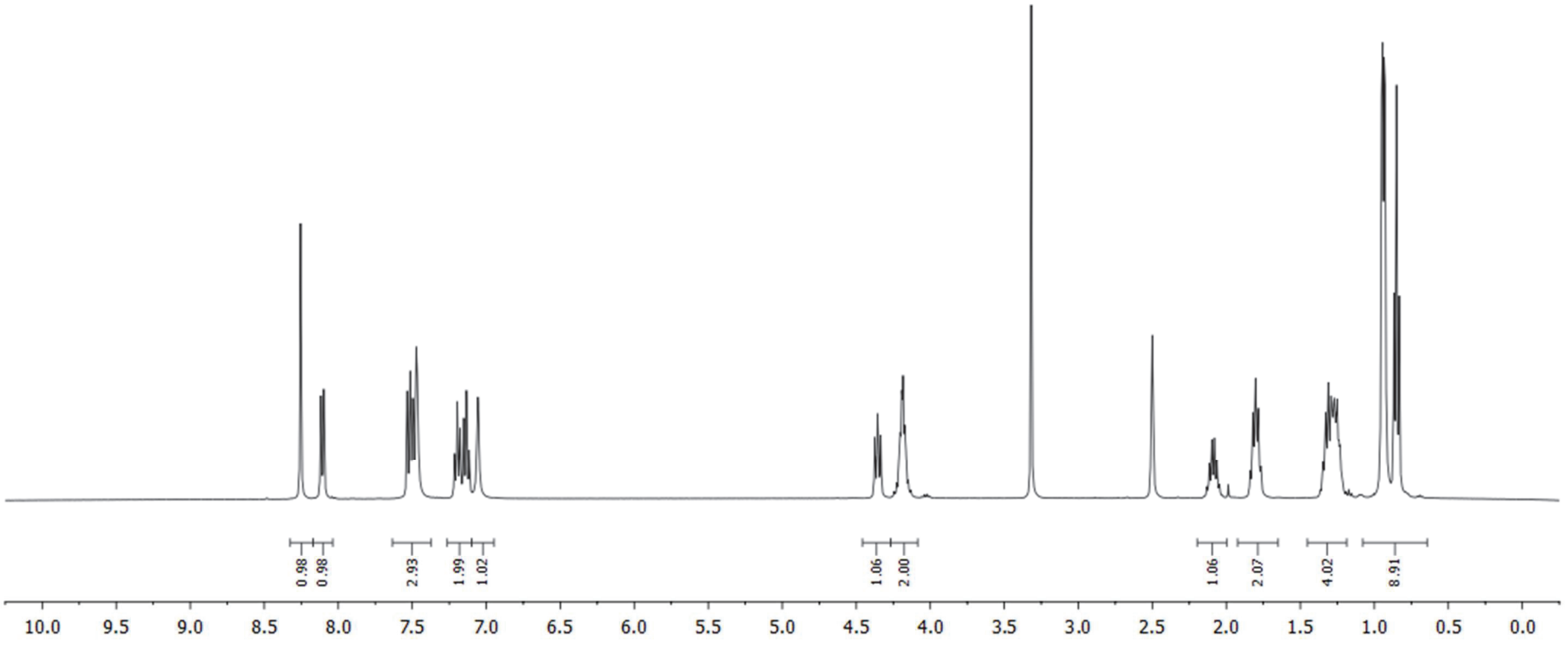

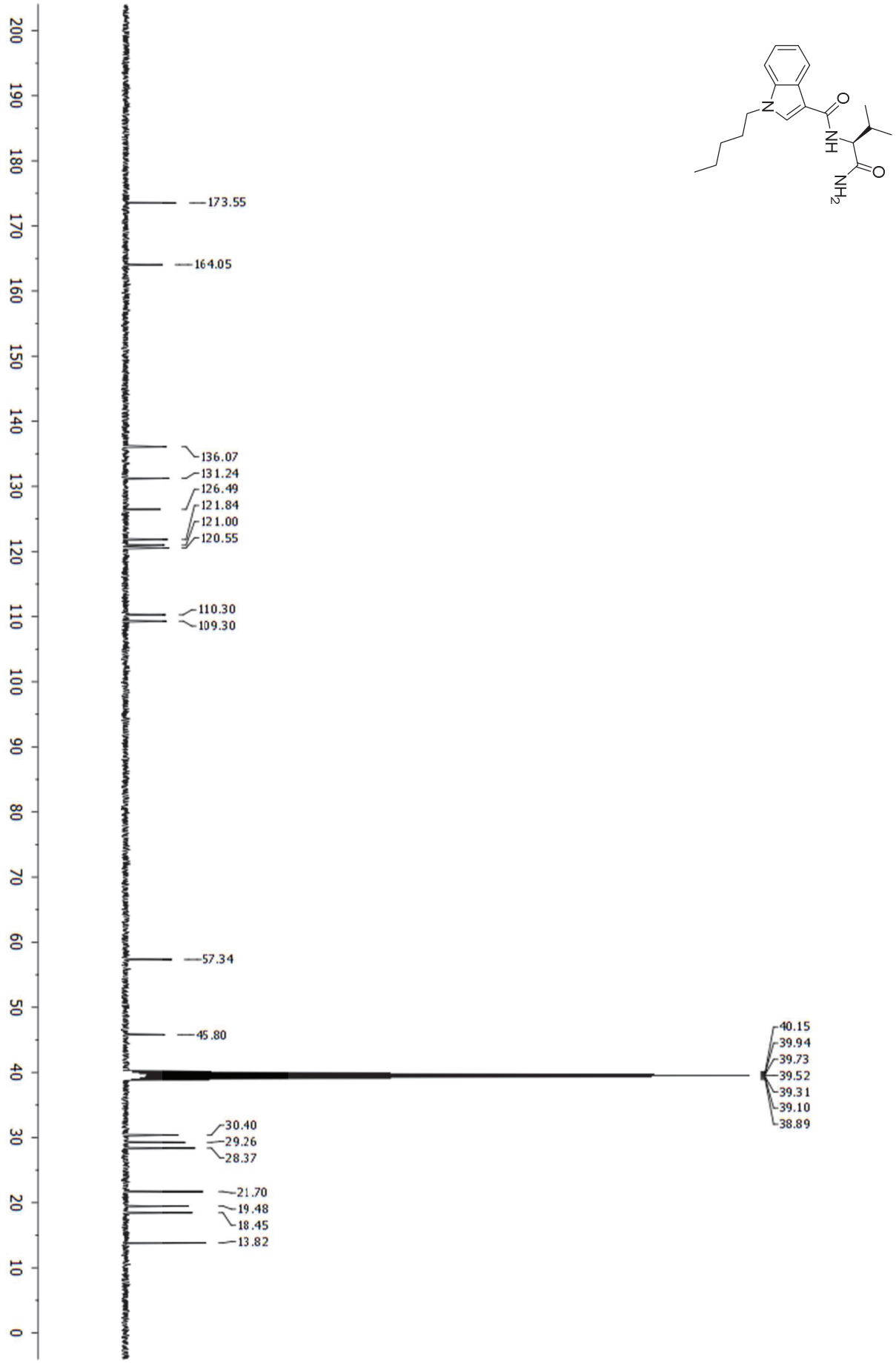

Figure S8. ^{13}C NMR spectrum (100 MHz, DMSO-d_6, 300 K) of AB-PICA (**15**).

Figure S9. ^{1}H NMR spectrum (400 MHz, DMSO-d_6, 300 K) of 5F-AB-PICA (**17**).

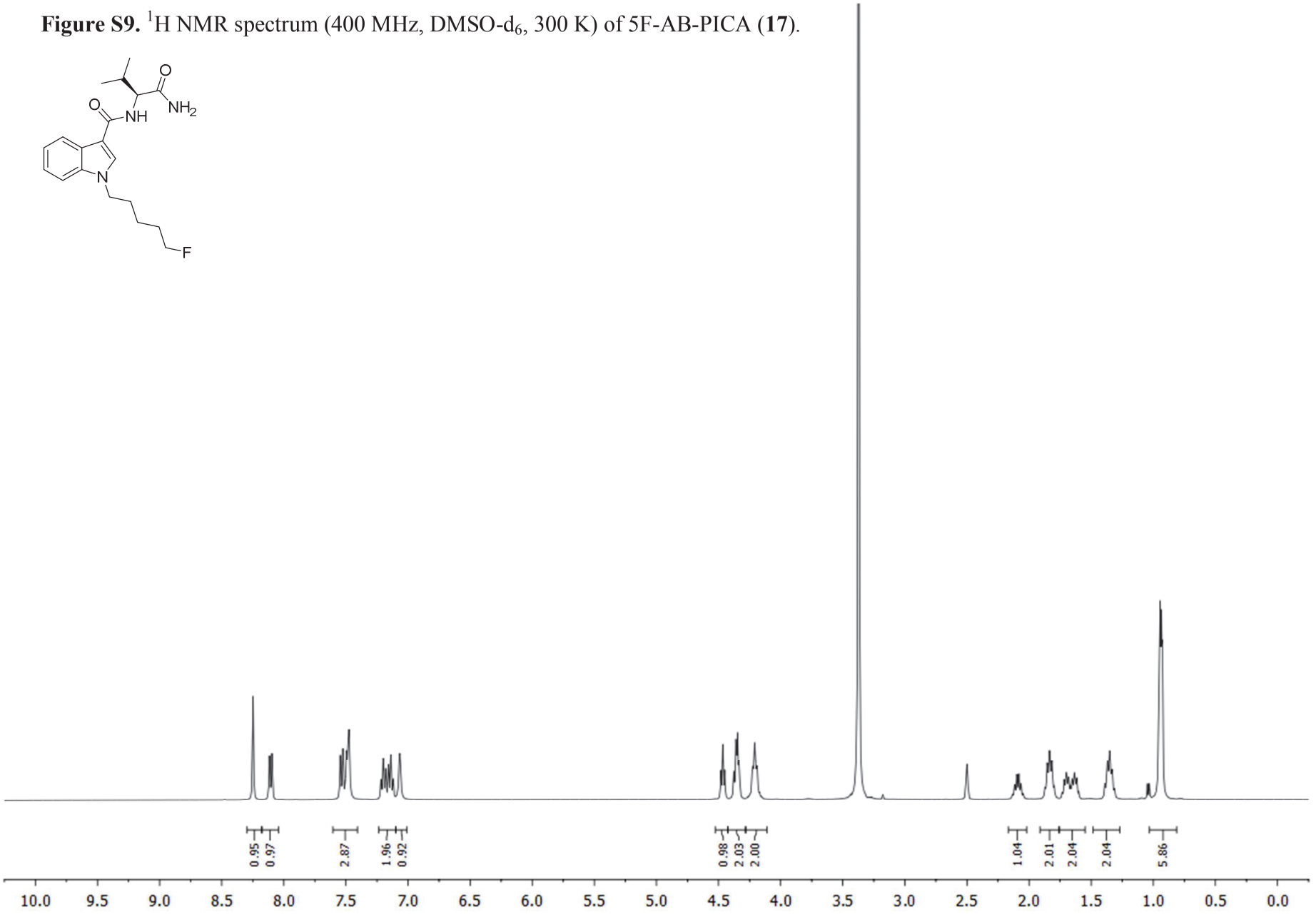

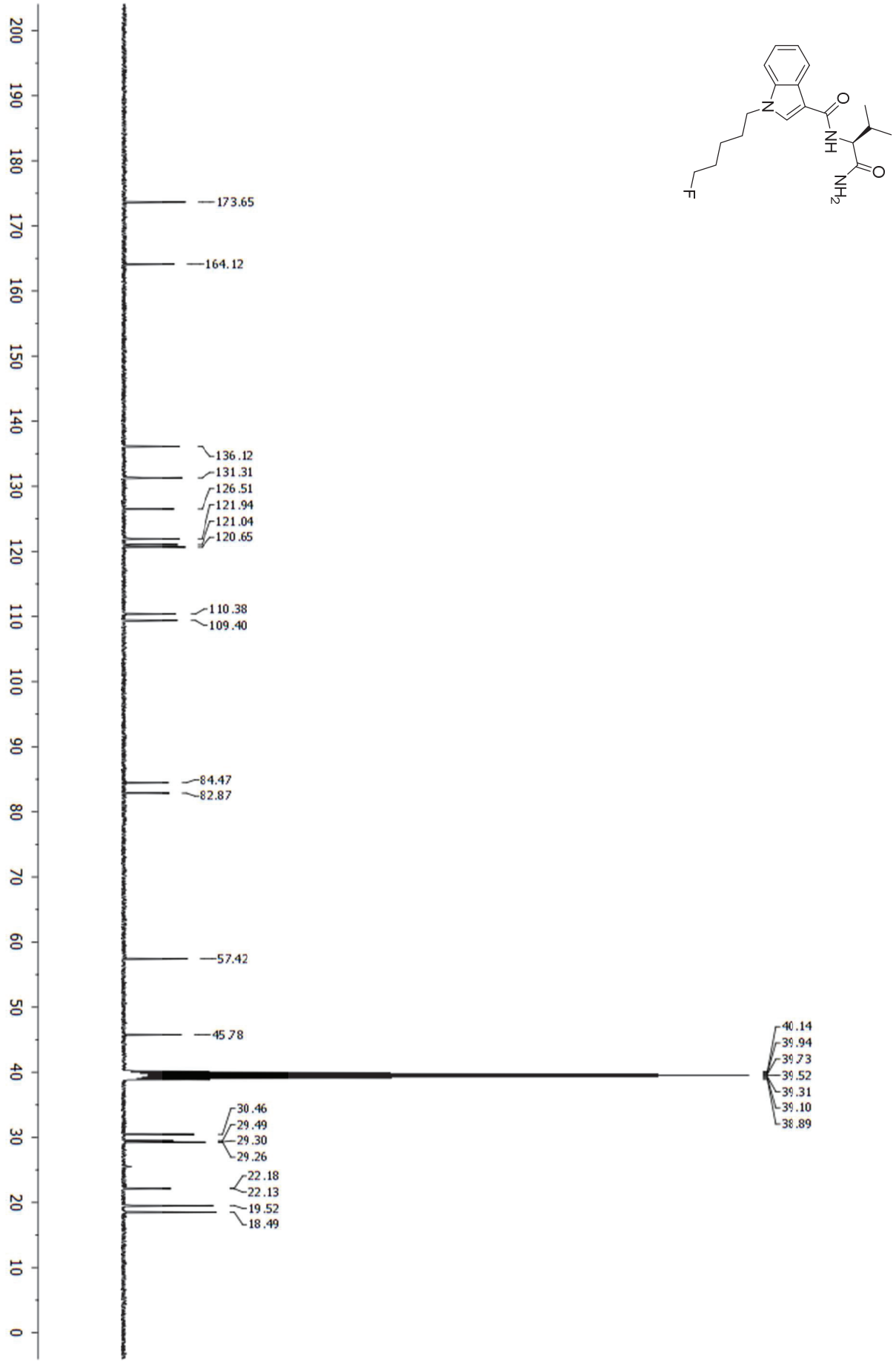

Figure S10. ^{13}C NMR spectrum (100 MHz, DMSO-d_6, 300 K) of 5F-AB-PICA (**17**).

Figure S11. ^{1}H NMR spectrum (400 MHz, $CDCl_3$, 300 K) of 5F-ADBICA (**18**).

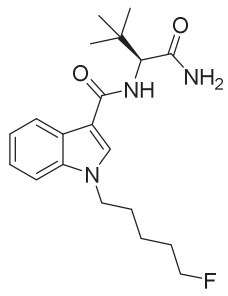

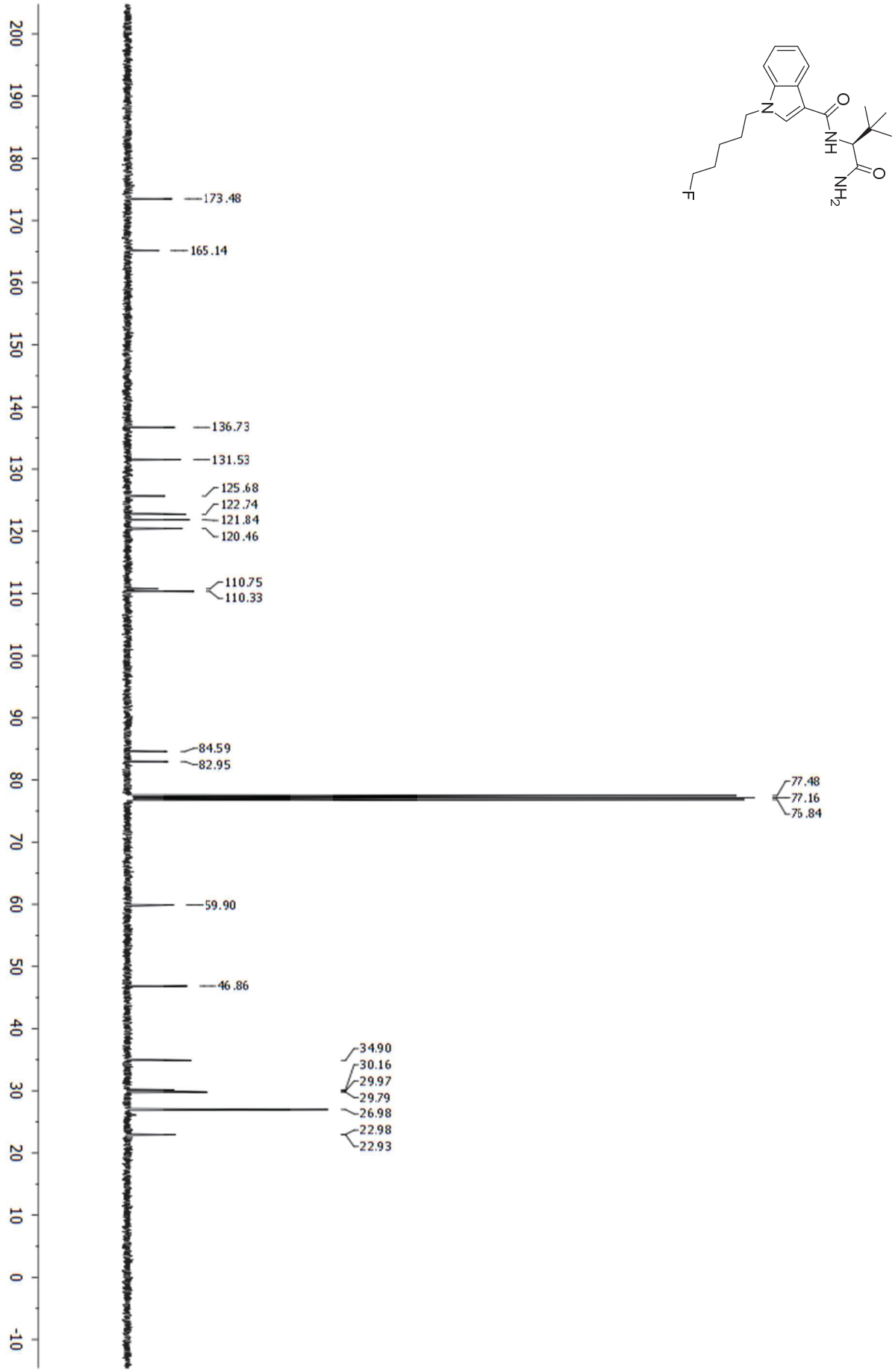

Figure S12. ^{13}C NMR spectrum (100 MHz, $CDCl_3$, 300 K) of 5F-ADBICA (**18**).

Figure S13. Mean area under the vehicle-vehicle baseline curve (AUC ± SEM) for body temperature for (A) AB-PINACA and (B) AB-FUBINACA (3 mg/kg), following pretreatment with vehicle, rimonabant (CB_1 antagonist, 3 mg/kg), or SR144528 (CB_2 antagonist, 3 mg/kg). The area was significantly reduced for both AB-PINACA and AB-FUBINACA by rimonabant but not SR144528. * $p < .05$ compared to vehicle.

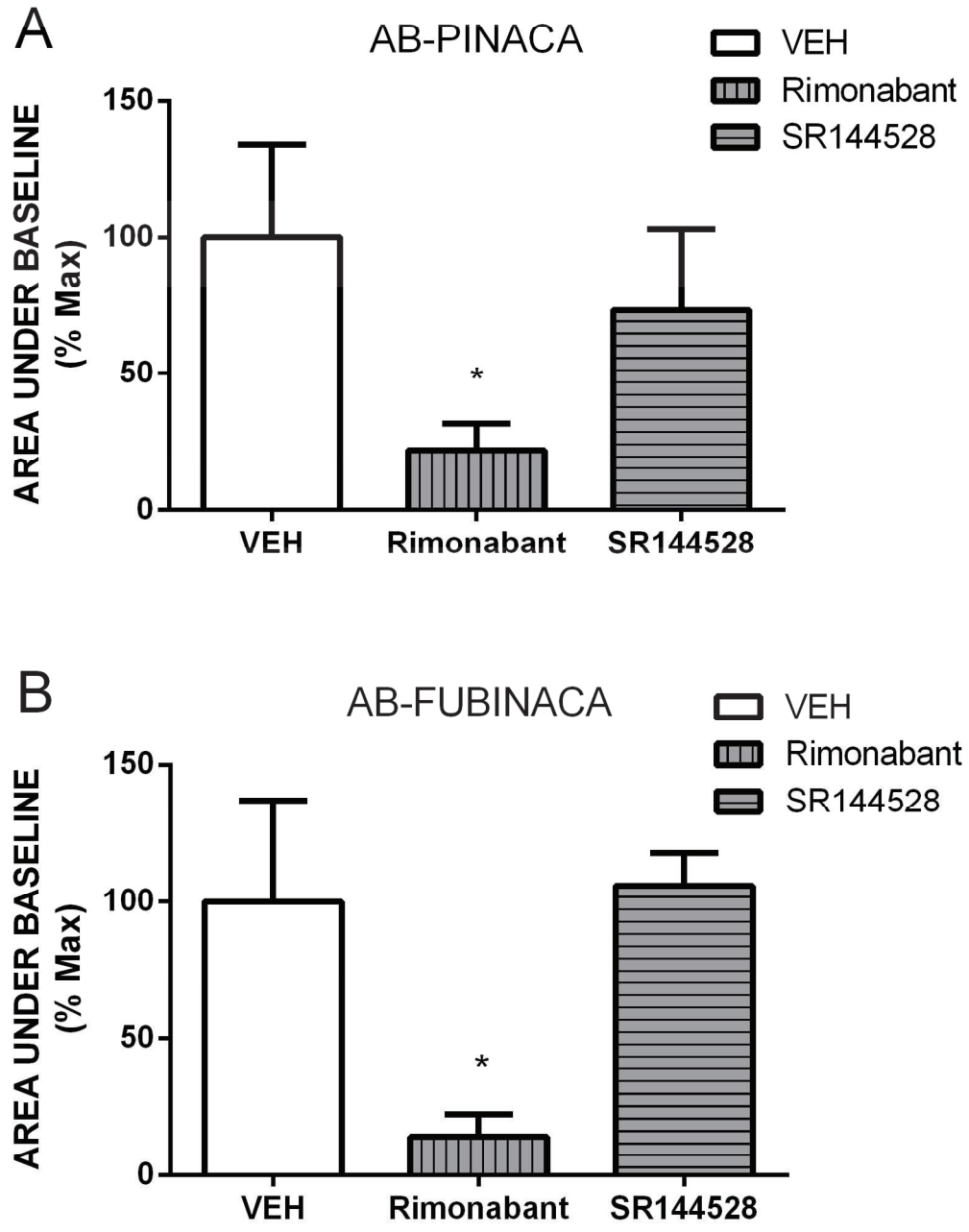

Pharmacology of Valinate and *tert*-Leucinate Synthetic Cannabinoids 5F-AMBICA, 5F-AMB, 5F-ADB, AMB-FUBINACA, MDMB-FUBINACA, MDMB-CHMICA, and Their Analogues

Samuel D. Banister, Mitchell Longworth, Richard Kevin, Shivani Sachdev, Marina Santiago, Jordyn Stuart, James B. C. Mack, Michelle Glass, Iain S. McGregor, Mark Connor, Michael Kassiou

Contents:

Table S1. IUPAC names, CAS numbers, and selected references for valinate- and *tert*-leucinate-derived indole and indazole synthetic cannabinoids.

	IUPAC	CAS	Notified to EMCDDA	Refs
5F-AMB-PICA (**10**)	methyl (*S*)-2-(1-(5-fluoropentyl)-1*H*-indole-3-carboxamido)-3-methylbutanoate	1616253-26-9 (racemate)	5 December 2014, Hungary	1-3
5F-MDMB-PICA (**11**)	methyl (*S*)-2-(1-(5-fluoropentyl)-1*H*-indole-3-carboxamido)-3,3-dimethylbutanoate	-	-	4
5F-AMB-PINACA (**12**)	methyl (*S*)-2-(1-(5-fluoropentyl)-1*H*-indazole-3-carboxamido)-3-methylbutanoate	1715016-74-2 (racemate) 1801552-03-3 (*S*-enantiomer)	18 June 2014, Hungary	2-9
5F-MDMB-PINACA (**13**)	methyl (*S*)-2-(1-(5-fluoropentyl)-1*H*-indazole-3-carboxamido)-3,3-dimethylbutanoate	1715016-75-3 (racemate) 1838134-16-9 (*R*-enantiomer)	-	2, 4, 10
AMB-FUBICA (**14**)	methyl (*S*)-2-(1-(4-fluorobenzyl)-1*H*-indole-3-carboxamido)-3-methylbutanoate	-	-	-
MDMB-FUBICA (**15**)	methyl (*S*)-2-(1-(4-fluorobenzyl)-1*H*-indole-3-carboxamido)-3,3-dimethylbutanoate	-		-
AMB-FUBINACA (**16**)	methyl (*S*)-2-(1-(4-fluorobenzyl)-1*H*-indazole-3-carboxamido)-3-methylbutanoate	1715016-76-4 (racemate)	-	2, 4
MDMB-FUBINACA (**17**)	methyl (*S*)-2-(1-(4-fluorobenzyl)-1*H*-indazole-3-carboxamido)-3,3-dimethylbutanoate	1715016-77-5 (racemate)	October 2014, Russian Federation[a]	2-4
AMB-CHMICA (**18**)	methyl (*S*)-2-(1-(cyclohexylmethyl)-1*H*-indole-3-carboxamido)-3-methylbutanoate	-	-	-
MDMB-CHMICA (**19**)	methyl (*S*)-2-(1-(cyclohexylmethyl)-1*H*-indole-3-carboxamido)-3,3-dimethylbutanoate	1863065-84-2 (racemate)	12 September 2014, Hungary[b]	2-3, 7, 11
AMB-CHMINACA (**20**)	methyl (*S*)-2-(1-(cyclohexylmethyl)-1*H*-indazole-3-carboxamido)-3-methylbutanoate	1863066-03-8 (racemate)	-	2
MDMB-CHMINACA (**21**)	methyl (*S*)-2-(1-(cyclohexylmethyl)-1*H*-indazole-3-carboxamido)-3,3-dimethylbutanoate	1715016-78-6 (racemate)	-	2, 4

		1185888-32-7 (*S*-enantiomer)		
AMB-PICA (**22**)	methyl (*S*)-2-(1-(pentyl)-1*H*-indole-3-carboxamido)-3-methylbutanoate	-	-	-
MDMB-PICA (**23**)	methyl (*S*)-2-(1-(pentyl)-1*H*-indole-3-carboxamido)-3,3-dimethylbutanoate	-	-	-
AMB-PINACA (**24**)	methyl (*S*)-2-(1-(pentyl)-1*H*-indazole-3-carboxamido)-3-methylbutanoate	1863066-06-1 (racemate) 1890250-13-1 (*S*-enantiomer)	10 December 2014, Sweden	2-3, 9
MDMB-PINACA (**25**)	methyl (*S*)-2-(1-(pentyl)-1*H*-indazole-3-carboxamido)-3,3-dimethylbutanoate	-		-

[a]An alert was issued after the EMCDDA identified media reports of two outbreaks of serious adverse events associated with consumption of MDMB-FUBINACA.

[b]Two alerts were issued in December 2014 after the Austrian national focal point reported 7 non-fatal intoxications associated with use of a product called 'Bonzai citrus' and/or 'Bonzai Winter Boost' (which allegedly contained MDMB-CHMICA) and after the Swedish national focal point reported 4 deaths and 6 non-fatal intoxications associated with the use of MDMB-CHMICA that occurred between September and November 2014.

References

1. Shevyrin, V. A., Morzherin, Y. Y., Melkozerov, V. P., Nevero, A. S. (2014) New Synthetic Cannabinoid – Methyl 2-{[1-(5-Fluoro-Pentyl)-3-Methyl-1H-Indol-3-Ylcarbonyl]-Amino}Butyrate – as a Designer Drug. *Chem Heterocycl Compd*. *50*, 583-586.
2. Akamatsu, S., Yoshida, M. (2016) Fragmentation of synthetic cannabinoids with an isopropyl group or a tert-butyl group ionized by electron impact and electrospray. *J Mass Spectrom*. *51*, 28-32.
3. European Monitoring Centre for Drugs and Drug Addiction (2015) *EMCDDA–Europol 2014 Annual Report on the implementation of Council Decision 2005/387/JHA*, Implementation reports, European Monitoring Centre for Drugs and Drug Addiction, Luxembourg.
4. Shevyrin, V., Melkozerov, V., Nevero, A., Eltsov, O., Shafran, Y., Morzherin, Y., Lebedev, A. T. (2015) Identification and analytical characteristics of synthetic cannabinoids with an indazole-3-carboxamide structure bearing a N-1-methoxycarbonylalkyl group. *Anal Bioanal Chem*. *407*, 6301-6315.

5. Uchiyama, N., Shimokawa, Y., Kawamura, M., Kikura-Hanajiri, R., Hakamatsuka, T. (2014) Chemical analysis of a benzofuran derivative, 2-(2-ethylaminopropyl)benzofuran (2-EAPB), eight synthetic cannabinoids, five cathinone derivatives, and five other designer drugs newly detected in illegal products. *Forensic Toxicol*. *32*, 266-281.
6. Hasegawa, K., Wurita, A., Minakata, K., Gonmori, K., Nozawa, H., Yamagishi, I., Watanabe, K., Suzuki, O. (2014) Postmortem distribution of AB-CHMINACA, 5-fluoro-AMB, and diphenidine in body fluids and solid tissues in a fatal poisoning case: usefulness of adipose tissue for detection of the drugs in unchanged forms. *Forensic Toxicol*. *33*, 45-53.
7. Langer, N., Lindigkeit, R., Schiebel, H.-M., Papke, U., Ernst, L., Beuerle, T. (2015) Identification and quantification of synthetic cannabinoids in "spice-like" herbal mixtures: update of the German situation for the spring of 2015. *Forensic Toxicol*. *34*, 94-107.
8. Dronova, M., Smolianitski, E., Lev, O. (2016) Electrooxidation of New Synthetic Cannabinoids: Voltammetric Determination of Drugs in Seized Street Samples and Artificial Saliva. *Anal Chem*. *88*, 4487-4494.
9. Andersson, M., Diao, X., Wohlfarth, A., Scheidweiler, K. B., Huestis, M. A. (2016) Metabolic profiling of new synthetic cannabinoids AMB and 5F-AMB by human hepatocyte and liver microsome incubations and high-resolution mass spectrometry. *Rapid Commun Mass Spectrom*. *30*, 1067-1078.
10. Hasegawa, K., Wurita, A., Minakata, K., Gonmori, K., Yamagishi, I., Nozawa, H., Watanabe, K., Suzuki, O. (2014) Identification and quantitation of 5-fluoro-ADB, one of the most dangerous synthetic cannabinoids, in the stomach contents and solid tissues of a human cadaver and in some herbal products. *Forensic Toxicol*. *33*, 112-121.
11. Grigoryev, A., Kavanagh, P., Pechnikov, A. (2016) Human urinary metabolite pattern of a new synthetic cannabimimetic, methyl 2-(1-(cyclohexylmethyl)-1H-indole-3-carboxamido)-3,3-dimethylbutanoate. *Forensic Toxicol*. doi: 10.1007/s11419-016-0319-8.

Figure S1. ^{1}H NMR spectrum (300 MHz, $CDCl_3$, 300 K) of 5F-AMB-PICA (**10**).

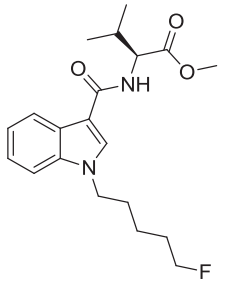

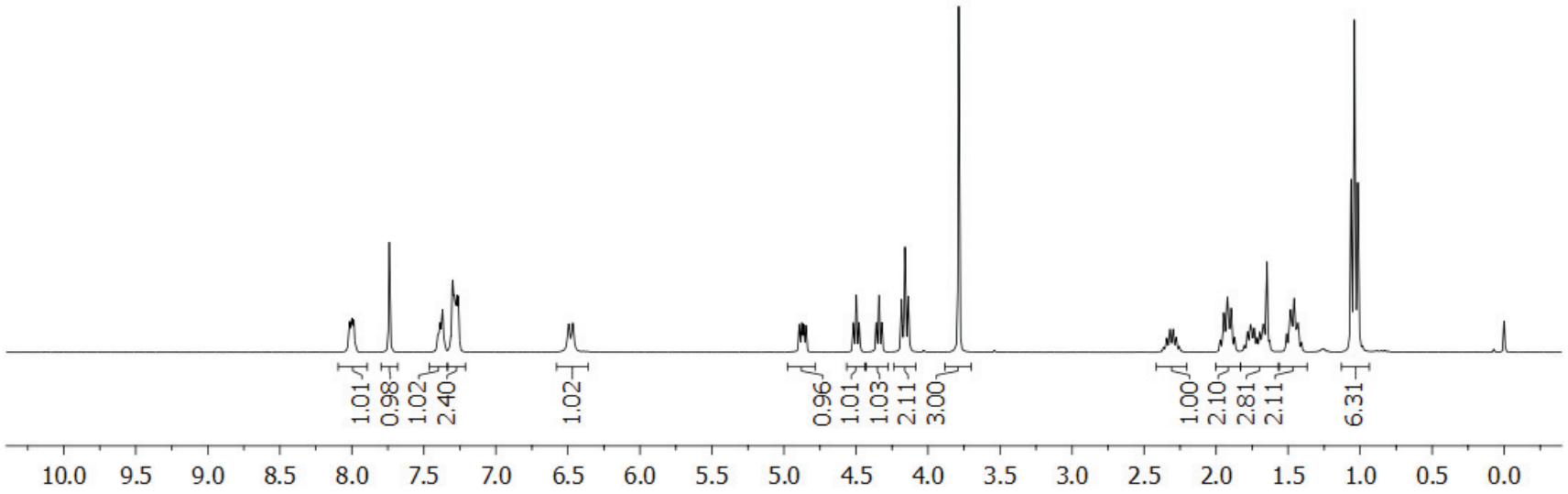

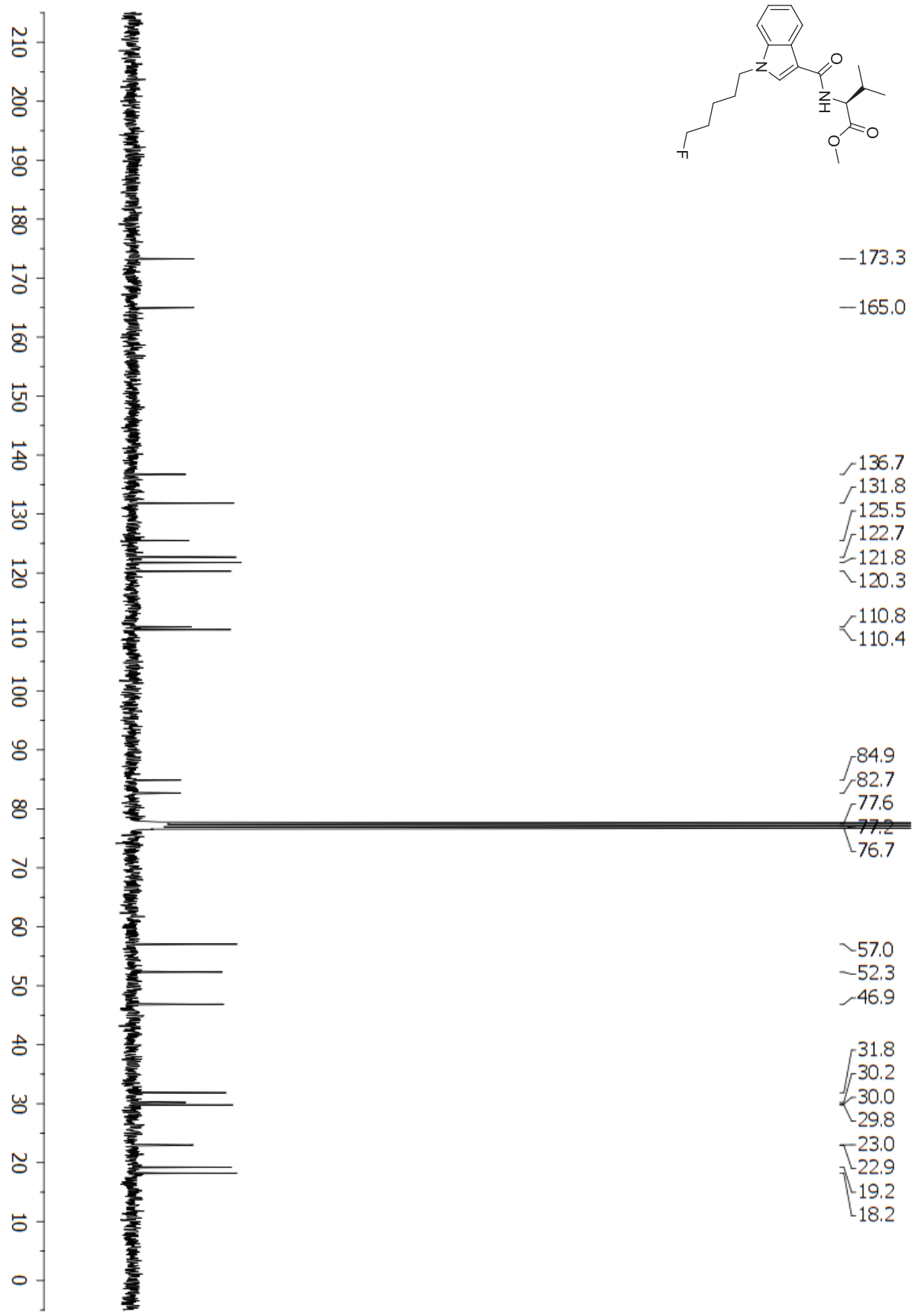

Figure S2. ^{13}C NMR spectrum (75 MHz, $CDCl_3$, 300 K) of 5F-AMB-PICA (**10**).

Figure S3. ^{1}H NMR spectrum (300 MHz, $CDCl_3$, 300 K) of 5F-MDMB-PICA (**11**).

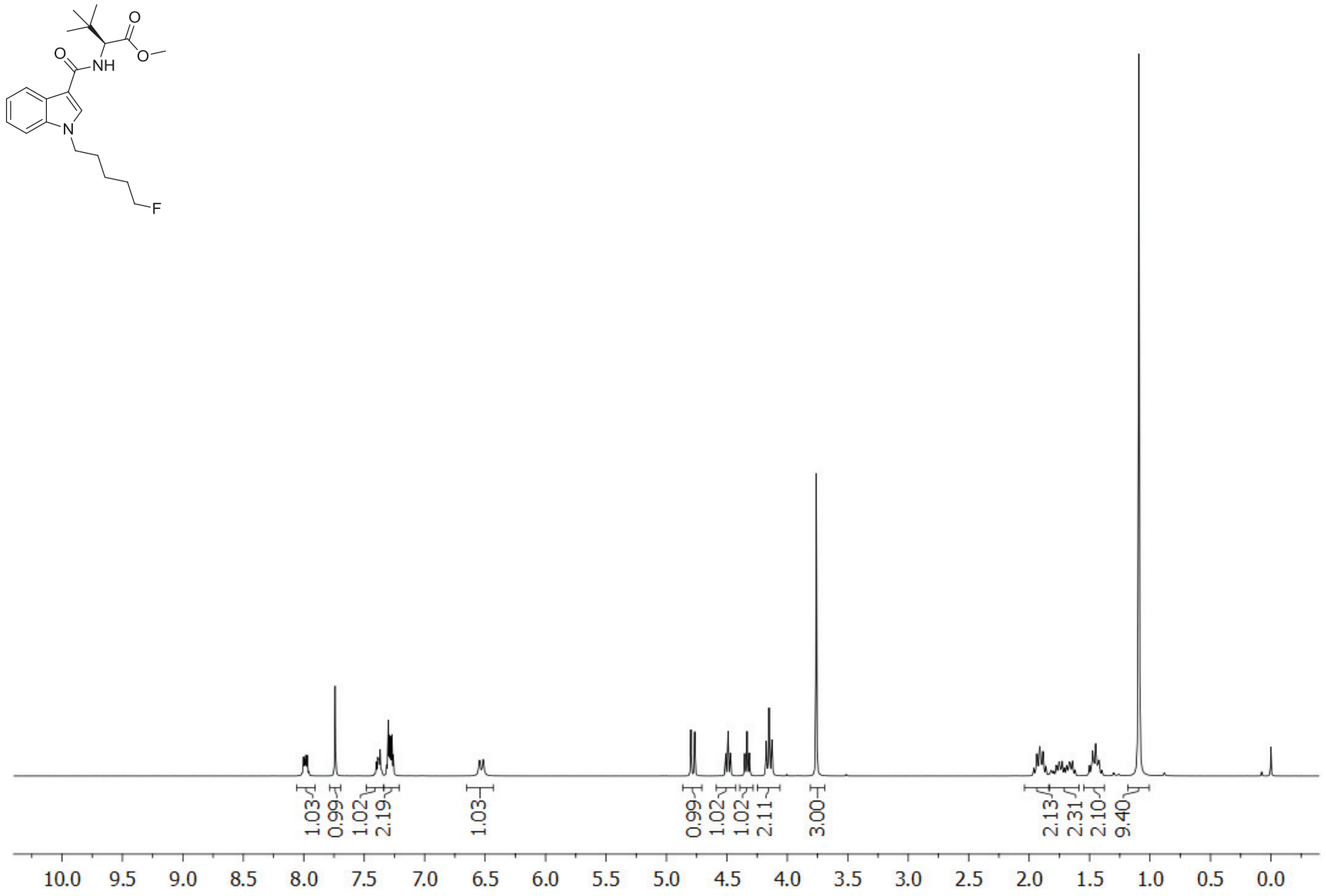

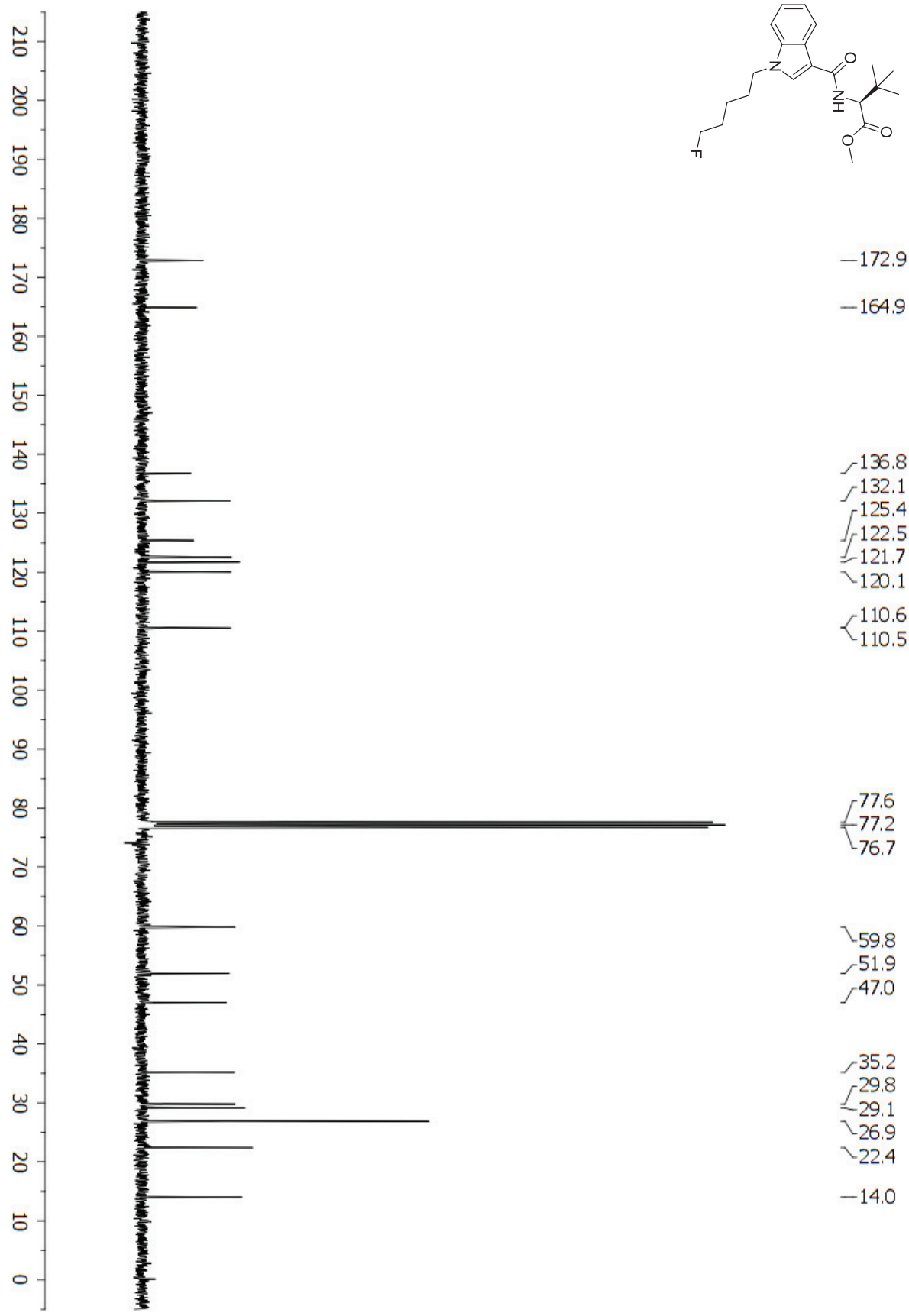

Figure S4. ^{13}C NMR spectrum (75 MHz, $CDCl_3$, 300 K) of 5F-MDMB-PICA (**11**).

Figure S5. ^{1}H NMR spectrum (300 MHz, $CDCl_3$, 300 K) of 5F-AMB-PINACA (**12**).

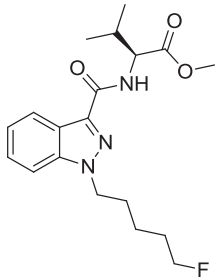

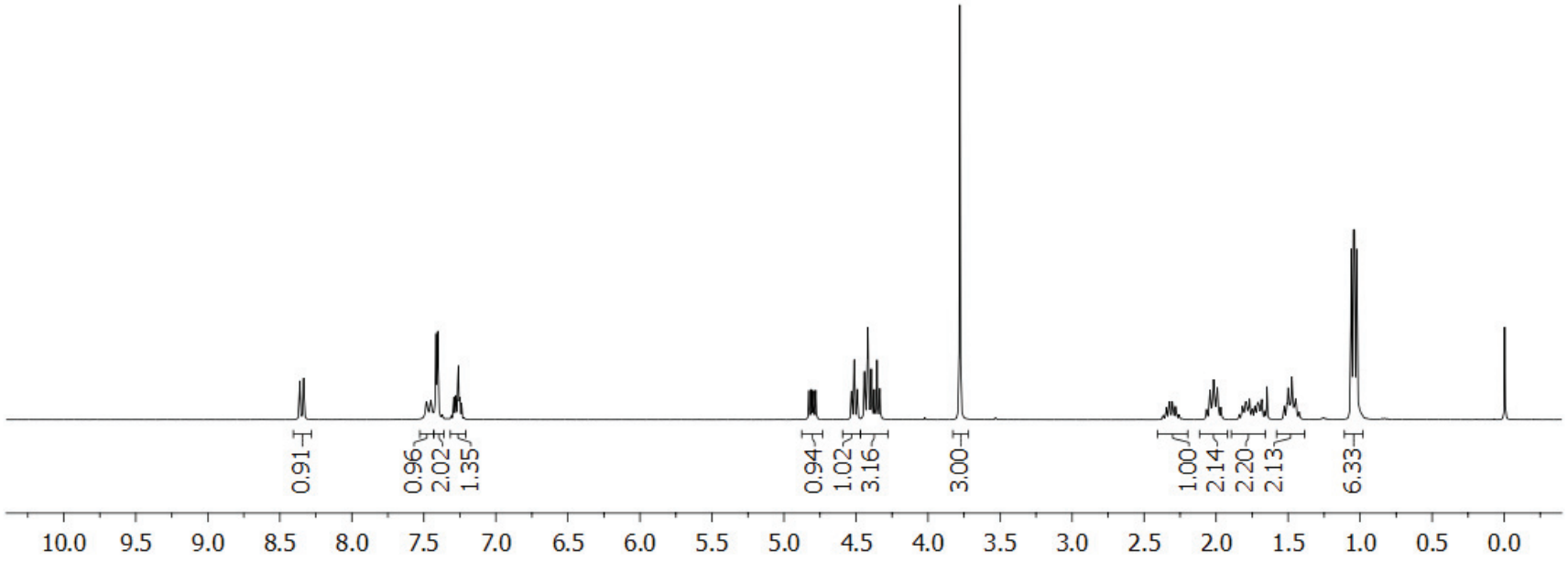

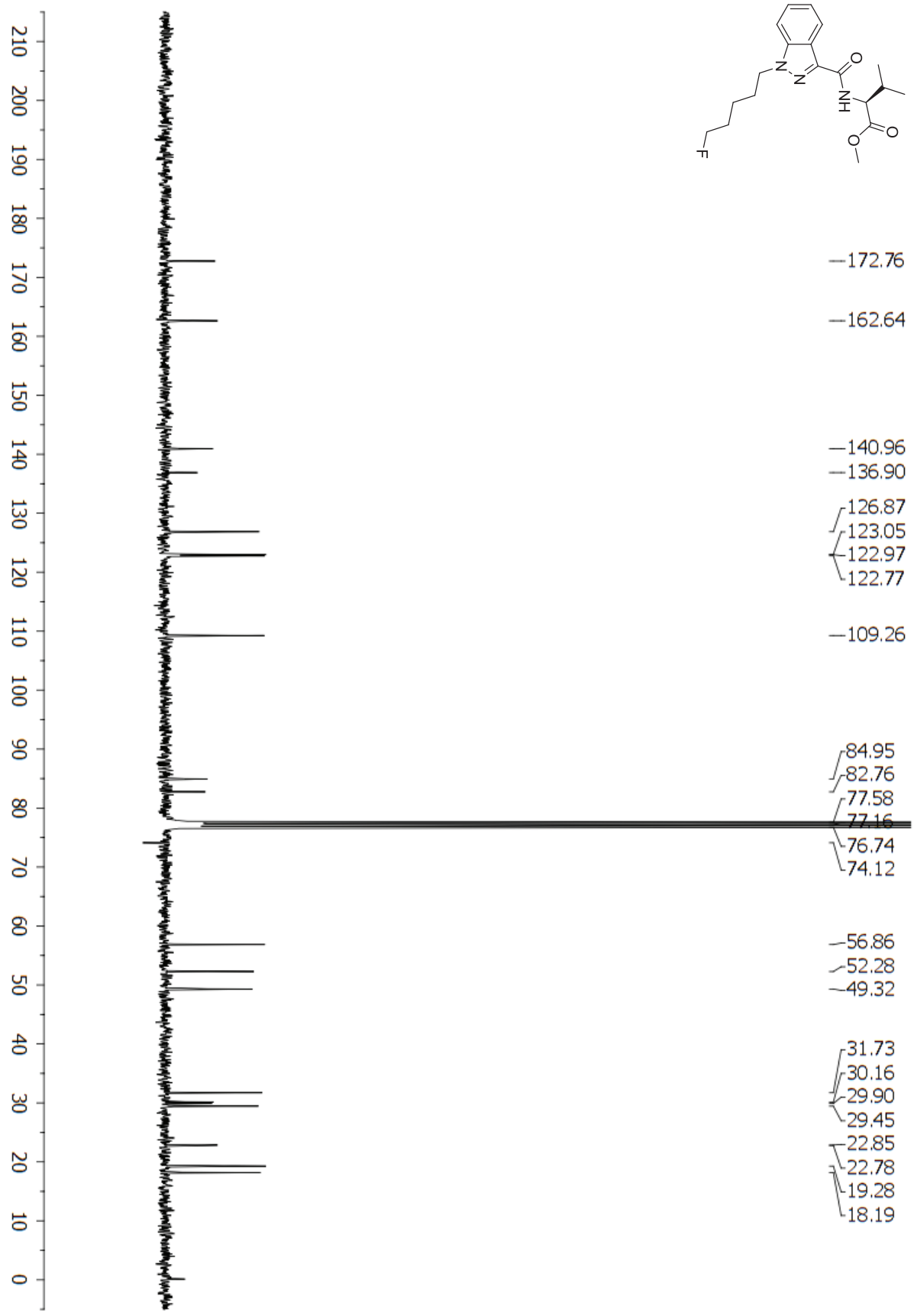

Figure S6. ^{13}C NMR spectrum (75 MHz, $CDCl_3$, 300 K) of 5F-AMB-PINACA (**12**).

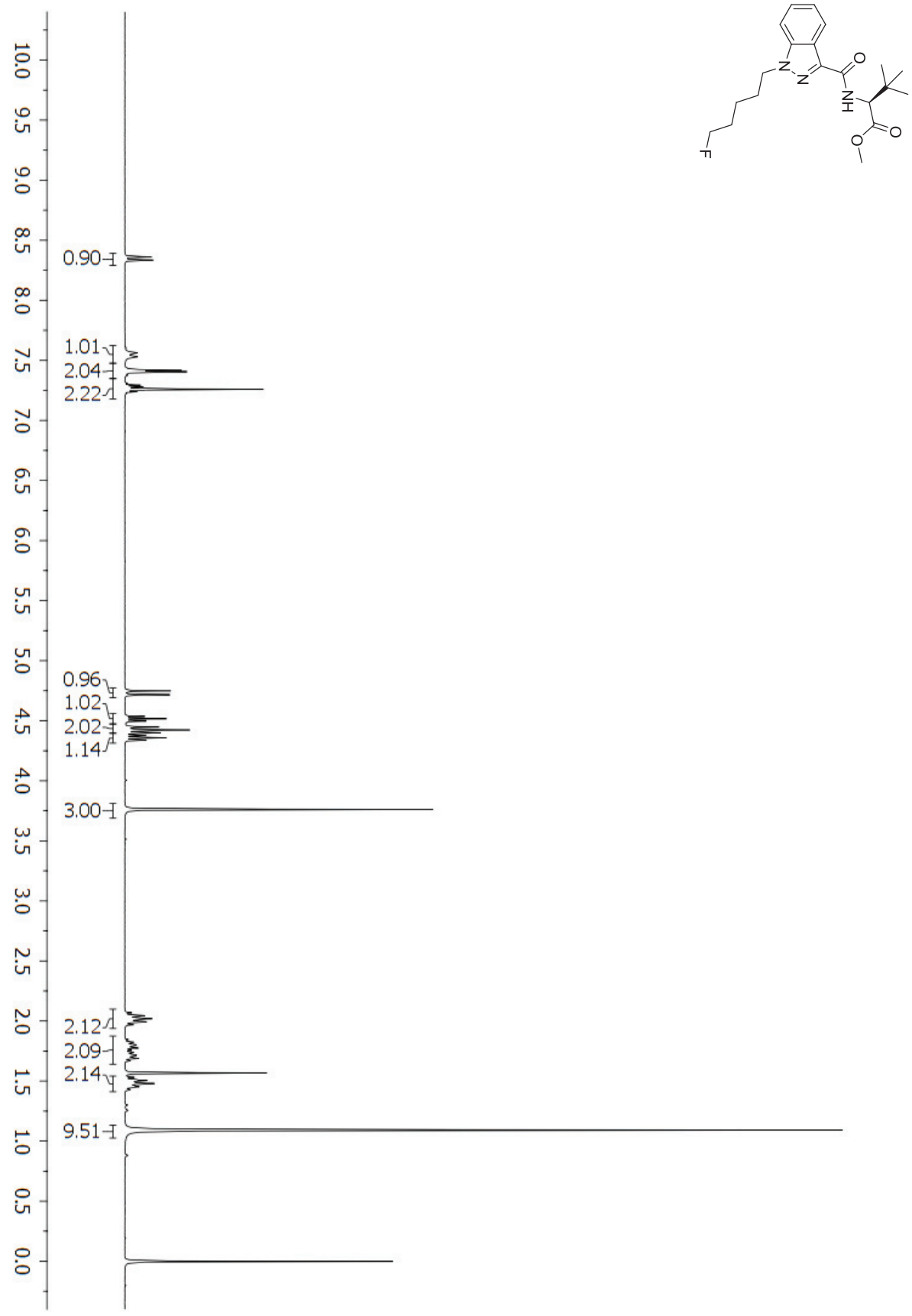

Figure S7. ^{1}H NMR spectrum (300 MHz, $CDCl_3$, 300 K) of 5F-MDMB-PINACA (**13**).

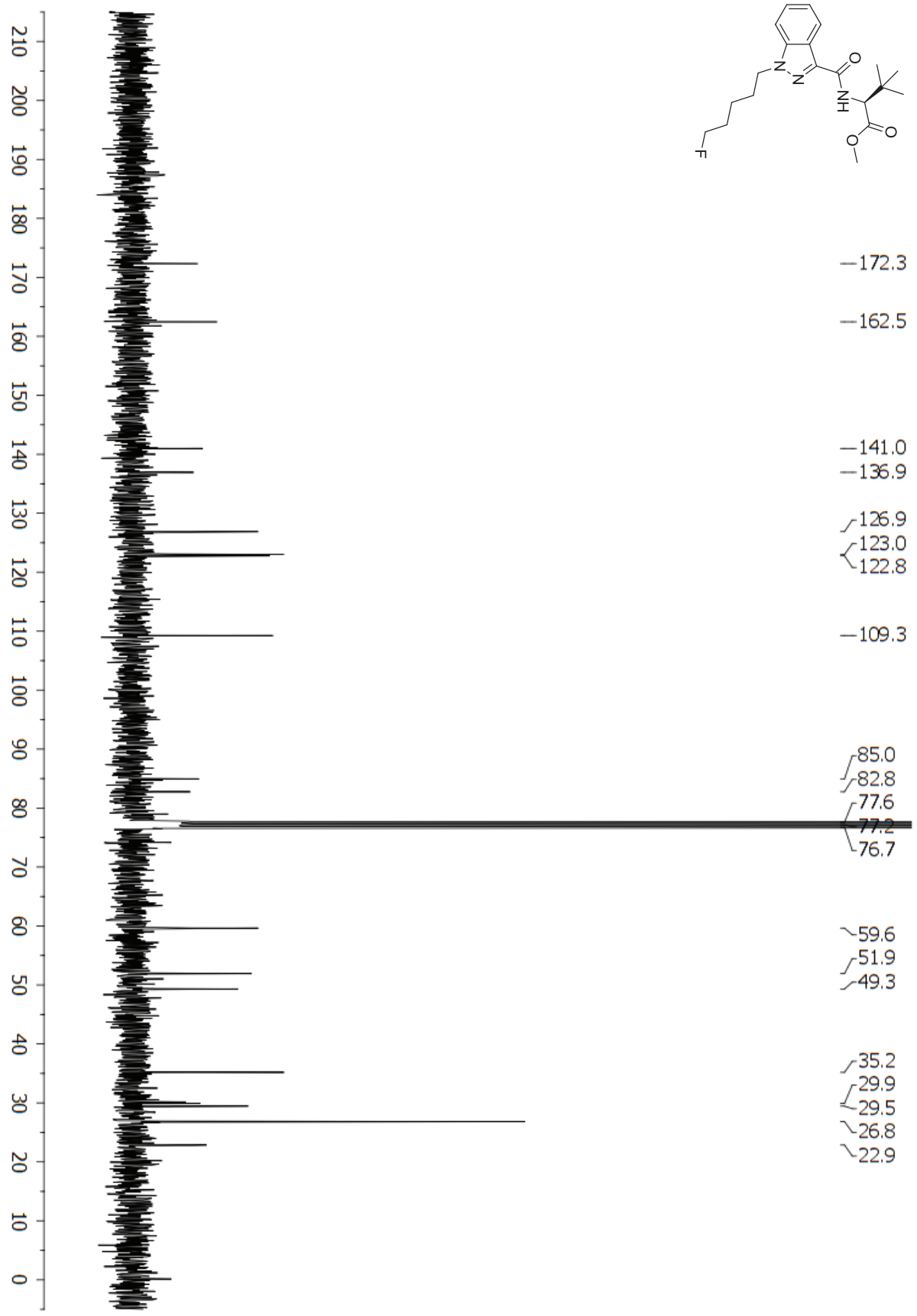

Figure S8. ^{13}C NMR spectrum (75 MHz, $CDCl_3$, 300 K) of 5F-MDMB-PINACA (**13**).

Figure S9. ^{1}H NMR spectrum (300 MHz, $CDCl_3$, 300 K) of AMB-FUBICA (**14**).

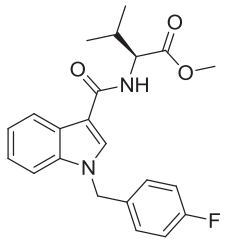

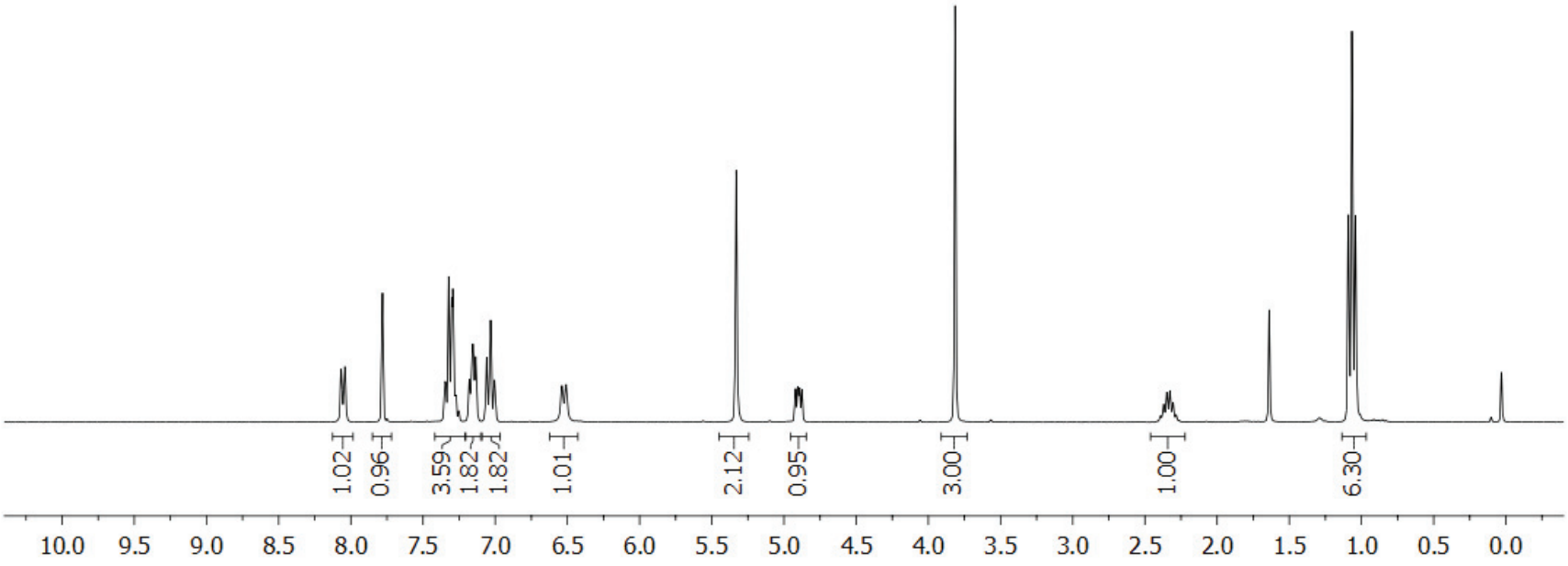

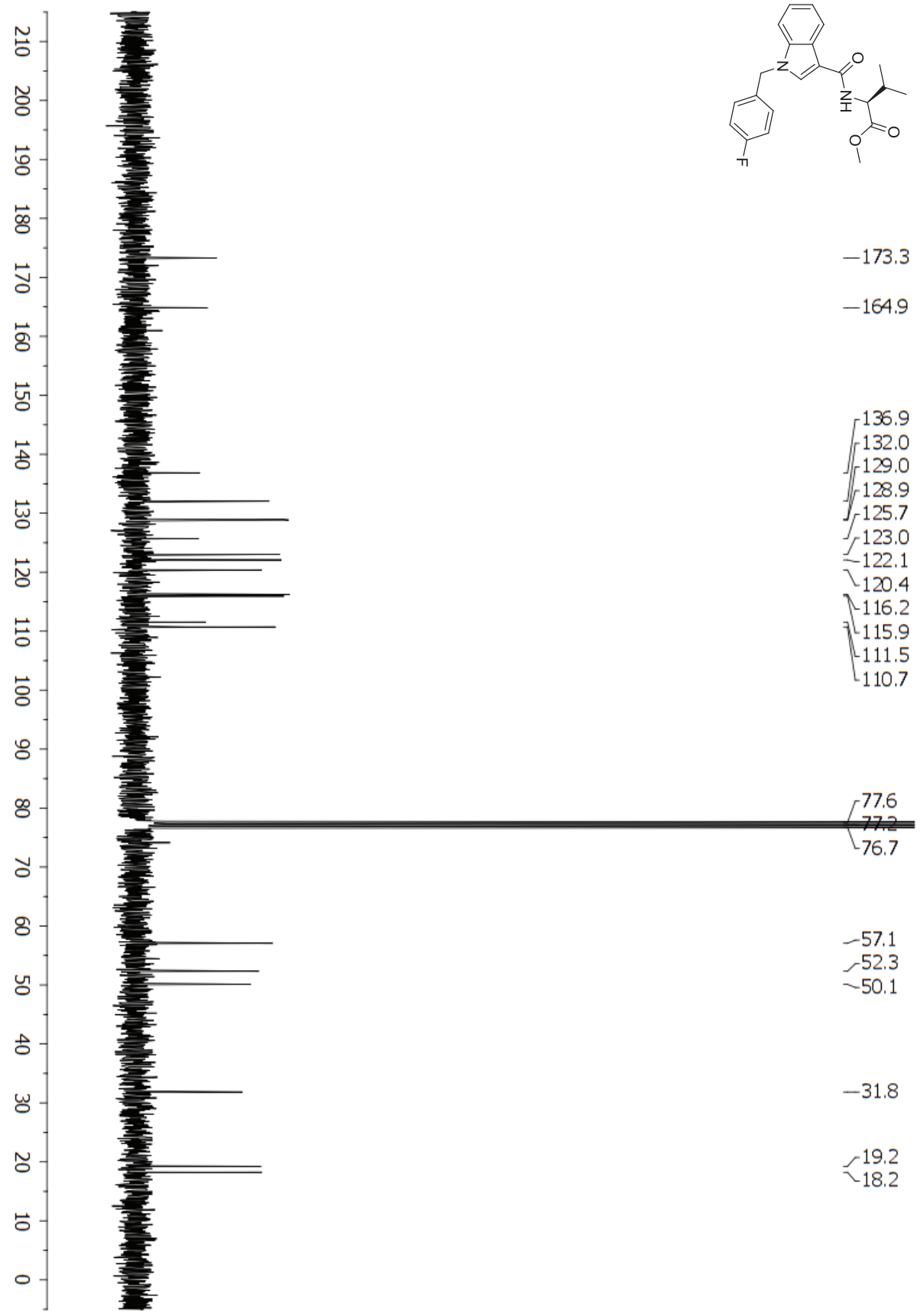

Figure S10. ^{13}C NMR spectrum (75 MHz, $CDCl_3$, 300 K) of AMB-FUBICA (**14**).

Figure S11. ^{1}H NMR spectrum (300 MHz, $CDCl_3$, 300 K) of MDMB-FUBICA (**15**).

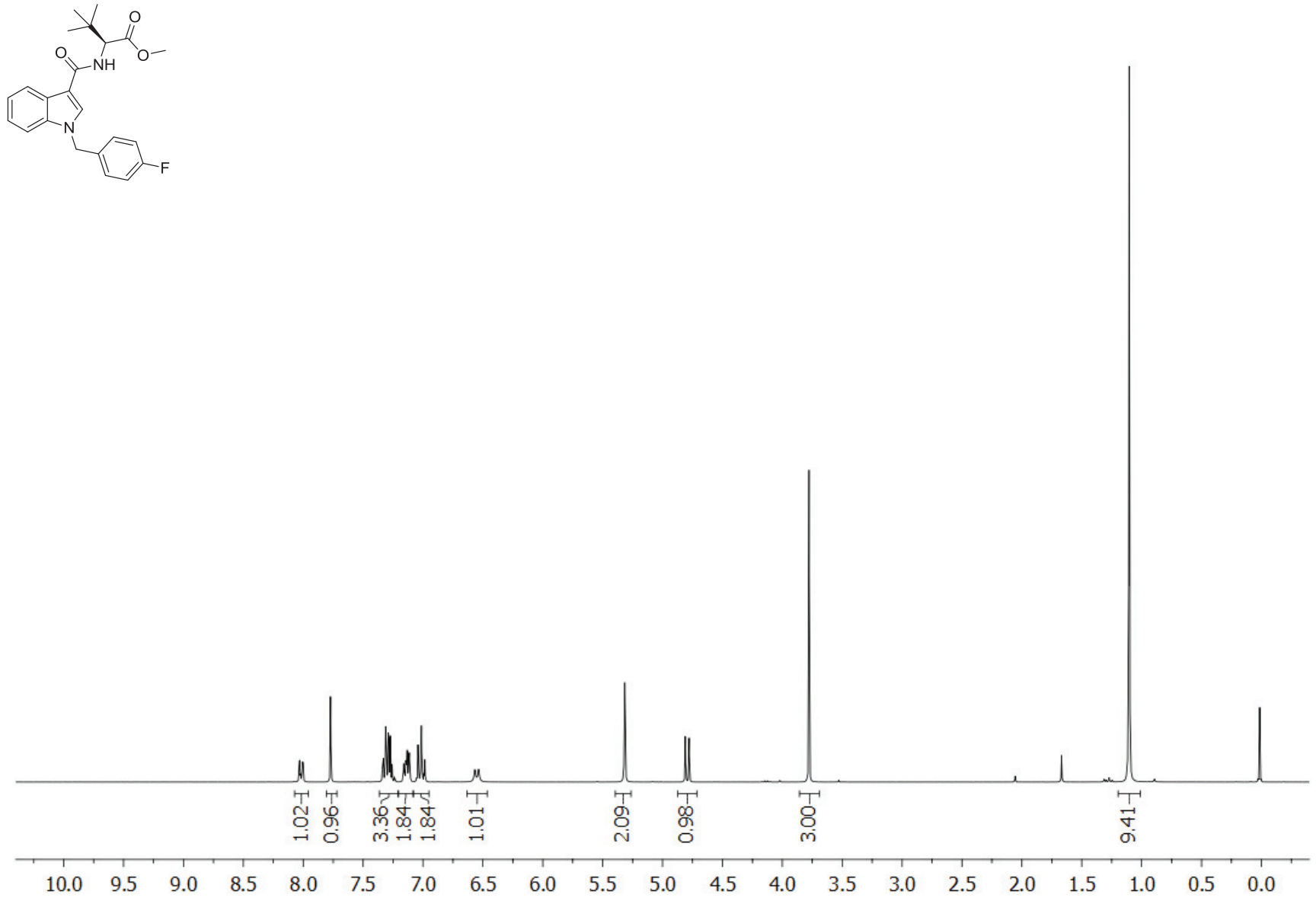

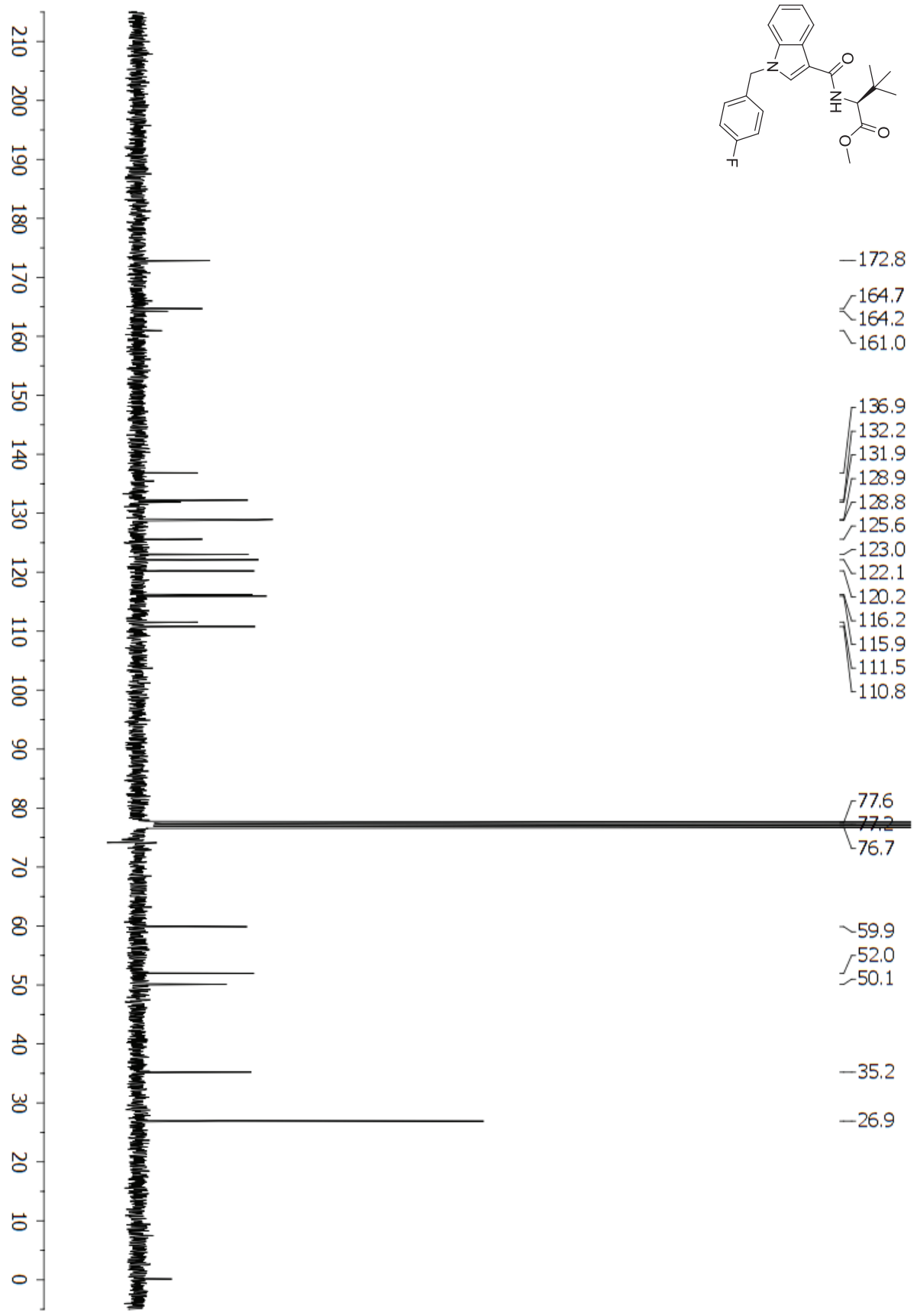

Figure S12. ^{13}C NMR spectrum (75 MHz, $CDCl_3$, 300 K) of MDMB-FUBICA (**15**).

Figure S13. ^{1}H NMR spectrum (300 MHz, $CDCl_3$, 300 K) of AMB-FUBINACA (**16**).

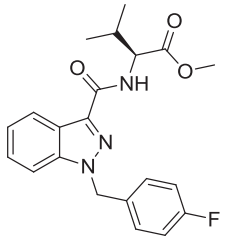

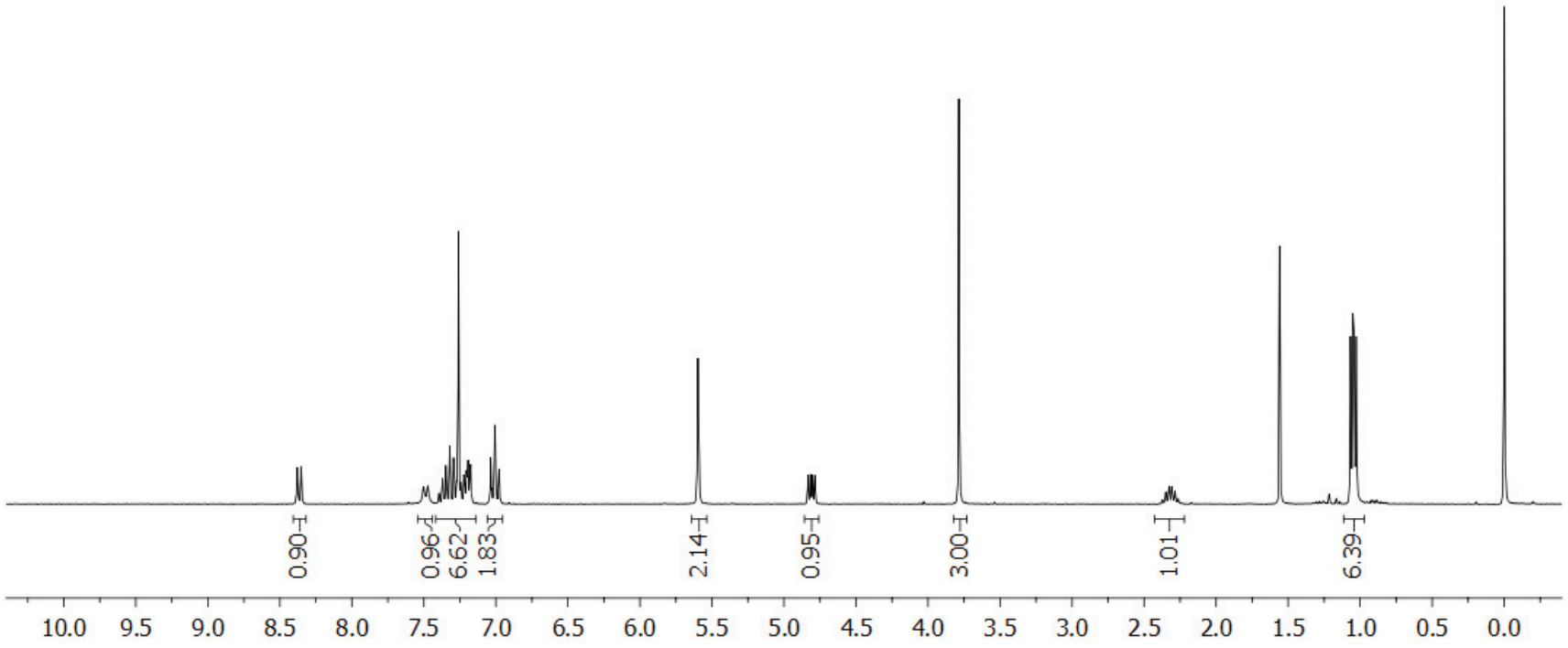

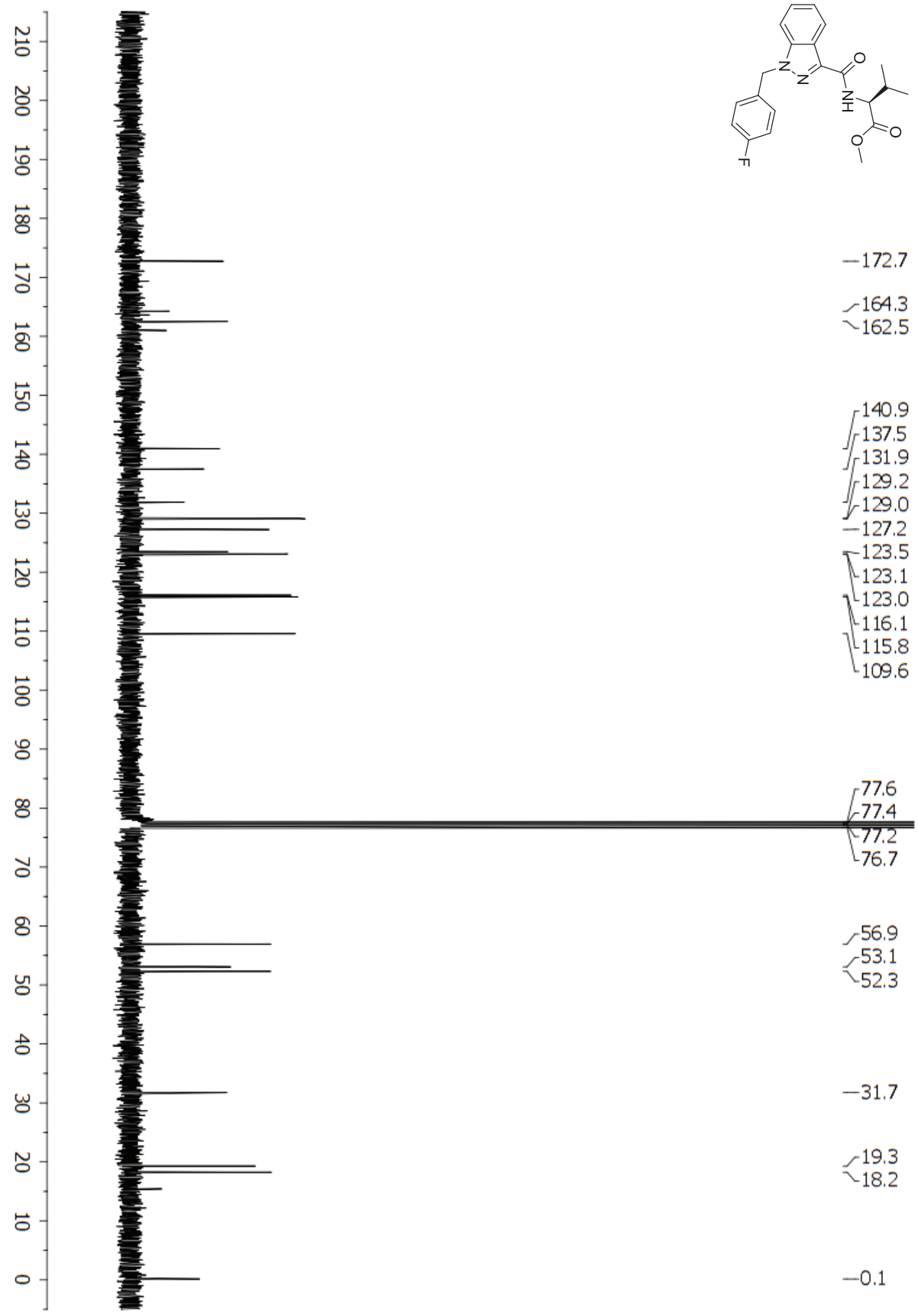

Figure S14. ^{13}C NMR spectrum (75 MHz, $CDCl_3$, 300 K) of AMB-FUBINACA (**16**).

Figure S15. ^{1}H NMR spectrum (300 MHz, $CDCl_3$, 300 K) of MDMB-FUBINACA (**17**).

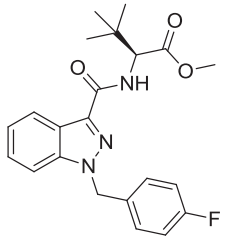

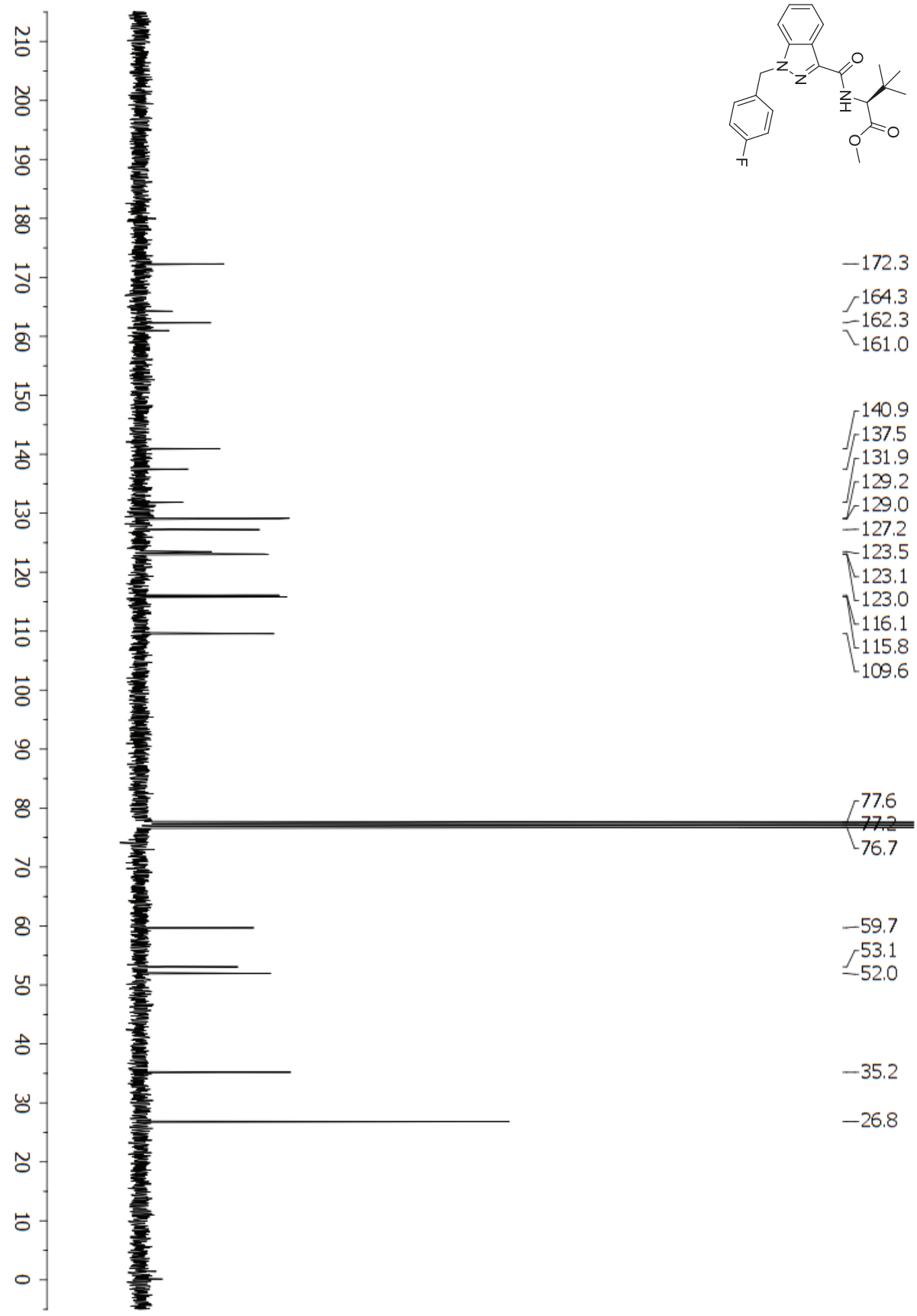

Figure S16. ^{13}C NMR spectrum (75 MHz, $CDCl_3$, 300 K) of MDMB-FUBINACA (**17**).

Figure S17. ^{1}H NMR spectrum (300 MHz, $CDCl_3$, 300 K) of AMB-CHMICA (**18**).

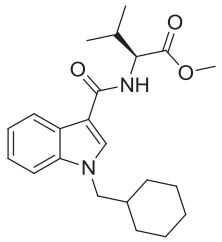

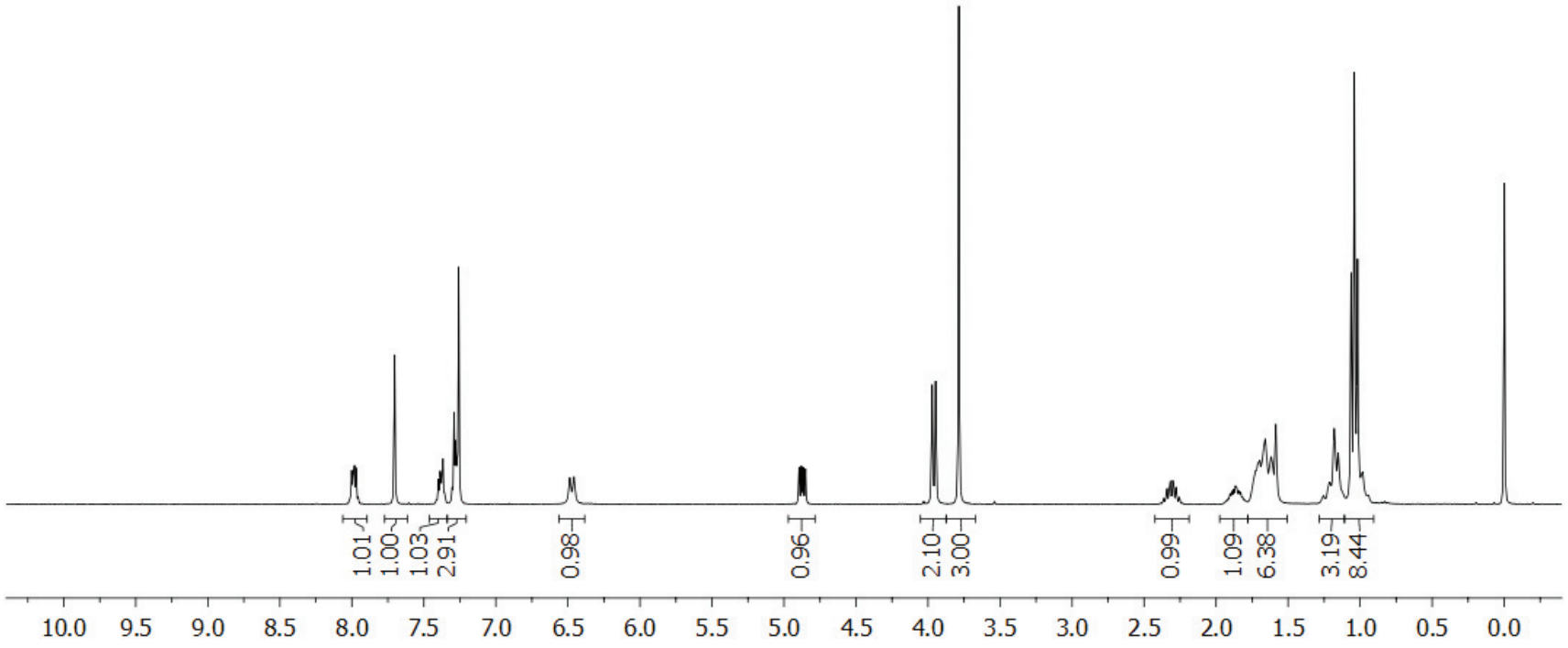

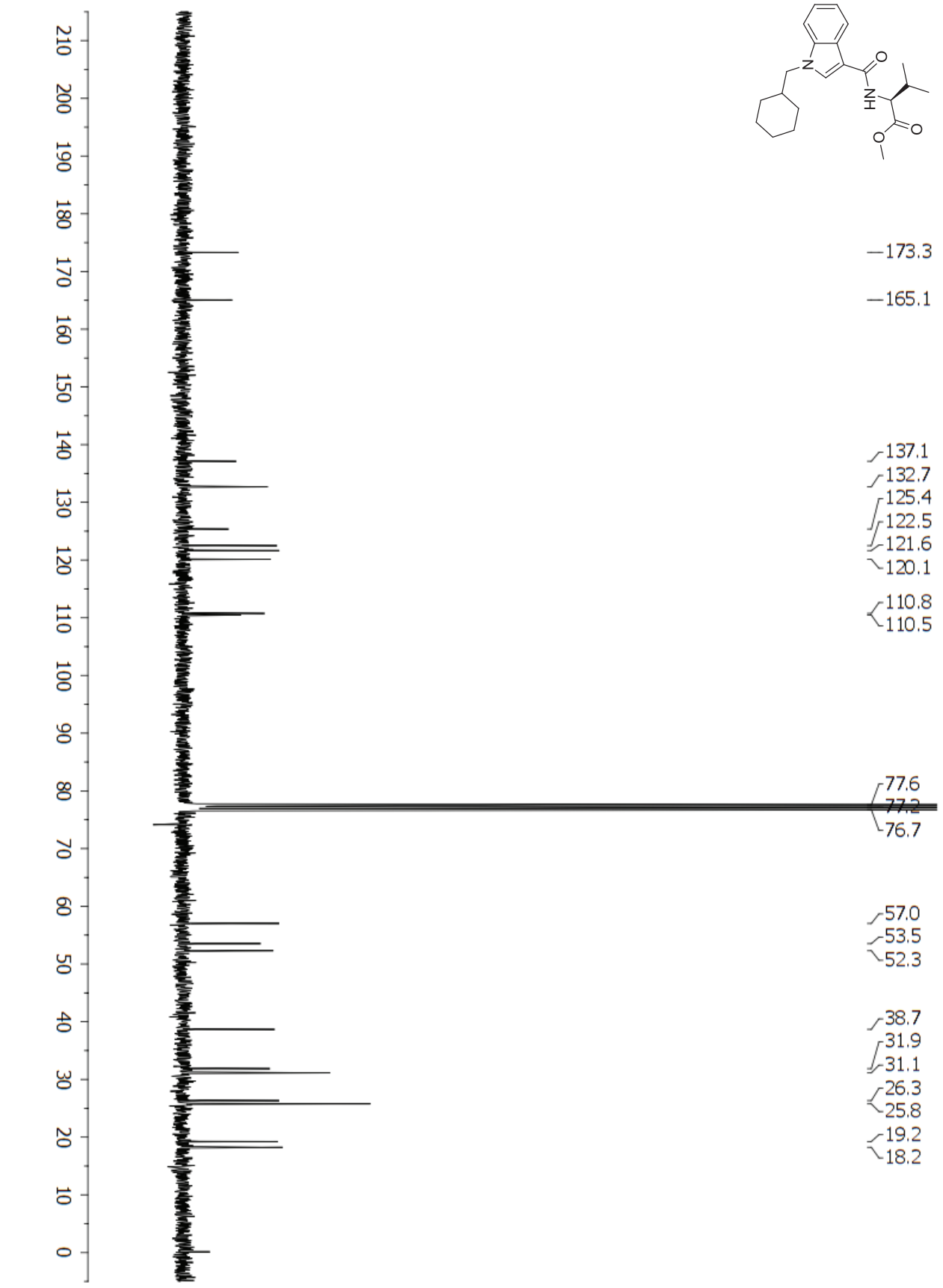

Figure S18. ^{13}C NMR spectrum (75 MHz, $CDCl_3$, 300 K) of AMB-CHMICA (**18**).

Figure S19. ^{1}H NMR spectrum (300 MHz, $CDCl_3$, 300 K) of MDMB-CHMICA (**19**).

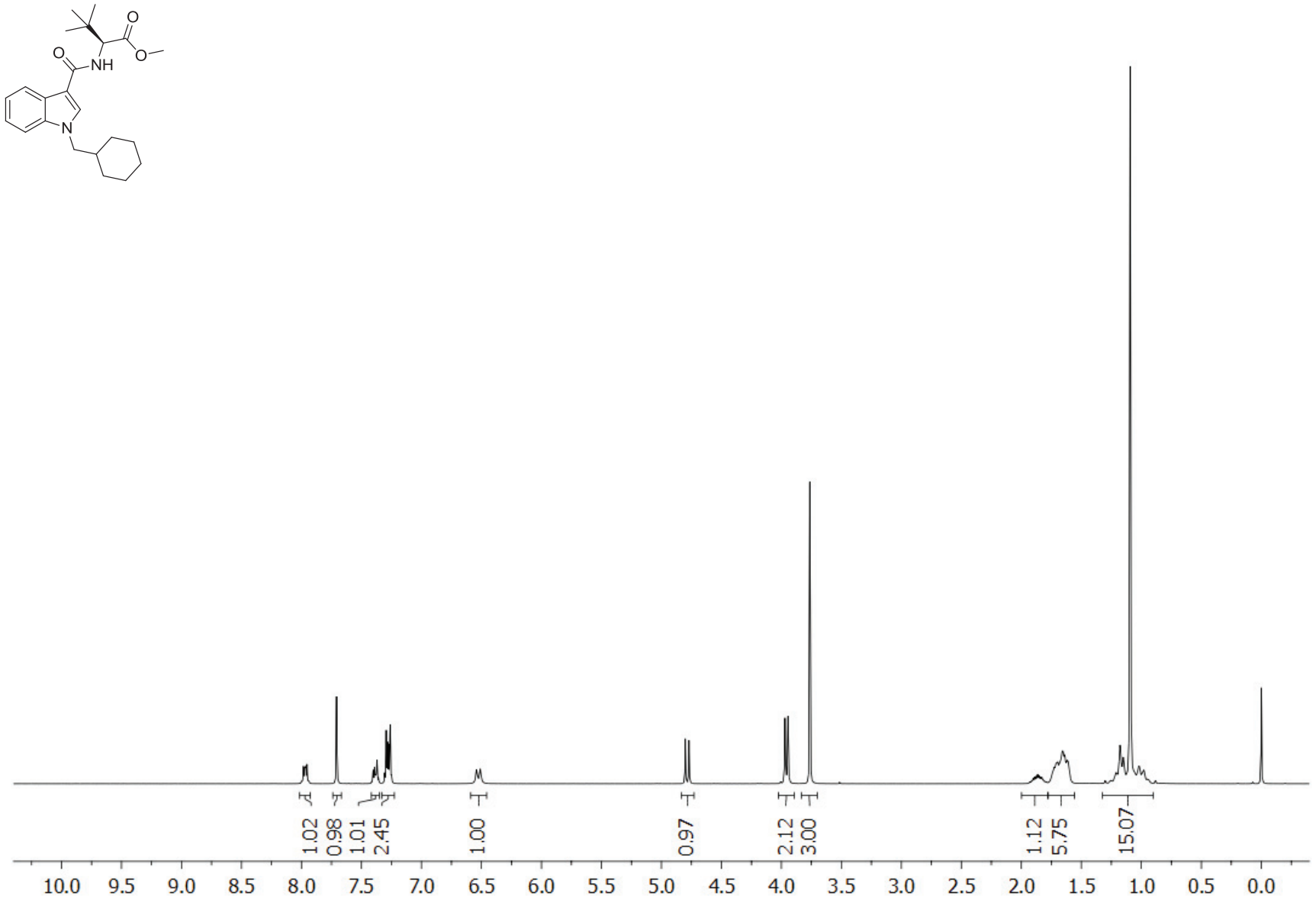

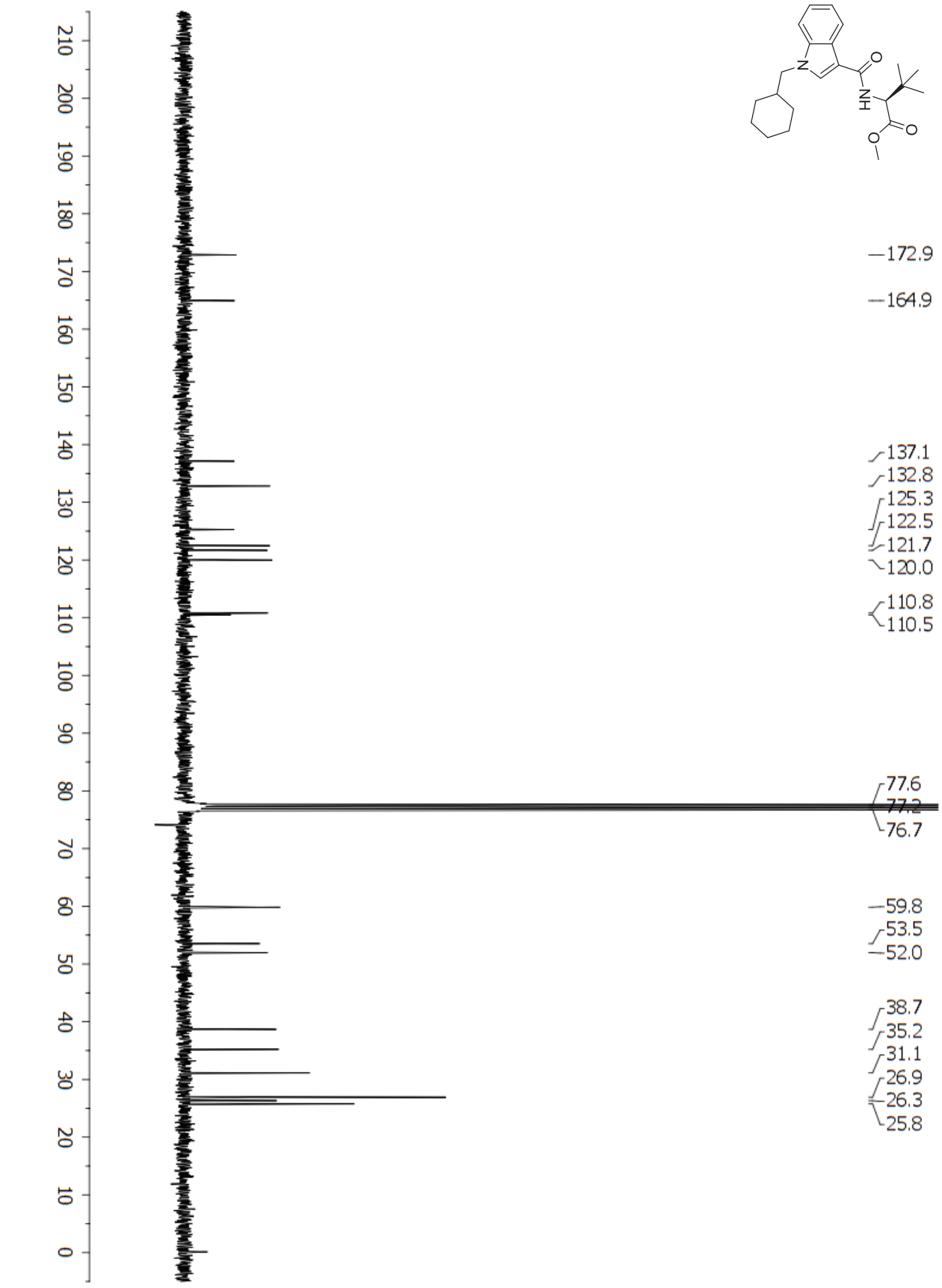

Figure S20. ^{13}C NMR spectrum (75 MHz, $CDCl_3$, 300 K) of MDMB-CHMICA (**19**).

Figure S21. ^{1}H NMR spectrum (300 MHz, $CDCl_3$, 300 K) of AMB-CHMINACA (**20**).

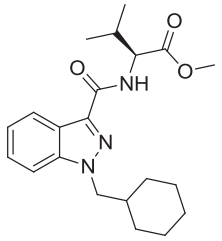

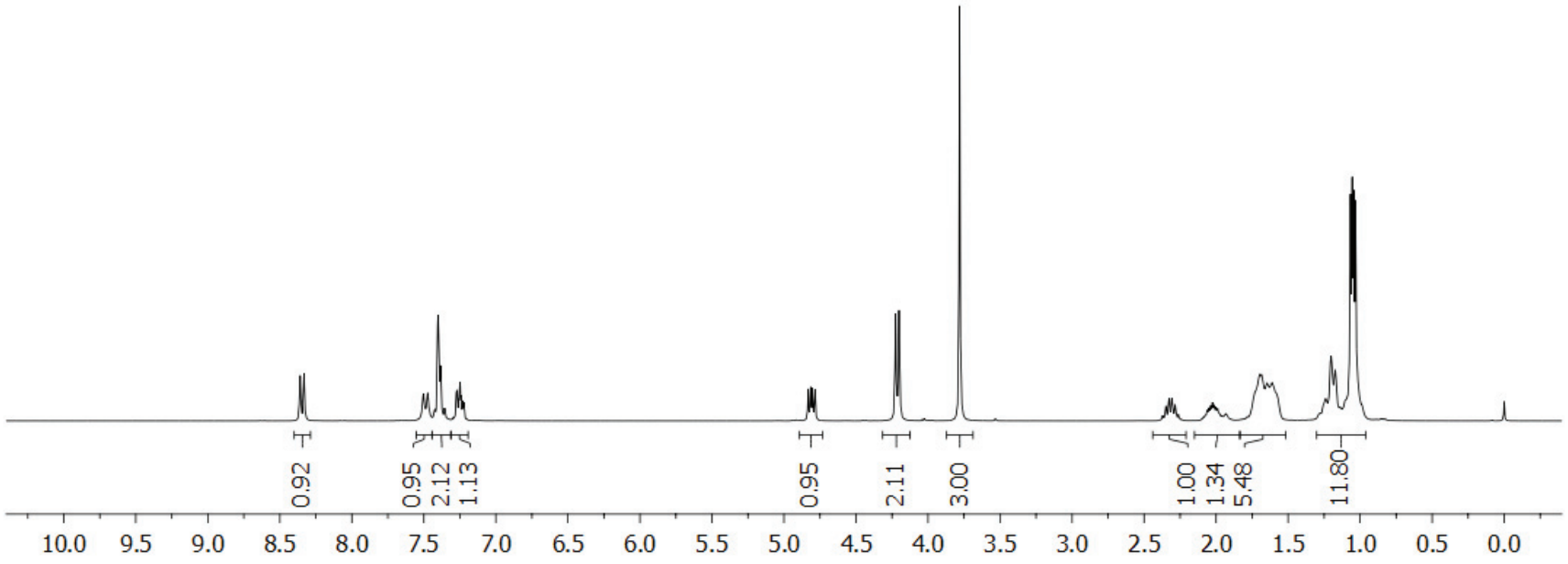

Figure S22. ^{13}C NMR spectrum (75 MHz, $CDCl_3$, 300 K) of AMB-CHMINACA (**20**).

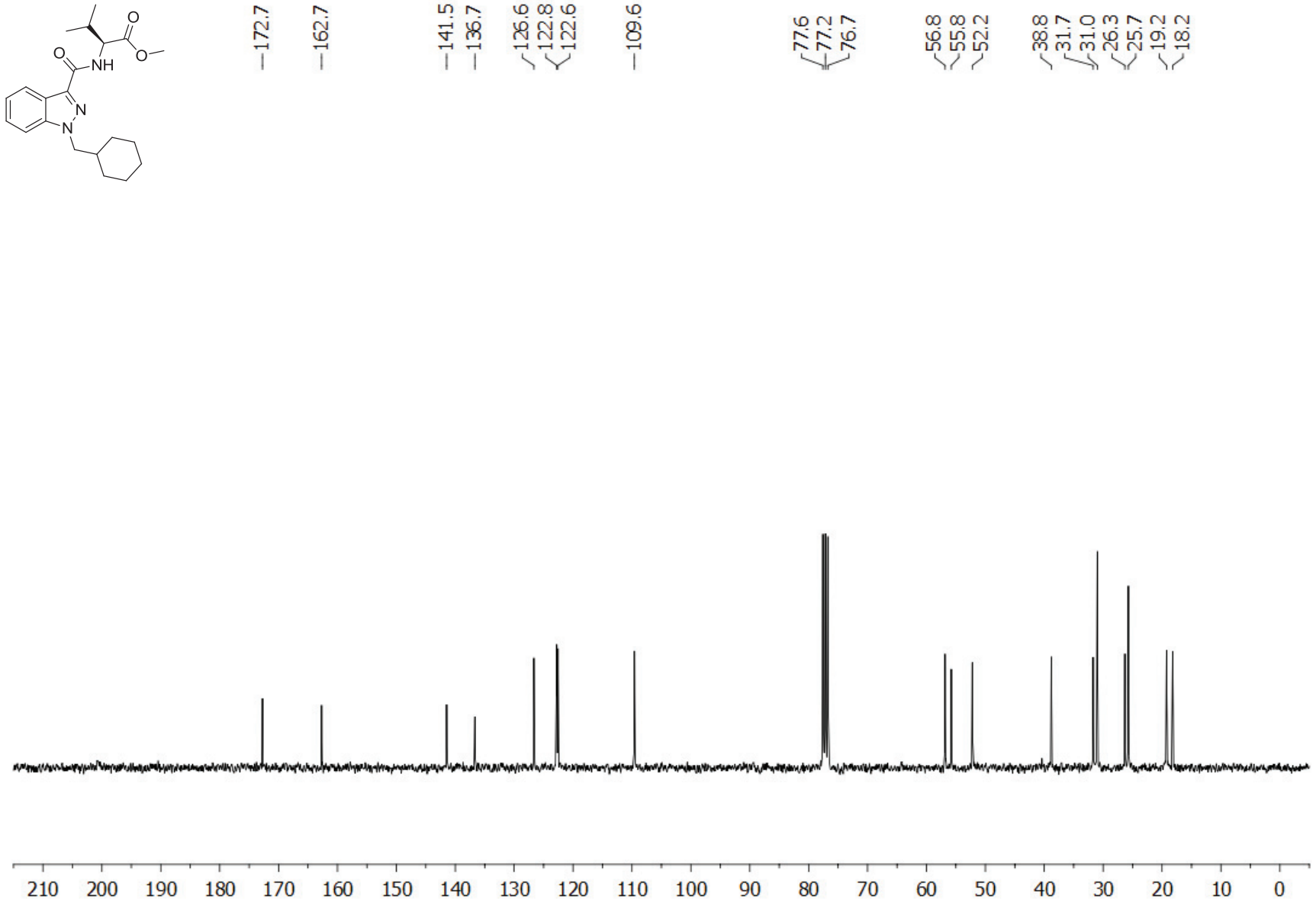

Figure S23. ^{1}H NMR spectrum (300 MHz, $CDCl_3$, 300 K) of MDMB-CHMINACA (**21**).

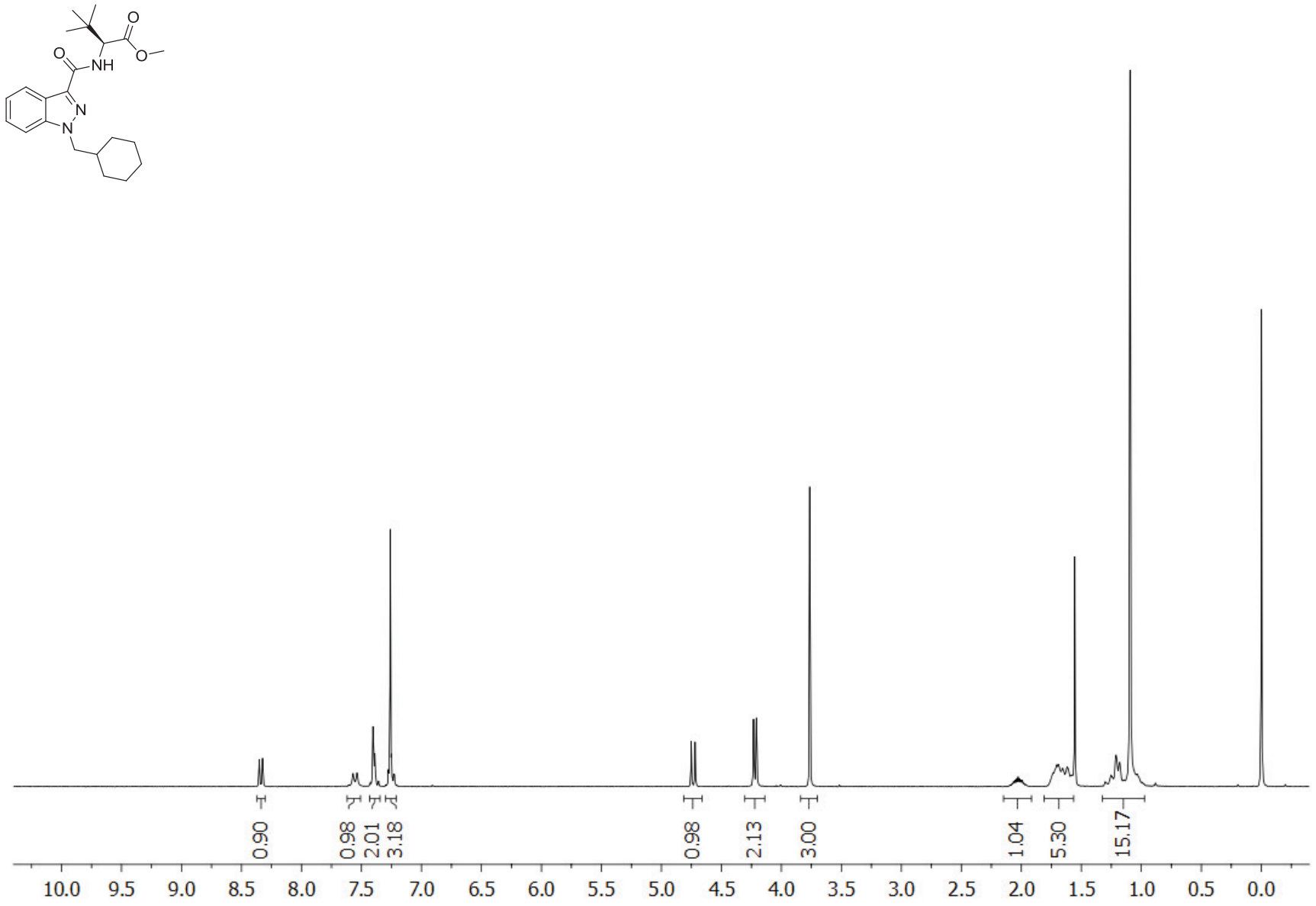

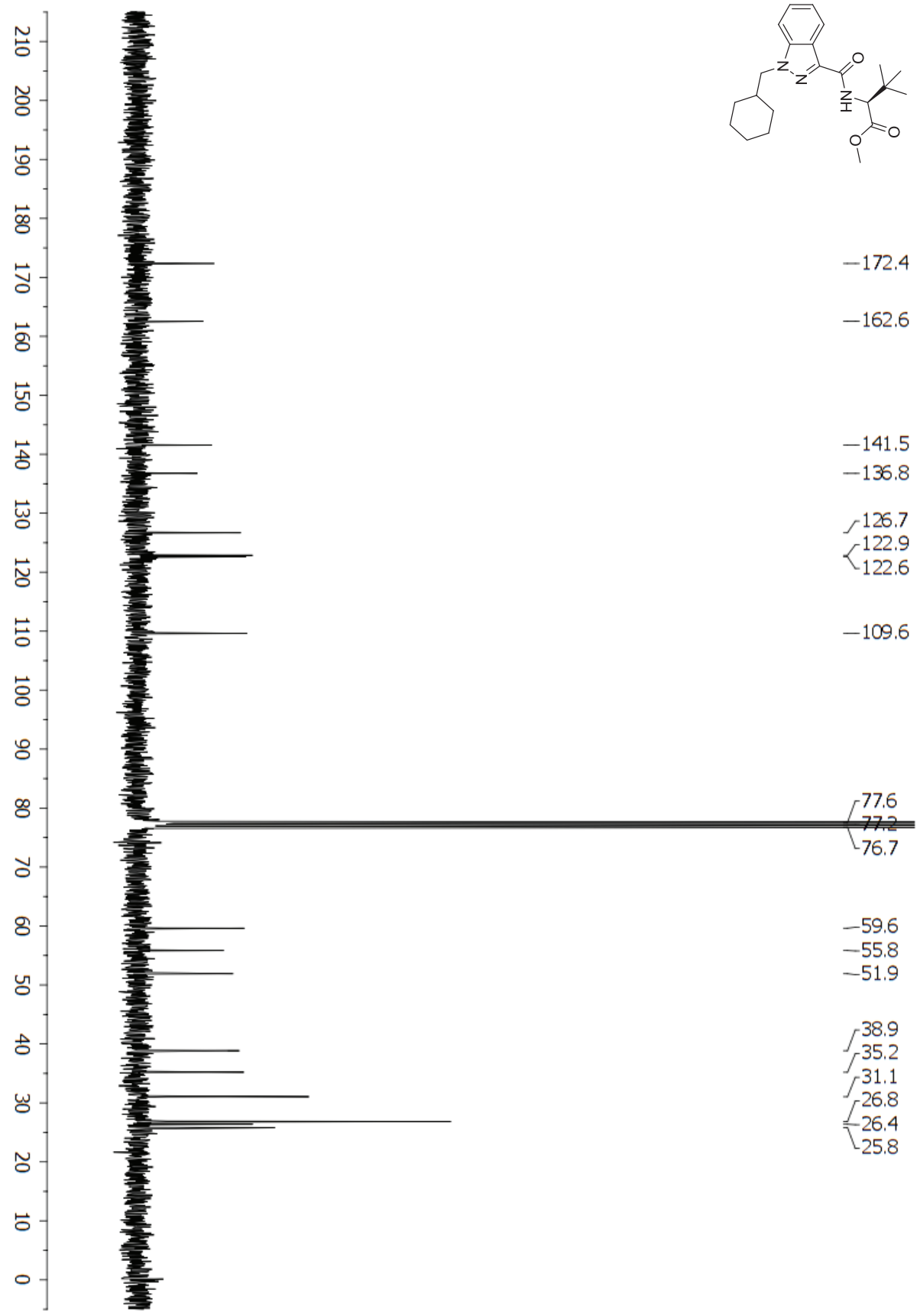

Figure S24. ^{13}C NMR spectrum (75 MHz, $CDCl_3$, 300 K) of MDMB-CHMINACA (**21**).

Figure S25. ^{1}H NMR spectrum (300 MHz, $CDCl_3$, 300 K) of AMB-PICA (**22**).

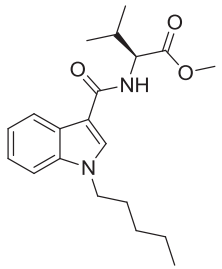

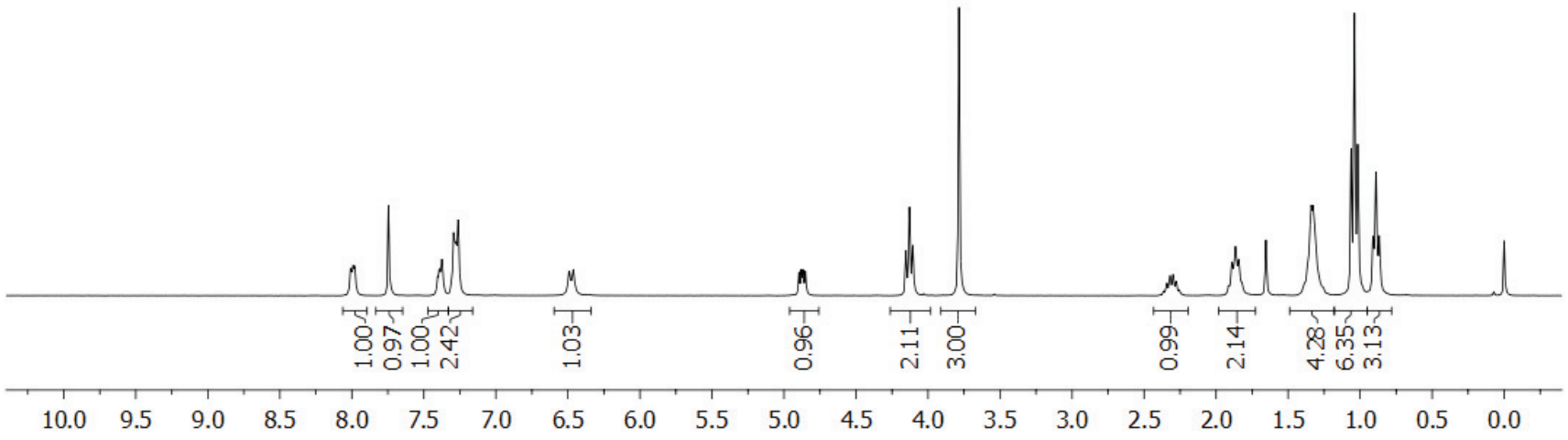

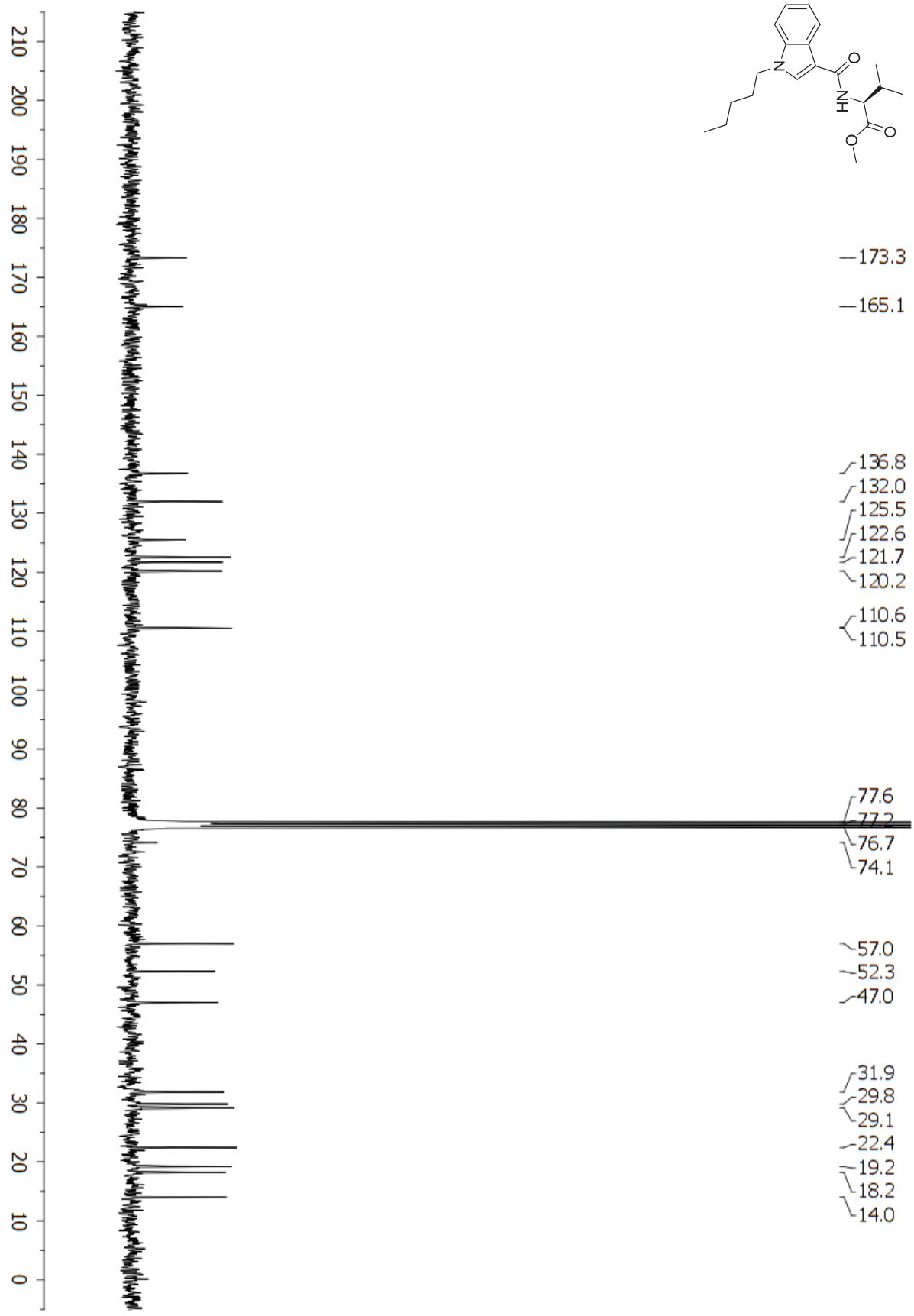

Figure S26. ^{13}C NMR spectrum (75 MHz, $CDCl_3$, 300 K) of AMB-PICA (**22**).

Figure S27. ^{1}H NMR spectrum (300 MHz, $CDCl_3$, 300 K) of MDMB-PICA (**23**).

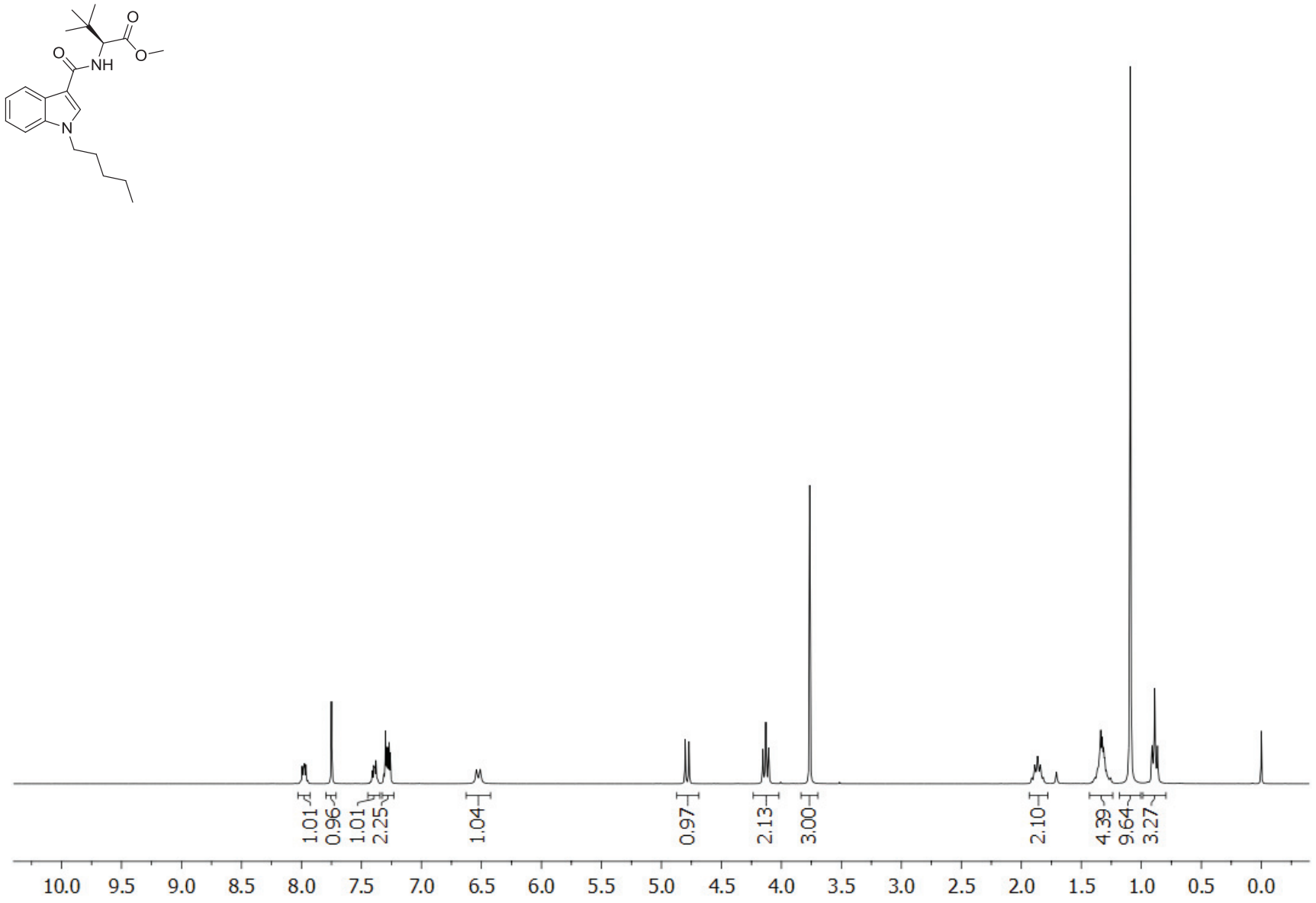

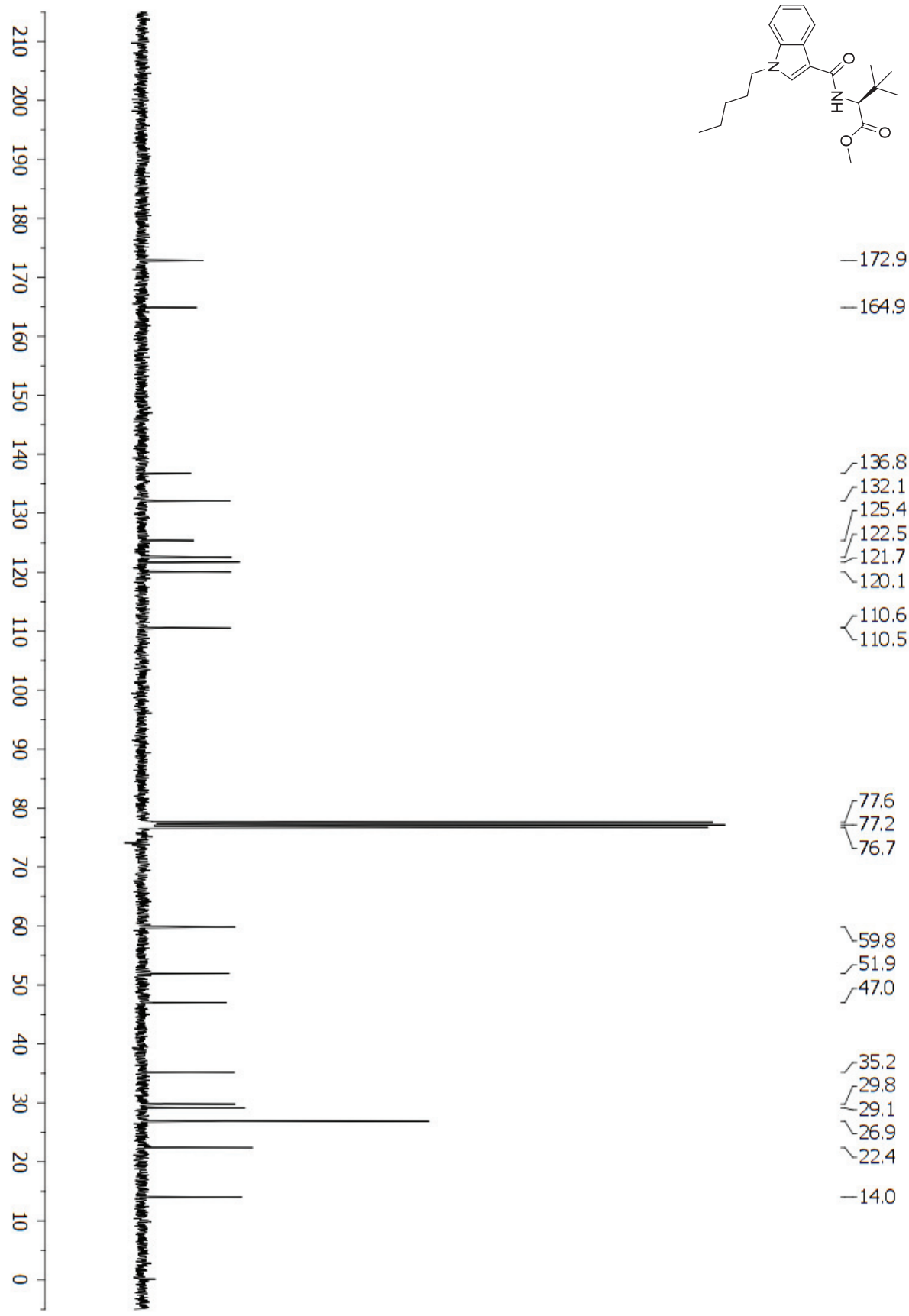

Figure S28. ^{13}C NMR spectrum (75 MHz, $CDCl_3$, 300 K) of MDMB-PICA (**23**).

Figure S29. ^{1}H NMR spectrum (300 MHz, $CDCl_3$, 300 K) of AMB-PINACA (**24**).

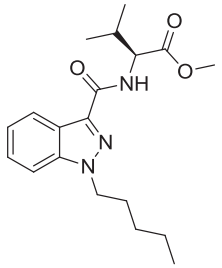

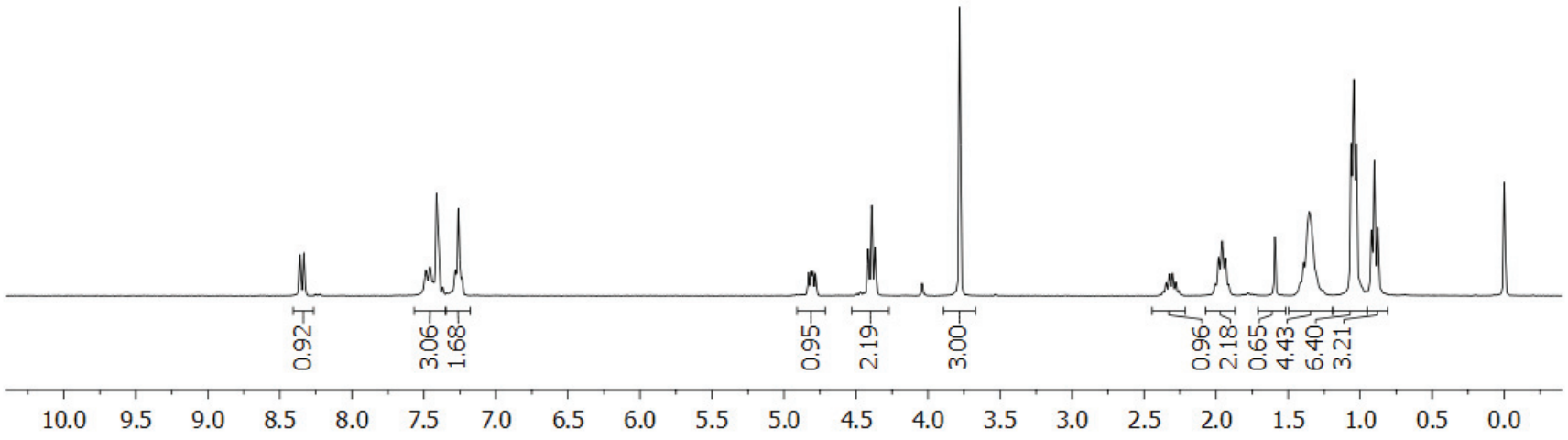

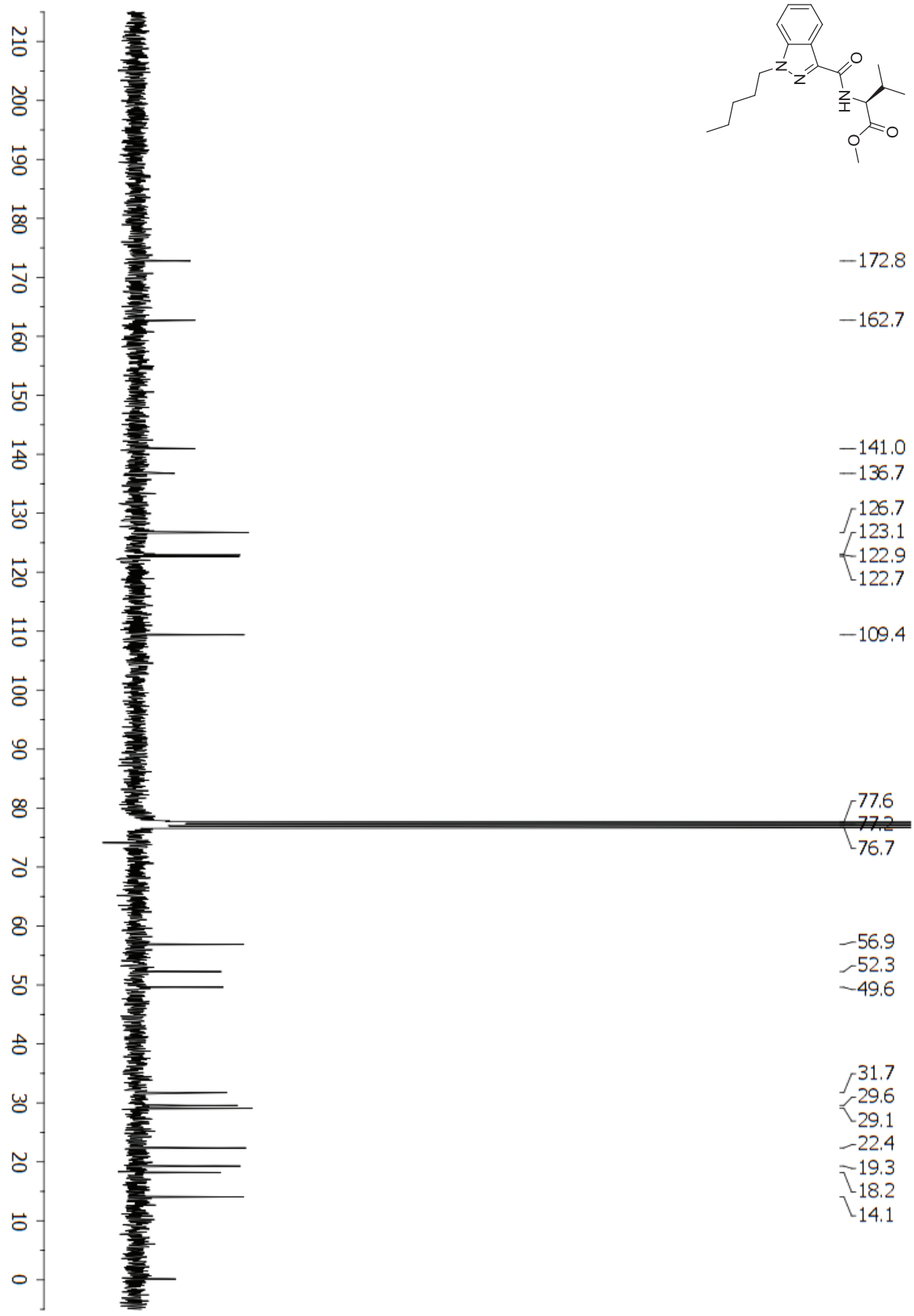

Figure S30. ^{13}C NMR spectrum (75 MHz, $CDCl_3$, 300 K) of AMB-PINACA (**24**).

Figure S31. ^{1}H NMR spectrum (300 MHz, $CDCl_3$, 300 K) of MDMB-PINACA (**25**).

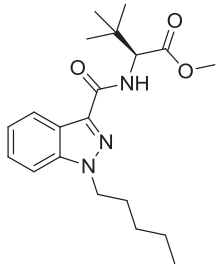

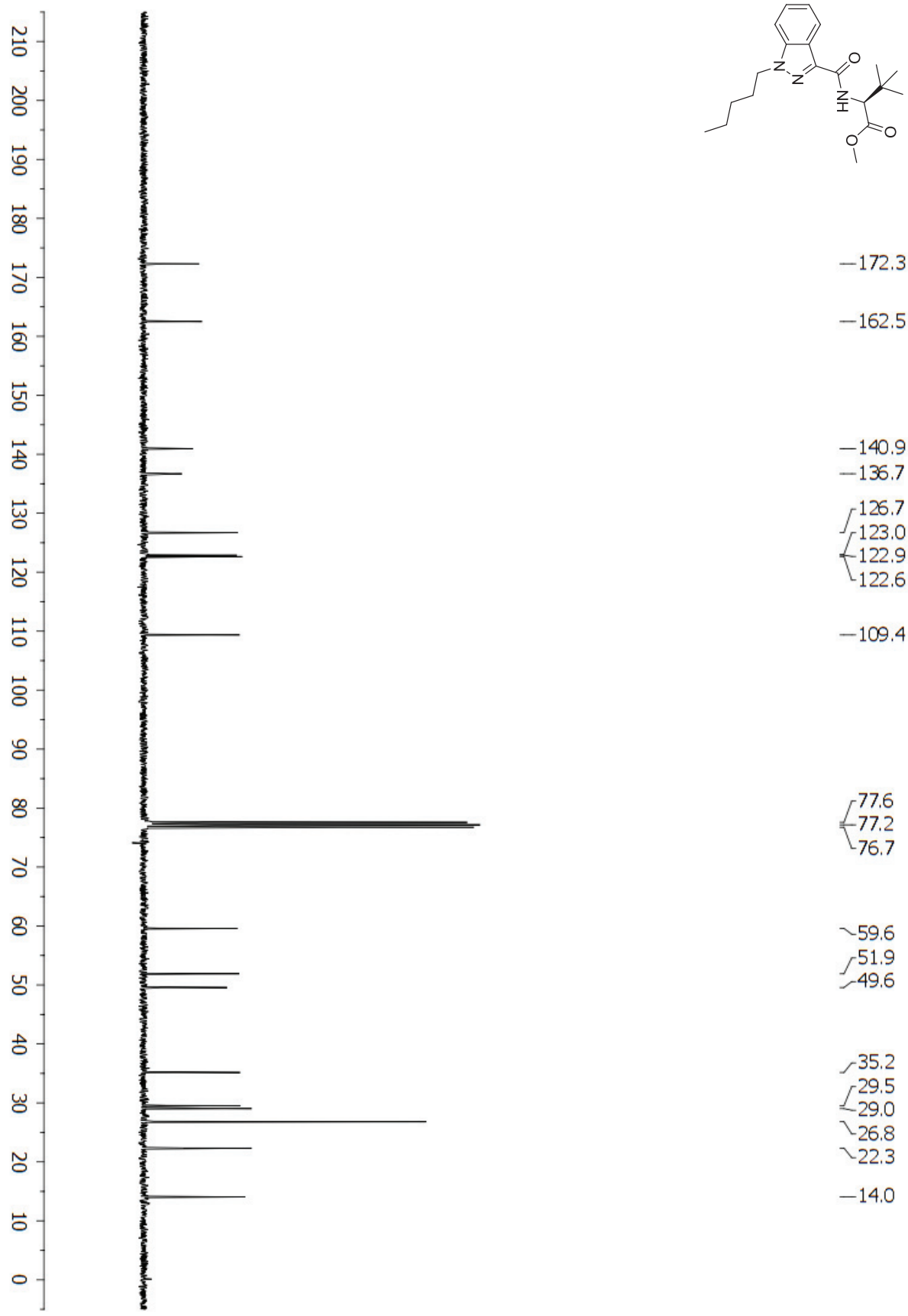

Figure S32. ^{13}C NMR spectrum (75 MHz, $CDCl_3$, 300 K) of MDMB-PINACA (**25**).

Figure S33. Mean normalized area under the vehicle baseline curve (AUC ± SEM) for (a) body temperature and (b) heart rate over the 6 hours immediately following doses of 0.1, 0.3, and 1 mg/kg MDMB-FUBINACA and 5F-AMB. MDMB-FUBINACA produced a larger hypothermic response compared to 5F-AMB at 0.3 and 1 mg/kg. * $P < .05$.

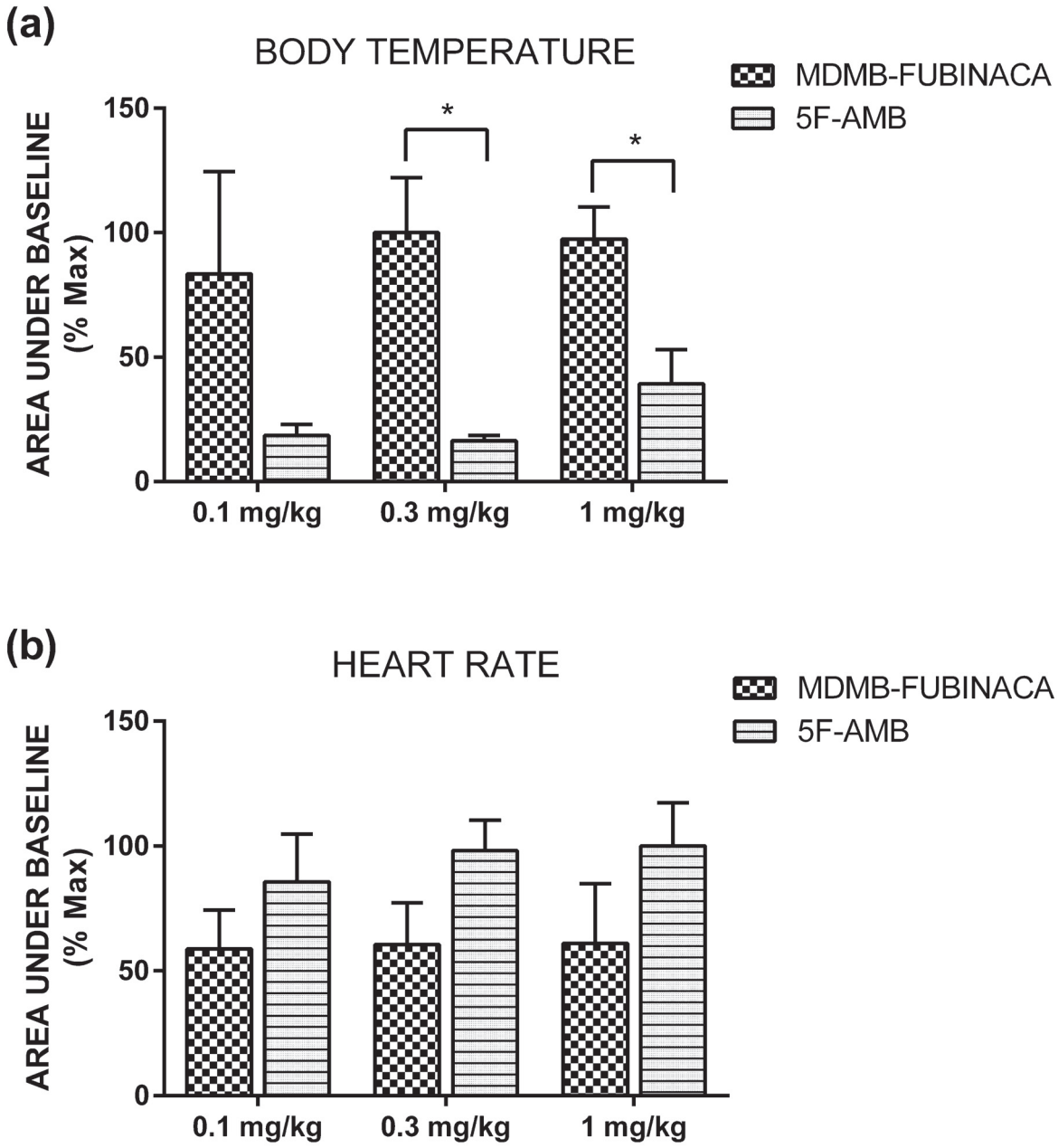

Figure S34. Body temperature data 24 hr following injection with 0.1 mg/kg MDMB-FUBINACA.Body temperature returned to baseline after 8 hr. Dashed line denotes time of intraperitoneal injection. Body temperature returned to baseline after 8 hr. Each point represents the mean ± SEM for four animals.

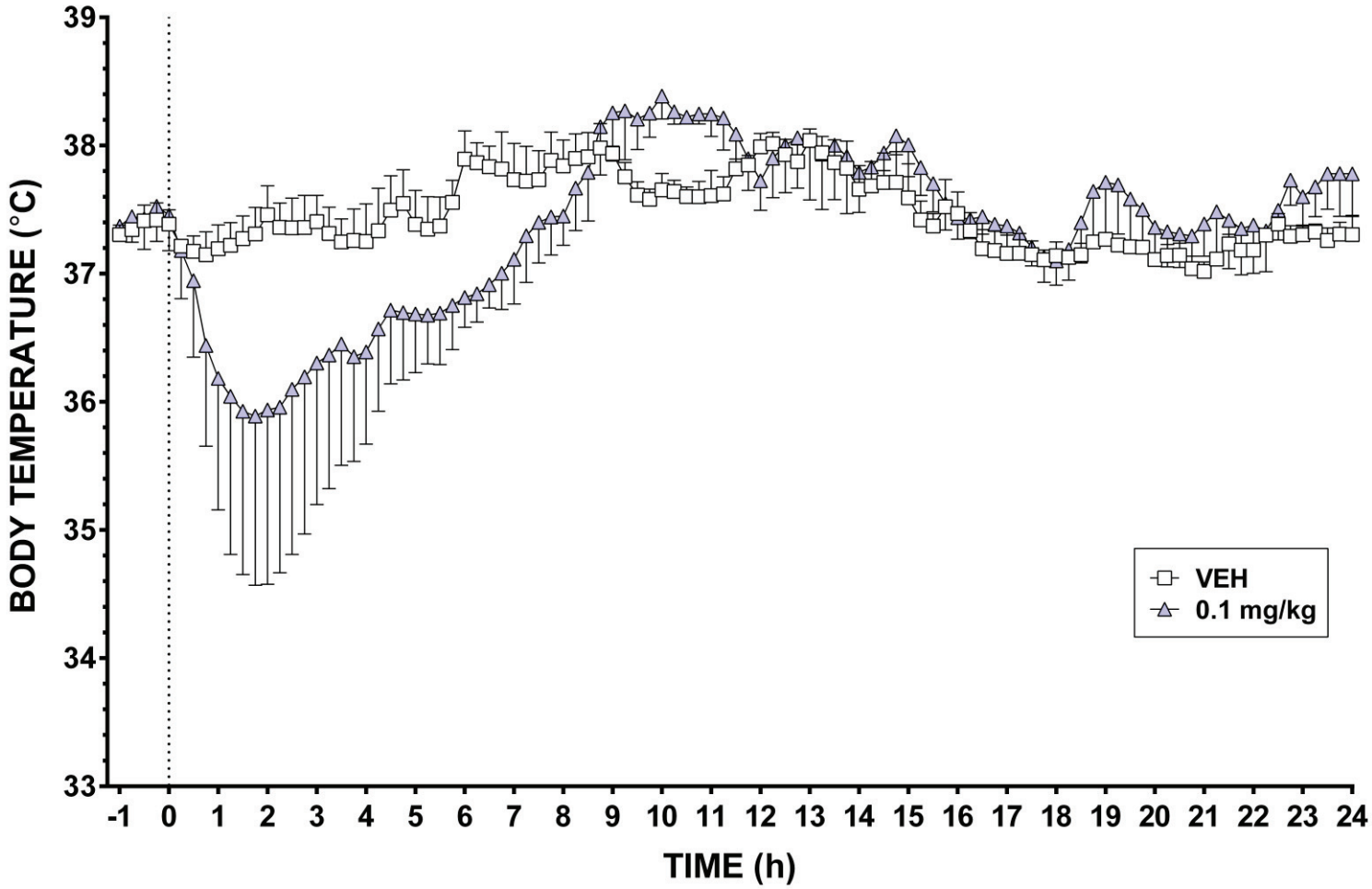

Figure S35. Mean area under the vehicle-vehicle baseline curve (AUC ± SEM) for body temperature for (a) 5F-AMB (3 mg/kg) and (b) MDMB-FUBINACA (1 mg/kg), following pretreatment with vehicle, rimonabant (CB_1 antagonist, 3 mg/kg), or SR144528 (CB_2 antagonist, 3 mg/kg). The area was significantly reduced for both 5F-AMB and MDMB-FUBINACA by rimonabant but not SR144528. * $p < .05$ compared to vehicle.

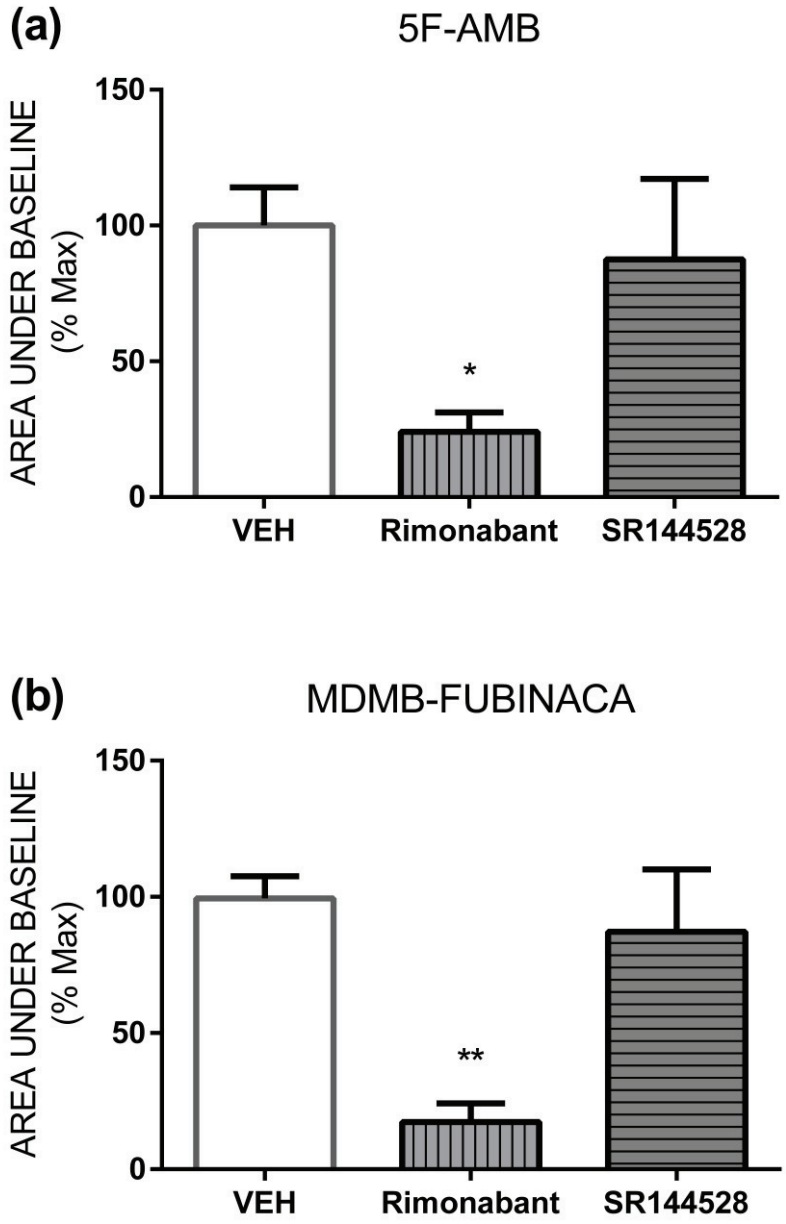

Appendix 2. Supplementary information for Chapter 5

Electronic supplementary material

Urinary cannabinoid levels during nabiximols (Sativex™)-medicated inpatient cannabis withdrawal

Richard C. Kevin, David J. Allsop, Nicholas Lintzeris, Adrian J. Dunlop, Jessica Booth and Iain S. McGregor*

*Address correspondence to:

Professor Iain McGregor, Professor of Psychopharmacology, School of Psychology, University of Sydney, A18, NSW 2006, Australia. Phone: +61 2 9351 3571; Fax +61 2 9351 8023; Email: iain.mcgregor@sydney.edu.au

Contents:

Table S1 Method validation and quantification parameters for urinary cannabinoid analysis using LC-MS/MS

Parameter	**CBD**	**THC**	**THC-COOH**	**11-OH-THC**
Internal Standard	CBD-d_3	THC-d_3	THC-COOH-d_9	11-OH-THC-d_3
LOQ (ng/mL)	1.0	1.0	125	10.0
LOD (ng/mL)	0.5	0.5	20.0	1.0
Linearity				
Quantification range (ng/mL)	1-1000	1-100	125-5000	10-500
r^2	.999	.996	.992	.993
Accuracy (%)				
Low QC	102	96.4	95.0	92.7
High QC	91.0	100	99.1	90.0
Precision %RSD, intra-day (n=3)				
Low QC	7.8	3.5	6.3	2.0
High QC	6.2	6.7	6.4	9.8
Precision %RSD, inter-day (n=3)				
Low QC	7.3	3.0	5.4	9.9
High QC	1.3	9.2	6.6	11.5

LOQ Limit of quantification, *LOD* limit of detection, *RSD* relative standard deviation. QCs were samples spiked to concentrations of each analyte at the top (high QC) and bottom (low QC) of the quantification range

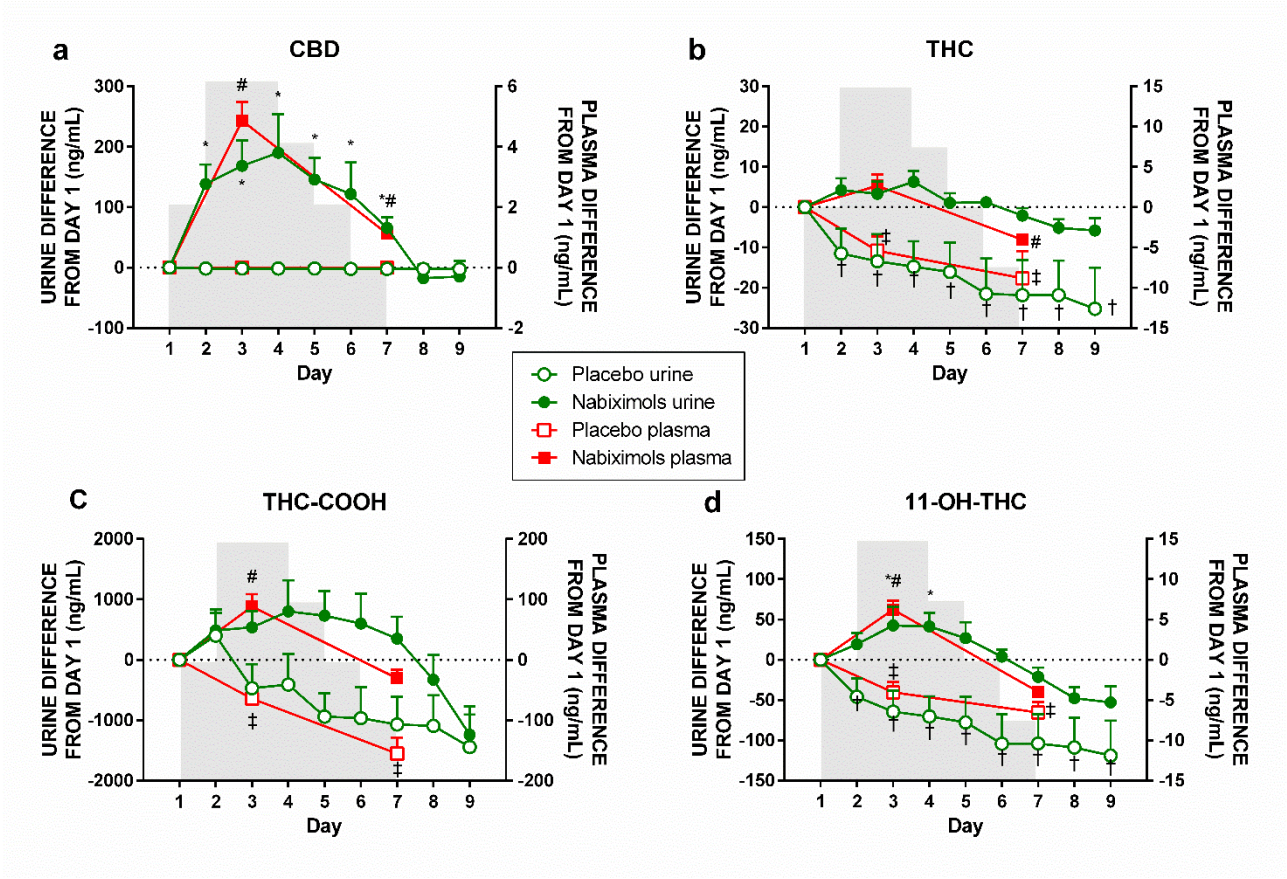

Fig. S1. Day 1 adjusted cannabidiol (CBD), Δ^9-tetrahydrocannabinol (THC), 11-nor-9-carboxy-THC (THC-COOH) and 11-hydroxy-THC (11-OH-THC) in plasma and urine of placebo (*n*=11) and nabiximols (*n*=11) treated patients. Shaded area indicates the tapered nabiximols dosing schedule, note that samples were taken in the morning and that day 1 samples were taken before the first nabiximols or placebo dose. * nabiximols urine significantly different from day 1 levels; # nabiximols plasma significantly different from day 1 levels; † placebo urine significantly different from day 1 levels; ‡ placebo plasma significantly different from day 1 levels.